

University of Mississippi

eGrove

---

Electronic Theses and Dissertations

Graduate School

---

1-1-2012

## Design and synthesis of HIV-1 integrase inhibitors

Sarah Chajkowski Scarry

*University of Mississippi*

Follow this and additional works at: <https://egrove.olemiss.edu/etd>



Part of the [Pharmacy and Pharmaceutical Sciences Commons](#)

---

### Recommended Citation

Scarry, Sarah Chajkowski, "Design and synthesis of HIV-1 integrase inhibitors" (2012). *Electronic Theses and Dissertations*. 1447.

<https://egrove.olemiss.edu/etd/1447>

This Dissertation is brought to you for free and open access by the Graduate School at eGrove. It has been accepted for inclusion in Electronic Theses and Dissertations by an authorized administrator of eGrove. For more information, please contact [egrove@olemiss.edu](mailto:egrove@olemiss.edu).

**DESIGN AND SYNTHESIS OF HIV-1 INTEGRASE INHIBITORS**

A Dissertation Presented in Partial Fulfillment of Requirements

for the Doctor of Philosophy in Pharmaceutical Sciences

The University of Mississippi

**Sarah Chajkowski Scarry**

May 2012

Copyright © 2012 by **Sarah Chajkowski Scarry**  
ALL RIGHTS RESERVED

## ABSTRACT

In recent years, HIV-1 integrase (IN) has emerged as an attractive target for the treatment of human immunodeficiency virus type 1 (HIV-1), the causative pathogen of acquired immunodeficiency syndrome (AIDS). Several classes of IN inhibitors are known but many of these compounds are toxic, do not show antiviral activity or display decreased potency. Therefore, new classes of potent IN inhibitors are desperately needed. The b-diketo (b-DK) class of compounds has emerged as one of the most successful classes of IN inhibitors. Although several b-DK inhibitors with potent antiviral activity are known, compounds containing b-DK motifs have limitations in drug development. The overall objective of this dissertation was to design and synthesize a novel series of IN inhibitors that retain the favorable characteristics of the b-DK scaffolds but are devoid of the “undruggable” properties. The design of the target molecules was established from crystal structure-based correlation and structure-activity relationship studies, which led to scaffolds containing three specific functional groups. Each molecule was designed to contain the core functional motif (a,b-diketoamide), optimal aryl groups (3-benzylphenyl or substituted 3-benzylphenyl) and a terminal group (proton donor or acceptor or amphoteric functional groups) in a planar or near planar configuration. Several oxalamate containing compounds were successfully designed and synthesized; and many of these synthetic analogs were sent to be screened for inhibitory activity against HIV-1 IN. The synthetic analogs described herein may elicit alluring antiviral activity, serve as potential lead molecules for future optimizations and ultimately elucidate mechanistic insight into HIV-1 IN inhibition.



## **DEDICATION**

I dedicate this dissertation to my family, especially...

to Brian for his patience and understanding and

to my parents for instilling the importance of hard work and for always encouraging me

## LIST OF ABBREVIATIONS

emim	3-methylimidazolium
3'-P	3'-processing
AZT	3'-azidothymidine
5-CITEP	1-(5-chloroindol-3-yl)-3-hydroxy-3-(2H-tetrazol-5-yl)-propanone
ART	antiretroviral therapy
ARV	antiretroviral
Asp	aspartic acid
BaP DE	benzo[a]pyrene 7,8-diol 9,10-epoxide
BnMe <sub>3</sub> N <sup>+</sup> CN <sup>-</sup>	benzyltrimethylammonium cyanide
CA	capsid
CAPE	caffeic acid phenyl ester
CBP	<i>CREB-binding protein</i>
CCD	catalytic core domain
CTD	carboxy-terminal domain
CCR5-C	C chemokine receptor 5-C
CD4	cluster of differentiation 4
cDNA	complementary DNA
CXCR4	chemokine receptor 4
CDK9	cyclin-dependent protein kinase
CYP450	cytochromeP450

Cys	cysteine
dba	dibenzalacetone
DDE	deoxynucleoside triphosphate (dNTP)
DHHS	Department of Health and Human Services
DMP	Dess-Martin periodinane
DAPY	diaryl-pyrimidine
DMSO	dimethyl sulfoxide
DKA	diketoacid
DNA	deoxyribonucleic acid
dsDNA	double-stranded DNA
DSIF	DRB sensitivity-inducing factor
Env	envelope glycoprotein-
FBS	fetal bovine serum
FDA	Food and Drug Administration
Glu	glutamic acid
gp41	glycoprotein 41
gp120	glycoprotein 120
GRID	gay-related immune deficiency
GSK	GlaxoSmithKline
HAART	highly active antiretroviral therapy
HCV	hepatitis C virus
HR2	heptad repeat 2
HMDS	hexamethyldisilazide

His	histidine
HIV-1	<i>human immunodeficiency virus type-1</i>
HPLC	high performance liquid chromatography
HSP60	heat-shock protein 60
HCl	hydrochloric acid
HCN	hydrogen cyanide
IC <sub>50</sub>	concentration that results in 50% inhibition
IDUs	injecting drug users
IL- $\beta$	interleukin-1 $\beta$
IN	integrase
Ini1	interactor 1
Inr	initiator
INSTIs	integrase strand inhibitors
KDa	kilodalton
LEDGF	lens epithelium-derived growth factor
LTR	long-terminal repeat
MA	matrix
MAP	mitogen activation protein
MOMCl	methyl chloromethyl ether
mRNA	messenger RNA
MS	mass spectrometry
MSM	men who have sex with men
MSM-IDU	men who have sex with men injection drug use

M-tropic	macrophagetropic
MAPK	p38 $\alpha$ mitogen-activated protein kinase
NCI	National Cancer Institute
NC	nucleocapsid
Nef	negative factor
NELF	negative elongation factor
NHS	normal human serum
Ni/C	nickel-on-charcoal
nM	nanomolar
NMR	nuclear magnetic resonance
NNRTIs	non-nucleoside reverse transcriptase inhibitors
NTD	N-terminal domain
NRTIs	nucleoside/nucleotide reverse transcriptase inhibitors
OHA	oxalohydroxamate
PCAF	p300/CREB-binding protein-associated factor
Pd	Palladium
PDB	protein data bank
PGL	persistent generalized lymphadenopathy
PIC	preintegration complex
PID	pelvic inflammatory disease
P-TEFb	positive transcription elongation factor b
PR	protease
PIs	protease inhibitors

PCC	pyridinium chlorochromate
RNA	ribonucleic acid
RNAPII	RNA polymerase II
RT	reverse transcriptase
SAR	structure-activity relationship
SeO <sub>2</sub>	selenium dioxide
SPA	scintillation proximity assay
ssDNA	single-stranded DNA
Sp1	specificity protein 1
ST	strand transfer
STI	strand transfer inhibitors
TLC	thin-layer chromatography
Tat	trans-activator of transcription
TNF- $\alpha$	tumor necrosis factor- $\alpha$
(Pd <sub>2</sub> (dba) <sub>3</sub> )	Tris(dibenzylideneacetone)dipalladium(0)
T20	enfuvirtide
TFAA	trifluoroacetic anhydride
UK	United Kingdom
Vif	viral infectivity factor
Vpr	viral protein R
WHO	World Health Organization
ZnBr <sub>2</sub>	zinc bromide
ZnCl <sub>2</sub>	zinc chloride

## ACKNOWLEDGMENTS

It would not have been possible for me to complete this dissertation without the support of many people. I owe my deepest appreciation to all of those who have made this work possible and because of whom my graduate career has been a rewarding and successful experience. First, and above all, I praise God, for allowing me this opportunity and for granting me the ability to complete this work.

My sincere gratitude goes to my advisor and mentor, Dr. John Rimoldi. Thank you for giving me that initial “second opportunity” to attend graduate school--for giving me that extra time to make one of the best decisions I’ve ever made. Thank you for your endless support, guidance, sense of humor and friendship. For encouraging me to teach, lead and be a successful and independent researcher. Most importantly, I thank you for knowing my strengths and abilities and for always challenging me to go beyond what I think I can do.

I would like to acknowledge the advice and insight from my committee members, Dr. Stephen Cutler, Dr. Christopher McCurdy and Dr. Takashi Tomioka. Thank you for providing me with genuine support and guidance throughout my graduate career. I would like to express my gratitude to all of the faculty members of the Department of Medicinal Chemistry. Dr. Robert Doerksen, Dr. Mitch Avery, and Dr. John Williamson, thank you for investing in my education, taking the time to teach me and for caring about my success as a future scientist.

Special thanks are due to the Rimoldi lab group members, past and present, for making it enjoyable to come to work every day and for being just like my family away from home. I

especially thank Dr. Rama Sarma Gadepalli for his willingness to always teach his laboratory skills and for being one of the kindest people I have ever met. I am grateful to have worked alongside Dr. S. Anand, Dr. Young Kim, Dr. Vanildo Braga, Dr. Stephen Slauson and Dr. Robert Smith. Thank you for always taking the time to teach me laboratory techniques, for insightful discussions in and out of the laboratory and for serving as role models for me. To my current lab mates, Brian Morgan, Eric Bow, Zarana Chauhan and Kimberly Foster it has been a true pleasure working with all of you and I will honestly miss being in lab 329 every day with each one of you. I owe a deep gratitude for the financial support provided by the National Science Foundation's Integrative Graduate Education and Research Traineeship Program (IGERT) program (Grant No. 0333136) and to the Department of Medicinal Chemistry (CDC/NIH-U50/CCU418839-01). A sincere thank you to our collaborator, Dr. John Babu and Panvirex, LLC. for providing us with this project and for the financial support that fueled this work (SBIR NIH-1R43AI080387-01). This dissertation certainly would not have been possible without Dr. John Babu's commitment to research.

I am extremely thankful to my wonderful family and many friends that have provided me with endless support every step of this journey. A very special thanks to the Cindy and Anthony Rimoldi for their friendship and for playing such an important role in my life. I express a sincere appreciation to my church family at College Hill Heights Baptist Church. My friends at work, Crystal and Jessica, thank you for all of our chats and for the occasional coffee breaks.

Thank you to my Mom and Dad, my sisters (Amy and Jenny) and my brother (David) for always believing in me and for providing endless encouragement. I am extremely thankful to my husband, Brian Scarry, for unselfishly loving and supporting me as I pursued my goals. This dissertation would simply be impossible to complete without the support of my loving family.



## TABLE OF CONTENTS

ABSTRACT .....	ii
DEDICATION .....	iv
LIST OF ABBREVIATIONS .....	v
ACKNOWLEDGMENTS .....	xvi
LIST OF TABLES .....	xviii
LIST OF FIGURES .....	xviii
LIST OF SCHEMES .....	xxii
I. INTRODUCTION .....	1
1.1. HIV AND AIDS BACKGROUND .....	1
1.1.1. History .....	1
1.1.2. Transmission .....	3
1.1.3. Statistics .....	6
1.1.4. Current Trends Worldwide .....	7
1.1.5. Current Trends in the United States .....	10
1.1.6. HIV-1 Structure and Genome .....	13
1.2. HIV-1 VIRAL LIFE CYCLE .....	14
1.2.1. Viral Entry Binding and Fusion .....	15
1.2.2. Reverse Transcription .....	17
1.2.3. Integration .....	18
1.2.4. Transcription .....	20

1.2.5. Assembly, Budding and Maturing .....	23
1.3. CURRENT THERAPY .....	23
1.3.1. Nucleotide/Nucleoside Reverse Transcriptase Inhibitors (NRTIs) .....	24
1.3.2. Protease Inhibitors (PIs).....	27
1.3.3. Non-Nucleoside Reverse Transcriptase Inhibitors (NNRTIs) .....	31
1.3.4. Highly Active Antiretroviral Therapy (HAART).....	32
1.3.5. Fusion inhibitors .....	33
1.3.6. Chemokine Receptor Antagonists.....	35
1.3.7. Integrase Inhibitors .....	36
1.3.8. Vaccines.....	37
1.4. ANTIRETROVIRAL DRUGS AND LABORATORY MONITORING .....	37
1.4.1. CD4 Testing.....	37
1.4.2. Quantitative Viral Load Testing .....	38
1.4.3. Drug Resistance Testing.....	38
1.4.4. Chemokine Receptor Tropism and HLA-B* Testing .....	38
1.5. COMPLICATIONS OF CURRENT ANTIRETROVIRAL THERAPIES.....	39
II. HIV-1 INTEGRASE INHIBITOR DEVELOPMENT .....	41
2.1. HIV-1 INTEGRASE: A TARGET FOR DRUG DISCOVERY .....	41
2.1.1. Challenges of HIV-1 IN as a Target .....	42
2.1.2. HIV-1 IN as a Valid and Attractive Target.....	43
2.2. THE EARLY YEARS OF DEVELOPMENT.....	45
2.2.1. The Development of an <i>In Vitro</i> Screening Assay .....	46
2.2.2. Hydroxylated Aromatics and Catechol-Containing Inhibitors .....	46

2.2.3. Non-Catechol-Containing Aromatic Inhibitors .....	48
2.2.4. An Assay to Identify Strand Transfer Inhibitors of HIV-1 IN.....	50
2.3. The $\beta$ -DIKETO ACID CLASS OF INHIBITORS .....	51
2.3.1. HIV-1 Integrase Inhibitors Enter Clinical Trials .....	54
2.4. HIV-1 IN INHIBITORS: FROM CLINCAL TRIALS TO MARKET .....	56
2.4.1. Raltegravir.....	56
2.4.2. Elvitegravir .....	58
2.4.3. GSK-364735 .....	59
2.4.4. Dolutegravir (S/GSK1349572).....	59
2.5. PERSPECTIVE.....	60
III. DESIGN AND SYNTHETIC APPROCHES TOWARDS THE	
DEVELOPMENT OF NOVEL HIV-1 INTEGRASE INHIBITORS .....	63
3.1. HIV-1 IN STRUCTURE AND FUNCTION.....	63
3.2. PROPOSED MECHANISMS OF ST INHIBITION.....	67
3.2.1. Biochemical Mechanisms .....	70
3.2.2. Molecular Mechanism .....	72
3.2.3. Proposed Mechanisms and Inhibitor Development .....	74
3.3. DISCOVERY OF THE AMINOCARBOXYALTE SYSTEM.....	75
3.3.1 Aromatic Substitutions of the DKAs .....	75
3.3.2. Keto-Enol Tautomerism of DKA IN Inhibitors.....	77
3.3.3. Aminocarboxylate: Alternative Surrogate for the $\beta$ -DK scaffold.....	79
3.3.4. Ligand Docking of Aminocarboxylate IN Inhibitors.....	82
3.3.5. Design of the Oxalamate IN inhibitors: Isosteric Replacement	

of the Hydroxamate.....	91
3.3.6. SAR of the Terminal Functional Groups of the Oxalamate Scaffolds .....	92
3.4. SYNTHETIC APPROACHES .....	95
3.4.1. Heteroaromatic $\alpha$ -Oxoacetic Acids: Cyanohydrin Chemistry .....	95
3.4.2. Heteroaromatic $\alpha$ -Oxoacetic Acids: Activation of Pyridium Salts for Electrophilic Acylation .....	102
3.4.3. Heteroaromatic $\alpha$ -Oxoacetic Acids: Heterocyclic $\alpha$ -Iminonitriles .....	104
3.4.4. Aryl $\alpha$ -Keto Esters and Acids .....	108
3.4.5. Negishi and Suzuki Cross-Coupling Reactions with Acid Chlorides.....	112
3.4.6. Friedel-Crafts Acylation .....	116
3.5. BIOLOGICAL EVALUATION .....	118
3.5.1. Determination of IN inhibition .....	118
3.5.2. Determination of Sensitivity to Known IN Inhibitor Mutations.....	120
3.5.3. Determination of Antiviral Efficacy .....	120
3.6 CONCLUSIONS AND FUTURE PERSPECTIVES .....	121
3.6.1. Alternative Strategy for the Synthesis of $\alpha$ , $\beta$ -diketo amides .....	122
3.6.2. Synthetic Strategies for Alternative Aryl Scaffolds.....	125
3.6.3. Opportunities for Alternative Biological Targets .....	127
3.6.3.1. Inhibitors of p38 $\alpha$ Mitogen-Activated Protein Kinase .....	127
3.6.3.2. Inhibitors of HIV-1 Attachment.....	128
IV. EXPERIMENTAL.....	129
BIBLIOGRAPHY.....	172
List of Appendices .....	207

Appendix: A.....	208
Appendix: B.....	366
VITA.....	414

## LIST OF TABLES

Table 1.1	CDC Classification System for HIV-1 Infection.....	5
Table 1.2	Selected Examples of Clinical Categories B and C Conditions .....	5
Table 1.3	WHO Clinical Staging of HIV-1/AIDS.....	6
Table 1.4	HIV-1 Prevalence and Incidence by Region.....	8
Table 1.5	Percentage of AIDS in U.S. among Various Ethnic Groups <sup>2</sup> Compared to Percentage of Population Each Ethnic Group Represents <sup>3,4</sup> .....	11
Table 1.6	Top Ten States by Cumulative AIDS Diagnosis and by AIDS Diagnosis Rate Per 100,000 .....	13
Table 1.7	Clinically Approved Nucleoside/Nucleotide Reverse Transcriptase Inhibitors (NRTIs) .....	27
Table 1.8	Clinically Approved Protease Inhibitors (PIs).....	28
Table 1.9	Clinically Approved Non-Nucleotide Reverse Transcriptase Inhibitors (NNRTIs).....	32
Table 1.10	Multi-Class HIV-1 Combination Drugs .....	33
Table 1.11	Clinically Approved HIV-1 Fusion Inhibitor .....	34
Table 1.12	Clinically Approved CCR5 Antagonist .....	36
Table 1.13	Clinically Approved HIV-1 Integrase Inhibitor.....	36
Table 2.1	Review Articles Detailing HIV-1 Integrase Inhibitors (1992-2011).....	41
Table 2.2	IN inhibitors in Clinic and Clinical Development .....	60
Table 3.1	Binding and Inhibition by Hybrid Integrase Inhibitors .....	73
Table 3.2	SAR of Aromatic Substitution on $\beta$ -DKA Scaffold .....	76
Table 3.3	SAR of $\beta$ -Diketo Compounds Lacking the Terminal Carboxylate.....	78

Table 3.4 SAR of Aminocarboxylate Scaffolds .....	80
Table 3.5 Summary of Hydrogen Bond Interactions with $\beta$ -BK and OHA Terminal Functional Groups .....	91
Table 3.6 Suzuki Methodology Summary with Acid Chlorides and Aryl Boronic Acids .....	115

## LIST OF FIGURES

Figure 1.1	Adults and Children Estimated to be Living with HIV-1, 2009.....	7
Figure 1.2	Estimated New HIV-1 Infections in the U.S., 2009 .....	10
Figure 1.3	Estimated Numbers of AIDS Diagnoses, All Ages, 2009.....	12
Figure 1.4	HIV-1 Genome .....	14
Figure 1.5	Schematic Representation of the HIV-1 Replication Cycle .....	15
Figure 1.6	Schematic description of early events occurring after HIV infection .....	17
Figure 1.7	The Two IN Catalytic Reactions .....	20
Figure 1.8	Stimulation of Transcriptional Elongation by HIV-1 Tat .....	21
Figure 1.9	The HIV-1 Replication Cycle and Drug Targets.....	24
Figure 1.10	Nucleoside/Nucleotide Reverse Transcriptase Inhibitors (NRTIs) .....	25
Figure 1.11	Structure of Natural Deoxynucleoside Triphosphates (dNTP) .....	26
Figure 1.12	Warfarin.....	29
Figure 1.13	Protease Inhibitors (PIs) .....	30
Figure 1.14	Non-Nucleotide Reverse Transcriptase Inhibitors (NNRTIs).....	31
Figure 1.15	Linear schematic of the HIV gp41 .....	34
Figure 1.16	CXCR4 and CCR5 Antagonists .....	35
Figure 1.17	HIV-1 Integrase Inhibitors .....	36
Figure 2.1	Calculated Druggability.....	44
Figure 2.2	Select Examples of DNA Binders and Topoisomerase Inhibitors .....	45
Figure 2.3	General Structure of Catechol Containing Inhibitors .....	46



Figure 2.4	Select Examples of Polyhydroxylated Aromatic IN inhibitors .....	47
Figure 2.5	Select Examples of Hydrazide-Based Inhibitors of IN .....	48
Figure 2.6	Select Examples of Sulfone-Based Inhibitors of IN .....	49
Figure 2.7	First Lead DKA IN Inhibitors with Selectivity for ST .....	51
Figure 2.8	5-CITEP Complexed with Crystal Structure .....	53
Figure 2.9	Instability of DKA in Aqueous Base .....	54
Figure 2.10	Replacement of DKA with Diaryl Diketones.....	54
Figure 2.11	Examples of Clinically Tested DKA IN Inhibitors .....	55
Figure 2.12	Discovery of Dihydropyrimidine Carboxamide (2.17) as an HIV-1 IN Inhibitor.....	57
Figure 2.13	Discovery of 4-quinolone-3-carboxylic acid as an IN inhibitor.....	58
Figure 2.14	Timeline of IN Inhibitor Milestones .....	62
Figure 3.1	Structural Domains of HIV-1 Integrase .....	64
Figure 3.2	Role of Divalent Metal Ions in Catalysis .....	65
Figure 3.3	The Mechanism of the 3'Processing and ST Reactions .....	66
Figure 3.4	Role of Major and Minor Grooves in IN Reactions.....	68
Figure 3.5	Important Components of IN/DNA Interactions .....	69
Figure 3.6	IN amino acids interacting with viral cDNA bases.....	69
Figure 3.7	Structure of 5-CITEP .....	70
Figure 3.8	Stereo Image of 5-CITEP Inhibitor/Protein Contacts. ....	70
Figure 3.9	Schematic of 5-CITEP and Interacting Residues .....	71
Figure 3.10	Structure of L-731,988 .....	71
Figure 3.11	Complexing Motifs for DKAs.....	72
Figure 3.12	Model for the Binding of Two Divalent Metals by DKA Inhibitors.....	74

Figure 3.13 Potent DKA ST Inhibitors with Antiviral Activity .....	75
Figure 3.14 Possible Tautomers of DKAs .....	77
Figure 3.15 Diol Derivative of DKA 3.6 .....	78
Figure 3.16 Potent DKA IN Inhibitors .....	79
Figure 3.17 Overlapping 3D Geometry of Compounds 3.6 and 3.16.....	81
Figure 3.18 Analysis of 5-CITEP bound in IN Crystal Structure (1QS4).....	84
Figure 3.19 Binding of the Carboxylate Derivative of 5-CITEP (3.5).....	84
Figure 3.20 The Overlapping Geometry of 5-CITEP .....	85
Figure 3.21 The Binding Orientation and Interactions of S-1360 and L-731,988. ....	86
Figure 3.22 Binding Orientation of Hydroxamate Containing Compound 3.16. ....	87
Figure 3.23 Hydroxamate 3.21 with Substituted Aryl Group.....	87
Figure 3.24 Binding Orientation of 3.2.....	88
Figure 3.25 Superimposed Crystal Structure 1QS4 and the Phosphate Ion Bound IN Structure 1K6Y. ....	89
Figure 3.26 Superimposed DNA Phosphate Backbone of dsDNA (1K6Y) with 1QS4.....	90
Figure 3.27 General SAR of Designed Oxalamate Scaffolds.....	92
Figure 3.28 The Interactions of $\beta$ -DK Class of IN Inhibitors with IN Amino Acids.....	92
Figure 3.29 Group A Proposed Scaffolds. ....	93
Figure 3.30 Group B Proposed Scaffolds .....	94
Figure 3.31 Group C Proposed Scaffolds. ....	94
Figure 3.32 The Ligand Docking Analysis of C9 (Ar-1 Aryl Group).....	95
Figure 3.33 Aryl Groups .....	95
Figure 3.34 Comparison of Estimated NMR Values to Reported NMR Values of 3.39.....	106

Figure 3.35 Synthesized Aryl Oxalamate Derivatives.....	109
Figure 3.36 TLC of Desired Product (B) and DBA (A) .....	115
Figure 3.37 Select Indole Glyoxamide HIV-1 Entry Inhibitors .....	116
Figure 3.38 Heterocyclic Oxalyl Amide MAPK inhibitor.....	127
Figure 3.39 Pyrazole $\alpha$ -Keto Amide Derivative .....	127

## LIST OF SCHEMES

Scheme 3.1 Proposed Route for the Synthesis of Heteroaromatic Oxalamate Derivatives.....	96
Scheme 3.2 Synthesis of 2-, 3- and 4- Pyridine Oxalamate Derivatives .....	96
Scheme 3.3 General Procedure for the Hydrolysis of Mandelonitrile.....	97
Scheme 3.4 Oxidation of 3-Pyridine $\alpha$ -Hydroxy Derivatives.....	98
Scheme 3.5 Synthesis of 5-Bromopyridine-2-oxalamate 3.49 .....	99
Scheme 3.6 Synthesis of 2-and 4-Imidazole Oxalamate Derivatives .....	100
Scheme 3.7 Approaches Towards the Synthesis of Furan $\alpha$ -Hydroxy .....	101
Scheme 3.8 Cyanide Ion and Pyridium Salts.....	102
Scheme 3.9 Synthesis of 3-Pyridine Oxalamate 3.44 .....	103
Scheme 3.10 Synthesis of $\alpha$ -Oxoacetic Acids .....	105
Scheme 3.11 Reaction Pathways for the Hydrolysis of the $\alpha$ -Iminonitrile 3.84 .....	107
Scheme 3.12 Alternative Route for the Synthesis of $\alpha$ -Oxoacetic Acids from $\alpha$ -Aminonitriles.....	108
Scheme 3.13 Three-step Sequential Procedure to Synthesize $\alpha$ -Keto Esters .....	108
Scheme 3.14 Synthesis of Aryl Oxalamate Scaffolds .....	109
Scheme 3.15 Pd-catalyzed Synthesis of Arylphosphonates .....	110
Scheme 3.16 Approach towards the Synthesis of 3- and 4-Arylphosphonates (3.111 and 3.112).....	110
Scheme 3.17 Alternative Approach for the Synthesis of Arylphosphonates.....	112
Scheme 3.18 Negishi Coupling of Diketo Acid Chloride with Zinc Bromides.....	112
Scheme 3.19 Synthesis of Furan Oxalamate 3.107 Using Negishi Coupling Conditions .....	113
Scheme 3.20 Suzuki Cross-coupling of Acid Chlorides with Arylboronic Acids.....	113

Scheme 3.21 Suzuki Cross-coupling of Diketo Acid Chlorides with Aryl Boronic Acids .....	114
Scheme 3.22 Friedel-Crafts Synthesis of Indole Derivatives 3.140-3.144.....	117
Scheme 3.23 Friedel-Crafts Synthesis of Azaindole Derivative 3.148 .....	118
Scheme 3.24 Summary of Synthetic Routes Explored .....	123
Scheme 3.25 Direct $\alpha$ -Oxidation of Amides and Esters Using Selenium Dioxide.....	124
Scheme 3.26 Sodium Bicarbonate Promoted Aerobic Oxidation Reaction .....	125
Scheme 3.27 Proposed Synthetic Route for 5-(2,4-difluorobenzyl)-2-isopropoxyaniline 3.157.....	126
Scheme 3.28 Pd-catalyzed Direct Benzylation of Fluoroarene 3.158 .....	127

## I. INTRODUCTION

Human immunodeficiency virus type-1 (HIV-1) is a lentivirus that infects CD4 (cluster of differentiation 4) positive (CD4+) T-lymphocytes (T-cells) and macrophages of the human immune system. Infection with the HIV-1 virus results in the progressive deterioration and impairment of the host immune system, leading to an 'immune deficiency'. A person infected with HIV-1 is easily susceptible to infections, most of which are rare among healthy people. Infections associated with an immunodeficiency are known as 'opportunistic infections' (OIs), because they take advantage of the weakened immune system.<sup>5</sup> HIV-1 is a slow disease that continues to cause progressive damage to the immune system from the time of infection to the manifestation of severe immunologic damage by OIs, neoplasms, wasting, or low CD4+ cell count that will eventually lead to acquired immunodeficiency syndrome (AIDS).<sup>6</sup>

### 1.1. HIV-1 AND AIDS BACKGROUND

#### 1.1.1. History

The simian version, simian immunodeficiency virus (SIV), of human immunodeficiency virus type 1 (HIV-1) was conceivably transferred from its natural host, the chimpanzee, to man in the early to middle years of the 20<sup>th</sup> century in the west central African countries of Cameroon and Gambia.<sup>7</sup> The spread of HIV-1 was initially slow and limited, but due to rapid urbanization in the post-colonial era, the disease rapidly spread worldwide appearing in at-risk individuals in most regions by the mid-to-late 1970s.<sup>8</sup>

HIV-1 infection was not recognized in medical publications until the clinical syndrome of advanced immune deficiency, later termed AIDS, was reported in the early 1980s.<sup>8</sup> Unusual cases of infection and illness among young, previously healthy individuals began to appear in large cities in the United States (U.S.) in 1981. Kaposi's Sarcoma (KS) was a rare form of relatively benign cancer that tended to occur in elderly people. In March 1981 at least eight cases of a more aggressive form of KS had transpired amid young homosexual men in New York.<sup>9</sup> On June 5, 1981, the first acquired immunodeficiency syndrome (AIDS) cases were reported by the Centers for Disease Control and Prevention (CDC): five cases of *Pneumocystis carinii* (now *P. jiroveci*) pneumonia (PCP) among previously healthy homosexual men in Los Angeles. The accompanying editorial suggested that the illness might be related to the men's sexual behavior.<sup>10</sup> Later in 1981, more cases of PCP and KS among homosexual men in New York and California were seen.<sup>11, 12</sup> When the CDC reported the new outbreak they called it "gay-related immune deficiency" (GRID) or "gay cancer", stigmatizing the gay community as carriers of this deadly disease.<sup>13</sup> However by December 1981, cases started appearing in heterosexuals, injecting drug users (IDUs) and people who received blood transfusions, also the first case of AIDS was reported in the United Kingdom (UK), proving the syndrome knew no boundaries.<sup>14, 15</sup> The disease continued to spread across the U.S. and by July 1982, a total of 452 cases from across the U.S. had been reported to the CDC.<sup>16</sup> By 1983 it was becoming increasingly clear that the disease was not limited to spreading across the U.S. Cases were also being reported in Europe, Uganda, Australia, Canada, Latin America and Japan.<sup>17</sup> It took eighteen months from the first report to identify the primary risk factors for AIDS; guidelines for prevention of occupational, drug-related and sexual transmission of the illness were issued by the CDC in March 1983.<sup>18</sup> It was later that year, that Luc Montangier and Francoise Barre-Sinoussi isolated the suspected

retrovirus<sup>19</sup> which was later confirmed to be the causative agent of AIDS by Robert Gallo in 1984.<sup>20, 21</sup> This virus was ultimately termed ‘human immunodeficiency virus’ (HIV).<sup>22</sup>

### **1.1.2. Transmission**

The transmission of HIV-1 from an infected person to an uninfected person occurs when an infected person’s bodily fluids, mainly semen, vaginal fluids, blood or breast milk enters an uninfected person’s body.<sup>23-25</sup> The most common routes of transmission are unprotected sexual intercourse, injection drug use (IDU), and from infected mother to infant.<sup>26</sup> Blood transfusions and organ transplants were initially a way that HIV-1 was spread, but now due to careful tests and screening the risk is extremely low.<sup>27</sup>

The first phase of HIV-1 infection is the asymptomatic incubation period. Most people that become infected with HIV-1 do not know that they have become infected because they do not feel ill immediately after infection.<sup>5</sup> However, some people at the time of seroconversion (development of antibodies to HIV-1; 1-6 weeks after HIV-1 infection) develop acute retroviral syndrome characterized by fever, malaise, generalized lymphadenopathy, pharyngitis, diarrhea, and rash.<sup>28</sup> An acute infection is often unrecognized because the complex of symptoms is easily confused with other illnesses and diseases (e.g., influenza or infectious mononucleosis).<sup>29</sup> In acute primary infection, plasma HIV-1 RNA (ribonucleic acid) concentrations can be very high, making secondary transmission a high risk if an infected individual continues to engage in behavior that could transmit HIV-1 to an uninfected person. After the symptoms of primary infection resolve, the infected person enters the second phase of HIV-1, the asymptomatic latent phase.<sup>8</sup> An infected person displays no symptoms and this stage can persist for several years (average eight to ten years), although rapid progression is usually common. During this stage,



HIV-1 is actively replicating and will continue to weaken the immune system. The symptomatic disease phase (one to three years) often emerges as the peripheral CD4+ cell count falls below 350 cells per  $\mu\text{L}$  and many people become susceptible to infections and begin to experience HIV-1 disease related symptoms. The last stage of infection is the progression of HIV-1 to AIDS when the immune-system's ability to fight infection on its own is lost. A diagnosis of AIDS is given when a patient CD4+ count falls below 200 cells per  $\mu\text{L}$  and individuals experience multiple OIs (pneumonia, neurological diseases and cancers). The CDC classification system is used to determine the severity and progression of HIV-1 and AIDS infection and disease (Table 1.1). This classification system is based on specific conditions that a patient has developed (Table 1.2).<sup>30, 31</sup>

The clinical staging and case definition for resource-constrained settings were developed by the World Health Organization (WHO) in 1990 and revised in 2007.<sup>32</sup> Staging is based on clinical findings that guide diagnosis, evaluation, and management of HIV-1 and AIDS and it does not require a CD4+ cell count. In many countries this staging will help to determine the eligibility for antiretroviral therapy (ART), particularly in locations where CD4+ testing is not available. Clinical stages, defined by clinical conditions, are categorized as 1 through 4, progressing from primary HIV-1 infection to advanced HIV-1 and AIDS (Table 1.3).<sup>32</sup>

CD4+ Cell Counts	Clinical Categories		
	<b>A</b> Asymptomatic, Acute HIV-1 or PGL*	<b>B</b> Symptomatic Conditions, not A or C	<b>C</b> AIDS-Indicator Conditions
$\geq 500$ cells/ $\mu\text{L}$	A1	B1	C1
200-499 cells/ $\mu\text{L}$	A2	B2	C2
$<200$ cells/ $\mu\text{L}$	A3	B3	C3

\*PGL= persistent generalized lymphadenopathy; Patients in categories A3, B3, C1-C3 are considered to have AIDS

**Table 1.1** CDC Classification System for HIV-1 Infection<sup>30, 31</sup>

Category B Symptomatic Condition Examples	Category C AIDS Indicator Conditions
<p>Symptomatic condition as are attributed to HIV infection or indicate a defect in cell-mediated immunity and/or</p> <p>They are considered to have a clinical management that is complicated by HIV infection</p> <p>Bacterial angiomatosis</p> <p>Oropharyngeal candidiasis (thrush)</p> <p>Vulvovaginal candidiasis, persistent/resistant</p> <p>Pelvic inflammatory disease (PID)</p> <p>Cervical dysplasia/ cervical carcinoma</p> <p>Hairy leukoplakia, oral</p> <p>Herpes zoster (shingles) <math>\geq 2</math> episodes</p> <p>Idiopathic thrombocytopenic purpura (low platelet count)</p> <p>Fever (<math>&gt;38.5^{\circ}\text{C}</math>) or diarrhea <math>&gt;1</math> month</p> <p>Peripheral neuropathy</p>	<p>Bacterial Pneumonia (<math>\geq 2</math> episodes in 12 months)</p> <p>Candidiasis of bronchi, trachea, or lungs</p> <p>Candidiasis, esophageal</p> <p>Cervical carcinoma, invasive</p> <p>Coccidioidomycosis (fungal disease)</p> <p>Cryptococcosis, extrapulmonary (fungal disease)</p> <p>Cryptosporidiosis, chronic intestinal <math>&gt;1</math> month (parasitic disease)</p> <p>Cytomegalovirus disease (other than liver, spleen, or nodes)</p> <p>Encephalopathy, HIV-1 related</p> <p>Herpes simplex: chronic ulcers (<math>&gt;1</math> month), or bronchitis, pneumonitis, or esophagitis</p> <p>Kaposi sarcoma</p> <p><i>Mycobacterium tuberculosis</i></p> <p><i>Salmonella</i> septicemia, recurrent (nontyphoid)</p> <p>Wasting syndrome caused by HIV (involuntary weight loss <math>&gt;10\%</math> of baseline body weight)</p>

**Table 1.2** Selected Examples of Clinical Categories B and C Conditions<sup>30, 31</sup>

Stage	Symptoms
Primary HIV-1 Infection	Asymptomatic, Acute retroviral syndrome
Clinical Stage 1	Asymptomatic, Persistent generalized lymphadenopathy (PGL)
Clinical Stage 2	Weight loss ( $<10\%$ measured body weight) Recurrent respiratory infections Herpes zoster Angular cheilitis (lesions) Recurrent oral ulceration Seborrheic dermatitis (inflammation) Fungal nail infection
Clinical Stage 3 Some persons with clinical stage 3 have AIDS	Severe weight loss ( $>10\%$ measured body weight) Chronic diarrhea $>1$ month Persistent fever $>1$ month Oral candidiasis Oral hairy leukoplakia Pulmonary tuberculosis Severe bacterial infections (pneumonia, bone or joint infection, meningitis) Anemia (hemoglobin $<8$ g/dL) Neutropenia (neutrophils $<500$ cells/ $\mu\text{L}$ ) Chronic thrombocytopenia (platelets $<50,000$ cells/ $\mu\text{L}$ )
Clinical Stage 4 Includes 22 opportunistic infections or cancers related to HIV-1. All persons with clinical stage 4 have AIDS.	HIV wasting syndrome ( $>10\%$ measured body weight) Pneumocystis pneumonia Recurrent severe bacterial pneumonia Chronic Herpes simplex infection Esophageal candidiasis Extrapulmonary tuberculosis Kaposi sarcoma Cytomegalovirus infection (retinitis or infection of other organs) Candidiasis of bronchi, trachea, esophagus or lungs Lymphoma (cerebral or B-cell non-Hodgkin) <i>Salmonella</i> septicemia, recurrent (nontyphoid) Cervical carcinoma, invasive Symptomatic HIV-associated nephropathy Symptomatic HIV-associated cardiomyopathy

**Table 1.3** WHO Clinical Staging of HIV-1/AIDS<sup>32</sup>

### 1.1.3. Statistics

Human immunodeficiency virus type 1 (HIV-1) is the etiological agent that causes AIDS. As of 2009, it is estimated that worldwide there are 33.3 million people living with HIV-1, with 22.5 million (68 % of the global total) in Sub-Saharan Africa (Figure 1.1).<sup>33</sup> The CDC has estimated that more than 1.1 million adults and adolescents were living with HIV infection in the U.S. at the end of 2006, the most recent year for which national prevalence estimates are available.<sup>26</sup> There is no cure for HIV-1 or AIDS and since the discovery of AIDS in 1981, it has led to the deaths of more than 30 million people.<sup>33</sup> HIV-1 is arguably the most intensely studied virus in the history of biomedical research. Despite the wealth of knowledge, however, HIV-1 infection remains a pandemic today and elusive in terms of a ‘cure’.<sup>34</sup>

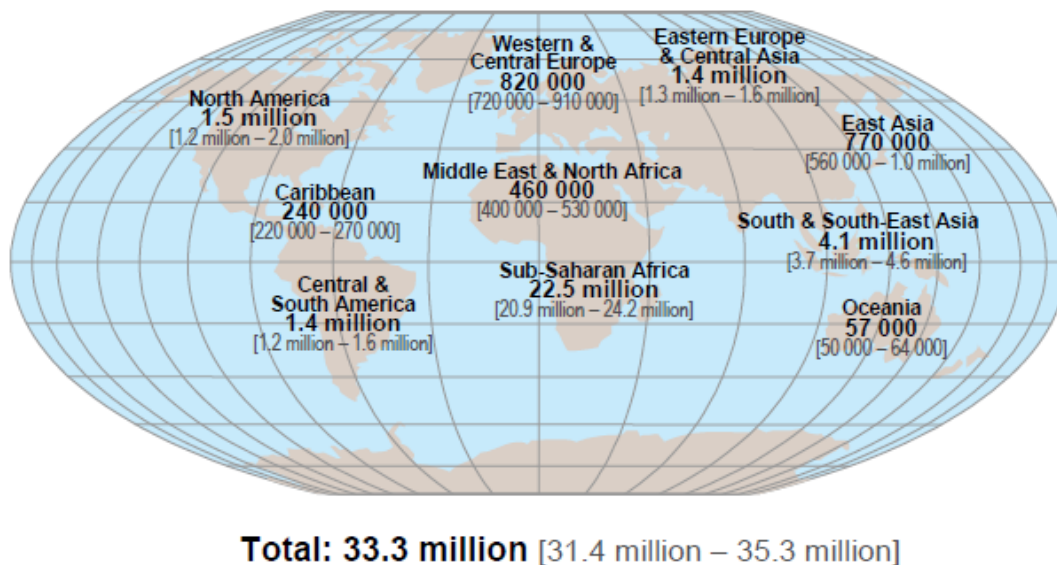


**Figure 1.1** Adults and Children Estimated to be Living with HIV-1, 2009<sup>33</sup>  
(Permission to reprint ID:87551 WHO, permissions@who.int; 02-20-2012)

### 1.1.4. Current Trends Worldwide

HIV-1 has become one of the most challenging and serious health concerns worldwide. When the first cases of HIV-1 and AIDS were reported in 1981, no one could have predicted

how the epidemic would spread around the world and how many millions of lives it would ultimately affect. Even though HIV-1 and AIDS cases have been reported in all regions of the world, about 95% of people living with HIV-1 and AIDS reside in low- and middle-income countries, where most new HIV-1 infections and AIDS-related deaths occur.<sup>33,35</sup> The major route of transmission worldwide is heterosexual sex, although risk factors vary within and across populations.<sup>36</sup> In several regions of the world, men who have sex with men (MSM), IDUs, and sex workers account for substantial proportions of infections.<sup>33</sup>

The most affected regions of the world are sub-Saharan Africa, Asia, Latin America and the Caribbean, Eastern Europe and Central Asia (Table 1.4).<sup>33,35,36</sup> Sub-Saharan Africa, the most severely affected region in the world, has two-thirds (68%, 22.5 million) of people living with HIV-1 but only about 12% of the world's population.<sup>37,38</sup> At the end of 2009, there were nine countries with more than 10% of adults are estimated to be HIV-positive.<sup>33</sup> Most children with HIV-1 live in this region (91%).<sup>39</sup> About 1.7 million people are estimated to be living with HIV-1 in Latin America and the Caribbean combined, including 112,000 newly infected in 2010.<sup>35</sup> The Caribbean itself, with an adult HIV-1 prevalence rate of nearly 1%, is the second most affected region in the world after sub-Saharan Africa.<sup>37</sup> Nearly 5 million people are living with HIV-1/AIDS across South/Southeast Asia and East Asia. While most national epidemics appear to have stabilized, HIV-1 prevalence is increasing in Bangladesh, Pakistan, and the Philippines.<sup>37</sup> An estimated 1.5 million people are living with HIV-1 in Eastern Europe and Central Asia, an increase of 250% since 2001.<sup>35,37</sup> The major transmission route for this epidemic is primarily caused by injecting drug use, although heterosexual transmission also plays an important role.<sup>35</sup>

Region	Total No. (%) Living with HIV end of 2010	Newly Infected in 2010	Adult Prevalence Rate 2010
<b>Global Total</b>	<b>34 million (100%)</b>	<b>2.7 million</b>	<b>0.8%</b>
Sub-Saharan Africa	22.9 million (67%)	1.9 million	5.0%
South/Southeast Asia	4.0 million (12%)	270,000	0.3%
Eastern Europe/Central Asia	1.5 million (4%)	160,000	0.9%
Latin America	1.5 million (4%)	100,000	0.4%
North America	1.3 million (4%)	58,000	0.6%
Western/Central Europe	840,000 (2%)	30,000	0.2%
East Asia	790,000 (2%)	88,000	0.1%
Middle East/North Africa	470,000 (1%)	59,000	0.2%
Caribbean	200,000 (0.6%)	12,000	0.9%
Oceania	54,000 (0.2%)	3,300	0.3%

**Table 1.4** HIV-1 Prevalence and Incidence by Region<sup>35</sup>

In the early years of the AIDS epidemic, it was quickly recognized that HIV-1 was having a severe impact on MSM. Currently, it is estimated that MSM accounts for between 5-10% of all HIV-1 infections worldwide.<sup>40</sup> Interestingly, more people have become infected with HIV-1 through male to male sex than through any other transmission route in many developed countries, such as U.S., Canada, Australia, New Zealand and many areas of Western Europe.<sup>41</sup> In many countries however, MSM are less observable. Sex between men is stigmatized, officially denied and criminalized in various parts of the world.<sup>41</sup> There are several factors that distort the statistics, in some countries the social identity of MSM is not acknowledged by the government and therefore they are simply counted as the general population. Also, it is not always possible to tell how a man initially became infected with HIV-1 especially if he is having sex with both men and women.<sup>41</sup> Many MSM often hide their same-sex relations from their families and friends to avoid persecution. Many have wives, or have sex with women, and this means that they may easily transmit HIV-1 to their female partners if they become infected. MSM is not an isolated problem but one that is potentially linked to countries' wider HIV-1 epidemics.<sup>42, 43</sup>

Women comprise an increasing proportion of people living with HIV-1 and AIDS. Globally, HIV-1/AIDS is the leading cause of death among women of reproductive age.<sup>44</sup> More

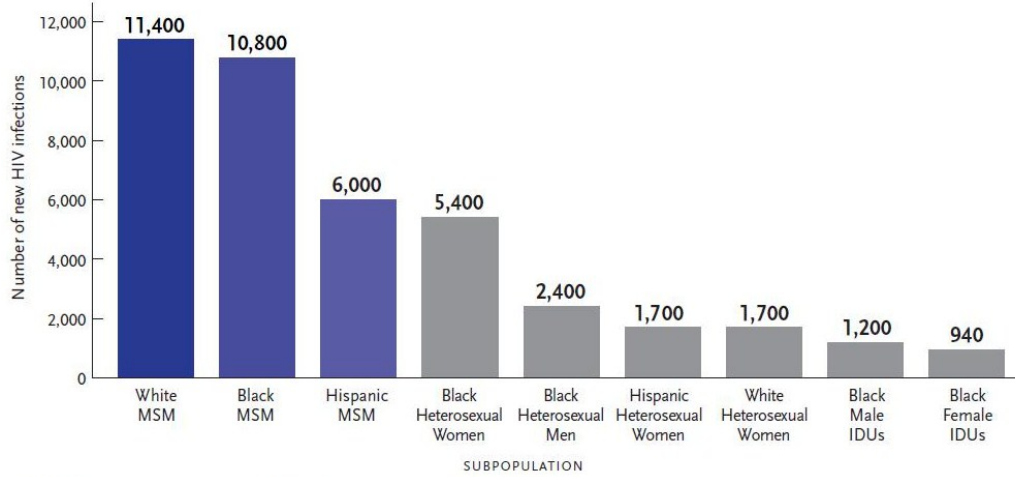
than half of the population of people living with HIV-1 globally is women, from whom the most usual route of infection is heterosexual intercourse.<sup>45</sup> This trend is occurring in most regions of the world, and is particularly pronounced in sub-Saharan Africa, where women represent 59% of all adults living with HIV-1 and AIDS.<sup>33</sup> In sub-Saharan Africa, more women than men are living with HIV, and young women aged 15-24 are about eight times more likely to be HIV-1 positive.<sup>45</sup> Gender inequalities in social and economic status and limited access to prevention and care services increase women's vulnerability to HIV-1.<sup>35</sup> Sexual violence also increases a women's risk to contract HIV-1 and women, especially young women, are biologically more susceptible to HIV-1 infection than men.

#### **1.1.5. Current Trends in the United States**

Homosexual, bisexual and other men of all races who have sex with men continue to be the risk group most severely affected by HIV-1 in the U.S. (Figure 1.2).<sup>46</sup> MSM represent approximately 2% of the U.S. population,<sup>47</sup> yet are the population most severely affected by HIV-1, and are the only risk group in which new HIV-1 infections have been increasing steadily since the early 1990s.<sup>48</sup> In 2006, more than half (53%) of all new HIV-1 infections in the U.S. were MSM. Additionally, MSM with a history of injection drug use (MSM-IDU) accounted for an additional 4% of new infections.<sup>48</sup> Since the beginning of the U.S. epidemic, MSM have consistently represented the largest percentage of persons diagnosed with AIDS and persons with an AIDS diagnosis who have died.<sup>48</sup>

**Estimated New HIV Infections in the U.S., 2009, for the Most-Affected Subpopulations\***

Gay and bisexual men of all races and black heterosexuals account for the greatest number of new HIV infections in the United States.



\*Subpopulations representing 2 percent or less of the overall U.S. epidemic are not reflected in this chart.

**Figure 1.2** Estimated New HIV-1 Infections in the U.S., 2009.<sup>49</sup>  
(Reprinted with Permission from CDC)

In the U.S., African Americans face the most severe burden of HIV-1 of all racial or ethnic groups (Table 1.5). Despite representing 14% of the US population in 2009, African Americans accounted for 44% of all new HIV-1 infections that year (Figure 1.2).<sup>50</sup> For both African American men and women, having unprotected sex with a man is the leading cause of HIV-1 infection, with injecting drug use being the second most likely infection route. Key factors such as high levels of poverty, limited access to healthcare, and stigma surrounding MSM shape the epidemic among African Americans.<sup>4</sup>

Hispanics/Latinos are also disproportionately affected by the HIV-1 and AIDS epidemic in America (Table 1.5). It is estimated that 1 in every 52 Hispanics/Latinos will be diagnosed with HIV-1 in their lifetime.<sup>51</sup> Interestingly, the risk for men and women differs widely; 1 in 36 Hispanic/Latino men will be diagnosed with HIV in their lifetime compared to 1 in 106 Hispanic/Latino women.<sup>52</sup> Language barriers, cultural factors, low access to healthcare and migration patterns have been identified as barriers to HIV-1 prevention and treatment within the Hispanic/Latino community.<sup>52</sup>

Race	Estimated % of new AIDS diagnosis in 2009	% of US population in 2008
White	27	65
African American/Black	47.9	12
Hispanic/Latino	21.2	15
Asian	1.2	4
American Indian/Alaska Native	<1	<1
Native Hawaiian/Other Pacific Islander	<1	<1
Multiple Races	2	2

**Table 1.5** Percentage of AIDS in U.S. among Various Ethnic Groups<sup>2</sup> Compared to Percentage of Population Each Ethnic Group Represents<sup>3,4</sup>

Geographic differences are a significant feature of the epidemic in the U.S. The epidemic was once concentrated primarily in the homosexual populations on the East and West coasts. However, in recent years HIV-1 has also become increasingly prevalent within African American and Hispanic/Latino communities in many Southern states as well as certain urban areas in the North-east and West-coast.<sup>4</sup> The map in Figure 1.3 shows the states with the number of people living with AIDS in 2009, relative to the population of each state. HIV-1 and AIDS remains mostly an urban disease, with the majority of individuals diagnosed with AIDS in 2009 residing in areas with more than 500,000 people. Areas hardest hit (by ranking of AIDS cases per 100,000 people) include Miami and Jacksonville, Florida; Baton Rouge, Louisiana; New York City, New York; and Washington, D.C.<sup>53</sup> Ten states account for 71% of AIDS diagnosis reported since the beginning of the AIDS epidemic. Nine of these states also rank in the top ten for new diagnosis in 2009 (Table 1.6).<sup>54</sup> As the epidemic has developed, it has become evident that the quality of prevention and treatment services than an individual receives is influenced by their socio-economic group and where they live. Poor urban communities are particularly affected by HIV-1 and AIDS in the US, which can be attributed to a number of factors including inadequate disease reporting, poverty, absence of adequate healthcare and lack of comprehensive sex education in schools.<sup>55</sup>



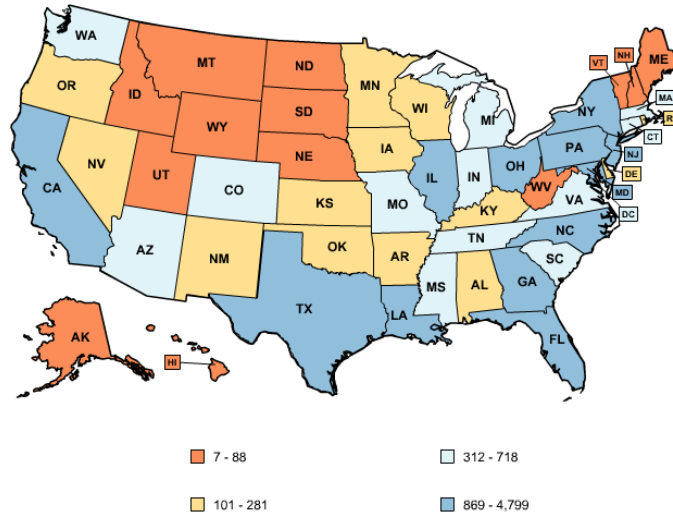


**Figure 1.3** Estimated Numbers of AIDS Diagnoses, All Ages, 2009<sup>56</sup>  
 (Permission to reprint Kaiser Family Foundation, 03-02-12)

State	Cumulative AIDS Diagnoses through 2009	State	AIDS Diagnosis Rate 2009
New York	201,871 (17.7%)	District of Columbia	119.8
California	161,695 (14.2%)	New York	24.6
Florida	122,278 (10.7%)	Florida	23.7
Texas	79,967 (7.0%)	Maryland	19.9
New Jersey	55,292 (4.8%)	Louisiana	19.4
Georgia	39,460 (3.5%)	Puerto Rico	18.5
Illinois	39,175 (3.4%)	Delaware	18.0
Pennsylvania	38,657 (3.4%)	New Jersey	16.9
Maryland	36,313 (3.2%)	South Carolina	15.6
Puerto Rico	33,277 (2.9%)	Georgia	14.1
Subtotal	807,985 (70.7%)	—	—
<b>U.S. Total</b>	<b>1,142,714 (100%)</b>	<b>U.S. Diagnosis Rate</b>	<b>11.2</b>

**Table 1.6** Top Ten States by Cumulative AIDS Diagnosis and by AIDS Diagnosis Rate Per 100,000<sup>2</sup>  
 (Requested permission to reprint Kaiser Family Foundation, 03-02-12)

New infections due to injection drug use has declined significantly over time and accounted for 9% of new infections in 2009.<sup>53, 57</sup> Throughout the epidemic, prevention efforts among IDUs has been controversial. For 21 years, programs where users exchange their needles for clean ones (needle exchange programs) were not permitted any federal funding, even though in some areas in the US these programs have been shown to reduce the rate of transmission.<sup>58, 59</sup>

The ban on federal funding for needle exchange programs was lifted in 2009, however, at the end of 2011, in a controversial action by Congress, the ban was later reinstated.<sup>60</sup>

#### **1.1.6. HIV-1 Structure and Genome**

HIV-1 is spherical in shape and has a diameter of 1/10,000 of a millimeter. The outer coat of the virus (the viral envelope) is composed of two layers of fatty acids, taken from the membrane of a human cell when a newly formed virus particle buds from the cell. Embedded within the viral envelope are proteins from the host cell, as well as about 72 copies of the complex protein envelope glycoprotein (Env). Env consists of a cap made of three molecules called glycoprotein 120 (gp120), and a stem consisting of three molecules gp41 that anchor the structure into the viral envelope. HIV-1 has three structural genes (gag, pol and Env) and six regulatory genes (tat (transcriptional activator), rev (regulator of viral gene expression), nef (negative effector), vif (viral infectivity factor), vpr (viral protein R), and vpu (viral protein U)) that contain information needed to produce proteins that control the ability for HIV-1 to infect a cell, produce new copies of virus, or cause disease (Figure 1.4). The ends of each strand of HIV-1 RNA contain an RNA sequence called the long terminal repeat (LTR). Regions in the LTR act as switches to control production of new viruses and can be triggered by proteins from either HIV-1 or the host cell.<sup>61</sup>

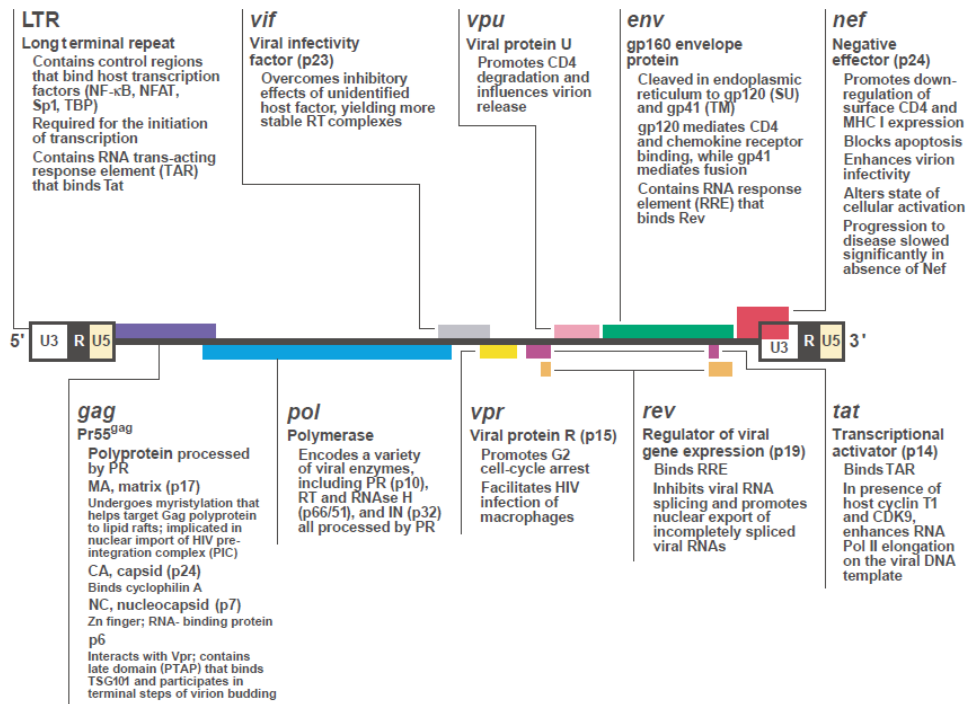


**Figure 1.4.** HIV-1 Genome: An overview of the organization of the ~9-kilobase genome of the HIV provirus and summary of its nine genes encoding 15 proteins. (Reprinted with permission from NPG: License 2863790720427)

## 1.2. HIV-1 VIRAL LIFE CYCLE

HIV-1 is a retrovirus (“slow virus”), which means it has genes composed of RNA molecules. Like all viruses, HIV-1 replicates inside host cells. It is considered a retrovirus because it uses an enzyme, reverse transcriptase (RT), to convert RNA into DNA, which can then be incorporated into the host cell’s genome.<sup>62</sup> The replication cycle of HIV-1 is a complex multistep process that depends on both viral and host cell factors (Figure 1.5). The HIV-1 replication cycle has two distinct phases. During an early pre-integration stage, the virus infects the cell, RT takes place and the proviral genome is transported into the nucleus and integrated into the host cell genome. In the subsequent post-integration stage, the integrated provirus expresses genes, and virus assembly and maturation takes place.<sup>63</sup>

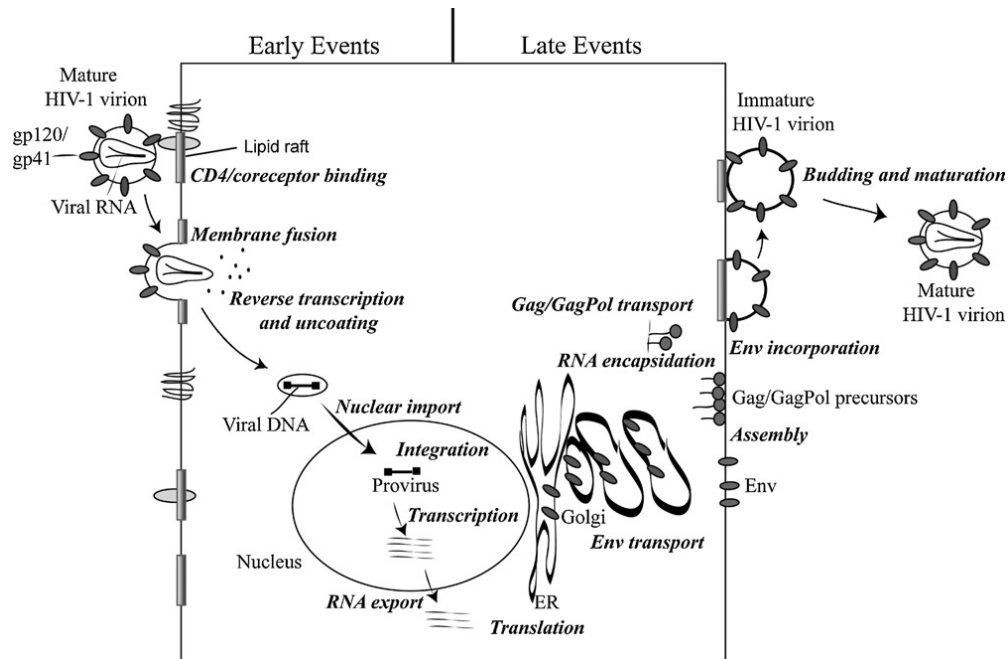


**Figure 1.5** Schematic Representation of the HIV-1 Replication Cycle<sup>64</sup>  
(Reprinted with permission from Elsevier license: 2857380636210)

### 1.2.1. Viral Entry Binding and Fusion

The life cycle of HIV-1 begins with adsorption of virions to the host cell (Figure 6), the viral envelope (Env) gp120 interacts nonspecifically with heparan sulfate, a sulfated polysaccharide widely expressed on animal cells and involved in virus cell binding of array of enveloped viruses.<sup>65-67</sup> This first interaction enables the virus to initially make contact with the host cell.<sup>68</sup> While attachment of HIV-1 to the cell surface can result for interactions with many surface molecules,<sup>69, 70</sup> specific binding of the gp120 subunit to CD4 is the first required step for viral infection.<sup>71</sup> CD4 is an integral membrane glycoprotein, belonging to the immunoglobulin gene superfamily, which is expressed mainly on the surface of T cells and cells of the macrophage/monocyte lineage.<sup>72</sup> CD4 binding alone is not sufficient for virus infection as it does not trigger the conformational changes needed for membrane fusion. For this to occur, the viral Env gp120 must interact with its coreceptor, CXCR4 (chemokine receptor 4) for T-cell line

tropic (T-tropic) or X4 HIV-1 strains or CCR5 (C-C chemokine receptor 5) for macrophagetropic (M-tropic) of R5 HIV-1 strains.<sup>71</sup> R5 virus strains typically infect macrophages and primary T cells, and are the virus type most commonly transmitted between individuals. The X4 virus strains tend to evolve years after infection in a subset of individuals as a consequence to mutation in Env, and infect primary T cells and transformed T cell lines.<sup>73, 74</sup> While the viral glycoprotein gp120 is responsible for viral interaction with the CD4 receptor and CCR5 or CXCR4 coreceptor, the viral glycoprotein gp41 (which has remained noncovalently attached to gp120 after their precursor glycoprotein gp160 has been cleaved by cellular proteases to yield the gp120/gp41 heterodimer ) is responsible for the fusion of viral envelope with the cell membrane.<sup>72</sup> The interaction of gp120 with CCR5 or CXCR4 coreceptor triggers a series of conformational changes in the gp120-gp41 complex that ultimately led to the formation of a ‘trimer-of-hairpins’ structure in gp41. The ‘trimer-of-hairpins’ is a bundle of six  $\alpha$ -helices: three  $\alpha$ -helices formed by the amino-terminal regions. The fusion-peptide region, located at the extreme amino terminus, will insert into the cellular membrane, while the carboxy-terminal region remains anchored in the viral envelope, thus, bringing the two membranes together.<sup>75</sup>

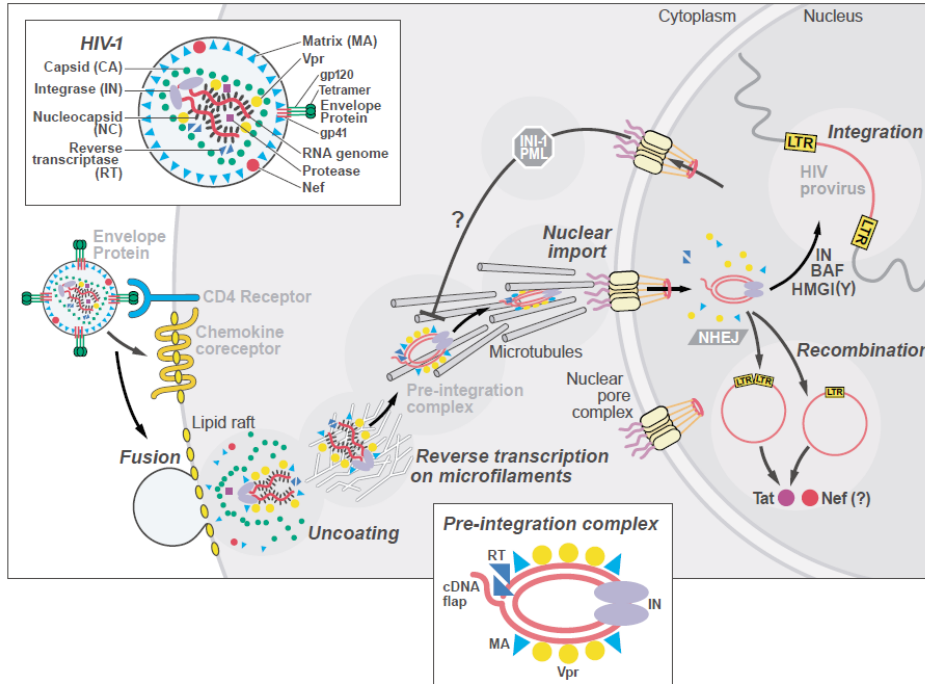


**Figure 1.6** Schematic description of early events occurring after HIV infection of a susceptible target cell including interactions between gp120, CD4 and chemokine receptors (CCR5 or CXCR4) leading to gp41 mediated fusion followed by virion uncoating, reverse transcription of the RNA genome, nuclear import of the viral preintegration complex (PIC), and integration of the double-stranded viral complementary DNA strain (cDNA) into the host chromosome thus establishing the provirus.<sup>76</sup> (Reprinted with permission from NPG: License 2863790346117)

## 1.2.2. Reverse Transcription

Once fusion delivers the viral core into the cytoplasm of the host cell, viral uncoating takes place. The viral core is composed of a capsid (CA) protein shell that encapsulates the single-stranded, dimeric viral RNA genome in complex with the viral nucleocapsid (NC) protein and the viral enzymes RT and integrase (IN) (Figure 1.6).<sup>77, 78</sup> Although the viral uncoating process is poorly understood, it likely involves the phosphorylation of matrix (MA) mediated by a mitogen activation protein (MAP) kinase<sup>79</sup> and additional actions of cyclophilin A,<sup>80</sup> and the viral negative factor (nef)<sup>81</sup> and viral infectivity factor (vif) proteins.<sup>82</sup> Successful uncoating generates the viral reverse transcription complex, which contains the diploid viral RNA genome, tRNA<sup>Lys</sup> (transfer RNA) primer, RT, IN, MA, NC, viral protein R (vpr) and various host proteins; the reverse-transcription complex is thus liberated from the plasma membrane.<sup>83</sup> Next,

the complex docks with actin microfilaments and this interaction, which is mediated by the phosphorylated MA, is required for efficient viral DNA synthesis.<sup>84</sup> HIV-1 now uses the enzyme RT to make a DNA copy of the RNA genome. Normal transcription in nature occurs when the DNA genome is transcribed into messenger RNA (mRNA) which is translated into protein. In HIV-1 RT, RNA is reverse-transcribed into DNA.<sup>68</sup> To convert viral RNA to pregenomic proviral DNA, three successive enzymatic reactions, all ensured by the p66 subunit of the p66/p51 RT heterodimer, are required. RT has three enzymatic activities: (i) it has RNA-dependent DNA polymerase activity that transcribes the viral (+) RNA strand to a (-) viral complementary DNA strand (cDNA); (ii) it has ribonuclease activity that degrades the (+) RNA strand during the synthesis of cDNA; and (iii) it has DNA-dependent DNA polymerase activity that copies the (-) cDNA strand into a (+) DNA strand to form a double-stranded DNA intermediate that enters the infected host cell's nucleus.<sup>68, 72</sup>

### **1.2.3. Integration**

Approximately 40-100 IN molecules are packaged within an HIV-1 particle.<sup>85</sup> The principal role of IN is to catalyze the insertion of the proviral DNA (cDNA) into the genome of infected host cells. Integration is essential for viral replication because efficient transcription of the viral genome and production of viral proteins require that the proviral DNA is fully integrated into the cellular genome (Figure 1.7).<sup>72</sup> Following RT, the proviral DNA is primed for integration by integrase-mediated 3'-processing, which correlates to an endonucleolytic cleavage of the 3' ends of the proviral DNA, thus generating CA-3'-hydroxyl ends. Following 3'-processing, IN remains bound to the proviral DNA as a multimeric complex that bridges both ends of viral DNA within intracellular particles termed preintegration complexes (PICs).<sup>72</sup>

Isolated PICs contain both viral and cellular proteins in addition to the IN-DNA complexes. The viral proteins RT, MA, NC and vpr can contribute to the transport of PICs through the nuclear envelope.<sup>86</sup> The cellular proteins packaged with the PICs, interactor 1 (Ini1),<sup>87</sup> lens epithelium-derived growth factor (LEDGF or p75),<sup>88</sup> embryonic ectoderm-development protein,<sup>89</sup> and heat-shock protein 60 (HSP60),<sup>90</sup> can bind to IN and stimulate its enzymatic activities.<sup>91</sup> Once in the nucleus, IN catalyzes the insertion of the proviral DNA into the host cell chromosome. This ‘stand transfer’ reaction consists of the ligation of the viral 3’-OH DNA ends (generated from 3’-processing) to the 5’-DNA phosphate of the host chromosome. Completion of integration can only take place after trimming of the last two nucleotides at the proviral DNA 5’-ends and extension (gap filling) from the 3’-OH end of the genomic DNA.<sup>86</sup>

The HIV-1 provirus can integrate into many different chromosomal locations in the cell and most infected cells harbor more than one provirus.<sup>76</sup> Integration can lead to either latent or transcriptionally active forms of infection,<sup>92</sup> which is determined by genetic factors of the viral strain, the type of cell infected, and the production of specific host cell proteins.<sup>68</sup> The majority of the proviral DNA is integrated into the chromosomes of activated CD4+ T cells. These generally comprise between 93% and 95% of infected cells and are productively infected, not latently infected. However, a small percentage of HIV-infected memory CD4+ T cells persist in a resting state because of a latent provirus. These, along with infected monocytes, macrophages, and dendritic cells, provide stable reservoirs of HIV-1 capable of escaping host defenses and Antiretroviral (ARV) chemotherapy.<sup>68</sup>



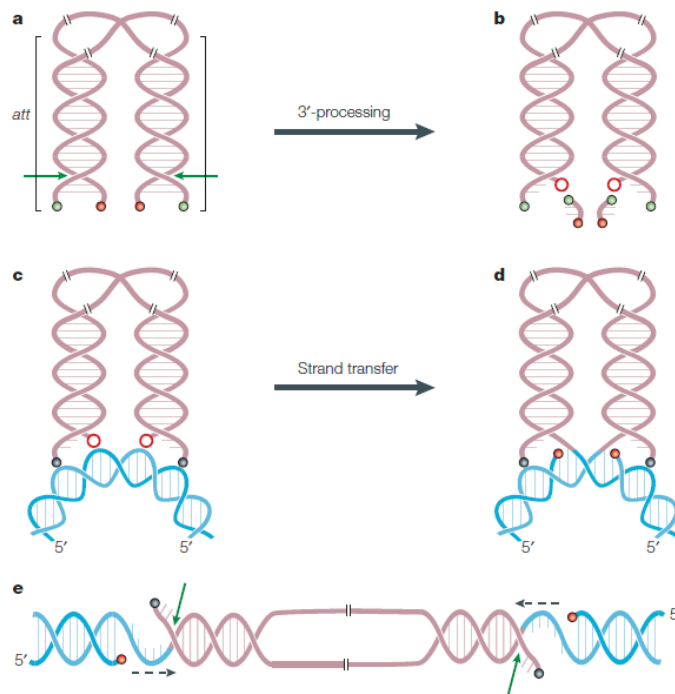


**Figure 1.7** The Two IN Catalytic Reactions (3'-Processing and Strand Transfer). The figure shows the viral DNA recombination attachment (*att*) sites. 3'-processing takes place in the cytoplasm following reverse transcription (Figure 1.) It is a water-mediated endonucleolytic cleavage (green arrow in a and BOX 1, figure part a) of the viral DNA immediately 3' from the conserved CA dinucleotide (BOX 1, figure part a.). 3'-processing generates reactive 3'-hydroxyls at both ends of the viral DNA (red circles (b); other 3'-hydroxyl ends and 5'-phosphate ends are shown as red and green dots, respectively.) IN multimers (not shown) remain bound to the ends of viral DNA as the PICs translocate to the nucleus. The second reaction (c to d) catalyzed by IN is strand transfer (3'-end joining), which inserts both viral DNA ends into a host-cell chromosome (acceptor DNA in blue). Strand transfer is coordinated in such a way that each of the two 3'-hydroxyl viral DNA ends (red circles) attacks a DNA phosphodiester bond on each strand of the host DNA acceptor with a five-base-pair stagger across the DNA major groove (d). Strand transfer leaves a five-base, single-stranded gap at each junction between the integrated viral DNA, and a two-base flap at the 5'-ends of the viral DNA (d and e). Gap filling and release of the unpaired 5'-ends of the viral DNA (arrows in e) are carried out in coordination with cellular repair enzymes.<sup>86</sup> (Reprinted with permission from NPG: License 2862620377001)

#### 1.2.4. Transcription

The vast majority of CD4+ T cells, which are productively infected, immediately begin to produce new viruses. In the case of resting memory CD4+ T cells, before replication can occur, the HIV-1 provirus must become activated. This activation is accomplished by such means as antigenic stimulation of the infected CD4+ T cells or their activation by factors such as cytokines, endotoxins and superantigens.<sup>68</sup>

Once integrated, the HIV-1 proviral genome is subject to transcriptional regulation by the host cell, as well as its own transcriptional control mechanism.<sup>63, 93</sup> In the host genome, the 5'

long-terminal repeat (LTR) functions like other eukaryotic transcriptional units. It contains downstream and upstream promoter elements, which include the initiator (Inr), TATA-box (T) and three Specificity Protein 1 (Sp1) sites.<sup>94</sup> These regions help position the RNA polymerase II (RNAPII) at the site of initiation of transcription and assemble the preinitiation complex. In the HIV-1 promoter, RNAPII activity is quickly stalled after initiation of transcription (Figure 1.8, Panel A). There are two cellular complexes, DRB sensitivity-inducing factor (DSIF) and negative elongation factor (NELF), that function together to block the elongation from occurring (Figure 1.8, Panel B).<sup>95, 96</sup> Although binding of DSIF and NELF to RNAPII shortly after initiating RNA synthesis leads to inhibition of elongation, this step is regulated by the phosphorylation of carboxy-terminal domain (CTD) of the largest subunit of RNAPII. Importantly, in the nuclear extract, DSIF and NELF tightly bind to hypophosphorylated RNAPII, but not to the hyperphosphorylated form, suggesting that phosphorylation of CTD caused dissociation of these negative factors from RNAPII.<sup>97</sup> The repression caused by DSIF and NELF is counteracted in HIV-1 transcription by trans-activator of transcription (tat), an 81-101-amino acid peptide (Figure 1.8, Panel C). In the absence of tat, HIV-1 transcription is highly inefficient because the

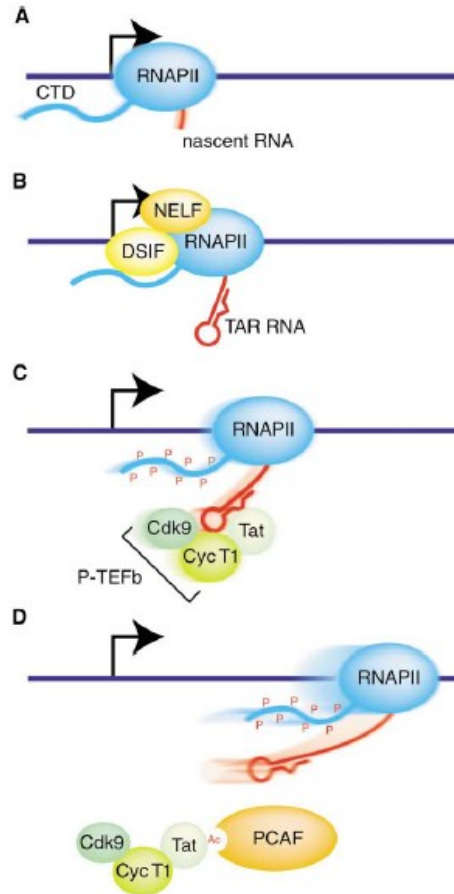


**Figure 1.8** Stimulation of Transcriptional Elongation by HIV-1 Tat (Reprinted with permission from NPG: License)

assembled RNAPII complex cannot elongate efficiently on the viral template.<sup>98</sup> First, tat forms a complex with the positive transcription elongation factor b (P-TEFb), which is composed of cyclin T1 and cyclin-dependent protein kinase 9 (CDK9). The complex of Tat with P-TEFb, which is composed of cyclin T1 and CDK9, then binds to the TAR (Tat response) element, thereby positioning CDK9 to phosphorylate the cellular RNA polymerase and this ensuring transcription elongation.<sup>97</sup> The tat protein is acetylated on lysine residues within its TAR-RNA-binding arginine rich motif by transcriptional coactivators/acetyltransferases, p300/CBP (CREB-binding protein), and PCAF (p300/CREB-binding protein-associated factor) which help to activate the HIV-1 promoter (Figure 1.8, Panel D).<sup>99</sup> Other phosphorylation and acetylation events accompany and may at least partially account for the activation of the HIV-1 transcription process.<sup>72</sup>

The integrated proviral DNA is transcribed to generate full-length progeny viral RNA and a number of spliced mRNA transcripts that are translated into the cytoplasm.<sup>100</sup> Transcription and translation, performed by cellular machinery, results in the synthesis of several major structural proteins: (i) the Gag polyprotein precursor, which is composed of four domains-MA, CA, NC and p6-and two spacer peptides, SP1 and SP2, (ii) the Gag-Pol polyprotein precursor, which is produced via a 1-ribosomal frameshift during gag translation and encodes the viral enzymes PR, RT and IN, and (iii) the Env glycoprotein precursor, gp160, which is cleaved into the gp120 and gp41 subunits by a host protease during trafficking through Golgi apparatus.<sup>100</sup> These protein components, together with full-length viral genomic RNA, are each transported to the site of virus particle assembly at the plasma membrane.<sup>77</sup>

### 1.2.5. Assembly, Budding and Maturing

After the transcription of the viral genome, more than a dozen HIV-specific transcripts are generated. Assembly is directed by Gag, which coordinates the incorporation of each of the viral components, together with a number of host cell factors, into the assembling particle.<sup>77</sup> All of the components of the virion are ultimately assembled at the plasma membrane of the host cell where budding occurs. Prior to budding the Env polyprotein (gp160) goes through the endoplasmic reticulum and is transported to the Golgi complex where it is cleaved by a protease and processed into the two HIV envelope glycoproteins gp41 and gp120. These envelope glycoproteins are transported to the plasma membrane of the host cell where gp41 anchors the gp120 to the membrane of the infected cell.<sup>68</sup> The Gag (p55) and Gag-Pol (p160) also interact with the inner surface of the plasma membrane along with HIV genomic RNA as the forming virion begins to bud from the host cell. Following budding from the plasma membrane, the viral protease cleaves the Gag and Gag-Pol precursors into their respective protein domains. Gag and Gag-Pol cleavage leads to virion maturation, a reassembly event that produces mature particles containing the condensed, conical core.<sup>77, 78</sup> In addition to the structural proteins listed above, HIV-1 encodes two regulatory gene products (tat and rev (regulation of viral gene expression)) and several accessory proteins: viral infectivity factor (vif), viral protein U (vpu), negative factor (nef), and viral protein R (vpr).<sup>100</sup> The various structural components then assemble to produce a mature HIV-1 virion which is now able to infect another cell.

## 1.3. CURRENT THERAPY

To date, there are 25 ARV drugs approved for the treatment of HIV-1 infection and AIDS. These drugs can be divided into six different mechanistic classes that target distinct steps

in the HIV-1 replication cycle (Figure 1.9): eight nucleoside/nucleotide reverse transcriptase inhibitors (NRTIs),<sup>101</sup> nine protease inhibitors (PIs),<sup>102</sup> five non-nucleoside reverse transcriptase inhibitors (NNRTIs),<sup>103</sup> one integrase inhibitor,<sup>104</sup> and two entry inhibitors.<sup>105</sup> There are two drugs that have been developed as entry inhibitors.

Enfuvirtide (T-20) is a fusion inhibitor that blocks viral fusion by targeting glycoprotein 41 (gp41) and maraviroc is an inhibitor of chemokine receptor CCR5, making it the only approved ARV drug that targets a host cell factor.<sup>105</sup> The remaining four mechanistic classes target each of the viral enzymes: RT, PR and IN.

### 1.3.1. Nucleotide/Nucleoside Reverse Transcriptase Inhibitors (NRTIs)

In 1986, there were 5,833 AIDS cases in the U.S. and the 1-year mortality was 51%-which translated to the public as ‘certain death’.<sup>34</sup> In 1987, four years after the identification of HIV,<sup>19</sup> 3'-azidothymidine (AZT, zidovudine), a nucleoside HIV-1 reverse transcriptase inhibitor (NRTI), was the first ARV drug approved by the U.S. Food and Drug Administration (FDA) for the treatment of AIDS. Over the course of over 25 years that followed after this

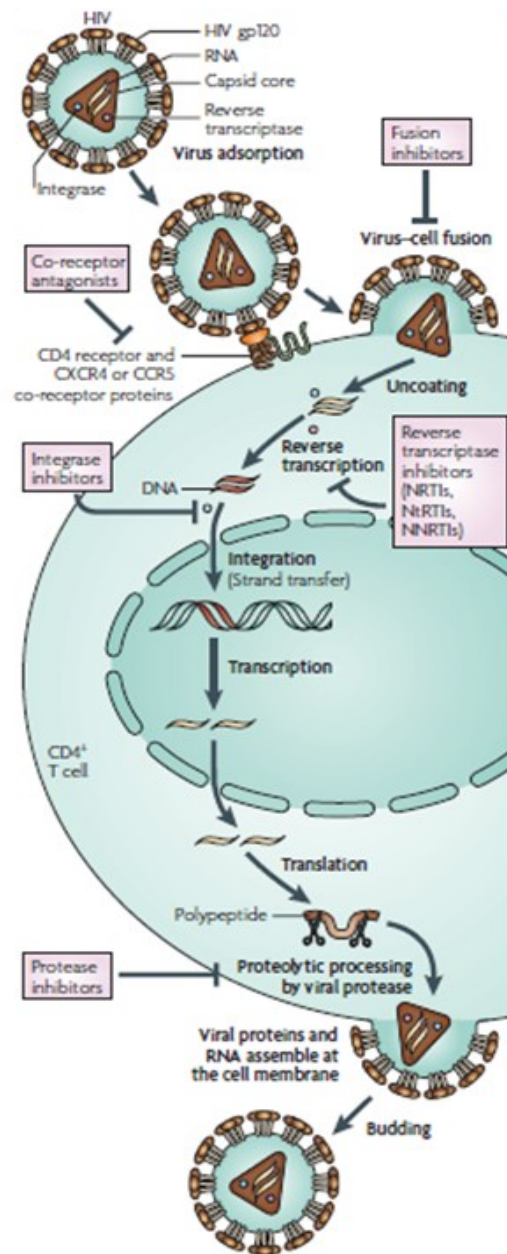


**Figure 1.9** The HIV-1 Replication Cycle and Drug Targets (Reprinted with permission from NPG)

seminal discovery, seven nucleosides and one nucleotide have been approved by the FDA for the treatment of HIV infection (Figure 1.10).

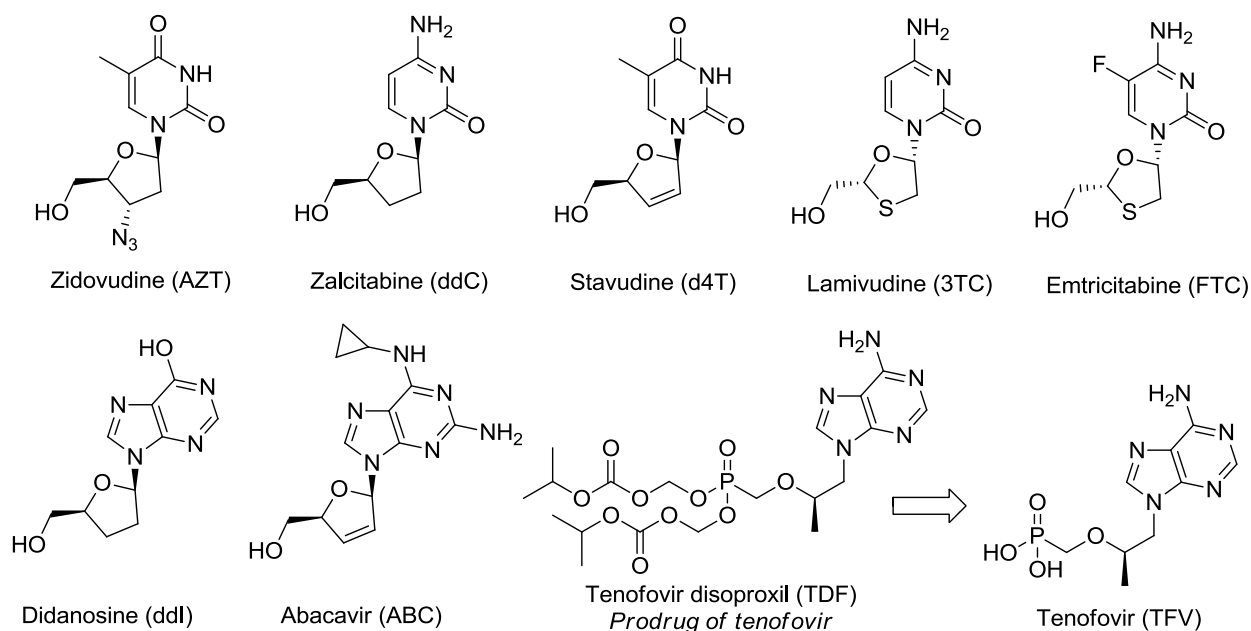


**Figure 1.10** Nucleoside/Nucleotide Reverse Transcriptase Inhibitors (NRTIs)

A total of thirteen NRTI drug products are available for clinical application: eight individual NRTIs, four fixed-dose combinations of two or three NRTIs, and one complete fixed-dose regimen containing two NRTIs and one non-nucleoside RT inhibitor (Table 1.7).<sup>101</sup> NRTIs target the HIV-1 RT, which offers two target sites for inhibitors: the catalytic substrate (deoxynucleoside triphosphate) binding site, and an allosteric site, which is distinct from (yet closely located to) the substrate binding site.<sup>106, 107</sup> NRTIs are analogues of endogenous 2'-deoxynucleosides and nucleotides (Figure 1.11). They are inactive in their parent forms and are first metabolized inside cells and then converted to their active 5'-triphosphate forms, which compete with the natural deoxynucleoside triphosphate (dNTP) substrates for HIV-1 RT and inhibit DNA polymerization.<sup>108-110</sup> In addition, after the drugs are incorporated into a growing viral DNA, they serve as chain-terminators of viral reverse transcripts owing to lack of a 3'-

hydroxy group (present in natural dNTPs) necessary for further DNA synthesis.<sup>110</sup> The NRTIs act early in the viral replication cycle by inhibiting a critical step of proviral DNA synthesis prior to integration into the host cell genome.

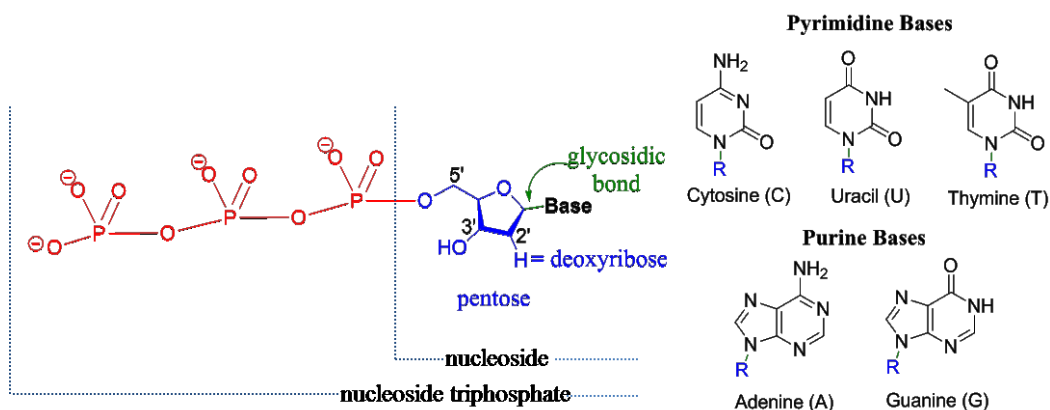


**Figure 1.11** Structure of Natural Deoxynucleoside Triphosphates (dNTP)

NRTIs are the backbone of current combination ART. The standard of care for HIV-1 patients is highly active antiretroviral therapy (HAART), which consists of three or more HIV-1 drugs. The common use of combinations of NRTIs has led to the clinical development of the fixed-dose combination pills (Table 1.7).<sup>101</sup> The success of NRTIs in HIV-1 therapy is due, at least in part, to the unique pharmacology and intracellular persistence. The intracellular retention of the active triphosphorylated NRTI metabolites allows for constant viral inhibition. Based on the Adult and Adolescent Antiretroviral Treatment Guidelines updated by the Department of Health and Human Services (DHHS) in October 2011, the two preferred NRTIs for the first-line regimens are TDF and FTC.<sup>111</sup>

While the unique pharmacology of NRTIs has helped them become a cornerstone of successful HAART treatment, the effectiveness of NRTIs can be limited by drug-drug interactions, emergence of drug resistance, and adverse side-effects of ART.<sup>101</sup> NRTIs are metabolized by complex and often overlapping pathways shared with the endogenous dNTPs

they compete with for activity, resulting in the potential for intra-class pharmacokinetic and pharmacodynamics drug interactions.<sup>112</sup> The error-prone reverse transcription due to lack of a proofreading function of RT<sup>113</sup> multiplied by the sheer number of replication cycles occurring in an infected individual facilitate the selection of drug resistant mutant strains of HIV-1.<sup>114</sup> A major toxicity that has been recognized for more than a decade is NRTI-related mitochondrial toxicity, which manifests as serious side effects such as hepatic failure and lactic acidosis.<sup>115</sup>

Trade Name	Generic Name	NRTI Base	Manufacturer	Approval Date
Retrovir	AZT, ZDV, azidothymidine, zidovudine	Pyrimidine	GlaxoSmithKline	19-Mar-87
Videx	ddI, didanosine, dideoxyinosine	Purine	Bristol Myers-Squibb	9-Oct-91
Hivid ( <i>Discontinued in 2006</i> )	ddC, zalcitabine, dideoxycytidine	Pyrimidine	Hoffman-La Roche	19-Jun-92
Zerit	d4T, stavudine	Pyrimidine	Bristol Myers-Squibb	24-Jun-94
Epivir	3TC, lamivudine	Pyrimidine	GlaxoSmithKline	17-Nov-95
Combivir	zidovudine + lamivudine		GlaxoSmithKline	27-Sep-97
Ziagen	ABC, abacavir sulfate	Purine	GlaxoSmithKline	17-Dec-98
Videx EC	ddI EC, enteric coated didanosine	Purine	Bristol Myers-Squibb	31-Oct-00
Trizivir	abacavir + zidovudine + lamivudine		GlaxoSmithKline	14-Nov-00
Viread ( <i>Supplied as a Prodrug, Nucleotide NRTI</i> )	TDF, tenofovir disoproxil fumarate	Purine	Gilead Sciences	26-Oct-01
Emtriva	FTC, emtricitabine	Pyrimidine	Gilead Sciences	2-Jul-03
Truvada	tenofovir disoproxil fumarate + emtricitabine		Gilead Sciences	2-Aug-04
Epzicom ( <i>or Kivexa</i> )	abacavir + lamivudine		GlaxoSmithKline	2-Aug-04

**Table 1.7** Clinically Approved Nucleoside/Nucleotide Reverse Transcriptase Inhibitors (NRTIs)<sup>101</sup>

### 1.3.2. Protease Inhibitors (PIs)

The discovery of HIV-1 protease inhibitors (PIs) in 1995 was a pivotal moment in the development of ARV therapy because the PIs made possible the dual class therapy a reality.

Currently, there are nine PIs approved by the FDA for clinical use and most of them are prescribed with a concomitant low dose of ritonavir as a boosting agent (Table 1.8).

HIV-1 PR, an aspartyl protease, plays a crucial role in the viral life cycle and is essential for the generation of mature infectious virus particles. PR generates mature infectious virus particles through the cleavage of the viral Gag and Gag-Pol precursor proteins.<sup>116</sup> The Gag precursor protein codes for all the structural viral proteins, MA, CA and NC, the p6 protein and the two



spacer proteins p2 (SP1) and p1 (SP2).<sup>117</sup> PIs have been designed to bind the viral PR with high affinity but tend to occupy more space than the natural substrates. HIV-1 PIs prevent cleavage of gag and gag-Pol precursors in acutely and chronically infected cells, arresting maturation and thereby blocking the infectivity of nascent virions.<sup>118, 119</sup>

Trade Name	Generic Name	Manufacturer	Approval Date
Invirase	SQV, saquinavir mesylate	Hoffman-La Roche	6-Dec-95
Norvir	RTV, ritonavir	Abbott Laboratories	1-Mar-96
Crixivan	IDV, indinavir	Merck	13-Mar-96
Viracept	NFV, nelfinavir mesylate	Agouron Pharmaceuticals	14-Mar-97
Fortovase	SQV, saquinavir	Hoffman-La Roche	7-Nov-97
Agenerase ( <i>Discontinued in 2007</i> )	APV, amprenavir	GlaxoSmithKline	15-Apr-99
Kaletra	LPV/RTV, lopinavir + ritonavir	Abbott Laboratories	15-Sep-00
Reyataz	ATV, atazanavir sulfate	Bristol-Myers Squibb	20-Jun-03
Lexiva ( <i>Prodrug of amprenavir</i> )	FOS-APV, Fosamprenavir Calcium	GlaxoSmithKline	20-Oct-03
Aptivus	TPV, tipranavir	Boehringer Ingelheim	22-Jun-05
Prezista	darunavir	Tibotec	23-Jun-06

**Table 1.8** Clinically Approved Protease Inhibitors (PIs)<sup>102</sup>

All of the FDA approved PIs, with the exception of tipranavir, are competitive peptidomimetic inhibitors, mimicking the natural substrate of viral PR (Figure 1.13).<sup>102</sup> The peptidomimetic inhibitors contain a hydroxyethylene core, which prohibits cleavage of the PI by the HIV-1 protease.<sup>120-127</sup> Instead of a peptidomimetic hydroxyethylene core, tipranavir contains a dihydropyrone ring as a central scaffold.<sup>128</sup>

Many of the first-generation PIs (saquinavir, indinavir, ritonavir and nelfinavir) suffered from low bioavailability and high protein binding, high pill burden (3-4 times per day dosing), the development of resistance and wide spectrum of side effects and toxicities.<sup>102</sup> Since one of the major initial problems with the PIs was poor bioavailability the second-generation drugs were developed in attempt to address this issue by reducing the molecular weight of the inhibitor and increasing the solubility.<sup>129</sup> In 1999, these attempts led to a smaller more bioavailable inhibitor, amprenavir. However, even though amprenavir was more bioavailable compared to the previous PIs it was not very soluble or potent and formulation led to a high pill burden. In 2003,

GSK introduced a phosphate prodrug fosamprenavir with improved solubility and a reduced pill burden.<sup>130</sup>

Another concerning issue that were revealed with PIs had was the development of a resistance profile. Lopinavir was developed with an alternative scaffold to try and overcome this problem. The isopropylthiazolyl group of ritonavir was removed and then a conformational constraint in the resulting urea by incorporation of a six-member ring was used in the scaffold. Although lopinavir was more potent than ritonavir and less affected by the mutation commonly found in ritonavir-resistant viruses, it suffered from poor bioavailability in humans.<sup>126</sup> A landmark breakthrough in the field of PIs was discovered with lopinavir. Since it is mainly metabolized by CYP3A4 it was discovered that dosing with ritonavir (CYP3A4 inhibitor) increased the bioavailability. This led to the development of a fixed-dose combination of the two, marketed as Kaletra. Lopinavir was the first boosted PI that compared head-to-head with an NNRTI as initial therapy.<sup>102</sup> Currently, Kaletra and atazanavir have the major share in the PI market. Atazanavir has good bioavailability and antiviral activity and a unique resistance profile, which sensitizes the virus to all other PIs.<sup>129</sup>

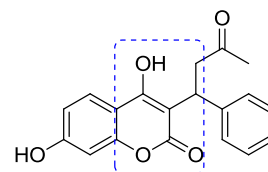


**Figure 1.12** Warfarin

After the screening of a compound library, warfarin (Figure 1.12) was discovered as a lead molecule and researchers realized that this pyrone derivative was a good start for nonpeptidic and low molecular weight analogs.<sup>129</sup> After extensive structure-activity relationship studies, tipranavir was discovered and approved in 2005. Tipranavir is effective against resistant mutants and has a good bioavailability profile but unfortunately suffers from significant incidences of side effects. Tipranavir is a strong CYP450 inducer, inducing its own metabolism and requiring double the usual boosting dose of ritonavir (200 mg), resulting in

multiple drug-drug interactions.<sup>131</sup> These problems are so great the use of tipranavir is largely restricted to deep salvage regimens.<sup>129</sup>

With the sole exception of tipranavir, the evolution of commercial PIs can be described in as incremental structural changes in the initially described leads that led to greater potency, increased activity against mutants, and in some cases improved bioavailability. The common practice of using ritonavir to boost blood levels and trough levels exemplifies the struggle to identify PIs with good bioavailability.<sup>129</sup>

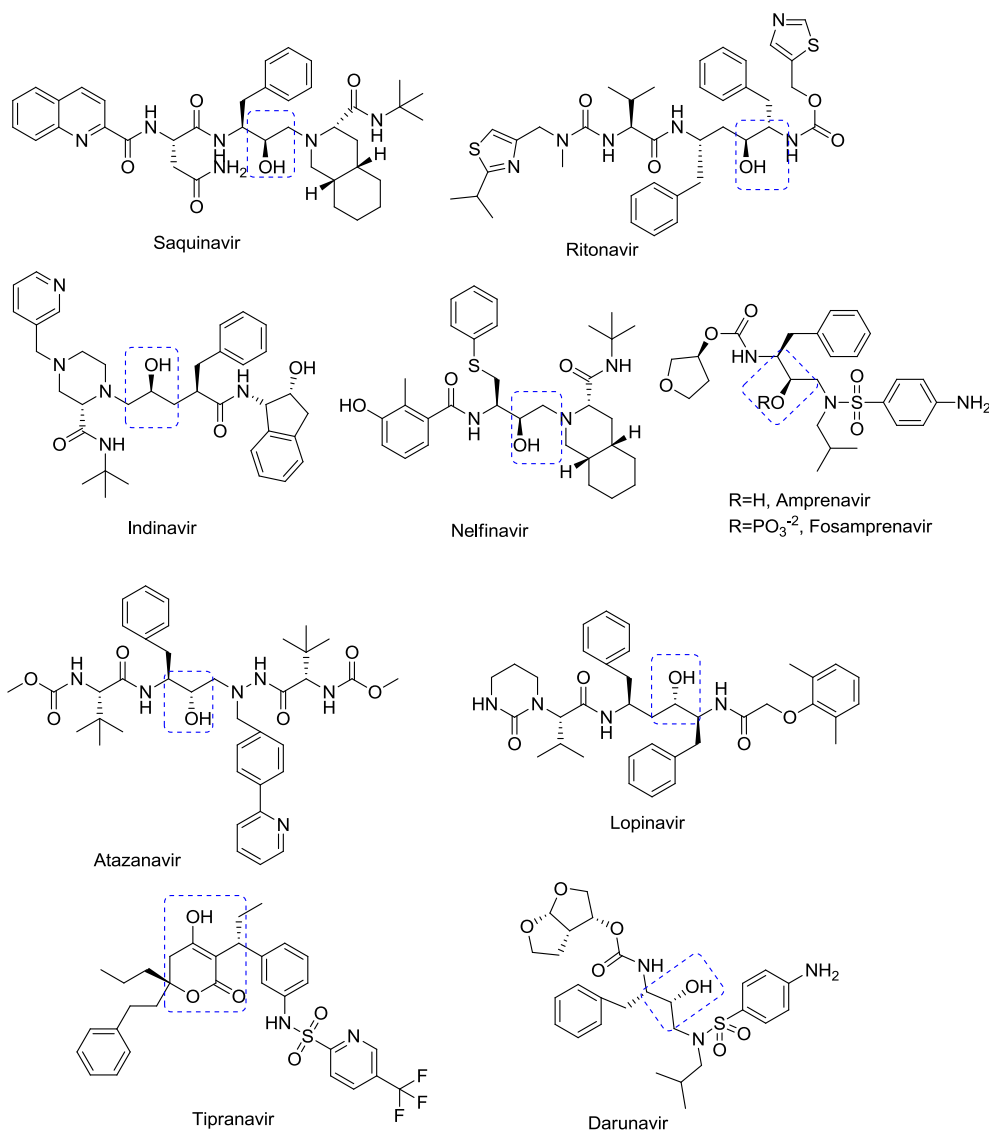


**Figure 1.13** Protease Inhibitors (PIs)(hydroxyethylene core/ dihydropyrene ring highlighted in blue)

### 1.3.3. Non-Nucleoside Reverse Transcriptase Inhibitors (NNRTIs)

Shortly after the approval of the first PI, non-nucleoside reverse transcriptase inhibitors (NNRTIs) quickly followed (Figure 1.14). NNRTIs inhibit RT by binding in a reversible and non-competitive manner to the enzyme in a hydrophobic pocket located close to the catalytic site. The interaction of the compounds with RT induces conformational changes that impact the catalytic activities of the enzyme.<sup>132</sup>

Unlike the NRTIs, NNRTIs are active as such, and do not need metabolized intracellularly to become active.<sup>103</sup> NNRTIs are highly specific for HIV-1 and are not active against other retroviruses.

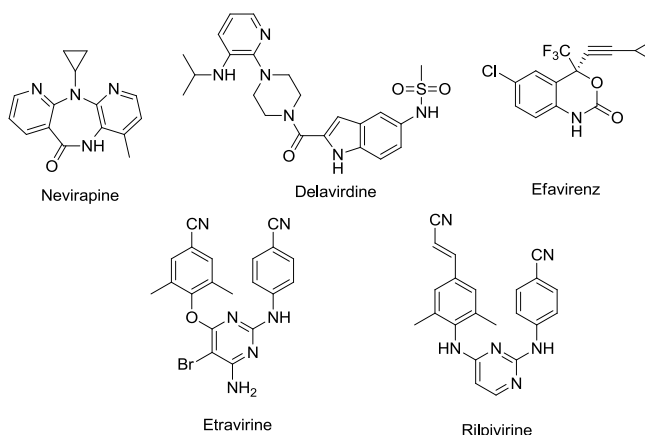


**Figure 1.14** Non-Nucleotide Reverse Transcriptase Inhibitors (NNRTIs)

The first generation of NNRTIs were approved in 1996 (nevirapine, NVP), 1997 (delavirdine, DLV), 1998 (efavirenz, EFV). Two NNRTIs, NVP and EFV are currently cornerstones of first line HAART, whereas DLV is rarely used today.<sup>103</sup> NVP is the drug of choice in developing countries and due to its reduced teratogenesis and pediatric toxicity it is also widely used in pregnant women and young children.<sup>133</sup> NNRTIs are generally characterized by a low genetic barrier to the development of resistance: they need to be combined with at least two other fully active non-NNRTI ARV drugs, and resistance to one of them precludes subsequent use of other first generation NNRTIs. They are generally well-tolerated and safe; however, hepatotoxicity and severe rash are associated with NVP<sup>134</sup> and central nervous system (CNS) side effects are associated with EFV that are sometimes difficult to overcome.<sup>135</sup> An

important consideration with the first generation NNRTIs is that they are metabolized by CYP450 and although the isoenzymes involved vary for each compound, there is a potential for drug-drug interactions with drugs that are also metabolized *via* the CYP450 pathway.

The success of the first-generation class of compounds prompted research for the discovery and development of the next generation of NNRTIs that would have a better resistance profile, in order to offer treatment experienced patients the option to benefit from the convenience and good safety profile of the NNRTI class of compounds. Etravirine was the first of the second generation class of compounds to be approved by the FDA. Etravirine and rilpivirine belong to the family of di-aryl-pyrimidine (DAPY) compounds and are reported to be clinically effective in HIV-1 strains that are resistant to other NNRTIs. They have a higher genetic barrier to resistance than the first generation NNRTI compounds.<sup>133</sup>

Trade Name	Generic Name	Manufacturer	Approval Date
Viramune ( <i>Immediate Release</i> )	NVP, nevirapine	Boehringer Ingelheim	21-Jun-96
Rescriptor	DLV, delavirdine	Pfizer	4-Apr-97
Sustiva	EFV, efavirenz	Bristol-Myers Squibb	17-Sep-98
Intelence	etravirine	Tibotec Therapeutics	18-Jan-08
Viramune XR ( <i>Extended Release</i> )	NVP, nevirapine	Boehringer Ingelheim	25-Mar-11
Edurant	rilpivirine	Tibotec Therapeutics	20-May-11

**Table 1.9** Clinically Approved Non-Nucleotide Reverse Transcriptase Inhibitors (NNRTIs)

#### 1.3.4. Highly Active Antiretroviral Therapy (HAART)

The combination of several classes of multiple classes of compounds, referred to as Highly Active Antiretroviral Therapy (HAART) or, more recently, as combined Antiretroviral Therapy (cART), reduces the viral load by sufficiently slowing the rate of viral replication, thus by restoring the immune system by increasing circulating levels of CD4+ T cells.<sup>133</sup> As a result, HAART has changed the prognosis for patients with HIV-1 infection from that of high morbidity and rapid mortality to, for many at least, a chronic, manageable, but still complicated

disease.<sup>136</sup> The key components of HAART are the RT inhibitors (NRTI or NNRTI) and PI, which target different stages of the viral replication cycle. The combination therapy optimizes the ARV effect of each drug and avoids genetic resistance.<sup>133</sup> There are several HAART strategies, which vary with the status of infection and/or patient characteristics, and are frequently updated. According to the current guidelines, initial regimens should be composed of two NRTIs with either a NNRTI or boosted PI.<sup>137</sup>

Over the past decade HAART has gradually evolved from drug regimens with more than 20 pills daily (i.e., stavudine plus lamivudine plus indinavir) in 1996 to 3 pills daily (i.e., zidovudine (Combivir<sup>®</sup>) twice daily and efavirenz once daily) in 2003 to 2 pills daily (i.e., emtricitabine/tenofovir disoproxil fumarate (Truvada<sup>®</sup>) and efavirenz) in 2004 and finally to one pill daily in 2006 (Atripla) and in 2011 (Complera<sup>®</sup>) (Table 1.10).<sup>138</sup>

Trade Name	Generic Name	Manufacturer	Approval Date
Atripla	efavirenz + emtricitabine + tenofovir disoproxil fumarate	Bristol-Myers Squibb & Gilead Sciences	12-Jul-06
Complera	emtricitabine + rilpivirine + tenofovir disoproxil fumarate	Gilead Sciences	10-Aug-11

**Table 1.10** Multi-Class HIV-1 Combination Drugs

### 1.3.5. Fusion inhibitors

Viral entry is a particularly attractive target for drug intervention since it involves the exposure of highly conserved domains in Env and depends on the cell surface receptors that can be targets for orally available small molecule inhibitors.<sup>71</sup> Enfuvirtide (Fuzeon<sup>®</sup>, DP-178, pentafuside, or T-20) is the first ARV fusion inhibitor approved for the treatment of HIV-1 infected patients. This new family of ARVs was eagerly awaited by the growing number of patients carrying drug-resistant viruses to RT and PR inhibitors.<sup>139</sup> Since the early 1990s it has been known that peptides synthesized on the basis of the amino acid sequence of heptad repeat 1 (HR1) and heptad repeat 2 (HR2) of gp41 may show antiviral properties against HIV-1.<sup>140-142</sup> In 1993, the *in vivo* potency of a peptide, D-178, which was synthesized on the basis of the amino

acid sequence of HR2, was demonstrated.<sup>139</sup> This molecule, enfuvirtide, is a synthetic peptide of 36 amino acids, which mimics the HR2 region of gp41 (Figure 1.15).<sup>143, 144</sup> It is homologous to the heptad repeat HR2 region of gp41 glycoprotein and, while T-20 will itself engage in a coiled-coil interaction with the heptad HR2 region of gp41, it prevents the six-helical bundle formation required to initiate the fusion process.<sup>72</sup> Enfuvirtide, the only HIV-1 drug injected subcutaneously, is generally used in combination with HAART regimens for the treatment of patients suffering failure to prior therapies. Although enfuvirtide is active in patients whose virus is resistant to other classes of ARVs, as in the case of all other ARVs, continued exposure, especially if the virus is not completely suppressed, can lead to emergence of viral resistance to enfuvirtide. It is by far the most complex ARV ever manufactured at such a large scale, which provides both production and economic challenges.<sup>145</sup>

Trade Name	Generic Name	Manufacturer	Approval Date
Fuzeon	T-20, enfuvirtide	Hoffmann-La Roche & Trimeris	13-Mar-03

**Table 1.11** Clinically Approved HIV-1 Fusion Inhibitor

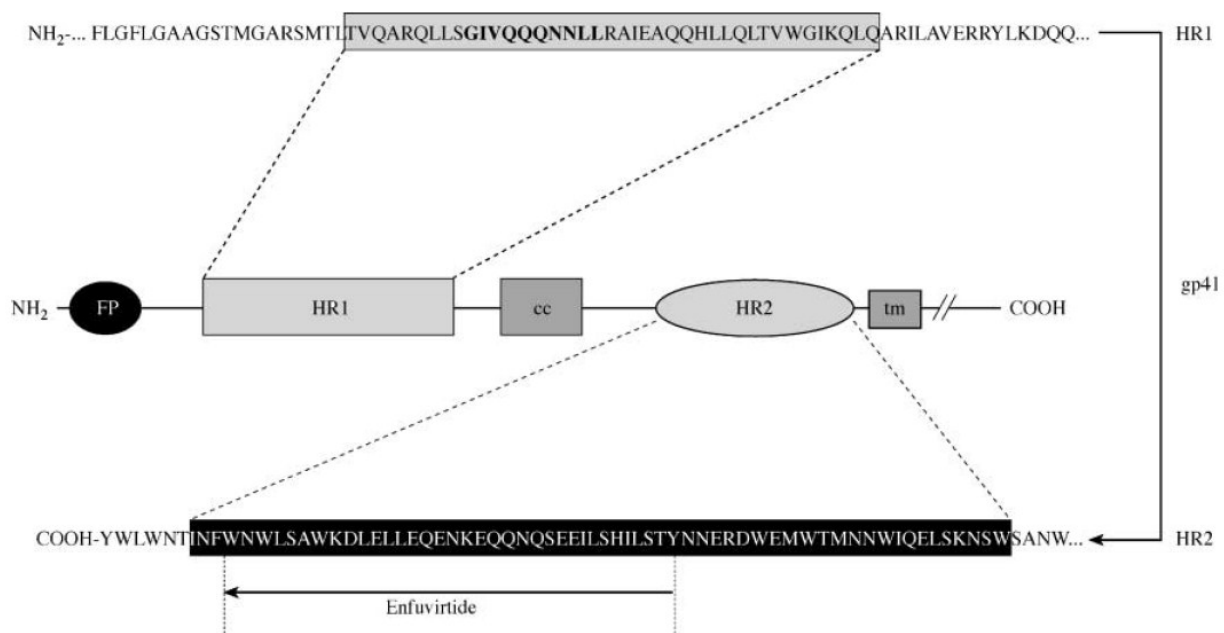


**Figure 1.15** Linear schematic of the HIV gp41. Four regions of functional importance are depicted: fusion peptide (FP), heptad repeat 1 (HR1), the cysteine residues (cc) that form disulphide bridges, heptad repeat 2 (HR2) and the transmembrane region (tm). The amino acid sequences of the HR1 and HR2 regions are shown in detail. Amino acids involved in the interaction between HR1 and HR2 are shown in bold, including those thought to be involved in resistance to enfuvirtide. The 36 amino acid region in HR2 corresponding to enfuvirtide indicated by a bold arrow.<sup>146</sup> (Reprinted with permission from Oxford Journals: License)

### 1.3.6. Chemokine Receptor Antagonists

The coincidental use of CXCR4 and CCR5 by HIV-1 as coreceptors to enter cells has prompted the search for CXCR4 and CCR5 antagonists (Figure 1.16), through blockade of the corresponding receptor, might be able to inhibit HIV entry into the cells.<sup>72</sup>

The most characterized of the CXCR4 antagonists is AMD3100 (JM3100, mozobil™). It was originally discovered as an anti-HIV agent with

strong inhibitory effect on the replication of X4 HIV-

1 strains<sup>147</sup> and was later found to inhibit X4 HIV-1

replication as a selective antagonist of CXCR4<sup>148</sup> then

found to specifically mobilize hematopoietic stem

CD34+ cells from bone marrow into the

bloodstream.

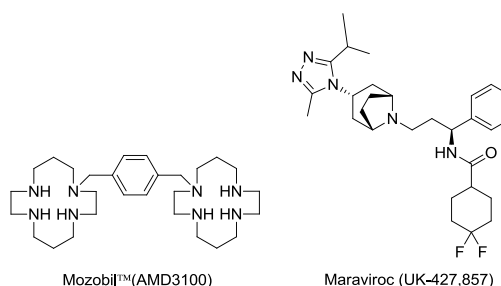


**Figure 1.16** CXCR4 and CCR5 Antagonists

Although several CCR5 antagonists have been evaluated in clinical trials only maraviroc has been approved for clinical use in the treatment of HIV-1 infected patients (Table 1.12).<sup>149</sup>

Maraviroc binds to CCR5, thereby blocking the HIV-1 protein gp120 from associating with the receptor and HIV-1 is unable to enter the host cell.<sup>150</sup> Since HIV-1 can also use other

coreceptors, such as CXCR4, and HIV-1 tropism test such as a trofile assay must be performed to determine if the drug will be effective.<sup>151</sup> Maraviroc has an extremely safe and tolerability

profile, however, the long-term safety of blocking CCR5 is not fully understood.<sup>152</sup> Despite

being approved in 2007, the optimal use of maraviroc has yet to be defined in HIV-1 therapy.

Unfortunately, one limitation to the clinical use of maraviroc is that it is only effective against

CCR5-using R5 HIV-1 strains. From dual (CCR5 and CXCR4)-tropic or mixed HIV-1

populations that use both CCR5 and CXCR4 (which are commonly used among highly treatment



experienced patients), maraviroc may select for the outgrowth of pure CXCR4-tropic X4 strains.<sup>153</sup> In addition, R5 HIV-1 strains may develop resistance to maraviroc while still utilizing the inhibitor-bound receptor for entry.<sup>154</sup> Evidently, to cope with dual-tropic or mixed X4/R5 HIV-1 populations, a combination of CXCR4inhibitors with CCR5 inhibitors will be needed.<sup>72</sup>

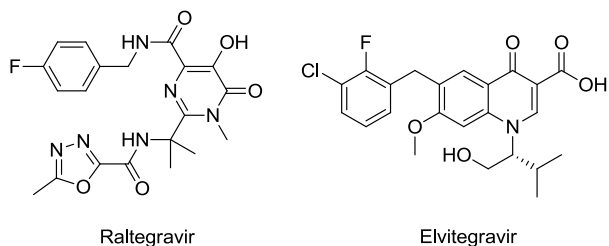
Trade Name	Generic Name	Manufacturer	Approval Date	Mechanism of Action
Selzentry	maraviroc	Pfizer	6-Aug-07	Non-competitive Inhibitor

**Table 1.12** Clinically Approved CCR5 Antagonist

### 1.3.7. Integrase Inhibitors

Among the furthest advanced IN inhibitors in clinical development are raltegravir (Isentress®, MK-0518) and elvitegravir (GS-9137) (Figure 1.17). Raltegravir was approved by the FDA in 2007 and elvitegravir's approval is

currently pending (Table 1.13).<sup>72</sup> Both compounds inhibit the strand transfer reaction in the integration process and were validated as



genuine HIV-1 IN inhibitors is cell culture assays.<sup>155</sup> When added onto an optimized

**Figure 1.17** HIV-1 Integrase Inhibitors

background regimen, raltegravir, offered better viral suppression than placebo over a 24-week treatment period.<sup>156</sup> Undoubtedly, the IN inhibitors may be welcomed (following NRTIs, NNRTIS, PIs, and virus entry inhibitors) as the next new class of anti-HIV drugs. However, just like all other classes of HIV-1 inhibitors, IN inhibitors should be carefully monitored for the emergence of drug-resistant virus strains.<sup>72</sup>

Trade Name	Generic Name	Manufacturer	Approval Date
Isentress	raltegravir	Merck	12-Oct-07

**Table 1.13** Clinically Approved HIV-1 Integrase Inhibitor

### **1.3.8. Vaccines**

There is currently little prospect of an effective vaccine for HIV-1 on the horizon. An HIV-1 and AIDS vaccine does not yet exist, but efforts to develop a vaccine against HIV-1, have been underway for many years. Since 1987, more than 30 vaccine candidates have been tested.<sup>157</sup> The development of an HIV-1 vaccine faces formidable scientific challenges related to high genetic variability in the virus, the lack of immune correlates of protection, lack of animal models and logistical problems associated with the conduct of multiple clinical trials.<sup>158</sup>

## **1.4. ANTIRETROVIRAL DRUGS AND LABORATORY MONITORING**

Antiretroviral drugs development was substantially accelerated by the development of accurate, reproducible, and inexpensive laboratory tests. These laboratory tests are used today to help individuals decide when to start ARV and continue to monitor the success of their anti-HIV therapy.

### **1.4.1. CD4 Testing**

The average CD4 T cell count of an uninfected adult is typically more than 500 cells per  $\mu\text{L}$ . Most OIs occur as the CD4 T cell counts fall below 200 cells per  $\mu\text{L}$ . Recent guidelines suggest the threshold of 350 cells per  $\mu\text{L}$  as a strong indicator for starting ARV.<sup>137</sup> Once treatment begins CD4 T cells typically increase rapidly for the first 3 months of treatment and then slowly increase by roughly 50-75 cells per  $\mu\text{L}$  per year, with rates declining CD4 T cell count reaches normal.<sup>159</sup> The biological and assay variability of the peripheral CD4 cell count is high, making it difficult to rely on one measurement.<sup>72</sup>

### **1.4.2. Quantitative Viral Load Testing**

Quantitative viral load, or concentrations of plasma HIV-1 RNA, is measured with PCR or related methods. Chronic established HIV-1 infection is often associated with a stable set point, which varies widely among individual patients. The viral set point is associated with the rate of CD4 T cell decline and the risk of AIDS and death.<sup>160, 161</sup> Viral load is measured before ARV therapy begins, but its primary value is monitoring treatment response or failure. The immediate goal of therapy is to reduce HIV-1 replication threshold below which the virus does not evolve and drug resistance does not emerge.<sup>8</sup>

### **1.4.3. Drug Resistance Testing**

Antiretroviral drug-resistance mutations will almost inevitably emerge if HIV-1 is allowed to replicate in the presence of ARV drug concentrations insufficient to exert complete suppression. The common resistance mutations for all drugs have been well characterized and their detection with reproducible commercial assays is straightforward, as long as the plasma viral load is at least 500-1000 copies per mL.<sup>162</sup>

### **1.4.4. Chemokine Receptor Tropism and HLA-B\* Testing**

HIV-1 enters the preferred target cells by binding to one of both of the chemokine receptors CXCR4 and CCR5. Nearly all patients with primary HIV-1 infection harbor a virus that binds to CCR5 (R5 virus). For unclear reasons, as the disease progresses overtime, many individuals develop a virus that also binds to CXCR4 (X4 virus).<sup>163</sup> Since one therapeutic drug specifically targets CCR5, testing is needed to define which tropism of the virus (CCR5 or CXCR4) is present.<sup>137</sup> The only validated tropism assay is an expensive phenotypic test that

takes 2-4 weeks and is only completed in a few specialized laboratories.<sup>164</sup> In view of these limitations, genotypic tropism assays are being developed and might gain widespread use.<sup>72</sup>

### 1.5. COMPLICATIONS OF CURRENT ANTIRETROVIRAL THERAPIES

Considering the low fidelity of HIV-1 RT coupled with the high replication of the virus, it is not surprising that even triple-class HAART therapy eventually fails in the majority of patients and is typically associated with the emergence of drug resistance. The success of HAART relies on a concerted multipoint attack that shuts down HIV replication so effectively that it reduces the likelihood that drug-resistant viral mutants will emerge. But if a patient doesn't follow the demanding regimen and concentrations of anti-HIV drugs in the blood taper off gradually, pressure on the virus is reduced, giving resistant strains a chance to emerge and crowd out "wild-type" virus.<sup>165</sup> Patients therefore need to be treated with sequential HAART regimens progressively, using up the diminishing pool of active drugs that are left available.<sup>145</sup> The combination of toxicity, "pill fatigue" and frequent changes in drug regimens has created the perfect conditions for the worst of all limitations: drug resistance.

The cost for most combination regimens approaches \$12,000 yearly. Despite the expense, ART is generally seen as cost effective, at least compared with other therapeutic strategies generally used.<sup>166</sup> In many resource-rich regions, treatment is often subsidized by public funding. There is a concern, however, in these countries, full and continuous access to ART could be threatened by a weak economy. Long waiting lists for access to publically supported treatment programs exist in many states within the US, and the lists seem to be getting longer.<sup>72</sup> The impact of the newly developed compounds incorporated in the HAART regimen remains to be seen. However, the fact that HIV-1 is now a chronic illness implies that therapies are

administered for life; therefore, their selection should be based not only on their efficacy but also on their toxicological profile.<sup>133</sup>

## II. HIV-1 INTEGRASE INHIBITOR DEVELOPMENT

Extensive reviews of HIV-1 integrase (IN) inhibitor design, development and mechanism of action have been previously published (Table 2.1). For the sake of brevity, a summary of significant contributions and discoveries that outline and provide a historical perspective as to the progression of the field of HIV-1 IN inhibition will be discussed.

Title	Reference
Design and Discovery of HIV-1 integrase inhibitors	<i>Drug Discovery Today</i> <b>1997</b> , 2, (11), 487-498.
HIV-1 integrase as a target for antiviral drugs	<i>Antiviral chemistry &amp; chemotherapy</i> <b>1997</b> , 8, 463-483.
Retroviral integrase inhibitors year 2000: update and perspectives	<i>Antiviral Research</i> <b>2000</b> , 47, (3), 139-148.
HIV-1 integrase inhibitors: past, present, and future	<i>Advances in Pharmacology</i> <b>2000</b> , 49, 147-165.
Patented small molecule inhibitors of HIV-1 integrase: a ten year saga	<i>Expert Opinion on Therapeutic Patents</i> <b>2002</b> , 12, (5), 709.
Small-molecule HIV-1 integrase inhibitors: the 2001-2002 update	<i>Current Pharmaceutical Design</i> <b>2003</b> , 9, (22), 1789.
Integrase inhibitors to treat HIV/AIDS	<i>Nature Reviews Drug Discovery</i> <b>2005</b> , 4, (3), 236-248.
HIV-1 integrase inhibitors: 2003-2004 update	<i>Medicinal Research Reviews</i> <b>2006</b> , 26, (3), 271-309.
HIV-1 integrase inhibitors: 2005-2006 update	<i>Medicinal Research Reviews</i> <b>2008</b> , 28, (1), 118-154.
HIV-1 IN inhibitors: 2010 update and perspectives	<i>Current Topics in Medicinal Chemistry</i> <b>2009</b> , 9, (11), 1016
HIV-1 integrase inhibitors: 2007-2008 update	<i>Medicinal Research Reviews</i> <b>2010</b> , 30, (6), 890-954.
HIV-1 integrase mechanism and inhibitor design	<i>Mechanism and Inhibitor Design</i> . 1 ed.; Wiley: <b>2011</b> ; p 528

**Table 2.1** Review Articles Detailing HIV-1 Integrase Inhibitors (1992-2011)

### 2.1. HIV-1 INTEGRASE: A TARGET FOR DRUG DISCOVERY

HIV-1 integrase (IN) was initially considered to be a difficult and “undruggable” target for antiretroviral (ARV) drug discovery and design. In comparison to HIV reverse transcriptase (RT) and protease (PR) inhibitors, where lead compounds were abundant in chemical repositories of major pharmaceutical companies, there were no authentic leads for IN inhibitors. The first decade of development in the field of HIV-1 IN inhibitor design was slow. The early lead IN inhibitors were not selective and in most cases were either inactive in blocking viral replication or too cytotoxic for further development.

### 2.1.1. Challenges of HIV-1 IN as a Target

The long process of HIV-1 IN inhibitor discovery and development can be attributed to the complexity of the IN and the integration reaction itself. Many copies of IN (50-100 copies) enter the cell with the infecting virus and only two integration events are required to produce the functional provirus.<sup>167</sup> Unlike RT, where several thousand enzymatic turnovers by RT are needed to complete the synthesis of viral RNA, providing numerous opportunities for NRTIs and NNRTIs to block RT, the relatively small number of events needed to complete integration potentially makes IN difficult to inhibit. Secondly, the absence of the crystal structure of the full length HIV-1 IN with viral or host DNA and its inhibitors has been an significant obstacle to the rational design of specific IN inhibitors.<sup>168</sup> Other challenges also include a shallow surface substrate binding site located on the surface of IN<sup>169, 170</sup> and its formation of a multimeric complex in preintegration complexes.<sup>171</sup> Finally, there were several initial technological complications that researchers encountered in respect to designing inhibitors of IN. Many of the early IN inhibitors were neither confirmed as antiviral nor specific inhibitors. Integrase can use either  $Mn^{2+}$  or  $Mg^{2+}$  as a metal cofactor to catalyze integration. It has always been a challenge to obtain good activity in the presence of  $Mg^{2+}$  and, therefore, most of the early inhibitors were reported using  $Mn^{2+}$  as cofactor.<sup>168</sup> It is now commonly acknowledged that  $Mg^{2+}$  is probably the biological cofactor of IN.<sup>86, 172</sup> Many of the early inhibitors screened in  $Mn^{2+}$  assays may have been responsible for a large number of false positives.

Collectively, the challenges were so significant that many in the field questioned the rationality of IN as a “druggable” target. Several recent studies predicting druggability still characterize the binding site of HIV-1 IN as not druggable.<sup>1, 169, 170</sup> In 2007, Cheng et al. used a model-based approach based on basic biophysical principles to predict the druggability of several

targets using the crystal structure of the target protein binding site.<sup>1</sup> They calculated values of the maximal affinity achievable by a drug-like molecule and correlated these values with expected drug-discovery outcomes. The group validated their theoretical data with experimental results against two targets using high-throughput screening of a diverse compound collection. They calculated druggability for a set of 27 protein target binding sites and remarkably HIV-1 IN was determined to be the most challenging and fundamentally “undruggable” target (Figure 2.1).<sup>1</sup>

### **2.1.2. HIV-1 IN as a Valid and Attractive Target**

With the long-term commitment of researchers dedicating time and resources to HIV-1 IN research, although once considered an invalid target, IN is now considered to be one of the promising new targets in preclinical and early clinical trials. HIV-1 IN enzyme is an attractive target for anti-HIV therapy for several reasons. First, IN specifically catalyzes the integration of proviral DNA into the host cell genome, which is an early and crucial step in the HIV-1 retroviral life cycle, and represents a point of no return.<sup>173, 174</sup> Upon inhibition of IN, the viral DNA is converted into circular DNA unable to be integrated into the host genome.<sup>175</sup> Moreover, a key component of the catalytic core of HIV IN is the highly conserved DDE motif which is composed of three amino acids: D64, D116 and E152.<sup>86</sup> A mutation in any of these conserved residues reduces the ability of the virus to replicate. Second, inhibitors of IN appear to be particularly promising since, unlike PR and RT, this enzyme does not have direct human homologs.<sup>176</sup> Therefore drug selectively targeting IN are expected to show low toxicity in the host. Third, reactions carried out by IN are unique, and sensitive assays exist for testing IN enzymatic activity *in vitro*.<sup>177</sup> In addition, crystal and nuclear magnetic resonance (NMR) structures are available for use in rational structure-based drug design.<sup>172, 178</sup> Lastly, combination



therapy with IN inhibitors and drugs directed against PR and RT was shown to be synergistic in several tested models.<sup>179</sup>

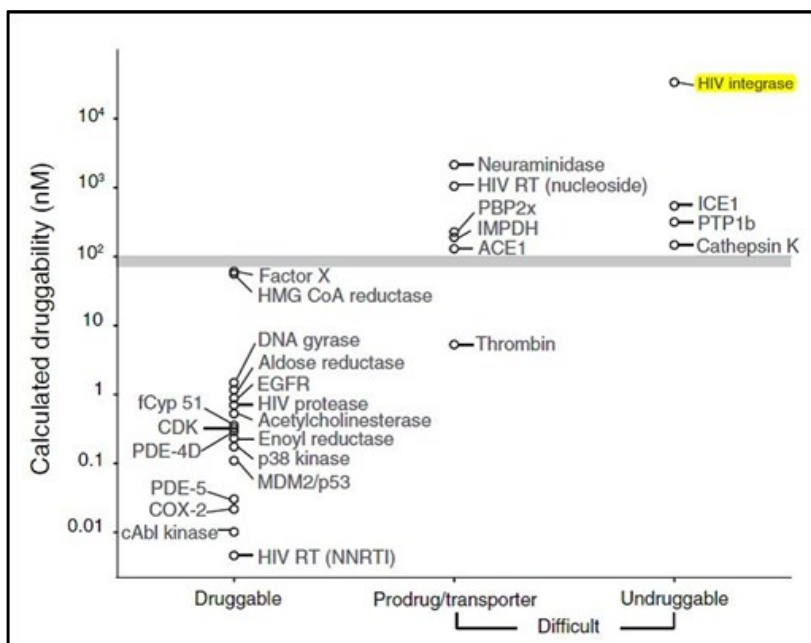


**Figure 2.1** Calculated Druggability. Calculated druggability for a set of 27 target binding sites. Known druggable protein targets are shown on the left vertical, whereas known difficult targets (prodrug and “undruggable”) are shown in the right verticals. Difficult and druggable target binding sites are effectively separated by the gray bar. The predicted druggability is the  $MAP_{pod}$  score calculated from the protein-ligand site structure. HMG-CoA, 3-hydroxy-3-methylglutaryl-CoA; EGFR, epidermal growth factor receptor kinase; CDK, cyclin-dependent kinase 2; PDE, phosphodiesterase; COX, cyclooxygenase; HIV RT, HIV reverse transcriptase; PBP2x, penicillin binding protein 2x; IMPDH, inosine monophosphate dehydrogenase; ACE-1, angiotensin-converting enzyme 1; ICE1, interleukin-1 $\beta$ -converting enzyme 1; PTP1b, phosphotyrosine phosphatase 1B.<sup>1</sup>

It is inconceivable to imagine that HIV-1 IN inhibitors were once considered an unattainable option for HIV-1 therapy. The continuous research in the IN field is responsible for the approval of the first marketed HIV-1 IN inhibitor and several other inhibitors emerging out of late stage clinical development. The 20 year journey from hypothetical concept to a proof-of-concept treatment option was not easy. The path was heavily laden with adversity and skepticism but dedication to the field led to a realistic and “druggable” target.

## 2.2. THE EARLY YEARS OF DEVELOPMENT

Concisely, prior to 1992, inhibition of HIV-1 had been considered as a treatment approach, but no specific IN inhibitor had been identified yet. Important biochemical studies on HIV-1 life cycle conducted during this period were fundamental for future IN inhibitor discovery.<sup>180-182</sup> Topoisomerase inhibitors and DNA-binding drugs were among the first drugs to be screened against IN (Figure 2.2).<sup>183</sup> However, the approach of using the DNA-binding drugs involved unfavorable risks and toxicity, and therefore, this route was quickly abandoned. Interestingly, topoisomerase II inhibitors, doxorubicin and mitoxantrone, inhibited HIV-1 IN catalytic activities but a topoisomerase I inhibitor, camptothecin, did not (Figure 2.2).<sup>183</sup> From these initial studies it was apparent that a common feature of the topoisomerase II inhibitors is the 5,8-dihydroxynaphthalene-1,4-dione (Figure 2.2). This was the first piece of evidence that compounds containing a keto-enol functionality (previously known to chelate divalent metal) inhibited HIV-1 IN activities.

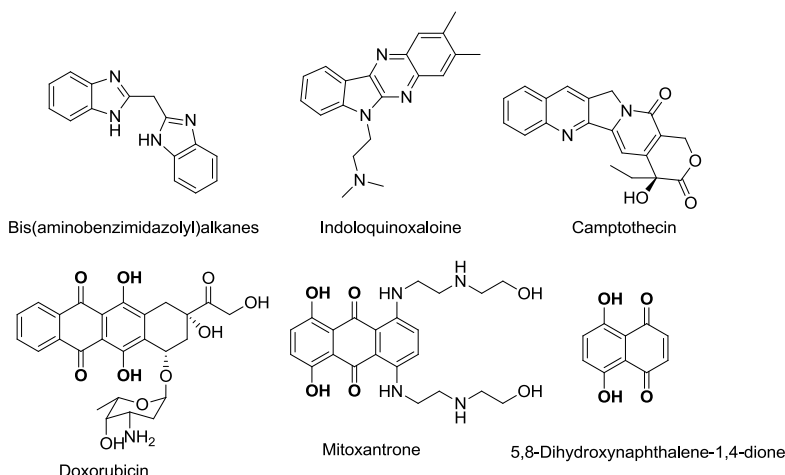


**Figure 2.2** Select Examples of DNA Binders and Topoisomerase Inhibitors

### 2.2.1. The Development of an *In Vitro* Screening Assay

During the period of 1992-1996, NRTIs, NNRTIs and PIs were already undergoing clinical testing or in an advanced phase of preclinical development and the discovery of IN inhibitors was just beginning.<sup>184</sup> These years would eventually lay the foundation for modern small molecule IN inhibitor discovery. A crucial step in the advancement of HIV-1 IN inhibitors was in 1992 with the development of an *in vitro* screening assay to identify inhibitors of IN.<sup>185</sup> This assay was based on labeled short oligonucleotide duplexes mimicking U5 and U3 viral DNA ends. These could act as mimics of both donor (e.g., viral) and target (e.g., cellular) DNA. Together with these methods used for producing purified recombinant retroviral integrases, this assay allowed to elucidate the first insights and several details regarding structure, catalytic activities and inhibitors of IN.

### 2.2.2. Hydroxylated Aromatics and Catechol-Containing

#### Inhibitors

In the mid-1990s several classes of IN inhibitors began to emerge and it became clear that a majority of compounds contained one or more catechol moieties were active against purified IN. Although the reported inhibitors are from unrelated structures, several of these compounds possessed multiple aromatic rings, with poly(arylhydroxylation), frequently in the 1,2-catechol arrangement. In many cases the aryl units of these compounds were separated by a variety of aromatic or aliphatic central linkers (Figure 2.3). By systemic screening using purified IN-based assays, several hydroxylated aromatic compounds (Figure 2.4) have been identified which include flavones and flavonoids,<sup>186, 187</sup> bis-catechols,<sup>188</sup> caffeic acid phenethyl ester (CAPE),<sup>189</sup>

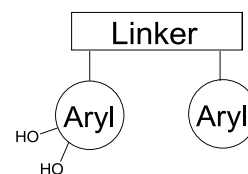


**Figure 2.3** General Structure of Catechol Containing Inhibitors

curcumin,<sup>186</sup> arctigenins,<sup>190</sup> tyrphostins,<sup>191</sup> styrylquinolines (SQLs) and chicoric acid and its derivatives.<sup>192, 193</sup> Although catechols as a group exhibit favorable inhibitory profiles in cell-free integrase assays, often these compounds have failed to have antiviral activity due to the dose-limiting toxicities in *in vitro* assays. Many polyhydroxylated aromatics showed considerable cytotoxicity, which obscures their potential antiviral activity.<sup>194</sup> One potential *in vivo* limitation is the cellular oxidation of the catechol to semiquinones or orthoquinones results in reactive

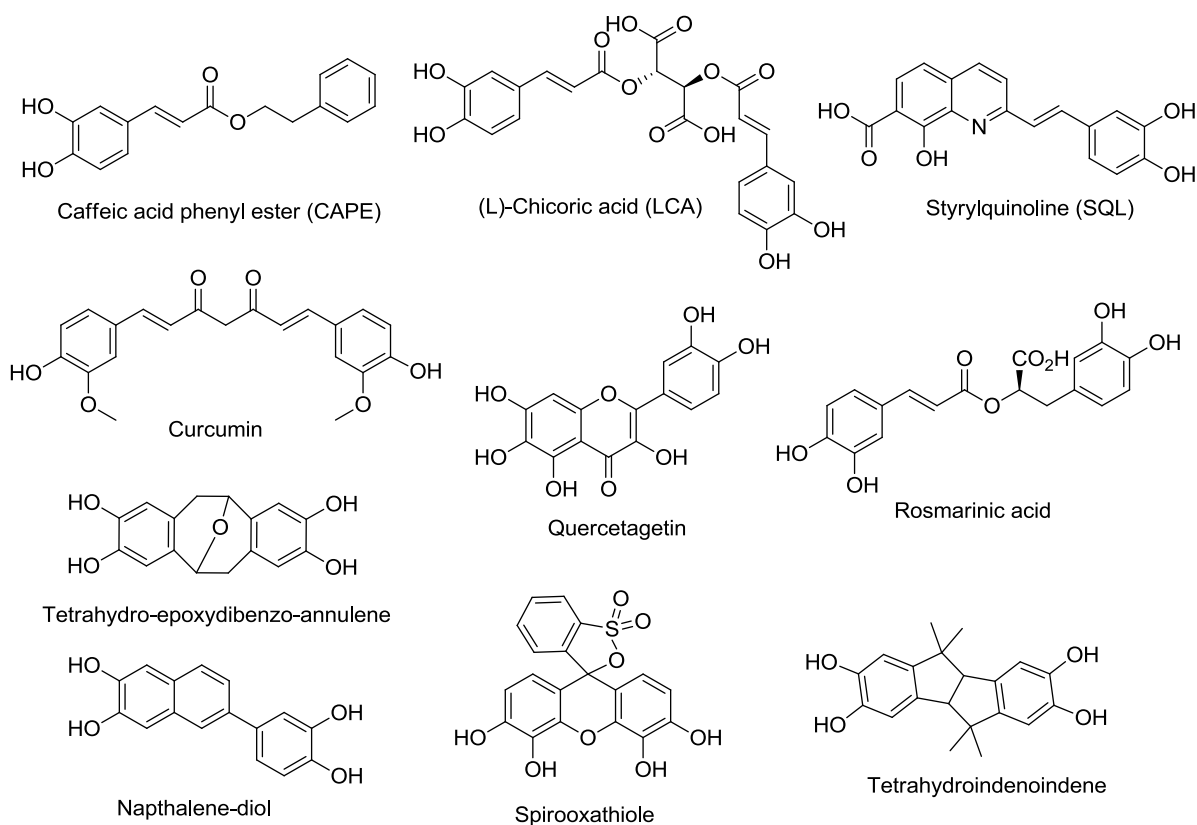


**Figure 2.4** Select Examples of Polyhydroxylated Aromatic IN inhibitors

intermediates that tend to cross-link to various cellular-targets.<sup>195</sup>

### 2.2.3. Non-Catechol-Containing Aromatic Inhibitors

Several classes of compounds lacking hydroxyl groups were developed in attempt to improve the toxicity and lack of antiviral activity of the catechol-containing compounds. These

compounds were tested in an effort to distinguish between mechanism of cytotoxicity and IN inhibition. In support of this endeavor, computer-assisted molecular modeling has been employed to identify potential inhibitors from among 206,876 open compounds contained within the National Cancer Institute (NCI) Drug Information System (DIS) database.<sup>196</sup>

An interesting detour in attempts to improve the profile and lack of antiviral activity of the catechol containing compounds led to the discovery of hydrazides (Figure 2.5). The *N, N'*-bis-salicylhydrazine (**H1**) generated fresh enthusiasm, albeit short lived, in synthetic exploration of its analogues.<sup>197, 198</sup> These hydrazide compounds are potent IN inhibitors, however, they do

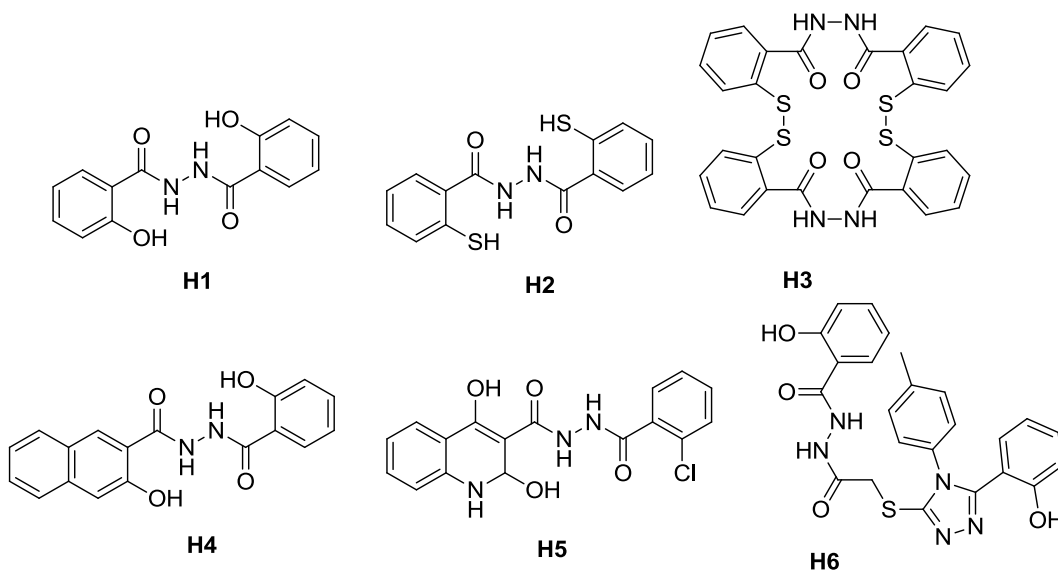


**Figure 2.5** Select Examples of Hydrazide-Based Inhibitors of IN

not show selectivity for 3'-P or ST. These compounds have been reported to inhibit IN through metal chelation but were only effective in assays using  $Mn^{2+}$  and not  $Mg^{2+}$  cofactors and lacked antiviral efficacy in HIV-1 infected cells.<sup>199, 200</sup>

The search for IN inhibitors that are superior to hydroxylated aromatics led to the discovery of several sulfones. Unfortunately, highly potent and selective inhibitors did not emerge from early structure-activity relationship studies of several screened sulfone analogues.

However, the search continued with other variations of sulfones such as sulfonates, sulfonamides and sulfides (Figure 2.6).<sup>194</sup> Among these, the mercaptobenzenesulfonamides and benzothiazines were shown to be promising for further optimization. In contrast to previously reported catechols, several of the sulfone analogues inhibited HIV-1 replication at a concentration below their cytotoxic concentrations. Furthermore, studies indicated that disulfones target an early-stage

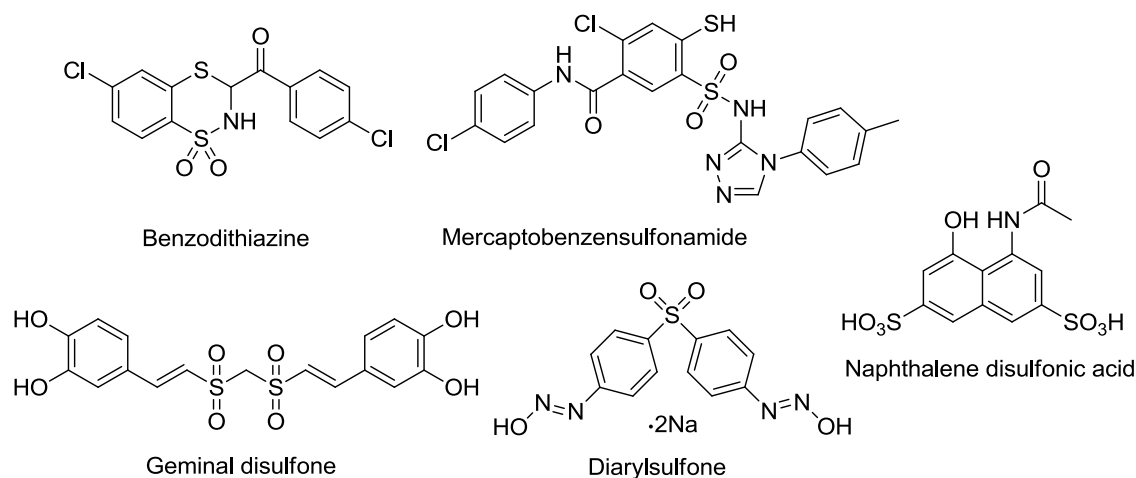


**Figure 2.6** Select Examples of Sulfone-Based Inhibitors of IN

HIV-1 replication event as well as a later step in virus replication, with IN as a possible target.<sup>201</sup>

Although, several compounds were found to inhibit IN function at low  $\mu\text{M}$  concentrations this endeavor was unsuccessful in yielding a selective bona fide lead.

#### 2.2.4. An Assay to Identify Strand Transfer Inhibitors of HIV-1 IN

Much of the earlier IN inhibition work led to the identification of compounds that interfered with the assembly and processing activities of IN in biochemical assays but did not show antiviral activity in cells.<sup>202</sup> In 1994, Merck researchers developed a novel rapid assay for the DNA strand-transfer activity of HIV-1 IN. This biochemical assay was able to separate the final strand transfer step from the earlier assembly and processing steps allowing high-throughput screening of compound libraries.<sup>175, 203</sup> This was achieved by allowing isolated IN enzyme to form an *in*

*vitro* IN-DNA-metal complex, also known as the preintegrase complex (PIC).<sup>204-206</sup> This assay allowed compounds to inhibit PIC-catalyzed strand transfer to a labeled “target” piece of DNA to be evaluated and ultimately evaluated for their ability to act exclusively as strand transfer inhibitors.<sup>207, 208</sup>

After about a decade of searching for a bona fide lead IN inhibitor it was apparent that there was an overwhelming sense of frustration among researchers. It had become apparent that the identification of a clinical candidate was noticeable more difficult than for other antiretroviral drug classes. In 1996, IN inhibitor research was overshadowed by the enthusiasm of the scientific community for the initial success of highly active antiretroviral treatment (HAART). The potential of HAART was initially overestimated due to the calculations forecasting the prolonged periods of HAART might lead to HIV eradication; therefore it was inevitable that main interest in drug companies was NRTIs, NNTIs and PIs. Merck was one of the few large pharmaceutical companies continuing huge efforts in IN research.<sup>209</sup> Despite the decay of interest in IN inhibitors, the assays optimized in the previous years allowed the screening of large numbers of molecules.<sup>209</sup>

### 2.3. The $\beta$ -DIKETO ACID CLASS OF INHIBITORS

The  $\beta$ -diketo acid (DKA) class of compounds represents one of the most promising classes of IN inhibitors and opened up a new frontier of IN antiviral drug discovery. A previous large-scale random screening of over 250,000 compounds yielded potent inhibitors, and the most active compounds proved to be 4-aryl-2,4-diketobutanoic acids, containing a distinct DKA functionality that was capable of coordinating metal ions in the active site of IN.<sup>175</sup> The DKA or keto-enol acid family of inhibitors were the first IN inhibitors reported with selectivity for the

strand transfer step of the integration reaction (STI),<sup>86</sup> high specificity for IN, and antiviral activity that could be related to IN inhibition.<sup>175</sup> During the time that the DKAs were first recognized, the hopes for HIV-1 eradication through HAART were definitively abandoned. Side effects became a serious problem affecting a large number of people. Thus, the interest in IN inhibitors in the scientific community was recharged.

The first small molecules (MW <500 Da) independently identified as potential HIV-1 IN STIs were L-731,988 (**2.1**) and L-708,906 (**2.2**) from Merck Research Laboratories,<sup>175, 210</sup> and 1-(5-chloroindol-3-yl)-3-hydroxy-3-(2H-tetrazol-5-yl)-propanone (5-CITEP, **2.3**) from Shionogi & Co. Ltd.<sup>211</sup> It was immediately clear that both the Merck and Shionogi compounds could be functionally classified together as DKAs.

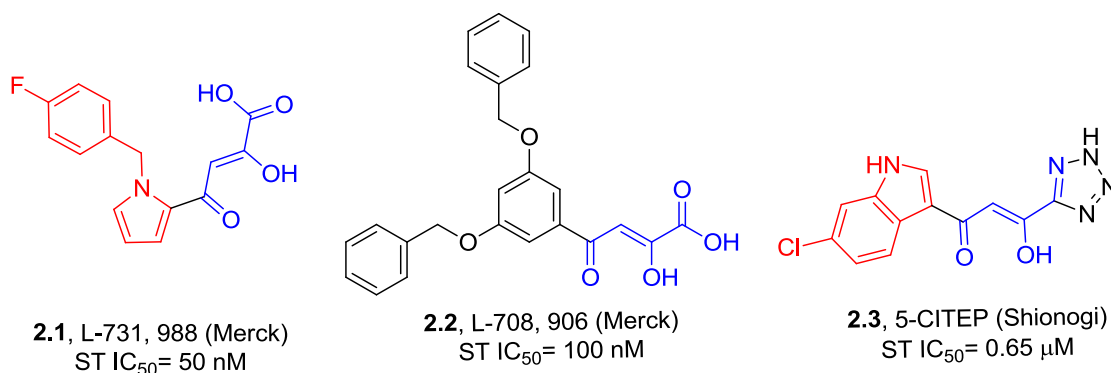


**Figure 2.7** First Lead DKA IN Inhibitors with Selectivity for ST

The DKAs from Merck (L-731,988 and L-708,906) were shown to selectively and potently inhibit both IN catalyzed ST and HIV-1 replication *in vitro*. Further studies of **2.1** and **2.2** showed that these compounds had no effect on viral entry, reverse transcription, PIC assembly, or 3' processing.<sup>175</sup> Additionally, upon serial passage of the HIV virus in cell culture in the presence of the two inhibitors, mutations that confer resistance to inhibition arose in the integrase active-site region (T66I/S153Y for **L-731,988**, T66I/M154I for **L-708,906**). These mutations are very near to the active-site amino acid residues D64 and E152, two of the three



amino acids critical for catalysis.<sup>175, 212</sup> This data was evidence that **2.1** and **2.2** were preventing integration by binding at the catalytic site.

The selectivity of these DKA containing compounds for ST inhibition over 3'P was greatly increased compared to previously reported IN inhibitors. For example, 5-CITEP presented an IC<sub>50</sub> value of 35 μM for 3'P and 0.65 μM for ST.<sup>211, 213</sup> Compound 5-CITEP (**2.3**) is a DKA bioisostere where the carboxylic acid group is replaced with its well-known isostere the tetrazole group.<sup>214</sup> The compound 5-CITEP was a breakthrough in the field of IN inhibitor research because it was co-crystallized with the catalytic core domain (CCD).<sup>211</sup> The electron density map clearly revealed the inhibitor bound in the center of the active site of the enzyme, lying between the three catalytic acidic residues D64, D166 and E152, suggesting that this binding mode might mimic interactions with the DNA substrate.<sup>211</sup> Of note, 5-CITEP was found to assume a planar conformation within the active site (Figure 2.8, panel A).<sup>211</sup>

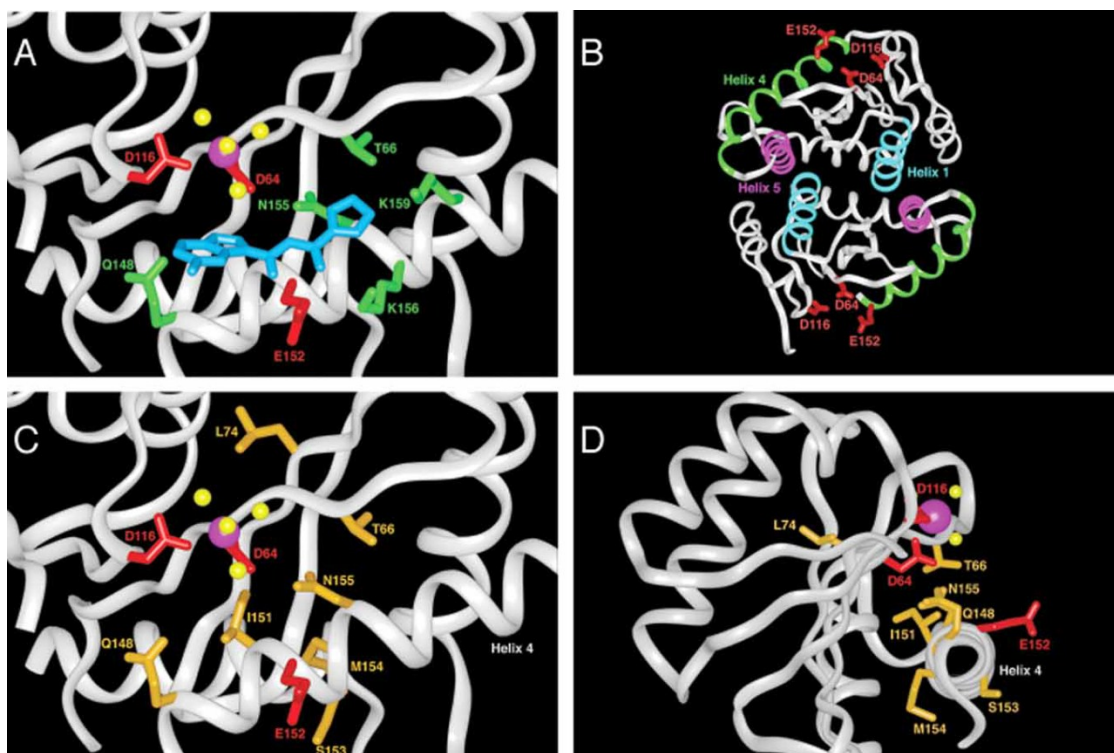


**Figure 2.8.** 5-CITEP Complexed with Crystal Structure. Panels A, B and C are derived from the crystal structure of the IN core domain complexed with 5-CITEP.<sup>211, 215</sup> The catalytic amino acids are shown in red, the magnesium ion is colored in magenta and the four coordinating water molecules are yellow. **A:** 5-CITEP interactions within the HIV-1 IN active site. Amino acids with direct interactions with 5-CITEP.<sup>211</sup> are highlighted in green. The view angle is the same in panel C. **B:** Crystal structure of the IN core domain dimer.<sup>216</sup> Alpha helices targeted by peptide inhibitors are colored and labeled. Helices 1 (cyan) and 5 (magenta) from the dimerization interface between two IN monomers. Helix 4 (green) is proximal to the active site and includes the catalytic amino acid E152. The three catalytic residues, D64, D116, and E152 are shown in red. **C and D:** Illustration of the amino acids that are mutated in the DKA resistant viruses. The side chains of the amino acids conferring resistance to DKA are highlighted in gold. Panel C is a view of the same orientation as in panel A. In panel D, the IN is rotated horizontally 90°.

The DKA derivatives mediate their antiviral activity through metal chelation.<sup>213, 217, 218</sup> It has been postulated that the integration mechanism involves two divalent metals (magnesium) in the catalytic site of the enzyme. The first magnesium atom, as observed in the different crystal structures, is coordinated by the two catalytic residues D64 and D116 (Figure 2.8) and the second would be coordinated either by D116 and E152.<sup>213, 217, 218</sup>

Extensive SAR of the DKA series of compounds would eventually lead to some most successful classes of IN inhibitors. The DKA integrase inhibitors **2.1-2.3** display a template of two carbonyl groups flanking a central enol moiety.<sup>175, 210, 212</sup> The DKA moiety was quickly recognized as important for activity, but it offered several liabilities as a drug candidate. The dicarbonyl portion was found to react reversibly with glutathione and the DKA was observed to

be unstable in the presence of aqueous base. Under these conditions the inactive methyl ketone

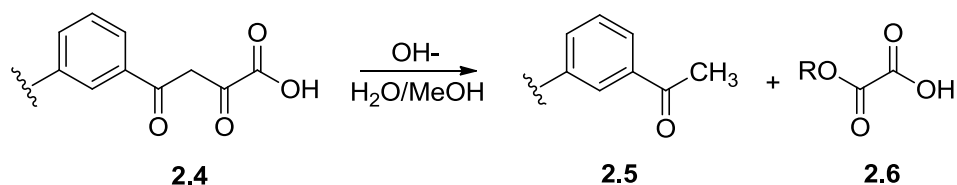


**Figure 2.9** Instability of DKA in Aqueous Base

was observed to form, as the result of loss of oxalate (Figure 2.9).<sup>219</sup> The terminal carboxyl group appears to act as a Lewis base rather than a Lewis acid, as has been confirmed by replacement by heterocyclic aromatic rings that have Lewis basic but not Lewis acid character (Figure 2.10).<sup>220</sup>

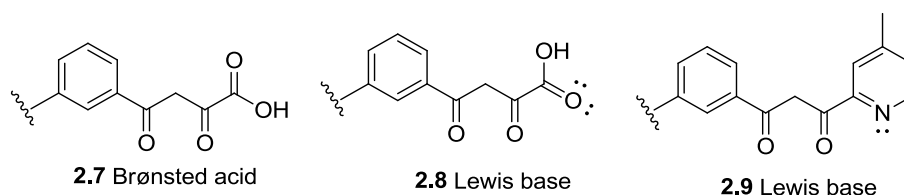


**Figure 2.10** Replacement of DKA with Diaryl Diketones

The discovery of compounds L-731,988 (**2.1**), L-708,906 (**2.2**) and 5-CITEP(**2.3**) represented a turning point in the IN inhibitor development because of their potent antiviral activity and well-characterized selectivity targeting integrase in HIV-infected cells.<sup>175</sup> From these initial series of DKAs several DKA derivatives advanced to clinical trials and ultimately the field of IN drug discovery started to gain momentum.

### 2.3.1. HIV-1 Integrase Inhibitors Enter Clinical Trials

The first IN inhibitor to enter clinical trials was S-1360 (**2.10**), a diaryl diketone derivative of 5-CITEP, developed by Shionogi & Co. Ltd in partnership with GlaxoSmithKline (GSK) (Figure 2.11).<sup>221, 222</sup> S-1360 proved that IN is indeed a “druggable” target, and results

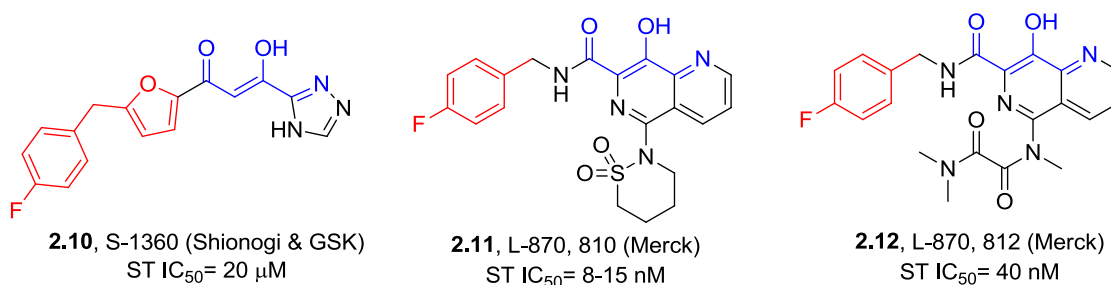


**Figure 2.11** Examples of Clinically Tested DKA IN inhibitors

with this drug in phase I clinical trials was very encouraging. Unfortunately, S-1360 failed phase II clinical trials due to lack of efficacy and pharmacokinetic problems.<sup>222</sup> It turned out that the DKA portion of the molecule, important for IN inhibition, was also a good substrate for aldo-keto reductase.<sup>223</sup> Although S-1360 did not proceed successfully through clinical trials it served as a good lead for structural optimization studies to identify more potent IN inhibitors.

Further optimization of the DKA series of compounds led to another class of IN inhibitors, the naphthyridine carboxamides (**2.11**) and (**2.12**) by Merck. In this series of compounds the carboxylate group was replaced with an appropriate heterocycle, which contained a lone pair donor atom such as an 8-hydroxy-1, 6-naphthyridine linked to a benzoyl substituent (Figure 2.11). Representative compounds from this class, L-870, 810 (**2.11**) and L-870-812 (**2.12**) show potent inhibition of the ST reaction with good antiviral potency.<sup>224, 225</sup> Most importantly these compounds provided the first proof-of-concept that IN inhibitors could prevent viral replication *in vivo*.<sup>226</sup> Unfortunately, following preliminary success in L-870, 810 (**2.11**) short-term monotherapy in both naïve and treatment experienced HIV-1 infected patients, the clinical development of this drug was terminated due to an observed long-term dosing toxicity in the liver and kidneys of dogs.<sup>227</sup> Additionally, L-870, 810 (**2.11**) exhibits a high affinity for serum protein binding, which may result in a lower effective plasma drug concentration. Although L-870, 812 (**2.12**) was one of the most extensively studied compounds of this series, the clinical

status has not been made public. Considering the structural similarity to L-870, 810 (**2.11**) it is assumed to display the same *in vivo* characteristics.

## 2.4. HIV-1 IN INHIBITORS: FROM CLINICAL TRIALS TO MARKET

### 2.4.1. Raltegravir

In October 2007, raltegravir (Isentress®, RAL, also known as MK-0518, **2.20**) was the first U. S. Food and Drug Administration (FDA) approved IN inhibitor to be used in combination with other ARV agents for the treatment of HIV-1 in treatment-experiences adults.<sup>228</sup> Raltegravir is the result of a long-term commitment by Merck Research Laboratories, West Point USA, and Istituto Ricerca Biologia Molecolare (IRBM) Italy in the development of IN inhibitors.<sup>229</sup> The medicinal chemistry behind the discovery of RAL by Merck Research Laboratories Rome (known as IRBM) relies on the understanding of the similarities of the mechanism of action of HIV-1 IN and another polynucleotidyl transferase, the NS5b RNA-dependent RNA polymerase of hepatitis C virus (HC V).<sup>230</sup> HIV-1 IN and HCV share the common feature of using two Mg<sup>2+</sup> ions in the active site as a key constituent of the catalytic mechanism. The two enzymes catalyze two different types of reactions, however, the amino acids within the catalytic site and the geometry of the catalytic metals are conserved. This observation was the basis of the integrated drug discovery program, where compounds designed as inhibitors for one viral target using the catalytic machinery, were screened across enzymes belonging to the same superfamily from other viruses.<sup>231</sup>

The research group working on hepatitis C virus polymerase discovered a simple DKA (**2.13**) and meconic acid (**2.14**) derivative as inhibitors of active site HCV NS5b RNA-

polymerase by random screening.<sup>232, 233</sup> Both classes (**2.13**) and (**2.14**) were liable to problems such as chemical instability, irreversible covalent

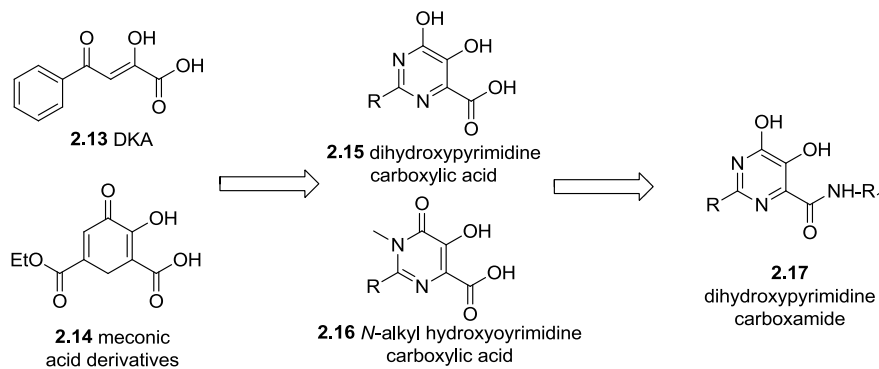


**Figure 2.12** Discovery of Dihydroxypyrimidine Carboxamide (**2.17**) as an HIV-1 IN Inhibitor

binding to protein, and poor stability in plasma. The constraint of the six member ring was an attractive template and a third class, dihydroxypyrimidine carboxylic acids (**2.15**) and N-alkyl hydroxypyrimidinone carboxylic acids (**2.16**), were designed to have more drug-like properties and maintain the correct geometry to bind the  $Mg^{2+}$  ions in the active site of HCV polymerase.<sup>232</sup> The mechanism of action of inhibition is likely due to the interaction with metals in the active site, resulting in a functional impairment by chelation of the critical metal cofactors.<sup>217</sup> Unfortunately, most of these inhibitors showed a suboptimal activity in the HCV cell assay resulting from compounds containing a free carboxylic acid.<sup>234</sup> Several carboxylic acid isostere derivatives, including amides (**2.17**), were synthesized to circumvent this problem. The dihydroxypyrimidine carboxamide that evolved from DKA in the HCV polymerase program<sup>232</sup> was a potent, reversible and selective HIV-1 INSTI while being completely inactive on the HCV polymerase.<sup>231</sup>

RAL was a result of continuous efforts to optimize these inhibitors, addressing pharmacokinetic, metabolic and antiviral activity issues presented by previously reported DKA inhibitors. RAL is an orally administered (400 mg twice daily), well-tolerated, highly potent, and with an excellent pharmacokinetic profile.<sup>228</sup> In July 2009, RAL was also approved by the FDA for use in first-line

antiretroviral (ARV) therapy and is undergoing Phase III studies in ARV treatment-naïve subjects including investigation of once daily dosing.<sup>104</sup>

#### 2.4.2. Elvitegravir

A second compound, elvitegravir (EVG, GS-9137 also known as JTK-303, **2.19**) is the next most advanced IN inhibitor in clinical development. EVG is a quinolone carboxylic acid derivative originally discovered by Japan Tobacco, Inc. that was subsequently licensed to Gilead Sciences for development outside of Japan. The 4-quinoline-3-glyoxlic acid scaffold was based on the idea that IN inhibitors with this scaffold maintain the co-planarity of DKA functional groups. Interestingly, the original developed scaffold (**2.18**) did not show activity, however, its precursor 4-quinoline-3-carboxylic acid (**2.19**) had IN inhibitory activity. This eventually led to the discovery of EVG. It is a potent, boosted, once-daily HIV-1 IN inhibitor with ARV activity

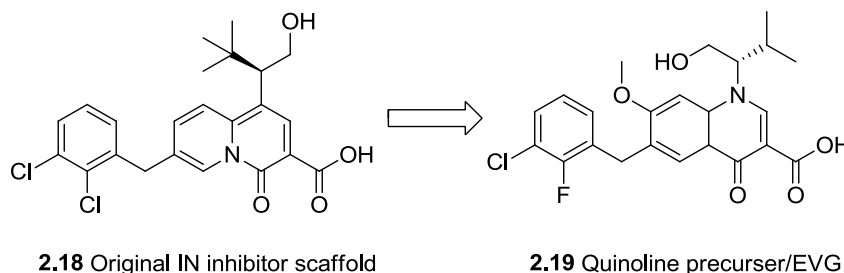


**Figure 2.13** Discovery of 4-quinolone-3-carboxylic acid as an IN inhibitor

against wild-type and drug-resistant strains on HIV-1. EVG is not yet approved by the FDA however; it is currently in Phase III clinical trials.<sup>235</sup> Unlike, RAL, EVG is primarily metabolized by cytochrome P450 3A4 isozyme and significant increases (boosts) in plasma exposure have been achieved by co-administering it with CYP3A4 inhibitors (e.g., ritonavir or cobicistat).<sup>236</sup> Boosting also results in a prolonged elimination half-life to ~9.5 hours, allowing once daily administration of a low 150 mg dose.<sup>236</sup> Structural modeling studies indicate that the efficient

binding of EVG to IN results from the  $\beta$ -ketone and carboxylic acid functional groups that have coplanar conformation similar to DKA derivatives.<sup>235</sup> RAL and EVG share the same mechanism of inhibitory action against IN.<sup>228, 237</sup>

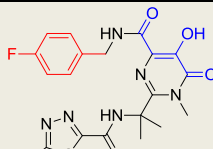
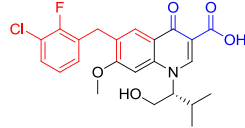
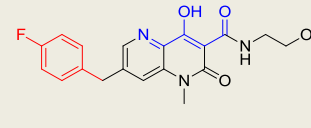
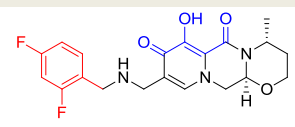
#### **2.4.3. GSK-364735**

Several studies to develop follow-on analogs of S-1360, the two groups involved jointly discovered a novel lead naphthyridinone-based inhibitor, GSK-364735 (**2.21**). This compound contains hydrophobic fluorobenzyl substituent flexibly linked to a chelatable quinolone region.<sup>238</sup> GSK-364735 exhibited ST inhibition comparable to RAL and EVG and demonstrated satisfactory results in a phase I clinical trial,<sup>239, 240</sup> but its clinical development was halted in a phase II clinical trial because of an unfavorable long-term safety profile.

#### **2.4.4. Dolutegravir (S/GSK1349572)**

The collaborative effort between Shionogi and GSK has advanced a Tricyclic hydroxypyridone carboxamide, S/GSK1349572 (**2.22**), into Phase IIb clinical trials. S/GSK1349572 is considered a second-generation HIV-1 IN inhibitor with demonstrates pharmacokinetic properties in humans consistent with once-daily unboosted dosing. Resistance data suggests that this compound may have an improved resistance profile on RAL and EVG selected mutations, which offers a potential therapeutic opportunity for patients suffering from RAL resistance.



Compound	Structural Class	IN inhibition profile	Anti-HIV activity	Pharmacokinetic Profile	Status
 2.20 Raltegravir	Pyrimidione carboxamide	IC <sub>50</sub> <sup>a</sup> = 2-7 nM	CIC <sub>95</sub> <sup>b</sup> = 19 nM (10% FBS) CIC <sub>95</sub> <sup>b</sup> = 33 nM (50 % NHS)	Rat: F <sub>absolute</sub> = 62% T <sub>1/2</sub> = <1 h Cl= 46 mL/min/kg Dog: F <sub>absolute</sub> = 62% T <sub>1/2</sub> = <1 h Cl= 46 mL/min/kg Human: F <sub>absolute</sub> = 32% T <sub>1/2</sub> (i.v.)= 1.4 h	Market
 2.19 Elvitegravir	4-Quinolone-3-carboxylic acid	IC <sub>50</sub> = 7 nM	EC <sub>50</sub> <sup>c</sup> = 0.7 nM EC <sub>90</sub> <sup>d</sup> = 1.7 nM (serum-adjusted)	Rat: F <sub>absolute</sub> = 34% T <sub>1/2</sub> = 2.3 h Cl= 8.3 mL/min/kg Dog: F <sub>absolute</sub> = 29.6% T <sub>1/2</sub> = 5.2 h Cl= 17 mL/min/kg	Phase III
 2.21 GSK-364735	1, 6-Naphthyridinone carboxamide	IC <sub>50</sub> = 8 nM	EC <sub>50</sub> = 1.2 nM EC <sub>90</sub> = 42 nM (serum-adjusted)	Rat: F <sub>absolute</sub> = 42% T <sub>1/2</sub> = 1.5 h Cl= 3.2 mL/min/kg Dog: F <sub>absolute</sub> = 12% T <sub>1/2</sub> = 1.6 h Cl= 8.6 mL/min/kg Rhesus: F <sub>absolute</sub> = 32% T <sub>1/2</sub> = 3.9 h Cl= 2 mL/min/kg	Halted Phase II
 2.22 Dolutegravir, S/GSK-1349572	Tricyclic hydroxy-pyridone carboxamide	IC <sub>50</sub> = 2.7 nM	EC <sub>50</sub> = 0.51 nM EC <sub>90</sub> = 2 nM	Human: F <sub>relative</sub> = 70% T <sub>1/2</sub> = 15 h	Phase IIb

<sup>a</sup>IC<sub>50</sub>—Concentration of compound that results in 50% inhibition of *in vitro* integrase assay

<sup>b</sup>CIC<sub>95</sub>—Concentration of compound that results in 95% inhibition of the spread of HIV-1 infection in cell culture

<sup>c</sup>EC<sub>50</sub>—Concentration of compound that results in 50% inhibition of *in vivo* viral replication

<sup>d</sup>EC<sub>90</sub>—Concentration of compound that results in 90% inhibition of *in vivo* viral replication

**Table 2.2** IN inhibitors in Clinic and Clinical Development<sup>223</sup>

## 2.5. PERSPECTIVE

Despite the clear successes of selective strand transfer IN inhibitors, the need for second-generation and new classes of inhibitors remains. Emergence of resistance leading to the treatment failure has already been reported for RAL and EVG.<sup>229, 241</sup> Consistent with selective targeting of IN by RAL and EVG, resistance pathways have been described in relationship with point mutations of IN residues surrounding the IN catalytic core site.<sup>215</sup> Three main resistance pathways involving the primary mutations Q148R/H/K, N155H and Y143R/C,<sup>241-243</sup> are

responsible for virological failure.<sup>244-248</sup> These pathways seem to be associated with secondary mutations that appear to rescue the viral fitness of those primary mutants for example G140S is observed together with Q148H, or G140A with Q148R.<sup>244, 248</sup> Several studies have shown the presence of significant genotypic and phenotypic cross-resistance between RAL and EVG, including mutations E92Q, Q148R/K/H, and N155H, suggesting that a common mechanism is involved in a resistance and potential cross-resistance of both IN inhibitors.<sup>249</sup> It is clear from the emergence of resistance from RAL and EVG in the clinic that second-generation HIV-1 IN inhibitors are needed.

After 20 years (Figure 2.14) IN is now a validated target for the development of anti-HIV therapies. However, our knowledge about its structure and function is still lacking. After the DKA series of compounds were discovered as STIs of IN and assay methods were refined, a plethora of compounds were revealed. These efforts have produced one marketed IN inhibitor (RAL) and several in late-stage clinical development, which validates IN as an effective target for the treatment of HIV/AIDS. Several companies, academic institutions and agencies continue to pursue novel scaffolds and inhibitors of HIV-1 IN.

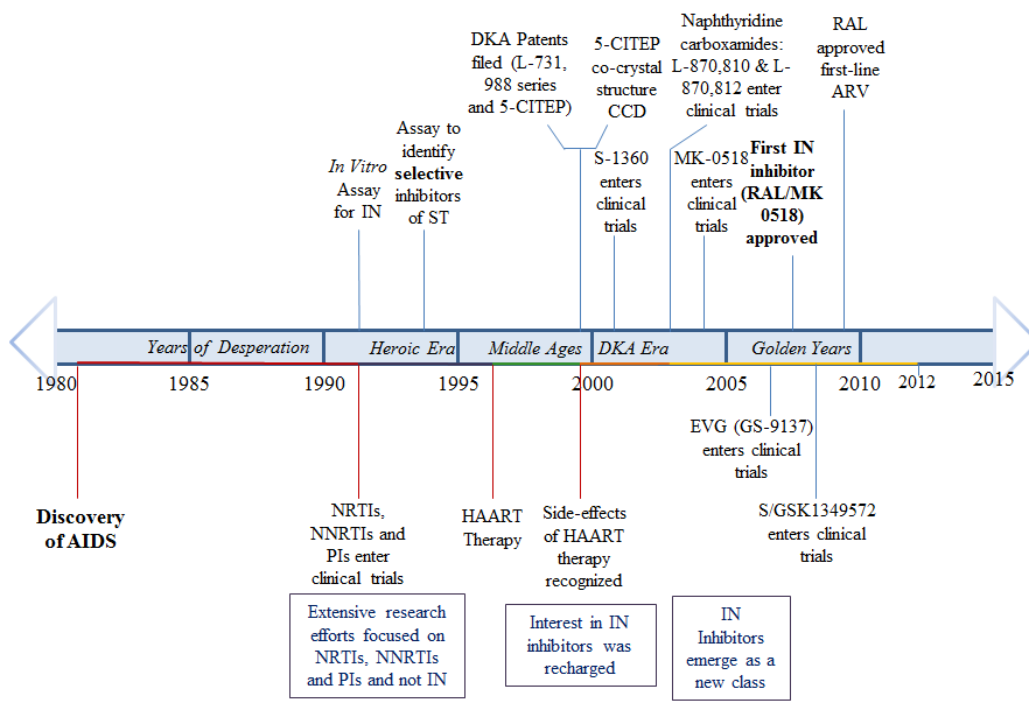


**Figure 2.14** Timeline of IN Inhibitor Milestones

### III. DESIGN AND SYNTHETIC APPROACHES TOWARDS THE DEVELOPMENT OF NOVEL HIV-1 INTEGRASE INHIBITORS

Despite the lack of valid structural information, several IN inhibitors have been discovered using *in vitro* assays specific to IN. The clinical success of selective ST inhibitors such as marketed raltegravir and the drug candidate elvitegravir, DKA-derived compounds, has validated IN as a rational ARV target. However, the exact mechanism of action of the DKA class of IN inhibitors has not yet been completely elucidated.<sup>250, 251</sup> Insights derived from studies in the field indicate several proposed mechanism of actions of IN inhibition by the DKA class of compounds. Several questions concerning the interactions of IN inhibitors with IN have remained unanswered<sup>86, 184</sup> and include: the docking site, possible interactions with metal ion(s) and viral DNA, the amino acids involved in IN binding, the role of drug resistance mutations, and the conformations assumed by the inhibitors in complex with the enzyme.<sup>252</sup> Clarification of these issues is critical, given the strict requirement of IN for insertion of proviral DNA into the host cell genome, leading to retroviral latency and persistence during therapy.<sup>253</sup>

#### 3.1. HIV-1 IN STRUCTURE AND FUNCTION

HIV-1 IN enzyme belongs to the DNA processing polynucleotide transferase superfamily, enzymes that cleave and join DNA by trans-esterification and is the key viral enzyme for catalyzing DNA integration.<sup>104</sup> HIV-1 IN is a 32 KDa enzyme that contains 288 amino acids, divided into three structural and functional domains. The three functional domains consist of the N-terminal domain (NTD), the catalytic core domain (CCD) and the C-terminal

domain (CTD).<sup>211, 254, 255</sup> Each IN monomer associates with another IN monomer to form a homo-dimer and these have been proposed to further associate into functional tetrameric or higher order IN complexes.<sup>254, 255</sup>

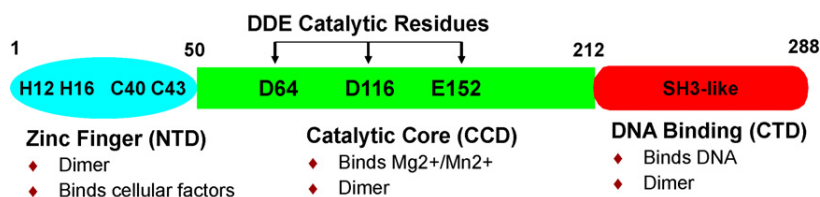


**Figure 3.1** Structural Domains of HIV-1 Integrase<sup>104</sup>

Reprinted with permission from Elsevier 2866750655927

Each of the three IN functional domains contains recognizable functional motifs (Figure 3.1). The NTD is composed of residues 1-50 and contains two histidine residues (His12 and His16) and two cysteine residues (Cys40 and Cys43), all of which are conserved and form a HHCC zinc finger motif that chelates one zinc atom per IN monomer.<sup>256, 257</sup> The NTD is essential for higher order multimer formation, a process which requires zinc. The zinc atom acts to stabilize the fold of the NTD and is necessary for the activity of IN.<sup>258</sup> The CCD is composed of residues 51-212 and contains three conserved negatively charged amino acids (residues Asp64 (D), Asp116 (D) and Glu152 (E), DDE motif). Mutation of any one of these three residues is sufficient to inactivate IN. These key catalytic residues are involved in coordinating divalent metal ions ( $Mg^{2+}$  or  $Mn^{2+}$ ) for catalysis of the chemical steps of DNA integration (Figure 3.2).<sup>259</sup> The crystal structure of the CCD shows that it consists of 5  $\beta$ -sheets and six  $\alpha$ -helices that are linked by flexible loops.<sup>211, 260, 261</sup> The CCD is essential for two key steps of the integration reaction, 3' processing (3'-P) of the viral DNA and the strand transfer (ST) reaction, in which it cleaves the phosphodiester bond of the host genomic DNA and subsequently joins the 3'-processed viral DNA ends to the host genomic DNA (Figure 3.3.). The CCD forms a dimer in solution and is a dimer in the functional IN enzyme.<sup>211, 260, 261</sup> The CTD is composed of residues

213-288 and has some structural homology with SH3 DNA binding domains and binds DNA nonspecifically.<sup>262</sup> The CTD is less conserved than the other two domains and has positively charged regions on its surface that are capable of binding DNA nonspecifically.<sup>255</sup> Coordinated action between the three domains is, however, necessary for the 3'-P and ST reactions to be catalyzed efficiently. Even though all three domains are required for full catalytic activity, site-directed mutagenesis studies have shown that the CCD is sufficient to promote a reverse integration *in vitro*, disintegration, indicating that this region contains the enzymatic catalytic center.<sup>263, 264</sup> The structures of the individual domains of IN have been determined but there still are no structures of the full-length protein and importantly, no structures with DNA substrate bound.<sup>265</sup>

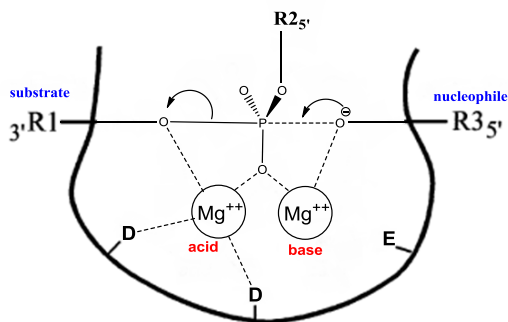


**Figure 3.2** Role of Divalent Metal Ions in Catalysis. This figure represents the catalytic pocket containing the pentacoordinated phosphate in the (hypothetical) transition state. One of the  $Mg^{2+}$  ions is proposed to act as a Lewis acid is shown to be coordinated with two aspartic acid residues and the oxyanion of the leaving group (R1 of nonbridging oxygen). The second  $Mg^{2+}$  is also shown to complex with the nonbridging oxygen and to act as a base for the deprotonization of the incoming nucleophile. The substrate is 3'R1-R25', and the product is 3'R3-R25'.

The DNA product formed after RT is a double-stranded linear DNA with LTR sequences at each end. This molecule is the substrate for integration and is acted upon in several biochemical and temporally discrete steps, before being co-linearly integrated in a host cell's chromosome. As soon as RT synthesizes double-stranded DNA, IN multimers will bind to DNA. IN will exert its catalytic activity when it recognizes an intact LTR end.<sup>266</sup> In the cytoplasm, HIV-1 IN recognizes and binds to a specific, imperfect, and inverted sequence in the LTR of the

reverse-transcribed DNA.<sup>86, 267</sup> IN then catalyzes the removal of a GT dinucleotide immediately 3' to the conserved CA dinucleotide at the 3' end of both strands of the viral cDNA (donor DNA) by a nucleophilic attack on the phosphodiester bond between deoxyguanosine and deoxyadenosine.<sup>181, 268, 269</sup> This initial step is called 3'-P and the IN remains bound to the LTR, forming a preintegration complex (PIC). The PIC containing viral proteins is then transported to the nucleus, where second reaction called 3'-end joining or ST occurs.

The ST reaction consists of a direct nucleophilic attack on the host chromosome (acceptor DNA) by the 3'-hydroxy recessed viral DNA, which are kept in close proximity, integrate at the 5'-ends of the host chromosomal DNA with a 5-base pair stagger.<sup>86, 269-271</sup> The two unpaired nucleotides at the 5'-ends of the viral DNA are removed, and the gaps at the

integration site on both termini are likely filled by host cellular repair enzymes.<sup>249, 272</sup> The ST reaction completes the viral DNA

integration into the host genome.

The integrated viral DNA (proviral DNA) becomes a template for virion synthesis, a process completed by host cellular machinery.<sup>249</sup>

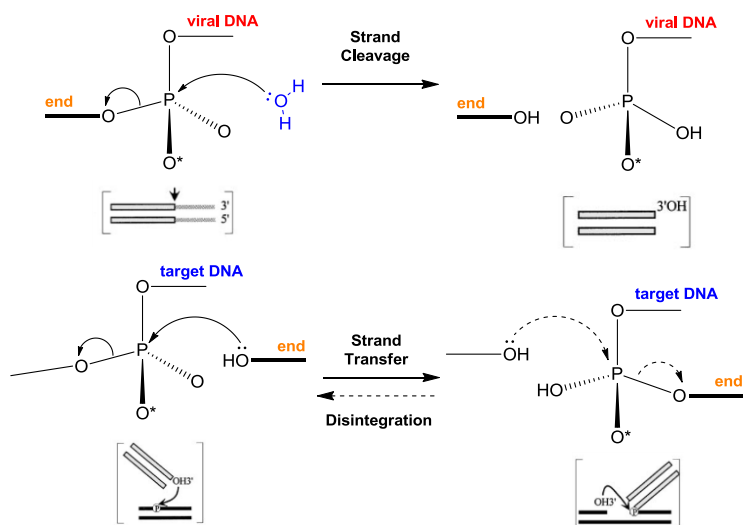


**Figure 3.3** The Mechanism of the 3'Processing and ST Reactions<sup>269</sup>

In general, IN inhibitors can be divided into dual inhibitors of 3'-P and ST (referred to as 3'P inhibitors), and selective strand transfer inhibitors (INSTIs). Based on several structural activity relationship studies, it was established that IN inhibitors bind to distinct regions of the IN

enzyme following conformational change induced under donor DNA binding, and then impair IN enzyme function by interaction with the catalytic triad.<sup>249</sup> The 3'-P inhibitors may contact both the donor and target DNA binding sites, whereas the ST inhibitors may bind selectively to the target DNA binding site.<sup>86,273</sup> IN inhibitors on the market and in advanced clinical trials are members of the INSTI class of compounds. Chemically, they possess a  $\beta$ -hydroxy carbonyl, thought to bind the two metal ions coordinating the three catalytic residues D64, D116 and E152.<sup>184,225</sup>

### 3.2. PROPOSED MECHANISMS OF ST INHIBITION

Interactions between HIV-1 IN and the HIV LTR are critical for IN-DNA binding, 3'-P, ST, and inhibitor interactions. Studies analyzing mutations in the IN amino acid or the LTR DNA base sequence provides insights into the structural requirements for IN 3'-P and ST. Collectively, understanding these IN-DNA interactions can provide useful information to aid in elucidating the interactions of IN inhibitors with IN. Although several synthetic and biological studies for DKA compounds have been reported, the mechanism by which they bind IN has not been well understood.

In order to increase the understanding of IN interactions with DNA, IN catalysis with oligonucleotides containing DNA backbone, base, and groove modifications were placed at unique positions surrounding the 3'-P site. IN sequence specifically recognizes the conserved 5'-CA in HIV LTR (Figure 3.4). Interactions between IN and the backbone of viral DNA have been



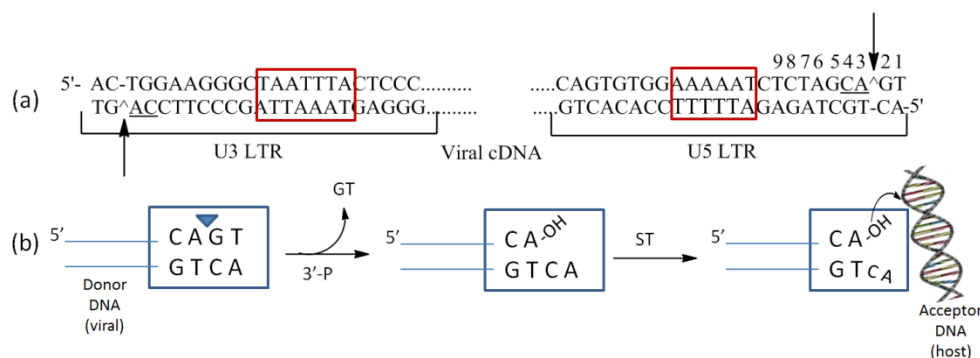


**Figure 3.4** Role of Major and Minor Grooves in IN Reactions. (a) Sequences of U3 and U5 LTRs. Nucleotide positions are indicated by numbers above the U5 LTR sequence. The 3'-P cleavage sites are indicated by vertical arrows, the conserved 5'-CA dinucleotides are underlined and the AT stretches are boxed. (b) Diagram of IN 3'-P and ST reactions.

examined by substituting conformationally constrained sugars into the 3'-P cleavage site.<sup>274</sup> The conformationally constrained sugar modifications prevented IN 3'-P, demonstrating that conformational restrictions at the 3'-P site block cleavage and suggesting DNA flexibility is required for 3'-P. From this study it was determined that IN has an open catalytic site that requires a flexible DNA backbone for 3'-P and ST.<sup>274, 275</sup> Several oligonucleotides were synthesized containing benzo[a]pyrene 7,8-diol 9,10-epoxide (BaP DE) adducts were tested to probe the effects of DNA groove occupancy on IN catalysis.<sup>274-276</sup> Only the adduct in the minor groove at the 3'-P site inhibited 3'-P, suggesting that the DNA minor groove surrounding the 3'-P site is important for IN-DNA interactions are important during 3'P.<sup>274</sup> The guanine/cytosine (GC) base-pair at the 3'-P site was replaced by the other 15 base-pair combinations to examine the importance of the base-pair sequence for IN reactions.<sup>274</sup> From this exercise it was determined that the interaction between cytosine (L2 cytosine or 5'-C) and Gln148 is critical for IN ST and plausible partners for hydrogen bonding.<sup>275</sup> From these studies several structural features of the viral cDNA that were found important for IN binding and reactions obtained from are summarized in Figure 3.5.<sup>274-278</sup>

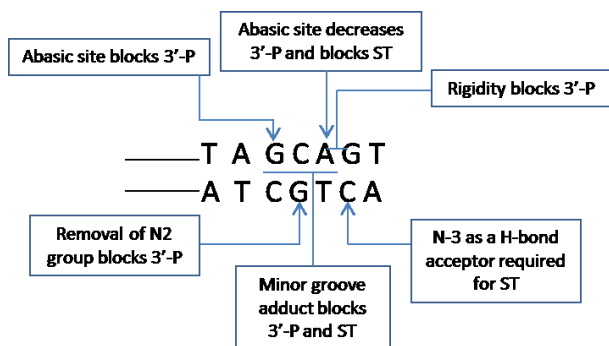


**Figure 3.5** Important Components of IN/DNA Interactions. The components that are critical to IN reactions are noted. A base is required at U3 adenine and U5 guanine positions. The L4 N2 guanine is required for 3'-P; the L2 cytosine N-3 group is required for ST. Interaction between IN and the cDNA minor groove is required for both 3'-P and ST.

Several IN amino acids have been identified to interact with specific viral cDNA bases (Figure 3.6).<sup>275</sup> The catalytic amino acids Glu152 and Asp64 interact with the U3 adenine and L3 thymine, respectively.<sup>279</sup> Lys159 interacts with the conserved U3 adenine<sup>280</sup> and the scissile phosphate.<sup>281</sup> The C-terminal domain residue Glu246 forms a disulfide cross-link with L7 adenine, and the IN monomer containing the active-site residues.<sup>282</sup> Gln148 interacts with the N-3 group of the L2 cytosine,<sup>277</sup> and Tyr143 forms a photo-cross-link with the terminal L1 adenine.<sup>280</sup> A specific viral LTR contact for the catalytic amino acid Asp116 has not been

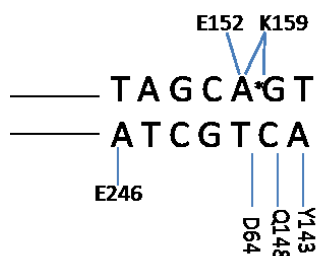


**Figure 3.6** IN amino acids interacting with viral cDNA bases.

identified.<sup>283</sup>

Integrase strand transfer inhibitors define a functionally distinct mechanistic class of compounds that selectively inhibit strand transfer *in vitro* and in infected cells.<sup>175</sup> The opinions on the mechanism of IN

inhibition by the  $\beta$ -DK class of compounds are divided. Previous studies have suggested that the binding of DKA inhibitors require that IN be assembled into a nucleoprotein complex competent to catalyze ST and that binding of the inhibitor and the target DNA are mutually exclusive.<sup>252, 284</sup> These studies suggest a biochemical basis for ST selectivity of these inhibitors. Alternative studies suggest a molecular basis of inhibition where there is interaction between IN inhibitor

and metal ion(s) in the IN active site, resulting in a functional sequestration of the critical cofactor(s).<sup>86, 217, 218, 275</sup>

### 3.2.1. Biochemical Mechanisms

In 1999, Goldgur *et al.* reported that the IN inhibitor, 5-CITEP (Figure 3.1, bound to the crystal structure of the CCD seems to mimic the DNA substrate/IN interaction.<sup>211</sup> The stereo view of 5-CITEP bound at the active site

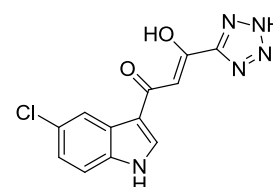


**Figure 3.7** Structure of 5-CITEP

represented in Figure 3.8, and a schematic of the contacting residues are shown in Figure 3.9. These figures depict the

inhibitor/active site interactions implicating several residues of importance for catalysis or DNA binding.<sup>211</sup> Gln148 forms a hydrogen bond to the nitrogen of the indole ring; Glu152 is within hydrogen-bonding distance of the enol hydroxyl. All four nitrogen atoms of the tetrazole ring are hydrogen bonded to Asn155, Thr66, Lys159 and Lys156. Although no direct contacts

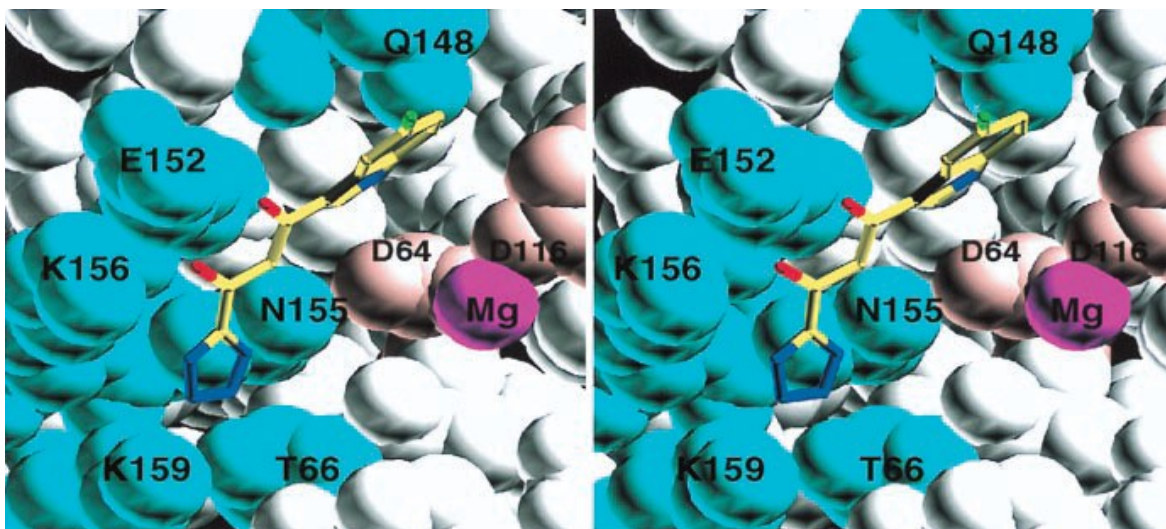


**Figure 3.8** Stereo Image of 5-CITEP Inhibitor/Protein Contacts. Contacting protein side chains are shown in cyan, with magnesium in purple and the catalytic residues Asp-64 and Asp-116 in pink.<sup>211</sup>

with the two catalytically essential aspartates are observed, one of the four water molecules coordinating the magnesium ion is close enough to the plane of the indole ring to be regarded as van der Waals interaction. Based on electron density mapping 5-CITEP is bound in the middle of

the active site between two aspartates, D64 and D116, and the glutamate E152, all three which

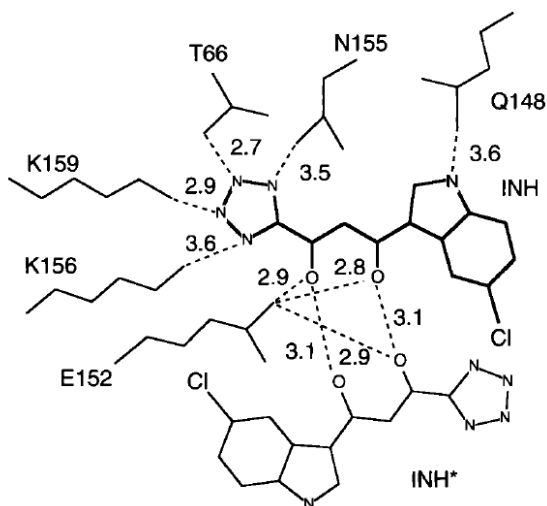


**Figure 3.9** Schematic of 5-CITEP and Interacting Residues. The contacting distances corresponding to the potential hydrogen bonds are shown. Note that for this subunit the inhibitor makes two hydrogen bonds with its symmetry-related neighbor. Also, one of the oxygens of Glu-152 is within contact distance of both inhibitors.

are required for IN catalysis. This study also revealed that the inhibitor does not displace the bound magnesium ion, which remains complexed to the two aspartic acid residues.<sup>211</sup>

It was speculated that the interactions between 5-CITEP and IN partially mimic the normal interactions with viral DNA substrate during the 3' processing reaction. The distance between the indole and tetrazole ring systems on the inhibitor is approximately 8 Å, a distance that could easily be spanned by two nucleotides, with the sugar

phosphate backbone containing the scissile bond passing between the active site carboxylates in close proximity to the bound magnesium ion. In this model the two bases adjacent to the scissile phosphate potentially would overlap the pockets in which the indole and tetrazole rings of the inhibitor are buried. It is postulated from this study that this DKA IN inhibitor, 5-CITEP, mimics the DNA substrate of the integration reaction and also interacts with unstacked DNA bases at the catalytic site.<sup>211</sup>

In 2000, Espeseth *et al.* developed a scintillation proximity assay (SPA) that allows analysis of radiolabeled IN inhibitor binding and IN function.<sup>284</sup> Investigations to aid in understanding the unique ability of DKA inhibitors to selectively inhibit the ST activity of IN in the absence of an effect on 3' end processing were investigated.

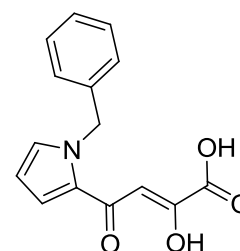
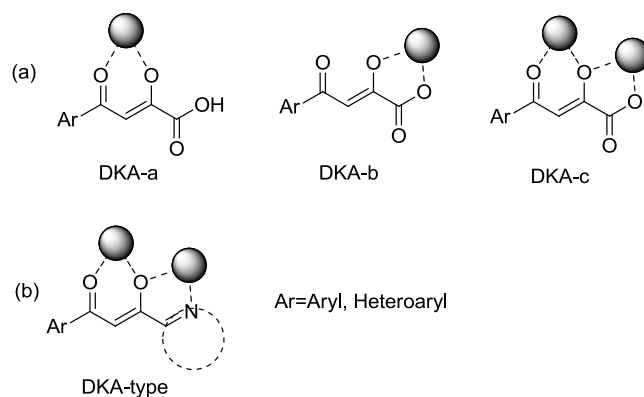


**Figure 3.10** Structure of L-731,988

Specifically, the mechanism of action of DKA, L-731,988 (Figure 3.10) and interactions of this inhibitor with IN were elucidated from this study.<sup>175, 284</sup> This study determined that L-731,988 binds within the IN active site and inhibits ST by competing with target DNA substrate. High-affinity binding of L-731,988 is shown to require the assembly of a specific complex on HIV-1 LTR. The interaction of L-731,988 with the complex and the efficacy of L-731,988 in ST can be abolished by the interaction with target substrates, suggesting competition between the inhibitor and target DNA. Although distinct from that of the viral donor substrate, the binding site for the DKA inhibitors is within the active site.<sup>284</sup> Given the results presented in this study it is surprising that 5-CITEP binds in the absence of donor substrate and that substantial conformational changes in the protein were not observed in the 5-CITEP complex.<sup>211</sup> Although it is not known if the mechanism of inhibition for 5-CITEP and L-731,988 is analogous, it is possible that the 5-CITEP represents the less interesting weak micromolar binding mode observed for the DKAs in the absence of substrate. Whether this interaction is predictive of the high-affinity DKA inhibited complex is therefore unclear.<sup>284</sup>

### 3.2.2. Molecular Mechanism

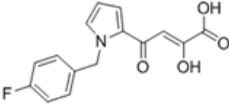
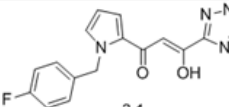
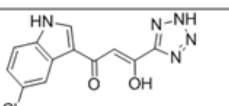
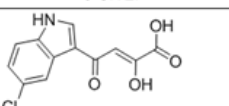
It is believed that the  $\beta$ -DKA pharmacophoric motif could be involved in a functional sequestration of one or both divalent metal ions (Figure 3.11) in the enzyme catalytic site<sup>86, 217</sup> to form a ligand- $M^{2+}$ -IN complex. This would subsequently block the transition state of the IN-DNA



**Figure 3.11** Complexing motifs for DKAs. (a) bidentate ligand (DKA-a and DKA-b), tridentate ligand (DKA-c), and (b) general scheme of two-metal-chelating state for DKA-type compounds. Dashed lines are the interactions with the metal ions (spheres).

complex by competing with the target DNA substrate.<sup>86, 284, 285</sup>

In 2002, Grobler *et al.* characterized the molecular basis of IN inhibition by using functional and binding assays to evaluate a series of DKA inhibitors.<sup>217</sup> Binding and mechanistic studies suggest that the DKAs and 5-CITEP are structural homologs.<sup>217, 250</sup> To explore the common functionalities in these compounds, carboxylate and tetrazole (isosteric replacement of carboxylate) containing compounds were synthesized and evaluated for binding and inhibition of IN. As shown in Table 3.1, both hybrid molecules were active; however, in the context of either

Compound	Competitive Binding Assay		Strand Transfer	
	IC <sub>50</sub> /Mn, nM	IC <sub>50</sub> /Mg, nM	IC <sub>50</sub> /Mn, nM	IC <sub>50</sub> /Mg, nM
 L-731,988	30	15	50	50
 3.1	110	3,100	60	470
 5-CITEP	320	50,000	400	4,000
 3.2	110	80	400	400

**Table 3.1** Binding and Inhibition by Hybrid Integrase Inhibitors

template, the carboxylate (L-731,988 and 3.2, respectively) was more potent. The choice of metal did not affect the affinity or potency of the carboxylate analogues. However, the tetrazole derivatives (3.1 and 5-CITEP) exhibited reduced binding and inhibition in Mg<sup>2+</sup> relative to Mn<sup>2+</sup>. This

observation can also in part explain the lack of antiviral activity in cellular system for the tetrazole containing DKAs, since Mg<sup>2+</sup> is the plausible metal *in vivo*.<sup>250</sup> The acidic tetrazole/carboxylate moiety therefore is not required for binding but it is essential for inhibition. It was demonstrated from this study that binding to IN is in part mediated by the interaction of the acid functionality with metals in the active site.<sup>217</sup> A model for the binding of the DKA analogs to IN that is consistent with the requirement for the acid functionality and observed

metal dependence of these inhibitors was developed (Figure 3.12). In this model, the inhibitor coordinates two metals bound at the active site by the conserved DDE motif of IN.<sup>217</sup> The bond lengths and angles for the acidic functional group used were based on the crystal structure of 5-CITEP.<sup>211</sup> Binding requires divalent metal and

additionally, resistance is metal dependent with active site mutants displaying resistance only when the enzymes are evaluated in the context of  $Mg^{2+}$ . The mechanism of action of these inhibitors is therefore

likely a consequence of the interaction between the acid moiety and metal ion(s) in the IN active site, resulting in a functional sequestration of the critical metal cofactor(s).<sup>217</sup>

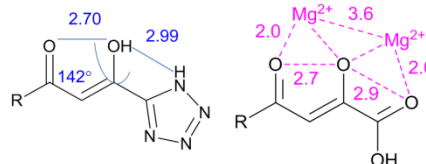


**Figure 3.12** Model for the Binding of Two Divalent Metals by DKA Inhibitors

### 3.2.3. Proposed Mechanisms and Inhibitor Development

Even if the exact mechanism of action of IN inhibitors has not been completely elucidated, it is generally more widely accepted that INSTIs bind to the host chromosomal DNA site of the enzyme and act by sequestering the metal ion(s) bound in the IN active site to form a ligand- $M^{2+}$ -IN complex.<sup>217, 286-288</sup> Furthermore, it has been believed that the inhibitors bind at the IN-DNA interface rather than to IN alone,<sup>243, 284</sup> thus acting as interfacial inhibitors of protein-nucleic acid interactions.<sup>86, 289, 290</sup> Almost all of the authentic HIV-1 IN inhibitors developed share similar chemical structural features. All of these compounds possess at least two distinct regions: an aromatic hydrophobic region and a metal chelating region.<sup>291</sup> Except for elvitegravir (GS-9137), the chelating region of all of these compounds is represented by a DKA motif or a bioisostere of DKA. In structural terms, these molecules have essentially three functional groups

in a coplanar conformation that are assumed to chelate two magnesium ions in the so-called two-metal-ion mechanism.<sup>217, 291</sup>

Research has focused on the molecular binding of INSTIs to IN complexes because of the increasing importance of selective INSTIs as ARV compounds and their unique mechanism of action.<sup>86</sup> Unfortunately, a full understanding of the inhibitor binding mode remains unclear. Although the X-ray crystal structure of 5-CITEP bound to the HIV-1 CCD has been investigated, the ligand forms a dimer with another molecule of 5-CITEP at a crystallographic dimer interface.<sup>211</sup> Therefore, the binding site of the inhibitor in the crystal is assumed rather unlikely to resemble the physiologically relevant binding configuration, especially considering that no DNA was observed in this structure.<sup>290</sup>

### 3.3. DISCOVERY OF THE AMINOCARBOXYALTE SYSTEM

#### 3.3.1. Aromatic Substitutions of the DKAs

One interesting trend noted with the  $\beta$ -DKA containing class of inhibitors is that several distinct compounds, while possessing various aromatic substitutions with the DKA scaffold (Figure 3.13), demonstrate potent ST inhibition and antiviral activity with remarkable fidelity.<sup>273, 288, 292</sup> For example, the  $\beta$ -DKA (carboxylate or tetrazole) compounds containing the aromatic groups diphenylmethane (**3.3**),<sup>293</sup> benzyl furan (**S-1360**),<sup>294</sup>

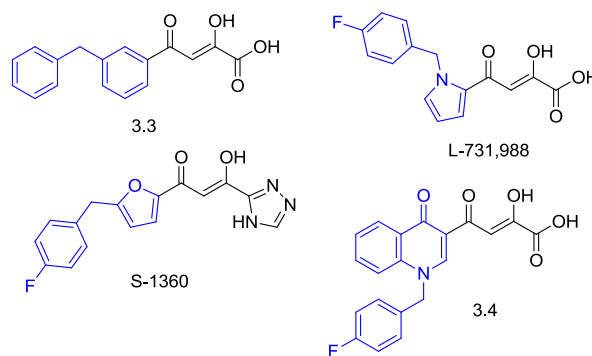


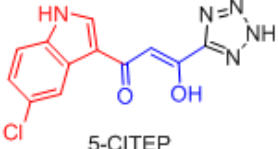
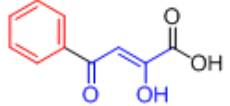
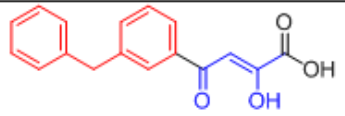
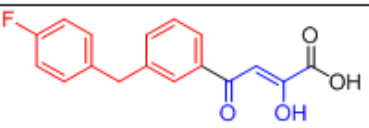
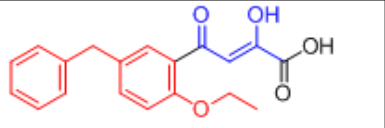
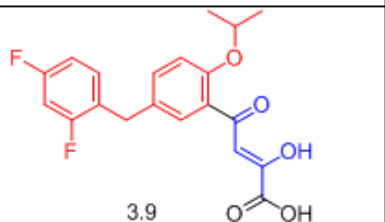
**Figure 3.13** Potent DKA ST inhibitors with Antiviral Activity. Aromatic substitutions highlighted in blue.



benzyl pyrrole (**L-731,988**)<sup>295</sup> or benzyl quinolone (**3.4**)<sup>292, 296</sup> demonstrate potent IN inhibition (<50 nM) with antiviral activity. However, compounds lacking a bulky aromatic group (Table 3.2) such as the indole derivative **5-CITEP** and phenyl containing DKA **3.5** did not show antiviral activity in cells even though they demonstrated potent ST inhibition.

In 2000, Wai *et al.* investigated

the SAR of a series of DKAs using **L-731,988** (Figure 3.13) as a lead molecule and replacing the central pyrrole ring with a series of aromatic systems.<sup>212</sup> This SAR study provided a series of potent 3-benzylphenyl DKA IN inhibitors (Table 3.2, compounds **3.6-3.8**) and revealed that by replacing the aromatic benzyl group with diphenylmethane or substituted diphenylmethane antiviral activity is significantly increased. For example, benzyl carboxylate **3.5** did not show any antiviral activity; however, when

Compound	ST IC <sub>50</sub> (μM)	CIC <sub>95</sub> (μM)
 5-CITEP	4	NONE
 3.5	5	NONE
 3.6	0.01	1.11
 3.7	0.01	0.69
 3.8	0.01	0.25
 3.9	0.01	0.05

**Table 3.2** SAR of Aromatic Substitution on β-DKA Scaffold

the aromatic group possesses an additional benzyl group (**3.6**) antiviral activity is observed.

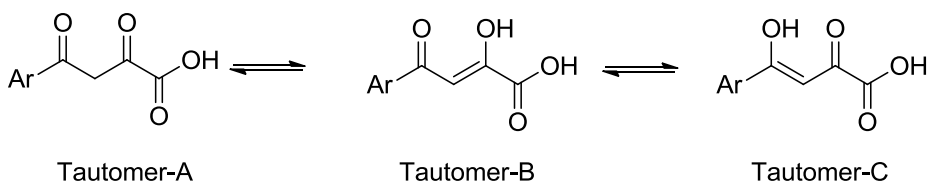
Furthermore, these compounds also show an increased selectivity for inhibition of ST reaction as

compared to 3'-P reaction and bind to IN only after viral DNA is bound.<sup>176, 284</sup> Substitutions on the phenyl and benzyl ring of diphenylmethane (**3.7-3.9**) further increase the antiviral activity of compounds to nM activity (**3.7-3.9**).<sup>212</sup> Compound **3.9** (2,4-difluoro-1-(4-isopropoxybenzyl)benzene) was synthesized and tested previously by our collaborators, Panvirex, LLC (*unpublished results*), lending a potent ST IN inhibitor that has better antiviral potency compared to the previously studied aromatic substituted series.<sup>212</sup> The mechanism of action of this series of compounds remains unknown but collectively, these studies suggest that the IN inhibitory potency is influenced by  $\beta$ -DKA motif of the molecule while the aryl substituents provide antiviral potency and ST specificity.

### 3.3.2. Keto-Enol Tautomerism of DKA IN Inhibitors

Several of the authentic IN inhibitors derived from the  $\beta$ -DKA class of compounds have multiple possible tautomers (Figure 3.14).<sup>297</sup> It is generally accepted that the  $\beta$ -DKA compounds exist most favorably in the tautomer-B form (Figure 3.14), which was noted as the most favorable

thermodynamic structure in the



inhibitor bound crystal

**Figure 3.14** Possible Tautomers of DKAs

structure (PDB:1QS4).<sup>211</sup> A lot of the early SAR work on the  $\beta$ -DKA compounds determined that the terminal carboxylate is involved in inhibitor binding and IN inhibition.<sup>217</sup> To date, developmental strategies for alternative heterocyclic structures assume that the  $\beta$ -diketo functional groups are essential in IN inhibitor design and functional groups of tautomer-B are retained in an empirical manner. Previous studies investigated by our collaborators (Panvirex,

LLC.) investigated the significance of the tautomeric state of the  $\beta$ -diketo functional groups. The diol derivative (**3.11**) of 3-benzylphenyl DKA (**3.6**) was synthesized and evaluated for ST inhibition. In the diol derivative (**3.11**) the carboxylate functional group involved in IN inhibition was retained and the diketo groups were converted into diols.

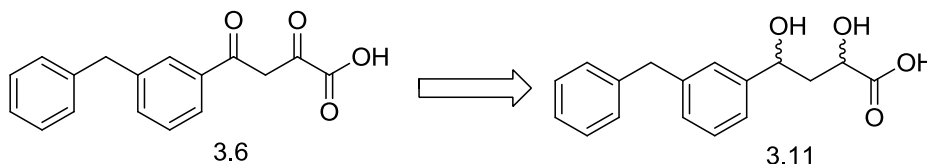


**Figure 3.15** Diol Derivative of DKA 3.6

The diol derivative is similar to the  $\beta$ -diketo compound **3.6** in the sense that contains all of the functional groups as they would be present in the tautomeric state. It was anticipated that the derivative would either demonstrate potent or moderate IN inhibition. Surprisingly, diol (**3.11**) was a poor inhibitor ( $IC_{50} >100 \mu M$ ), although it

Compound	Competitive Binding Assay ( $Mg^{2+}$ ) $IC_{50}$ , nM	Strand Transfer ( $Mg^{2+}$ ) $IC_{50}$ , nM
 L-731,988	15	50
 3.11	1, 120	>100,000
 3.12	3,590	>100,000
 3.13	590	>100,000
 3.14	>100,000	>100,000
 3.15	>100,000	>100,000

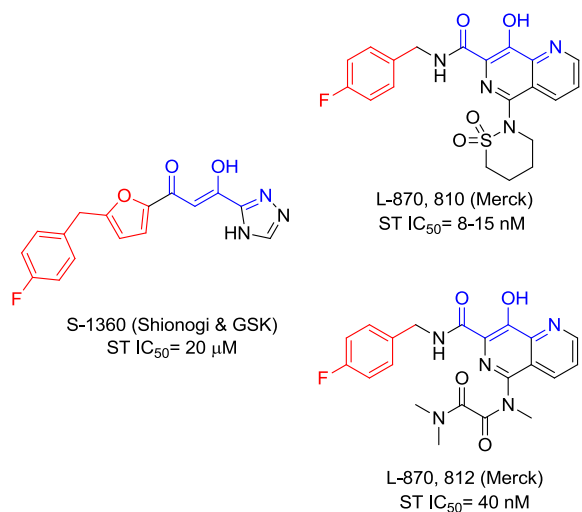
**Table 3.3** SAR of  $\beta$ -Diketo Compounds Lacking the Terminal Carboxylate

contained all of the functional group requirements of the DKA **3.6** (Panvirex, *unpublished data*). The lack of ST inhibition of **3.11** in conjunction with data from previously studied compounds containing the  $\beta$ -diketo functional group devoid of a terminal carboxylate (Table 3.3)<sup>217</sup>

collectively indicate that potent IN inhibition is influenced by the tautomeric state of  $\beta$ -diketo groups together with the terminal functional group. One of the consequences in loss of the enolic configuration of the  $\beta$ -diketo functional group is that the intermolecular interaction between the keto groups is likely disrupted resulting in a non-planar configuration of the functional motif. From this study, it was assumed that the planar geometry of the functional motif is essential in a potent IN inhibitor.

### 3.3.3. Aminocarboxylate: Alternative Surrogate for the $\beta$ -DK scaffold

Despite the success of selective ST inhibition, potency and antiviral activity of the  $\beta$ -DKA class of IN inhibitors several serious limitations in regards to the development of drug candidates exist. For example, the  $\beta$ -DKA class of compounds contains two reactive keto groups

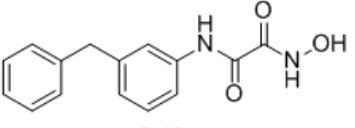
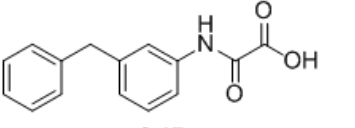
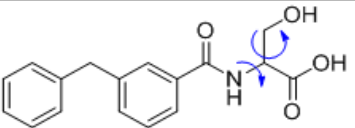
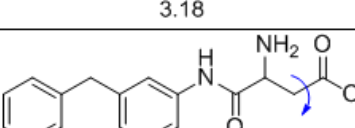
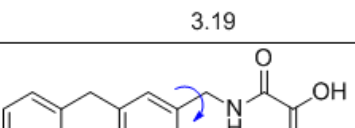


**Figure 3.16** Potent DKA IN Inhibitors

that react irreversibly with plasma proteins. The lead candidate **S-1360** failed Phase II clinical trials due to lack of efficacy resulting from 99% of the drug being bound irreversibly to plasma proteins.<sup>178</sup> Thus, compounds containing “druggable” characteristics while retaining the  $\beta$ -DK motif functional groups were explored with heterocyclic systems using the geometry of the  $\beta$ -DK motif. Using this approach, the  $\beta$ -DK characteristics were retained in the fused heterocyclic structures and evolution of the naphthyridine carboxamides (**L-870, 810** and **L-870,812**) led to potent ST inhibition and good antiviral potency. However, development of these compounds was suspended due to long-term cardiotoxicity in Phase II clinical trials.<sup>251</sup> Alternative suitable

surrogates to the reactive  $\beta$ -DKA functional group may overcome the pharmacological limitations of these compounds. To date, there have been no reports of a functional domain that can serve as a surrogate for the  $\beta$ -DKA motif of IN inhibitors.

The work described in this dissertation project is focused on the development novel HIV-1 IN inhibitors that contain an aminocarboxylate functional group to serve as a surrogate for the  $\beta$ -DKA functional motif. In the design towards a lead molecule several key findings discussed in

Compound	ST IC <sub>50</sub> ( $\mu$ M)
 <p>3.16</p>	0.19
 <p>3.17</p>	None
 <p>3.18</p>	>100
 <p>3.19</p>	>100
 <p>3.20</p>	>100

**Table 3.4** SAR of Aminocarboxylate Scaffolds

the preceding section were considered. The planar configuration of the functional domain was given high priority and less consideration was given to retaining the  $\beta$ -DK characteristics previously retained in the development of heterocyclic scaffolds (e.g., naphthyridine carboxamides, **L-870, 810** and **L-870,812**). Compound **L-708,810 (3.6)** was selected as the starting building block, since the aryl group, 3-benzylphenyl, does not contain any additional substitutions. In this regard, it was anticipated that the ST inhibition response would rely solely on the role of the aminocarboxylate functional groups under evaluation. Several compounds containing the aminocarboxylate functional group

the preceding section were considered. The planar configuration of the functional domain was given high priority and less consideration was given to retaining the  $\beta$ -DK characteristics previously retained in the development of heterocyclic scaffolds (e.g., naphthyridine carboxamides, **L-870, 810** and **L-870,812**). Compound **L-708,810 (3.6)** was selected as the starting building block, since the aryl group, 3-

(28 total compounds) were evaluated in an all or non-response ST inhibition assay by our collaborators and the results of a few closely related compounds are summarized in Table 3.4 (Panvirex, *unpublished results*). Among the various compounds analyzed, only **3.16** containing the oxalohydroxamate (OHA) motif showed potent ST inhibition, whereas all others were

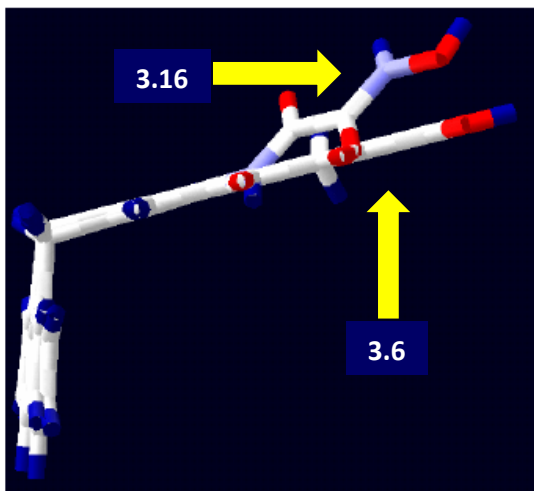


**Figure 3.17** Overlapping 3D Geometry of Compounds **3.6** and **3.16**. The compounds are overlaid on their 3-benzylphenyl aryl groups.

negative. From this SAR data, it was noted that the hydroxyl group of the terminal hydroxamic acid is critical to obtain potent ST inhibition.

Interestingly, compounds containing a terminal carboxylate (**3.17-3.20**), previously considered to be essential for binding affinity and potent IN inhibition,<sup>217</sup> did not show IN inhibition (Table 3.4). In the serine amide derivative **3.18**, the assumed  $\alpha$ -keto group of the  $\beta$ -diketo motif hydroxyl (tautomer-B) is one carbon length

away from its normal position. In the glycine amide **3.19** and oxalamic acid containing compound **3.20**, all of the functional groups are present yet no IN inhibition was observed. It can be considered that the lack of IN inhibition shown from these compounds is a result of deviation of the functional motif from the planar configuration due to the free rotational bond (Table 3.4, highlighted with blue arrows). Such assumption is further supported by the observation that diol **3.11** containing all of the groups of the functional motif also did not show inhibition of IN. However, the requirement of the planar geometry of the functional group is not absolute as it is previously assumed in the inhibitor. The 3-benzylphenyl aryl group of **3.16** distorts the functional domain from the absolute planarity of the prototypical  $\beta$ -DKA inhibitor **3.6** or as in

the naphthyridine carboxamides (**L-870, 810** and **L-870,812**) as illustrated by the overlapping geometry in Figure 3.17. The moderate deviation appears to be tolerable without losing the potent IN inhibitor characteristics. Collectively, the structural observations of the OHA motif containing compounds suggests that the isosteric functional group of the  $\beta$ -diketo motif in moderate planar configuration (**3.16**) is sufficient for IN inhibition but significant deviation from planar or near planar configuration abolishes IN inhibitory potency (Table 3.4).

### 3.3.4. Ligand Docking of Aminocarboxylate IN Inhibitors

Although the chelation model (Figure 3.12) of ST inhibition by the  $\beta$ -DKA class of compounds has been widely accepted as a plausible mechanism of IN inhibition several studies have surfaced, based largely on SAR and IN crystal structure studies, prompting investigators to revisit the proposed mechanisms of inhibition. In previous studies, the  $\beta$ -DKA **3.6** has demonstrated progressive drug resistant viral mutations beginning at T66I and it is followed with concomitant mutations of either amino residues S153Y, M154I or N155S.<sup>175</sup> The T66I mutation alone is significant enough to render IN inhibitors less effective. Studies have also shown that the tetrazole  $\beta$ -diketo isoster, **5-CITEP** (Figure 3.7), and carboxylate  $\beta$ -DKA, **L-731,988** (Figure 3.10), although having different aryl groups are ineffective to the same drug mutations (T66I/M154I) in IN.<sup>211, 217</sup> These findings suggest that regardless of the aryl and terminal functional groups (tetrazole or carboxylate) present in the  $\beta$ -DKA molecule, the compounds appear to bind at the same site. Interestingly, the drug resistant mutations described above are in the vicinity of the tetrazole terminal functional group of **5-CITEP** bound in the IN CCD and are located 180° opposite to the Mg<sup>2+</sup> ion bound to the catalytic residues D64 and D116.<sup>211</sup> In the chelation model, compound 5-CITEP should bind in an opposite orientation compared to the

orientation observed when bound in the IN CCD crystal structure (PDB: 1QS4). Also, the aryl group should contact the IN residues that undergo drug resistance mutations and the  $\beta$ -diketo functional groups should interact with the  $Mg^{2+}$  metal ions. It was suggested that the drug resistance mutations are capable of causing distortion of the molecule and result in loss of interaction with the  $Mg^{2+}$  ions. The inhibitor binding site has adequate room and compounds can be easily docked without steric hindrance in support of the chelation model and manual docking is sometimes utilized to demonstrate the likely scenario of metal ion chelation.<sup>225</sup> Alternatively, since compounds containing both tetrazole and carboxylate terminal functional groups and are resistant to the same mutations, it is also possible that the binding orientation is the same. In collaboration with Panvirex, molecular docking studies were carried out to investigate the mechanism of IN inhibition. Ultimately, clarity of the binding orientation of  $\beta$ -DKA class of compounds is essential to aid in the elucidation of the role of the terminal functional groups of the novel aminocarboxylate IN inhibitors and lead to the design of novel IN inhibitors.

The structural similarities between **5-CITEP** and **3.5** (Table 3.2) and the availability of 5-CITEP bound IN crystal structure provide an opportunity to understand the role of the terminal functional group interactions. In collaboration with Panvirex, molecular docking experiments were carried out in rigid ligand conformation since the planar or near planar configuration of the inhibitors was discovered essential in our previous SAR studies (Table 3.4 and diol derivative **3.11**). In all of the docking experiments, the 5-CITEP bound region was chosen as the inhibitor binding site. The validity of the ligand docking was established by our collaborators by comparing the orientation and geometry of our docking of 5-CITEP to the previously reported 5-CITEP bound IN crystal structure. From this comparison it was determined that the structural interactions are essentially the same as previously reported in the crystal structure.<sup>211</sup> The major



focus of our docking studies is the hydrogen bonding interactions of the terminal functional group and the binding orientation of the inhibitors.

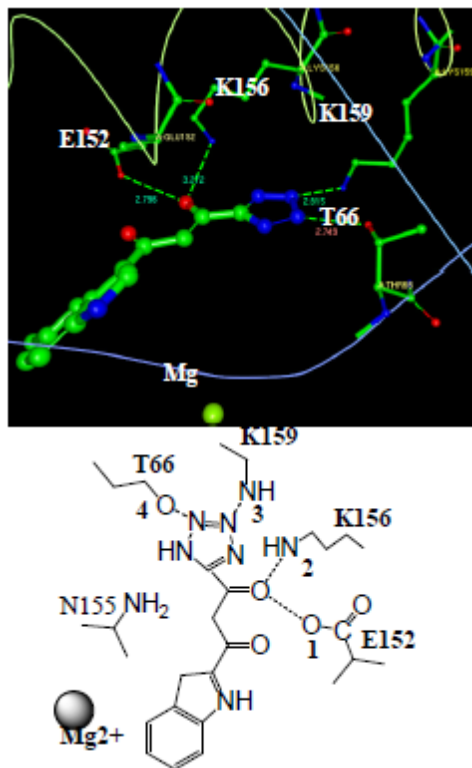


**Figure 3.18** Analysis of 5-CITEP bound in IN Crystal Structure (1QS4).

In the initial analysis of 5-CITEP bound IN crystal structure all of the possible interactions of 5-CITEP were mentioned. However, analysis of the crystal structure in Ligand Explorer<sup>298</sup> within the hydrogen bonding threshold (3.3Å) with all of the residues including the water molecules that are present in the IN crystal structure suggest that the tetrazole functional can only form two hydrogen bonds with T66 and K159. The enolic  $\alpha$ -keto group provides hydrogen bond interactions with E-152 carbonyl and K156 side chain nitrogen (Figure 3.18). The interaction of the  $\alpha$ -keto group is not mentioned in the initial docking studies of 5-CITEP. The only possible

interaction of the  $\gamma$ -keto group is with a water molecule which is about 5Å distance away. There

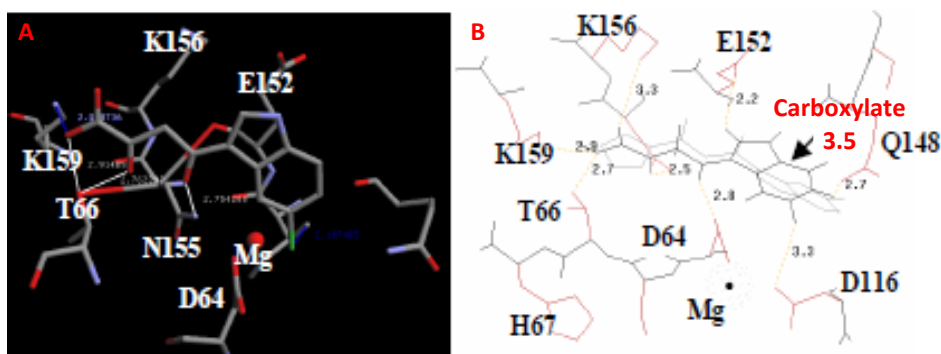


**Figure 3.19** Binding of the Carboxylate Derivative of 5-CITEP (3.5) (A) The flipped orientation binding of 3.5 in ligand docking (B) The hydrogen bonding interactions of 3.5.

were no hydrogen bond interactions noted with the nitrogen atoms of the tetrazole or indole although they can interact electrostatically with the nearby N155 and Q148 (Figure 3.18). In contrast, the carboxylate derivative of 5-CITEP (**3.5**) binds in a flipped orientation in the ligand docking but the carboxylate terminal functional group interacts with the same IN amino acid residues as that of the tetrazole (Figure 3.19A). The acid carbonyl oxygen of the carboxylate can form two bonds between the side chains of K159 and T66. The carbonyl oxygen of the carboxylate interacts with K156. In the flipped orientation the  $\alpha$ -keto functional group of **3.5** interacts with N155 (Figure 3.19B). The interaction between E152 and the  $\alpha$ -keto functional group of **3.5** is lost in the flipped configuration. However, the interaction of E152 is regained by the hydrogen atom or nitrogen atom of the indole ring. The  $\gamma$ -keto group is within hydrogen bonding distances with the D64 carbonyl but the carbonyl-carbonyl interactions are considered unlikely. The aryl group is flanked by the region occupied by E152, D64, D116 and Q148 and is within hydrogen bonding distances. In the ligand docking studies the compounds are in rigid conformation but the aryl group is expected to undergo some degree of rotation following enzyme binding as observed in the crystal structure bound 5-CITEP (Figure 3.20) and optimal interactions with any one of the residues is possible.

The binding orientations of the tetrazole containing S-1360 and the carboxylate containing compound L-731, 988 having different aryl groups were also compared (Figure 3.21). These compounds bind essentially in the same orientation as observed with 5-CITEP and the interactions with the functional motifs were essentially identical. The tetrazole group of S-1360 interacts with T66, K156 and K159 (Figure 3.21B) as

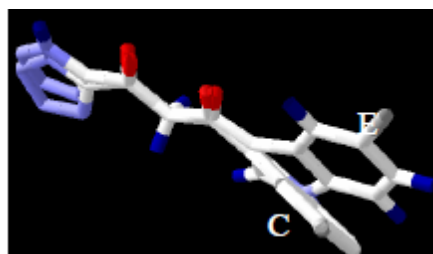
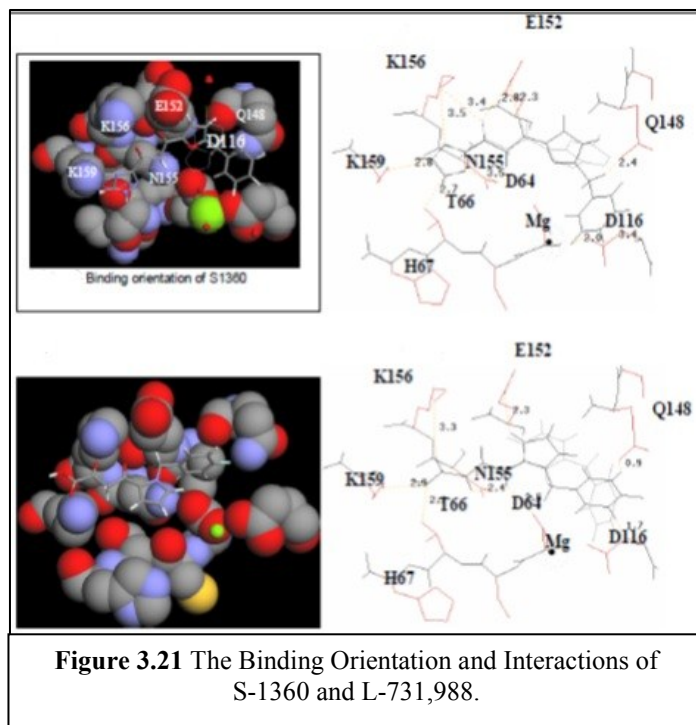


**Figure 3.20** The Overlapping Geometry of Crystal Structure Bound 5-CITEP (C) and Energy Minimized Structure (E)

seen previously with 5-CITEP and L-731,988. The terminal functional group interactions of L-731,988 is essentially the same with coordination to K159 and T66 with the acid carbonyl of the

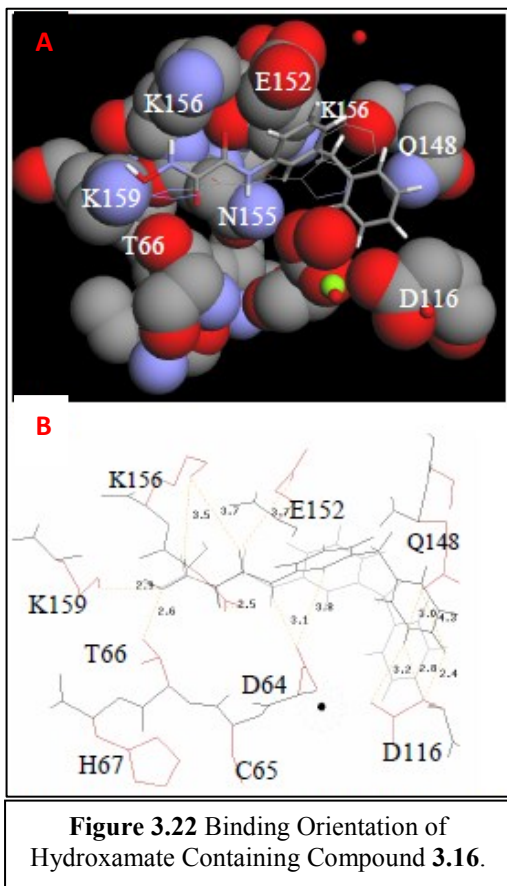
carboxylate interacting with N155

(Figure 3.21D).



The potent ST inhibition exhibited with hydroxamate containing **3.16** and complete loss of ST inhibition with closely related **3.17** (Table 3.4), lacking the hydroxamate terminal functional group, provides an opportunity to assess how the ST inhibition potential of an IN inhibitor is attained by docking the compounds in

the crystal structure and comparing the interactions. The compounds containing the OHA motif bind in the 5-CITEP binding direction but in a flipped orientation similar to the carboxylate derivative of 5-CITEP (**3.5**). In this configuration, the hydroxamate is centrally located between K156, K159 and T66 but only K159 and T66 residues can interact with the hydroxyl group (Figure 3.22B). The K156 is located 4.5Å from the nitrogen atom and 3.5Å from the hydrogen atom of the hydroxamate. The oxamate carbonyl in the *trans* position can interact with N155 as that of the carboxylate in the  $\beta$ -DK motif. The aryl group of **3.16** is in proximity of the D64, D116, E152 and Q148 residues (Figure 3.22B).



In this configuration it is easy to understand why **3.17**, a compound lacking a hydroxamic acid group, did not show IN inhibition. Compound **3.17** binds in the same configuration as that of **3.16** but the hydroxyl group of **3.17** did not have any interactions with K159 or T66. Moreover, the hydroxyl group of hydroxamate of **3.16** provides optimal hydrogen bonding interactions with K159 and T66. Thus, it is assumed that minimal terminal functional group interactions with T66 and K159 may be considered as the defining parameters of gain or loss of IN inhibition. This observation is supported by the consistent interactions of both the carboxylate and

tetrazole terminal functional group with K159 and T66. The interactions with K156 and N155 and all of the other interactions may be necessary for inhibitor binding. The binding orientation of **3.21** containing an aryl group with substitutions (2, 4-difluoro-1-(4-isopropoxybenzyl) benzene, Figure 3.23) is comparable to the orientation observed in the core compound **3.16**.

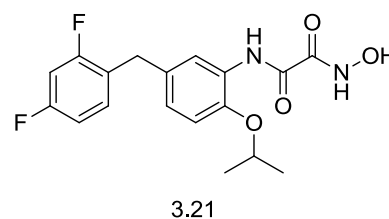


**Figure 3.23** Hydroxamate **3.21** with Substituted Aryl Group.

The hydroxamate terminal group of **3.21** also interacts with K159 and T66 and the oxamate carbonyl interacts with N155. The benzyl functional group occupies the position between D64 and D116 and the isopropoxy of the phenyl ring occupies the region surrounded by K156, E152 and Q158 (Figure 3.24).

Ligand docking in the absence of DNA bound IN crystal structure has its limitations. However, it can provide insight towards the preferred orientation of compound binding. Although, the binding configurations of various compounds are different, the terminal functional group interactions with K159 and T66 are consistently noticed. Also, as previously mentioned, several of the  $\beta$ -DKA inhibitors are rendered ineffective when there is a mutation at T66I.

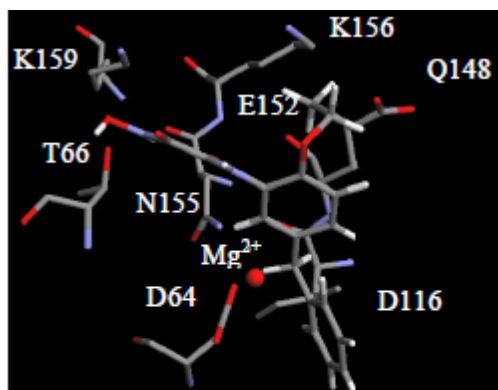


**Figure 3.24** Binding Orientation of 3.21. E152, Q148 and D116 are not shown for clarity but locations are indicated.

The similarity of these compounds to interact with T66 suggests that the terminal functional group interaction with T66 together with K159 prevents ST reactions. The progressive N155S mutation encountered together with T66I as originally observed in the early carboxylate containing compounds<sup>175</sup> and the interactions of the functional domains with these residues suggest selective evolutionary pressure to undergo drug resistance. Additional interactions contributed by the diketo or oxamate functional domain with K156 or N155 along with E152 and aryl group interactions with D64, D116 and Q148 can provide better binding affinity. These ligand docking studies are more aligned with the proposed biochemical mechanism<sup>211</sup> of IN inhibition compared to the proposed chelation model<sup>217</sup> of IN inhibition.

Studies indicate that the mutations of K156 or K159 impair DNA binding and mutation of either of these amino acid residues is lethal to HIV-1 virus.<sup>280, 299</sup> In the IN crystal structure (PDB: 1K6Y) phosphate ion binding is observed between T66, H67 and C65 residues. The preferential interactions of these amino acids with a phosphate ion led to the assumption that these amino acid residues contact the phosphate backbone in DNA.<sup>281</sup> The K156 and K159 bind equally to both viral LTR end and host DNA. However, photo-cross-linking with the viral DNA

end shows specific interaction of K159 and K156 with viral adenine<sup>280</sup> adjacent to the scissile phosphate of the CA dinucleotide at the 3'-end of the strand that undergoes 3'-processing reaction. Based on this observation it was proposed that the K156 and K159 are involved in viral DNA binding<sup>280</sup> and the phosphate ion in the crystal structure (PDB: 1K6Y) could represent the viral DNA.<sup>281</sup> In this context, 5-CITEP inhibitor bound crystal structure (PDB:1QS4) was superimposed with the phosphate ion bound IN structure (PDB: 1K6Y) to obtain a spatial configuration of inhibitor interactions. Superimposed structures indicate juxtaposed position of the inhibitor terminal residue with phosphate ion indicating that the site of viral DNA interaction and inhibitor terminal functional group is the same (Figure 3.25). The superimposed crystal structures docked with the 5-LTR end double-stranded DNA (dsDNA) phosphate backbone on the phosphate ion of the phosphate ion bound IN structure (PDB: 1K6Y) suggests that the inhibitor binding site spans between the binding sites of the two strands. Interestingly, the terminal functional group of the inhibitor and the DNA phosphate backbone of 3'-P strand cross at T66 and K159. The scissile phosphate 5'-to the GT dinucleotide that undergoes 3'-P is exactly

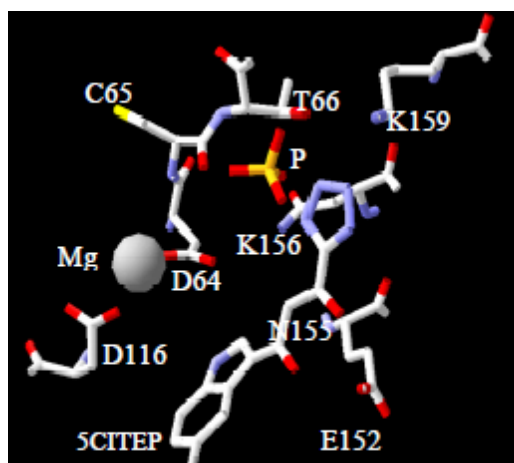


**Figure 3.25** Superimposed 5-CITEP inhibitor bound crystal structure (1QS4) and the phosphate ion bound IN structure (1K6Y).

on the catalytic site at the  $Mg^{2+}$  ion (Figure 3.26 arrow). It is observed in the docking study that the dsDNA confirmation is essential and it is consistent with the observation that single-stranded DNA (ssDNA) fail to bind to IN. The DNA sugar residue of the strand that undergoes 3'-P contact the K159 and its complementary strand sugar residues contact K156, E152, S157 and Q148. Studies have shown that the CA dinucleotide overhang of the complementary strand of the viral DNA that undergoes the 3'-P (T66 and K159 binding strand) forms a stable complex with Q148<sup>204</sup> and mutation of Q148I abolishes viral DNA binding.<sup>279</sup> From this study, it is indicated that the inhibitor terminal functional group interactions between T66, K156 and K159 and the aryl moiety is likely to interact with the Q148 and the viral DNA bridges the viral LTR end and prevents them from undergoing the ST reaction. Goldgur *et al.* proposed that the inhibitor may bind between the unstacked bases mimicking DNA substrate interactions.<sup>211</sup> This view is consistent with the model (Figure 3.26) and the inhibitor functional motif is wedged between the bases of the two strands and the aryl group occupies the position in which the viral DNA bases undergo unstacking during the 3'-P reaction. It is apparent that the rigid conformation of the

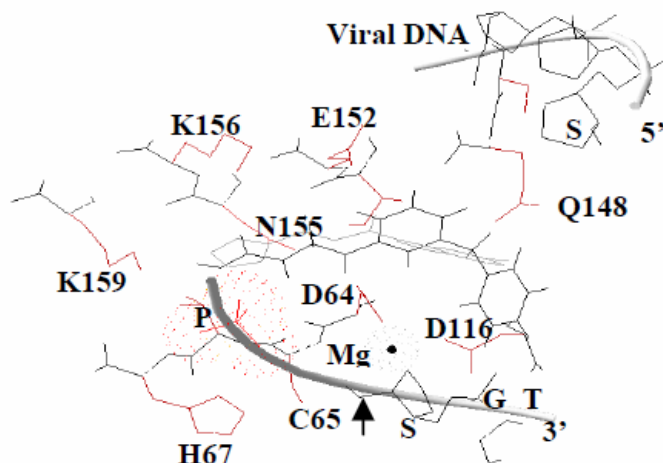


**Figure 3.26** Superimposed DNA Phosphate Backbone of dsDNA (1K6Y) with 1QS4. The orientation of 3.16 docked in the 5-CITEP binding site is shown. P:phosphate ion of 1K6Y and DNA; S: Sugar Residue in DNA; Arrow: scissile phosphate; GT: nucleotides

inhibitors is essential for wedging between the bases.

It has been reported in the literature that the  $\beta$ -DK inhibitors should be considered as “interfacial inhibitors” because they interfere with host DNA binding.<sup>86</sup> The structure based analysis of SAR functions of various compounds is in agreement with the view of interfacial inhibitors and provides a molecular mechanism of interaction. In comparing the interactions of the terminal functional groups, only the carboxylate containing compounds additionally interacts with N155 as compared to the tetrazole containing inhibitor (Table 3.5). In the OHA containing inhibitors, the oxamate is shown to interact with residue N155; however, there is not a noticeable interaction of the hydroxamate with K156. The interaction of the oxamate carbonyl with N155 suggests that the addition of a suitable terminal functional group can provide interaction with K156 which is likely missing from the hydroxamate functional group.

	T66	E152	K156	K159	N155	# of bonds
$\beta$ -DK carboxylate	+	+	+	+	+	5
$\beta$ -DK tetrazole	+	+	+	+	-	4
OHA	+	+	-	+	+	4

**Table 3.5** Summary of Hydrogen Bond Interactions with  $\beta$ -BK and OHA Terminal Functional Groups

### 3.3.5. Design of the Oxalamate IN inhibitors: Isosteric Replacement of the Hydroxamate

Crystal structure based correlation of SAR studies indicate that the IN inhibitor interactions are essentially acid-base interactions. One of the major focuses of this project is to investigate the role of the terminal functional group interactions with the amino acid residues of IN. The design of the target molecules is envisioned to contain three specific functional groups. Each molecule is designed to contain the core functional motif ( $\alpha$ ,  $\beta$ -diketoamide), optimal aryl groups (3-benzylphenyl or substituted 3-benzylphenyl) and a terminal group (proton donor or acceptor or amphoteric functional groups) in a planar or near planar configuration (Figure 3.27).



The molecular docking studies on the OHA motif completed in collaboration with Panvirex have led to the identification of an oxamate serving as a suitable surrogate for the  $\beta$ -DK functional group. The tetrazole and pyridine were identified as carboxylate isosters in the  $\beta$ -DK class of compounds and the OHA motif studies indicate that the hydroxamate can also serve as an isosteric replacement. It is likely that the tetrazole and pyridine can also function as a hydroxamate isoster in the oxamate scaffold. In addition, various terminal functional groups will be investigated for their potential to serve as isosteric replacements of the hydroxamate and the interactions with the IN amino acids can be determined.

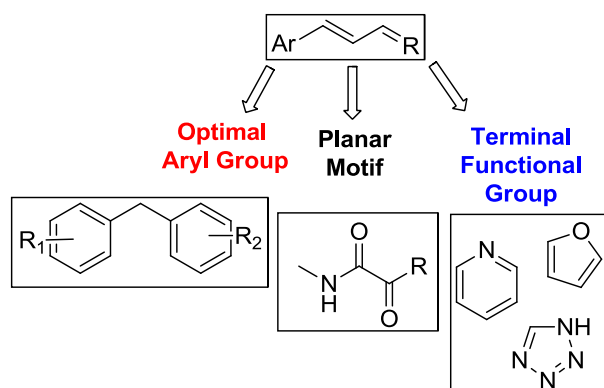


**Figure 3.27** General SAR of Designed Oxalamate Scaffolds

### 3.3.6. SAR of the Terminal Functional Groups of the Oxalamate Scaffolds

The oxalamate derivatives to be investigated and synthesized can be classified in three groups (A-C) based upon the expected interactions of the terminal functional groups with the HIV-1 IN binding site (Figure 3.28). The group A terminal functional groups are expected to

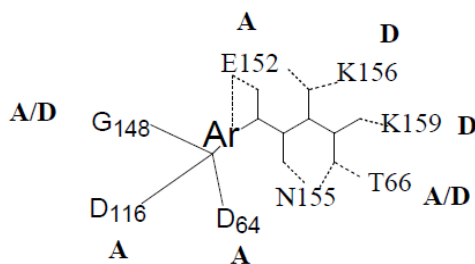
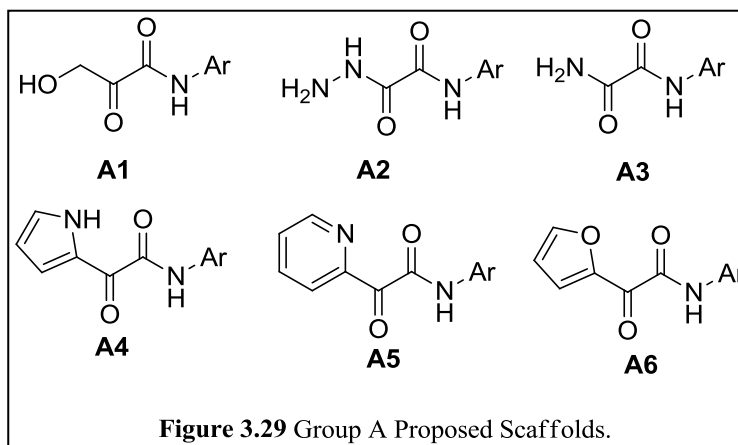


**Figure 3.28** The interactions of  $\beta$ -DK class of IN inhibitors with IN amino acids and their donor (D) and acceptor (A) functions.

have the same interactions as the hydroxamate (Figure 3.29). While the position of the terminal amine of **A2** is similar to that of

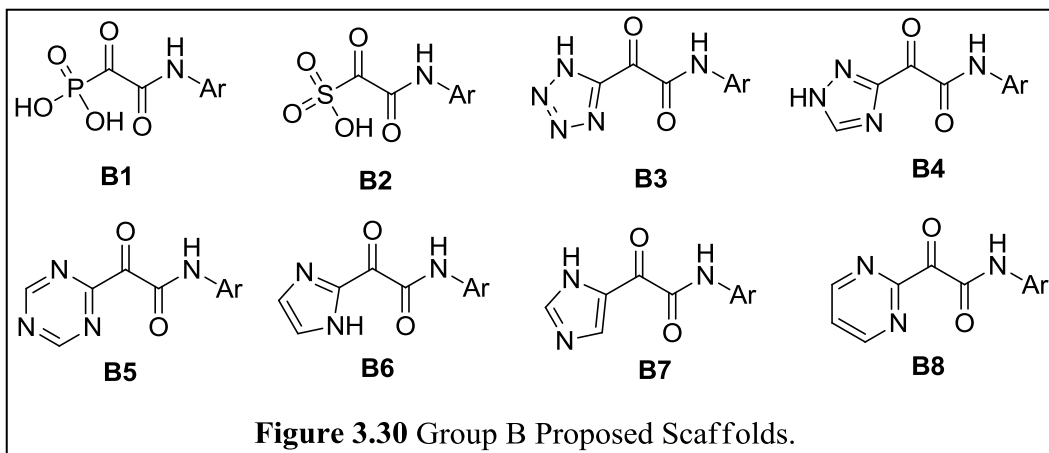
hydroxamate **3.16**, the terminal amine of **A3** is one carbon shorter.

Compound **A3** is expected to have potential electrostatic interactions with T66 and K159. The group B compounds **B1** and **B2** (Figure

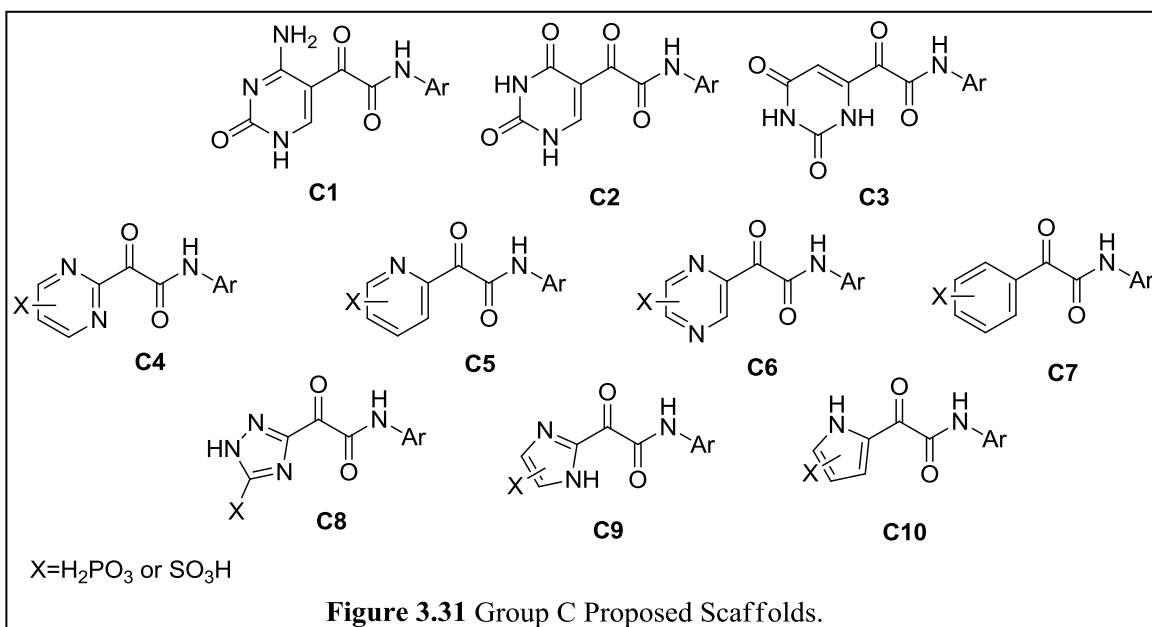


3.30) contain a phosphate or sulfate functional group and due to the position of the terminal functional group interaction is expected with the phosphate ion binding residue (Figure 3.25).

The interactions of **B1-B5** are expected to be similar to the carboxylate or tetrazole interactions with T66, K159 and K156. Additional interactions that are absent in the group A compounds are expected from the imidazole derivatives (**B6** and **B7**) and the pyrimidine derivative (**B8**). The group C compounds (Figure 3.31) are of interest because the terminal functional groups cytosine and uracil (**C1-C3**) of these compounds are expected to provide interactions. In biochemical studies of viral LTR interaction uracil was found to interact with K156 and K159.<sup>280</sup> The carbonyl atom of the nucleotide and the phosphate or sulfate substituted in the pyrimidine (**C4**), pyridine (**C5**), pyrazine (**C6**), triazole (**C8**) and imidazole (**C9** and **C10**) can coordinate additionally to the H67 and the amide nitrogen of the H67-T66 peptide bond. Ligand docking with phosphate substituted imidazole in the oxamate motif of **C9** containing the aryl group **Ar-1** (Figure 3.33) shows interactions with H67, T66, K156, K159, N155, and E152 (Figure 3.32). The phosphate of **C9** interacts with backbone carbonyl of H67, the peptide bond nitrogen and hydroxyl group of T66.



The compounds from the three groups (A-C) will be synthesized in phases. For the initial evaluation of the various terminal functional groups, the compounds that will be synthesized will contain the **Ar-1** aryl scaffold (Figure 3.33). The response of these compounds will be a direct reflection of the terminal functional group under evaluation. The compounds that demonstrate potent ST inhibition (<500 nM) will have the substituted aryl scaffold (**Ar-2**) incorporated in place of **Ar-1**, which was determined to be necessary for potent antiviral activity (Table 3.2, 3.9).



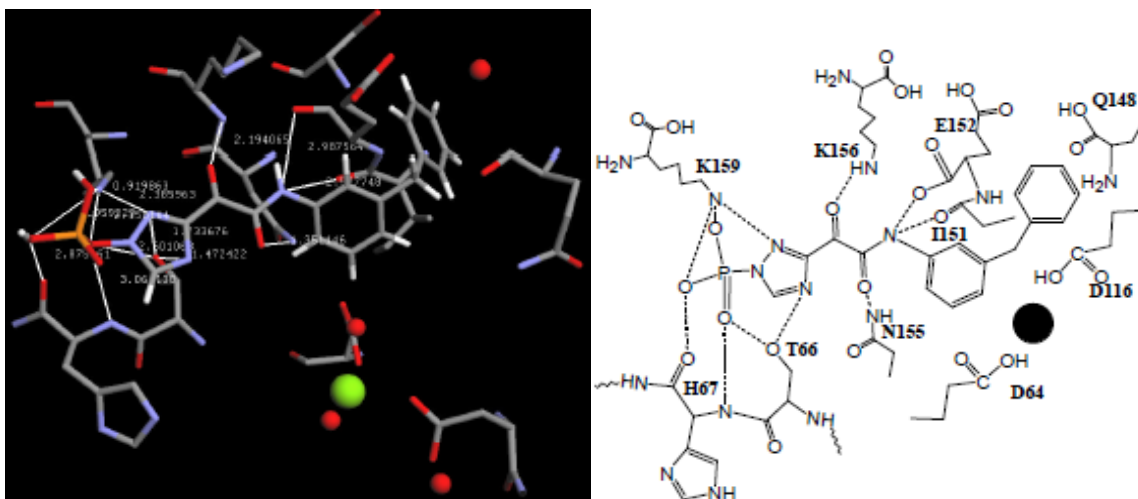


**Figure 3.32** The Ligand Docking Analysis of **C9** (**Ar-1** Aryl Group)

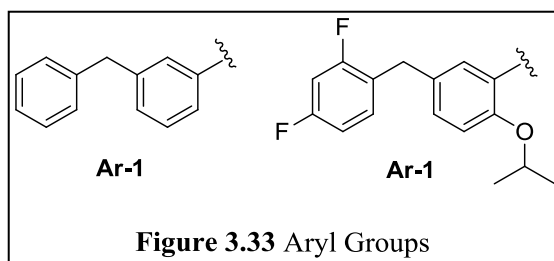
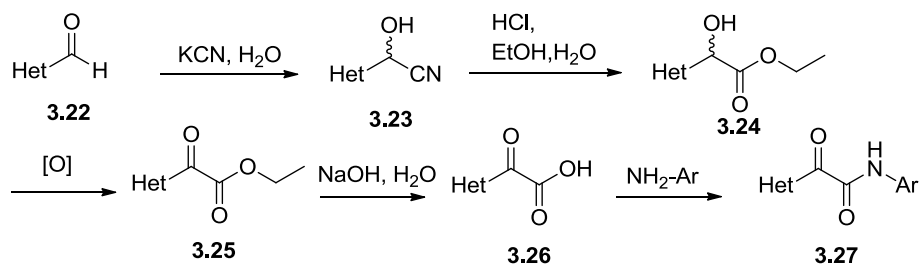


**Figure 3.33** Aryl Groups

### 3.4 SYNTHETIC APPROACHES

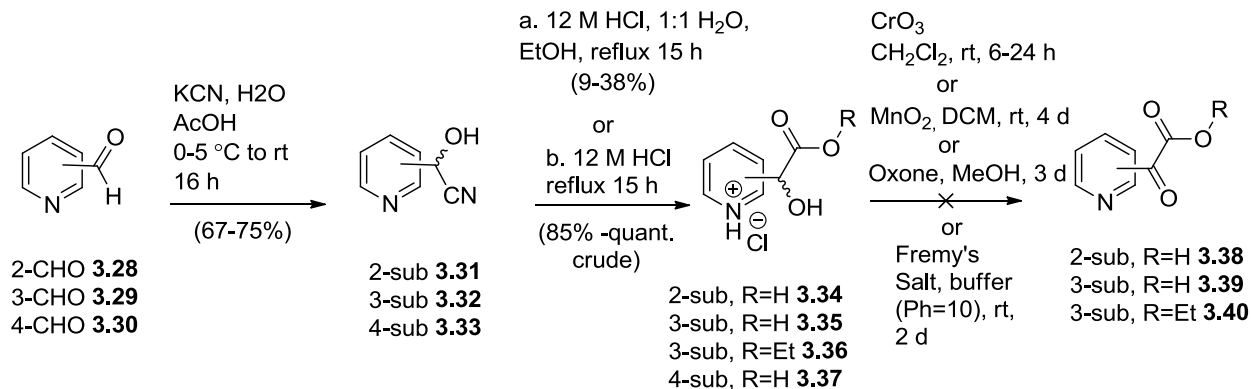
#### 3.4.1. Heteroaromatic $\alpha$ -Oxoacetic Acids: Cyanohydrin Chemistry

At the onset of this project we began to focus our attention on the synthesis of the several of the heteroaromatic  $\alpha$ -oxoacetic acids. It was envisioned that several of these compounds could be obtained through cyanohydrin chemistry as proposed in Scheme 3.1. In general, commercially available heteroaromatic aldehydes (**3.22**) could be synthesized into corresponding cyanohydrins (**3.23**)<sup>300, 301</sup> followed by hydrolysis of the cyanohydrin to obtain the  $\alpha$ -hydroxy esters (**3.24**).<sup>302</sup> The  $\alpha$ -hydroxy esters could then be oxidized<sup>303</sup> to obtain the  $\alpha,\beta$ -diketo derivatives (**3.25**) that could then undergo ester hydrolysis<sup>304, 305</sup> to afford the desired  $\alpha$ -oxoacetic acids (**3.26**). With



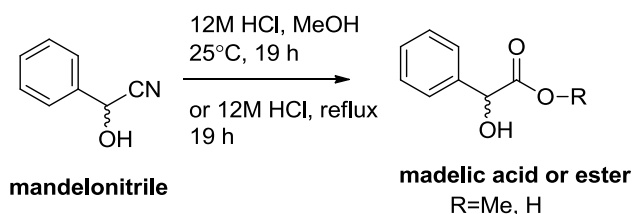
**Scheme 3.1** Proposed route for the synthesis of heteroaromatic oxalamate derivatives access to the  $\alpha$ -oxoacetic acids the final compounds (**3.27**) could easily be made utilizing amide coupling conditions with desired aniline aryl scaffolds.<sup>306</sup>

Of particular interest was the synthesis of the 2-, 3-, and 4-pyridine heterocyclic scaffolds. The availability of the pyridine carboxaldehydes and inexpensive reagents and solvents made this an attractive route for synthesizing the pyridine series of compounds (Scheme 3.2). Sequential addition of potassium cyanide in water and acetic acid to the 2-, 3-, or 4-pyridine carboxaldehyde (**3.28**, **3.29** or **3.30**) afforded the corresponding racemic cyanohydrin (**3.31**, **3.32** or **3.33**).<sup>300</sup> Cyanohydrins are well-documented as unstable and under basic conditions they can be converted back to the carbonyl compound or racemize through reversible loss of hydrogen cyanide (HCN).<sup>307</sup> Therefore, it was necessary to proceed forward to the next reaction step, hydrolysis of the cyanohydrins, immediately following cyanohydrin isolation. The initial procedure (Scheme 3.2, method a) attempted for the hydrolysis of cyanohydrin derivatives



**Scheme 3.2.** Synthesis of 2-, 3- and 4- pyridine oxalamate derivatives

(**3.31-3.33**) was a method reported for the acid-catalyzed hydrolysis of mandelonitrile, the cyanohydrin of benzaldehyde, to obtain mandelic acid or the  $\alpha$ -hydroxy ester (Scheme 3.3).<sup>302</sup> Although, hydrolysis of the cyanohydrins (**3.31-3.33**) did occur there were several issues with isolating the desired  $\alpha$ -hydroxy acid and ester products (**3.34-3.37**) and yields were much lower than anticipated (9-38% yield). This was due primarily as a consequence of working with a heteroaromatic (pyridine) scaffold with acid/base properties and trying to adapt a procedure used for the synthesis of an aryl aromatic scaffold. In order to move the synthesis forward with optimal yields it was necessary to try and obtain a reaction procedure that included compounds possessing similar chemical properties as to the heteroaromatic scaffolds. Also, any examples found in the literature would allow us to gain an understanding on efficient work-up procedures and product isolation techniques for our heteroaromatic scaffolds, which had previously been our limiting factor. To our delight, a procedure from a 1986 patent was found for the synthesis of pyrid-3-yl-hydroxyacetic acid (**3.35**) from the corresponding pyrid-3-yl cyanohydrin (**3.32**) (Scheme 3.2, method b).<sup>308</sup> The  $\alpha$ -hydroxyacetic acids (**3.34**, **3.35** and **3.37**) were obtained by refluxing the corresponding cyanohydrin in concentrated hydrochloric acid (HCl). Instead of isolating compounds using an acid/base work-up, as previously utilized,<sup>302</sup> after reaction completion (monitored by mass spectrometry (MS)) the HCl was removed and products were simply obtained as pyridium chloride salts (**3.34-3.37**). Although, MS product peaks were



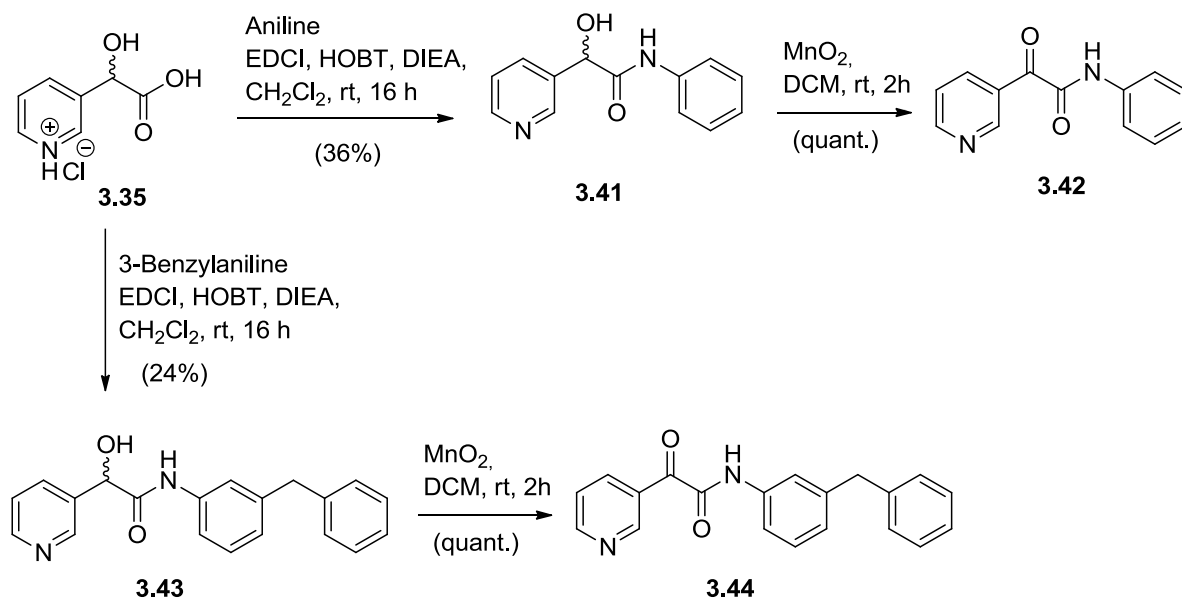
**Scheme 3.3.** General procedure for the hydrolysis of mandelonitrile

identified for all three isomers (**3.34**, **3.35** and **3.37**) the NMR for the pyrid-4-yl-hydroxyacetic acid (**3.37**) remains unclear, possibly due to

impurities from the crude product, therefore, only the 2- and 3- derivatives (**3.34** and **3.35**) were

carried forward in the synthesis. In addition to obtaining the  $\alpha$ -hydroxyacetic acids (**3.34** and **3.35**), the procedure was easily modified by adding ethanol as a solvent and obtaining the ethyl ester products. Only ethyl pyrid-3-ylhydroxyacetate (**3.36**) was successfully obtained using this method. With the  $\alpha$ -hydroxyacetic acids (**3.34** and **3.35**) or ester (**3.37**) in hand, the next logical step in our linear sequence was to oxidize the  $\alpha$ -hydroxy to the  $\alpha$ -keto acid or ester (**3.25**). Oxidative conditions using Collins reagent,<sup>303</sup> Oxone,<sup>309</sup> Fremy's salt,<sup>310</sup> and manganese dioxide<sup>311</sup> proved unsuccessful for the conversion of the  $\alpha$ -hydroxyacetic acids (**3.34**, **3.35** and **3.36**) to  $\alpha$ ,  $\beta$ -diketones. The unsuccessful attempts for this conversion is assumed to be a result of reactivity issues with the pyridine series of compounds as well as solubility issues with the starting  $\alpha$ -hydroxy compounds.

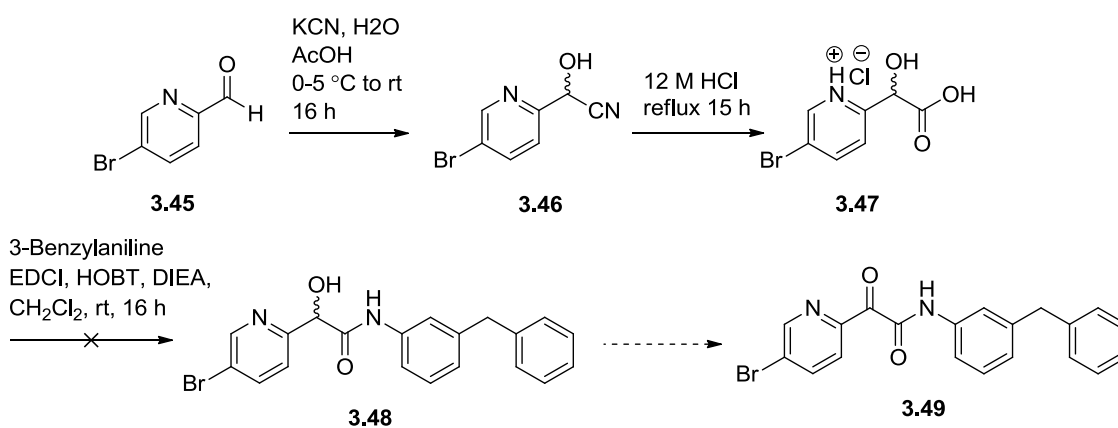
An alternative route was required to obtain the desired oxoacetic acids. It was hypothesized that a reasonable step to proceed forward was to first complete the amide coupling reaction with  $\alpha$ -hydroxyacetic **3.35** and aniline to obtain **3.43** (Scheme 3.3). Once **3.43** was synthesized attempts to oxidize the  $\alpha$ -hydroxy to ketone and provide **3.44** could be easily



**Scheme 3.4.** Oxidation of 3-pyridine  $\alpha$ -hydroxy derivatives

pursued. There were several advantages to using this route, the  $\alpha$ -hydroxyacetic acids could be used as their pyridinium chloride salts and the terminal carboxylic acid functional group would be removed and replaced by the amide bond and therefore solubility issues may be dealt with. Also, unlike the  $\alpha$ -hydroxyacetic acids, compounds **3.41** and **3.43** could be easily purified by column chromatography. Initially, these reactions were rehearsed with aniline and once validated a practical approach to the reaction was then performed with 3-benzylaniline, primarily due to cost factors (3-benzylaniline 1g=\$49.00; aniline 1g=\$0.03). The reactions were conducted on both the 2- and 3-pyridine series of compounds; however, the 2-pyridine oxamide was not successfully isolated from the reaction mixture. The amide coupling of pyrid-3-yl-hydroxyacetic acid (**3.35**) and aniline or benzylaniline was completed with ease using standard amide coupling conditions to obtain **3.41** and **3.43**, respectively.<sup>306</sup> To our delight, a recent publication utilizing MnO<sub>2</sub> as the oxidant for  $\alpha$ -hydroxyacetic amides to oxamides was identified which led to the successful synthesis of **3.42** and **3.44** (Scheme 3.3).<sup>312</sup>

Once this route was determined to be feasible to obtain the desired oxamide **3.44** for the pyridine series of compounds it was of interest to explore other heteroaromatic scaffolds using

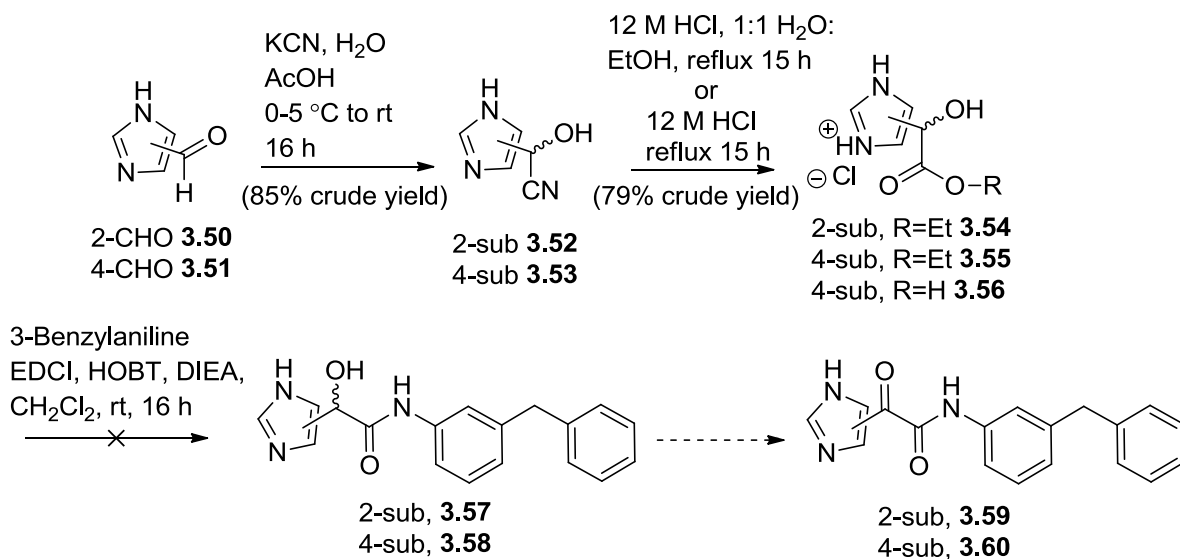


**Scheme 3.5** Synthesis of 5-Bromopyridine-2-oxalamate **3.49**



the same methodology. Starting with 5-bromo-2-carbaldehyde we employed the same reaction conditions as previously noted in Scheme 3.5. The reactions proceeded forward smoothly until the amide bond formation between  $\alpha$ -hydroxyacetic acid (**3.47**) and 3-benzylaniline.<sup>306</sup> Although it had appeared as if product had formed by monitoring the reaction with MS analysis, column chromatography purification and isolation of all products from the reaction mixture demonstrated that the production of **3.48** was unsuccessful. The reaction was repeated several times with varying conditions but unfortunately, compound **3.48** was not isolated.

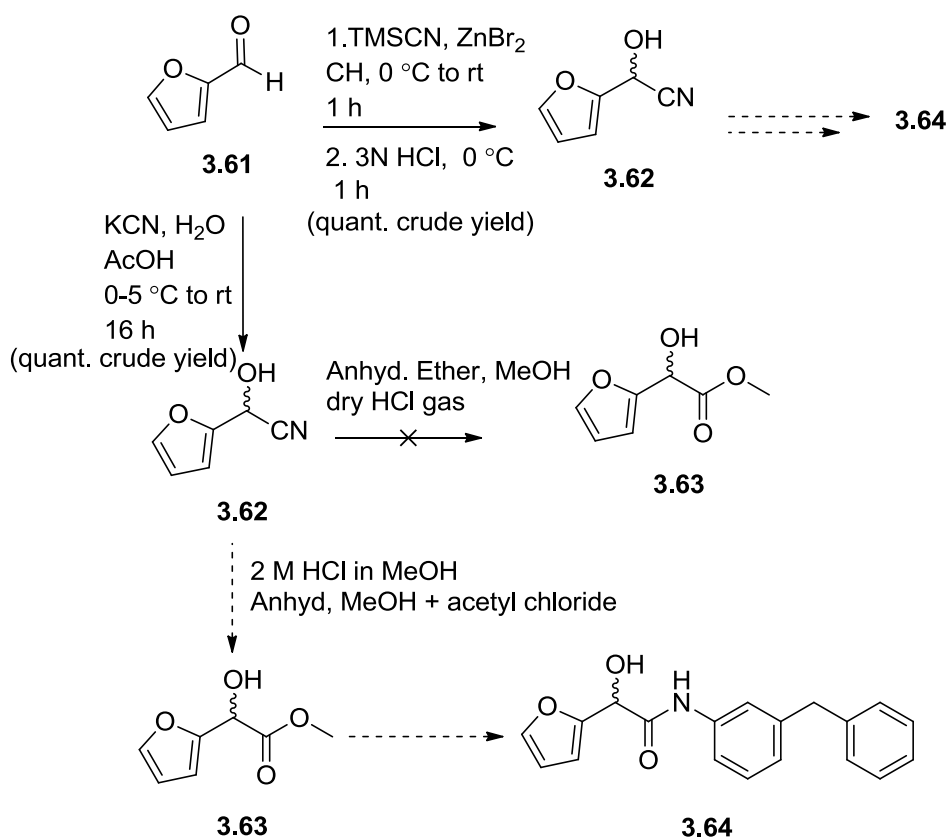
Similarly, the same cyanohydrin chemistries were employed with imidazole-2-carboxaldehyde (**3.50**) and imidazole-4-carboxaldehyde (**3.51**) derivatives (Scheme 3.6). Unfortunately, using the previously noted procedure for the pyridine series the conversion of imidazole-2-carboxaldehyde **3.50** to desired imidazole-2-cyanohydrin **3.52** was not successful. However, success was demonstrated with the conversion of imidazole-4-carboxaldehyde **3.51** to imidazole-4-cyanohydrin **3.53** using this procedure.<sup>300, 301</sup> The imidazole-4-cyanohydrin **3.53** was successively hydrolyzed to the  $\alpha$ -hydroxyacetic acid **3.56** and also as the ethyl ester **3.55**.<sup>308</sup>



**Scheme 3.6** Synthesis of 2- and 4-imidazole oxalamate derivatives

Analogous to problems faced with several of the other heteroaromatic derivatives previously noted at this stage, the amide coupling of  $\alpha$ -hydroxyacetic acid **3.56** with 3-benzylaniline was unsuccessful and **3.58** was not isolated.<sup>306</sup>

The synthesis of the furan oxalamate derivative began with the conversion of furfural (**3.61**) to the cyanohydrin **3.62** (Scheme 3.7).<sup>313, 314</sup> An attempt to convert the cyanohydrin **3.62** to the methyl ester **3.63** via the corresponding imidate through a modified Pinner reaction<sup>315</sup> was unsuccessful and alternative routes to obtain **3.63** were explored.<sup>316</sup> However, due to the instability of the furan scaffold, especially under acidic conditions, this route was abandoned and more favorable routes were pursued (Scheme 3.13 and 3.19, compound **3.98**).

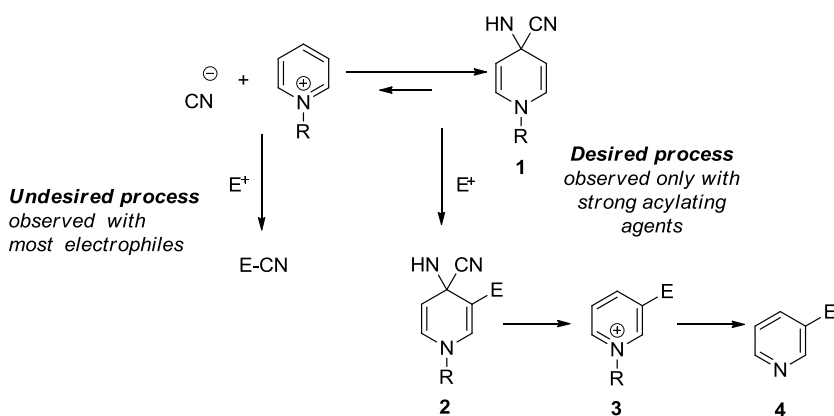


**Scheme 3.7** Approaches towards the synthesis of furan  $\alpha$ -hydroxy **3.64**

### 3.4.2. Heteroaromatic $\alpha$ -Oxoacetic Acids: Activation of Pyridium Salts for Electrophilic Acylation

At the same time that the cyanohydrin chemistries were underway, alternative routes to obtain the pyridine derivatives were also being investigated. It is well-known that electrophilic aromatic substitution reactions of pyridines are extraordinarily challenging. Instead of C-substitution at the pyridine ring, the electrophile typically forms an adduct with the pyridine nitrogen, which even further deactivates the already electron deficient pyridine ring toward electrophilic substitution. For example, the direct nitration of pyridine requires a reaction temperature of 330°C to provide only a 15% yield of 3-nitropyridine.<sup>317</sup>

To overcome the lack of reactivity of pyridines, pyridines can be converted into a temporarily activated electron rich 1,4-dihydropyridine which features strongly enhanced reactivity towards electrophiles at the 3-position.<sup>318-322</sup> Klapars *et al.* recently reported an indirect



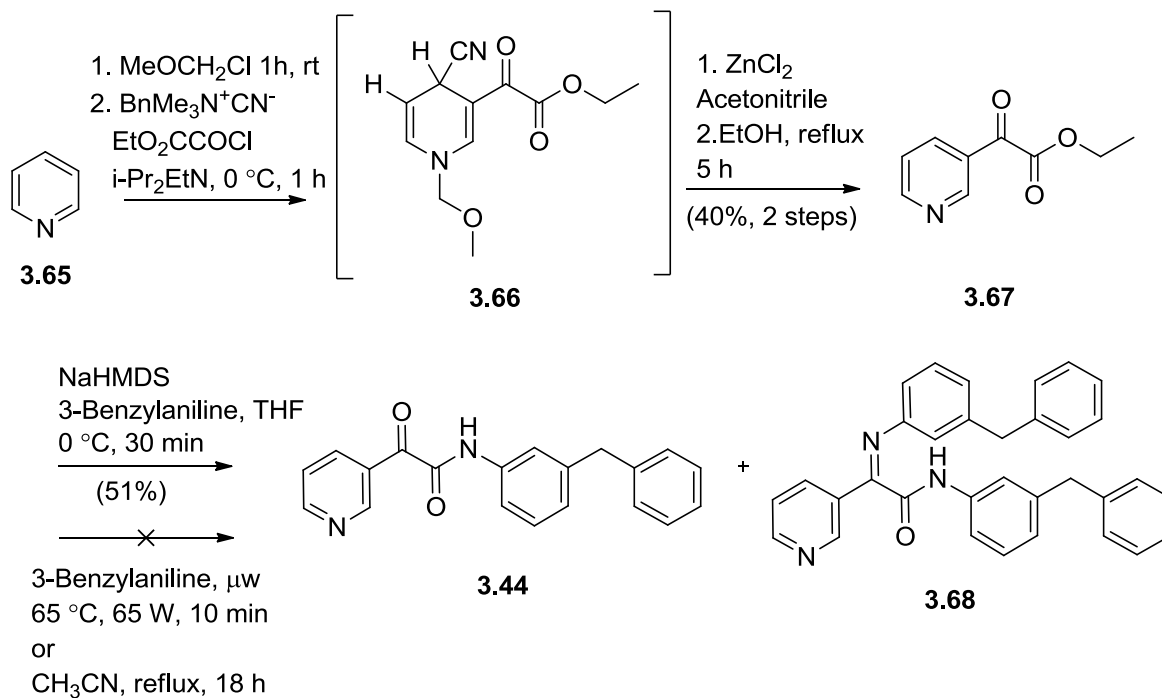
Scheme 3.8 Cyanide ion and pyridium salts

method for the 3-acylation of pyridines by converting recalcitrant pyridinium salts into Reissert-type 4-cyano-1,4-dihydropyridines in a one-pot procedure. In general, this method works

favorably if the equilibrium mixtures are treated with strong acylating agents such as ethyl oxalyl chloride. However, treatment with weaker acylating agents does not provide the desired dihydropyridines. Instead, products resulting from the reaction of the cyanide ion, present in the equilibrium mixture, can be observed (Scheme 3.8). This method was a good alternative to the

cyanohydrin chemistry and was used to obtain ethyl 3-pyridineglyoxylate (**3.67**) which was used for the synthesis of the 3-pyridine oxalamate derivative (**3.68**).<sup>323</sup>

The optimized procedure (Scheme 3.9) starting with pyridine (**3.65**) followed the sequence of N-alkylation with methyl chloromethyl ether (MOMCl) and addition of the soluble cyanide source benzyltrimethylammonium cyanide ( $\text{BnMe}_3\text{N}^+\text{CN}^-$ ) to generate the activated dihydropyridine **3.66**, and C-acylation with ethyl oxalyl chloride in the presence of Hünig's base. The aromatization of dihydropyridine **3.66** to the desired 3-acyl pyridine **3.67** was accomplished with the help of zinc chloride ( $\text{ZnCl}_2$ ) as a mild cyanophile. Upon addition of  $\text{ZnCl}_2$  to **3.66**, a rapid decyanation to the pyridinium salt which activated the MOM group toward deprotection via nucleophilic displacement. This was accomplished by refluxing the crude pyridinium salt mixture in ethanol, resulting in the formation of ethyl 3-pyridineglyoxylate **3.67** in moderate yields.



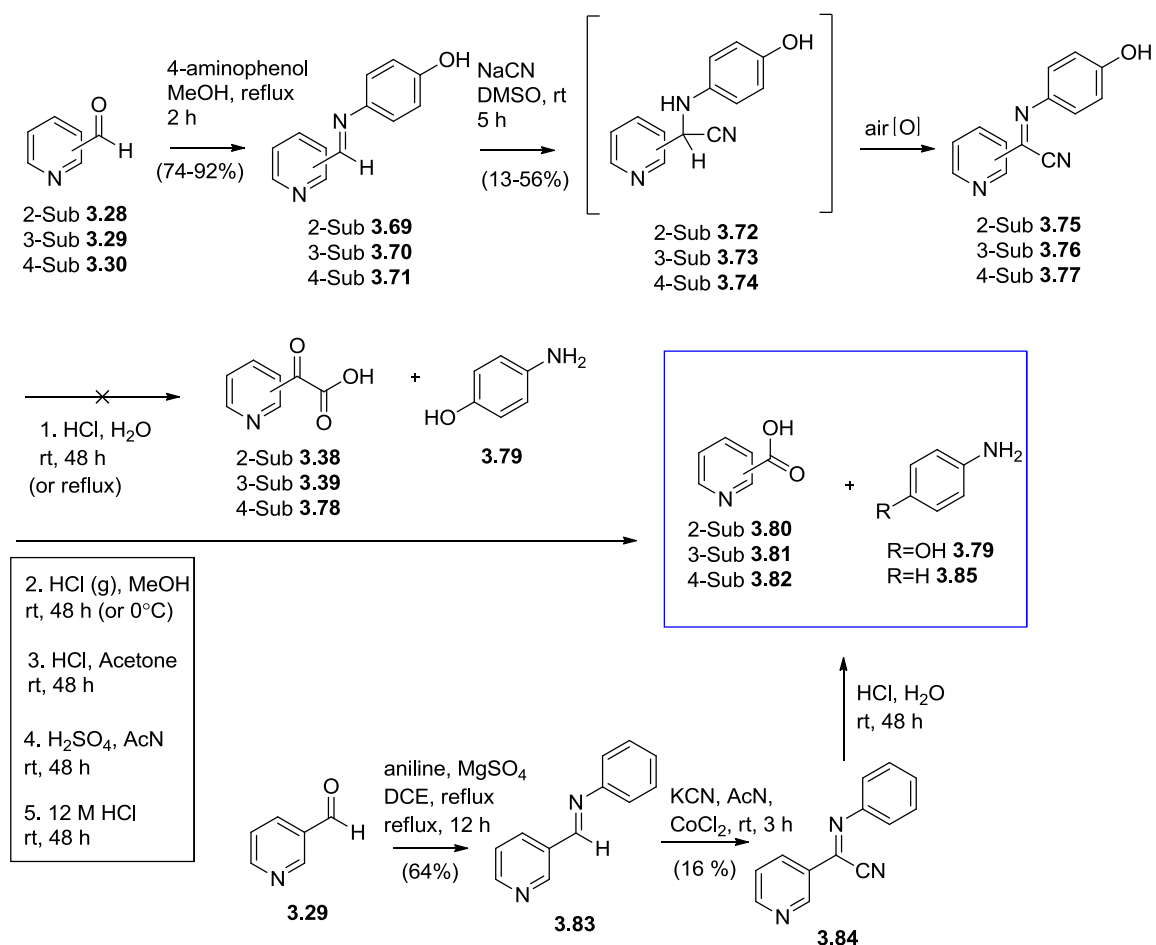
**Scheme 3.9.** Synthesis of 3-pyridine oxalamate **3.44**

Initial attempts of amide formation by heating ethyl ester **3.67** in the presence of 3-benzylaniline in a CEM microwave synthesizer for 10 min at 65 °C and an initial power of 65 W or refluxing the reaction mixture overnight did not give corresponding oxamide (**3.44**) and only starting material (**3.67**) remained.<sup>324</sup> The ethyl 3-pyridineglyoxylate **3.67** was then subjected to amide coupling conditions using sodium hexamethyldisilazide (NaHMDS) to deprotect the aniline and then to react with the ethyl ester to give the required amide **3.44**. Although, the desired amide was obtained, the product was contaminated with an undesired Schiff-base product **3.68**. The thin-layer chromatography (TLC) profile of the isolated product from the reaction mixture appeared as one spot; however, NMR and HPLC analysis revealed both products **3.44** and **3.68** (50:50 ratio).

### **3.4.3. Heteroaromatic $\alpha$ -Oxoacetic Acids: Heterocyclic $\alpha$ -Iminonitriles**

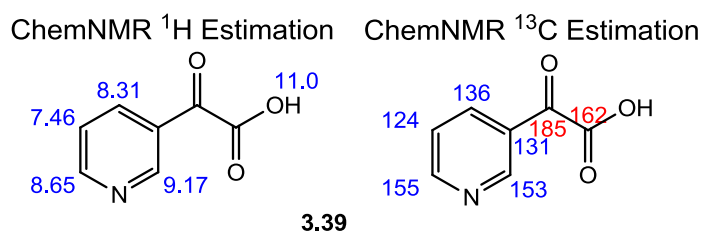
There are several synthetic procedures for the preparation of  $\alpha$ -Iminonitriles (Schiff-bases), however, most of them are multistep processes and have a limited application scope.<sup>325-</sup><sup>337</sup> Jursic *et al.* reported this procedure as for the conversion of heterocyclic aldehydes (**3.28-3.30**) into heterocyclic methylened-*p*-hydroxyanilines, heterocyclic  $\alpha$ -iminonitriles (**3.75-3.77**), and finally into heterocyclic  $\alpha$ -oxoacetic acids (**3.38, 3.39** and **3.78**).<sup>338</sup> Initially, this route was anticipated as an efficient three-step route for the synthesis of heteroaromatic  $\alpha$ -oxoacetic acids (Scheme 3.10).<sup>338</sup> A simple reaction of 2-, 3- and 4-pyridine carboxaldehydes (**3.28-3.30**) with *p*-aminophenol in methanol resulted in the corresponding heterocyclic imines (**3.69-3.71**) in high purity and yields. The heterocyclic imines were then treated with sodium cyanide and dimethyl sulfoxide (DMSO) and subjected to air oxidation to yield the  $\alpha$ -iminonitriles (**3.75-3.77**). Following the reported procedure, preparation of **3.77** was straight-forward and product was

identified with ease in high yield. Interestingly, it was extremely difficult to identify and purify both of the 2- and 3- pyridine  $\alpha$ -iminonitrile derivatives (**3.75** and **3.76**) following the reported procedure. However, after carefully modifying the purification method both of the desired  $\alpha$ -iminonitriles (**3.75** and **3.76**) were identified successfully. With all three  $\alpha$ -iminonitriles available the next step invoked hydrolysis to the desired heterocyclic- $\alpha$ -oxoacetic acids (**3.38**, **3.39** and **3.78**). The  $\alpha$ -iminonitriles represent a class of compounds that should hydrolyze rather easily to the desired heterocyclic- $\alpha$ -oxoacetic acids.<sup>338, 339</sup> However, following the reported approach of stirring an aqueous hydrochloric acid suspension of heterocyclic  $\alpha$ -iminonitrile followed by separation of the heterocyclic- $\alpha$ -oxoacetic acid (**3.38**, **3.39** and **3.78**) from *p*-aminophenol (**3.79**)



**Scheme 3.10** Synthesis of  $\alpha$ -oxoacetic acids from  $\alpha$ -iminonitriles

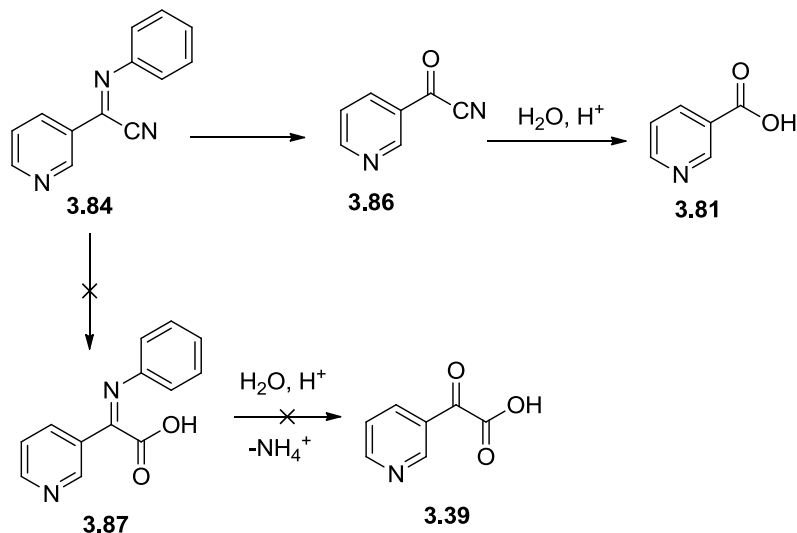
failed. Hydrolysis was attempted several times with varying reaction conditions, times and temperatures.<sup>339-342</sup> Collectively, the hydrolysis methods tested did not yield the desired heterocyclic- $\alpha$ -oxoacetic acids (**3.38**, **3.39** and **3.78**), and the products identified from the hydrolysis reactions were nicotinic acid (**3.80-3.82**) and *p*-aminophenol (**3.79**) co-eluting as a mixture (Scheme 3.10). After reviewing the literature it became apparent that mechanistically, the hydrolysis of the  $\alpha$ -imino functional group happens at a faster reaction rate compared to the nitrile functional group and therefore leading to the formation of nicotinic acid instead to  $\alpha$ -oxoacetic acids (3.11).<sup>339-342</sup> Although the published method reports the synthesis of  $\alpha$ -oxoacetic acids there is skepticism due to the lack of reproducibility. It is worth mentioning that since the publication of this preliminary report there have been no other reports using this method to obtain  $\alpha$ -oxoacetic acids in the literature. Also, comparing the reported NMR values for **3.39** in this paper<sup>338</sup> to known and estimated values of **3.39** shows discrepancy (Figure 3.35).



Reported NMR values:

<sup>1</sup>H NMR (DMSO-*d*6)  $\delta$  9.144 (1 H, d,  $J=2.1$  Hz, pyridine 2-H), 8.907 (1H, dd,  $J_1=5.4$  Hz,  $J_2=2.1$  Hz, pyridine 6-H), 8.535 (1H, dt,  $J_1=7.8$  Hz,  $J_2=2.1$  Hz, pyridine 4-H), 7.790 (1H, dd,  $J_1=7.8$  Hz,  $J_2=5.4$  Hz, pyridine 5-H);  
<sup>13</sup>C NMR (DMSO-*d*6)  $\delta$  161.633, 146.560, 143.869, 136.855, 124.432, 121.692, and 96.019 ppm

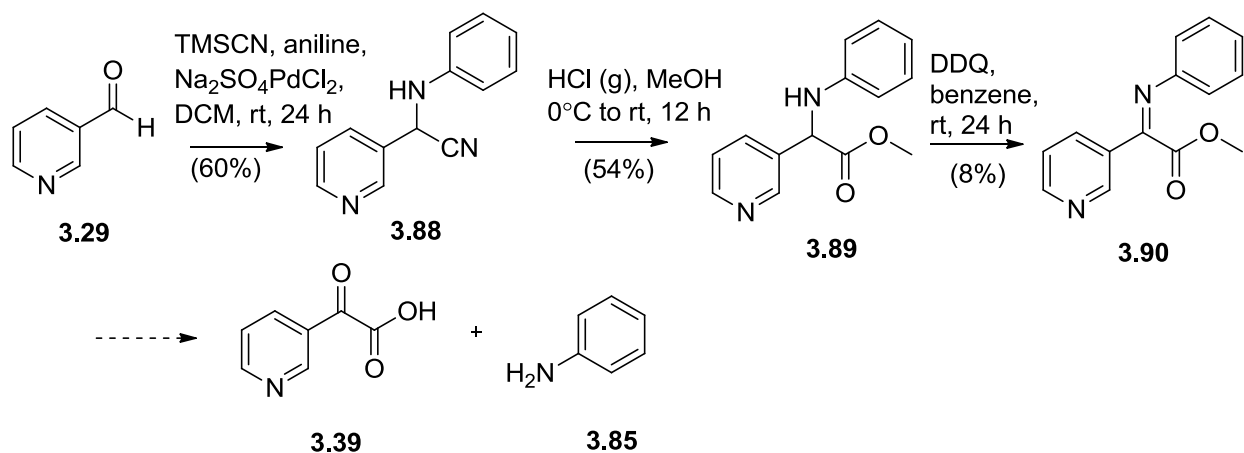
**Figure 3.34** Comparison of estimated NMR values to reported NMR values of **3.39** (Discrepancies highlighted in red)



**Scheme 3.11** Reaction pathways for the hydrolysis of the  $\alpha$ -iminonitrile **3.84**

In order to elucidate a reason for this and potentially come to a more reliable reaction protocol, we chose to investigate alternative reaction conditions. Additionally, when aniline **3.85** was used as an alternative to the *p*-aminophenol **3.79**, containing an electron donating hydroxyl group, the same reaction products were obtained (Scheme 3.10). We decided to use the lessons learned from this chemistry to explore an alternative route to obtain the  $\alpha$ -oxoacetic acids (Scheme 3.12). It was evident that the major hurdle to overcome was the competing hydrolysis reaction rate of the  $\alpha$ -imino group compared to that of the nitrile functional group. We envisioned that a more robust route would invoke an  $\alpha$ -amino group in place of the  $\alpha$ -imino group. Therefore, a simple and efficient one-pot, three component method was used for the synthesis of  $\alpha$ -aminonitrile **3.88**.<sup>343</sup> The  $\alpha$ -aminonitrile **3.88** was subjected to Pinner synthesis to hydrolyze the nitrile and afford the amino ester **3.89**.<sup>344</sup> The next step towards the synthesis of the  $\alpha$ -oxoacetic acid **3.39** was to oxidize the  $\alpha$ -amino to an  $\alpha$ -imino functional group with 2, 3-dichloro-5, 6-dicyano-1, 4-benzoquinone (DDQ)<sup>345, 346</sup> to furnish **3.90**, in preparation of hydrolysis of both the ester and  $\alpha$ -imino functional group to provide  $\alpha$ -oxoacetic acid **3.39**.<sup>338</sup>

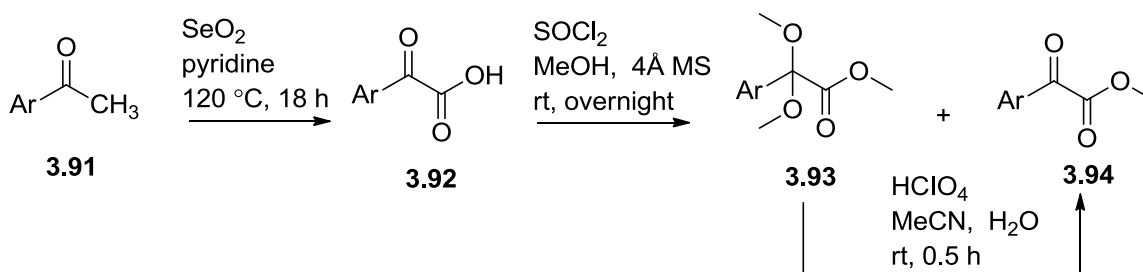




**Scheme 3.12** Alternative route for the synthesis of  $\alpha$ -oxoacetic acids from  $\alpha$ -iminonitriles

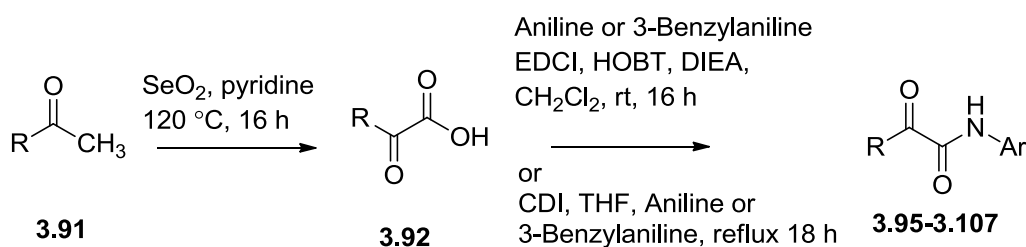
### 3.4.4. Aryl $\alpha$ -Keto Esters and Acids

In the past several decades, much attention focused on the synthesis of  $\alpha$ -keto esters. Several routes were reported including the oxidation of  $\alpha$ -hydroxy esters with either pyridinium chlorochromate (PCC) or Dess-Martin periodinane (DMP),<sup>347, 348</sup> Friedel-Crafts acylation,<sup>349</sup> oxidative cleavage of cyano keto phosphoranes,<sup>350</sup> hydrolysis and esterification of acyl cyanides,<sup>351</sup> the reaction of organometallic species with oxalic ester derivatives,<sup>352</sup> and acylation or alkylation of mono-substituted 1,3-dithianes.<sup>353</sup> The most common route for the synthesis of  $\alpha$ -keto esters is the reaction of Grignard reagents with oxalyl chloride.<sup>354</sup> However, all of these methods involve either strict reaction conditions, complicated procedures, or in some instances low yields. Collectively, all of the drawbacks associated with these procedures have limited the



**Scheme 3.13** Three-step sequential procedure to synthesize  $\alpha$ -keto esters

synthetic application of these methods to obtain  $\alpha$ -keto esters. Recently, Zhaung *et al.* reported an efficient one-pot synthesis of  $\alpha$ -keto acids and  $\alpha$ -keto esters by using selenium dioxide to oxidize aryl ketones (Scheme 3.13).<sup>355</sup> Although there are several routes for the synthesis of aryl  $\alpha$ -keto esters as noted above, this method provided a convenient and efficient route for the synthesis of our aryl  $\alpha$ -keto acids (Figure 3.34). With the synthesis outlined in Scheme 3.14, numerous compounds could be effortlessly synthesized starting with readily available aryl ketones **3.91** to obtain the  $\alpha$ -ketoacids **3.92**. The  $\alpha$ -ketoacids produced could then be used in subsequent amide coupling reactions<sup>306</sup> with aniline or 3-benzylaniline to obtain target compounds **3.93-3.105** (Figure 3.34).



**Scheme 3.14** Synthesis of aryl oxalamate scaffolds

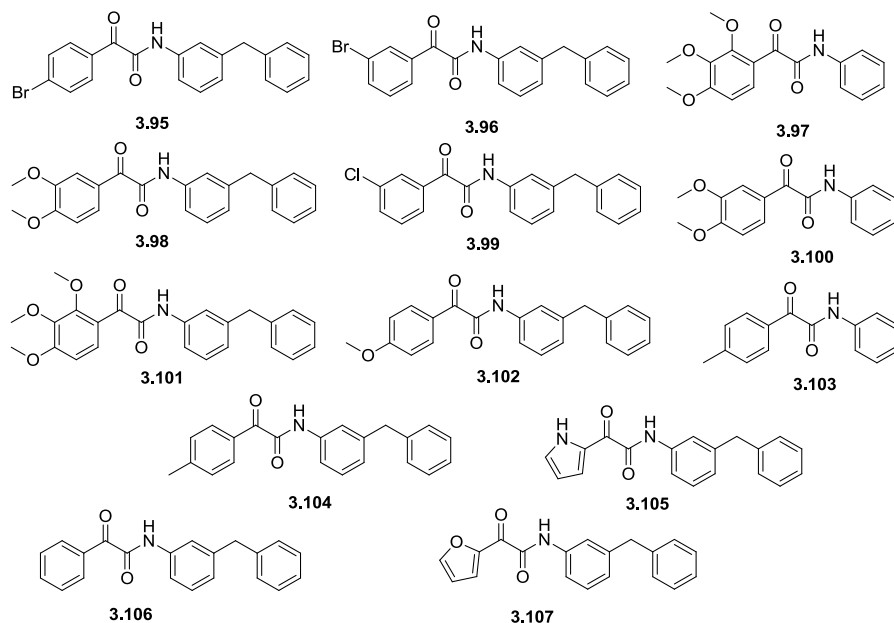


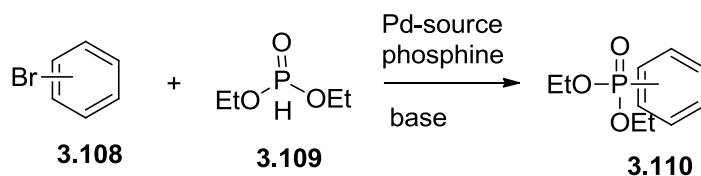
**Figure 3.35** Synthesized aryl oxalamate derivatives

The brominated aryl

oxalamate compounds **3.95** and **3.96**

were of particular interest because

they are viable precursors for the



**Scheme 3.15** Pd-catalyzed synthesis of arylphosphonates

palladium-catalyzed cross-coupling reaction with dialkyl phosphites (Scheme 3.15).<sup>356</sup>

Traditional synthetic methods for aryl- and vinylphosphonic acid class of compounds include

Friedel-Crafts reactions,<sup>357</sup> Cu-catalyzed reactions of diazonium salts with  $\text{PCl}_3$ ,<sup>324, 358</sup>

nucleophilic substitution reactions of activated aryl halides and sodium dialkylphosphites,<sup>359</sup> Ni-

or Cu-mediated couplings between aryl halides and trialkyl phosphites,<sup>360-364</sup> and reaction of

arylmethyl derivatives and trialkyl phosphites.<sup>365-367</sup> However, due to the aggressive and harsh

reaction conditions required, these transformations tend to be incompatible with sensitive

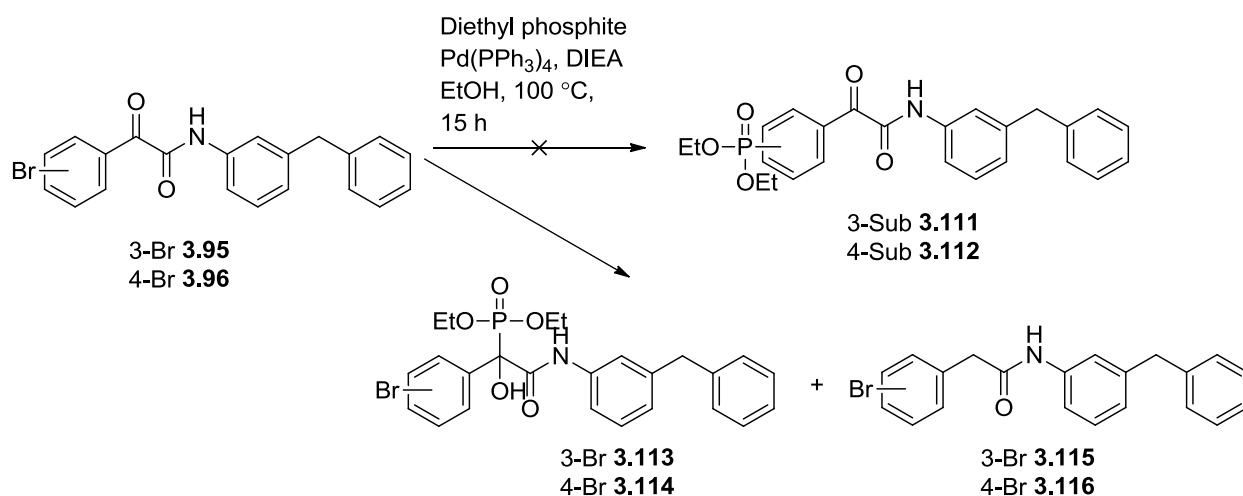
functionalities.<sup>356</sup> A potentially more general access to dialkyl arylphosphonates based on

palladium-catalyzed reaction of aryl halides with dialkyl phosphite has been previously reported

by Hirao *et al.* (Scheme 3.15).<sup>368-372</sup> Unfortunately, when Gooßen *et al.* employed these

previously published procedures for the preparation of various functionalized aryl phosphonates

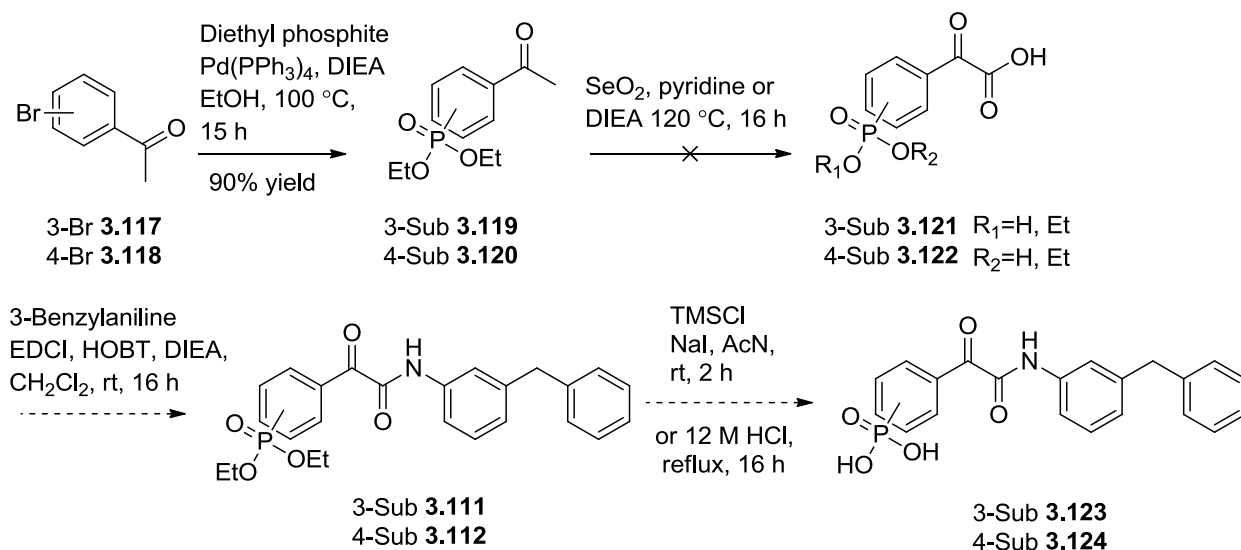
the reactions provided unsatisfactory yields.<sup>356</sup> Therefore it was necessary to explore alternative



**Scheme 3.16** Approach towards the synthesis of 3- and 4-arylphosphonates (**3.111** and **3.112**)

reaction conditions to develop an efficient and broadly applicable approach for the cross-coupling of aryl bromides with dialkyl phosphites. The best results were obtained using Pd(OAc)<sub>2</sub> as the Pd-source, triphenylphosphine as the phosphine source, a sterically demanding tertiary amine as the base, and use of the protic solvent ethanol. Remarkably clean reactions were observed even with functionalized molecules bearing keto, nitro, ester, thioether, nitrile and even hydroxyl functional groups.<sup>356</sup> Therefore, this method seemed reasonable to follow with the  $\alpha$ ,  $\beta$ -diketo containing oxoamide starting materials **3.95** or **3.96** (Scheme 3.16). After reaction completion and subsequent purification by column chromatography, two products were isolated. Unfortunately, neither product was the desired aryl phosphonate (**3.111** or **3.112**), as determined by spectroscopic methods of analysis. The products isolated from both the 3- and 4-substituted derivatives were **3.113** and **3.115** or **3.114** and **3.116**, respectively (Scheme 3.16). It appears from the reaction mechanism that products **3.113** and **3.114** are a result of nucleophilic addition to the reactive  $\alpha$ -keto carbonyl with diethyl phosphite, happening at a faster reaction rate than the phosphorus-carbon bond coupling reaction. Products **3.115** and **3.116** are a result from the diethyl phosphite acting as a hydride source and reducing the  $\alpha$ -keto carbonyl group. Therefore, it can be concluded that both products are a result from the reactivity of the  $\alpha$ -carbonyl ketone. A solution for this problem was to install the phosphonate ester first (**3.119** or **3.120**, Scheme 3.17) and then oxidize the aryl ketone to obtain the  $\alpha$ -hydroxyacetic acid (**3.121** or **3.122**).<sup>306, 355</sup> Once the phosphonate  $\alpha$ -hydroxyacetic acid derivatives were available, amide bond formation with 3-benzylamine (**3.111** or **3.112**) and deprotection of the phosphonates under mild conditions to afford the phosphoric acid oxalamate derivatives **3.123** or **3.124**.<sup>306, 373</sup> Unexpectedly, the reaction yielded a mixture of multiple products of mono-dealkylated, di-dealkylated instead of the phosphonate ester  $\alpha$ -keto acids (**3.121** and **3.122**). It was quickly apparent from the two

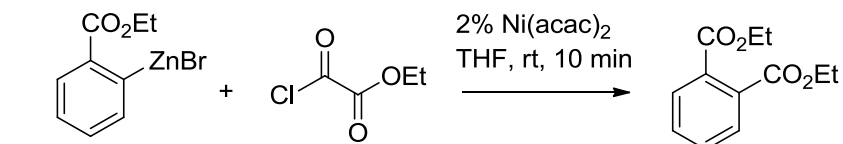
methods employed that an alternative route was warranted for the synthesis of the phosphoric acid oxalamate derivatives.



**Scheme 3.17** Alternative approach for the synthesis of arylphosphonates

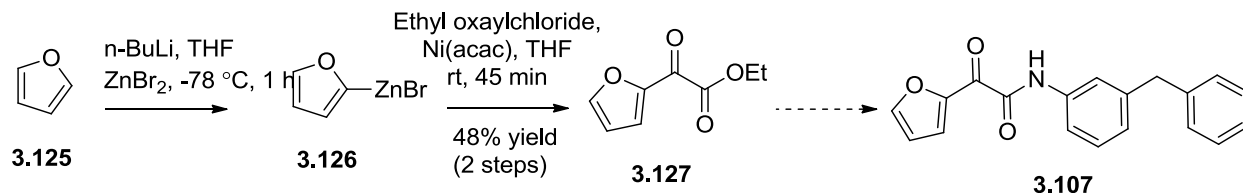
### 3.4.5. Negishi and Suzuki Cross-Coupling Reactions with Acid Chlorides

In 2011, Kim *et al.* published a procedure for a Ni-catalyzed cross-coupling reaction of organozinc reagents with acid chlorides.<sup>374</sup> From the series of compounds derived from this study, of particular interest was the Negishi cross-coupling reaction between ethyl 2-oxalyl chloride and an aryl zinc bromide (Scheme 3.18). This was of interest because the reaction conditions reported were well-tolerated by the acid chloride which contained two ester functionalities. This procedure seemed to be a feasible method for the synthesis of the furan oxalamate scaffold **3.107** (Scheme 3.19). The furan zinc bromide **3.126** was



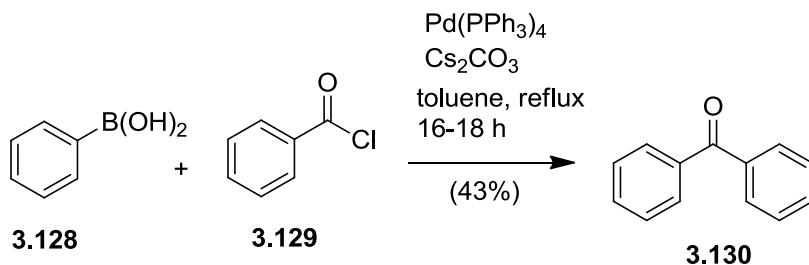
**Scheme 3.18** Negishi coupling of diketo acid chloride with zinc bromides

synthesized<sup>375</sup> and subjected to Ni-catalyzed cross-coupling conditions to afford **3.127** in moderate yield. During the time that this synthetic route was being pursued an alternative route to synthesize the furan oxalamate **3.107** (Scheme 3.14) was discovered and this route was abandoned. However, the use of acid chlorides, specifically diketo acid chloride prompted us to pursue alternative interesting and less exploited cross-coupling reactions (Scheme 3.21).



**Scheme 3.19** Synthesis of furan oxalamate **3.107** using Negishi coupling conditions

Currently, there is no procedure reported for the Suzuki cross-coupling of diketo acid chlorides with arylboronic acids. In 1999, a procedure by Haddach *et al.* for the Pd-catalyzed cross-coupling of acid chlorides with arylboronic acids was reported (Scheme 3.20).<sup>376</sup> This method provided a convenient route to ketones, since boronic acids and acid chlorides are inexpensive commercially available starting reagents. The Suzuki coupling reaction is generally carried out as a two-phase Pd-catalyzed reaction in ethanol, toluene and water.<sup>377</sup> These conditions are not suitable for the coupling of acid chlorides with boronic acids. However, this procedure synthesis ketones from acid chlorides and boronic acids under anhydrous Suzuki

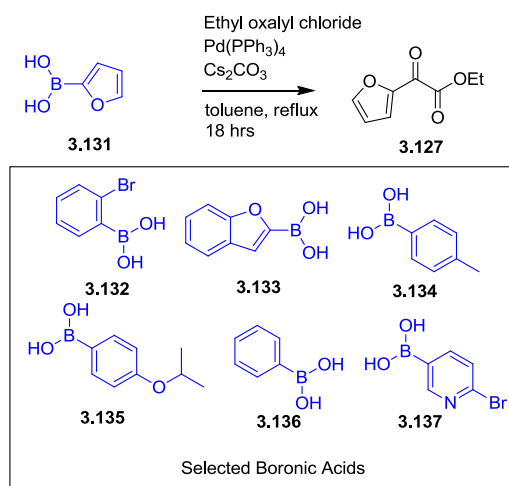


**Scheme 3.20** Suzuki cross-coupling of acid chlorides with arylboronic acids

cross-coupling reaction conditions with Pd-catalyst and cesium carbonate in toluene (Scheme 3.20).<sup>376</sup>

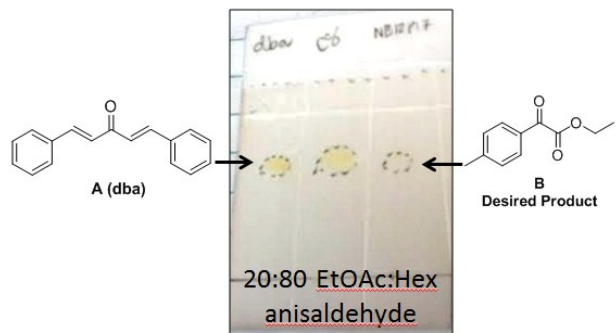
It was projected that Suzuki cross-coupling with diketo acid chlorides and boronic acids, derived from this seminal paper,<sup>376</sup> would offer the ability to synthesize a library of oxalamate derivative scaffolds for this project. Several boronic acids with ethyl oxalyl chloride (Scheme 3.21, Table 3.6 ) were subjected to Pd-catalyzed cross-coupling conditions using similar reaction conditions as reported in the literature. Both NMR and mass spectral analysis of the products isolated from the performed reactions determined that although in several instances the desired diketo ester product had formed it was in undesirable yields (0-28% yield). The anticipated products in the crude reaction mixture were among several byproducts. One of the most commonly observed byproducts formed from these reactions was the homocoupling of the boronic acid to itself rather than boronic acid coupling to the acid chloride. An interesting observation was noted when Tris(dibenzylideneacetone)dipalladium(0) ( $\text{Pd}_2(\text{dba})_3$ ) was used as the catalyst for these Suzuki-cross coupling reactions. The ( $\text{Pd}_2(\text{dba})_3$ ) catalyzed reactions provided some of the higher yields

compared to the reactions using alternative palladium catalysts. However, when the desired products were isolated they were co-eluted as inseparable mixtures with dibenzalacetone (dba) that had been dissociated from the ( $\text{Pd}_2(\text{dba})_3$ ) catalyst (Figure 3.35). Due to the

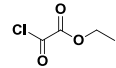
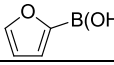
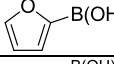
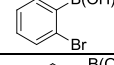
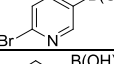
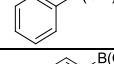
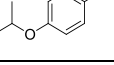
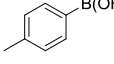
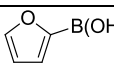
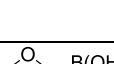
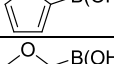
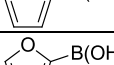
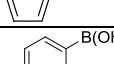
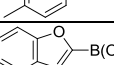
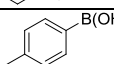


Scheme 3.21 Suzuki cross-coupling of diketo acid chlorides with arylboronic acids

undesirable yields and complicated reaction mixtures these chemistries were not continued as a method for obtaining the oxalamate scaffolds.



**Figure 3.36** TLC of Desired Product **B** co-eluting with dba **A**

Reference	Boronic Acid	Boronic Acid Eq		Cs <sub>2</sub> CO <sub>3</sub>	Catalyst	Catalyst Eq	Results
NB11P53		1	2	2.5	Pd(PPh <sub>3</sub> ) <sub>4</sub>	2.57 mol%	Several products (homocoupling)
NB11P57		1	3	2.5	Pd(PPh <sub>3</sub> ) <sub>4</sub>	1.61 mol%	Isolated major product (byproduct)
NB11P60		1	3	2.5	Pd(PPh <sub>3</sub> ) <sub>4</sub>	1.04 mol%	Several products
NB11P66		1	2	2.5	Pd(PPh <sub>3</sub> ) <sub>4</sub>	4 mol%	Several products
NB11P83		1	2	5	Pd(PPh <sub>3</sub> ) <sub>4</sub>	5 mol%	homocoupling
NB11P86		1	2	5	Pd(PPh <sub>3</sub> ) <sub>4</sub>	5 mol%	Several products (could not isolate prod)
NB11P87		1	2	5	Pd(PPh <sub>3</sub> ) <sub>4</sub>	5 mol%	Several products (could not isolate prod)
NB11P93		1	2	2.62	Pd(PPh <sub>3</sub> ) <sub>4</sub>	5 mol%	Several products Mass spec shows product
NB11P97		1	3	3	Pd(PPh <sub>3</sub> ) <sub>4</sub>	5 mol%	homocoupling
NB12P03		1	3	3	Pd <sub>2</sub> (dba) <sub>3</sub>	5 mol%	TLC matches Negishi NMR-shows but w/dba
NB12P05		1	3	3	Pd(OAc) <sub>2</sub>	5 mol%	homocoupling
NB12P07		1	3	3	Pd <sub>2</sub> (dba) <sub>3</sub>	5 mol%	TLC-one bright spot NMR-mixture w/dba
NB12P15		1	3	3	Pd <sub>2</sub> (dba) <sub>3</sub>	5 mol%	TLC-one bright spot NMR-mixture w/dba
NB12P17		1	3	3	Pd <sub>2</sub> (dba) <sub>3</sub>	5 mol%	TLC-one bright spot NMR-mixture w/dba

**Table 3.6** Suzuki Methodology Summary of Coupling with Acid Chlorides and Aryl Boronic Acids



### 3.4.6. Friedel-Crafts Acylation

In the early 2000s, with the emergence of resistance from the commonly prescribed marketed HIV therapeutics, Bristol-Myers Squibb (BMS) implemented a screening program to identify new classes of HIV-1 inhibitors that acted against novel drug targets without bias for a particular mechanism of action.<sup>378</sup> This initiative produced a number of compounds that interfered with HIV-1 replication in cell culture without overt cytotoxicity. Most of the compounds discovered were characterized as NNRTIs. However, one compound, the simple indole glyoxamide (**A**, Figure 3.36), emerged as a molecule with a unique mechanistic profile.<sup>379,</sup><sup>380</sup> Time-of-addition experiments eventually elucidated that the indole glyoxamides (Figure 3.36) inhibited an early event in HIV infection that was subsequently determined to be interference with the binding of HIV-1 gp120 to the host-cell receptor CD4.<sup>380</sup>

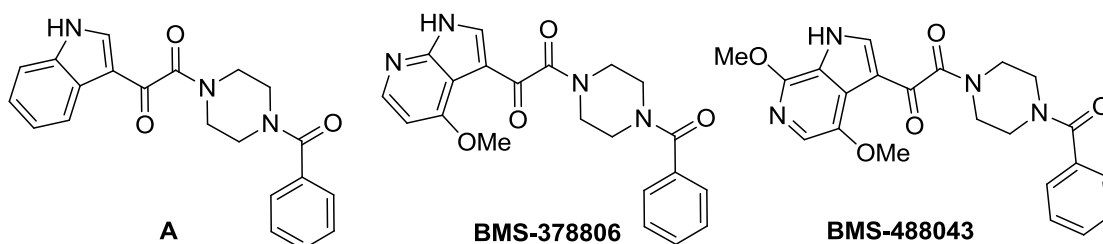
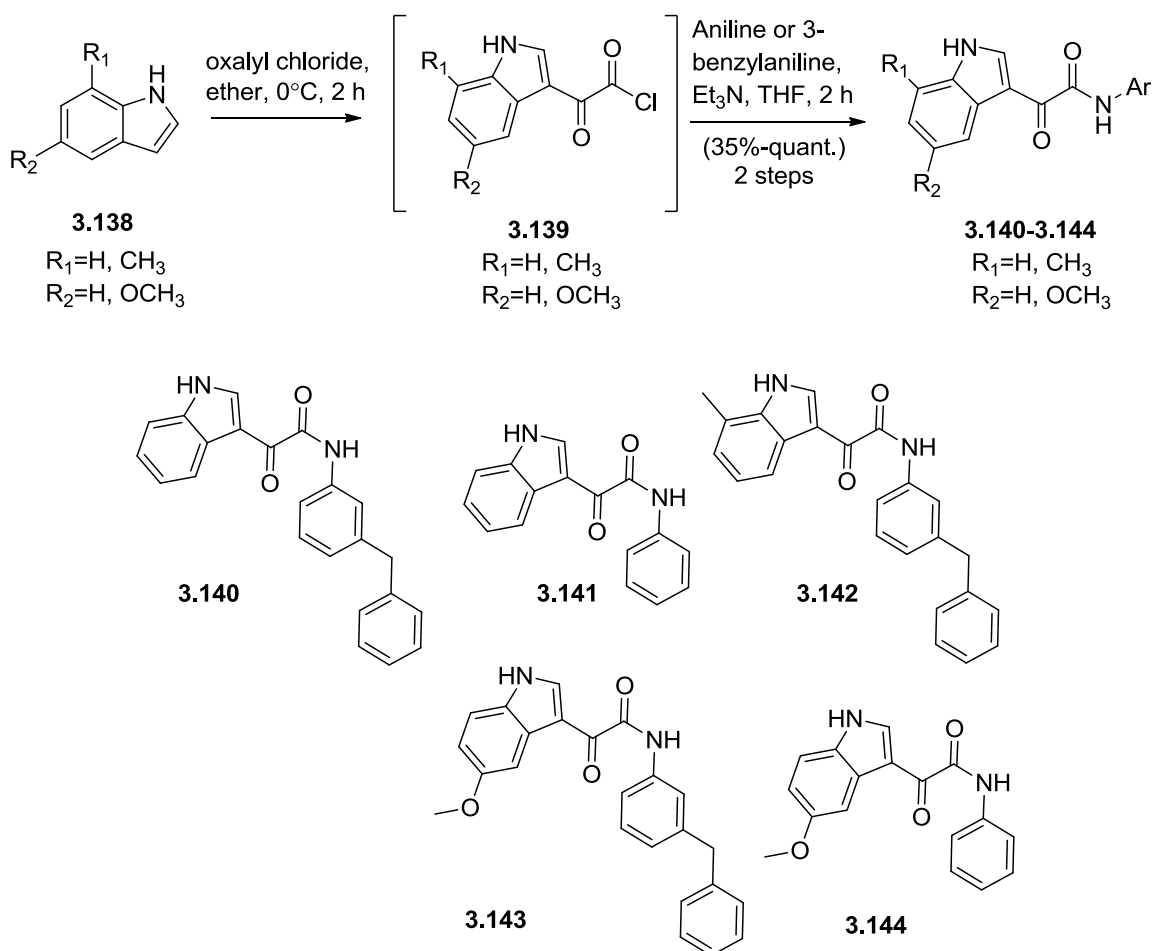


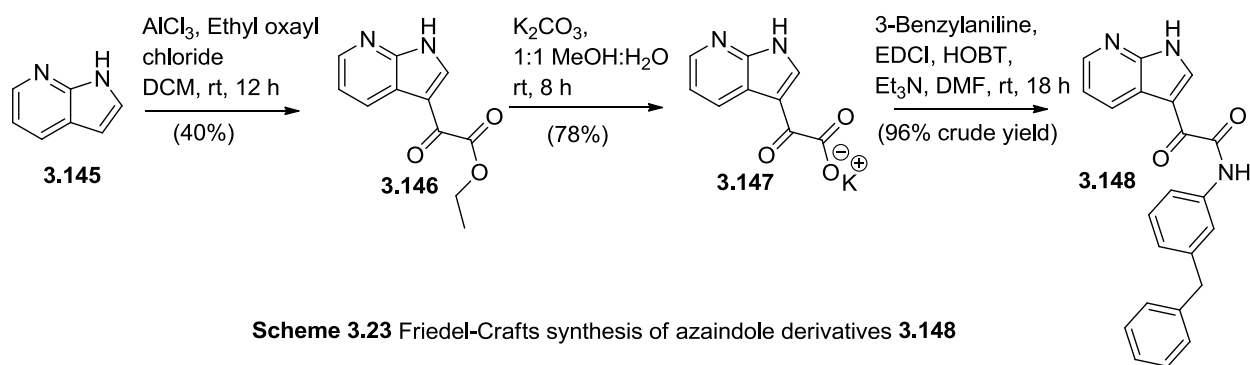
**Figure 3.37** Select Indole Glyoxamide HIV-1 Entry Inhibitors

The ease of the synthesis for the indole glyoxamide class of compounds using Friedel-Crafts acylation chemistry, their advent as HIV-1 entry inhibitors with similar structural features to our proposed molecules made these scaffolds interesting molecules to pursue and test as HIV-1 IN inhibitors. Moreover, considering the analogous structural features of the library of synthesized molecules from this dissertation project it may be worthwhile to also evaluate our compounds as HIV-1 entry inhibitors.

As shown in Scheme 3.22 and 3.23, Friedel-Crafts acylation of substituted indoles led to the synthesis of several indole glyoxamides. Due to the high nucleophilic character at the 3-position of indole, the treatment with oxalyl chloride of appropriate indoles **3.138** produced the corresponding 2-(1H-indol-3-yl)-2-oxoacetyl chloride intermediates **3.139** which were then coupled with aniline or 3-benzylaniline in alkaline medium in a one-pot procedure to give the desired indole oxalamate derivatives **3.140-3.144** (Scheme 3.22).<sup>381, 382</sup> The synthesis of azaindole (**3.148**) is depicted in Scheme 3.23 and is initiated by acylating 7-azaindole (**3.145**) with ethyl chlorooxoacetate in the presence of AlCl<sub>3</sub> to afford **3.146**.<sup>383</sup> Hydrolysis of the resulting ester, using K<sub>2</sub>CO<sub>3</sub> in aqueous MeOH,<sup>305</sup> followed by coupling with 3-benzylaniline afforded the azaindole glyoxamide **3.148**.<sup>306</sup>



**Scheme 3.22** Friedel-Crafts synthesis of indole derivatives **3.140-3.144**



**Scheme 3.23** Friedel-Crafts synthesis of azaindole derivatives **3.148**

### 3.5. BIOLOGICAL EVALUATION

The compounds designed and synthesized from this dissertation project were completed with an agreement between the University of Mississippi and Panvirex, LLC. In summary, several of the compounds (**3.41-3.44**, **3.95-3.107**, **3.113-3.115**, **3.140-3.144** and **3.148**) that were synthesized during the course of this project have been submitted to our collaborators at Panvirex, LLC. and the biological data is currently pending at the time of writing this dissertation. The synthetic analogues will undergo biological screening to determine the IN inhibitory activity, the sensitivity to known IN inhibitor mutations and analyzed for their antiviral efficacy.

#### 3.5.1. Determination of IN inhibition

The selectivity of  $\beta$ -DKA class of IN inhibitors towards the inhibition of the ST-reaction provides specificity to the viral enzyme mediated reaction. Several types of assays to determine IN inhibition have been previously described in the literature.<sup>203, 384-389</sup> The high-throughput electrochemiluminescent (ECL) based determination of the ST inhibition reaction and the solid phase ELISA assay (Biomek® robotic system) will be used for the evaluation of the synthesized chemical scaffolds (Figure 3.37). The principles of the ECL and ELISA assays are essentially the

same, however, in the solid-phase ELISA assay either biotin or fluorescent FTC (fluorescein-5-thiosemicarbazide) labeled DNA is used and in the ECL assay the DNA label is a chemiluminescence molecule. The high-throughput ECL assay (BioVeris Inc., Gaithersburg, MD) is commercially available and will be used in routine analysis of IC<sub>50</sub> potency of the synthesized compounds.

Both the solid-phase ELISA assay and high-throughput ECL can only determine the inhibition of the ST reaction, which is important from a drug development perspective. However, it is important to also determine the inhibitor selectivity of the ST-reaction over the 3'-P reaction. The traditional gel-based assay containing the labeled 21-mer duplex oligonucleotide corresponding to the U5 end of the HIV LTR sequence can determine both ST-inhibition and 3'-P inhibition. Although this assay is cumbersome and tedious, it will be of great importance from a mechanistic perspective. The evaluated compounds that show ST inhibition from the high-throughput ECL assay will be evaluated using this gel-based assay to determine if any inhibition of the 3'-P reaction is also seen.

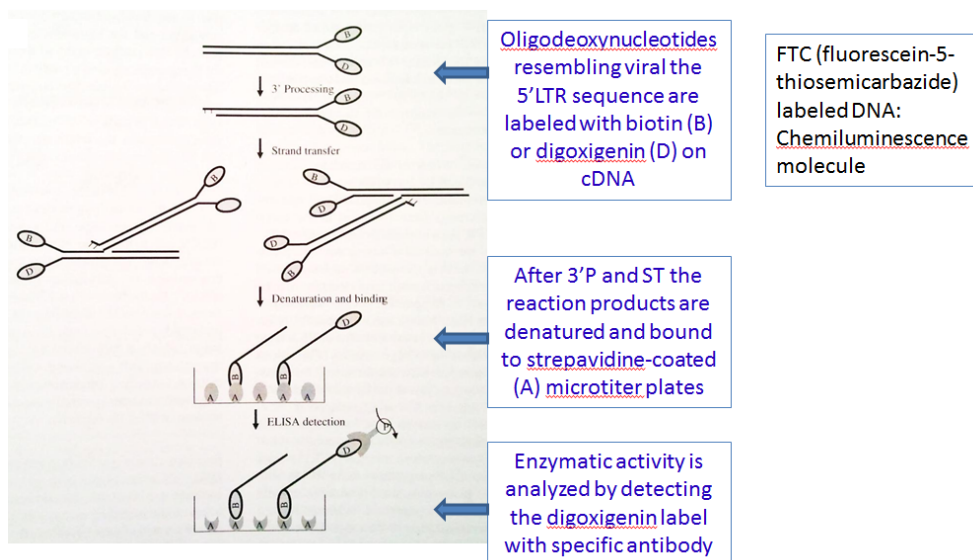


Figure 3.37 Standard ELISA ST IN Assay<sup>251</sup>

### 3.5.2. Determination of Sensitivity to Known IN Inhibitor Mutations

It has been previously reported that the  $\beta$ -DKA class of compounds induce progressive drug resistance mutations of T66I/S153Y, T66I/M154I or T66I/S153Y/N155S. These mutations in the enzyme do not alter the enzyme efficiency as observed with the emergence of drug resistant viruses and also established by *in vitro* studies. In this regard, compounds synthesized will be evaluated against the IN enzyme containing either an individual mutation or a combination of mutations. Analysis of ST inhibition in IN mutations of K156 and K159 or Q148 are not meaningful because these residues are involved in host and viral DNA binding and ST inhibition is lost if these residues are mutated. Similarly, mutations of the residues in the catalytic triad, E152, D64 and D116, are not possible. The histidine (His) Tag-recombinant cDNA clones of the IN enzyme containing T66I, S153Y and M154I are readily available at Panvirex, LLC and the combination of mutants were obtained as a gift from Dr. Vinay Pathak, at the National Cancer Institute (NCI).

### **3.5.3 Determination of Antiviral Efficacy**

The antiviral activity of the compounds determined to have  $IC_{50}$  values of  $<500$  nM will be determined in multiple rounds of replication inhibition assays comparable to a Phase I clinical study. The cytotoxicity of the newly synthesized molecules will also be evaluated prior to being subjected to the antiviral inhibition assay. Briefly, cells infected with HXB-2 or CEM-TART cells infected with HIV-1 MC99IIIB $\Delta$ Tat-Rev viral strains<sup>390</sup> will be added to uninfected cells and the extent of viral replication will be determined using commercially available ELISA kits. The  $EC_{50}$  will be determined by comparing the viral replication of cells exposed to synthesized inhibitors to no inhibitor control.

### 3.6 CONCLUSIONS AND FUTURE DIRECTIONS

The identification and characterization of HIV-1 as the causative pathogen of AIDS in 1984 triggered an enthusiastic effort to identify antiviral drugs capable of interrupting replication of the virus that in absence of therapeutic intervention represents a death sentence.<sup>391, 392</sup> HIV-1 encodes three enzymes that are required for viral replication: reverse transcriptase (RT), protease (PR) and integrase (IN). To date, there are 25 ARV drugs approved for the treatment of HIV-1 infection and AIDS. FDA-approved therapies target three steps of the HIV life cycle: reverse transcription, proteolytic maturation and fusion. Triple therapy, commonly referred to as highly active antiretroviral therapy (HAART) is the standard treatment for HIV. HAART consists of a protease inhibitor (PI) or a non-nucleoside reverse transcriptase inhibitor (NNRTI) in combination with two nucleoside reverse transcriptase inhibitors (NRTI.)<sup>86</sup> HAART, however, is often not well tolerated by patients, requires discipline, is expensive and leads to multidrug resistance and cross-resistance.<sup>86, 165, 393</sup> Despite the quantity of marketed antiretroviral HIV-1 drugs, there are only a limited number of mechanistic drug classes to build combinations from. HIV-1 exhibits poor fidelity of replication which eventually leads to the emergence of resistance viruses and treatment failure making the development of new inhibitors essential for continued therapy.

The third viral enzyme, IN, has emerged as an attractive target because it is necessary for stable infection and has no cellular human equivalent.<sup>86</sup> Substantial progress has been achieved since IN was first recognized as an important antiretroviral drug target. In October 2007, the FDA approved raltegravir, the first example of a drug active against IN, validated the enzyme as a new target in the field of anti-HIV drug research.<sup>227, 228, 394</sup> Over the last decade, a number of IN inhibitors have been discovered but many of these compounds are toxic, do not show antiviral

activity or display decreased potency. Therefore, new classes of potent IN inhibitors are desperately needed. The  $\beta$ -diketo ( $\beta$ -DK) class of compounds has emerged as one of the most successful classes of IN inhibitors. Although several  $\beta$ -DK inhibitors with potent antiviral activity are known, compounds containing  $\beta$ -DK motifs have limitations in drug development.

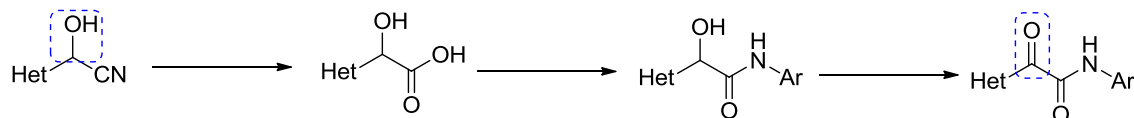
The overall objective of this dissertation was to design and synthesize a novel series of IN inhibitors that retain the favorable characteristics of the  $\beta$ -DK scaffolds but are devoid the “undruggable” properties. Several analogs proposed from crystal structure-based correlation and structure-activity relationship studies were synthesized during the course of this dissertation project. Many of the originally projected synthetic pathways to obtain these inhibitors, although initially appearing as reasonable routes, failed in the practical setting. These challenges led to the exploration of alternative chemistries and allowed us to gain new insight into alternative chemistries as a mechanism to synthesize several of the oxalamate scaffolds.

### **3.6.1. Alternative Strategy for the Synthesis of $\alpha$ , $\beta$ -diketo Amides**

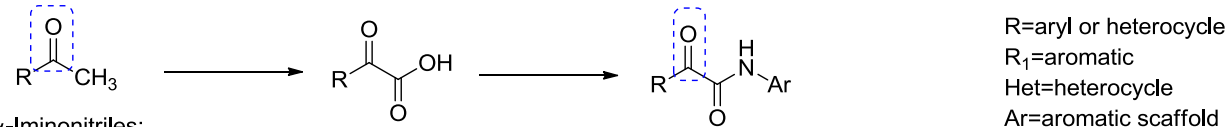
A common strategy employed for the synthesis of the majority of desired  $\alpha$ ,  $\beta$ -diketo amide desired compounds was to establish the  $\alpha$ -hydroxy or  $\alpha$ -carbonyl in the early stages of compound synthesis (Scheme 3.24). Although these routes seemed feasible originally, and several compounds were obtained through these methods, there were also several problems encountered when exploiting these synthetic routes. For example, the initial attempts to oxidize the  $\alpha$ -hydroxy functional group of  $\alpha$ -hydroxy acetic acids were not straightforward (Scheme 3.2), the anticipated Pd-catalyzed coupling of aryl bromides with diethyl phosphite failed due to the reactivity of the electrophilic  $\alpha$ -carbonyl functional group (Scheme 3.16), and hydrolysis of the  $\alpha$ -iminonitriles to provide diketo acids was unsuccessful because the hydrolysis reaction rate of

the  $\alpha$ -imino functional group was faster than that of the nitrile functional group (Scheme 3.11). A common theme observed with these unexpected difficulties was the involvement of the  $\alpha$ -hydroxy or  $\alpha$ -carbonyl functional group. In terms of optimizing and planning a more efficient synthetic route to obtain  $\alpha$ ,  $\beta$ -diketo amide derivatives the reactivity of the  $\alpha$ -functional groups was considered. An alternative synthetic route the observed byproduct (compounds **3.115** and **3.116**) isolated from the phosphonate coupling reaction and the challenges associated with the chemistries described above was to begin the synthesis without the  $\alpha$ -hydroxy or  $\alpha$ -carbonyl functional group in place and then oxidize to the  $\alpha$ -keto amides at a later step in the linear synthesis (Scheme 3.25 and 3.26).

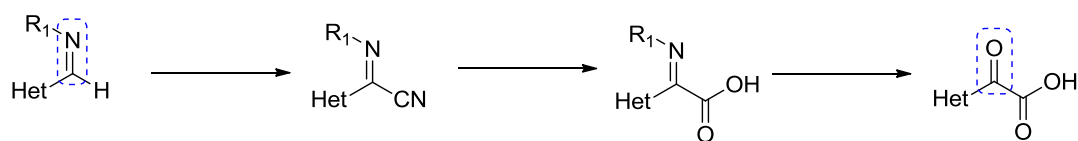
Cyanohydrin Chemistry:



Selenium Dioxide Oxidation:



$\alpha$ -Iminonitriles:

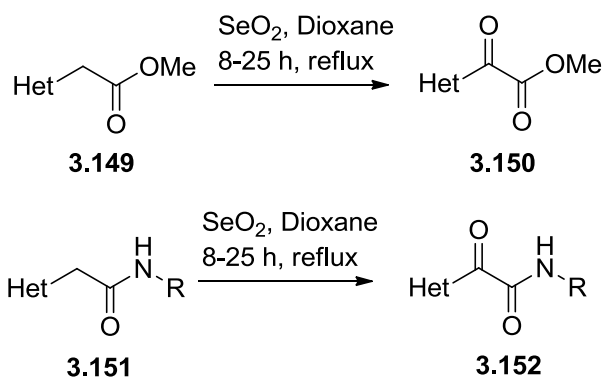


**Scheme 3.24** Summary of synthetic routes explored: establishing  $\alpha$ -hydroxy or  $\alpha$ -carbonyl early in synthesis

After reviewing the literature for chemistries that are concurrent with the new synthetic approach a few appealing synthetic opportunities were discovered. One option for the new synthetic route is to do a direct  $\alpha$ -oxidation of amides or esters using  $\text{SeO}_2$  as a metal oxidant.<sup>395-</sup>  
<sup>399</sup> This oxidation of the methylene group adjacent to the carbonyl using  $\text{SeO}_2$  is generally referred to as a Riley oxidation and this method has been reported previously with a variety of aromatic and heterocyclic scaffolds.<sup>395-399</sup> It would be beneficial to employ this reaction using

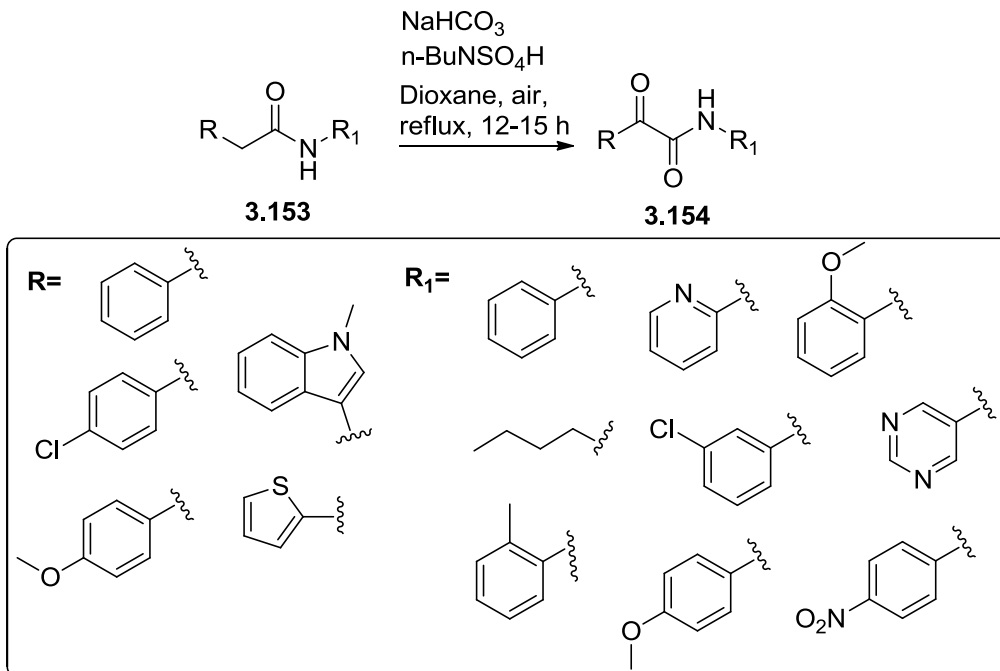


commercially available or easily synthesized aryl- or heteroarylacetamides or esters (Scheme 3.25).



**Scheme 3.25** Direct  $\alpha$ -oxidation of amides and esters using selenium dioxide

In 2012, Shao *et al.*<sup>400</sup> reported a simple synthetic route using a sodium bicarbonate promoted aerobic oxidation reaction to prepare  $\alpha$ -keto amides from easily available aryl- or heteroarylacetamides (Scheme 3.26). This method was explored on a variety of functionalized molecules that were tolerated and readily to give the corresponding  $\alpha$ -keto amides in good yields. The oxidation reaction was not limited to simple benzene-containing aromatics, substrates containing the substructure of naphthalene, pyrimidine, pyridine, and aliphatic chains also gave good yields. This route would potentially offer the ability to synthesize several structurally diverse compounds conveniently without the use of toxic reagents and harsh conditions.



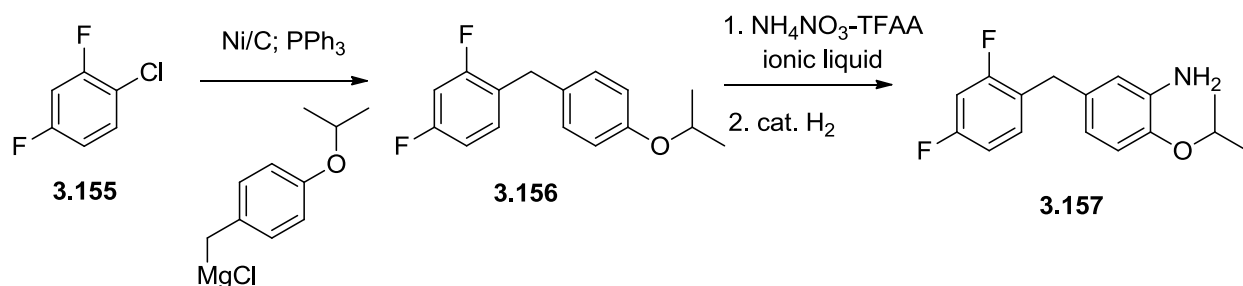
**Scheme 3.26** Sodium bicarbonate promoted aerobic oxidation reaction to prepare  $\alpha$ -keto amides

### 3.6.2. Synthetic Strategies for Alternative Aryl Scaffolds

The main focus of the compounds synthesized to date was to determine the SAR and role of the terminal functional group in regards to IN inhibition. Almost all of the compounds developed contained either an aniline or diphenylmethane as the aromatic functional group. One of the long term goals of this project is to develop analogues with “decorated” aromatic substituted scaffolds in place of the diphenylmethane scaffold (Figure 3.33). Preliminary data showed that substitutions on the phenyl and benzyl ring of diphenylmethane further increase the antiviral activity of compounds to nM activity (**3.7-3.9**, Table 3.2).

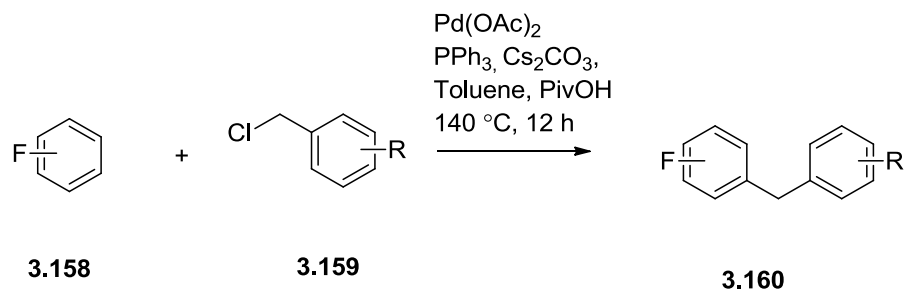
It was originally proposed that (2,4-difluoro-1-(4-isopropoxybenzyl)benzene) could be synthesized using a three-step protocol (Scheme 3.27). Initially, a Kumada coupling of 1-chloro-2,4-difluorobenzene (**3.155**) and the appropriate Grignard reagent using Ni/C catalyst to afford diaryl methane (**3.156**).<sup>401, 402</sup> Electrophilic nitration of **3.156** with ammonium nitrate/TFAA

utilizing the ionic liquid 3-methylimidazolium (emim) to produce the nitration product, and subsequent catalytic hydrogenation will afford aniline **3.157**.<sup>403</sup> However, initial attempts by the Rimoldi research group to synthesize **3.157** using this method were unsuccessful. Therefore, alternative routes to obtain substituted aryl scaffolds were considered.



**Scheme 3.27** Proposed synthetic route for 5-(2,4-difluorobenzyl)-2-isopropoxyaniline **3.157**

In 2010, Fan *et al.*<sup>404</sup> published an efficient and practical method to a wide range of perfluorinated unsymmetrical diarylmethanes with good to excellent yields and high regioselectivity using a direct Pd-catalyzed benzylation (Scheme 3.28). The most widely used approaches to this functional group array rely on cross-couplings of a stoichiometric amount of organometallic aryl with electrophiles.<sup>405</sup> However, this “prefunctionalization” process suffers from the requirement of additional steps for the preparation of organometallic reagents and the incompatibility of functional groups.<sup>404</sup> In this regard, direct benzylation of arenes and heteroarenes has been successfully discovered recently and this current method provides a method for the direct benzylation of highly electron-deficient perfluorenes with various functional groups.<sup>404, 406-408</sup> Collectively, these methods may provide access to a variety of substituted aromatic scaffolds.



**Scheme 3.28** Pd-catalyzed direct benzylation of fluoroarene **3.158** with various benzylchlorides **3.159**

### 3.6.3. Opportunities for Alternative Biological Targets

#### 3.6.3.1 p38 $\alpha$ Mitogen-Activated Protein Kinase Inhibitors

The p38 $\alpha$  mitogen-activated protein kinase (MAPK) is a serine-threonine protein kinase and is recognized as a highly attractive target for therapeutic intervention. It is well established the proinflammatory cytokines, tumor necrosis factor- $\alpha$  (TNF- $\alpha$ ) and interleukin-1 $\beta$  (IL- $\beta$ ), play an important role in the pathogenesis of various inflammatory diseases and that the stress-activated signal transduction pathway leading to these cytokines is in part regulated by p38 $\alpha$  MAPK.

Recent publications like that of Mavunkel *et al.*<sup>409</sup> report the design and synthesis of MAPK inhibitors based on 4-fluorobenzylpiperidine heterocyclic oxalyl amides (Figure 3.38). In 2008,

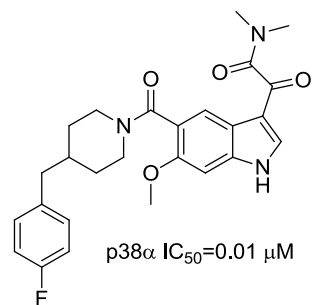


**Figure 3.38** Heterocyclic oxalyl amide MAPK inhibitor

Montalban *et al.*<sup>410</sup> identified a novel series of p38 $\alpha$  MAPK inhibitors through structure-based design and interestingly the  $\alpha$ -ketoamide series of compounds were examined for p38 $\alpha$  MAPK inhibition. Although, the representative molecule (Figure 3.39) only showed

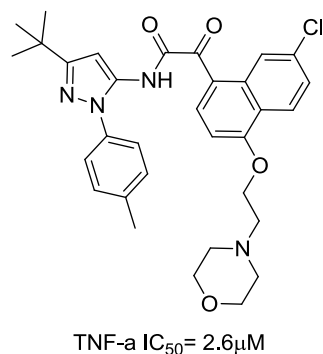


**Figure 3.39** Pyrazole  $\alpha$ -ketoamide derivative

moderate TNF- $\alpha$  inhibition it may eventually be used as a lead molecule towards the development of more potent p38 $\alpha$  MAPK inhibitors. Although the synthesized  $\alpha$ -ketoamides from this dissertation project were designed as HIV-1 IN inhibitors it would be interesting to examine the activity of the molecules as MAPK inhibitors, considering the similar structural features of the compound. Additionally, numerous studies have shown that the MAPK signal pathway can regulate the replication of HIV-1, but exactly how each MAPK pathway affects HIV-1 infection and replication is not fully understood.<sup>411</sup>

### 3.6.3.2 Inhibitors of HIV-1 Attachment

The interaction of HIV-1 surface glycoprotein gp120 with CD4, a glycoprotein receptor expressed in mammalian cells, is the critical first step of a series of several events that allows virus access to the host cells.<sup>71</sup> As mentioned previously in this dissertation with the synthesis of the indole glyoxamide derivatives, several structurally similar indole glyoxamides (**A**, Figure 3.36) were determined previously to inhibit an early event in HIV infection. These inhibitors were subsequently shown to be interfering with the binding of HIV-1 gp120 to the host-cell receptor CD4.<sup>379, 380</sup> With the apparent similarities of the indole glyoxamide HIV-1 attachment inhibitors and the  $\alpha$ ,  $\beta$ -diketo amides class of compounds, it is likely that the synthetic analogs of this dissertation project may possess inhibitory activity against HIV-1 attachment.

## IV. EXPERIMENTAL

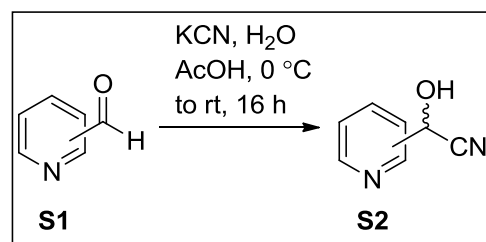
### General Methods:

Moisture and oxygen sensitive reactions were carried out in flame-dried glassware under an inert argon atmosphere. Anhydrous tetrahydrofuran (THF), diethyl ether (Et<sub>2</sub>O), and 1,4-dioxane were distilled over sodium metal in the presence of benzophenone indicator. Anhydrous dichloromethane (DCM, CH<sub>2</sub>Cl<sub>2</sub>), acetonitrile (AcN) and toluene were distilled over calcium hydride (CaH<sub>2</sub>). All commercially available starting materials and reagents were purchased at the highest commercial quality and used without further purification, unless otherwise noted. Reactions were monitored by thin-layer chromatography (TLC) carried out on 225 μm aluminum backed TLC sheets coated with silica gel 60 F254 (EMD Chemicals Inc. Gibbstown, NJ, USA). TLCs were visualized under UV (254 nm) and by staining with either *p*-anisaldehyde, phosphomolybdic acid (PMA), iodine, or Dragendorff's reagent. NMR spectra were recorded at room temperature on Bruker Avance DRX 400 (400 MHz) and DRX 500 (400 MHz) spectrometers. The following abbreviations were used to explain the multiplicities: s = singlet, d = doublet, t = triplet, q = quartet and m = multiplet. Infrared (IR) spectra were recorded on Bruker Vector 33 FT-IR spectrometer. Electrospray ionization (ESI) mass spectrometry (MS) experiments were performed on a Waters Micromass ZQ single quadrupole mass spectrometer. High-resolution mass spectra (HR-MS) were recorded using a Waters Micromass quadrupole time of flight (Q-TOF) micro mass spectrometer. High-performance liquid chromatography liquid chromatography (HPLC) analysis was conducted using a Waters Delta Prep 4000 System with a 77725I Rheodyne injector, a Waters 2487 Dual Wavelength Absorbance Detector, and an

XTerra™ MS C18 5  $\mu\text{m}$  4.6 x 100 mm column. Elemental Analysis was obtained using a PerkinElmer 2400 Series II CHNS/O Analyzer.

### General Procedure for the Synthesis of 2-, 3- and 4-pyridineacetonitriles (S2):

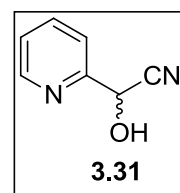
Using an adapted procedure from Sauerberg *et al.*,<sup>300</sup> to a solution of potassium cyanide (KCN) (1.33 g, 0.0205 mol, 1.10 eq) in water (8.39 mL) was added pyridinecarboxaldehyde **S1** (2.0 g, 0.0187 mol, 1.0 eq)



over 30 minutes at 5-10 °C. To the reaction mixture was added AcOH (1.17 mL, 0.0205 mol, 1.10 eq) over 30 minutes at 5-10 °C. The reaction mixture was stirred at room temperature for 16 hours and then cooled to 0 °C. The precipitate was filtered using a Buchner funnel and the 2-, 3- and 4-pyridineacetonitriles (**S2**) solid products were collected, washed with cold water and used immediately. **CAUTION:** potassium cyanide is highly toxic. Care should be taken when handling this reagent.<sup>412</sup>

### 2-Pyridineacetonitrile, $\alpha$ -hydroxy- (**3.31**)

Synthesized using the general procedure described for **S2**. Light yellow solid (41% crude yield);  $R_f$  = 0.30 (50:50 EtOAc: hexanes);  $^1\text{H NMR}$  (400 MHz, DMSO)  $\delta$  8.59 (d,  $J$  = 3.2 Hz, 1H), 7.90 (t,  $J$  = 7.7 Hz, 1H), 7.58 (d,  $J$  = 7.8 Hz,



1H), 7.45 – 7.39 (m, 1H), 5.81 (s, 1H);  $^{13}\text{C NMR}$  (101 MHz, DMSO)  $\delta$  156.39, 149.35, 137.60, 123.93, 120.72, 120.38, 63.74; **DEPT-135** 101 MHz, DMSO)  $\delta$  149.54, 138.09, 124.39, 121.02, 64.12; **ESI+ MS:**  $m/z$  134  $[\text{MH}]^+$ .

### 3-Pyridineacetonitrile, $\alpha$ -hydroxy- (3.32)

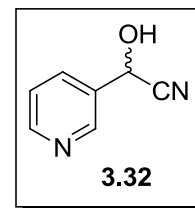
Synthesized using the general procedure described for **S2**. Pale yellow crystalline solid (67 % crude yield);  $R_f$  = 0.30 (50:50 EtOAc: hexanes);  $^1\text{H}$

**NMR** (400 MHz, DMSO)  $\delta$  8.72 (s, 1H), 8.63 (s, 1H), 7.93 (d,  $J$  = 5.2 Hz,

1H), 7.51 (s, 1H), 7.30 (s, 1H), 5.90 (s, 1H);  $^{13}\text{C}$  **NMR** (101 MHz, DMSO)  $\delta$  150.54, 148.12,

134.77, 133.42, 124.33, 120.41, 60.45; **DEPT-135** (101 MHz, DMSO)  $\delta$  150.55, 148.13, 134.79,

124.34, 60.45; **ESI+ MS**:  $m/z$  134  $[\text{MH}]^+$ .



### 4-Pyridineacetonitrile, $\alpha$ -hydroxy- (3.33)

Synthesized using the general procedure described for **S2**. Light orange-pink clay-like solid (81% crude yield);  $R_f$  = 0.30 (50:50 EtOAc: hexanes);  $^1\text{H}$  **NMR**

(400 MHz, DMSO)  $\delta$  8.65 (d,  $J$  = 4.9 Hz, 2H), 8.53 (d,  $J$  = 4.9 Hz, 1H), 7.53 (d,

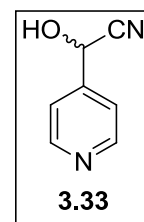
$J$  = 5.0 Hz, 2H), 7.39 (d,  $J$  = 4.9 Hz, 2H), 5.48 (s, 1H), 4.79 (s, 1H);  $^{13}\text{C}$  **NMR** (101 MHz,

DMSO)  $\delta$  150.92, 150.62, 150.04, 149.19, 148.45, 123.68, 123.25, 121.72, 121.37, 119.75,

76.92, 76.66; **DEPT-135** (101 MHz, DMSO)  $\delta$  150.91, 150.60, 150.03, 149.54, 149.18, 149.01,

123.67, 123.24, 123.17, 122.47, 121.76, 121.71, 121.36, 76.66, 76.30; **ESI+ MS**:  $m/z$  135

$[\text{MH}]^+$ .

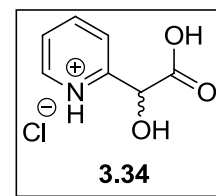


### 2-Pyridineacetic acid, $\alpha$ -hydroxy-, hydrochloride (3.34)

Using an adapted procedure from Ward *et al.*,<sup>308</sup> a suspension of crude cyanohydrin **3.31** (500 mg, 3.73 mmol) in 5 mL of concentrated HCl was

refluxed for 15 hours. The concentrated HCl was removed under reduced pressure (0.03 mmHg)

with slight heating (60 °C). The residue was washed with water and the water was removed

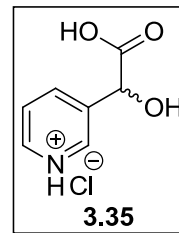




under reduced pressure (0.03 mmHg) with slight heating (60 °C) to yield **3.34** as an orange-brown solid powder (96% crude yield). No further purification was used; **ESI+ MS**:  $m/z$  153  $[MH]^+$ ; **ESI- MS**:  $m/z$  151  $[M-H]^-$ .

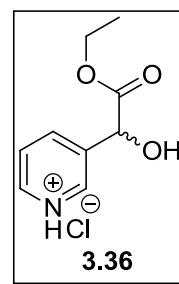
### 3-Pyridineacetic acid, $\alpha$ -hydroxy-, hydrochloride (**3.35**)

Using an adapted procedure from Ward *et al.*,<sup>308</sup> a suspension of crude cyanohydrin **3.32** (500 mg, 3.73 mmol) in 5 mL of concentrated HCl was refluxed for 15 hours. The concentrated HCl was removed under reduced pressure (0.03 mmHg) with slight heating (60 °C). The residue was washed with water and the water was removed under reduced pressure (0.03 mmHg) with slight heating (60 °C) to yield **3.35** as a pale yellow solid (63% crude yield). No further purification was used.; **<sup>1</sup>H NMR** (400 MHz, D<sub>2</sub>O)  $\delta$  8.94 (s, 1H), 8.79 (d,  $J = 5.6$  Hz, 1H), 8.74 (d,  $J = 8.2$  Hz, 1H), 8.12 (dd,  $J = 7.9, 6.1$  Hz, 1H), 5.65 (s, 1H); **<sup>13</sup>C NMR** (101 MHz, D<sub>2</sub>O)  $\delta$  173.46, 145.03, 140.83, 139.43, 139.07, 127.34, 69.33; **DEPT-135** (101 MHz, D<sub>2</sub>O)  $\delta$  145.03, 140.84, 139.43, 127.34, 69.33. **ESI+ MS**:  $m/z$  154 $[MH]^+$ ; **ESI- MS**:  $m/z$  151  $[M-H]^-$ .



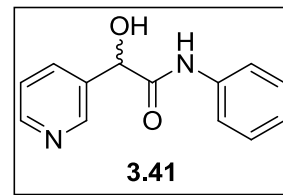
### 3-Pyridineacetic acid, $\alpha$ -hydroxy-, ethyl ester, hydrochloride (**3.36**)

Using an adapted procedure from Ward *et al.*,<sup>308</sup> and Baeza *et al.*,<sup>302</sup> to a solution of crude cyanohydrin **3.32** (500 mg, 3.73 mmol) in ethanol (11 mL) and water (11 mL) was slowly added concentrated HCl (22 mL). The reaction flask was fitted with a reflux condenser and refluxed for 15 hours. The solvents were removed under reduced pressure (0.03 mmHg) with slight heating (50-60 °C) to yield **3.36** as a white solid (91% crude yield). No further purification was used; **ESI+ MS**:  $m/z$  181  $[MH]^+$ .



### 2-hydroxy-N-phenyl-2-(pyridin-3-yl) acetamide (3.41)

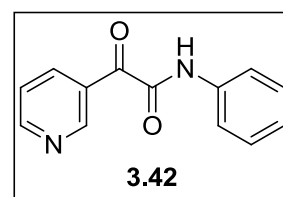
Using a modified procedure from Martyn *et al.*,<sup>306</sup> to a mixture of crude **3.35** (250 mg, 1.33 mmol, 1.0 eq) and freshly distilled aniline (0.134 mL, 1.47 mmol, 1.1 eq) in anhydrous DCM (14 mL) was added



1-(3-dimethylaminopropyl)-3-ethylcarbodiimide hydrochloride (331.80 mg, 1.73 mmol, 1.3eq) and 1-hydroxybenzotriazole hydrate (HOBT) (269.6 mg, 1.96 mmol, 1.5 eq) at room temperature. The reaction mixture was yellow and cloudy in appearance. *N,N*-Diisopropylethylamine (0.256 mL, 1.47 mmol, 1.1 eq) was added dropwise and the reaction mixture stirred at room temperature for 18 hours. The reaction was quenched with H<sub>2</sub>O (5 mL) and stirred for 30 minutes at room temperature. The solution was diluted with DCM (10 mL), washed with 1N HCl (3 x 10 mL), water (3 x 10 mL), and the combined aqueous washings were back-extracted with fresh DCM (3 x 10 mL). The combined organic fractions were dried over Na<sub>2</sub>SO<sub>4</sub> and the solvent was removed *in vacuo* to afford crude product. Flash-column chromatography on silica using a gradient of 10:90 EtOAc:Hexanes to 100% EtOAc followed by 10:90 MeOH:EtOAc afforded **3.41** as a brown “caramel-color” sticky oil (110.3 mg, 36%); **R<sub>f</sub>** = 0.34 (10:90 MeOH:EtOAc; stains white with anisaldehyde/orange spot with Dragendorff reagent); **<sup>1</sup>H NMR** (400 MHz, CDCl<sub>3</sub>); **<sup>13</sup>C NMR** (101 MHz, CDCl<sub>3</sub>); **DEPT-135** (101 MHz, CDCl<sub>3</sub>); **ESI+ MS**: *m/z* 229 [MH]<sup>+</sup>; **ESI- MS**: *m/z* 227 [M-H]<sup>-</sup>.

### 2-oxo-N-phenyl-2-(pyridin-3-yl) acetamide (3.42)

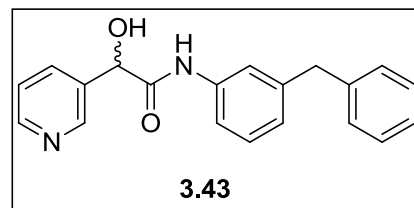
Using a modified procedure from Bou-Hamdan *et al.*,<sup>312</sup> to a solution of **3.41** (24.3 mg, 0.107 mmol, 1.0 eq) in anhydrous DCM (1 mL) was added MnO<sub>2</sub> (93.03 mg, 1.07 mmol, 10 eq) and the mixture was stirred



at room temperature for 1 hour. The mixture was filtered through a short pad of silica gel and the silica layer was washed with fresh DCM (20 mL). Concentration of the filtrate afforded 24 mg (**quant. yield**) of **3.42** as a solid; **ESI+ MS**:  $m/z$  227 [MH]<sup>+</sup>.

### N-(3-benzylphenyl)-2-hydroxy-2-(pyridin-3-yl) acetamide (**3.43**)

Using a modified procedure from Martyn *et al.*,<sup>306</sup> to a mixture of crude **3.35** (132.9 mg, 0.703 mmol, 1.0 eq) and 3-benzylaniline (141.66 mg, 0.773, 1.1 eq) in anhydrous DCM

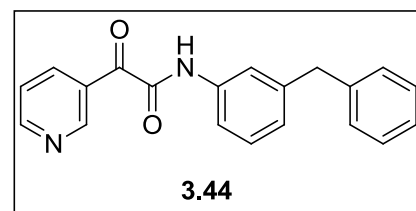


(9.52 mL) was added 1-(3-dimethylaminopropyl)-3-ethylcarbodiimide hydrochloride (175.29 mg, 0.914 mmol, 1.3eq) and 1-hydroxybenzotriazole hydrate (HOBT) (142.43 mg, 1.054 mmol, 1.5 eq) at room temperature. The reaction mixture was an orange-pink color. N, N-Diisopropylethylamine (0.202 mL, 1.15 mmol, 1.65 eq) was added dropwise (reaction mixture became yellow in color) and the reaction mixture stirred at room temperature for 24 hours. The reaction was quenched with H<sub>2</sub>O (5 mL) and stirred for 30 minutes at room temperature. The solution was diluted with DCM (10 mL), washed with 1N HCl (3 x 10 mL), water (3 x 10 mL), and the combined aqueous washings were back-extracted with fresh DCM (3 x 10 mL). The combined organic fractions were dried over Na<sub>2</sub>SO<sub>4</sub> and the solvent was removed *in vacuo* to afford crude product. Flash-column chromatography on silica using a gradient of 10:90 EtOAc:Hexanes to 100% EtOAc afforded **3.43** as a pale yellow sticky oil (54 mg, 24%); **R<sub>f</sub>** = 0.53 (100% EtOAc; stains white with anisaldehyde/orange spot with Dragendorff reagent); **<sup>1</sup>H NMR** (400 MHz, CDCl<sub>3</sub>) δ 8.92 (s, 1H), 8.49 (s, 1H), 8.33 (d, *J* = 3.6 Hz, 1H), 7.87 (d, *J* = 7.8 Hz, 1H), 7.47 – 7.35 (m, 3H), 7.30 – 7.13 (m, 5H), 6.95 (d, *J* = 7.4 Hz, 1H), 5.15 (s, 1H), 3.92 (s, 2H); **<sup>13</sup>C NMR** (101 MHz, CDCl<sub>3</sub>) δ 169.64, 148.23, 147.15, 142.29, 140.72, 137.16, 136.37,

135.56, 129.19, 128.91, 128.53, 126.22, 125.44, 124.00, 120.25, 117.62, 71.76, 41.86; **DEPT-135** (101 MHz, CDCl<sub>3</sub>)  $\delta$  148.23, 147.15, 135.56, 129.19, 128.91, 128.53, 126.22, 125.44, 123.99, 120.25, 117.62, 71.76, 41.86; **ESI- MS**:  $m/z$  317 [M-H]<sup>-</sup>.

#### **N-(3-benzylphenyl)-2-oxo-2-(pyridin-3-yl) acetamide (3.44)**

Using a modified procedure from Bou-Hamdan *et al.*,<sup>312</sup> to a solution of **3.43** (17.5 mg, 1.0 eq, 0.0550) in anhydrous DCM (1 mL) was added freshly prepared MnO<sub>2</sub> (119 mg, 25 eq,

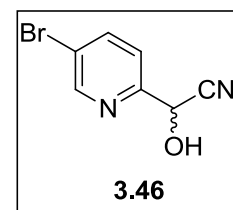


1.375 mmol) and the mixture was stirred at room temperature for 16 hours. The mixture was filtered through a short pad of silica gel and the silica layer was washed with fresh DCM.

Concentration of the filtrate afforded 17 mg (quant yield) of **3.42** as a yellow solid residue; **R<sub>f</sub>** = 0.75 (100% EtOAc); <sup>1</sup>H NMR (400 MHz, DMSO)  $\delta$  10.90 (s, 1H), 9.22 (s, 1H), 8.88 (s, 1H), 8.43 (d,  $J$  = 7.2 Hz, 1H), 7.38 – 7.14 (m, 10H), 3.97 (s,  $J$  = 22.7 Hz, 2H).; **ESI- MS**:  $m/z$  315 [M-H]<sup>-</sup>.

#### **2-(5-bromopyridin-2-yl)-2-hydroxyacetonitrile (3.46)**

Using an adapted procedure from Sauerberg *et al.*,<sup>300</sup> to a solution of KCN (192.34 mg, 2.959 mmol, 1.10 eq) in water (2.08 mL) was added 5-bromopyridine-2-carboxaldehyde (500 mg, 2.69 mmol, 1.0 eq) over 30

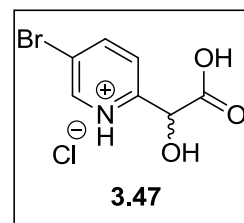


minutes at 5-10 °C. To the reaction mixture was added AcOH (0.169 mL, 2.959 mmol, 1.10 eq) over 30 minutes at 5-10 °C. The reaction mixture was stirred at room temperature for 16 hours. After 16 hours, the reaction mixture was cooled to 0°C and the solids were collected via vacuum filtration in a Buchner funnel to afford **3.46** as a yellow-brown golden solid (575 mg,

quantitative crude yield) Compound **3.46** was used immediately without any additional purification. ESI- MS:  $m/z$  124 [M-H]<sup>-</sup>.

### 2-Pyridineacetic acid, 5-bromo- $\alpha$ -hydroxy-, hydrochloride (**3.47**)

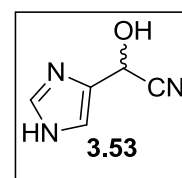
Using a modified procedure from Baeza *et al.*,<sup>302</sup> compound **3.46** (515 mg, 2.417 mmol) was dissolved in a 1.5:1 mixture of EtOH:H<sub>2</sub>O (5 mL) at room temperature. To this mixture was slowly added concentrated HCl (5



mL). The reaction flask was fitted with a reflux condenser and refluxed for 24 hours. The reaction was cooled to room temperature and neutralized with saturated NaHCO<sub>3</sub> (pH ~6). The aqueous mixture was extracted with EtOAc (3 x 20 mL) and the organic layers were combined, dried over Na<sub>2</sub>SO<sub>4</sub> and concentrated *in vacuo* to afford crude **3.47** as a red-brown solid (253.1 mg, 45% crude yield). No further purification was used. ESI+ MS:  $m/z$  253, 252 [MH]<sup>+</sup>.

### 1H-Imidazole-4-acetonitrile, $\alpha$ -hydroxy- (**3.53**)

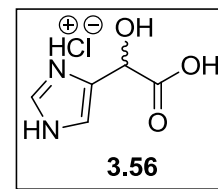
Using an adapted procedure from Sauerberg *et al.*,<sup>300</sup> to a solution of KCN (372.74 mg, 5.724 mmol, 1.10 eq) in water (2.094 mL) was added imidazole-4-carboxaldehyde (500 mg, 5.203 mmol, 1.0 eq) over 30 minutes at 5-10 °C.



To the reaction mixture was added AcOH (0.327 mL, 5.724 mmol, 1.10 eq) over 30 minutes at 5-10 °C. The reaction mixture was stirred at 0 °C for 18 hours. After 18 hours, the solvents were removed under reduced pressure (0.03 mmHg) with slight heating (45 °C) to afford **3.53** as orange-yellow solid (598 mg, 85% crude yield). Compound **3.53** was used immediately without any additional purification. ESI- MS:  $m/z$  124 [M-H]<sup>-</sup>.

### 1*H*-Imidazole-4-acetic acid, $\alpha$ -hydroxy-(3.56)

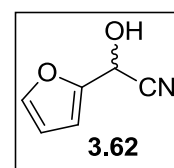
Using an adapted procedure from Ward *et al.*,<sup>308</sup> to a suspension of crude cyanohydrin **3.53** (540 mg, 4.38 mmol) in 10 mL of EtOH: H<sub>2</sub>O (5mL:5mL) was slowly added 10 mL of concentrated HCl. The reaction



flask was fitted with a reflux condenser and refluxed for 16 hours. The concentrated HCl was removed under reduced pressure (0.03 mmHg) with slight heating (50 °C). The residue was washed with water and the water was removed under reduced pressure (0.03 mmHg) with slight heating (50 °C) to yield **3.56** as a pale yellow solid (600.4 mg, 79% crude yield). No further purification was used. <sup>1</sup>H NMR (400 MHz, MeOD)  $\delta$  8.91 (d,  $J$  = 1.4 Hz, 1H), 7.55 (s, 2H), 5.42 (d,  $J$  = 0.8 Hz, 2H); <sup>1</sup>H NMR (400 MHz, DMSO)  $\delta$  9.12 (s, 1H), 7.64 (s, 1H), 5.32 (s, 1H); <sup>13</sup>C NMR (101 MHz, DMSO)  $\delta$  171.80, 134.60, 132.42, 116.93, 64.76; DEPT-135 (101 MHz, DMSO)  $\delta$  134.59, 116.92, 64.75; ESI- MS:  $m/z$  140 [M-H]<sup>-</sup>.

### 2-Furanacetonitrile, $\alpha$ -hydroxy-(3.62)

Using an adapted procedure from Felfer *et al.*,<sup>314</sup> trimethylsilyl cyanide (TMSCN) (0.333 mL, 2.496 mmol, 1.2 eq) was added to freshly distilled furfural (0.172 mL, 2.08 mmol, 1.0 eq) in anhydrous DCM at 0 °C. After the



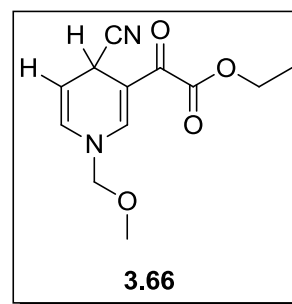
addition of a few crystals of ZnBr the reaction was stirred at 0 °C for 15 minutes before it was allowed to warm to room temperature. The reaction stirred for 45 minutes at room temperature. The TMS protected cyanohydrin was subjected to acid-hydrolysis by the addition of 3N HCl (3.75 g) at 0 °C. The mixture was stirred for 1 hour at room temperature. The crude reaction mixture was extracted with ether (3 x 20 mL), combined, dried over Na<sub>2</sub>SO<sub>4</sub> and concentrated *in vacuo* to afford crude product as an orange yellow oil (307.1 mg, quantitative crude yield); **R<sub>f</sub>**=

0.71 (50:50 EtOAc: hexanes);  $^1\text{H NMR}$  (400 MHz,  $\text{CDCl}_3$ )  $\delta$  7.59 – 7.39 (m, 1H), 6.59 (d,  $J$  = 3.3 Hz, 1H), 6.42 (dd,  $J$  = 3.3, 1.9 Hz, 1H), 5.55 (s, 1H), 3.80 (s, 1H).

### Ethyl 4-cyano-1-methoxymethyl-1, 4-dihydro-3-pyridineglyoxylate (3.66)

#### Preparation of Benzyltrimethylammonium Cyanide ( $\text{BnMe}_3\text{N}^+\text{CN}^-$ ):

was prepared according to a procedure by Vedejs and Monahan<sup>413</sup> with modification. Benzyltrimethylammonium chloride (1.33 grams, 7.18 mmol) was dried at 0.5 mmHg vacuum and dissolved in anhydrous MeOH (1.67 mL). The resulting solution was transferred *via* syringe into a stirring



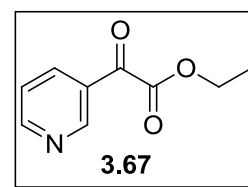
solution of NaCN (525 mg, 10.71 mmol) in 10 mL of anhydrous MeOH. After stirring for 30 minutes at room temperature, the white suspension was carefully concentrated by rotary evaporation with minimal exposure to atmospheric moisture. The white residue was treated with 10 mL of hot anhydrous AcN and the resulting suspension was filtered hot through a fritted glass filter under argon. The filtrate was carefully concentrated by rotary evaporation at room temperature to dryness and collected and dried under reduced pressure (0.03 mmHg) to yield white hygroscopic crystals (373.10 mg, 29%).

Using an adapted procedure from Klapars and Vedejs,<sup>323</sup> to a solution of anhydrous pyridine (0.33 mL, 4.08 mmol) in 10 mL of anhydrous  $\text{CHCl}_3$  at room temperature was added methoxymethyl chloride (0.34 mL, 4.48 mmol). After stirring at room temperature for 1 hour, the colorless solution was transferred via syringe into a 50 mL flame-dried round bottom flask charged with  $\text{BnMe}_3\text{N}^+\text{CN}^-$  (660 mg, 3.74 mmol). The resulting clear solution was cooled in an ice-bath to 0 °C, and diisopropylethylamine (0.80 mL, 4.59 mmol) was added followed by ethyl oxalyl chloride (0.48 mL, 4.30 mmol). After stirring at 0 °C for 1 hour, the orange solution was

poured into 50 mL of ether and washed with 2 x 20 mL of H<sub>2</sub>O. The bright yellow organic layer was dried over Na<sub>2</sub>SO<sub>4</sub> and concentrated by rotary evaporation to give crude dihydropyridine **3.66**, which was used immediately in the next step without further purification. Yellow-orange oil; **R<sub>f</sub>** = 0.47 (50:50 acetone:hexanes); **<sup>1</sup>H NMR** (400 MHz, CDCl<sub>3</sub>) δ 7.98 (s, 1H), 6.26 (d, *J* = 7.9 Hz, 1H), 5.20 (dd, *J* = 7.9, 4.5 Hz, 1H), 4.64 (s, 2H), 4.60 (d, *J* = 4.5 Hz, 1H), 4.35 (d, *J* = 7.1 Hz, 2H), 3.36 (s, 3H), 1.39 (t, *J* = 7.1 Hz, 3H); **ESI+ MS**: *m/z* 251 [MH]<sup>+</sup>.

### 3-Pyridineacetic acid, $\alpha$ -oxo-, ethyl ester (**3.67**)

The crude dihydropyridine **3.66** was dissolved in anhydrous AcN (5 mL, including syringe washings), and the solution was transferred *via* syringe into a 25 mL round bottom flask charged with ZnCl<sub>2</sub> (1.05g, 7.70 mmol).

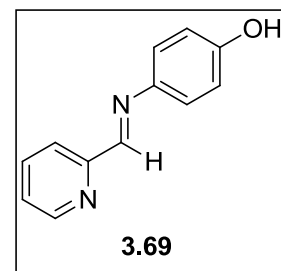


After stirring at room temperature for 5 hours, the yellow suspension was filtered through Celite eluting 2 x 2 mL of anhydrous AcN. Anhydrous EtOH (10 mL) was added to the filtrate, the resulting tan solution was refluxed for 15 hours, cooled to room temperature, and poured into 10% aqueous solution of NaHCO<sub>3</sub> (20 mL) at 0°C (ice-bath). The resulting suspension was filtered through Celite eluting with 2 x 10 mL of EtOH. The tan filtrate was extracted with DCM (3 x 30 mL). The combined organic phase was dried over Na<sub>2</sub>SO<sub>4</sub>, concentrated by rotary evaporation, and the orange-red residue was purified by flash chromatography on silica gel using 4:1 hexanes:acetone to yield **3.67** yellow solid (147.2 mg, 82%); **<sup>1</sup>H NMR** (400 MHz, CDCl<sub>3</sub>) δ 9.26 (d, *J* = 1.7 Hz, 1H), 8.86 (dd, *J* = 4.8, 1.6 Hz, 1H), 8.37 (d, *J* = 8.0 Hz, 1H), 7.61 – 7.37 (m, 1H), 4.48 (q, *J* = 7.1 Hz, 2H), 1.43 (dd, *J* = 23.4, 16.3 Hz, 3H); **ESI+ MS**: *m/z* 359 [M+MH]<sup>+</sup>.



### Phenol, 4-[(2-pyridinylmethylene) amino] - (3.69)

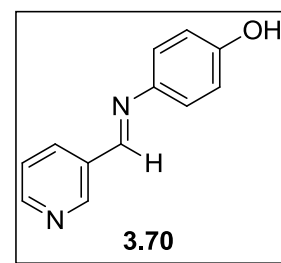
Using an adapted procedure from Jursic *et al.*,<sup>338</sup> a mixture of 2-pyridine-carboxaldehyde (0.446 mL, 500 mg, 4.66 mmol) and 4-aminophenol (509 mg, 4.66 mmol) in methanol (93 mL) was refluxed for 2 hours. The solvent was reduced to 1/10 of its original volume (~10



mL). The resulting suspension was cooled in an ice-water bath. The bright yellow crystalline solid was separated by filtration, washed with cold methanol (3x10 mL) and dried under high-vacuum to afford **3.69** (687.2 mg, 74 %). No further purification was needed for the next step.  $R_f$  = 0.30 (50:50 EtOAc: hexanes);  $^1\text{H NMR}$  (400 MHz, DMSO)  $\delta$  9.67 (s, 1H), 8.70 (d,  $J$  = 4.6 Hz, 1H), 8.62 (s, 1H), 8.14 (d,  $J$  = 7.9 Hz, 1H), 7.92 (dd,  $J$  = 11.0, 4.2 Hz, 1H), 7.49 (dd,  $J$  = 6.8, 5.4 Hz, 1H), 7.32 (d,  $J$  = 8.7 Hz, 2H), 6.86 (d,  $J$  = 8.7 Hz, 2H);  $^{13}\text{C NMR}$  (101 MHz, DMSO)  $\delta$  157.53, 157.40, 155.02, 149.99, 141.97, 137.32, 125.50, 123.40, 121.14, 116.29; **DEPT-135** (101 MHz, DMSO)  $\delta$  157.40, 149.99, 137.32, 125.51, 123.40, 121.14, 116.29; **ESI+ MS**:  $m/z$  199  $[\text{MH}]^+$ .

### Phenol, 4-[(3-pyridinylmethylene) amino] - (3.70)

Prepared by the procedure described for **3.69**. Pale yellow fluffy solid (8.55 g, 92 %)  $R_f$  = 0.37 (70:30 EtOAc: hexanes);  $^1\text{H NMR}$  (400 MHz, DMSO)  $\delta$  9.59 (s, 1H), 9.03 (d,  $J$  = 1.5 Hz, 1H), 8.70 (s, 1H), 8.67 (dd,  $J$



= 4.7, 1.5 Hz, 1H), 8.27 (dd,  $J$  = 7.9, 1.7 Hz, 1H), 7.52 (dd,  $J$  = 7.8, 4.8 Hz, 1H), 7.26 (d,  $J$  = 8.7 Hz, 2H), 6.83 (d,  $J$  = 8.7 Hz, 2H);  $^{13}\text{C NMR}$  (101 MHz, DMSO)  $\delta$  157.14, 155.14, 151.79, 150.48, 142.64, 134.95, 132.41, 124.42, 123.14, 116.18; **DEPT-135** (101 MHz, DMSO)  $\delta$  155.15, 151.80, 150.50, 134.96, 124.43, 123.16, 116.20; **ESI+ MS**:  $m/z$  199  $[\text{MH}]^+$ .

### Phenol, 4-[(4-pyridinylmethylene) amino] - (3.71)

Prepared by the procedure described for **3.69**. Gold-yellow solid (7.11 g,

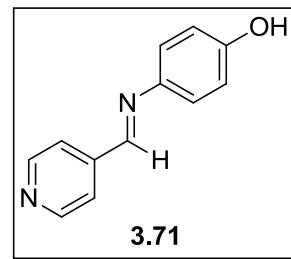
76%)  $R_f = 0.28$  (70:30 EtOAc: Hexanes);  $^1\text{H NMR}$  (400 MHz, DMSO)

$\delta$  9.69 (s, 1H), 8.72 (d,  $J = 5.7$  Hz, 2H), 8.68 (s, 1H), 7.81 (d,  $J = 5.8$  Hz,

2H), 7.31 (d,  $J = 8.6$  Hz, 2H), 6.85 (d,  $J = 8.6$  Hz, 2H);  $^{13}\text{C NMR}$  (101

MHz, DMSO)  $\delta$  157.68, 155.55, 150.80, 143.45, 142.04, 123.53, 122.32, 116.26; **DEPT-135**

(101 MHz, DMSO)  $\delta$  155.55, 150.80, 123.53, 122.32, 116.26; ; **ESI+ MS**:  $m/z$  199  $[\text{MH}]^+$ .



### 4-Pyridineacetonitrile, $\alpha$ -[(4-hydroxyphenyl) imino] - (3.77)

Using an adapted procedure from Jursic *et al.*,<sup>338</sup> a DMSO (20 mL)

solution of **3.71** (600 mg, 3.02 mmol) and sodium cyanide (162.8 mg,

3.32 mmol) stirred at room temperature for 24 hours. In the first 5

minutes, the solution went from yellow to orange then to deep red. After 24 hours at room

temperature, the DMSO was evaporated at reduced pressure (0.03 mmHg) with slight heating

(60 °C). A dark burgundy residue remained which was then dissolved in THF (slight heating 40-

50 °C was needed). The solution was immediately filtered through a pad of silica gel in a fritted

Buchner funnel and washed with fresh THF (6 x 50 mL). Immediately it was noted that a bright

orange solid was crashing out of the THF solution. The combined THF filtrates were evaporated

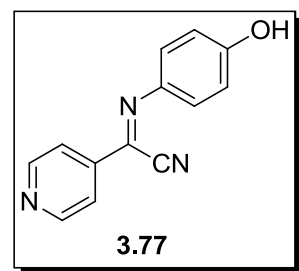
to a solid. The solid residue was slurred in MeOH (50 mL) and the resulting suspension was

heated at 50 °C for 10 minutes, cooled down in an ice-water bath and the fluorescent-orange

solid was collected by vacuum filtration and washed with ice-cold MeOH (3x20 mL) and dried

under high-vacuum to afford **3.77** (381 mg, 56 %). No further purification was needed for the

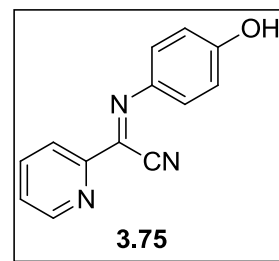
next step.;  $R_f = 0.60$  (70:30 EtOAc: hexanes; stains bright yellow with *p*-anisaldehyde);  $^1\text{H}$



**NMR** (400 MHz, DMSO)  $\delta$  10.16 (s, 1H), 8.94 – 8.68 (m, 2H), 8.12 – 7.69 (m, 2H), 7.43 (d,  $J$  = 8.8 Hz, 2H), 6.94 (d,  $J$  = 8.8 Hz, 2H);  **$^{13}\text{C}$  NMR** (101 MHz, DMSO)  $\delta$  159.37, 151.18, 141.20, 139.68, 133.65, 124.75, 121.21, 116.41, 112.10; **DEPT-135** (101 MHz, DMSO)  $\delta$  151.18, 124.75, 121.21, 116.42. **ESI+ MS**:  $m/z$  224 [MH] $^+$ .

### 2-Pyridineacetonitrile, $\alpha$ -[(4-hydroxyphenyl) imino] - (3.75)

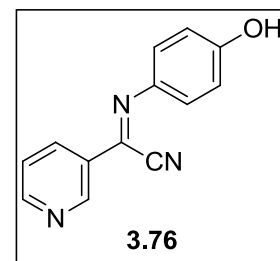
Prepared by the procedure described for **3.77**, with modification of the purification method. Unlike previously reported, no solid residue formed to be filtered and collected as product. Therefore, the MeOH solution was concentrated *in vacuo* to afford crude product. Purification was



achievable via flash-column chromatography (20:80 to 50:50 EtOAc: Hexanes) to yield bright yellow solid “saw dust” (95.4 mg, 42 %)  $R_f$  = 0.77 (70:30 EtOAc: hexanes; stains bright yellow with *p*-anisaldehyde);  **$^1\text{H}$  NMR** (400 MHz, DMSO)  $\delta$  10.08 (s, 1H), 8.79 (d,  $J$  = 4.3 Hz, 1H), 8.20 (d,  $J$  = 7.9 Hz, 1H), 8.02 (t,  $J$  = 7.7 Hz, 1H), 7.71 – 7.56 (m, 1H), 7.42 (d,  $J$  = 8.7 Hz, 2H), 6.94 (d,  $J$  = 8.7 Hz, 2H).  **$^{13}\text{C}$  NMR** (101 MHz, DMSO)  $\delta$  158.96, 152.50, 149.95, 139.52, 138.03, 136.53, 126.83, 124.52, 121.63, 116.33, 112.49; **DEPT-135** (101 MHz, DMSO)  $\delta$  149.95, 138.03, 126.82, 124.52, 121.63, 116.33; **ESI+ MS**:  $m/z$  224 [MH] $^+$ .

### 3-Pyridineacetonitrile, $\alpha$ -[(4-hydroxyphenyl) imino] - (3.76)

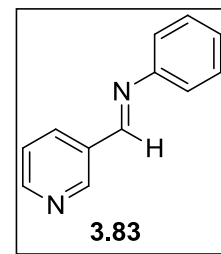
Prepared by same procedure described for **3.75**. Burnt orange solid (88.9 mg, 13%);  $R_f$  = 0.71 (70:30 EtOAc: hexanes; stains bright yellow with *p*-anisaldehyde);  **$^1\text{H}$  NMR** (400 MHz, DMSO)  $\delta$  10.07 (s, 1H), 9.16 (s, 1H), 8.80 (d,  $J$  = 3.8 Hz, 1H), 8.36 (d,  $J$  = 8.0 Hz, 1H), 7.64 (dd,  $J$  = 7.9, 4.8 Hz, 1H),



7.37 (d,  $J = 8.6$  Hz, 2H), 6.93 (d,  $J = 8.7$  Hz, 2H);  $^{13}\text{C}$  NMR (101 MHz, DMSO)  $\delta$  158.70, 152.96, 148.75, 140.15, 135.25, 133.87, 130.27, 124.57, 124.20, 116.31, 111.97; **DEPT-135** (101 MHz, DMSO)  $\delta$  152.96, 148.75, 135.25, 124.57, 124.21, 116.31; **ESI+ MS**:  $m/z$  224  $[\text{MH}]^+$ .

### Benzenamine, *N*-(3-pyridinylmethylene) - (**3.83**)

Using an adapted procedure from Dickson *et al.*,<sup>414</sup> freshly distilled aniline (0.294 mL, 300 mg, 3.22 mmol) and freshly distilled 3-pyridine carboxaldehyde (0.324 mL, 369.7 mg, 3.38 mmol) were dissolved in anhydrous 1, 2-dichloroethane (38.34 mL), and magnesium sulfate (461.4

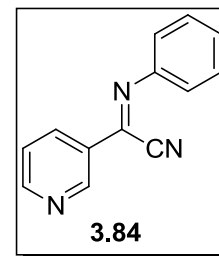


mg, 3.83 mmol) was added. The reaction flask was fitted with a reflux condenser and refluxed for 18 hours. The solution was filtered to remove the magnesium sulfate and the solvents were concentrated under reduced pressure to yield crude product as a viscous dark orange oil. Flash-column chromatography on silica using a gradient of 20:80 EtOAc:hexanes to 30:70

EtOAc:hexanes afforded **3.83** as a bright orange oil (498 mg, 84%); ( $R_f = 0.38$  (50:50 EtOAc:Hexanes; stains bright yellow with *p*-anisaldehyde)  $^1\text{H}$  NMR (400 MHz,  $\text{CDCl}_3$ )  $\delta$  9.01 (d,  $J = 1.2$  Hz, 1H), 8.70 (d,  $J = 3.5$  Hz, 1H), 8.49 (s, 1H), 8.29 (d,  $J = 7.9$  Hz, 1H), 7.47 – 7.36 (m, 3H), 7.30 – 7.19 (m, 3H);  $^{13}\text{C}$  NMR (101 MHz,  $\text{CDCl}_3$ )  $\delta$  157.18, 151.99, 151.43, 150.94, 134.89, 131.82, 129.25, 126.55, 123.80, 120.85; **DEPT-135** (101 MHz,  $\text{CDCl}_3$ )  $\delta$  157.18, 151.99, 151.43, 150.94, 134.89, 131.82, 129.25, 126.55, 123.80, 120.85; **ESI+ MS**:  $m/z$  183  $[\text{MH}]^+$ .

### 3-Pyridineacetonitrile, $\alpha$ -(phenylimino) - (3.84)

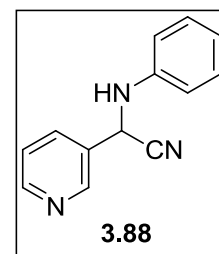
Using an adapted procedure from Surya K. De.,<sup>415</sup> a mixture of freshly distilled 3-pyridinecarboxaldehyde (0.103 mL, 1.073 mmol, 1.0 eq), freshly distilled aniline (1.022 mL, 1.073 mmol, 1.0 eq), KCN (104.9 mg, 1.609



mmol, 1.5 eq) and CoCl<sub>2</sub> (14.36 mg, 10 mol%) in anhydrous AcN (20 mL) was stirred at room temperature for 3 hours. After reaction completion, the reaction mixture was extracted with EtOAc (2 x 20 mL). The organic layers were washed with water (20 mL), brine (20 mL), dried over Na<sub>2</sub>SO<sub>4</sub>, and concentrated by rotary evaporation to yield crude yellow-orange oil. The residue was purified by flash-column chromatography on silica using a gradient of 10:90 EtOAc:hexanes to 100% EtOAc to afford **3.84** as an orange-yellow waxy residue (36.4 mg, 16 %); **R<sub>f</sub>** = 0.58 (50:50 EtOAc: hexanes; stains light yellow with *p*-anisaldehyde); **<sup>1</sup>H NMR** (400 MHz, CDCl<sub>3</sub>)  $\delta$  9.36 (s, 1H), 8.82 (d, *J* = 3.7 Hz, 1H), 8.41 (dd, *J* = 6.2, 1.9 Hz, 1H), 7.55 – 7.44 (m, 3H), 7.36 (t, *J* = 7.4 Hz, 1H), 7.29 – 7.21 (m, 2H); **<sup>13</sup>C NMR** (101 MHz, CDCl<sub>3</sub>)  $\delta$  153.19, 149.53, 148.47, 137.09, 135.22, 129.53, 129.41, 128.09, 123.71, 120.59, 110.32; **DEPT-135** (101 MHz, CDCl<sub>3</sub>)  $\delta$  153.20, 149.53, 135.22, 129.41, 128.09, 123.71, 120.59. **ESI+ MS**: *m/z* 210 [MH]<sup>+</sup>; **ESI- MS**: *m/z* 208 [MH]<sup>-</sup>.

### 3-Pyridineacetonitrile, $\alpha$ -(phenylamino) - (3.88)

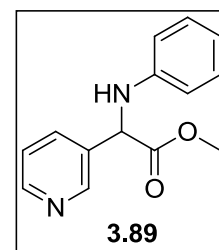
Using a modified procedure from Jarusiewicz *et al.*,<sup>343, 414</sup> to a mixture of PdCl<sub>2</sub> (14.89 mg, 3 mol%), freshly distilled 3-pyridinecarboxaldehyde (0.268 mL, 2.80 mmol, 1.0 eq), freshly distilled aniline (0.255 mL, 2.80 mmol, 1.0 eq), and Na<sub>2</sub>SO<sub>4</sub> (1.39 g, 9.80 mmol, 3.5 eq) in anhydrous DCM (4 mL) was added dropwise TMSCN (0.700 mL, 5.60 mmol, 2.0 eq). The reaction was stirred at



room temperature for 24 hours. After completion the mixture was filtered and the filtrate was concentrated under reduced pressure to yield a pale yellow solid (712.8 mg, 60%). Product was used in the subsequent reaction without further purification;  $R_f = 0.35$  (50:50 EtOAc: hexanes; stains bright yellow with *p*-anisaldehyde);  $^1\text{H NMR}$  (400 MHz,  $\text{CDCl}_3$ )  $\delta$  8.82 (d,  $J = 1.7$  Hz, 1H), 8.66 (d,  $J = 4.6$  Hz, 1H), 7.94 (d,  $J = 7.9$  Hz, 1H), 7.38 (dd,  $J = 7.9, 4.9$  Hz, 1H), 7.28 (t,  $J = 7.9$  Hz, 2H), 6.93 (t,  $J = 7.4$  Hz, 1H), 6.82 – 6.76 (m, 2H), 5.49 (s, 1H), 4.34 (s, 1H);  $^{13}\text{C NMR}$  (400 MHz,  $\text{CDCl}_3$ )  $\delta$  150.63, 148.58, 144.26, 135.03, 130.08, 129.67, 123.97, 120.78, 117.32, 114.46, 48.19; **DEPT-135**  $^{13}\text{C NMR}$  (101 MHz,  $\text{CDCl}_3$ )  $\delta$  150.63, 148.58, 135.03, 129.67, 123.97, 120.78, 114.46, 48.19; **ESI+ MS**:  $m/z$  210  $[\text{MH}]^+$ ; **ESI- MS**:  $m/z$  209  $[\text{M-H}]^-$ .

### 3-Pyridineacetic acid, $\alpha$ -(phenylamino)-, methyl ester (**3.89**)

Using a modified procedure from Burkhardt *et al.*,<sup>344</sup> the  $\alpha$ -amino nitrile **3.88** (199.5 mg, 0.953 mmol) was dissolved in anhydrous MeOH (5 mL) and cooled to 0°C with an ice-bath. Anhydrous HCl gas was bubbled into the

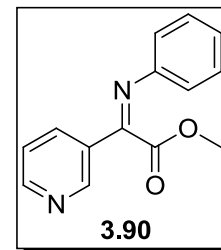


solution for 30 minutes until the solution was completely saturated. The reaction was warmed to room temperature and stirred for 12 hours. After completion the reaction was neutralized with saturated  $\text{NaHCO}_3$  and the extracted with EtOAc (3 x 20 mL). The organic layers were collected, dried over  $\text{Na}_2\text{SO}_4$  and evaporated under reduced pressure. The caramel-colored crude residue was purified by flash-column chromatography on silica using a gradient of 10:90 EtOAc:hexanes to 100% EtOAc to yield **3.89** as a yellow-orange oil (65.0 mg, 54%);  $R_f = 0.54$  (70:30 EtOAc: hexanes, stains pink with *p*-anisaldehyde);  $^1\text{H NMR}$  (400 MHz,  $\text{CDCl}_3$ )  $\delta$  8.81 (s, 1H), 8.58 (d,  $J = 3.9$  Hz, 1H), 7.85 (d,  $J = 7.9$  Hz, 1H), 7.31 (dd,  $J = 7.8, 4.9$  Hz, 1H), 7.12 (t,  $J = 7.9$  Hz, 2H), 6.72 (t,  $J = 7.3$  Hz, 1H), 6.54 (d,  $J = 7.7$  Hz, 2H), 5.14 (s, 1H), 3.75 (s, 3H);  $^{13}\text{C NMR}$  (101

MHz, CDCl<sub>3</sub>)  $\delta$  171.29, 148.85, 148.60, 145.31, 135.21, 134.00, 129.36, 124.07, 118.64, 113.51, 58.47, 53.18; **DEPT-135** (101 MHz, CDCl<sub>3</sub>)  $\delta$  148.85, 148.60, 135.21, 129.36, 124.08, 118.64, 113.51, 58.47, 53.18; **ESI+ MS**:  $m/z$  243 [MH]<sup>+</sup>.

### 3-Pyridineacetic acid, $\alpha$ -(phenylimino)-, methyl ester (**3.90**)

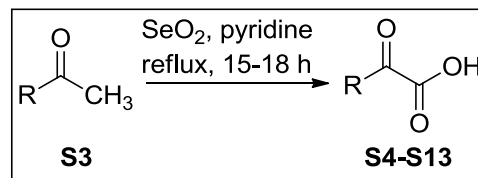
Using a modified procedure from Vu *et al.*,<sup>416</sup> a mixture of **3.89** (25.0 mg, 0.103 mmol, 1.0 eq) and DDQ (25.71mg, 0.113 mmol, 1.1 eq) in anhydrous benzene (3 mL) was stirred at room temperature for 24 hours. Initially, the reaction mixture was yellow then went to green followed by a dark maroon



color. After reaction completion the solvent was removed by rotary evaporation and immediately purified using flash-column chromatography on basic alumina using a gradient of 100% hexanes to 10:90 EtOAc:hexanes to yield **3.90** as a yellow oil (2.0 mg, 8%);  $R_f$  = 0.62 (50:50 EtOAc:hexanes; stains yellow with *p*-anisaldehyde); <sup>1</sup>H NMR (400 MHz, CDCl<sub>3</sub>)  $\delta$  9.09 (s, 1H), 8.79 (s, 1H), 8.25 (d,  $J$  = 8.0 Hz, 1H), 7.56 – 7.42 (m, 1H), 7.36 (t,  $J$  = 7.9 Hz, 2H), 7.19 (dd,  $J$  = 14.0, 6.6 Hz, 1H), 6.99 – 6.94 (m, 2H), 3.67 (s, 3H).; **ESI+ MS**:  $m/z$  241 [MH]<sup>+</sup>.

### General Procedure A for the Synthesis of Aryl $\alpha$ -Keto Acids (**S4-S13**):

Using an adapted procedure from Zhuang *et al.*,<sup>355</sup> in a 15 mL oven-dried pressure tube was added aryl ketone **S3** (1.0 eq), selenium dioxide (2.0 eq) and anhydrous

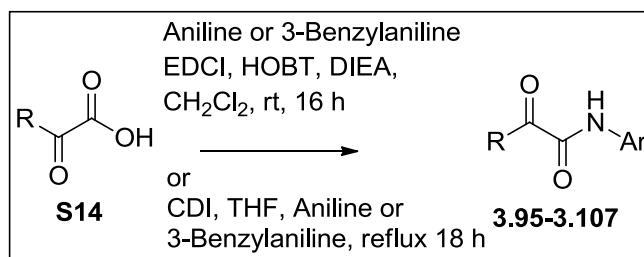


pyridine (6.25 eq) under argon. The reaction was heated between 110°C-120°C for 15 hours. The reaction was cooled and filtered through a pad of Celite eluting 2 x 2 mL of EtOAc and the filtrate was concentrated by rotary evaporation. The crude residue was dissolved in EtOAc, transferred into a separatory funnel and washed with 2 M NaOH (3 x 10 mL). The aqueous

layers were combined, cooled to 0°C and acidified with concentrated HCl (pH 1-2) and back-extracted with fresh EtOAc (3 x 20 mL). The organic layers were combined dried over Na<sub>2</sub>SO<sub>4</sub> and concentrated *in vacuo* to afford crude product **S4-S13** which were used without any additional purification.

### General Procedure B for the Synthesis of Aryl Oxalamate Scaffolds (3.95-3.107)

Using an adapted procedure from Martyn *et al.*,<sup>306</sup> to a mixture of crude **S14** (1.0 eq) and 3-benzylaniline or aniline(1.1 eq) in anhydrous DCM (213 eq) was added 1-(3-



dimethylaminopropyl)-3-ethylcarbodiimide hydrochloride (1.3eq) and 1-hydroxybenzotriazole hydrate (HOBT) (1.5 eq) at room temperature. *N,N*-Diisopropylethylamine (1.1 eq) was added dropwise and the reaction mixture stirred at room temperature for 24 hours. The reaction was quenched with H<sub>2</sub>O (5 mL) and stirred for 30 minutes at room temperature. The solution was diluted with DCM (10 mL), washed with 1N HCl (3 x 10 mL), water (3 x 10 mL), and the combined aqueous washings were back-extracted with fresh DCM (3 x 10 mL). The combined organic fractions were dried over Na<sub>2</sub>SO<sub>4</sub> and the solvent was removed *in vacuo* to afford crude product. Flash-column chromatography on silica using a gradient of 10:90 EtOAc:hexanes to 100% EtOAc afforded **3.95-3.107** as pure oxalamates.



### 2-(4-bromophenyl)-2-oxoacetic acid (S4)

Synthesized using the general procedure A described for aryl  $\alpha$ -keto acids. Salmon-pink solid

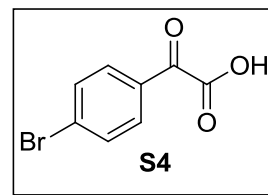
(1.48 g, quantitative crude yield);  $R_f$  = 0.17 (20:80 EtOAc: hexanes);

$^1\text{H NMR}$  (400 MHz,  $\text{CDCl}_3$ )  $\delta$  9.81 (s, 1H), 8.17 (d,  $J$  = 8.6 Hz, 2H),

7.66 (dd,  $J$  = 17.9, 8.5 Hz, 2H);  $^{13}\text{C NMR}$  (101 MHz,  $\text{CDCl}_3$ )  $\delta$

183.56, 162.35, 132.47, 132.44, 131.63, 130.47; **DEPT-135** (101 MHz,  $\text{CDCl}_3$ )  $\delta$  132.47,

132.44; **ESI- MS**:  $m/z$  227, 229[M-H] $^-$ ; **ESI+ MS**:  $m/z$  456, 458 [MNa] $^+$ .



### N-(3-benzylphenyl)-2-(4-bromophenyl)-2-oxoacetamide (3.95)

Synthesized using the general procedure B described for

aryl oxalamate scaffolds with modification. Flash-

column chromatography on silica using a gradient of

50:50  $\text{CHCl}_3$ :hexanes to 100%  $\text{CHCl}_3$  afforded **3.95** as a pale yellow solid (192 mg, 54%);  $R_f$  =

0.50 (50:50  $\text{CHCl}_3$ : hexanes, stains yellow with *p*-anisaldehyde);  $^1\text{H NMR}$  (400 MHz,  $\text{CDCl}_3$ )  $\delta$

8.88 (s, 1H), 8.30 (d,  $J$  = 8.6 Hz, 2H), 7.64 (d,  $J$  = 8.6 Hz, 2H), 7.56 (d,  $J$  = 8.0 Hz, 1H), 7.48 (s,

1H), 7.30 (td,  $J$  = 7.4, 3.9 Hz, 3H), 7.21 (t,  $J$  = 7.1 Hz, 3H), 7.03 (d,  $J$  = 7.5 Hz, 1H), 4.00 (s,

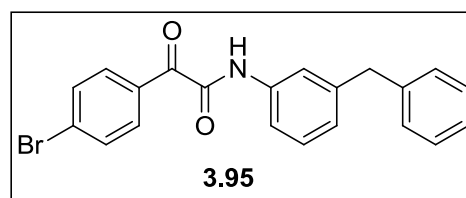
2H);  $^{13}\text{C NMR}$  (101 MHz,  $\text{CDCl}_3$ )  $\delta$  186.29, 158.46, 142.56, 140.54, 136.60, 132.97, 131.96,

131.82, 130.45, 129.36, 128.94, 128.58, 126.30, 126.11, 120.40, 117.78, 41.87; **DEPT-135** (101

MHz,  $\text{CDCl}_3$ )  $\delta$  132.97, 131.96, 129.36, 128.93, 128.58, 126.30, 126.11, 120.40, 117.78, 41.87;

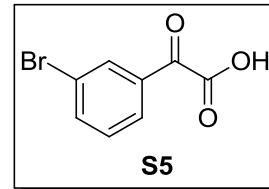
**ESI- MS**:  $m/z$  392, 394 [M-H] $^-$ ; **Elemental Analysis**: Calc. for  $\text{C}_{21}\text{H}_{16}\text{BrNO}_2$ : C, 63.97; H, 4.09;

N, 3.55. Found: C, 63.75; H, 3.91; N, 3.49; **melting point**: 110-112  $^\circ\text{C}$ .



### 2-(3-bromophenyl)-2-oxoacetic acid (**S5**)

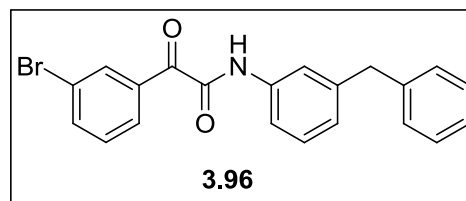
Synthesized using the general procedure **A** described for aryl  $\alpha$ -keto acids. Yellow solid (844.8 mg, 64% crude yield);  $R_f$  = 0.17 (20:80 EtOAc: hexanes);  $^1\text{H NMR}$  (400 MHz,  $\text{CDCl}_3$ )  $\delta$  9.30 (s, 1H), 8.51 –



8.31 (m, 1H), 8.22 (d,  $J$  = 7.9 Hz, 1H), 7.82 (dd,  $J$  = 8.0, 0.9 Hz, 1H), 7.52 – 7.37 (m, 1H).  $^{13}\text{C NMR}$  (101 MHz,  $\text{CDCl}_3$ )  $\delta$  183.63, 162.59, 138.30, 133.57, 130.50, 129.64, 123.20; **DEPT-135** (101 MHz,  $\text{CDCl}_3$ )  $\delta$  138.30, 133.57, 130.50, 129.64; **ESI- MS**:  $m/z$  226, 228 [M-H] $^-$ .

### *N*-(3-benzylphenyl)-2-(3-bromophenyl)-2-oxoacetamide (**3.96**)

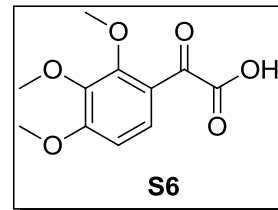
Synthesized using the general procedure **B** described for aryl oxalamate scaffolds with modification. Flash-column chromatography on silica using a gradient of



50:50  $\text{CHCl}_3$ :hexanes to 100%  $\text{CHCl}_3$  afforded **3.96** as a pale yellow crystalline solid (302.2 mg, 71%);  $R_f$  = 0.50 (50:50  $\text{CHCl}_3$ : hexanes; stains yellow with *p*-anisaldehyde);  $^1\text{H NMR}$  (400 MHz,  $\text{CDCl}_3$ )  $\delta$  8.89 (s, 1H), 8.56 (s, 1H), 8.39 (d,  $J$  = 7.9 Hz, 1H), 7.79 (d,  $J$  = 8.0 Hz, 1H), 7.60 (d,  $J$  = 7.9 Hz, 1H), 7.51 (s, 1H), 7.42 – 7.20 (m, 8H), 4.02 (s, 2H);  $^{13}\text{C NMR}$  (101 MHz,  $\text{CDCl}_3$ )  $\delta$  186.01, 158.20, 142.56, 140.52, 137.41, 136.54, 134.73, 134.15, 130.09, 129.36, 128.93, 128.58, 126.30, 126.15, 122.71, 120.41, 117.80, 41.87; **DEPT-135** (101 MHz,  $\text{CDCl}_3$ )  $\delta$  137.42, 134.16, 130.11, 129.37, 128.94, 128.59, 126.31, 126.16, 120.42, 117.81, 41.87. **ESI- MS**:  $m/z$  391, 393 [M-H] $^-$ ; **Elemental Analysis**: Calc. for  $\text{C}_{21}\text{H}_{16}\text{BrNO}_2$ : **C**, 63.97; **H**, 4.09; **N**, 3.55. Found: **C**, 63.27; **H**, 3.86; **N**, 3.46; **melting point**: 103-105°C.

### 2-oxo-2-(2,3,4-trimethoxyphenyl)acetic acid (S6)

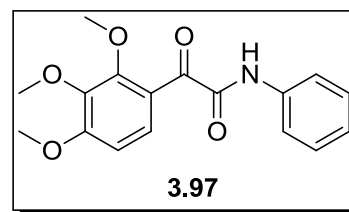
Synthesized using the general procedure A described for aryl  $\alpha$ -keto acids. Yellow solid (240.2 mg, quantitative crude yield);  $R_f = 0.10$



(50:50 EtOAc: hexanes);  $^1\text{H NMR}$  (400 MHz,  $\text{CDCl}_3$ )  $\delta$  10.97 (s, 3H), 7.73 (d,  $J = 8.9$  Hz, 1H), 6.80 (d,  $J = 8.9$  Hz, 1H), 3.99 (s, 3H), 3.96 (s, 2H), 3.87 (s, 3H);  $^{13}\text{C NMR}$  (101 MHz,  $\text{CDCl}_3$ )  $\delta$  184.50, 169.85, 160.22, 155.48, 141.18, 126.44, 119.66, 107.84, 61.52, 60.85, 56.35; **DEPT-135** (101 MHz,  $\text{CDCl}_3$ )  $\delta$  126.43, 107.83, 61.51, 60.85, 56.34; **ESI- MS**:  $m/z$  239  $[\text{M-H}]^-$ .

### 2-oxo-N-phenyl-2-(2,3,4-trimethoxyphenyl)acetamide (3.97)

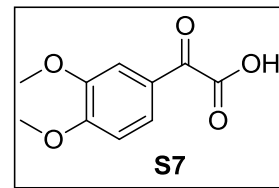
Synthesized using the general procedure B described for aryl oxalamate scaffolds. Orange-brown oil (45 mg, 34%);  $R_f = 0.68$



(50:50 EtOAc: hexanes);  $^1\text{H NMR}$  (400 MHz,  $\text{CDCl}_3$ )  $\delta$  8.46 (s, 1H), 7.70 – 7.66 (m, 2H), 7.58 (d,  $J = 8.8$  Hz, 1H), 7.38 (t,  $J = 7.9$  Hz, 2H), 7.17 (t,  $J = 7.4$  Hz, 1H), 6.75 (d,  $J = 8.8$  Hz, 1H), 3.97 (s, 3H), 3.93 (s, 3H), 3.85 (s, 3H);  $^{13}\text{C NMR}$  (101 MHz,  $\text{CDCl}_3$ )  $\delta$  189.78, 161.00, 158.79, 154.68, 141.67, 137.02, 129.17, 127.05, 124.95, 121.55, 119.80, 106.99, 61.79, 60.76, 56.24; **DEPT-135** (101 MHz,  $\text{CDCl}_3$ )  $\delta$  129.17, 127.06, 124.95, 120.16, 119.80, 106.99, 61.78, 60.76, 56.24. **ESI+ MS**:  $m/z$  316  $[\text{MH}]^+$ ; **Elemental Analysis**: Calc. for  $\text{C}_{17}\text{H}_{17}\text{NO}_5$ : **C**, 64.75; **H**, 5.43; **N**, 4.44. Found: **C**, 64.22; **H**, 5.81; **N**, 4.06.

### 2-(3,4-dimethoxyphenyl)-2-oxoacetic acid (S7)

Synthesized using the general procedure A described for aryl  $\alpha$ -keto acids. Off-white powder (466.5 mg, quantitative crude yield);  $R_f = 0.11$

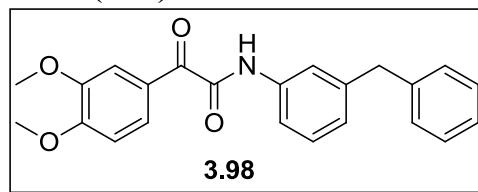


(50:50 EtOAc: hexanes);  $^1\text{H NMR}$  (400 MHz,  $\text{CDCl}_3$ )  $\delta$  9.15 (s, 1H), 8.19 (dd,  $J = 8.5, 1.9$  Hz, 1H), 7.79 (d,  $J = 1.8$  Hz, 1H), 6.95 (d,  $J = 8.6$  Hz, 1H), 3.98 (d,  $J = 15.7$  Hz, 6H);  $^{13}\text{C NMR}$  (101

MHz, CDCl<sub>3</sub>) δ 182.32, 162.12, 155.82, 149.29, 128.08, 124.80, 112.11, 110.48, 99.99, 56.30, 56.07; DEPT-135 (101 MHz, CDCl<sub>3</sub>) δ 128.08, 112.10, 110.48, 56.30, 56.07; **ESI+ MS: ESI-MS: *m/z* 209 [M-H]<sup>-</sup>.**

***N*-(3-benzylphenyl)-2-(3,4-dimethoxyphenyl)-2-oxoacetamide (3.98)**

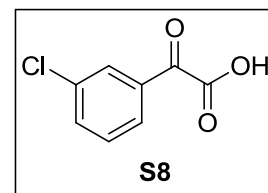
Synthesized using the general procedure **B** described for aryl oxalamate scaffolds. Brown-orange sticky residue (42.5 mg, 79%); **R<sub>f</sub>** = 0.603 (50:50 EtOAc: hexanes;



stains orange-yellow with *p*-anisaldehyde); **<sup>1</sup>H NMR** (400 MHz, CDCl<sub>3</sub>) δ 8.97 (s, 1H), 8.33 (dd, *J* = 8.6, 1.9 Hz, 1H), 7.92 (d, *J* = 1.8 Hz, 1H), 7.59 (d, *J* = 8.0 Hz, 1H), 7.49 (s, 1H), 7.35 – 7.26 (m, 3H), 7.21 (t, *J* = 5.5 Hz, 3H), 7.02 (d, *J* = 7.5 Hz, 1H), 6.92 (d, *J* = 8.6 Hz, 1H), 4.00 (s, 2H), 3.97 (s, 3H), 3.95 (s, 3H); **<sup>13</sup>C NMR** (101 MHz, CDCl<sub>3</sub>) δ 185.07, 159.48, 154.92, 148.88, 142.44, 140.62, 136.89, 129.30, 128.93, 128.56, 127.72, 126.26, 126.16, 125.87, 120.44, 117.82, 112.92, 110.25, 56.18, 56.03, 41.87; **DEPT-135** (101 MHz, CDCl<sub>3</sub>) δ 129.28, 128.92, 128.54, 127.71, 126.24, 125.86, 120.43, 117.80, 112.91, 110.24, 56.17, 56.03, 41.86; **Elemental Analysis:** Calc. for C<sub>23</sub>H<sub>21</sub>NO<sub>4</sub>: **C**, 73.58; **H**, 5.64; **N**, 3.73. Found: **C**, 71.86 **H**, 6.37 **N**, 3.15.

**2-(3-chlorophenyl)-2-oxoacetic acid (S8)**

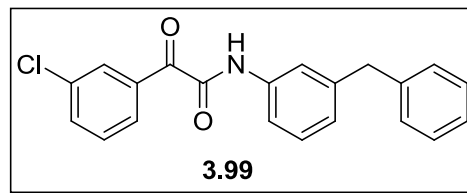
Synthesized using the general procedure **A** described for aryl α-keto acids. Light tan solid (240.1 mg, quantitative crude yield); **R<sub>f</sub>** = 0.10 (30:70 EtOAc: hexanes); **<sup>1</sup>H NMR** (400 MHz, CDCl<sub>3</sub>) δ 10.57 (s, 1H), 8.32 – 7.98 (m, 2H), 7.63 (dd, *J* = 21.0, 7.7 Hz, 1H), 7.56 – 7.38 (m, 1H); **<sup>13</sup>C NMR** (101 MHz, CDCl<sub>3</sub>) δ 183.42, 163.33, 135.40, 135.32, 133.29, 130.52, 130.30, 129.04; **DEPT-135** (101



MHz, CDCl<sub>3</sub>)  $\delta$  135.40, 134.22, 130.52, 130.31, 129.93, 129.04, 128.41 **ESI- MS**:  $m/z$  182, 184 [M-H].

### **N-(3-benzylphenyl)-2-(3-chlorophenyl)-2-oxoacetamide (3.99)**

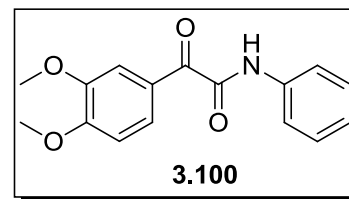
Using an adapted procedure from Kumar et al.,<sup>417</sup> carbonyldiimidazole (CDI) (66.32 mg, 0.409 mmol, 1.5 eq) was dissolved in anhydrous THF (3 mL) and stirred



at room temperature. To this mixture was slowly added **S8** (75.54 mg, 0.409 mmol, 1.5 eq). The reaction mixture was further stirred for 10 minutes at room temperature and then after the evolution of CO<sub>2</sub> ceased, 3-benzylaniline (50 mg, 0.273 mmol, 1.0 eq) was added. The stirring was continued for an additional 10 minutes at room temperature and then refluxed for 16 hours. After completion of the reaction, monitored by TLC, reaction mixture was concentrated *in vacuo* to obtain crude product as orange-brown oil. The crude product was immediately purified by flash-column chromatography using a gradient of 10:90 EtOAc: hexanes to 30:70 EtOAc:hexanes to afford **3.99** (54.6 mg, 38%) as a yellow oil. **R<sub>f</sub>** = 0.89 (30:70 EtOAc: hexanes; stains yellow with *p*-anisaldehyde); **<sup>1</sup>H NMR** (400 MHz, CDCl<sub>3</sub>)  $\delta$  8.87 (s, 1H), 8.39 (d,  $J$  = 1.6 Hz, 1H), 8.32 (d,  $J$  = 7.8 Hz, 1H), 7.65 – 7.54 (m, 2H), 7.49 (s, 1H), 7.43 (t,  $J$  = 7.9 Hz, 1H), 7.30 (dd,  $J$  = 12.8, 7.4 Hz, 3H), 7.21 (t,  $J$  = 6.8 Hz, 3H), 7.04 (d,  $J$  = 7.5 Hz, 1H), 4.00 (s, 2H); **<sup>13</sup>C NMR** (101 MHz, CDCl<sub>3</sub>)  $\delta$  186.12, 158.24, 142.56, 140.52, 136.54, 134.80, 134.51, 131.27, 129.86, 129.63, 129.36, 128.93, 128.57, 126.29, 126.15, 120.41, 117.80, 41.86; **DEPT-135** (101 MHz, CDCl<sub>3</sub>)  $\delta$  134.51, 131.27, 129.86, 129.64, 129.36, 128.93, 128.57, 126.29, 126.15, 120.41, 117.80, 41.86; **ESI- MS**:  $m/z$  209 [M-H].

### 2-(3,4-dimethoxyphenyl)-2-oxo-N-phenylacetamide (3.100)

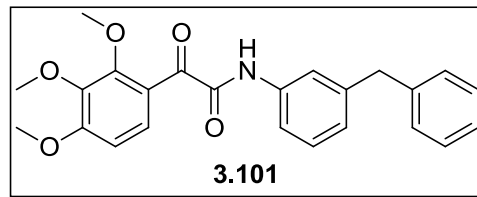
Synthesized using the general procedure **B** described for aryl oxalamate scaffolds. Yellow crystalline solid (51 mg, 53%);  $R_f = 0.72$  (50:50 EtOAc: hexanes);  $^1\text{H NMR}$  (400 MHz,  $\text{CDCl}_3$ )  $\delta$  9.05



(s, 1H), 8.33 (dd,  $J = 8.6, 1.9$  Hz, 1H), 7.93 (d,  $J = 1.8$  Hz, 1H), 7.69 (d,  $J = 7.9$  Hz, 2H), 7.39 (t,  $J = 7.9$  Hz, 2H), 7.18 (t,  $J = 7.4$  Hz, 1H), 6.92 (d,  $J = 8.6$  Hz, 1H), 3.97 (s, 3H), 3.95 (s, 3H);  $^{13}\text{C NMR}$  (101 MHz,  $\text{CDCl}_3$ )  $\delta$  185.09, 159.56, 154.91, 148.86, 136.76, 129.19, 127.70, 126.15, 125.19, 120.00, 112.91, 110.26, 56.16, 56.00; **DEPT-135** (101 MHz,  $\text{CDCl}_3$ )  $\delta$  129.19, 127.70, 125.19, 120.00, 112.91, 110.26, 56.16, 56.00; **Elemental Analysis:** Calc. for  $\text{C}_{16}\text{H}_{15}\text{NO}_4$ : **C**, 67.36; **H**, 5.30; **N**, 4.91. Found: **C**, 66.85; **H**, 5.0; **N**, 4.90.

### N-(3-benzylphenyl)-2-oxo-2-(2,3,4-trimethoxyphenyl)acetamide (3.101)

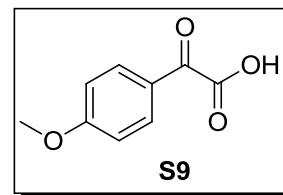
Synthesized using the general procedure **B** described for aryl oxalamate scaffolds. Pale yellow oil (15.3 mg, 18 %);  $R_f = 0.85$  (50:50EtOAc: hexanes);  $^1\text{H NMR}$  (400



MHz,  $\text{CDCl}_3$ )  $\delta$  8.37 (s, 1H), 7.57 (t,  $J = 7.1$  Hz, 2H), 7.45 (s, 1H), 7.25 (dt,  $J = 24.6, 7.7$  Hz, 5H), 7.01 (d,  $J = 7.5$  Hz, 1H), 6.73 (d,  $J = 8.8$  Hz, 1H), 3.99 (s, 2H), 3.93 (d,  $J = 4.4$  Hz, 6H), 3.84 (s, 3H);  $^{13}\text{C NMR}$  (101 MHz,  $\text{CDCl}_3$ )  $\delta$  189.71, 160.84, 158.76, 142.44, 140.60, 137.14, 129.27, 128.96, 128.54, 127.03, 126.24, 125.58, 121.61, 120.25, 117.62, 106.99, 61.77, 60.76, 56.23, 41.85; **DEPT-135** (101 MHz,  $\text{CDCl}_3$ )  $\delta$  129.26, 128.95, 128.53, 127.02, 126.23, 125.57, 120.24, 117.61, 106.98, 61.76, 60.75, 56.23, 41.85; **Elemental Analysis:** Calc. for  $\text{C}_{24}\text{H}_{23}\text{NO}_5$ : **C**, 71.10; **H**, 5.72; **N**, 3.45. Found: **C**, 70.38 **H**, 5.87 **N**, 3.30.

### 2-(4-methoxyphenyl)-2-oxoacetic acid (S9)

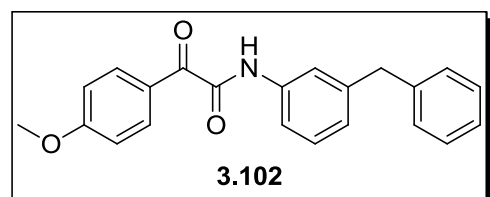
Synthesized using the general procedure A described for aryl  $\alpha$ -keto acids. Pale pink-orange oil (479 mg, quantitative crude yield);  $R_f$  = 0.106 (50:50 EtOAc: hexanes);  $^1\text{H NMR}$  (400 MHz,  $\text{CDCl}_3$ )  $\delta$  12.56 (s, 1H),



8.07 (d,  $J$  = 8.9 Hz, 2H), 6.93 (d,  $J$  = 8.9 Hz, 2H), 3.86 (s, 3H);  $^{13}\text{C NMR}$  (101 MHz,  $\text{CDCl}_3$ )  $\delta$  188.68, 168.43, 164.57, 132.70, 114.01, 55.54; **DEPT-135** (101 MHz,  $\text{CDCl}_3$ )  $\delta$  132.70, 114.01, 55.54; **ESI- MS**:  $m/z$  179  $[\text{M-H}]^-$ .

### N-(3-benzylphenyl)-2-(4-methoxyphenyl)-2-oxoacetamide (3.102)

Synthesized using the general procedure B described for aryl oxalamate scaffolds. Pale yellow oil (18 mg, 24 %);



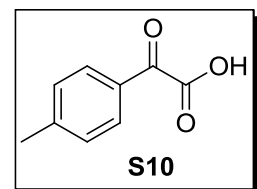
$R_f$  = 0.80 (50:50 EtOAc: hexanes; stains red/pink with *p*-

anisaldehyde);  $^1\text{H NMR}$  (400 MHz,  $\text{CDCl}_3$ )  $\delta$  8.98 (s, 3H), 8.48 (d,  $J$  = 9.0 Hz, 2H), 7.58 (d,  $J$  = 8.3 Hz, 1H), 7.51 (s, 1H), 7.30 (t,  $J$  = 8.2 Hz, 3H), 7.20 (d,  $J$  = 7.8 Hz, 3H), 7.02 (d,  $J$  = 7.5 Hz, 1H), 6.96 (d,  $J$  = 9.0 Hz, 2H), 4.00 (s, 2H), 3.89 (s, 3H);  $^{13}\text{C NMR}$  (101 MHz,  $\text{CDCl}_3$ )  $\delta$  185.18, 164.89, 159.43, 142.44, 140.62, 136.89, 134.27, 129.30, 128.94, 128.57, 126.26, 126.07, 125.81, 120.33, 117.70, 113.92, 55.62, 41.88; **DEPT -135** (101 MHz,  $\text{CDCl}_3$ )  $\delta$  134.27, 129.30, 128.94, 128.57, 126.26, 125.81, 120.33, 117.70, 113.95, 113.92, 55.63, 55.62, 41.89, 41.88.

### 2-oxo-2-(*p*-tolyl) acetic acid (S10)

Synthesized using the general procedure A described for aryl  $\alpha$ -keto acids.

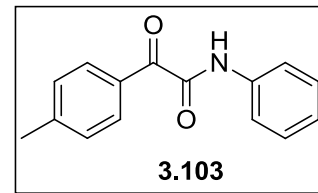
Golden yellow solid (402.8 mg, quantitative crude yield);  $R_f$  = 0.17 (50:50 EtOAc: hexanes);  $^1\text{H NMR}$  (400 MHz,  $\text{CDCl}_3$ )  $\delta$  9.23 (s, 1H), 8.12 (d,  $J$  =



8.1 Hz, 2H), 7.31 (d,  $J = 8.0$  Hz, 2H), 2.44 (s, 3H);  $^{13}\text{C}$  NMR (101 MHz,  $\text{CDCl}_3$ )  $\delta$  184.88, 164.23, 147.05, 131.06, 129.72, 129.38, 21.96; **DEPT-135** (101 MHz,  $\text{CDCl}_3$ )  $\delta$  131.05, 129.70, 21.96; **ESI- MS**:  $m/z$  163  $[\text{M-H}]^-$ .

### 2-oxo-N-phenyl-2-(p-tolyl) acetamide (3.103)

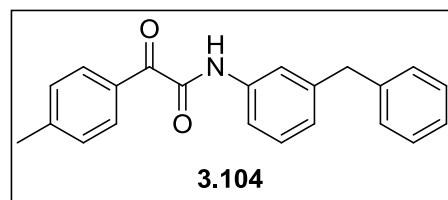
Synthesized using the general procedure **B** described for aryl oxalamate scaffolds. Bright yellow solid (42 mg, 41%);  $R_f = 0.86$  (30:70 EtOAc: hexanes)  $^1\text{H}$  NMR (400 MHz,  $\text{CDCl}_3$ )  $\delta$  8.99 (s, 1H),



8.34 (d,  $J = 8.3$  Hz, 2H), 7.81 – 7.58 (m, 2H), 7.40 (dd,  $J = 10.8, 5.2$  Hz, 2H), 7.31 (d,  $J = 8.0$  Hz, 2H), 7.19 (dd,  $J = 10.6, 4.2$  Hz, 1H), 2.44 (s, 3H);  $^{13}\text{C}$  NMR (101 MHz,  $\text{CDCl}_3$ )  $\delta$  186.83, 159.13, 146.00, 136.69, 131.67, 130.54, 129.35, 129.22, 125.23, 119.89, 21.98; **DEPT-135**  $^{13}\text{C}$  NMR (400 MHz,  $\text{CDCl}_3$ )  $\delta$  197.38, 196.79, 196.76, 195.76, 194.42, 169.78; **melting point**: 119–122 °C.

### N-(3-benzylphenyl)-2-oxo-2-(p-tolyl) acetamide (3.104)

Synthesized using the general procedure **B** described for aryl oxalamate scaffolds. Bright yellow crystalline solid (43.8 mg, 72%);  $R_f = 0.75$  (30:70 EtOAc: hexanes);  $^1\text{H}$



NMR (400 MHz,  $\text{CDCl}_3$ )  $\delta$  8.91 (s, 1H), 8.32 (d,  $J = 8.2$  Hz, 2H), 7.58 (d,  $J = 7.8$  Hz, 1H), 7.50 (s, 1H), 7.28 (d,  $J = 8.1$  Hz, 5H), 7.20 (d,  $J = 7.5$  Hz, 2H), 7.01 (d,  $J = 7.5$  Hz, 1H), 3.99 (s, 2H), 2.43 (s, 3H);  $^{13}\text{C}$  NMR (101 MHz,  $\text{CDCl}_3$ )  $\delta$  186.80, 159.11, 145.92, 142.45, 140.60, 136.86, 131.65, 130.60, 129.31, 128.93, 128.56, 126.26, 125.86, 120.37, 117.74, 41.88, 21.93; **DEPT-135** (101 MHz,  $\text{CDCl}_3$ )  $\delta$  131.66, 129.31, 128.93, 128.56, 126.26, 125.86, 120.37, 117.74, 41.88,



21.93; **ESI+ MS:**  $m/z$  352  $[\text{MNa}]^+$ ; **ESI- MS:**  $m/z$  328  $[\text{MH}]^+$ ; **Elemental Analysis:** Calc. for  $\text{C}_{22}\text{H}_{19}\text{NO}_2$ : **C**, 80.22; **H**, 5.81; **N**, 4.25. Found: **C**, 80.0; **H**, 5.65; **N**, 4.25.

### 2-oxo-2-(1H-pyrrol-2-yl) acetic acid (S11)

Synthesized using the general procedure **A** described for aryl  $\alpha$ -keto acids.

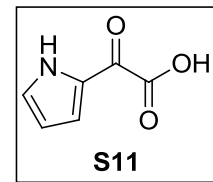
Dark red-orange solid (318 mg, quantitative crude yield);  $R_f = 0.075$  (90:10

DCM: MeOH; stains dark brown with *p*-anisaldehyde);  $^1\text{H NMR}$  (400 MHz,

DMSO)  $\delta$  12.22 (s, 1H), 7.28 (s, 1H), 7.12 (s, 1H), 6.27 (s, 1H);  $^{13}\text{C NMR}$  (101 MHz, DMSO)  $\delta$

175.39, 172.49, 165.35, 129.35, 128.88, 121.89, 111.62; **DEPT-135** (101 MHz, DMSO)  $\delta$

129.34, 121.87, 111.61; **ESI- MS:**  $m/z$  137  $[\text{MH}]^+$ .



### *N*-(3-benzylphenyl)-2-oxo-2-(1H-pyrrol-2-yl) acetamide (3.105)

Synthesized using the general procedure **B** described for aryl

oxalamate scaffolds. Light yellow solid powder (45.5 mg,

22%);  $R_f = 0.59$  (30:70 EtOAc: hexanes; stains dark orange-

brown with *p*-anisaldehyde);  $^1\text{H NMR}$  (500 MHz, DMSO)  $\delta$  12.24 (s, 1H), 10.57 (s, 1H), 7.71

(s, 1H), 7.63 (d,  $J = 7.9$  Hz, 1H), 7.38 – 7.15 (m, 8H), 7.02 (d,  $J = 7.5$  Hz, 1H), 6.35 – 6.27 (m,

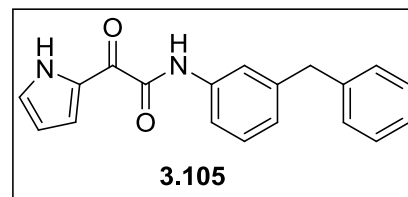
1H), 3.94 (s, 2H);  $^{13}\text{C NMR}$  (126 MHz, DMSO)  $\delta$  162.37, 142.34, 141.50, 138.46, 129.26,

129.17, 128.97, 128.91, 126.49, 125.29, 121.05, 118.54, 111.69, 41.68; **DEPT-135** (126 MHz,

DMSO)  $\delta$  129.26, 129.17, 128.91, 126.49, 125.29, 122.34, 121.05, 118.54, 111.70, 41.68;

**Elemental Analysis:** Calc. for  $\text{C}_{19}\text{H}_{16}\text{N}_2\text{O}_2$ : **C**, 74.98; **H**, 5.30; **N**, 9.20. Found: **C**, 74.66; **H**,

5.31; **N**, 8.64; **melting point:** 148-150 °C.



### 2-oxo-2-phenylacetic acid (S12)

Synthesized using the general procedure A described for aryl  $\alpha$ -keto acids.

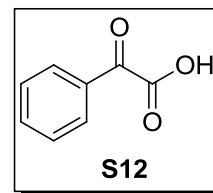
Pale yellow oil (312 mg, quantitative crude yield);  $R_f = 0.57$  (20:80 EtOAc:

Hexanes);  $^1\text{H NMR}$  (400 MHz,  $\text{CDCl}_3$ )  $\delta$  10.00 (s, 1H), 8.22 (d,  $J = 7.7$  Hz,

2H), 7.77 – 7.64 (m, 1H), 7.58 – 7.43 (m, 2H);  $^{13}\text{C NMR}$  (101 MHz,  $\text{CDCl}_3$ )  $\delta$  185.20, 163.99,

135.55, 131.79, 130.90, 130.35, 128.99, 128.61; **DEPT-135** (101 MHz,  $\text{CDCl}_3$ )  $\delta$  135.55,

130.90, 130.35, 128.99, 128.61; **ESI-MS**:  $m/z$  148 [M-H].



### *N*-(3-benzylphenyl)-2-oxo-2-phenylacetamide (3.106)

Synthesized using the general procedure B described for aryl

oxalamate scaffolds. Light yellow solid (46 mg, 44%);  $R_f =$

0.57 (20:80 EtOAc: hexanes);  $^1\text{H NMR}$  (400 MHz, )  $\delta$  8.91 (s, 1H), 8.54 – 8.23 (m, 2H), 7.62

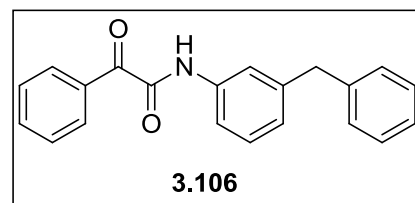
(dd,  $J = 15.7, 8.5$  Hz, 2H), 7.53 – 7.44 (m, 3H), 7.34 – 7.25 (m, 3H), 7.21 (dd,  $J = 11.1, 6.7$  Hz,

3H), 7.02 (d,  $J = 7.6$  Hz, 1H), 3.99 (s, 2H);  $^{13}\text{C NMR}$  (101 MHz,  $\text{CDCl}_3$ )  $\delta$  187.45, 158.93,

142.51, 140.63, 136.84, 134.62, 133.13, 131.48, 129.34, 128.97, 128.60, 128.57, 126.31, 125.97,

120.44, 117.82, 41.91. **DEPT-135** (101 MHz,  $\text{CDCl}_3$ )  $\delta$  134.61, 131.47, 129.33, 128.96, 128.59,

128.56, 126.29, 125.96, 120.43, 117.80, 41.90; **ESI-MS**:  $m/z$  313 [M-H].



### 2-(furan-2-yl)-2-oxoacetic acid (S13)

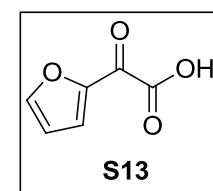
Synthesized using the general procedure A described for aryl  $\alpha$ -keto acids.

Yellow solid (313 mg, quantitative crude yield);  $R_f = 0.15$  (50:50 EtOAc:

hexanes);  $^1\text{H NMR}$  (400 MHz,  $\text{CDCl}_3$ )  $\delta$  9.21 (s, 1H), 8.15 (s, 1H), 7.86 (s,

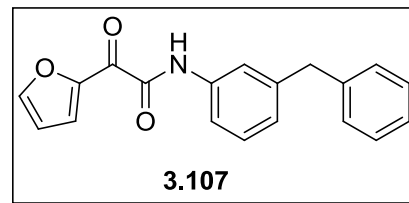
1H), 6.70 (s, 1H);  $^{13}\text{C NMR}$  (101 MHz,  $\text{CDCl}_3$ )  $\delta$  169.76, 159.54, 150.67, 128.07, 120.12,

113.39; **DEPT-135** (101 MHz,  $\text{CDCl}_3$ )  $\delta$  150.68, 127.76, 113.09; **ESI-MS**:  $m/z$  138[M-H].



***N*-(3-benzylphenyl)-2-(furan-2-yl)-2-oxoacetamide (3.107)**

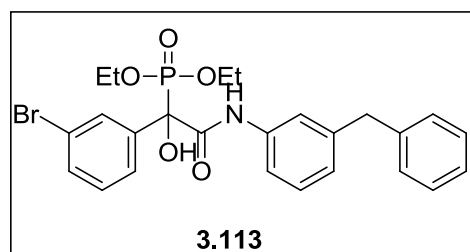
Synthesized using the general procedure **B** described for aryl oxalamate scaffolds. Bright yellow solid (15.3 mg, 14%)  $R_f = 0.55$  (30:70 EtOAc: hexanes; stains purple with *p*-



anisaldehyde);  $^1\text{H NMR}$  (400 MHz,  $\text{CDCl}_3$ )  $\delta$  9.04 (s, 1H), 8.25 (d,  $J = 3.6$  Hz, 1H), 7.76 (s, 1H), 7.58 (d,  $J = 8.0$  Hz, 1H), 7.49 (s, 1H), 7.30 (dd,  $J = 11.4, 5.5$  Hz, 3H), 7.20 (t,  $J = 6.6$  Hz, 3H), 7.02 (d,  $J = 7.6$  Hz, 1H), 6.63 (dd,  $J = 3.5, 1.4$  Hz, 1H), 3.99 (s, 2H);  $^{13}\text{C NMR}$  (101 MHz,  $\text{CDCl}_3$ )  $\delta$  173.50, 157.53, 149.73, 149.30, 142.51, 140.57, 136.56, 129.34, 128.94, 128.58, 127.39, 126.29, 126.05, 120.42, 117.79, 113.36, 41.86; **DEPT-135** (101 MHz,  $\text{CDCl}_3$ )  $\delta$  149.73, 129.34, 128.94, 128.58, 127.39, 126.29, 126.05, 120.42, 117.79, 113.36, 41.86; **ESI+MS**:  $m/z$  328  $[\text{MNa}]^+$ . **Elemental Analysis**: Calc. for  $\text{C}_{15}\text{H}_{13}\text{NO}_2$ : **C**, 75.30; **H**, 5.48; **N**, 5.85. Found: **C**, 73.68; **H**, 4.91; **N**, 4.52.

**Diethyl (2-((3-benzylphenyl) amino)-1-(3-bromophenyl)-1-hydroxy-2-oxoethyl) phosphonate (3.113)**

Using an adapted procedure from Gooßen and Dezfuli,<sup>356</sup> in a flame-dried round flask was added *Tetrakis*(triphenylphosphine)palladium(0) (2 mol%) and  $\text{PPh}_3$  (3.99 mg, 6 mol%). The reaction vessel was fitted

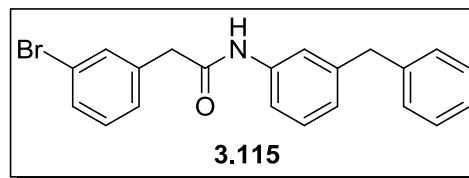


with a reflux condenser and purged with argon. Subsequently, anhydrous EtOH (3 mL), **3.96** (100 mg, 0.254 mmol, 1.0 eq), *N, N*-Diisopropylethylamine (49.5 mg, 66.7  $\mu\text{L}$ , 0.381 mmol, 1.5 eq) and diethylphosphite (42.1 mg, 39.2  $\mu\text{L}$ , 0.305 mmol, 1.2 eq) were added. The reaction mixture was heated to 80°C overnight (16 hours). After the disappearance of the starting

material, the reaction was quenched with 1 N HCl (5 mL) and EtOAc was added (5 mL). The mixture was transferred into a separatory funnel and the organic layer was washed with water (3 x 10 mL) and brine (2 x 10 mL). The organic layers were dried over Na<sub>2</sub>SO<sub>4</sub> and concentrated by rotary evaporation. The crude residue was purified by flash-column chromatography using a gradient of 10:90 EtOAc:hexanes to 70:30 EtOAc:hexanes to yield **3.113** (80.8 mg, 70%) and **3.115** (10.9 mg, 11 %). **3.113**: White crystalline solid  $R_f = 0.13$  (30:70 EtOAc: Hexanes); <sup>1</sup>H NMR (500 MHz, CDCl<sub>3</sub>) δ 9.09 (s, 1H), 7.74 (s, 1H), 7.51 (d,  $J = 7.7$  Hz, 1H), 7.48 – 7.38 (m, 7H), 7.28 – 7.11 (m, 7H), 6.91 (d,  $J = 7.5$  Hz, 1H), 5.89 (d,  $J = 8.5$  Hz, 1H), 4.10 (dddd,  $J = 24.8, 21.7, 11.0, 4.8$  Hz, 4H), 3.90 (s, 2H), 1.43 – 1.11 (m, 2H); <sup>13</sup>C NMR (126 MHz, CDCl<sub>3</sub>) δ 165.88, 165.83, 142.09, 140.77, 138.04, 138.00, 137.49, 132.24, 130.25, 130.05, 129.03, 128.88, 128.49, 126.16, 125.79, 125.38, 122.69, 120.50, 117.83, 77.82, 77.78, 64.90, 64.85, 64.73, 64.69, 41.92, 16.07, 16.04, 16.02, 15.99; **DEPT-135** (126 MHz, CDCl<sub>3</sub>) δ 132.26, 132.24, 130.28, 130.25, 130.05, 129.08, 129.03, 128.90, 128.88, 128.50, 126.16, 125.79, 125.37, 120.50, 117.83, 77.82, 77.78, 77.75, 64.86, 64.74, 64.68, 41.93, 41.92; **Elemental Analysis**: Calc. for C<sub>25</sub>H<sub>27</sub>BrNO<sub>5</sub>P: C, 56.40; H, 5.11; N, 2.63. Found: C, 56.37; H, 4.93 N, 2.52; **melting point**: 93-95 °C.

***N*-(3-benzylphenyl)-2-(3-bromophenyl) acetamide (3.115)**

Prepared by procedure described for **3.113**. White fluffy powder (10.9 mg, 11 %);  $R_f = 0.52$  (30:70 EtOAc: hexanes); <sup>1</sup>H NMR (400 MHz, DMSO) δ 10.11 (s, 1H),

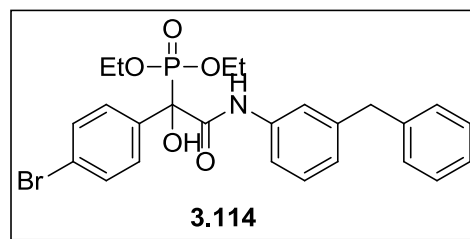


7.52 (s, 1H), 7.44 (dd,  $J = 8.4, 2.6$  Hz, 3H), 7.29 (dt,  $J = 14.1, 7.1$  Hz, 4H), 7.24 – 7.13 (m, 4H), 6.92 (d,  $J = 7.5$  Hz, 1H), 3.89 (s, 2H), 3.62 (s, 2H); <sup>13</sup>C NMR (101 MHz, DMSO) δ 168.91,

142.30, 141.52, 139.63, 139.11, 132.37, 130.85, 129.86, 129.22, 129.14, 128.88, 128.75, 126.45, 121.89, 119.84, 117.35, 43.04, 41.62, 40.61, 40.40, 40.19, 39.99, 39.78, 39.57, 39.36; **DEPT-135** (101 MHz, DMSO)  $\delta$  132.36, 130.85, 129.85, 129.22, 129.14, 129.11, 128.87, 128.85, 128.74, 128.70, 126.44, 124.26, 124.23, 119.83, 119.81, 117.35, 117.31, 43.05, 43.02, 41.63, 41.61; **ESI- MS**:  $m/z$  378, 380 [M-H].

**Diethyl (2-((3-benzylphenyl) amino)-1-(4-bromophenyl)-1-hydroxy-2-oxoethyl) phosphonate (3.114)**

Using an adapted procedure from Gooßen and Dezfuli,<sup>356</sup> in a flame-dried round flask was added Pd(OAc)<sub>2</sub> (2 mol%) and PPh<sub>3</sub> (2.75 mg, 6 mol%). The reaction vessel

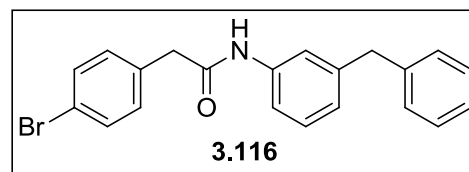


was fitted with a reflux condenser and purged with argon. Subsequently, anhydrous EtOH (4 mL), **3.95** (68.9 mg, 0.175 mmol, 1.0 eq), *N, N*-Diisopropylethylamine (33.93 mg, 45.7  $\mu$ L, 0.263 mmol, 1.5 eq) and diethylphosphite (29 mg, 27.1  $\mu$ L, 0.210mmol, 1.2 eq) were added. The reaction mixture was heated to 80°C overnight (16 hours). After the disappearance of the starting material, the reaction was quenched with 1 N HCl (5 mL) and EtOAc was added (5 mL). The mixture was transferred into a separatory funnel and the organic layer was washed with water (3 x 10 mL) and brine (2 x 10 mL). The organic layers were dried over Na<sub>2</sub>SO<sub>4</sub> and concentrated by rotary evaporation. The crude residue was purified by flash-column chromatography using a gradient of 10:90 EtOAc:hexanes to 70:30 EtOAc:hexanes to yield **3.114** (24.6 mg, 26%) and **3.116** (17.2 mg, 25%). **3.114**: white crystalline solid;  $R_f$  = 0.13 (30:70 EtOAc: hexanes); **<sup>1</sup>H NMR** (500 MHz, CDCl<sub>3</sub>)  $\delta$  9.04 (s, 1H), 7.43 (dt,  $J$  = 24.3, 7.9 Hz, 6H), 7.24 (t,  $J$  = 7.4 Hz, 2H), 7.21 – 7.10 (m, 4H), 6.91 (d,  $J$  = 7.4 Hz, 1H), 5.87 (d,  $J$  = 8.5 Hz, 1H), 4.22 – 3.97 (m, 4H), 3.89 (s, 2H), 1.24 (dt,  $J$  = 14.4, 7.0 Hz, 6H); **<sup>13</sup>C NMR** (126 MHz, CDCl<sub>3</sub>)  $\delta$  166.03, 165.98, 142.11,

140.78, 137.48, 134.94, 134.90, 131.86, 129.06, 128.89, 128.81, 128.51, 126.18, 125.41, 123.41, 120.48, 117.82, 78.00, 77.96, 64.86, 64.81, 64.68, 64.63, 41.92, 16.09, 16.05, 16.03, 16.00; **DEPT-135** (126 MHz, CDCl<sub>3</sub>)  $\delta$  131.87, 129.06, 128.89, 128.81, 128.51, 126.18, 125.41, 120.48, 117.82, 78.00, 77.95, 64.86, 64.81, 64.68, 64.64, 41.92. **Elemental Analysis:** Calc. for C<sub>25</sub>H<sub>27</sub>BrNO<sub>5</sub>P: C, 56.40; H, 5.11; N, 2.63. Found: C, 56.45; H, 5.02 N, 2.54; **melting point:** 97-100 °C.

### ***N*-(3-benzylphenyl)-2-(4-bromophenyl) acetamide (3.116)**

Prepared by procedure described for **3.114**. White fluffy powder (17.2 mg, 25%); **R<sub>f</sub>** = 0.52 (30:70 EtOAc: hexanes); **<sup>1</sup>H NMR** (400 MHz, DMSO)  $\delta$  10.15 (s, 1H),

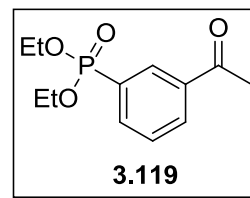


7.57 – 7.39 (m, 4H), 7.32 – 7.23 (m, 4H), 7.24 – 7.13 (m, 4H), 6.92 (d,  $J$  = 7.4 Hz, 1H), 3.88 (s, 2H), 3.60 (s, 2H); **<sup>13</sup>C NMR** (101 MHz, DMSO)  $\delta$  169.03, 142.29, 141.52, 139.67, 135.83, 131.87, 131.57, 129.22, 129.14, 128.88, 126.44, 124.23, 120.20, 119.78, 117.31, 42.94, 41.63; **DEPT-135** (101 MHz, DMSO)  $\delta$  131.87, 131.57, 129.22, 129.14, 128.87, 126.44, 124.22, 119.78, 117.31, 42.94, 41.63; **ESI- MS:**  $m/z$  378, 380 [M-H]<sup>-</sup>.

### **Diethyl (3-acetylphenyl) phosphonate (3.119)**

Using an adapted procedure from Gooßen and Dezfuli,<sup>356</sup> a flame-dried round bottom flask fitted with a reflux condenser charged with Pd(OAc)<sub>2</sub> (13.5 mg, 2 mol%) and PPh<sub>3</sub> (47.48 mg, 6 mol%) was evacuated and purged with argon. Subsequently, anhydrous EtOH (15 mL), 3'-bromoacetophenone (600 mg, 3.014 mmol, 1.0 eq), *N,N*-Diisopropylethylamine (587 mg, 792  $\mu$ L, 4.52 mmol, 1.5 eq) and diethylphosphite (500 mg, 466  $\mu$ L, 3.62 mmol, 1.2 eq) were added.

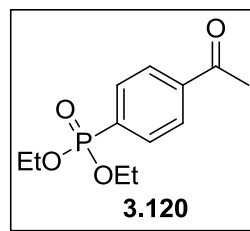
The reaction mixture was heated to 80°C overnight (16 hours). After the disappearance of the starting material, the reaction was quenched with 1 N HCl (5 mL) and EtOAc was added (5 mL). The mixture was transferred



into a separatory funnel and the organic layer was washed with water (3 x 10 mL) and brine (2 x 10 mL). The organic layers were dried over Na<sub>2</sub>SO<sub>4</sub> and concentrated by rotary evaporation. The crude residue was purified by flash-column chromatography using 75:25 EtOAc:hexanes to yield **3.119** as a colorless oil (563 mg, 73%);  $R_f$  = 0.30 (70:30 EtOAc: hexanes); <sup>1</sup>H NMR (400 MHz, CDCl<sub>3</sub>) δ 8.39 (d,  $J$  = 13.8 Hz, 1H), 8.16 (d,  $J$  = 7.8 Hz, 1H), 8.03 (d,  $J$  = 7.6 Hz, 1H), 7.61 (dd,  $J$  = 7.6, 4.0 Hz, 1H), 4.17 (dddd,  $J$  = 24.2, 10.1, 7.3, 2.6 Hz, 4H), 2.65 (s, 3H), 1.35 (t,  $J$  = 7.0 Hz, 6H); <sup>13</sup>C NMR (101 MHz, CDCl<sub>3</sub>) δ 197.08, 137.18, 137.04, 136.02, 135.92, 131.99, 131.84, 131.81, 131.68, 131.58, 130.29, 128.99, 128.84, 128.41, 62.44, 62.38, 26.63, 16.31, 16.25; **DEPT-135** (101 MHz, CDCl<sub>3</sub>) δ 136.02, 135.92, 131.99, 131.84, 131.81, 131.68, 131.58, 128.99, 128.84, 62.44, 62.38, 26.63, 16.31, 16.25; **ESI+MS**:  $m/z$  257 [MH]<sup>+</sup>,  $m/z$  279 [MNa]<sup>+</sup>.

### Diethyl (4-acetylphenyl)phosphonate (**3.120**)

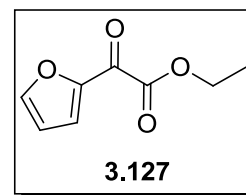
Same procedure for was used as described for **3.119** except using 4'-bromoacetophenone as the starting material. Colorless oil (601 mg, 78%);



$R_f$  = 0.32 (70:30 EtOAc: hexanes); <sup>1</sup>H NMR (400 MHz, CDCl<sub>3</sub>) δ 8.08 – 7.99 (m, 2H), 7.92 (dd,  $J$  = 12.8, 8.4 Hz, 2H), 4.20 – 4.06 (m, 4H), 2.64 (s, 3H), 1.34 (t,  $J$  = 7.1 Hz, 6H); <sup>13</sup>C NMR (101 MHz, CDCl<sub>3</sub>) δ 197.49, 139.82, 134.20, 132.34, 132.10, 132.00, 128.57, 128.45, 128.10, 127.95, 62.48, 62.43, 26.77, 16.32, 16.26; **DEPT-135** (101 MHz, CDCl<sub>3</sub>) δ 132.08, 132.01, 131.98, 128.56, 128.44, 128.09, 127.94, 62.47, 62.42, 26.77, 16.33, 16.32, 16.25; **ESI+MS**:  $m/z$  257 [MH]<sup>+</sup>,  $m/z$  279 [MNa]<sup>+</sup>.

### Ethyl 2-(furan-2-yl)-2-oxoacetate (3.127)

Using an adapted procedure from Cheng *et al.*<sup>1</sup> and Kim *et al.*,<sup>374</sup> to a solution of furan (0.191 mL, 3.00 mmol, 1.0 eq) in anhydrous THF (4 mL) was added slowly *n*-butyl lithium (2.373 mL, 3.15 mmol, 1.05 eq)

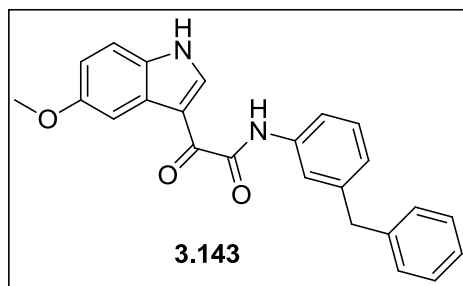


at -78°C. The reaction mixture was stirred at -78°C for 30 minutes. After 30 minutes, a solution (cooled to -78°C) of ZnBr<sub>2</sub> (532.0 mg, 3.6 mmol, 1.20 eq) in anhydrous THF (2 mL) was added to the reaction flask slowly and stirred for 30 minutes. To a separate reaction flask containing Ni(acac) (11.3 mg, 2 mol%) was added 6.9 mL of the ZnBr<sub>2</sub> reagent mixture (6.9 mL, 2.197 mmol, 1.2 eq) at -78°C. This reaction stirred for 15 minutes and then a solution of ethyl oxalyl chloride (0.205 mL, 1.831 mmol, 1.0 eq) in anhydrous THF (2 mL) was added and stirred for 30 minutes. After 30 minutes, the reaction was quenched with a saturated NH<sub>4</sub>Cl solution (10 mL) and extracted with EtOAc. The combined organic layers were washed with a saturated Na<sub>2</sub>S<sub>2</sub>O<sub>3</sub> solution (2 x 10 mL), brine (2 x 10 mL), dried over Na<sub>2</sub>SO<sub>4</sub> and concentrated by rotary evaporation to afford crude orange yellow oil. The crude oil was purified by flash-column chromatography using a gradient of 10:90 EtOAc:hexanes to 50:50 EtOAc:hexanes to afford 3.129 as a dark yellow oil (21.4 mg, 4 %); **R<sub>f</sub>** = 0.32 (10:90 EtOAc: hexanes; stains white with *p*-anisaldehyde); **<sup>1</sup>H NMR** (400 MHz, CDCl<sub>3</sub>) δ 7.79 (dd, *J* = 1.6, 0.7 Hz, 1H), 7.74 (dd, *J* = 3.7, 0.6 Hz, 1H), 6.65 (dd, *J* = 3.7, 1.7 Hz, 1H), 4.44 (q, *J* = 7.1 Hz, 2H), 1.45 (td, *J* = 7.1, 2.8 Hz, 3H); **<sup>13</sup>C NMR** (101 MHz, CDCl<sub>3</sub>) δ 171.12, 161.01, 149.75, 149.50, 149.49, 124.68, 112.99, 62.69, 13.98; **ESI+ MS**: *m/z* 169 [MH]<sup>+</sup>, *m/z* 191 [MNa]<sup>+</sup>.



***N*-(3-benzylphenyl)-2-(5-methoxy-1*H*-indol-3-yl)-2-oxoacetamide (3.143)**

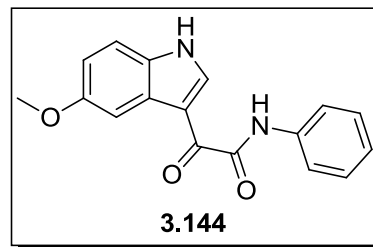
Using an adapted procedure from Lee *et al.*<sup>418</sup> and Marchand *et al.*,<sup>419</sup> a mixture of 5-methoxyindole (30 mg, 21.4  $\mu$ L 0.204 mmol, 1.0 eq) and anhydrous ether



(1 mL) was cooled to 0°C and stirred for 30 minutes. After 30 minutes, oxalyl chloride (31.09 mg, 21  $\mu$ L, 0.245 mmol, 1.2 eq) was added slowly dropwise at 0°C. Solution went from light orange in color to an intense orange-red color. The mixture was stirred for 2 hours at 0°C. After 2 hours, the solvent was carefully removed by rotary evaporation and to the crude residue was added anhydrous THF (1 mL) and 3-benzylaniline (37.38 mg, 0.204 mmol, 1.0 eq) and 1 drop (catalytic amount) of triethylamine. The reaction mixture became golden yellow and cloudy and was stirred at room temperature for 2 hours. The mixture was quenched with saturated NaHCO<sub>3</sub> (10 mL) then extracted with EtOAc (3 x 10 mL). The organic layers were combined, dried over Na<sub>2</sub>SO<sub>4</sub> and concentrated *via* rotary evaporation. The crude solid was then recrystallized from EtOAc:hexanes to yield pure **3.121** as a golden yellow solid (27.6 mg, 35%); <sup>1</sup>H NMR (400 MHz, CDCl<sub>3</sub>)  $\delta$  8.98 (s, 3H), 8.48 (d, *J* = 9.0 Hz, 2H), 7.58 (d, *J* = 8.3 Hz, 1H), 7.51 (s, 1H), 7.30 (t, *J* = 8.2 Hz, 3H), 7.20 (d, *J* = 7.8 Hz, 3H), 7.02 (d, *J* = 7.5 Hz, 1H), 6.96 (d, *J* = 9.0 Hz, 2H), 4.00 (s, 2H), 3.89 (s, 3H); <sup>13</sup>C NMR (101 MHz, CDCl<sub>3</sub>)  $\delta$  185.18, 164.89, 159.43, 142.44, 140.62, 136.89, 134.27, 129.30, 128.94, 128.57, 126.26, 126.07, 125.81, 120.33, 117.70, 113.92, 55.62, 41.88; DEPT-135 (101 MHz, CDCl<sub>3</sub>)  $\delta$  134.27, 129.30, 128.94, 128.57, 126.26, 125.81, 120.33, 117.70, 113.95, 113.92, 55.63, 55.62, 41.89, 41.88; ESI+MS: *m/z* 383 [MH]<sup>+</sup>; **Elemental Analysis:** Calc. for C<sub>24</sub>H<sub>20</sub>N<sub>2</sub>O<sub>3</sub>: C, 74.98; H, 5.24; N, 7.29. Found: C, 73.49; H, 4.98 N, 7.08.

***N*-(3-benzylphenyl)-2-(5-methoxy-1*H*-indol-3-yl)-2-oxoacetamide (3.144)**

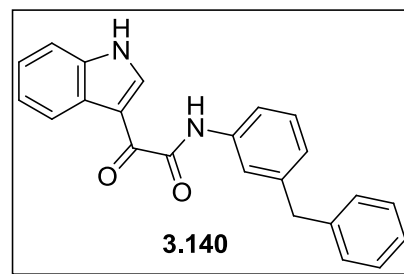
Using an adapted procedure from Lee *et al.*<sup>418</sup> and Marchand *et al.*<sup>419</sup> a mixture of 5-methoxyindole (50 mg, 35.7  $\mu$ L, 0.339 mmol) and anhydrous ether (1 mL) was cooled to 0°C and stirred for 30 minutes. After 30 minutes, oxalyl chloride (51.75



mg, 35  $\mu$ L, 0.408 mmol) was added slowly dropwise at 0°C. Solution went from light orange in color to an intense orange-red color. The mixture was stirred for 2 hours at 0°C. After 2 hours, the solvent was carefully removed by rotary evaporation and to the crude residue was added anhydrous THF (2 mL) and aniline (31.59 mg, 30.9  $\mu$ L, 0.339 mmol, 1.0 eq) and 1 drop (catalytic amount) of triethylamine. The reaction mixture became golden yellow and cloudy and was stirred at room temperature for 2 hours. The mixture was quenched with saturated NaHCO<sub>3</sub> then extracted with EtOAc (3 x 10 mL). The organic layers were combined, dried over Na<sub>2</sub>SO<sub>4</sub> and concentrated *via* rotary evaporation. The crude orange yellow solid was then recrystallized from EtOAc:hexanes to yield pure **3.122** as a light tan powder (53.5 mg, 53%); **R<sub>f</sub>** = 0.333 (20:80 EtOAc: hexanes); **<sup>1</sup>H NMR** (400 MHz, DMSO)  $\delta$  12.26 (s, 1H), 10.66 (s, 1H), 8.72 (s, 1H), 7.86 (dd, *J* = 17.6, 5.0 Hz, 3H), 7.48 (d, *J* = 8.8 Hz, 1H), 7.39 (t, *J* = 7.8 Hz, 2H), 7.15 (t, *J* = 7.3 Hz, 1H), 6.94 (dd, *J* = 8.7, 2.3 Hz, 1H), 3.83 (s, 3H); **<sup>13</sup>C NMR** (101 MHz, DMSO)  $\delta$  182.22, 162.87, 156.56, 138.97, 138.53, 131.60, 129.19, 127.64, 124.67, 120.65, 113.89, 113.43, 112.30, 103.83, 55.71; **DEPT-135** (101 MHz, DMSO)  $\delta$  138.97, 129.19, 124.67, 120.65, 113.89, 113.43, 103.83, 55.71; **Elemental Analysis:** Calc. for C<sub>23</sub>H<sub>18</sub>N<sub>2</sub>O<sub>2</sub>: **C**, 77.95; **H**, 5.12; **N**, 7.90. Found: **C**, 77.47; **H**, 4.92 **N**, 7.78; **melting point:** 243-245 °C (decomp).

### ***N*-(3-benzylphenyl)-2-(1*H*-indol-3-yl)-2-oxoacetamide (3.140)**

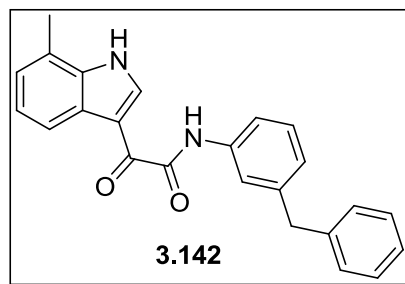
Using an adapted procedure from Lee *et al.*<sup>418</sup> and Marchand *et al.*<sup>419</sup> a mixture of indole (50 mg, 0.427 mmol, 1.0 eq) and anhydrous ether (1.14 mL) was cooled to 0°C and stirred for 30 minutes. After 30 minutes, oxalyl chloride (65 mg, 43.9



μL, 0.512 mmol, 1.2 eq) was added slowly dropwise at 0°C. Solution was bright yellow in color. The mixture was stirred for 2 hours at 0°C. After 2 hours, the solvent was carefully removed by rotary evaporation and to the crude residue was added anhydrous THF (2 mL) and 3-benzylaniline (78.2 mg, 0.427 mmol, 1.0 eq) and 1 drop (catalytic amount) of triethylamine. The reaction mixture became an orange brown color and was stirred at room temperature for 2 hours. The mixture was quenched with saturated NaHCO<sub>3</sub> (10 mL) then extracted with EtOAc (3 x 10 mL). The organic layers were combined, dried over Na<sub>2</sub>SO<sub>4</sub> and concentrated *via* rotary evaporation to yield **3.140** as a light tan powder (155.1 mg, quantitative yield); **R<sub>f</sub>** = 0.333 (20:80 EtOAc: hexanes; stains light brown with *p*-anisaldehyde); **<sup>1</sup>H NMR** (400 MHz, DMSO) δ 12.34 (s, 1H), 10.61 (s, 1H), 8.76 (s, 1H), 8.29 (dd, *J* = 6.2, 2.6 Hz, 1H), 7.79 (s, 1H), 7.69 (d, *J* = 8.1 Hz, 1H), 7.61 – 7.51 (m, 1H), 7.37 – 7.14 (m, 9H), 7.02 (d, *J* = 7.5 Hz, 1H), 3.95 (s, 2H); **<sup>13</sup>C NMR** (101 MHz, DMSO) δ 182.42, 162.80, 142.29, 141.52, 139.04, 138.62, 136.85, 129.23, 129.15, 128.89, 126.64, 126.47, 125.17, 124.02, 123.16, 121.69, 121.04, 118.53, 113.12, 112.41; **DEPT-135** 101 MHz, DMSO) δ 139.04, 129.23, 129.15, 128.89, 126.47, 125.17, 124.02, 123.16, 121.69, 121.04, 118.53, 113.12; **Elemental Analysis:** Calc. for C<sub>23</sub>H<sub>18</sub>N<sub>2</sub>O<sub>2</sub>: **C**, 77.95; **H**, 5.12; **N**, 7.90. Found: **C**, 77.47; **H**, 4.92 **N**, 7.78.

### ***N*-(3-benzylphenyl)-2-(7-methyl-1*H*-indol-3-yl)-2-oxoacetamide (3.142)**

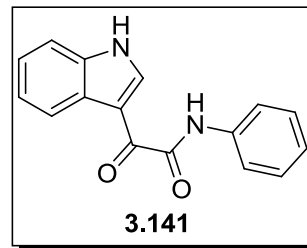
Using an adapted procedure from Lee *et al.*<sup>418</sup> and Marchand *et al.*<sup>419</sup> a mixture of 7-methylindole (30 mg, 0.229 mmol, 1.0 eq) and anhydrous ether (1 mL) was cooled to 0°C and stirred for 30 minutes. After 30 minutes, oxalyl chloride (34.84 mg, 23.6



μL, 0.274 mmol, 1.2 eq) was added slowly dropwise at 0°C. The mixture was stirred for 2 hours at 0°C. After 2 hours, the solvent was carefully removed by rotary evaporation and to the crude residue was added anhydrous THF (2 mL) and 3-benzylaniline (41.9 mg, 0.229 mmol, 1.0 eq) and 1 drop (catalytic amount) of triethylamine. The reaction mixture was stirred at room temperature for 2 hours. The mixture was quenched with saturated NaHCO<sub>3</sub> (10 mL) then extracted with EtOAc (3 x 10 mL). The organic layers were combined, dried over Na<sub>2</sub>SO<sub>4</sub> and concentrated *via* rotary evaporation to yield **3.142** as a brown tan solid (155.1 mg, quantitative yield); **R<sub>f</sub>** = 0.333 (20:80 EtOAc: hexanes; stains light brown with *p*-anisaldehyde); **<sup>1</sup>H NMR** (400 MHz, DMSO) δ 12.39 (s, 1H), 10.74 (s, 1H), 10.60 (s, 1H), 8.71 (s, 1H), 8.12 (d, *J* = 7.8 Hz, 1H), 7.78 (d, *J* = 6.1 Hz, 2H), 7.67 (t, *J* = 8.9 Hz, 2H), 7.32 – 7.19 (m, 5H), 7.09 (d, *J* = 7.1 Hz, 1H), 7.06 – 6.98 (m, 1H), 3.94 (d, *J* = 6.1 Hz, 2H), 2.53 (s, 2H); **<sup>13</sup>C NMR** (101 MHz, DMSO) δ 182.41, 162.80, 158.98, 142.35, 142.27, 141.53, 141.43, 138.62, 138.18, 136.28, 129.17, 128.90, 126.48, 125.47, 124.67, 123.37, 122.49, 121.17, 119.25, 118.64, 112.75, 41.70, 17.09; **DEPT-135** (101 MHz, DMSO) δ 138.55, 129.21, 129.17, 128.90, 126.48, 125.47, 125.17, 124.67, 123.37, 121.17, 121.04, 119.25, 118.64, 118.53, 41.70, 17.09; **ESI- MS**: *m/z* 367 [MH]<sup>+</sup>; **Elemental Analysis**: Calc. for C<sub>24</sub>H<sub>20</sub>N<sub>2</sub>O<sub>2</sub>: **C**, 78.24; **H**, 5.47; **N**, 7.60. Found: **C**, 77.98; **H**, 5.46; **N**, 7.02.

### 2-(1H-indol-3-yl)-2-oxo-N-phenylacetamide (3.141)

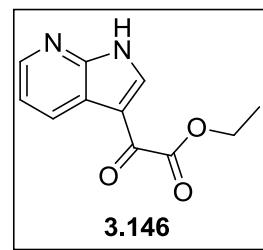
Using an adapted procedure from Lee *et al.*<sup>418</sup> and Marchand *et al.*,<sup>419</sup> a mixture of indole (200 mg, 1.71 mmol, 1.0 eq) and anhydrous ether (4.57 mL) was cooled to 0°C and stirred for 30 minutes. After 30



minutes, oxalyl chloride (260.46 mg, 175 mL, 0.512 mmol, 1.2 eq) was added slowly dropwise at 0°C. Solution was bright yellow in color. The mixture was stirred for 2 hours at 0°C. After 2 hours, the solvent was carefully removed by rotary evaporation and to the crude residue was added anhydrous THF (4 mL) and freshly distilled aniline (54.5 mg, 53.4 μL, 0.171 mmol, 1.0 eq) and 1 drop (catalytic amount) of triethylamine. The reaction mixture became an orange yellow color and was stirred at room temperature for 2 hours. The mixture was quenched with saturated NaHCO<sub>3</sub> (20 mL) then extracted with EtOAc (3 x 20 mL). The organic layers were combined, dried over Na<sub>2</sub>SO<sub>4</sub> and concentrated *via* rotary evaporation to yield **3.141** as a golden-yellow solid (335.9 mg, 94% yield);  $R_f = 0.77$  (50:50 EtOAc: hexanes; stains purple/pink with *p*-anisaldehyde); <sup>1</sup>H NMR (400 MHz, DMSO) δ 12.37 (s, 1H), 10.69 (s, 1H), 8.80 (d, *J* = 2.3 Hz, 1H), 8.33 (dd, *J* = 5.8, 2.3 Hz, 1H), 7.90 (d, *J* = 8.0 Hz, 2H), 7.66 – 7.56 (m, 1H), 7.41 (t, *J* = 7.9 Hz, 2H), 7.37 – 7.30 (m, 2H), 7.17 (t, *J* = 7.3 Hz, 1H); <sup>13</sup>C NMR (101 MHz, DMSO) δ 182.45, 162.82, 139.05, 138.52, 136.86, 129.19, 126.64, 124.69, 124.04, 123.18, 121.69, 120.72, 113.13, 112.43; DEPT-135 (101 MHz, DMSO) δ 139.05, 129.19, 124.69, 124.04, 123.18, 121.69, 120.73, 113.13.3; **Elemental Analysis:** Calc. for C<sub>16</sub>H<sub>12</sub>N<sub>2</sub>O<sub>2</sub>: **C**, 72.72; **H**, 4.58; **N**, 10.60. Found: **C**, 72.19; **H**, 4.30 **N**, 10.45; **melting point:** 240-242 °C (decomp).

### Ethyl 2-oxo-2-(1H-pyrrolo[2,3-b]pyridin-3-yl)acetate (3.146)

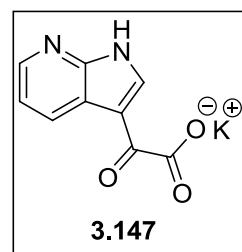
Using an adapted procedure from Zhang *et al.*,<sup>383</sup> azaindole (250 mg, 2.12 mmol, 1 eq) was added to a stirred suspension of AlCl<sub>3</sub> (1.413 g, 10.6 mmol, 5 eq) in anhydrous DCM (50 mL). After the mixture stirred at room temperature for 1 hour, ethyl oxalyl chloride (1.18 mL, 10.6 mmol, 5



eq) was added dropwise. It was noted that as the ethyl oxalyl chloride was added the solution went from yellow color to an orange color. After 12 hours of stirring at room temperature the reaction flask was placed in an ice-water and MeOH was slowly added dropwise to quench the reaction. The color of the solution went from an orange yellow cloudy color to a light brownish orange clear color. DCM was added and the organic layer was separated, washed with saturated NaHCO<sub>3</sub> (3 x 20 mL), H<sub>2</sub>O (2 x 20 mL) and brine (2 x 20 mL). The organic layers were combined, dried over Na<sub>2</sub>SO<sub>4</sub> and concentrated by rotary evaporation to afford an orange-yellow solid. The solid was washed with ice-cold ether to obtain **3.146** as an off-white powder (186.9 mg, 40%); **R<sub>f</sub>** = 0.77 (10:1 EtOAc: MeOH; stains white with *p*-anisaldehyde); **<sup>1</sup>H NMR** (400 MHz, CDCl<sub>3</sub>) δ 13.51 (s, 1H), 8.76 (dd, *J* = 7.9, 1.4 Hz, 1H), 8.72 (s, 1H), 7.34 (dd, *J* = 7.9, 4.9 Hz, 1H), 4.45 (q, *J* = 7.1 Hz, 2H), 4.36 (q, *J* = 7.1 Hz, 1H), 1.46 (t, *J* = 7.1 Hz, 3H), 1.38 (t, *J* = 7.1 Hz, 1H); **<sup>13</sup>C NMR** (101 MHz, CDCl<sub>3</sub>) δ 178.03, 162.31, 149.13, 144.00, 137.57, 131.99, 119.82, 119.12, 112.68, 63.16, 62.31, 14.09, 13.91; DEPT-135 (101 MHz, CDCl<sub>3</sub>) δ 143.99, 137.56, 131.98, 119.11, 63.15, 62.30, 14.09, 13.90; **ESI+MS**: *m/z* 219 [MH]<sup>+</sup>;

### Potassium 2-oxo-2-(1H-pyrrolo[2,3-b]pyridin-3-yl)acetate (**3.147**)

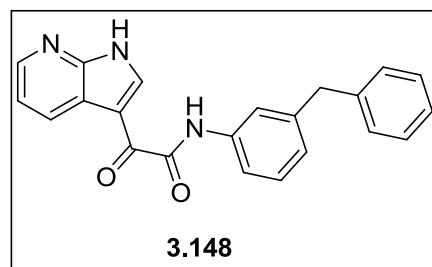
Using an adapted procedure from Wang *et al.*,<sup>305</sup> K<sub>2</sub>CO<sub>3</sub> (151.36 mg, 0.916 mmol, 2.0 eq) was added to a solution of **3.126** (100 mg, 0.458 mmol, 1 eq) in 1:1 mixture of MeOH:H<sub>2</sub>O (2 mL), and the mixture stirred at room temperature for 8 hours. The white precipitate was collected and washed



with cold H<sub>2</sub>O (5 mL) to afford **3.147** as an off-white crystalline powder (68.2 mg, 78%), which was used in the next step without further purification; <sup>1</sup>H NMR (400 MHz, DMSO) δ 8.35 (s, 1H), 8.18 (s, 1H), 7.07 (s, 1H); ESI- MS: *m/z* 189 [M-H]<sup>-</sup>;

### *N*-(3-benzylphenyl)-2-oxo-2-(1H-pyrrolo[2,3-b]pyridin-3-yl)acetamide (**3.148**)

Using an adapted procedure from Martyn *et al.*,<sup>306</sup> to a mixture of **3.148** (43.9 mg, 0.193 mmol, 1.0 eq) and 3-benzylaniline (38.85 mg, 0.212 mmol, 1.1 eq) in anhydrous DMF (2 mL) was added 1-(3-dimethylaminopropyl)-3-



ethylcarbodiimide hydrochloride (48.12, 0.251 mmol, 1.3eq) and 1-hydroxybenzotriazole hydrate (HOBT) (39.12, 0.289, 1.5 eq) at room temperature. *N,N*-Diisopropylethylamine (37.0 μL, 27.40 mg, 0.212 mmol, 1.1 eq) was added dropwise and the reaction mixture stirred at room temperature for 16 hours. The reaction was quenched with H<sub>2</sub>O (5 mL) and stirred for 30 minutes at room temperature. The solution was diluted with EtOAc (10 mL) and the organic layer was washed with H<sub>2</sub>O (5 x 100 mL), saturated NaHCO<sub>3</sub> and brine. The organic layers were combined, dried over Na<sub>2</sub>SO<sub>4</sub> and concentrated to afford an orange-yellow crude solid product **3.128** (66 mg, 96% crude yield); ESI- MS: *m/z* 354 [M-H]<sup>-</sup>.

## **BIBLIOGRAPHY**



1. Cheng, A. C.; Coleman, R. G.; Smyth, K. T.; Cao, Q.; Soulard, P.; Caffrey, D. R.; Salzberg, A. C.; Huang, E. S., Structure-based maximal affinity model predicts small-molecule druggability. *Nature Biotechnology* **2007**, *25*, (1), 71-75.
2. CDC HIV/AIDS Surveillance Report: Diagnoses of HIV Infection and AIDS in the United States and Dependent Areas, 2009. <http://www.cdc.gov/hiv/surveillance/resources/reports/2009report/index.htm> (March 1, 2012),
3. United States Census Bureau 2008 American Community Survey. <http://factfinder2.census.gov/faces/nav/jsf/pages/index.xhtml> (March 1, 2012),
4. AVERT HIV and AIDS in America. [www.avert.org/america.htm](http://www.avert.org/america.htm) (March 1, 2012),
5. UNAIDS Fast Facts about HIV. <http://www.unaids.org/en/resources/presscentre/factsheets/> (February 28, 2012),
6. Osmond, D. H. Epidemiology of Disease Progression in HIV. <http://hivinsite.ucsf.edu/InSite?page=kb-03-01-04> (February 28, 2012),
7. Keele, B. F.; Van Heuverswyn, F.; Li, Y.; Bailes, E.; Takehisa, J.; Santiago, M. L.; Bibollet-Ruche, F.; Chen, Y.; Wain, L. V.; Liegeois, F.; Loul, S.; Ngole, E. M.; Bienvenue, Y.; Delaporte, E.; Brookfield, J. F. Y.; Sharp, P. M.; Shaw, G. M.; Peeters, M.; Hahn, B. H., Chimpanzee Reservoirs of Pandemic and Nonpandemic HIV-1. *Science* **2006**, *313*, (5786), 523-526.
8. Volberding, P. A.; Deeks, S. G., Antiretroviral therapy and management of HIV infection. *The Lancet* **2010**, *376*, (9734), 49-62.
9. History of AIDS Up to 1986. <http://www.avert.org/aids-history-86.htm> (February 25, 2012),
10. CDC *Pneumocystis Pneumonia --- Los Angeles, MMWR*; 1981; pp 250-252.
11. Altman, L. K., Rare Cancer Seen in 41 Homosexuals *The New York Times* 1981.
12. CDC *Kaposi's Sarcoma and Pneumocystis Pneumonia among Homosexual Men- New York City and California, MMWR*; 1981; pp 305-308.
13. Altman, L. K., New Homosexual Disorder Worries Health Officials *The New York Times* 1982.
14. du Bois, R.; Branthwaite, M.; Mikhail, J.; Batten, J., Primary *Pneumocystis carinii* and cytomegalovirus infections. *Lancet* **1981**, *2*, 1339.
15. Masur, H.; Michelis, M. A.; Greene, J. B.; Onorato, I.; Stouwe, R. A.; Holzman, R. S.; Wormser, G.; Brettman, L.; Lange, M.; Murray, H. W.; Cunningham-Rundles, S., An Outbreak of community acquired *Pneumocystis carinii* pneumonia: initial manifestation of cellular immune dysfunction. *The New England Journal Of Medicine* **1981**, *305*, (24), 1431-1438.

16. CDC *Kaposi's sarcoma (KS), Pneumocystis pneumonia (PCP), and other opportunistic infections (01): case reported to CDC as of July 8th 1982, MMWR 31; 1982; pp 507-508, 513-514.*
17. WHO *Acquired Immune Deficiency Syndrome Emergencies, Report of a WHO Meeting; Geneva, 1983.*
18. CDC *Current trends prevention of Acquired Immune Deficiency Syndrome (AIDS): report of interagency recommendations, MMWR; 1983; pp 101-103.*
19. Barre-Sinoussi, F.; Chermann, J. C.; Rey, F.; Nugeyre, M. T.; Chamaret, S.; Gruest, J.; Dauguet, C.; Axler-Blin, C.; Vezinet-Brun, F.; Rouzioux, C.; Rozenbaum, W.; Montagnier, L., Isolation of a T-lymphotropic retrovirus from a patient at risk for acquired immune deficiency syndrome (AIDS). *Science* **1983**, 220, (4599), 868-871.
20. Marx, J. L., Strong new candidate for AIDS agent. *Science* **1984**, 224, (4648), 475-477.
21. Popovic, M.; Sarngadharan, M. G.; Read, E.; Gallo, R. C., Detection, isolation, and continuous production of cytopathic retroviruses (HTLV-III) from patients with AIDS and pre-AIDS. *Science* **1984**, 224, (4648), 497-500.
22. Coffin, J.; Haase, A.; Levy, J. A.; Montagnier, L., Oroszlan, S.; Teich, N.; Temin, H.; Toyoshima, K.; Varmus, H.; Vogt, P., et al., What to call the AIDS virus? *Nature* **1986**, 321.
23. Hardy, A. M.; Allen, J. R.; Morgan, W. M.; Curran, J. W., The incidence rate of acquired immunodeficiency syndrome in selected populations *JAMA : the journal of the American Medical Association* **1985**, 253, (2), 215-220.
24. Cameron, D. W.; D'Costa, L.; Maitha, G.; Cheang, M.; Piot, P.; Simonsen, J. N.; Ronald, A.; Gakinya, M.; Ndinya-Achola, J. O.; Brunham, R.; Plummer, F., Female to Male Transmission of Human Immunodeficiency Virus Type 1: Risk Factors for Seroconversion in Men. *The Lancet* **1989**, 334, (8660), 403-407.
25. Kingsley, L.; Kaslow, R.; Rinaldo, C.; Detre, K.; Odaka, N.; Vanraden, M.; Detels, R.; Polk, B. F.; Chmiel, J.; Kelsey, S.; Ostrow, D.; Visscher, B., Risk Factors for Seroconversion to Human Immunodeficiency Virus Among Male Homosexuals. *The Lancet* **1987**, 329, (8529), 345-349.
26. CDC HIV/AIDS. <http://www.cdc.gov/hiv/default.htm>
27. What is Aids? <http://www.aids.org/topics/aids-factsheets/aids-background-information/what-is-aids/> (February 27, 2012),
28. Schacker, T.; Collier, A. C.; Hughes, J.; Shea, T.; Corey, L., Clinical and epidemiologic features of primary HIV infection. *Annals of Internal Medicine* **1996**, 125, 257-264.

29. Weintrob, A.; Giner, J.; Menezes, P.; Patrick, E.; Benjamin, D. J.; J, L.; CD, P.; JJ, E.; CB, H., Infrequent diagnosis of primary human immunodeficiency virus infection: missed opportunities in acute care settings. *Archives of Internal Medicine* **2003**, 163, 2097-3100.
30. CDC, 1993 revised classification system for HIV infection and expanded surveillance case definition for AIDS among adolescents and adults. *MMWR Recomm Rep* **1992**, 18, (44(RR-17)), 1-19.
31. CDC, Guidelines for national human immunodeficiency virus case surveillance, including monitoring for human immunodeficiency virus infection and acquired immunodeficiency syndrome. . *MMWR Recomm Rep* **1999**, 10, (48(RR-13)), 1-27, 29-31.
32. WHO WHO Case Definitions of HIV for Surveillance and Revised Clinical Staging and Immunological Classification of HIV-Related Disease in Adults and Children. <http://www.who.int/hiv/pub/guidelines/HIVstaging150307.pdf> (February 28, 2012),
33. UNAIDS *Joint United Nations Programme on HIV/AIDS (UNAIDS) Global report: UNAIDS report on the global AIDS epidemic* Switzerland, 2010.
34. Schader, S. M.; Wainberg, M. A., Insights into HIV-1 pathogenesis through drug discovery: 30 years of basic research and concerns for the future. *HIV & AIDS Review* **2011**, 10, (4), 91-98.
35. The Henry J. Kaiser Family Foundation U.S. Global Health Policy: The Global HIV/AIDS Epidemic Fact Sheet. <http://www.kff.org/hivaids/upload/3030-16.pdf> (March 1, 2012),
36. The Henry J. Kaiser Family Foundation HIV/AIDS Policy Fact Sheet: The Global HIV/AIDS Epidemic. <http://www.kff.org/hivaids/upload/3030-07.pdf> (March 1, 2012),
37. UNAIDS World AIDS Day Report. [http://www.unaids.org/en/media/unaids/contentassets/documents/unaidspublication/2011/JC2216\\_WorldAIDSday\\_report\\_2011\\_en.pdf](http://www.unaids.org/en/media/unaids/contentassets/documents/unaidspublication/2011/JC2216_WorldAIDSday_report_2011_en.pdf) (March 1, 2012),
38. WHO Tuberculosis and HIV. <http://www.who.int/hiv/topics/tb/en/index.html> (March 1, 2012),
39. UNAIDS Core Slides: Global Summary of the AIDS Epidemic. <http://www.unaids.org/en/dataanalysis/epidemiology/epidemiologyslides/> (March 1, 2012),
40. UNAIDS Policy Brief: HIV and Sex Between Men. [http://www.unaids.org/en/media/unaids/contentassets/dataimport/publications/irc-pub07/jc1269-policybrief-msm\\_en.pdf](http://www.unaids.org/en/media/unaids/contentassets/dataimport/publications/irc-pub07/jc1269-policybrief-msm_en.pdf) (February 29, 2012),
41. AVERT HIV, AIDS and Men Who Have Sex with Med. <http://www.avert.org/men-sex-men.htm> (March 1, 2012),

42. UNAIDS New Same Sex and Transgender Action Framework. <http://www.unaids.org/en/Resources/PressCentre/Featurestories/2009/May/20090515ActionFramework/> (March 1, 2012),
43. MSMGF Top Ten Key Global Policy Developments in 2010: Reflections from the Global Forum on MSM & HIV <http://www.msngf.org/index.cfm/id/11/aid/3027/langID/1/> (March 1, 2012),
44. WHO Women and health: today's evidence tomorrow's agenda. <http://www.who.int/gender/documents/9789241563857/en/index.html> (March 2, 2012),
45. UNAIDS AIDS SCORECARD Overview: UNAIDS Report on the Global AIDS Epidemic 2010. [http://www.unaids.org/documents/20101123\\_AIDS\\_scorecards\\_em.pdf](http://www.unaids.org/documents/20101123_AIDS_scorecards_em.pdf) (February 27, 2012),
46. CDC HIV/AIDS among men who have sex with men. <http://www.cdc.gov/nchhstp/newsroom/docs/fastfacts-msm-final508comp.pdf> (February 29, 2012),
47. Purcell, D. W.; Johnson, C.; Lansky, A.; Prejean, J.; Stein, R.; Denning, Z.; Weinstock, G. H.; Su, J.; Crepaz, N. In *Calculating HIV and Syphilis Rates for Risk Groups: Estimating the National Population Size of Men Who Have Sex with Men*, National STD Prevention Conference, Atlanta, 2010; Atlanta, 2010.
48. CDC HIV among Gay, Bisexual and Other Men Who Have Sex with Men (MSM). <http://www.cdc.gov/hiv/topics/msm/index.htm> (February 29, 2012),
49. CDC Fact Sheet: Estimates of New HIV Infections in the United States, 2006-2009. <http://www.cdc.gov/nchhstp/newsroom/docs/HIV-Infections-2006-2009.pdf> (February 29, 2012),
50. Hall, H. I.; Song, R.; Rhodes, P.; Prejean, J.; An, Q.; Lee, L. M.; Karon, J.; Brookmeyer, R.; Kaplan, E. H.; McKenna, M. T.; Janssen, R. S., Estimation of HIV Incidence in the United States. *JAMA: The Journal of the American Medical Association* **2008**, 300, (5), 520-529.
51. CDC Estimated Lifetime Risk for Diagnosis of HIV Infection Among Hispanics/Latinos --- 37 States and Puerto Rico, 2007. <http://www.cdc.gov/mmwr/preview/mmwrhtml/mm5940a2.htm> (March 1, 2012),
52. CDC HIV among Latinos. <http://www.cdc.gov/hiv/latinos/index.htm> (March 1, 2012),
53. CDC HIV in the United States: An Overview. <http://www.cdc.gov/hiv/topics/surveillance/resources/factsheets/incidence-overview.htm> (March 2, 2012),
54. The Henry J. Kaiser Family Foundation. HIV/AIDS Policy: The HIV/AIDS Epidemic in the United States. <http://www.kff.org/hivaids/upload/3029-12.pdf> (March 2, 2012),

55. McEnery, R. Why is HIV Ravaging D.C.? <http://www.iavireport.org/archives/2010/Pages/IAVI-Report-14%286%29-HIV-In-DC.aspx> (March 1, 2012),
56. The Henry J. Kaiser Family Foundation. Estimated Numbers of AIDS Diagnoses, All Ages, 2009. <http://www.statehealthfacts.org/comparemaptable.jsp?ind=508&cat=11&sub=119&yr=92&typ=1&sort=a> (March 2, 2012),
57. Prejean, J.; Song, R.; Hernandez, A.; Ziebell, R.; Green, T.; Walker, F.; Lin, L. S.; An, Q.; Mermin, J.; Lansky, A.; Hall, H. I., Estimated HIV Incidence in the United States, 2006-2009. *PLoS ONE* **2011**, 6, (8), e17502.
58. Monterroso, E. R.; Hamburger M E ; Vlahov, D.; Des Jarlais, D. C.; Ouellet, L. J.; Altice, F. L.; Byers, R. H.; Kerndt, P. R.; Watters, J. K.; Bowser, B. P.; Fernando, M. D.; Holmberg, S. D., Prevention of HIV infection in street-recruited injection drug users. The Collaborative Injection Drug User Study (CIDUS). *Journal of Acquired Immune Deficiency Syndromes* **2000**, 25, (1), 63-70.
59. Des Jarlais, D. C.; Perlis, T.; Arasteh, K.; Torian, L. V.; Beatrice, S.; Milliken, J.; Mildvan, D.; Yancovitz, S.; Friedman, S. R., HIV Incidence Among Injection Drug Users in New York City, 1990 to 2002: Use of Serologic Test Algorithm to Assess Expansion of HIV Prevention Services. *American Journal of Public Health* **2005**, 95, (8), 1439-1444.
60. Barr, S. Kaiser Health News: Needle-Exchange Programs Face New Federal Funding Ban <http://www.kaiserhealthnews.org/Stories/2011/December/21/needle-exchange-federal-funding.aspx> (March 2, 2012),
61. NIAID HIV/AIDS: Structure of HIV. <http://www.niaid.nih.gov/topics/HIVAIDS/Understanding/Biology/Pages/structure.aspx> (March 7, 2012),
62. NIAID HIV/AIDS. <http://www.niaid.nih.gov/TOPICS/HIVAIDS/UNDERSTANDING/HOWHIVCAUSESAIDS/Pages/howhiv.aspx> (March 3, 2012),
63. Jonathan, K., Tackling Tat. *Journal of Molecular Biology* **1999**, 293, (2), 235-254.
64. Freed, E. O., HIV-1 and the host cell: an intimate association. *Trends in Microbiology* **2004**, 12, (4), 170-177.
65. Vives, R. R.; Imberty, A.; Sattentau, Q. J.; Lortat-Jacob, H., Heparan Sulfate Targets the HIV-1 Envelope Glycoprotein gp120 Coreceptor Binding Site. *The Journal of Biological Chemistry* **2005**, 280, (22), 21353-21357.
66. Shukla, D.; Liu, J.; Blaiklock, P.; Shworak, N. W.; Bai, X.; Esko, J. D.; Cohen, G. H.; Eisenberg, R. J.; Rosenberg, R. D.; Spear, P. G., A Novel Role for 3-O-Sulfated Heparan Sulfate in Herpes Simplex Virus 1 Entry. *Cell* **1999**, 99, (1), 13-22.

67. Chen, Y.; Maguire, T.; Hileman, R. E.; Fromm, J. R.; Esko, J. D.; Linhardt, R. J.; Marks, R. M., Dengue virus infectivity depends on envelope protein binding to target cell heparan sulfate. *Nature Medicine* **1997**, 3, (8), 866-871.
68. Kaiser, G. E. IV. Viruses: Animal Virus Life Cycles-The Life Cycle of HIV. <http://faculty.cbcmd.edu/courses/bio141/lecguid/unit3/viruses/hivlc.html> (March 4, 2012),
69. Geijtenbeek, T. B. H.; Kwon, D. S.; Torensma, R.; van Vliet, S. J.; van Duijnhoven, G. C. F.; Middel, J.; Cornelissen, I. L. M. H. A.; Nottet, H. S. L. M.; KewalRamani, V. N.; Littman, D. R.; Figdor, C. G.; van Kooyk, Y., DC-SIGN, a Dendritic Cell-Specific HIV-1-Binding Protein that Enhances trans-Infection of T Cells. *Cell* **2000**, 100, (5), 587-597.
70. Mondor, I.; Ugolini, S.; Sattentau, Q. J., Human Immunodeficiency Virus Type 1 Attachment to HeLa CD4 Cells Is CD4 Independent and gp120 Dependent and Requires Cell Surface Heparans. *Journal of Virology* **1998**, 72, (5), 3623-3634.
71. Doms, R. W., Beyond Receptor Expression: The Influence of Receptor Conformation, Density, and Affinity in HIV-1 Infection. *Virology* **2000**, 276, (2), 229-237.
72. De Clercq, E., HIV Life Cycle: Targets for Anti-HIV Agents. In *HIV-1 Integrase: Mechanism and Inhibitor Design*, 1 ed.; Neamati, N., Ed. John Wiley & Sons: 2011; pp 1-14.
73. Connor, R. I.; Sheridan, K. E.; Ceradini, D.; Choe, S.; Landau, N. R., Change in Coreceptor Use Correlates with Disease Progression in HIV-1-Infected Individuals. *The Journal of Experimental Medicine* **1997**, 185, (4), 621-628.
74. Scarlatti, G. T., Eleonora; Bjorndal, Asa; Fredriksson, Robert; Colognesi, Claudia; Deng, Hong Kui; Malnati, Mauro S.; Plebani, Anna; Siccardi, Antonio G.; Littman, Dan R.; Fenyo, Eva Maria; Lusso, Paolo In vivo evolution of HIV-1 co-receptor usage and sensitivity to chemokine-mediated suppression. *Nature Medicine* **1997**, 3, (11), 1259-1265.
75. De Clercq, E., Strategies in the Design of Antiviral Drugs *Nature Reviews Drug Discovery* **2002**, 1, 13-25.
76. Greene, W. C.; Peterlin, B. M., Charting HIV's remarkable voyage through the cell: Basic science as a passport to future therapy. *Nature Medicine* **2002**, 8, (7), 673.
77. Adamson, C. S.; Freed, E. O., Advances in Pharmacology, HIV-1: Molecular Biology and Pathogenesis: Viral Mechanisms. In [Online] Jeang, K.-T., Ed. Elsevier: 2007.
78. Ganser-Pornillos, B. K.; Yeager, M.; Sundquist, W. I., The structural biology of HIV assembly. *Current Opinion in Structural Biology* **2008**, 18, (2), 203-217.
79. Cartier, C.; Sivard, P.; Tranchat, C.; Decimo, D.; Desgranges, C.; Boyer, V. r., Identification of Three Major Phosphorylation Sites within HIV-1 Capsid. *Journal of Biological Chemistry* **1999**, 274, (27), 19434-19440.

80. Franke, E. K.; Yuan, H. E. H.; Luban, J., Specific incorporation of cyclophilin A into HIV-1 virions. *Nature (London)* **1994**, 372, (6504), 359-362.
81. Schaeffer, E.; Geleziunas, R.; Greene, W. C., Human Immunodeficiency Virus Type 1 Nef Functions at the Level of Virus Entry by Enhancing Cytoplasmic Delivery of Virions. *Journal of Virology* **2001**, 75, (6), 2993-3000.
82. Ohagen, A.; Gabuzda, D., Role of Vif in Stability of the Human Immunodeficiency Virus Type 1 Core. *Journal of Virology* **2000**, 74, (23), 11055-11066.
83. Karageorgos, L. L., Peng; Burrell, Chris, Characterization of HIV replication complexes early after cell-to-cell infection. *AIDS Research and Human Retroviruses* **1993**, 9, (9), 817-823.
84. Bukrinskaya, A.; Brichacek, B.; Mann, A.; Stevenson, M., Establishment of a Functional Human Immunodeficiency Virus Type 1 (HIV-1) Reverse Transcription Complex Involves the Cytoskeleton. *The Journal of Experimental Medicine* **1998**, 188, (11), 2113-2125.
85. Duyk, G.; Leis, J.; Longiaru, M.; Skalka, A. M., Selective cleavage in the avian retroviral long terminal repeat sequence by the endonuclease associated with the alpha beta form of avian reverse transcriptase. *Proceedings of the National Academy of Sciences* **1983**, 80, (22), 6745-6749.
86. Pommier, Y.; Johnson, A. A.; Marchand, C., Integrase inhibitors to treat HIV/Aids. *Nature Reviews Drug Discovery* **2005**, 4, (3), 236-248.
87. Kalpana, G. V.; Marmon, S.; Wang, W.; Crabtree, G. R.; Goff, S. P., Binding and stimulation of HIV-1 integrase by a human homolog of yeast transcription factor SNF5. *Science* **1994**, 266, (5193), 2002-2006.
88. Cherepanov, P.; Maertens, G.; Proost, P.; Devreese, B.; Van Beeumen, J.; Engelborghs, Y.; De Clercq, E.; Debyser, Z., HIV-1 Integrase Forms Stable Tetramers and Associates with LEDGF/p75 Protein in Human Cells. *Journal of Biological Chemistry* **2003**, 278, (1), 372-381.
89. Violot, S. b.; Hong, S. S.; Rakotobe, D.; Petit, C.; Gay, B.; Moreau, K.; Billaud, G. v.; Priet, S. p.; Sire, J. p.; Schwartz, O.; Mouscadet, J.-F. o.; Boulanger, P., The Human Polycomb Group EED Protein Interacts with the Integrase of Human Immunodeficiency Virus Type 1. *Journal of Virology* **2003**, 77, (23), 12507-12522.
90. Parissi, V.; Calmels, C.; De Soultrait, V. R.; Caumont, A.; Fournier, M.; Chaignepain, S. p.; Litvak, S., Functional Interactions of Human Immunodeficiency Virus Type 1 Integrase with Human and Yeast HSP60. *Journal of Virology* **2001**, 75, (23), 11344-11353.
91. Turlure, F. D., Eric; Silver, Pamela A.; Engelman, Alan Human cell proteins and human immunodeficiency virus DNA integration. *Frontiers in bioscience* **2004**, 9, (suppl.), 3187-3208.
92. Jordan, A.; Defechereux, P.; Verdin, E., The site of HIV-1 integration in the human genome determines basal transcriptional activity and response to Tat transactivation. *EMBO J* **2001**, 20, (7), 1726-1738.



93. Stevens, M.; De Clercq, E.; Balzarini, J., The regulation of HIV-1 transcription: Molecular targets for chemotherapeutic intervention. *Medicinal Research Reviews* **2006**, 26, (5), 595-625.
94. Taube, R.; Fujinaga, K.; Wimmer, J.; Barboric, M.; Peterlin, B. M., Tat Transactivation: A Model for the Regulation of Eukaryotic Transcriptional Elongation. *Virology* **1999**, 264, (2), 245-253.
95. Yamaguchi, Y.; Takagi, T.; Wada, T.; Yano, K.; Furuya, A.; Sugimoto, S.; Hasegawa, J.; Handa, H., NELF, a Multisubunit Complex Containing RD, Cooperates with DSIF to Repress RNA Polymerase II Elongation. *Cell* **1999**, 97, (1), 41-51.
96. Yamaguchi, Y.; Filipovska, J.; Yano, K.; Furuya, A.; Inukai, N.; Narita, T.; Wada, T.; Sugimoto, S.; Konarska, M. M.; Handa, H., Stimulation of RNA Polymerase II Elongation by Hepatitis Delta Antigen. *Science* **2001**, 293, (5527), 124-127.
97. Yamaguchi, Y., HIV-1 Transcription: Activation Mediated by Acetylation of Tat. *Structure* **2002**, 10, 443-446.
98. Garber, M. E.; Jones, K. A., HIV-1 Tat: coping with negative elongation factors. *Current Opinion in Immunology* **1999**, 11, 460-465.
99. Wong, K.; Sharma, A.; Awasthi, S.; Matlock, E. F.; Rogers, L.; Van Lint, C.; Skiest, D. J.; Burns, D. K.; Harrod, R., HIV-1 Tat Interactions with p300 and PCAF Transcriptional Coactivators Inhibit Histone Acetylation and Neurotrophin Signaling through CREB. *Journal of Biological Chemistry* **2005**, 280, (10), 9390-9399.
100. Adamson, C. S.; Freed, E. O., Novel approaches to inhibiting HIV-1 replication. *Antiviral Research* **2010**, 85, (1), 119-141.
101. Cihlar, T.; Ray, A. S., Nucleoside and nucleotide HIV reverse transcriptase inhibitors: 25 years after zidovudine. *Antiviral Research* **2011**, 85, (1), 39-58.
102. Wensing, A. M. J. v. M., Noortje M; Nijhuis, Monique Fifteen years of HIV Protease Inhibitors: raising the barrier to resistance. *Antiviral research* **2010**, 85, (1), 59-74.
103. de Bethune, M.-P., Non-nucleoside reverse transcriptase inhibitors (NNRTIs), their discovery, development, and use in the treatment of HIV-1 infection: A review of the last 20 years (1989-2009). *Antiviral Research* **2010**, 85, (1), 75-90.
104. McColl, D. J.; Chen, X., Strand transfer inhibitors of HIV-1 integrase: Bringing IN a new era of antiretroviral therapy. *Antiviral Research* **2010**, 85, (1), 101-118.
105. Tilton, J. C.; Doms, R. W., Entry inhibitors in the treatment of HIV-1 infection. *Antiviral Research* **2010**, 85, (1), 91-100.
106. Tantillo, C. D., Jianping; Jacobo-Molina, Alfredo; Nanni, Raymond G.; Boyer, Paul L.; Hughes, Stephen H.; Pauwels, Rudi; Andries, Koen; Janssen, Paul A. J.; Arnold, Edward



Locations of Anti-AIDS Drug Binding Sites and Resistance Mutations in the Three-dimensional Structure of HIV-1 Reverse Transcriptase Implications for Mechanisms of Drug Inhibition and Resistance. *Journal of Molecular Biology* **1994**, 243, (3), 369-387.

107. Rudi, P., New non-nucleoside reverse transcriptase inhibitors (NNRTIs) in development for the treatment of HIV infections. *Current Opinion in Pharmacology* **2004**, 4, (5), 437-446.

108. Furman, P. A.; Fyfe, J. A.; St Clair, M. H.; Weinhold, K.; Rideout, J. L.; Freeman, G. A.; Lehrman, S. N.; Bolognesi, D. P.; Broder, S.; Mitsuya, H., Phosphorylation of 3'-azido-3'-deoxythymidine and selective interaction of the 5'-triphosphate with human immunodeficiency virus reverse transcriptase. *Proceedings of the National Academy of Sciences* **1986**, 83, (21), 8333-8337.

109. Cheng, Y. C.; Dutschman, G. E.; Bastow, K. F.; Sarngadharan, M. G.; Ting, R. Y., Human immunodeficiency virus reverse transcriptase. General properties and its interactions with nucleoside triphosphate analogs. *Journal of Biological Chemistry* **1987**, 262, (5), 2187-2189.

110. St Clair, M. H.; Richards, C. A.; Spector, T.; Weinhold, K.; Miller, W. H.; Langlois, A. J.; Furman, P. A., 3'-Azido-3'-deoxythymidine triphosphate as an inhibitor and substrate of purified human immunodeficiency virus reverse transcriptase. *Antimicrob. Agents Chemother.* **1987**, 31, (12), 1972-1977.

111. DHHS Guidelines for the Use of Antiretroviral Agents in HIV-1-Infected Adults and Adolescents. [http://aidsinfo.nih.gov/contentfiles/AA\\_Tables.pdf](http://aidsinfo.nih.gov/contentfiles/AA_Tables.pdf) (March 8, 2012),

112. Ray, A. S., Intracellular interactions between nucleos(t)ide inhibitors of HIV reverse transcriptase. *AIDS Reviews* **2005**, 7, 113-125.

113. Roberts, J. D.; Bebenek, K.; Kunkel, T. A., The accuracy of reverse transcriptase from HIV-1. *Science* **1988**, 242, 1171-1173.

114. Coffin, J. M., HIV population dynamics in vivo: implications for genetic variation, pathogenesis, and therapy. *Science* **1995**, 267, 483-489.

115. Lewis, W.; Day, B. J.; Copeland, W. C., Mitochondrial Toxicity of NRTI Antiviral Drugs: An Integrated Cellular Perspective. *Nature Reviews Drug Discovery* **2003**, 2, 812-822.

116. Kohl, N. E.; Emimi, E. A.; Schleif, W. A.; Davis, L. J.; Heimbach, J. C.; Dixon, R. A.; Scolnick, E. M.; Sigal, I. S., Active human immunodeficiency virus protease is required for viral infectivity. *Proceedings of the National Academy of Sciences* **1988**, 85, (13), 4686-4690.

117. Jacks, T. P., Michael D.; Masiarz, Frank R.; Luciw, Paul A.; Barr, Philip J.; Varmus, Harold E., Characterization of ribosomal frameshifting in HIV-1 gag-pol expression. *Nature* **1988**, 331, (6153), 280-283.

118. Karacostas, V.; Nagashima, K.; Gonda, M. A.; Moss, B., Human immunodeficiency virus-like particles produced by a vaccinia virus expression vector. *Proceedings of the National Academy of Sciences* **1989**, 86, 8964-8967.
119. Roberts, N. A.; Martin, J. A.; Kinchington, D.; Broadhurst, A. V.; Craig, J. C.; Duncan, I. B.; Galpin, S. A.; Handa, B. K.; Kay, J.; Kröhn, A.; Lambert, R. W.; Merrett, J. H.; Mills, J. S.; Parkes, K. E. B.; Redshaw, S.; Ritchie, A. J.; Taylor, D. L.; Thomas, G. J.; Machin, P. J., Rational Design of Peptide-Based HIV Proteinase Inhibitors. *Science* **1990**, 248, (4953), 358-361.
120. Craig, J. C. D., I. B.; Hockley, D.; Grief, C.; Roberts, N. A.; Mills, J. S. , Antiviral properties of Ro 31-8959, an inhibitor of human immunodeficiency virus (HIV) proteinase. *Antiviral Research* **1991**, 16, (4), 295-305.
121. Kempf, D. J. M., Kennan C.; Denissen, Jon F.; McDonald, Edith; Vasavanonda, Sudthida; Flentge, Charles A.; Green, Brian E.; Fino, Lynnmarie; Park, Chang H.; Kong, Xiang-Peng; Wideburg, Norman E.; Saldivar, Ayda; Ruiz, Lisa; Kati, Warren M.; Sham, Hing L.; Robins, Terry; Stewart, Kent D.; Hsu, Ann; Plattner, Jacob J.; Leonard, John M.; Norbeck, Daniel W., ABT-538 is a Potent Inhibitor of Human Immunodeficiency Virus Protease and has High Oral Bioavailability in Humans. *PNAS : Proceedings of the National Academy of Sciences* **1995**, 92, (7), 2484-2488.
122. Koh, Y. N., Hiroto; Maeda, Kenji; Ogata, Hiromi; Bilcer, Geoffrey; Devasamudram, Thippeswamy; Kincaid, John F.; Boross, Peter; Wang, Yuan-Fang; Tie, Yunfeng; Volarath, Patra; Gaddis, Laquasha; Harrison, Robert W.; Weber, Irene T.; Ghosh, Arun K.; Mitsuya, Hiroaki Novel bis-Tetrahydrofuranylurethane-Containing Nonpeptidic Protease Inhibitor (PI) UIC-94017 (TMC114) with Potent Activity against Multi-PI-Resistant Human Immunodeficiency Virus In Vitro. *Antimicrobial Agents and Chemotherapy* **2003**, 47, (10), 3123-3129.
123. Partaledis, J. A. Y., Koushi; Tisdale, Margaret; Blair, Edward E.; Falcione, Cristina; Maschera, Barbara; Myers, Richard E.; Pazhanisamy, S.; Futer, Olga; Cullinan, Aine B.; Stuver, Cameron M.; Byrn, Randal A.; Livingston, David J., In vitro selection and characterization of human immunodeficiency virus type 1 (HIV-1) isolates with reduced sensitivity to hydroxyethylamino sulfonamide inhibitors of HIV-1 aspartyl protease. *Journal of Virology* **1995**, 69, (9), 5228.
124. Patick, A. K.; Mo, H.; Markowitz, M.; Appelt, K.; Wu, B.; Musick, L.; Kalish, V.; Kaldor, S.; Reich, S.; Ho, D.; Webber, S., Antiviral and resistance studies of AG1343, an orally bioavailable inhibitor of human immunodeficiency virus protease. *Antimicrobial Agents and Chemotherapy* **1996**, 40, (2), 292-7.
125. Robinson, B. S.; Riccardi, K. A.; Gong, Y.-f.; Guo, Q.; Stock, D. A.; Blair, W. S.; Terry, B. J.; Deminie, C. A.; Djang, F.; Colonno, R. J.; Lin, P.-f., BMS-232632, a Highly Potent Human Immunodeficiency Virus Protease Inhibitor That Can Be Used in Combination with Other Available Antiretroviral Agents. *Antimicrobial Agents and Chemotherapy* **2000**, 44, (8), 2093-2099.

126. Sham, H. L.; Kempf, D. J.; Molla, A.; Marsh, K. C.; Kumar, G. N.; Chen, C.-M.; Kati, W.; Stewart, K.; Lal, R.; Hsu, A.; Betebenner, D.; Korneyeva, M.; Vasavanonda, S.; McDonald, E.; Saldivar, A.; Wideburg, N.; Chen, X.; Niu, P.; Park, C.; Jayanti, V.; Grabowski, B.; Granneman, G. R.; Sun, E.; Japour, A. J.; Leonard, J. M.; Plattner, J. J.; Norbeck, D. W., ABT-378, a Highly Potent Inhibitor of the Human Immunodeficiency Virus Protease. *Antimicrobial Agents and Chemotherapy* **1998**, 42, (12), 3218-3224.
127. Vacca, J. P. D., B.D.; Schleif, W.A.; Levin, R.B.; McDaniel, S.L.; Darke, P.L.; Zugay, J.; Quintero, J.C.; Blahly, O.M.; Roth, E., L-735,524: An Orally Bioavailable Human Immunodeficiency Virus Type 1 Protease Inhibitor. *Proceedings of the National Academy of Sciences* **1994**, 91, (9), 4096-4100.
128. Turner, S. R.; Strohbach, J. W.; Tommasi, R. A.; Aristoff, P. A.; Johnson, P. D.; Skulnick, H. I.; Dolak, L. A.; Seest, E. P.; Tomich, P. K.; Bohanon, M. J.; Horng, M.-M.; Lynn, J. C.; Chong, K.-T.; Hinshaw, R. R.; Watenpaugh, K. D.; Janakiraman, M. N.; Thaisrivongs, S., Tipranavir (PNU140690): a potent, orally bioavailable nonpeptidic HIV protease inhibitor of the 5,6-dihydro-4hydroxy-2-pyrone sulfonamide class. *Journal of Medicinal Chemistry* **1998**, 41, (18), 3467-3476.
129. Gulnik, S. V., HIV-1 Protease Inhibitors as Antiretroviral Agents. In *Enzyme Inhibition in Drug Discovery and Development*, Lu, C.; Li, A. P. L., Eds. John Wiley & Sons, Inc.: Hoboken, NJ, 2010; pp 749-810.
130. Furfine, E. S.; Baker, C. T.; Hale, M. R.; Reynolds, D. J.; Salisbury, J. A.; Searle, A. D.; Studenberg, S. D.; Todd, D.; Tung, R. D.; Spaltenstein, A., Preclinical Pharmacology and Pharmacokinetics of GW433908, a Water-Soluble Prodrug of the Human Immunodeficiency Virus Protease Inhibitor Amprenavir. *Antimicrobial Agents and Chemotherapy* **2004**, 48, (3), 791-798.
131. King, J. R.; Acosta, E. P., Tipranavir: a novel peptidic protease inhibitor of HIV. *Clinical Pharmacokinetics* **2006**, 45, 665-682.
132. Sluis-Cremer, N.; Temiz, N. A.; Bahar, I., Conformational changes in HIV-1 reverse transcriptase induced by nonnucleoside reverse transcriptase inhibitor binding. *Current HIV Research* **2004**, 2, 323-332.
133. Blas-Garcia, A.; Esplugues, J. V.; Apostolova, N., Twenty Years of HIV-1 Non-Nucleoside Reverse Transcriptase Inhibitors: Time to Reevaluate their Toxicity. *Current Medicinal Chemistry* **2011**, 18, 2186-2195.
134. Podzamczar, D.; Fumero, E., The role of nevirapine in the treatment of HIV-1 disease. *Expert Opinion in Pharmacotherapy* **2001**, 2, 2065-2078.
135. Best, B. M.; Goicoechea, M., Efavirenz-still first-line king? *Expert Opinion in Drug Metabolism & Toxicology* **2008**, 4, 965-972.

136. Kitchen, C. M.; Kitchen, S. G.; Dubin, J. A.; Gottlieb, M. S., Initial Virological and Immunologic Response to Highly Active Antiretroviral Therapy Predicts Long-Term Clinical Outcome. *Clinical Infectious Diseases* **2001**, 33, (4), 466-472.
137. Hammer, S. M.; Eron, J. J.; Reiss, P.; Schooley, R. T.; Thompson, M. A.; Walmsley, S.; Cahn, P.; Fischl, M. A.; Gatell, J. M.; Hirsch, M. S.; Jacobsen, D. M.; Montaner, J. S. G.; Richman, D. D.; Yeni, P. G.; Volberding, P. A., Antiretroviral Treatment of Adult HIV Infection. *JAMA: The Journal of the American Medical Association* **2008**, 300, (5), 555-570.
138. Clercq, E. D., From adefovir to Atripla™ via tenofovir, Viread™ and Truvada™. *Future Virology* **2006**, 1, (6), 709-715.
139. Poveda, E.; Briz, V.; Soriano, V., Enfuvirtide, the First Fusion Entry Inhibitor to Treat HIV Infection. *AIDS Reviews* **2005**, 7, 139-147.
140. Wild, C.; Oas, T.; McDanal, C.; Bolognesi, D.; Matthews, T., A synthetic peptide inhibitor of human immunodeficiency virus replication: correlation between solution structure and viral inhibition. *Proceedings of the National Academy of Sciences* **1992**, 89, (21), 10537-10541.
141. Wild, C. T.; Shugars, D. C.; Greenwell, T. K.; McDanal, C. B.; Matthews, T. J., Peptides corresponding to a predictive alpha-helical domain of human immunodeficiency virus type 1 gp41 are potent inhibitors of virus infection. *Proceedings of the National Academy of Sciences* **1994**, 91, (21), 9770-9774.
142. Jiang, S.; Li, K.; Strik, N.; Neurath, A., HIV-1 inhibition by a peptide. *Nature* **1993**, 365, (6442), 113-113.
143. Dietrich, U., HIV-1 Entry Inhibitors. *AIDS Reviews* **2001**, 3, 89-97.
144. Weiss, C., HIV-1 gp41: Mediator of Fusion and Target for Inhibition. *AIDS Reviews* **2003**, 5, 214-221.
145. Matthews, T.; Salgo, M.; Greenberg, M.; Chung, J.; DeMasi, R.; Bolognesi, D., Enfuvirtide: the first therapy to inhibit the entry of HIV-1 into host CD4 lymphocytes. *Nat Rev Drug Discov* **2004**, 3, (3), 215-225.
146. Greenberg, M. L.; Cammack, N., Resistance to enfuvirtide, the first HIV fusion inhibitor. *Journal of Antimicrobial Chemotherapy* **2004**, 54, (2), 333-340.
147. De Clercq, E.; Yamamoto, N.; Pauwels, R.; Balzarini, J.; Witvrouw, M.; De Vreese, K.; Debyser, Z.; Rosenwirth, B.; Peichl, B.; Datema, R.; Thornton, D.; Skerlj, R.; Gaul, F.; Padmanabhan, S.; Bridger, G.; Henson, G.; Abrams, M., Highly potent and selective inhibition of human immunodeficiency virus by the bicyclam derivative JM3100. *Antimicrobial Agents and Chemotherapy* **1994**, 38, 668-674.

148. Schols, D.; Struyf, S.; J., V. D.; Esté, J. A.; Henson, G.; De Clercq, E., Inhibition of T-trophic HIV strains by selective antagonization of the chemokine receptor CXCR4. *Journal of Experimental Medicine* **1997**, 186, 1383-1388.
149. Perros, M., CCR5 antagonists for the treatment of HIV infection and AIDS. In *Advances in Antiviral Drug Design*, Elsevier: Amsterdam, 2007; Vol. 5, pp 185-212.
150. Levy, J. A., HIV pathogenesis: 25 years of progress and persistent challenges. *AIDS* **2009**, 23, (2), 147-160.
151. Biswas, P.; Tambussi, G.; Lazzarin, A., Access denied? The status of co-receptor inhibition to counter HIV entry. *Expert Opinion in Pharmacotherapy* **2007**, 8, (7), 923-933.
152. Emmelkamp, J.; Rockstroh, J., CCR5 antagonists: comparison of efficacy, side effects, pharmacokinetics and interactions--review of the literature. *European Journal of Medical Research* **2007**, 12, (9), 409-417.
153. Westby, M.; Lewis, M.; Whitcomb, J.; Youle, M.; Pozniak, A. L.; James, I. T.; Jenkins, T. M.; Perros, M.; van der Ryst, E., Emergence of CXCR4-Using Human Immunodeficiency Virus Type 1 (HIV-1) Variants in a Minority of HIV-1-Infected Patients following Treatment with the CCR5 Antagonist Maraviroc Is from a Pretreatment CXCR4-Using Virus Reservoir. *Journal of Virology* **2006**, 80, (10), 4909-4920.
154. Westby, M.; Smith-Burchnell, C.; Mori, J.; Lewis, M.; Mosley, M.; Stockdale, M.; Dorr, P.; Ciaramella, G.; Perros, M., Reduced Maximal Inhibition in Phenotypic Susceptibility Assays Indicates that Viral Strains Resistant to the CCR5 Antagonist Maraviroc Utilize Inhibitor-Bound Receptor for Entry. *Journal of Virology* **2007**, 81, (5), 2359-2371.
155. Daelemans, D.; Lu, R.; De Clercq, E.; Engelman, A., Characterization of a Replication-Competent, Integrase-Defective Human Immunodeficiency Virus (HIV)/Simian Virus 40 Chimera as a Powerful Tool for the Discovery and Validation of HIV Integrase Inhibitors. *Journal of Virology* **2007**, 81, (8), 4381-4385.
156. Grinsztejn, B.; Nguyen, B.-Y.; Katlama, C.; Gatell, J. M.; Lazzarin, A.; Vittecoq, D.; Gonzalez, C. J.; Chen, J.; Harvey, C. M.; Isaacs, R. D., Safety and efficacy of the HIV-1 integrase inhibitor raltegravir (MK-0518) in treatment-experienced patients with multidrug-resistant virus: a phase II randomised controlled trial. *The Lancet* **2007**, 369, (9569), 1261-1269.
157. Ross, A. L.; Brave, A.; Scarlatti, G.; Manrique, A.; Buonaguro, L., Progress towards development of an HIV vaccine: report of the AIDS Vaccine 2009 Conference. *Lancet Infectious Diseases* **2010**, 10, (5), 305-316.
158. Jesil, A. M.; Palanimuthu Vasanth Raj, A. M.; Rao, J. V., HIV Vaccines: Present Scenario and Future Prospects. *Pharmacologyonline* **2011**, 2, 90-103.
159. Mocroft, A.; Phillips, A. N.; Gatell, J.; Ledergerber, B.; Fisher, M.; Clumeck, N.; Losso, M.; Lazzarin, A.; Fatkenheuer, G.; Lundgren, J. D., Normalisation of CD4 counts in patients

with HIV-1 infection and maximum virological suppression who are taking combination antiretroviral therapy: an observational cohort study. *The Lancet* **2007**, 370, (9585), 407-413.

160. Rodriguez, B.; Sethi, A. K.; Cheruvu, V. K.; Mackay, W.; Bosch, R. J.; Kitahata, M.; Boswell, S. L.; Mathews, W. C.; Bangsberg, D. R.; Martin, J.; Whalen, C. C.; Sieg, S.; Yadavalli, S.; Deeks, S. G.; Lederman, M. M., Predictive Value of Plasma HIV RNA Level on Rate of CD4 T-Cell Decline in Untreated HIV Infection. *JAMA: The Journal of the American Medical Association* **2006**, 296, (12), 1498-1506.

161. Mellors, J. W.; Margolick, J. B.; Phair, J. P.; Rinaldo, C. R.; Detels, R.; Jacobson, L. P.; Munoz, A., Prognostic Value of HIV-1 RNA, CD4 Cell Count, and CD4 Cell Count Slope for Progression to AIDS and Death in Untreated HIV-1 Infection. *JAMA: The Journal of the American Medical Association* **2007**, 297, (21), 2349-2350.

162. Johnson, V.; Brun-Vezinet, F.; Clotet, B.; Gunthard, H.; Kuritzkes, D.; Pillay, D.; Schapiro, J.; Richman, D., Update of the drug resistance mutations in HIV-1: December 2009. *Top HIV Med* **2009**, 17, (5), 138-145.

163. Moore, J. P.; Kitchen, S. G.; Pugach, P.; Zack, J. A., The CCR5 and CXCR4 Coreceptors—Central to Understanding the Transmission and Pathogenesis of Human Immunodeficiency Virus Type 1 Infection *AIDS Research and Human Retroviruses* **2004**, 20, (1), 111-126.

164. Hirsch, M. S.; Gunthard, H. F.; Schapiro, J. M.; Vezinet, F. B.; Clotet, B.; Hammer, S. M.; Johnson, V. A.; Kuritzkes, D. R.; Mellors, J. W.; Pillay, D.; Yeni, P. G.; Jacobsen, D. M.; Richman, D. D., Antiretroviral Drug Resistance Testing in Adult HIV-1 Infection: 2008 Recommendations of an International AIDS Society-USA Panel. *Clinical Infectious Diseases* **2008**, 47, (2), 266-285.

165. Cohen, J., Confronting the Limits of Success. *Science* **2002**, 296, (5577), 2320-2324.

166. Freedberg, K. A.; Losina, E.; Weinstein, M. C.; Paltiel, A. D.; Cohen, C. J.; Seage, G. R.; Craven, D. E.; Zhang, H.; Kimmel, A. D.; Goldie, S. J., The Cost Effectiveness of Combination Antiretroviral Therapy for HIV Disease. *New England Journal of Medicine* **2001**, 344, (11), 824-831.

167. Asante-Appiah, E.; Skalka, A. M., Molecular mechanisms in retrovirus DNA integration. *Antiviral Research* **1997**, 36, (3), 139-156.

168. Liao, C.; Marchand, C.; Burke, T. R.; Pommier, Y.; Nicklaus, M. C., Authentic HIV-1 integrase inhibitors. *Future Medicinal Chemistry* **2010**, 2, (7), 1107-1122.

169. Halgren, T. A., Identifying and Characterizing Binding Sites and Assessing Druggability. *Journal of Chemical Information and Modeling* **2009**, 49, (2), 377-389.

170. Schmidtke, P.; Barril, X., Understanding and Predicting Druggability. A High-Throughput Method for Detection of Drug Binding Sites. *Journal of Medicinal Chemistry* **2010**, 53, (15), 5858-5867.

171. Miller, M. D.; Farnet, C. M.; Bushman, F. D., Human immunodeficiency virus type 1 preintegration complexes: studies of organization and composition. *Journal of Virology* **1997**, 71, (7), 5382-8390.
172. Chiu, P.; Craigie, R.; Davies, D. R., Structure and Function of HIV-1 integrase. *Current Topics in Medicinal Chemistry* **2004**, 4, 965-977.
173. Engelman, A.; Mizuuchi, K.; Craigie, R., HIV-1 DNA integration: Mechanism of viral DNA cleavage and DNA strand transfer. *Cell* **1991**, 67, (6), 1211-1221.
174. Schroder, A. R. W.; Shinn, P.; Chen, H.; Berry, C.; Ecker, J. R.; Bushman, F., HIV-1 Integration in the Human Genome Favors Active Genes and Local Hotspots. *Cell* **2002**, 110, (4), 521-529.
175. Hazuda, D. J.; Felock, P.; Witmer, M.; Wolfe, A.; Stillmock, K.; Grobler, J. A.; Espeseth, A.; Gabryelski, L.; Schleif, W.; Blau, C.; Miller, M. D., Inhibitors of Strand Transfer That Prevent Integration and Inhibit HIV-1 Replication in Cells. *Science* **2000**, 287, (5453), 646-650.
176. Asante-Appiah, E.; Skalka, A. M.; Karl Rlaramorosch, F. A. M.; Aaron, J. S., HIV-1 Integrase: Structural Organization, Conformational Changes, and Catalysis. In *Advances in Virus Research*, Academic Press: 1999; Vol. Volume 52, pp 351-369.
177. Bushman, F. D.; Craigie, R., Activities of human immunodeficiency virus (HIV) integration protein in vitro: specific cleavage and integration of HIV DNA. *Proceedings of the National Academy of Sciences* **1991**, 88, (4), 1339-1343.
178. Neamati, N., Structure-based HIV-1 integrase inhibitor design: a future perspective. *Expert opinion on investigational drugs* **2001**, 10, (2), 281-296.
179. Deng, J.; Kelley, J. A.; Barchi, J. J.; Sanchez, T.; Dayam, R.; Pommier, Y.; Neamati, N., Mining the NCI antiviral compounds for HIV-1 integrase inhibitors. *Bioorganic & Medicinal Chemistry* **2006**, 14, (11), 3785-3792.
180. Bushman, F. D.; Fujiwara, T.; Craigie, R., Retroviral DNA integration directed by HIV integration protein in vitro. *Science* **1990**, 249, (4976), 1555-1558.
181. Sherman, P. A.; Fyfe, J. A., Human immunodeficiency virus integration protein expressed in Escherichia coli possesses selective DNA cleaving activity. *Proceedings of the National Academy of Sciences* **1990**, 87, (13), 5119-5123.
182. Farnet, C. M.; Haseltine, W. A., Integration of human immunodeficiency virus type 1 DNA in vitro. *Proceedings of the National Academy of Sciences* **1990**, 87, (11), 4164-4168.
183. Fesen, M. R.; Kohn, K. W.; Leteurtre, F.; Pommier, Y., Inhibitors of human immunodeficiency virus integrase. *Proceedings of the National Academy of Sciences* **1993**, 90, (6), 2399-2403.

184. Savarino, A., A Historical Sketch of the Discovery and Development of HIV-1 Integrase Inhibitors. *Expert opinion on Investigational Drugs* **2006**, 15, (12), 1507-1522.
185. Craigie, R.; Bushman, F.; Mizuchi, K. Retroviral in vitro integration assay for screening for inhibitors of integration factors. WO 9203578, March 5, 1992.
186. Fesen, M. R.; Pommier, Y.; Leteurtre, F.; Hiroguchi, S.; Yung, J.; Kohn, K. W., Inhibition of HIV-1 integrase by flavones, caffeic acid phenethyl ester (CAPE) and related compounds. *Biochemical Pharmacology* **1994**, 48, (3), 595-608.
187. Kim, H. J.; Woo, E.-R.; Shin, C.-G.; Park, H., A New Flavonol Glycoside Gallate Ester from *Acer okamotoanum* and Its Inhibitory Activity against Human Immunodeficiency Virus-1 (HIV-1) Integrase. *Journal of Natural Products* **1998**, 61, (1), 145-148.
188. LaFemina, R. L.; Graham, P. L.; LeGrow, K.; Hastings, J. C.; Wolfe, A.; Young, S. D.; Emini, E. A.; Hazuda, D. J., Inhibition of human immunodeficiency virus integrase by bis-catechols. *Antimicrobial agents and chemotherapy* **1995**, 39, (2), 320-324.
189. Mazumder, A.; Wang, S.; Neamati, N.; Nicklaus, M.; Sunder, S.; Chen, J.; Milne, G. W. A.; Rice, W. G.; Burke, T. R.; Pommier, Y., Antiretroviral Agents as Inhibitors of both Human Immunodeficiency Virus Type 1 Integrase and Protease. *Journal of Medicinal Chemistry* **1996**, 39, (13), 2472-2481.
190. Eich, E.; Pertz, H.; Kaloga, M.; Schulz, J.; Fesen, M. R.; Mazumder, A.; Pommier, Y., (-)-Arctigenin as a Lead Structure for Inhibitors of Human Immunodeficiency Virus Type-1 Integrase. *Journal of Medicinal Chemistry* **1996**, 39, (1), 86-95.
191. Mazumder, A.; Gazit, A.; Levitzki, A.; Nicklaus, M.; Yung, J.; Kohlhagen, G.; Pommier, Y., Effects of Tyrphostins, Protein Kinase Inhibitors, on Human Immunodeficiency Virus Type 1 Integrase. *Biochemistry* **1995**, 34, (46), 15111-15122.
192. Robinson, W. E.; Cordeiro, M.; Abdel-Malek, S.; Jia, Q.; Chow, S. A.; Reinecke, M. G.; Mitchell, W. M., Dicaffeoylquinic acid inhibitors of human immunodeficiency virus integrase: inhibition of the core catalytic domain of human immunodeficiency virus integrase. *Molecular Pharmacology* **1996**, 50, (4), 846-855.
193. Robinson, W. E.; Reinecke, M. G.; Abdel-Malek, S.; Jia, Q.; Chow, S. A., Inhibitors of HIV-1 replication that inhibit HIV integrase. *Proceedings of the National Academy of Sciences* **1996**, 93, (13), 6326-6331.
194. Neamati, N.; Sunder, S.; Pommier, Y., Design and discovery of HIV-1 integrase inhibitors. *Drug Discovery Today* **1997**, 2, (11), 487-498.
195. Stanwell, C.; Ye, B.; Yuspa, S. H.; Burke, T. R., Cell Protein Cross-linking by Erbstatin and Related Compounds. *Biochemical Pharmacology* **1996**, 52, 475-480.



196. Nicklaus, M. C.; Neamati, N.; Hong, H.; Mazumder, A.; Sunder, S.; Chen, J.; Milne, G. W. A.; Pommier, Y., HIV-1 Integrase Pharmacophore: Discovery of Inhibitors through Three-Dimensional Database Searching. *Journal of Medicinal Chemistry* **1997**, 40, (6), 920-929.
197. Zhao, H.; Neamati, N.; Sunder, S.; Hong, H.; Wang, S.; Milne, G. W.; Pommier, Y.; Burke, T. R., Hydrazide-containing inhibitors of HIV-1 integrase. *Journal of Medicinal Chemistry* **1997**, 40, 937-941.
198. Neamati, N.; Hong, H.; Owen, J. M.; Sunder, S.; Winslow, H. E.; Christensen, J. L.; Zhao, H.; Burke, T. R.; Milne, G. W.; Pommier, Y., Salicylhydrazine-containing inhibitors of HIV-1 integrase: Implication for a selective chelation in the integrase active site. *Journal of Medicinal Chemistry* **1998**, 41, 3202-3209.
199. Hong, H.; Neamati, N.; Wang, S.; Nicklaus, M. C.; Mazumder, A.; Zhao, H.; Burke, T. R.; Pommier, Y.; Milne, G. W., Discovery of HIV-1 integrase inhibitors by pharmacophore searching. *Journal of Medicinal Chemistry* **1997**, 40, (6), 930-936.
200. Zhao, X. Z.; Semenova, E. A.; Vu, B. C.; Maddali, K.; Marchand, C.; Hughes, S. H.; Pommier, Y.; Burke, T. R., 2,3-Dihydro-6,7-dihydroxy-1H-isindol-1-one-Based HIV-1 Integrase Inhibitors. *Journal of Medicinal Chemistry* **2008**, 51, (2), 251-259.
201. Dayam, R.; Neamati, N., Small-Molecule HIV-1 Integrase Inhibitors: the 2001-2002 Update. *Current Pharmaceutical Design* **2003**, 9, (22), 1789.
202. Pommier, Y.; Neamati, N., Inhibitors of human immunodeficiency virus integrase. *Advances in Virus Research* **1999**, 52, 427-458.
203. Hazuda, D. J.; Felock, P. J.; Hastings, J. C.; Pramanik, B.; Wolfe, A. L., Differential Divalent Cation Requirements Uncouple the Assembly and Catalytic Reactions of Human Immunodeficiency Virus Type 1 Integrase. *Journal of Virology* **1997**, 71, (9), 7005-7011.
204. Ellison, V.; Brown, P. O., A stable complex between integrase and viral DNA ends mediates human immunodeficiency virus integration in vitro. *Proceedings of the National Academy of Sciences* **1994**, 91, (15), 7316-7320.
205. Parrill, A. L., HIV-1 Integrase Inhibition: Binding Sites, Structure Activity Relationships and Future Perspectives. *Current Medicinal Chemistry* **2003**, 10, (18), 1811.
206. Asante-Appiah, E.; Skalka, A. M., A Metal-induced Conformational Change and Activation of HIV-1 Integrase. *Journal of Biological Chemistry* **1997**, 272, (26), 16196-16205.
207. Wolfe, A. L.; Felock, P. J.; Hastings, J. C.; Blau, C. U.; Hazuda, D. J., The role of manganese in promoting multimerization and assembly of human immunodeficiency virus type 1 integrase as a catalytically active complex on immobilized long terminal repeat substrates. *Journal of Virology* **1996**, 70, (3), 1424-1432.
208. Hazuda, D. J.; Hastings, J. C.; Wolfe, A. L.; Emini, E. A., A novel assay for the DNA strand-transfer reaction of HIV-1 integrase. *Nucleic Acids Research* **1994**, 22, (6), 1121-1122.

209. Singh, S. B.; Pelaez, F.; Hazuda, D. J.; Lingham, R. B., Discovery of natural product inhibitors of HIV-1 integrase at Merck. *Drugs of the Future* **2005**, 30, (3), 277-299.
210. Selnick, H. G.; Hazuda, D. J.; Egbertson, M.; Guare, J. P., Jr.; Wai, J. S.; Young, S. D.; Clark, D. L.; Medina, J. C. Preparation of nitrogen-containing 4-heteroaryl-2,4-dioxobutyric acids useful as HIV integrase inhibitors. WO 9962513 A1, 1999.
211. Goldgur, Y.; Craigie, R.; Cohen, G. H.; Fujiwara, T.; Yoshinaga, T.; Fujishita, T.; Sugimoto, H.; Endo, T.; Murai, H.; Davies, D. R., Structure of the HIV-1 integrase catalytic domain complexed with an inhibitor: A platform for antiviral drug design. *Proceedings of the National Academy of Sciences* **1999**, 96, (23), 13040-13043.
212. Wai, J. S.; Egbertson, M. S.; Payne, L. S.; Fisher, T. E.; Embrey, M. W.; Tran, L. O.; Melamed, J. Y.; Langford, H. M.; Guare, J. P.; Zhuang, L.; Grey, V. E.; Vacca, J. P.; Holloway, M. K.; Naylor-Olsen, A. M.; Hazuda, D. J.; Felock, P. J.; Wolfe, A. L.; Stillmock, K. A.; Schleif, W. A.; Gabryelski, L. J.; Young, S. D., 4-Aryl-2,4-dioxobutanoic Acid Inhibitors of HIV-1 Integrase and Viral Replication in Cells. *Journal of Medicinal Chemistry* **2000**, 43, (26), 4923-4926.
213. Pais, G. C. G.; Zhang, X.; Marchand, C.; Neamati, N.; Cowansage, K.; Svarovskaia, E. S.; Pathak, V. K.; Tang, Y.; Nicklaus, M.; Pommier, Y.; Burke, T. R., Jr., Structure Activity of 3-Aryl-1,3-diketo-Containing Compounds as HIV-1 Integrase Inhibitors. *Journal of Medicinal Chemistry* **2002**, 45, (15), 3184-3194.
214. Neamati, N., Patented small molecule inhibitors of HIV-1 integrase: a 10-year saga. *Expert Opinion on Therapeutic Patents* **2002**, 15, (5), 709-724.
215. Marchand, C.; Maddali, K.; Métifiot, M.; Pommier, Y., HIV-1 IN Inhibitors: 2010 Update and Perspectives. *Current Topics in Medicinal Chemistry* **2009**, 9, (11), 1016-1037.
216. Dyda, F.; Hickman, A. B.; Jenkins, T. M.; Craige, R.; Davies, D. R., Crystal Structure of the Catalytic Domain of HIV-1 Integrase: Similarity of Other Polynucleotide Transferases. *Science* **1994**, 266, 1981-1986.
217. Grobler, J. A.; Stillmock, K.; Hu, B.; Witmer, M.; Felock, P.; Espeseth, A. S.; Wolfe, A.; Egbertson, M.; Bourgeois, M.; Melamed, J.; Wai, J. S.; Young, S.; Vacca, J.; Hazuda, D. J., Diketo acid inhibitor mechanism and HIV-1 integrase: Implications for metal binding in the active site of phosphotransferase enzymes. *Proceedings of the National Academy of Sciences* **2002**, 99, (10), 6661-6666.
218. Marchand, C.; Johnson, A. A.; Karki, R. G.; Pais, G. C. G.; Zhang, X.; Cowansage, K.; Patel, T. A.; Nicklaus, M. C.; Burke, T. R.; Pommier, Y., Metal-Dependent Inhibition of HIV-1 Integrase by  $\hat{\text{I}}^2$ -Diketo Acids and Resistance of the Soluble Double-Mutant (F185K/C280S). *Molecular Pharmacology* **2003**, 64, (3), 600-609.
219. Egbertson, M. S.; Anthony, N. J.; Summa, V., HIV-Integrase Inhibitor Design: From Diketo Acids to Heterocyclic Templates: History of HIV Integrase Medicinal Chemistry at Merck West Point and Merck Rome (IRBM) Leading to Discovery of Raltegravir. In *HIV-1*

*Integrase: Mechanism and Inhibitor Design*, Neamati, N., Ed. John Wiley & Sons, Inc.: 2011; pp 197-229.

220. Young, S. D.; Egbertson, M.; Payne, L. S.; Wai, J. S.; Fisher, T. E.; Guare, J. P., Jr.; Embrey, M. W.; Tran, L.; Zhuang, L.; Vacca, J. P.; Langford, M.; Melamed, J.; Clark, D. L.; Medina, J. C.; Jaen, J. Preparation of aromatic and heteroaromatic 4-aryl-2,4-dioxobutyric acid derivatives useful as HIV integrase inhibitors. WO 9962520, Dec 9, 1999.

221. Uenaka, M.; Kawata, K.; Nagai, M.; Endoh, T. Novel processes for the preparation of substituted propenone derivatives. . WO 2000075122, Dec 14, 2000.

222. Billich, A., S-1360(Shionogi-GlaxoSmithKline). *Current Opinion in Investigational Drugs (Thomson Current Drugs)* **2003**, 4, (2), 206-209.

223. Ramkumar, K.; Serrao, E.; Odde, S.; Neamati, N., HIV-1 integrase inhibitors: 2007–2008 update. *Medicinal Research Reviews* **2010**, 30, (6), 890-954.

224. Embrey, M. W.; Wai, J. S.; Funk, T. W.; Homnick, C. F.; Perlow, D. S.; Young, S. D.; Vacca, J. P.; Hazuda, D. J.; Felock, P. J.; Stillmock, K. A.; Witmer, M. V.; Moyer, G.; Schleif, W. A.; Gabryelski, L. J.; Jin, L.; Chen, I. W.; Ellis, J. D.; Wong, B. K.; Lin, J. H.; Leonard, Y. M.; Tsou, N. N.; Zhuang, L., A series of 5-(5,6)-dihydrouracil substituted 8-hydroxy-[1,6]naphthyridine-7-carboxylic acid 4-fluorobenzylamide inhibitors of HIV-1 integrase and viral replication in cells. *Bioorganic & Medicinal Chemistry Letters* **2005**, 15, (20), 4550-4554.

225. Hazuda, D. J.; Anthony, N. J.; Gomez, R. P.; Jolly, S. M.; Wai, J. S.; Zhuang, L.; Fisher, T. E.; Embrey, M.; Guare, J. P.; Egbertson, M. S.; Vacca, J. P.; Huff, J. R.; Felock, P. J.; Witmer, M. V.; Stillmock, K. A.; Danovich, R.; Grobler, J.; Miller, M. D.; Espeseth, A. S.; Jin, L.; Chen, I. W.; Lin, J. H.; Kassahun, K.; Ellis, J. D.; Wong, B. K.; Xu, W.; Pearson, P. G.; Schleif, W. A.; Cortese, R.; Emini, E.; Summa, V.; Holloway, M. K.; Young, S. D., A naphthyridine carboxamide provides evidence for discordant resistance between mechanistically identical inhibitors of HIV-1 integrase. *Proceedings of the National Academy of Sciences of the United States of America* **2004**, 101, (31), 11233-11238.

226. Hazuda, D. J.; Young, S. D.; Guare, J. P.; Anthony, N. J.; Gomez, R. P.; Wai, J. S.; Vacca, J. P.; Handt, L.; Motzel, S. L.; Klein, H. J.; Dornadula, G.; Danovich, R. M.; Witmer, M. V.; Wilson, K. A. A.; Tussey, L.; Schleif, W. A.; Gabryelski, L. S.; Jin, L.; Miller, M. D.; Casimiro, D. R.; Emini, E. A.; Shiver, J. W., Integrase Inhibitors and Cellular Immunity Suppress Retroviral Replication in Rhesus Macaques. *Science* **2004**, 305, (5683), 528-532.

227. Dayam, R.; Gundla, R.; Al-Mawsawi, L. Q.; Neamati, N., HIV-1 integrase inhibitors: 2005–2006 update. *Medicinal Research Reviews* **2008**, 28, (1), 118-154.

228. Summa, V.; Petrocchi, A.; Bonelli, F.; Crescenzi, B.; Donghi, M.; Ferrara, M.; Fiore, F.; Gardelli, C.; Gonzalez Paz, O.; Hazuda, D. J.; Jones, P.; Kinzel, O.; Laufer, R.; Monteagudo, E.; Muraglia, E.; Nizi, E.; Orvieto, F.; Pace, P.; Pescatore, G.; Scarpelli, R.; Stillmock, K.; Witmer, M. V.; Rowley, M., Discovery of Raltegravir, a Potent, Selective Orally Bioavailable HIV-

- Integrase Inhibitor for the Treatment of HIV-AIDS Infection. *Journal of Medicinal Chemistry* **2008**, 51, (18), 5843-5855.
229. Pace, P., Integrase inhibitors for the treatment of HIV infection. *Current opinion in drug discovery & development* **2008**, 11, (4), 471-479.
230. Kazmierski, W. M., *Antiviral Drugs: From Basic Discovery through Clinical Trials*. 1 ed.; John Wiley & Sons, Inc.: 2011.
231. Summa, V.; Petrocchi, A.; Matassa, V. G.; Gardelli, C.; Muraglia, E.; Rowley, M.; Paz, O. G.; Laufer, R.; Monteagudo, E.; Pace, P., 4,5-Dihydroxypyrimidine Carboxamides and N-Alkyl-5-hydroxypyrimidinone Carboxamides Are Potent, Selective HIV Integrase Inhibitors with Good Pharmacokinetic Profiles in Preclinical Species. *Journal of Medicinal Chemistry* **2006**, 49, (23), 6646-6649.
232. Summa, V.; Petrocchi, A.; Matassa, V. G.; Taliani, M.; Laufer, R.; De Francesco, R.; Altamura, S.; Pace, P., HCV NS5b RNA-dependent RNA polymerase inhibitors: from alpha,gamma-diketoacids to 4,5-dihydroxypyrimidine- or 3-methyl-5-hydroxypyrimidinonecarboxylic acids. Design and synthesis. *Journal of Medicinal Chemistry* **2004**, 47, (22), 5336-5339.
233. Pace, P.; Nizi, E.; Pacini, B.; Pesci, S.; Matassa, V.; De Francesco, R.; Altamura, S.; Summa, V., The monoethyl ester of meconic acid is an active site inhibitor of HCV NS5B RNA-dependent RNA polymerase. *Bioorganic & Medicinal Chemistry Letters* **2004**, 14, (12), 3257-3261.
234. Koch, U.; Attenni, B.; Malancona, S.; Colarusso, S.; Conte, I.; Di Filippo, M.; Harper, S.; Pacini, B.; Giomini, C.; Thomas, S.; Incitti, I.; Tomei, L.; De Francesco, R.; Altamura, S.; Matassa, V. G.; Narjes, F., 2-(2-Thienyl)-5,6-dihydroxy-4-carboxypyrimidines as Inhibitors of the Hepatitis C Virus NS5B Polymerase: Discovery, SAR, Modeling, and Mutagenesis. *Journal of Medicinal Chemistry* **2006**, 49, (5), 1693-1705.
235. Shimura, K.; Kodama, E. N., Elvitegravir: a new HIV integrase inhibitor. *Antiviral Chemistry & Chemotherapy* **2009**, 20, (2), 79-85.
236. Ramanathan, S., Clinical Pharmacokinetic and Pharmacodynamic Profile of the HIV Integrase Inhibitor Elvitegravir. *Clinical Pharmacokinetics* **2011**, 50, (4), 229-244.
237. Sato, M.; Motomura, T.; Aramaki, H.; Matsuda, T.; Yamashita, M.; Ito, Y.; Kawakami, H.; Matsuzaki, Y.; Watanabe, W.; Yamataka, K.; Ikeda, S.; Kodama, E.; Matsuoka, M.; Shinkai, H., Novel HIV-1 Integrase Inhibitors Derived from Quinolone Antibiotics. *Journal of Medicinal Chemistry* **2006**, 49, (5), 1506-1508.
238. Serrao, E.; Odde, S.; Ramkumar, K.; Neamati, N., Raltegravir, Elvitegravir, and Metoogravir: the birth of "me-too" HIV-1 integrase inhibitors. *Retrovirology* **2009**, 6, 1-14.
239. Reddy, Y. S.; Min, S. S.; Borland, J.; Song, I.; Lin, J.; Palleja, S.; Symonds, W. T., Safety and Pharmacokinetics of GSK364735, a Human Immunodeficiency Virus Type 1 Integrase

Inhibitor, following Single and Repeated Administration in Healthy Adult Subjects. *Antimicrob. Agents Chemother.* **2007**, 51, (12), 4284-4289.

240. Garvey, E. P.; Johns, B. A.; Gartland, M. J.; Foster, S. A.; Miller, W. H.; Ferris, R. G.; Hazen, R. J.; Underwood, M. R.; Boros, E. E.; Thompson, J. B.; Weatherhead, J. G.; Koble, C. S.; Allen, S. H.; Schaller, L. T.; Sherrill, R. G.; Yoshinaga, T.; Kobayashi, M.; Wakasa-Morimoto, C.; Miki, S.; Nakahara, K.; Noshi, T.; Sato, A.; Fujiwara, T., The Naphthyridinone GSK364735 Is a Novel, Potent Human Immunodeficiency Virus Type 1 Integrase Inhibitor and Antiretroviral. *Antimicrobial Agents and Chemotherapy* **2008**, 52, (3), 901-908.

241. Shimura, K.; Kodama, E.; Sakagami, Y.; Matsuzaki, Y.; Watanabe, W.; Yamataka, K.; Watanabe, Y.; Ohata, Y.; Doi, S.; Sato, M.; Kano, M.; Ikeda, S.; Matsuoka, M., Broad Antiretroviral Activity and Resistance Profile of the Novel Human Immunodeficiency Virus Integrase Inhibitor Elvitegravir (JTK-303/GS-9137). *Journal of Virology* **2008**, 82, (2), 764-774.

242. Kobayashi, M.; Nakahara, K.; Seki, T.; Miki, S.; Kawauchi, S.; Suyama, A.; Wakasa-Morimoto, C.; Kodama, M.; Endoh, T.; Oosugi, E.; Matsushita, Y.; Murai, H.; Fujishita, T.; Yoshinaga, T.; Garvey, E.; Foster, S.; Underwood, M.; Johns, B.; Sato, A.; Fujiwara, T., Selection of diverse and clinically relevant integrase inhibitor-resistant human immunodeficiency virus type 1 mutants. *Antiviral Research* **2008**, 80, (2), 213-222.

243. Marinello, J.; Marchand, C.; Mott, B. T.; Bain, A.; Thomas, C. J.; Pommier, Y., Comparison of Raltegravir and Elvitegravir on HIV-1 Integrase Catalytic Reactions and on a Series of Drug-Resistant Integrase Mutants *Biochemistry* **2008**, 47, (36), 9345-9354.

244. Delelis, O.; Malet, I.; Na, L.; Tchertanov, L.; Calvez, V.; Marcelin, A.-G.; Subra, F.; Deprez, E.; Mouscadet, J.-F. o., The G140S mutation in HIV integrases from raltegravir-resistant patients rescues catalytic defect due to the resistance Q148H mutation. *Nucleic Acids Research* **2009**, 37, (4), 1193-1201.

245. Malet, I.; Delelis, O.; Valantin, M.-A.; Montes, B.; Soulie, C.; Wirden, M.; Tchertanov, L.; Peytavin, G.; Reynes, J.; Mouscadet, J.-F. o.; Katlama, C.; Calvez, V.; Marcelin, A.-G. v., Mutations Associated with Failure of Raltegravir Treatment Affect Integrase Sensitivity to the Inhibitor In Vitro. *Antimicrobial Agents and Chemotherapy* **2008**, 52, (4), 1351-1358.

246. Delelis, O.; Thierry, S.; Subra, F.; Simon, F.; Malet, I.; Alloui, C.; Sayon, S.; Calvez, V.; Deprez, E.; Marcelin, A.-G.; Tchertanov, L.; Mouscadet, J.-F., Impact of Y143 HIV-1 Integrase Mutations on Resistance to Raltegravir In Vitro and In Vivo. *Antimicrobial Agents and Chemotherapy* **2009**, 54, (1), 491-501.

247. Sichtig, N.; Sierra, S.; Kaiser, R.; Däumer, M.; Reuter, S.; Schülter, E.; Altmann, A.; Fätkenheuer, G.; Dittmer, U.; Pfister, H.; Esser, S., Evolution of raltegravir resistance during therapy. *Journal of Antimicrobial Chemotherapy* **2009**, 64, (1), 25-32.

248. Malet, I.; Delelis, O.; Soulie, C.; Wirden, M.; Tchertanov, L.; Mottaz, P.; Peytavin, G.; Katlama, C.; Mouscadet, J.-F.; Calvez, V.; Marcelin, A.-G., Quasispecies variant dynamics during emergence of resistance to raltegravir in HIV-1-infected patients. *Journal of Antimicrobial Chemotherapy* **2009**, 63, (4), 795-804.

249. Jegede, O.; Babu, J.; Di Santo, R.; McColl, D. J.; Weber, J.; Quiñones-Mateu, M., HIV type 1 integrase inhibitors: from basic research to clinical implications. *AIDS Reviews* **2008**, *10*, (3), 172-189.
250. Sechi, M.; Carcelli, M.; Rogolino, D.; Neamati, N., Role of Metals in HIV-1 Integrase Inhibitor Design. In *HIV-1 Integrase: Mechanism and Inhibitor Design*, 1 ed.; Neamati, N., Ed. John Wiley & Sons, Inc.: 2011; pp 287-307.
251. Neamati, N., *HIV-1 Integrase: Mechanism and Inhibitor Design*. 1 ed.; Wiley: 2011; p 528.
252. Savarino, A., In-Silico Docking of HIV-1 Integrase Inhibitors Reveals a Novel Drug Type Acting on an Enzyme/DNA Reaction Intermediate. *Retrovirology* **2007**, *4*, (21), 1-15.
253. Sharkey, M.; Triques, K.; Kuritzkes, D. R.; Stevenson, M., In Vivo Evidence for Instability of Episomal Human Immunodeficiency Virus Type 1 cDNA. *Journal of Virology* **2005**, *79*, (8), 5203-5210.
254. Ellison, V.; Gerton, J.; Vincent, K. A.; Brown, P. O., An Essential Interaction between Distinct Domains of HIV-1 Integrase Mediates Assembly of the Active Multimer. *Journal of Biological Chemistry* **1995**, *270*, (7), 3320-3326.
255. Engelman, A.; Bushman, F. D.; Craigie, R., Identification of discrete functional domains of HIV-1 integrase and their organization within an active multimeric complex. *EMBO J* **1993**, *12*, (8), 3269-3275.
256. Burke, C. J.; Sanyal, G.; Bruner, M. W.; Ryan, J. A.; LaFemina, R. L.; Robbins, H. L.; Zeff, A. S.; Middaugh, C. R.; Cordingley, M. G., Structural implications of spectroscopic characterization of a putative zinc finger peptide from HIV-1 integrase. *Journal of Biological Chemistry* **1992**, *267*, (14), 9639-9644.
257. Cai, M. Z., Ronglan; Caffrey, Michael; Craigie, Robert; Clore, G. Marius; Gronenborn, Angela M., Solution structure of the N-terminal zinc binding domain of HIV-1 integrase. *Nature structural biology* **1997**, *4*, (7), 567-577.
258. Zheng, R.; Jenkins, T. M.; Craigie, R., Zinc folds the N-terminal domain of HIV-1 integrase, promotes multimerization and enhances catalytic activity. *Proceedings of the National Academy of Sciences* **1996**, *93*, 13659-13664.
259. Engelman, A.; Craigie, R., Identification of conserved amino acid residues critical for human immunodeficiency virus type 1 integrase function in vitro. *Journal of Virology* **1992**, *66*, (11), 6361-6369.
260. Chen, J. C. H.; Krucinski, J.; Miercke, L. J. W.; Finer-Moore, J. S.; Tang, A. H.; Leavitt, A. D.; Stroud, R. M., Crystal structure of the HIV-1 integrase catalytic core and C-terminal domains: A model for viral DNA binding. *Proceedings of the National Academy of Sciences* **2000**, *97*, (15), 8233-8238.

261. Lubkowski, J.; Yang, F.; Alexandratos, J.; Wlodawer, A.; Zhao, H.; Burke, T. R.; Neamati, N.; Pommier, Y.; Merkel, G.; Skalka, A. M., Structure of the catalytic domain of avian sarcoma virus integrase with a bound HIV-1 integrase-targeted inhibitor. *Proceedings of the National Academy of Sciences* **1998**, 95, (9), 4831-4836.
262. Vink, C.; Plasterk, R. H. A., The human immunodeficiency virus integrase protein. *Trends in Genetics* **1993**, 9, (12), 433-437.
263. Bushman, F. D.; Engelman, A.; Palmer, I.; Wingfield, P.; Craigie, R., Domains of the integrase protein of human immunodeficiency virus type 1 responsible for polynucleotidyl transfer and zinc binding. *Proceedings of the National Academy of Sciences* **1993**, 90, (8), 3428-3432.
264. Chow, S. A.; Vincent, K. A.; Ellison, V.; Brown, P. O., Reversal of integration and DNA splicing mediated by integrase of human immunodeficiency virus. *Science* **1992**, 255, (5045), 723-726.
265. Craigie, R., Integrase Mechanism and Function. In *HIV-1 Integrase: Mechanism and Inhibitor Design*, 1 ed.; Neamati, N., Ed. John Wiley & Sons: 2011; pp 23-34.
266. Pluymers, W.; De Clercq, E.; Debyser, Z., HIV-1 Integration as a Target for Antiretroviral Therapy: A Review. *Current Drug Targets - Infectious Disorders* **2001**, 1, 133-149.
267. Colicelli, J.; Goff, S., Sequence and spacing requirements of a retrovirus integration site. *Journal of Molecular Biology* **1988**, 199, (1), 47-59.
268. LaFemina, R. L.; Callahan, P.; Cordingley, M. G., Substrate specificity of recombinant HIV integrase protein. *Journal of Virology* **1991**, 65, 5624-5630.
269. Haren, L.; Ton-Hoang, B., Integrating DNA: Transposases and retroviral integrases. *Annual Review of Microbiology* **1999**, 53, (1), 245.
270. Johnson, A.; Marchand, C.; Pommier, Y., HIV-1 integrase inhibitors: a decade of reserach and two drugs in cliniclal trial. *Current Topics in Medicinal Chemistry* **2004**, 4, 1059-1077.
271. Leavitt, A. D.; Rose, R. B.; Varmus, H. E., Both substrate and target oligonucleotide sequences affect in vitro integration mediated by human immunodeficiency virus type 1 integrase protein produced in *Saccharomyces cerevisiae*. *Journal of Virology* **1992**, 66, (4), 2359-2368.
272. Yoder, K.; Bushman, F., Repair of gaps in the retroviral DNA integration intermediates. *Journal of Virology* **2000**, 74, 11191-11200.
273. Marchand, C.; Zhang, X.; Pais, G. C. G.; Cowansage, K.; Neamati, N.; Burke, T. R.; Pommier, Y., Structural Determinants for HIV-1 Integrase Inhibition by  $\beta$ -Diketo Acids. *Journal of Biological Chemistry* **2002**, 277, (15), 12596-12603.

274. Johnson, A. A.; Sayer, J. M.; Yagi, H.; Patil, S. S.; Debart, F. o.; Maier, M. A.; Corey, D. R.; Vasseur, J.-J.; Burke, T. R.; Marquez, V. E.; Jerina, D. M.; Pommier, Y., Effect of DNA Modifications on DNA Processing by HIV-1 Integrase and Inhibitor Binding. *Journal of Biological Chemistry* **2006**, 281, (43), 32428-32438.
275. Johnson, A.; Marchand, C.; Pommier, Y., Insights into HIV-1 Integrase-DNA Interactions. In *HIV-1 Integrase: Mechanism and Inhibitor Design*, 1 ed.; Neamati, N., Ed. John Wiley & Sons: 2011; pp 83-94.
276. Johnson, A. A.; Sayer, J. M.; Yagi, H.; Kalena, G. P.; Amin, R.; Jerina, D. M.; Pommier, Y., Position-specific Suppression and Enhancement of HIV-1 Integrase Reactions by Minor Groove Benzo[a]pyrene Diol Epoxide Deoxyguanine Adducts. *Journal of Biological Chemistry* **2004**, 279, (9), 7947-7955.
277. Johnson, A. A.; Santos, W.; Pais, G. C. G.; Marchand, C.; Amin, R.; Burke, T. R.; Verdine, G.; Pommier, Y., Integration requires a specific interaction of the donor DNA terminal 5'-cytosine with glutamine 148 of the HIV-1 integrase flexible loop. *Journal of Biological Chemistry* **2006**, 281, (1), 461-467.
278. Mazumder, A.; Pommier, Y., Processing of deoxyuridine mismatches and abasic sites by human immunodeficiency virus type- integrase. *Nucleic Acids Research* **1995**, 23, (15), 2865-2871.
279. Gerton, J. L.; Ohgi, S.; Olsen, M.; DeRisi, J.; Brown, P. O., Effects of Mutations in Residues near the Active Site of Human Immunodeficiency Virus Type 1 Integrase on Specific Enzyme-Substrate Interactions. *Journal of Virology* **1998**, 72, (6), 5046-5055.
280. Jenkins, T. M.; Esposito, D.; Engelman, A.; Craigie, R., Critical contacts between HIV-1 integrase and viral DNA identified by structure-based analysis and photo-crosslinking. *EMBO J* **1997**, 16, 6849-6859.
281. Wang, J.-Y.; Ling, H.; Yang, W.; Craigie, R., Structure of a two-domain fragment of HIV-1 integrase: implications for domain organization in the intact protein. *EMBO J* **2001**, 20, (24), 7333-7343.
282. Gao, K.; Butler, S. L.; Bushman, F., Human immunodeficiency virus type 1 integrase: arrangement of protein domains in active cDNA complexes. *EMBO J* **2001**, 20, (13), 3565-3576.
283. Johnson, T. W.; Tanis, S. P.; Butler, S. L.; Dalvie, D.; DeLisle, D. M.; Dress, K. R.; Flahive, E. J.; Hu, Q.; Kuehler, J. E.; Kuki, A.; Liu, W.; McClellan, G. A.; Peng, Q.; Plewe, M. B.; Richardson, P. F.; Smith, G. L.; Solowiej, J.; Tran, K. T.; Wang, H.; Yu, X.; Zhang, J.; Zhu, H., Design and Synthesis of Novel N-Hydroxy-Dihydronaphthyridinones as Potent and Orally Bioavailable HIV-1 Integrase Inhibitors. *Journal of Medicinal Chemistry* **2011**, 54, (9), 3393-3417.
284. Espeseth, A. S.; Felock, P.; Wolfe, A.; Witmer, M.; Grobler, J.; Anthony, N.; Egbertson, M.; Melamed, J. Y.; Young, S.; Hamill, T.; Cole, J. L.; Hazuda, D. J., HIV-1 integrase inhibitors



- that compete with the target DNA substrate define a unique strand transfer conformation for integrase. *Proceedings of the National Academy of Sciences* **2000**, 97, (21), 11244-11249.
285. Pais, G. C. G.; Burke, T. R., Novel aryl diketo-containing inhibitors of HIV-1 integrase. *Drugs of the Future* **2002**, 27, 1101-1111.
286. Johns, B. A.; Svolto, A. C., Advances in two-metal chelation inhibitors of HIV integrase. *Expert Opinion on Therapeutic Patents* **2008**, 18, (11), 1225-1237.
287. Kawasuji, T.; Fuji, M.; Yoshinaga, T.; Sato, A.; Fujiwara, T.; Kiyama, R., A platform for designing HIV integrase inhibitors. Part 2: A two-metal binding model as a potential mechanism of HIV integrase inhibitors. *Bioorganic & Medicinal Chemistry* **2006**, 14, (24), 8420-8429.
288. Marchand, C.; Johnson, A. A.; Karki, R. G.; Pais, G. C. G.; Zhang, X.; Cowansage, K.; Patel, T. A.; Nicklaus, M. C.; Burke, T. R.; Pommier, Y., Metal-Dependent Inhibition of HIV-1 Integrase by  $\beta$ -Diketo Acids and Resistance of the Soluble Double-Mutant (F185K/C280S) *Molecular Pharmacology* **2003**, 64, (3), 600-609.
289. Pommier, Y.; Cherfils, J., Interfacial inhibition of macromolecular interactions: nature's paradigm for drug discovery. *Trends in Pharmacological Sciences* **2005**, 26, (3), 138-145.
290. Barreca, M. L.; Iraci, N.; De Luca, L.; Chimirri, A., Induced-Fit Docking Approach Provides Insight into the Binding Mode and Mechanism of Action of HIV-1 Integrase Inhibitors. *ChemMedChem* **2009**, 4, (9), 1446-1456.
291. Liao, C.; Nicklaus, M. C., Tautomerism and Magnesium Chelation of HIV-1 Integrase Inhibitors: A Theoretical Study. *ChemMedChem* **2010**, 5, (7), 1053-1066.
292. Di Santo, R.; Costi, R.; Roux, A.; Miele, G.; Crucitti, G. C.; Iacovo, A.; Rosi, F.; Lavecchia, A.; Marinelli, L.; Di Giovanni, C.; Novellino, E.; Palmisano, L.; Andreotti, M.; Amici, R.; Galluzzo, C. M.; Nencioni, L.; Palamara, A. T.; Pommier, Y.; Marchand, C., Novel Quinolinonyl Diketo Acid Derivatives as HIV-1 Integrase Inhibitors: Design, Synthesis, and Biological Activities. *Journal of Medicinal Chemistry* **2008**, 51, (15), 4744-4750.
293. Sato, M.; Kawakami, H.; Motomura, T.; Aramaki, H.; Matsuda, T.; Yamashita, M.; Ito, Y.; Matsuzaki, Y.; Yamataka, K.; Ikeda, S.; Shinkai, H., Quinolone Carboxylic Acids as a Novel Monoketo Acid Class of Human Immunodeficiency Virus Type 1 Integrase Inhibitors. *Journal of Medicinal Chemistry* **2009**, 52, (15), 4869-4882.
294. Fujishita, T.; Yoshinaga, T.; Sato, A. Preparation of aromatic heterocycle compounds having HIV integrase inhibiting activities. WO 2000039086, 2000.
295. Vacca, J. P.; Dorsey, B. D.; Schleif, W. A.; Levin, R. B.; McDaniel, S. L.; Darke, P. L.; Zugay, J.; Quintero, J. C.; Blahy, O. M.; Roth, E., L-735,524: an orally bioavailable human immunodeficiency virus type 1 protease inhibitor. *Proceedings of the National Academy of Sciences* **1994**, 91, (9), 4096-4100.

296. Di Santo, R. P., Yves; Marchand, Christophe; Artico, Marino; Costi, Roberta Preparation of quinolin-4-ones as inhibitors of retroviral integrase for the treatment of HIV, AIDS and aids related complex (ARC). WO 2005087759, 2005.
297. Pospisil, P.; Ballmer, P.; Scapozza, L.; Folkers, G., Tautomerism in Computer-Aided Drug Design. *Journal of Receptors and Signal Transduction* **2003**, 23, (4), 361-371.
298. Moreland, J.; Gramada, A.; Buzko, O.; Zhang, Q.; Bourne, P., The Molecular Biology Toolkit (MBT): a modular platform for developing molecular visualization applications. *BMC Bioinformatics* **2005**, 6, (1), 21.
299. Wiskerchen, M.; Muesing, M. A., Human immunodeficiency virus type 1 integrase: effects of mutations on viral ability to integrate, direct viral gene expression from unintegrated viral DNA templates, and sustain viral propagation in primary cells. *Journal of Virology* **1995**, 69, (1), 376-86.
300. Sauerberg, P.; Olesen, P. H.; Nielsen, S.; Treppendahl, S.; Sheardown, M. J.; Honor, T.; Mitch, C. H.; Ward, J. S.; Pike, A. J.; Bymaster, F. P.; Sawyer, B. D.; Shannon, H. E., Novel functional M1 selective muscarinic agonists. Synthesis and structure-activity relationships of 3-(1,2,5-thiadiazolyl)-1,2,5,6-tetrahydro-1-methylpyridines. *Journal of Medicinal Chemistry* **1992**, 35, (12), 2274-2283.
301. Kane, B. E.; Grant, M. K. O.; El-Fakahany, E. E.; Ferguson, D. M., Synthesis and evaluation of xanomeline analogs—Probing the wash-resistant phenomenon at the M1 muscarinic acetylcholine receptor. *Bioorganic & Medicinal Chemistry* **2008**, 16, (3), 1376-1392.
302. Baeza, A.; Casas, J.; Nájera, C.; Sansano, J. M.; Saá, J. M., Enantioselective Synthesis of O-Methoxycarbonyl Cyanohydrins: Chiral Building Blocks Generated by Bifunctional Catalysis with BINOLAM-AlCl. *European Journal of Organic Chemistry* **2006**, 2006, (8), 1949-1958.
303. Subramanyam, C.; Noguchi, M.; Weinreb, S. M., An approach to amphimedine and related marine alkaloids utilizing an intramolecular Kondrat'eva pyridine synthesis *Journal of Organic Chemistry* **1989**, 54, (23), 5580-5585.
304. Yeung, K.-S.; Farkas, M. E.; Kadow, J. F.; Meanwell, N. A.; Taylor, M.; Johnston, D.; Coulter, T. S.; Wright; Kim, J. J. Indole, azaindole and related heterocyclic N-substituted piperazine derivatives and their preparation and use for the treatment of HIV infection. US 8039486, 2011.
305. Wang, T.; Yin, Z.; Zhang, Z.; Bender, J. A.; Yang, Z.; Johnson, G.; Yang, Z.; Zadjura, L. M.; D'Arienzo, C. J.; DiGiugno Parker, D.; Gesenberg, C.; Yamanaka, G. A.; Gong, Y.-F.; Ho, H.-T.; Fang, H.; Zhou, N.; McAuliffe, B. V.; Eggers, B. J.; Fan, L.; Nowicka-Sans, B.; Dicker, I. B.; Gao, Q.; Colonno, R. J.; Lin, P.-F.; Meanwell, N. A.; Kadow, J. F., Inhibitors of human immunodeficiency virus type 1 (HIV-1) attachment. 5. An evolution from indole to azaindoles leading to the discovery of 1-(4-benzoylpiperazin-1-yl)-2-(4,7-dimethoxy-1H-pyrrolo[2,3-c]pyridin-3-yl)ethane-1,2-dione (BMS-488043), a drug candidate that demonstrates antiviral activity in HIV-1-infected subjects. *Journal of Medicinal Chemistry* **2009**, 52, (23), 7778-7787.

306. Martyn, D.; Abell, A., N-[5-(3-Phenylpropionyl)-1H-pyrrole-2-carbonyl]-L-proline Methyl Ester. *Molbank* **2003**, (3), M338.
307. DeSantis, G.; Zhu, Z.; Greenberg, W. A.; Wong, K.; Chaplin, J.; Hanson, S. R.; Farwell, B.; Nicholson, L. W.; Rand, C. L.; Weiner, D. P.; Robertson, D. E.; Burk, M. J., An Enzyme Library Approach to Biocatalysis: Development of Nitrilases for Enantioselective Production of Carboxylic Acid Derivatives. *Journal of the American Chemical Society* **2002**, 124, (31), 9024-9025.
308. Ward, C. E. Herbicidal 2-(Nitrogen Heterocycle)5-Amino-3-Oxo-4-(Substituted-Phenyl)-2,3-Dihydrofurans. 1986.
309. Travis, B. R.; Sivakumar, M.; Hollist, G. O.; Borhan, B., Facile Oxidation of Aldehydes to Acids and Esters with Oxone. *Organic Letters* **2003**, 5, (7), 1031-1034.
310. Garcia-Raso, A.; Deya, P. M.; Saa, J. M., Oxidation of  $\alpha$ -amino acids and  $\alpha$ -hydroxy acids by Fremy's salt. A model for oxidases? *The Journal of Organic Chemistry* **1986**, 51, (22), 4285-4287.
311. Zhou, Y.; Bourque, E.; Zhu, Y.; McEachern, E. J.; Harwig, C.; Skerlj, R. T.; Bridger, G. J.; Li, T.-S.; Metz, M. Substituted imidazolidinones and related compounds as chemokine receptor binding compounds and their preparation, pharmaceutical compositions and use in the treatment of infection of target cells by human immunodeficiency virus. WO 2007022371, 2007.
312. Bou-Hamdan, F. R.; Leighton, J. L., Highly Enantioselective Pictet–Spengler Reactions with  $\alpha$ -Ketoamide-Derived Ketimines: Access to an Unusual Class of Quaternary  $\alpha$ -Amino Amides. *Angewandte Chemie International Edition* **2009**, 48, (13), 2403-2406.
313. Montalban, A. G.; Boman, E.; Chang, C.-D.; Ceide, S. C.; Dahl, R.; Dalesandro, D.; Delaet, N. G. J.; Erb, E.; Gibbs, A.; Kahl, J.; Kessler, L.; Lundström, J.; Miller, S.; Nakanishi, H.; Roberts, E.; Saiah, E.; Sullivan, R.; Wang, Z.; Larson, C. J., 'Reverse' [alpha]-ketoamide-based p38 MAP kinase inhibitors. *Bioorganic & Medicinal Chemistry Letters* **2008**, 18, (20), 5456-5459.
314. Felfer, U.; Strauss, U. T.; Kroutil, W.; Fabian, W. M. F.; Faber, K., Substrate spectrum of mandelate racemase: Part 2. (Hetero)-aryl-substituted mandelate derivatives and modulation of activity. *Journal of Molecular Catalysis B: Enzymatic* **2001**, 15, (4-6), 213-222.
315. Brussee, J.; Loos, W. T.; Kruse, C. G.; Van Der Gen, A., Synthesis of optically active silyl protected cyanohydrins. *Tetrahedron* **1990**, 46, (3), 979-986.
316. Bull, J. A.; Balskus, E. P.; Horan, R. A. J.; Langner, M.; Ley, S. V., Total Synthesis of Potent Antifungal Marine Bisoxazole Natural Products Bengazoles A and B. *Chemistry – A European Journal* **2007**, 13, (19), 5515-5538.
317. Friedl, F., Preparation of Nitropyridine. *Berichte der Deutschen Chemischen Gesellschaft* **1912**, 45, 428-430.

318. Acheson, R. M.; Wright, N. D.; Tasker, P. A., Addition reactions of heterocyclic compounds. LI. Cyclobuta[b]pyridines from reactions of dimethyl acetylenedicarboxylate with 1-alkyl-1,4-dihydropyridines and the cycloelimination of amide and carboxy groups. *Perkin transactions. I* **1972**, (23), 2918.
319. Comins, D. L.; Mantlo, N. B., Synthesis of 3-acylpyridines utilizing a friedel-crafts reaction. *Tetrahedron Letters* **1983**, 24, (35), 3683-3686.
320. Tsuge, O.; Kanemasa, S.; Naritomi, T.; Tanaka, J., Regioselective alkyl group introduction at the 3-position of pyridine via 1,4-bis(trimethylsilyl)-1,4-dihydropyridine. *Chemistry letters* **1984**, (7), 1255-1258.
321. Haase, M.; Goerls, H.; Anders, E., Synthesis of PO(OR)<sub>2</sub>- and PR<sub>3</sub>-disubstituted pyridines via N-(trifluoromethylsulfonyl)pyridinium triflates. *Synthesis (Stuttgart)* **1998**, (2), 195-200.
322. Bannasar, M. L. s.; Juan, C. l.; Bosch, J., Synthesis of 3,5-diacyl-4-phenyl-1,4-dihydropyridines. *Tetrahedron Letters* **1998**, 39, (50), 9275-9278.
323. Klapars, A.; Vedejs, E., Activation of pyridinium salts for electrophilic acylation: A method for conversion of pyridines into 3-acylpyridines *Chemistry of Heterocyclic Compounds* **2004**, 40, (6), 759-766.
324. Jones, I. L.; Schofield, D. J.; Strevens, R. R.; Horton, P. N.; Hursthouse, M. B.; Tomkinson, N. C. O., Novel steroid mimics: synthesis of tri- and tetra-substituted oxamides and oxoamides. *Tetrahedron Letters* **2007**, 48, (4), 521-525.
325. De Corte, B.; Denis, J. M.; De Kimpe, N., A convenient synthesis of C-unsubstituted and C-monoalkylated ketene imines by dehydrocyanation of imidoyl cyanides using vacuum gas-solid reactions. *The Journal of Organic Chemistry* **1987**, 52, (6), 1147-1149.
326. Maruoka, K.; Miyazaki, T.; Ando, M.; Matsumura, Y.; Sakane, S.; Hattori, K.; Yamamoto, H., Organoaluminum-promoted Beckmann rearrangement of oxime sulfonates. *Journal of the American Chemical Society* **1983**, 105, (9), 2831-2843.
327. Takahashi, K.; Kimura, S.; Ogawa, Y.; Yamada, K.; Iida, H., A convenient synthesis of  $\alpha,\beta$ -disubstituted cinnamionitriles (1-anilino-2-cyano-1,2-diphenylethenes). *Synthesis (Stuttgart)* **1978**, (12), 892.
328. Boyer, J. H.; Dabek, H., Iminoacetonitriles, a new family of compounds. N-t-butyliminoacetonitrile. *Journal of the Chemical Society D: Chemical Communications* **1970**, (18), 1204.
329. De Kimpe, N.; Verhe, R.; De Buyck, L.; Chys, J.; Schamp, N., Synthesis of  $\alpha$ -iminonitriles (imidoyl cyanides). *Synthesis (Stuttgart)* **1978**, (12), 895-897.

330. Drenkard, S.; Ferris, J.; Eschenmoser, A., Chemistry of  $\alpha$ -aminonitriles. 2. Aziridine-2-carbonitrile: photochemical formation from 2-aminopropenenitrile. *Helvetica chimica acta* **1990**, 73, (5), 1373-1390.
331. Smith, J. G.; Irwin, D. C.,  $\alpha$ -Iminonitriles (imidoyl cyanides); their preparation using phase-transfer catalysis and their reductive dimerization. *Synthesis (Stuttgart)* **1978**, (12), 894-895.
332. Dutta, D. K.; Prajapati, D.; Sandhu, J. S.; Baruah, J. N., A new facile method for the preparation of  $\alpha$ -iminonitriles from aldonitrone and cyanotrimethylsilane. *Synthetic communications* **1985**, 15, (4), 335-339.
333. Konwar, D.; Goswami, B. N.; Borthakur, N., Organic synthesis with anion exchange resins: synthesis of  $\alpha$ -imino nitriles from nitrones. *Journal of chemical research. Synopses* **1999**, (3), 242-243.
334. Pochat, F., A new method for the preparation of  $\alpha$ -iminonitriles from aromatic aldehydes. *Tetrahedron Letters* **1981**, 22, (10), 955-956.
335. Saegusa, T.; Takaishi, N.; Ito, Y., Cationic isomerization and oligomerization of isocyanide. *The Journal of Organic Chemistry* **1969**, 34, (12), 4040-4046.
336. Pellissier, H.; Gil, G., Reaction of isocyanides. III. Synthesis of  $\beta$ -alkoxy imidoyl cyanides from acetals. *Tetrahedron Letters* **1989**, 30, (2), 171-172.
337. Tobisu, M.; Kitajima, A.; Yoshioka, S.; Hyodo, I.; Oshita, M.; Chatani, N., Bronsted Acid Catalyzed Formal Insertion of Isocyanides into a C-O Bond of Acetals. *Journal of the American Chemical Society* **2007**, 129, (37), 11431-11437.
338. Jursic, B. S.; Douelle, F.; Bowdy, K.; Stevens, E. D., A new facile method for preparation of heterocyclic  $\alpha$ -iminonitriles and  $\alpha$ -oxoacetic acid from heterocyclic aldehydes, p-aminophenol, and sodium cyanide. *Tetrahedron Letters* **2002**, 43, (30), 5361-5365.
339. Masui, M.; Ohmori, H.; Ueda, C.; Yamauchi, M., Hydrolysis of  $\alpha$ -cyanobenzylideneanilines. I. Kinetic studies in acidic media. *Perkin transactions. 2* **1974**, (12), 1448-1453.
340. Okuyama, T.; Pletcher, T. C.; Sahn, D. J.; Schmir, G. L., Hydrolysis of imidate esters derived from weakly basic amines. Influences of structure and pH on the partitioning of tetrahedral intermediates. *Journal of the American Chemical Society* **1973**, 95, (4), 1253-1265.
341. Okuyama, T.; Sahn, D. J.; Schmir, G. L., Hydrolysis of imidate esters derived from weakly basic amines. II. Influence of general acid-base catalysis on the partitioning of tetrahedral intermediates. *Journal of the American Chemical Society* **1973**, 95, (7), 2345-2352.
342. Culbertson, J. B., Factors Affecting the Rate of Hydrolysis of Ketimines. *Journal of the American Chemical Society* **1951**, 73, (10), 4818-4823.

343. Jarusiewicz, J.; Choe, Y.; Yoo, K. S.; Park, C. P.; Jung, K. W., Efficient Three-Component Strecker Reaction of Aldehydes/Ketones via NHC-Amidate Palladium(II) Complex Catalysis. *The Journal of Organic Chemistry* **2009**, *74*, (7), 2873-2876.
344. Burkhart, D. J.; McKenzie, A. R.; Nelson, J. K.; Myers, K. I.; Zhao, X.; Magnusson, K. R.; Natale, N. R., Catalytic Asymmetric Synthesis of Glutamate Analogues. *Organic Letters* **2004**, *6*, (8), 1285-1288.
345. Vu, C. B. C., Rebecca L. Preparation of 8-substituted quinolines and related analogs as sirtuin modulators. WO 2010101949, 2010.
346. Vu, C. B. D., Jeremy S.; Springer, Stephanie K.; Blum, Charles A.; Perni, Robert B. Quinolines and related analogs as sirtuin modulators and their preparation, pharmaceutical compositions and use in the treatment of diseases. WO 2009134973, 2009.
347. Yamada, K.; Kato, M.; Iyoda, M.; Hirata, Y., Total synthesis of (+)-4-isoavenaciolide, a metabolite of *Aspergillus avenaceus*. *Journal of the Chemical Society. Chemical communications* **1973**, (14), 499-500.
348. Burkhart, J. P.; Peet, N. P.; Bey, P., Oxidation of  $\alpha$ -hydroxy esters to  $\alpha$ -keto esters using the Dess-Martin periodinane reagent. *Tetrahedron Letters* **1988**, *29*, (28), 3433-3436.
349. Micetich, R. G., Arylglyoxylic esters. Friedel-Crafts reaction. *Organic preparations and procedures* **1970**, *2*, (4), 249-252.
350. Wasserman, H. H.; Ho, W.-B., (Cyanomethylene)phosphoranes as Novel Carbonyl 1,1-Dipole Synthons: An Efficient Synthesis of  $\alpha$ -Keto Acids, Esters, and Amides. *The Journal of Organic Chemistry* **1994**, *59*, (16), 4364-4366.
351. Photis, J. M. M., Halide-directed nitrile hydrolysis. *Tetrahedron Letters* **1980**, *21*, (37), 3539-3540.
352. Singh, J.; Kissick, T. P.; Mueller, R. H., Improved procedure for the one-step synthesis of  $\alpha$ -keto esters. *Organic Preparations and Procedures International* **1989**, *21*, (4), 501-504.
353. Corey, E. J.; Erickson, B. W., Oxidative hydrolysis of 1,3-dithiane derivatives to carbonyl compounds using N-halosuccinimide reagents. *The Journal of Organic Chemistry* **1971**, *36*, (23), 3553-3560.
354. Babudri, F.; Fiandanese, V.; Marchese, G.; Punzi, A., A general and straightforward approach to  $\alpha,\omega$ -ketoesters. *Tetrahedron* **1996**, *52*, (42), 13513-13520.
355. Zhuang, J.; Wang, C.; Xie, F.; Zhang, W., One-pot efficient synthesis of aryl  $\alpha$ -keto esters from aryl-ketones. *Tetrahedron* **2009**, *65*, (47), 9797-9800.
356. GooBen, L. J.; Dezfuli, M. K., Practical Protocol for Palladium-Catalyzed Synthesis of Arylphosphonates from Bromoarenes and Diethyl Phosphite. *Synlett* **2005**, *3*, 0445-0448.

357. Kosolapoff, G. M., The Chemistry of Phosphonic Acids with Aromatic Nuclei. I. Orientation of Phosphorus in Friedel-Crafts Synthesis. *Journal of the American Chemical Society* **1952**, 74, (16), 4119-4120.
358. Freedman, L. D.; Doak, G. O., The Preparation of the Isomeric Ethylphenylphosphonic Acids. *Journal of the American Chemical Society* **1955**, 77, (1), 173-174.
359. Boumekouez, A.; About-Jaudet, E.; Collignon, N.; Savignac, P., A remarkable accelerating effect of iodide ions in the photostimulated phosphorylation of bromoaromatic compounds. *Journal of organometallic chemistry* **1992**, 440, (3), 297-301.
360. Yuan, C.; Feng, H., Studies on organophosphorus compounds. XL. A one-pot procedure for the mono-O-alkylation of phosphonic acid: a facile synthesis of alkyl hydrogen p-substituted phenylphosphonates. *Synthesis (Stuttgart)* **1990**, (2), 140-141.
361. Tavs, P., Reaction of aryl halides with trialkyl phosphites or dialkyl phenylphosphonites to aromatic phosphonates or phosphinates by nickel salt catalyzed arylation. *Chemische Berichte* **1970**, 103, (8), 2428-2436.
362. Tavs, P., Preparation of aromatic phosphonic acid esters from aryl halides and trialkyl phosphites. *Tetrahedron* **1967**, 23, (12), 4677-4679.
363. Gelman, D.; Jiang, L.; Buchwald, S. L., Copper-Catalyzed C-P Bond Construction via Direct Coupling of Secondary Phosphines and Phosphites with Aryl and Vinyl Halides. *Organic Letters* **2003**, 5, (13), 2315-2318.
364. Osuka, A.; Ohmasa, N.; Yoshida, Y.; Suzuki, H., Synthesis of arenephosphonates by copper(I) iodide-promoted arylation of phosphite anions. *Synthesis (Stuttgart)* **1983**, (1), 69-71.
365. Burger, A.; Dawson, N. D., The Reaction of Dialkyl Chlorophosphates with Arylmagnesium Halides. *The Journal of Organic Chemistry* **1951**, 16, (8), 1250-1254.
366. Edmundson, R. S.; Wrigley, J. O. L., Cyclic organophosphorus compounds. IV. Cleavage of 1,3,2-dioxaphospholane and 1,3,2-dioxaphosphorinane rings by Grignard reagents. *Tetrahedron* **1967**, 23, (1), 283-290.
367. Freeman, S.; Harger, M. J. P., Influence of ortho methyl and isopropyl substituents on the reactivity of N-tert-butyl P-arylphosphonamidic chlorides with isopropylamine and tert-butylamine. Steric acceleration of metaphosphonimidate formation by an elimination-addition mechanism. Contrasting behavior of N,N-dimethyl-P-arylphosphonamidic chlorides. *Perkin transactions. I* **1987**, (6), 1399-1406.
368. Hirao, T.; Masunaga, T.; Ohshiro, Y.; Agawa, T., A novel synthesis of dialkyl arenephosphonates. *Synthesis (Stuttgart)* **1981**, (1), 56.
369. Hirao, T.; Masunaga, T.; Yamada, N.; Ohshiro, Y.; Agawa, T., Palladium-catalyzed new carbon-phosphorus bond formation. *Bulletin of the Chemical Society of Japan* **1982**, 55, (3), 909-913.

370. Petrakis, K. S.; Nagabhushan, T. L., Palladium-catalyzed substitutions of triflates derived from tyrosine-containing peptides and simpler hydroxyarenes forming 4-(diethoxyphosphinyl)phenylalanines and diethyl arylphosphonates. *Journal of the American Chemical Society* **1987**, 109, (9), 2831-2833.
371. Ngo, H. L.; Lin, W., Chiral Crown Ether Pillared Lamellar Lanthanide Phosphonates. *Journal of the American Chemical Society* **2002**, 124, (48), 14298-14299.
372. Beletskaya, I. P. P., Palladium catalyzed C-C and C-heteroatom bond formation reactions. *Pure and applied chemistry* **1997**, 69, (3), 471-476.
373. Sabitha, G.; Reddy, B. V. S.; Abraham, S.; Yadav, J. S., Deprotection of sulfonamides using iodotrimethylsilane. *Tetrahedron Letters* **1999**, 40, (8), 1569-1570.
374. Kim, S.-H.; Rieke, R. D., Preparation of aryl ketones via Ni-catalyzed Negishi-coupling reactions with acid chlorides. *Tetrahedron Letters* **2011**, 52, (13), 1523-1526.
375. Cheng, G.; Fan, R.; Hernandez-Torres, J. M.; Boulineau, F. P.; Wei, A., syn Additions to 4 $\alpha$ -Epoxy pyranosides: Synthesis of l-Idopyranosides. *Organic Letters* **2007**, 9, (23), 4849-4852.
376. Haddach, M.; McCarthy, J. R., A new method for the synthesis of ketones: The palladium-catalyzed cross-coupling of acid chlorides with arylboronic acids. *Tetrahedron Letters* **1999**, 40, (16), 3109-3112.
377. Ohe, T.; Miyaura, N.; Suzuki, A., Palladium-catalyzed cross-coupling reaction of organoboron compounds with organic triflates. *The Journal of Organic Chemistry* **1993**, 58, (8), 2201-2208.
378. Blair, W. S.; Spicer, T. P. HIV-1 reporter viruses and their use in assaying anti-viral compounds. WO 2001096610, 2001.
379. Blair, W. S.; Deshpande, M.; Fang, H.; Lin, P.-f.; Spicer, T. P.; Wallace, O. B.; Wang, H.; Wang, T.; Zhang, Z.; Yeung, K.-s. Preparation of antiviral indoleoxoacetyl piperazine derivatives. WO 2000076521, 2000.
380. Wang, T.; Zhang, Z.; Wallace, O. B.; Deshpande, M.; Fang, H.; Yang, Z.; Zadjura, L. M.; Tweedie, D. L.; Huang, S.; Zhao, F.; Ranadive, S.; Robinson, B. S.; Gong, Y.-F.; Ricarrdi, K.; Spicer, T. P.; Deminie, C.; Rose, R.; Wang, H.-G. H.; Blair, W. S.; Shi, P.-Y.; Lin, P.-f.; Colonna, R. J.; Meanwell, N. A., Discovery of 4-Benzoyl-1-[(4-methoxy-1H-pyrrolo[2,3-b]pyridin-3-yl)oxoacetyl]-2-(R)-methylpiperazine (BMS-378806): A Novel HIV-1 Attachment Inhibitor That Interferes with CD4-gp120 Interactions *Journal of Medicinal Chemistry* **2003**, 46, (20), 4236-4239.
381. Gitto, R.; Luca, L. D.; Ferro, S.; Citraro, R.; Sarro, G. D.; Costa, L.; Ciranna, L.; Chimirri, A., Development of 3-substituted-1H-indole derivatives as NR2B/NMDA receptor antagonists. *Bioorganic & Medicinal Chemistry* **2009**, 17, (4), 1640-1647.



382. Vermeulen, E. S.; van Smeden, M.; Schmidt, A. W.; Sprouse, J. S.; Wikstroem, H. V.; Grol, C. J., Novel 5-HT<sub>7</sub> Receptor Inverse Agonists. Synthesis and Molecular Modeling of Arylpiperazine- and 1,2,3,4-Tetrahydroisoquinoline-Based Arylsulfonamides. *Journal of Medicinal Chemistry* **2004**, 47, (22), 5451-5466.
383. Zhang, Z.; Yang, Z.; Wong, H.; Zhu, J.; Meanwell, N. A.; Kadow, J. F.; Wang, T., An Effective Procedure for the Acylation of Azaindoles at C-3. *The Journal of Organic Chemistry* **2002**, 67, (17), 6226-6227.
384. Carteau, S.; Mouscadet, J. F.; Goulaouic, H.; Subra, F.; Auclair, C., Quantitative in Vitro Assay for Human Immunodeficiency Virus Deoxyribonucleic Acid Integration. *Archives of biochemistry and biophysics* **1993**, 300, (2), 756-760.
385. Chow, S. A., In Vitro Assays for Activities of Retroviral Integrase. *Methods* **1997**, 12, (4), 306-317.
386. Debyser, Z., Assays for the evaluation of HIV-1 integrase inhibitors. *Methods in molecular biology (Clifton, N.J.)* **2001**, 160, (nuclease methods and protocols), 139.
387. Zhimin, G.; Hongshan, C., [HIV-1 integrase enzyme linked immunosorbent assay and inhibitors]. *Zhonghua shi yan he lin chuang bing du xue za ji* **2002**, 16, (2), 119-23.
388. Hwang, Y.; Rhodes, D.; Bushman, F., Rapid microtiter assays for poxvirus topoisomerase, mammalian type IB topoisomerase and HIV-1 integrase: application to inhibitor isolation. *Nucleic Acids Research* **2000**, 28, (24), 4884-4892.
389. Chang, Y.-C.; Ching, T.-T.; Syu, W., Jr., Assaying the activity of HIV-1 integrase with DNA-coated plates. *Journal of Virological Methods* **1996**, 59, (1-2), 135-140.
390. Chen, H.; Boyle, T. J.; Malim, M. H.; Cullen, B. R.; Lyerly, H. K., Derivation of a Biologically Contained Replication System for Human Immunodeficiency Virus Type 1. *Proceedings of the National Academy of Sciences of the United States of America* **1992**, 89, (16), 7678-7682.
391. Gallo, R. C.; Montagnier, L., The Discovery of HIV as the Cause of AIDS. *New England Journal of Medicine* **2003**, 349, (24), 2283-2285.
392. Pomerantz, R. J.; Horn, D. L., Twenty years of therapy for HIV-1 infection. *Nat Med* **2003**, 9, (7), 867-873.
393. Moyle, G.; Gatell, J.; Perno, C.-F.; Ratanasuwan, W.; Schechter, M.; Tsoukas, C., Potential for new antiretrovirals to address unmet needs in the management of HIV-1 infection. *AIDS patient care and STDs* **2008**, 22, (6), 459-471.
394. Markowitz, M.; Evering, T. H., Raltegravir (MK-0518): An integrase inhibitor for the treatment of HIV-1. *Drugs Today* **2007**, 43, (12), 1699-3993.

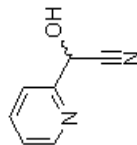
395. Buu-Hoi, N. P.; Saint-Ruf, G.; Bourgeade, J. C., Phthalonimides (1,3,4-trioxo-1,2,3,4-tetrahydroisoquinolines) of potential biological interest. *Journal of heterocyclic chemistry* **1968**, 5, (4), 545-547.
396. Chen, Y.-H.; Zhang, Y.-H.; Zhang, H.-J.; Liu, D.-Z.; Gu, M.; Li, J.-Y.; Wu, F.; Zhu, X.-Z.; Li, J.; Nan, F.-J., Design, Synthesis, and Biological Evaluation of Isoquinoline-1,3,4-trione Derivatives as Potent Caspase-3 Inhibitors. *Journal of Medicinal Chemistry* **2006**, 49, (5), 1613-1623.
397. Zaitso, K.; Nakazono, M.; Tani, K. Preparation of of fluorescent compound with bis(benzofuranyl)maleimide structure. JP 2011162546, 2011.
398. Kozikowski, A. P.; Gaysina, I. Benzofuran-3-yl(indol-3-yl)maleimides as potent GSK3 inhibitors and their preparation, and use in the treatment of diseases. US 20100004308, 2010.
399. Wang, L.; Hubert, J. A.; Lee, S. J.; Pan, J.; Qian, S.; Reitman, M. L.; Strack, A. M.; Weingarh, D. T.; MacNeil, D. J.; Weber, A. E.; Edmondson, S. D., Discovery of pyrimidine carboxamides as potent and selective CCK1 receptor agonists. *Bioorganic & Medicinal Chemistry Letters* **2011**, 21, (10), 2911-2915.
400. Shao, J.; Huang, X.; Wang, S.; Liu, B.; Xu, B., A straightforward synthesis of N-monosubstituted  $\alpha$ -keto amides via aerobic benzylic oxidation of amides. *Tetrahedron* **2012**, 68, (2), 573-579.
401. Park, S. Y.; Kang, M.; Yie, J. E.; Kim, J. M.; Lee, I.-M., A novel and efficient route to diarylmethanes catalyzed by nickel(II) ion on nanoporous carbon. *Tetrahedron Letters* **2005**, 46, (16), 2849-2852.
402. Tasler, S.; Lipshutz, B. H., Nickel-on-Charcoal-Catalyzed Aromatic Aminations and Kumada Couplings: Mechanistic and Synthetic Aspects. *The Journal of Organic Chemistry* **2002**, 68, (4), 1190-1199.
403. Laali, K. K.; Gettewert, V. J., Electrophilic Nitration of Aromatics in Ionic Liquid Solvents. *The Journal of Organic Chemistry* **2000**, 66, (1), 35-40.
404. Fan, S.; He, C.-Y.; Zhang, X., Direct Pd-catalyzed benzylation of highly electron-deficient perfluoroarenes. *Chemical Communications* **2010**, 46, (27), 4926-4928.
405. Liegault, B.; Renaud, J.-L.; Bruneau, C., Activation and functionalization of benzylic derivatives by palladium catalysts. *Chemical Society Reviews* **2008**, 37, (2), 290-299.
406. Martins, A.; Lautens, M., Aromatic ortho-Benzylation Reveals an Unexpected Reductant. *Organic Letters* **2008**, 10, (21), 5095-5097.
407. Verrier, C.; Hoarau, C.; Marsais, F., Direct palladium-catalyzed alkenylation, benzylation and alkylation of ethyl oxazole-4-carboxylate with alkenyl-, benzyl- and alkyl halides. *Organic & Biomolecular Chemistry* **2009**, 7, (4), 647-650.

408. Mukai, T.; Hirano, K.; Satoh, T.; Miura, M., Palladium-Catalyzed Direct Benzoylation of Azoles with Benzyl Carbonates. *Organic Letters* **2010**, 12, (6), 1360-1363.
409. Mavunkel, B. J.; Perumattam, J. J.; Tan, X.; Luedtke, G. R.; Lu, Q.; Lim, D.; Kizer, D.; Dugar, S.; Chakravarty, S.; Xu, Y.-j.; Jung, J.; Licican, A.; Levy, D. E.; Tabora, J., Piperidine-based heterocyclic oxalyl amides as potent p38 $\alpha$  MAP kinase inhibitors. *Bioorganic & Medicinal Chemistry Letters* **2009**, 20, (3), 1059-1062.
410. Montalban, A. G.; Boman, E.; Chang, C.-D.; Ceide, S. C.; Dahl, R.; Dalesandro, D.; Delaet, N. G. J.; Erb, E.; Ernst, J. T.; Gibbs, A.; Kahl, J.; Kessler, L.; Lundström, J.; Miller, S.; Nakanishi, H.; Roberts, E.; Saiah, E.; Sullivan, R.; Wang, Z.; Larson, C. J., The design and synthesis of novel  $\beta$ -ketoamide-based p38 MAP kinase inhibitors. *Bioorganic & Medicinal Chemistry Letters* **2008**, 18, (6), 1772-1777.
411. Gong, J.; Shen, X.-h.; Chen, C.; Qiu, H.; Yang, R.-g., Down-regulation of HIV-1 infection by inhibition of the MAPK signaling pathway. *Virologica Sinica* **2012**, 26, (2), 114-122.
412. *National Research Council (US) Committee on Prudent Practices in the Laboratory. National Prudent Practices in the Laboratory: Handling and Management of Chemical Hazards: Updated Version.* National Academies Press (US): Washington (DC), 2011.
413. Vedejs, E.; Monahan, S. D., Competing Pathways in the Azomethine Ylide Route to Indoloquinones: An Improved Procedure for the Generation of a Transient 4-Oxazoline from the Oxazolium Salt. *The Journal of Organic Chemistry* **1997**, 62, (14), 4763-4769.
414. Dickson, S. J.; Biagini, S. C. G.; Steed, J. W., Anion binding in (arene)ruthenium(ii)-based hosts. *Chemical Communications* **2007**, (46), 4955-4957.
415. De, S. K., Cobalt(II) chloride catalyzed one-pot synthesis of  $\alpha$ -aminonitriles. *Beilstein J. Org. Chem.* **2005**, 1, (8), 1-3.
416. Chi B. Vu, J. S. D., Stephanic K. Springer, Charles A. Blum, Robert B. Perni Quinolines and related analogs as sirtuin modulators and their preparation, pharmaceutical compositions and use in the treatment of diseases. WO 2009134973, 2011.
417. Kumar, A.; Narasimhan, B.; Kumar, D., Synthesis, antimicrobial, and QSAR studies of substituted benzamides. *Bioorganic & Medicinal Chemistry* **2007**, 15, (12), 4113-4124.
418. Lee, Y.-J.; Han, Y.-R.; Park, W.; Nam, S.-H.; Oh, K.-B.; Lee, H.-S., Synthetic analogs of indole-containing natural products as inhibitors of sortase A and isocitrate lyase. *Bioorganic & Medicinal Chemistry Letters* **2010**, 20, (23), 6882-6885.
419. Marchand, P.; Antoine, M.; Baut, G. L.; Czech, M.; Baasner, S.; Guenther, E., Synthesis and structure-activity relationships of N-aryl(indol-3-yl)glyoxamides as antitumor agents. *Bioorganic & Medicinal Chemistry* **2009**, 17, (18), 6715-6727.

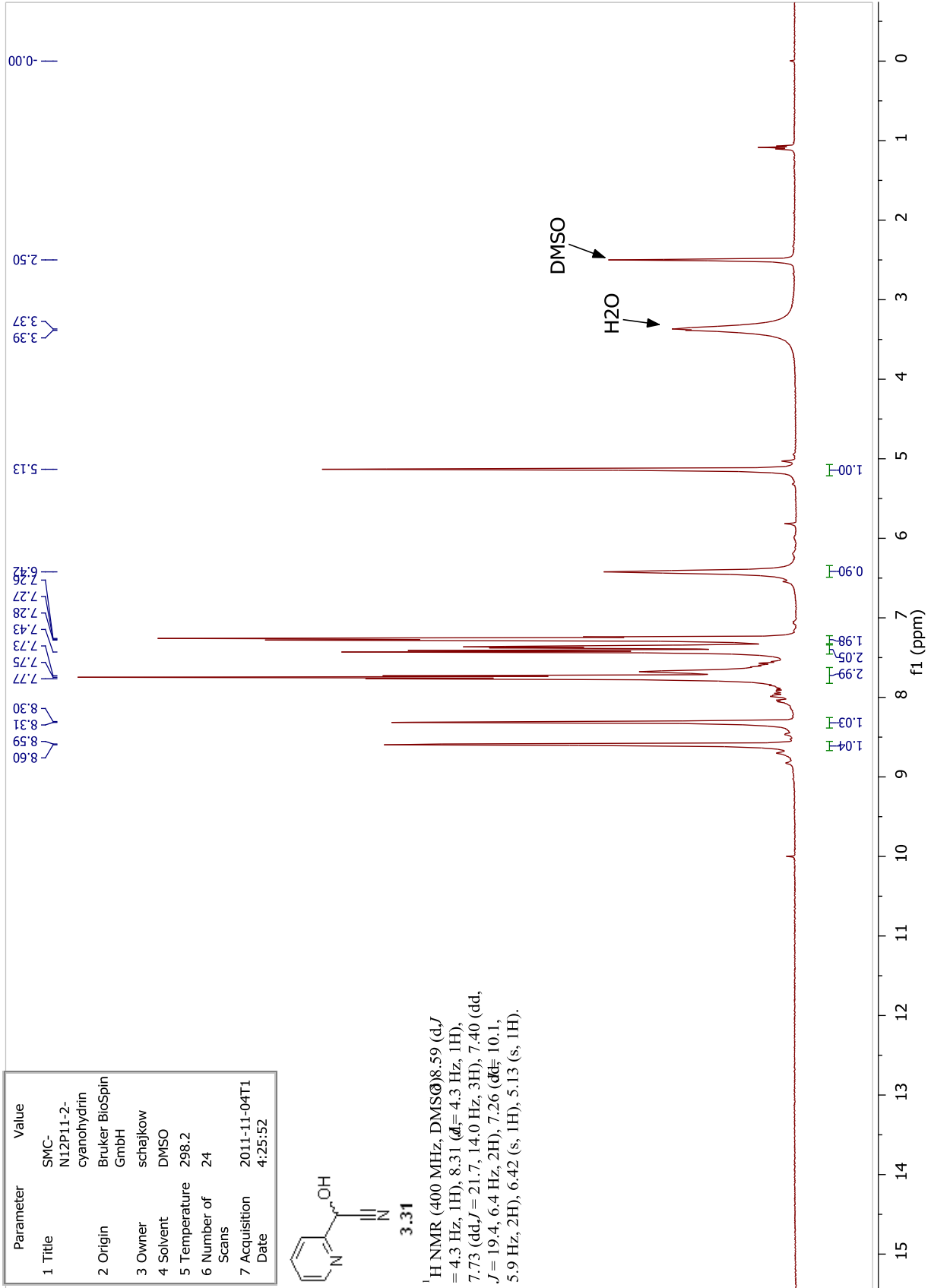
## **List of Appendices**

**Appendix: A**  
**Spectral Data**

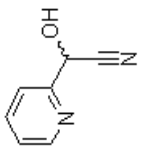
Parameter	Value
1 Title	SMC-NI2P11-2-cyanohydrin
2 Origin	Bruker BioSpin GmbH
3 Owner	schajkowi
4 Solvent	DMSO
5 Temperature	298.2
6 Number of Scans	24
7 Acquisition Date	2011-11-04T14:25:52



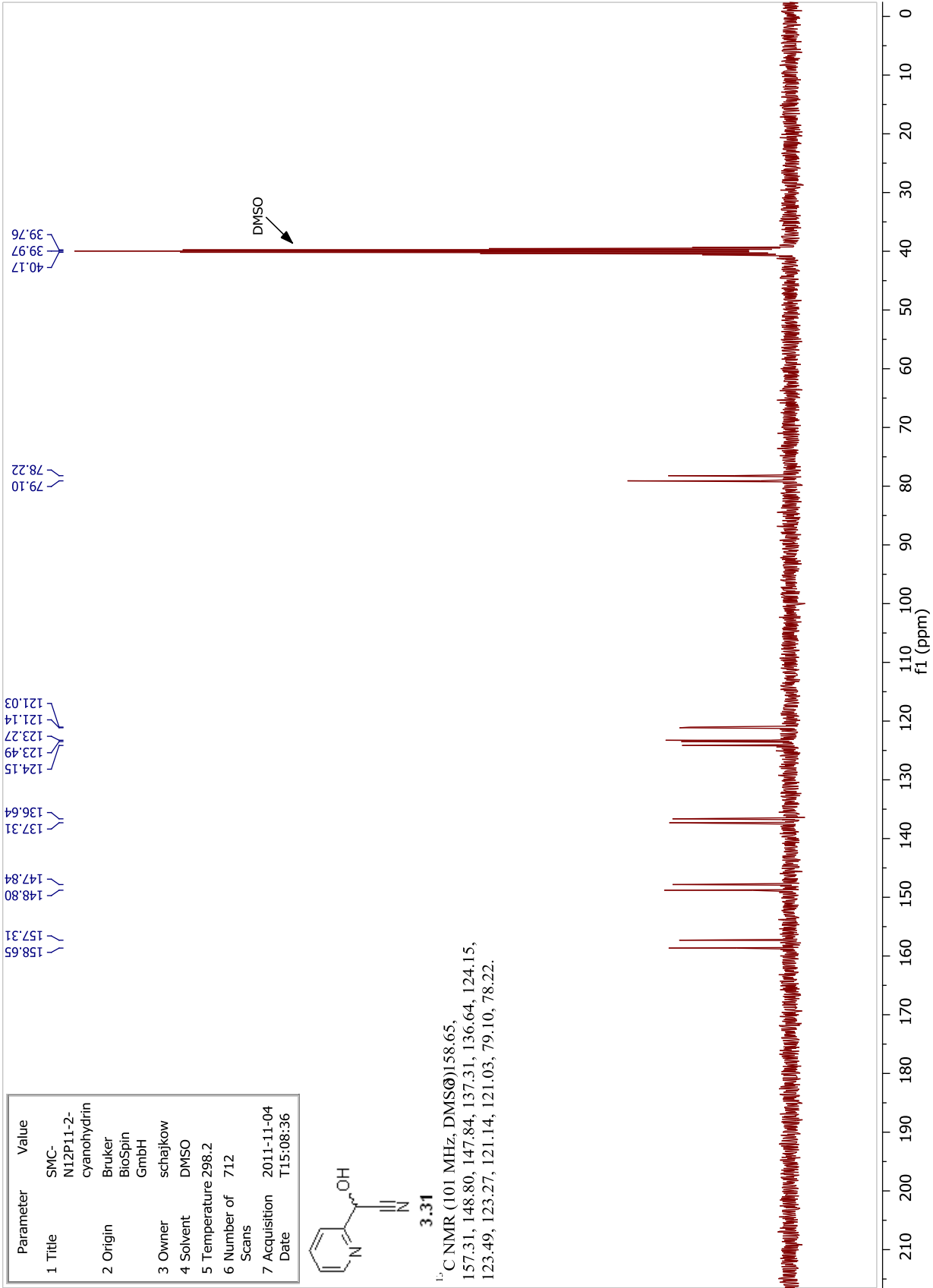
<sup>1</sup>H NMR (400 MHz, DMSO-d<sub>6</sub>) 8.59 (d, J = 4.3 Hz, 1H), 8.31 (d, J = 4.3 Hz, 1H), 7.73 (dd, J = 21.7, 14.0 Hz, 3H), 7.40 (dd, J = 19.4, 6.4 Hz, 2H), 7.26 (dd, J = 10.1, 5.9 Hz, 2H), 6.42 (s, 1H), 5.13 (s, 1H).



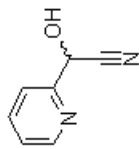
Parameter	Value
1 Title	SMC-NI2P11-2-cyanohydrin
2 Origin	Bruker BioSpin GmbH
3 Owner	schajkow
4 Solvent	DMSO
5 Temperature	298.2
6 Number of Scans	712
7 Acquisition Date	2011-11-04 T15:08:36



<sup>13</sup>C NMR (101 MHz, DMSO-d<sub>6</sub>) 158.65, 157.31, 148.80, 147.84, 137.31, 136.64, 124.15, 123.27, 121.14, 121.03, 79.10, 78.22.

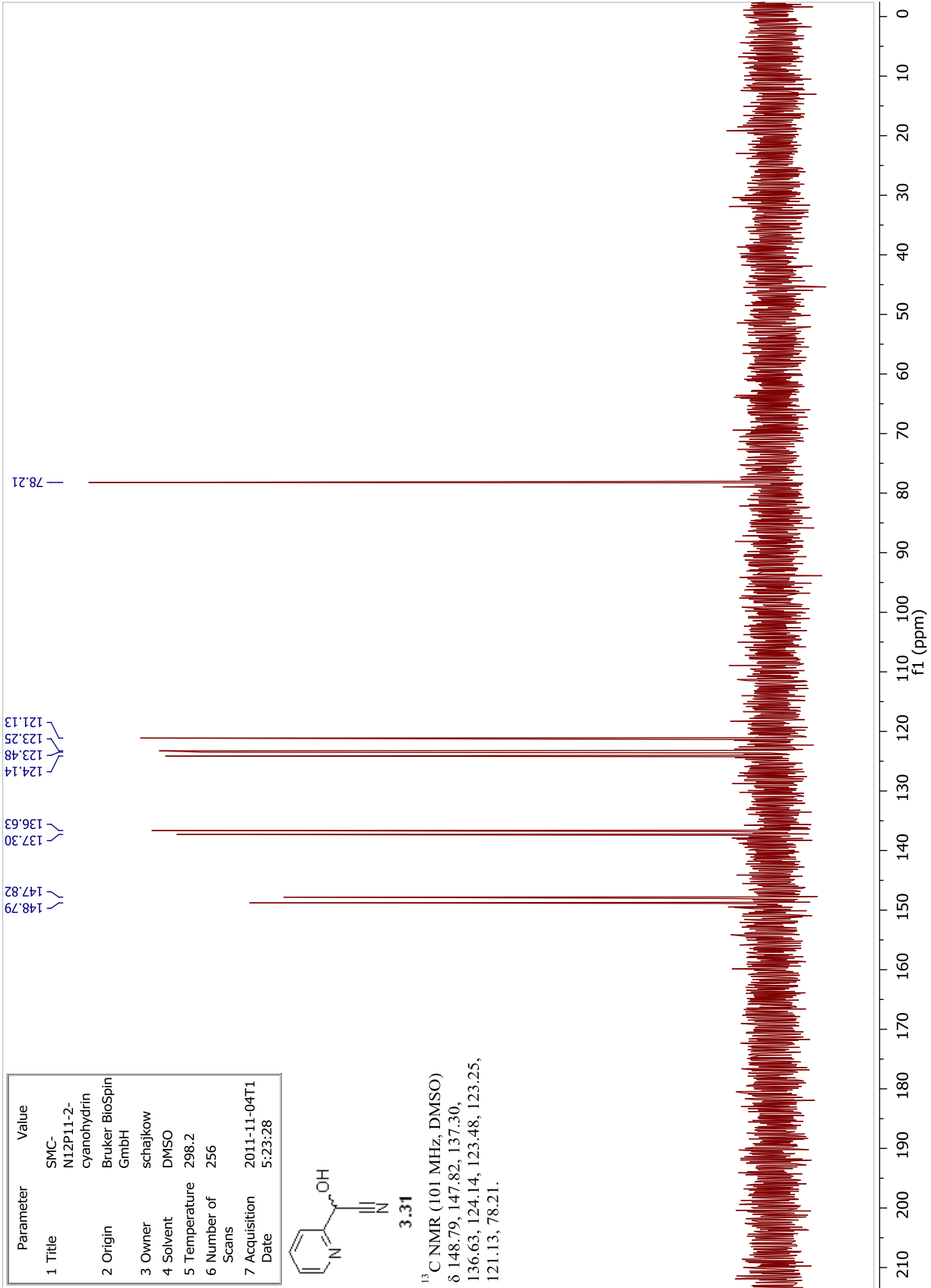


Parameter	Value
1 Title	SMC- NI2P11-2- cyanohydrin
2 Origin	Bruker BioSpin GmbH
3 Owner	schajkow
4 Solvent	DMSO
5 Temperature	298.2
6 Number of Scans	256
7 Acquisition Date	2011-11-04T1 5:23:28



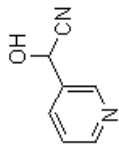
**3.31**

<sup>13</sup>C NMR (101 MHz, DMSO)  
 δ 148.79, 147.82, 137.30,  
 136.63, 124.14, 123.48, 123.25,  
 121.13, 78.21.

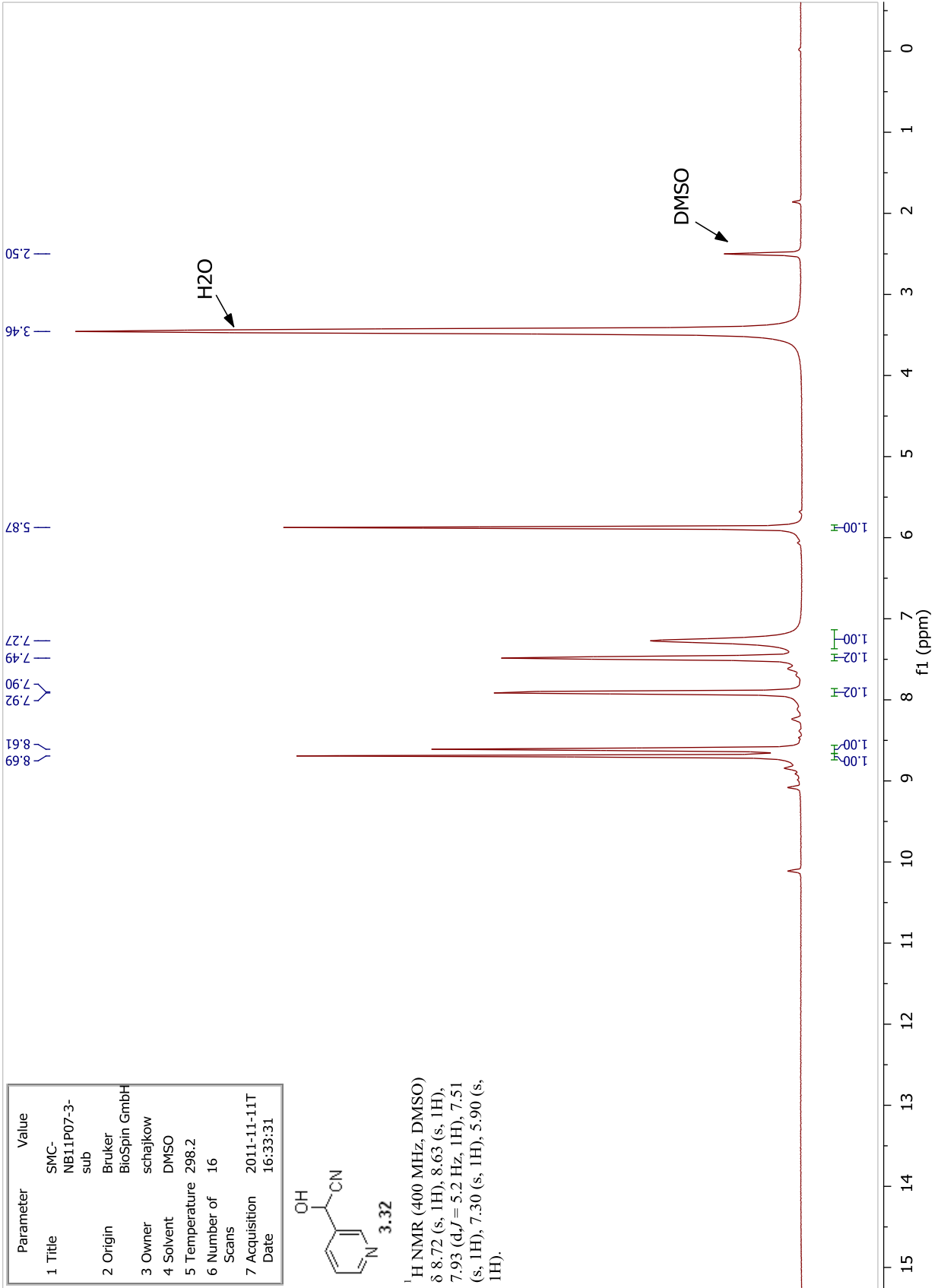




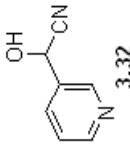
Parameter	Value
1 Title	SMC-NB11P07-3-sub
2 Origin	Bruker BioSpin GmbH
3 Owner	schajkow
4 Solvent	DMSO
5 Temperature	298.2
6 Number of Scans	16
7 Acquisition Date	2011-11-11T16:33:31



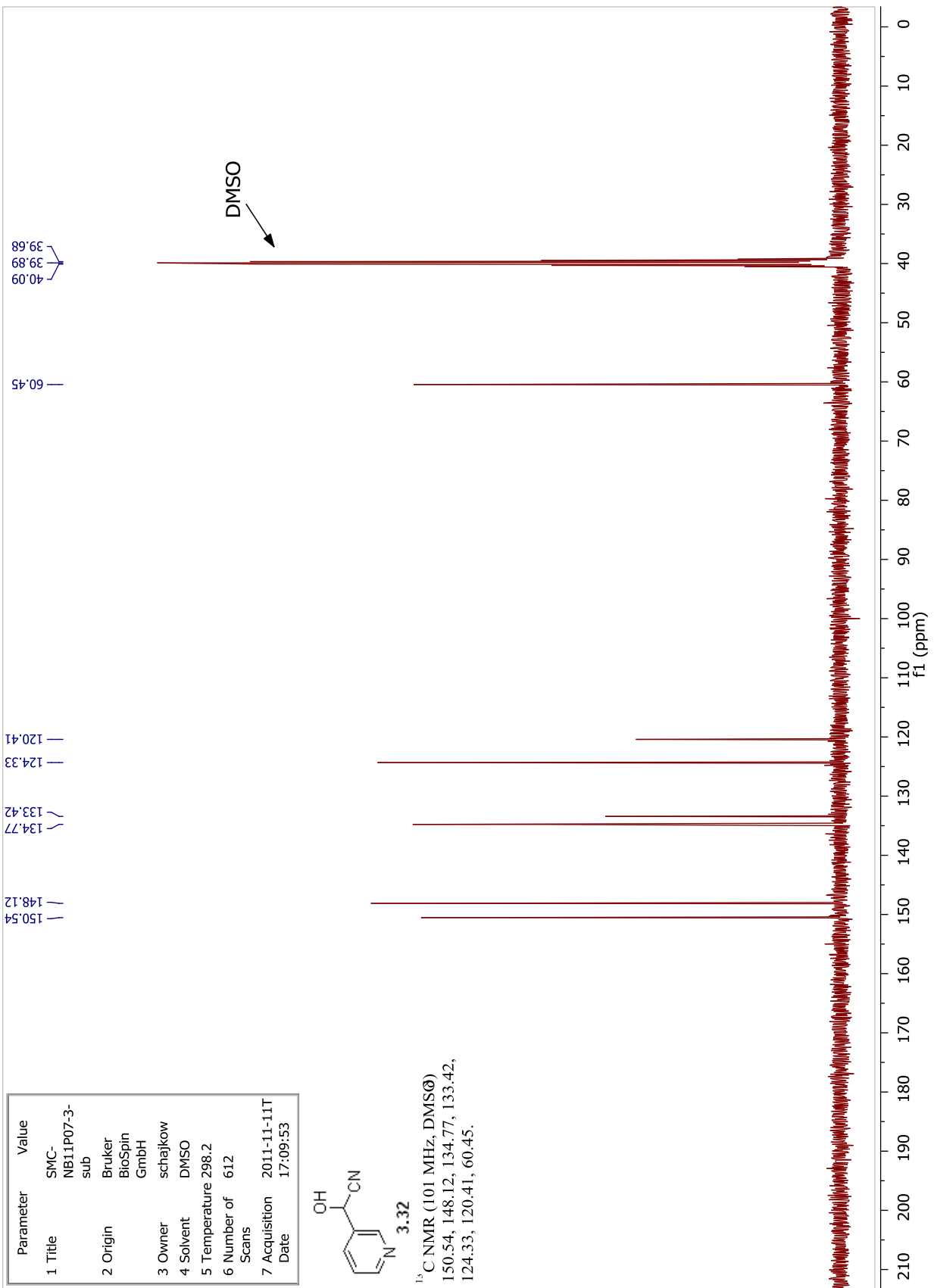
<sup>1</sup>H NMR (400 MHz, DMSO)  
 $\delta$  8.72 (s, 1H), 8.63 (s, 1H),  
7.93 (d,  $J$  = 5.2 Hz, 1H), 7.51  
(s, 1H), 7.30 (s, 1H), 5.90 (s,  
1H).



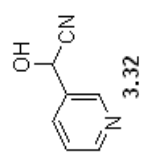
Parameter	Value
1 Title	SMC-NB11P07-3-sub
2 Origin	Bruker BioSpin GmbH
3 Owner	schajkow
4 Solvent	DMSO
5 Temperature	298.2
6 Number of Scans	612
7 Acquisition Date	2011-11-11T17:09:53



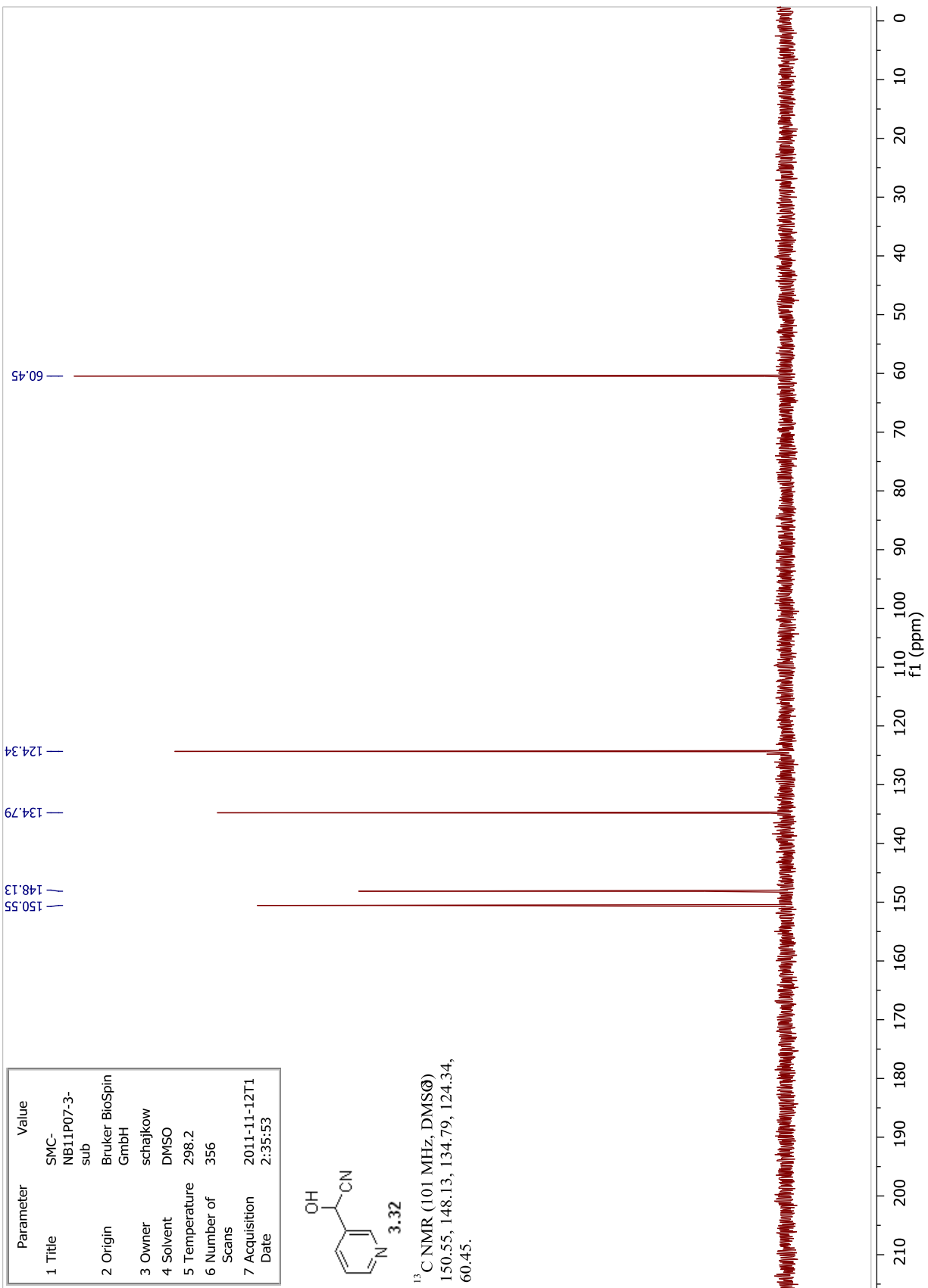
<sup>13</sup>C NMR (101 MHz, DMSO- $d_6$ )  
150.54, 148.12, 134.77, 133.42,  
124.33, 120.41, 60.45.



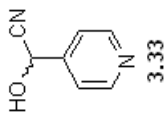
Parameter	Value
1 Title	SMC-NB11P07-3-sub
2 Origin	Bruker BioSpin GmbH
3 Owner	schajkowi
4 Solvent	DMSO
5 Temperature	298.2
6 Number of Scans	356
7 Acquisition Date	2011-11-12T1 2:35:53



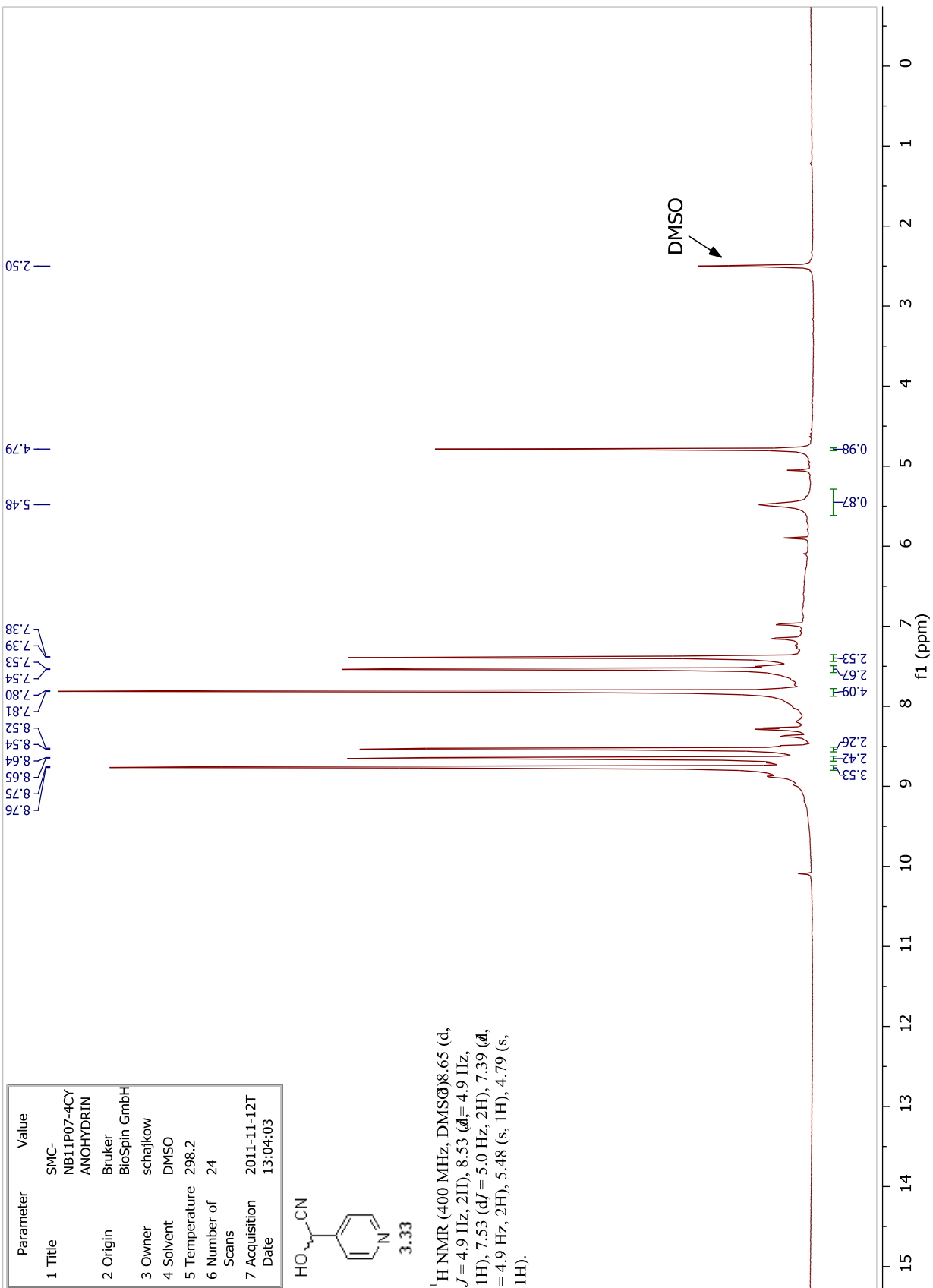
<sup>13</sup>C NMR (101 MHz, DMSO)  
 150.55, 148.13, 134.79, 124.34,  
 60.45.



Parameter	Value
1 Title	SMC-NB11P07-4CY ANOXYDRIN
2 Origin	Bruker BioSpin GmbH
3 Owner	schajkow
4 Solvent	DMSO
5 Temperature	298.2
6 Number of Scans	24
7 Acquisition Date	2011-11-12T13:04:03



<sup>1</sup>H NMR (400 MHz, DMSO-d<sub>6</sub>) 8.65 (d, J = 4.9 Hz, 2H), 8.53 (d, J = 4.9 Hz, 1H), 7.53 (d, J = 5.0 Hz, 2H), 7.39 (d, J = 4.9 Hz, 2H), 5.48 (s, 1H), 4.79 (s, 1H).

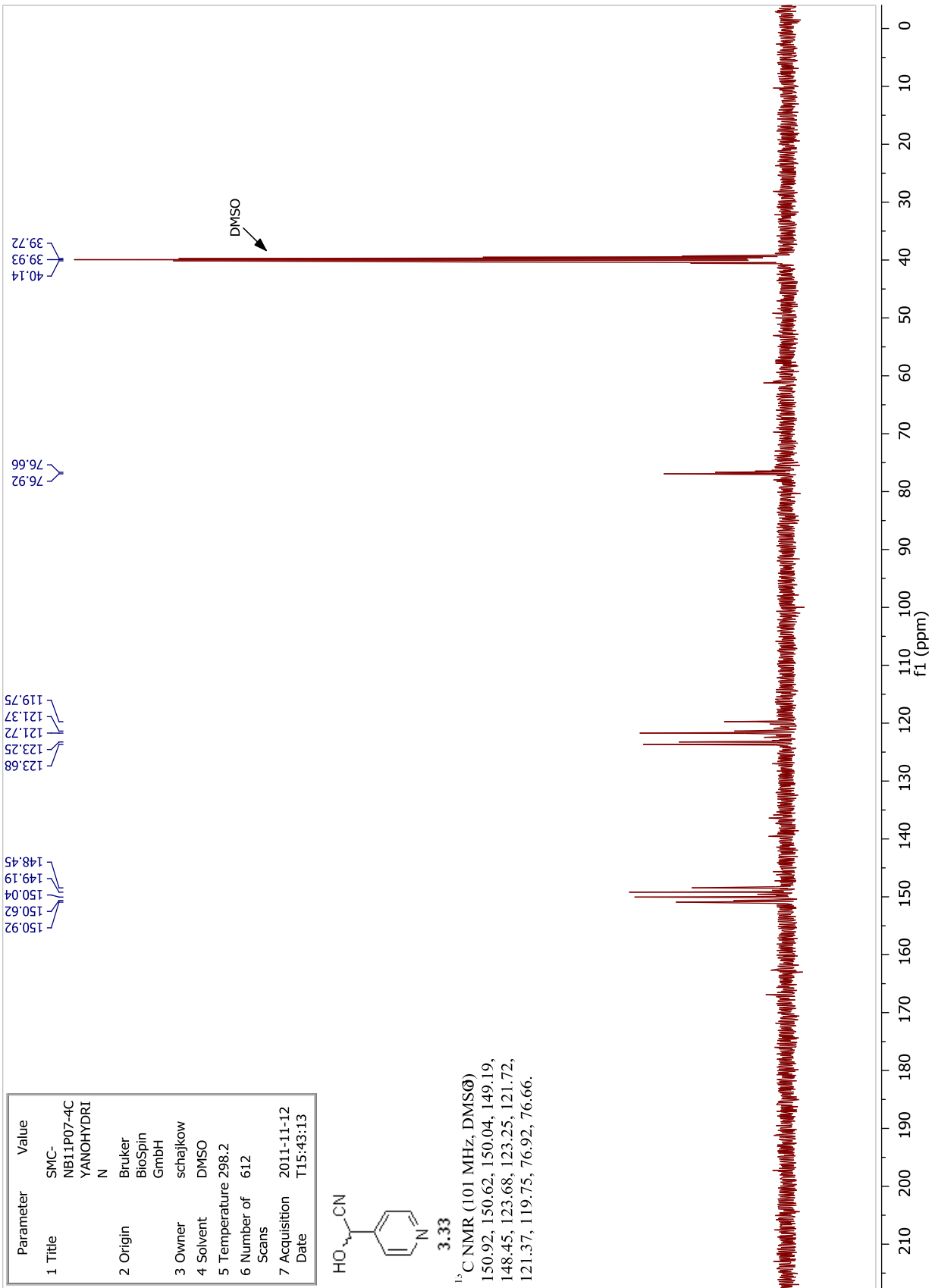


Parameter	Value
1 Title	SMC- NB11P07-4C YANOHYDRI N
2 Origin	Bruker BioSpin GmbH
3 Owner	schajkow
4 Solvent	DMSO
5 Temperature	298.2
6 Number of Scans	612
7 Acquisition Date	2011-11-12 T15:43:13

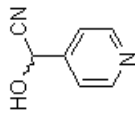


**3.33**

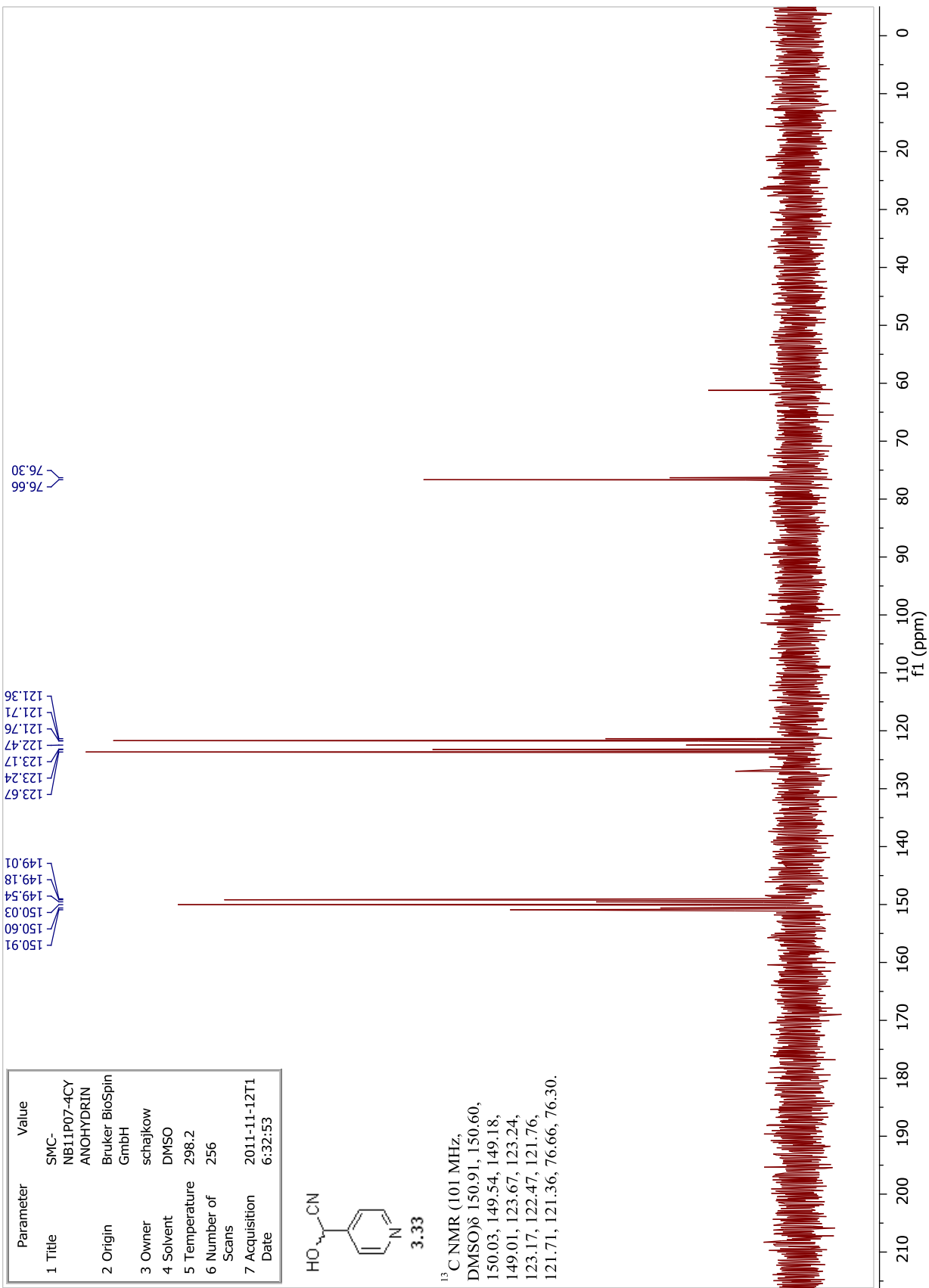
<sup>13</sup>C NMR (101 MHz, DMSO)  
150.92, 150.62, 150.04, 149.19,  
148.45, 123.68, 123.25, 121.72,  
121.37, 119.75, 76.92, 76.66.



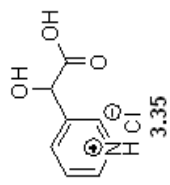
Parameter	Value
1 Title	SMC- NB11P07-4CY ANOHYDRIN
2 Origin	Bruker BioSpin GmbH
3 Owner	schajkow
4 Solvent	DMSO
5 Temperature	298.2
6 Number of Scans	256
7 Acquisition Date	2011-11-12T1 6:32:53



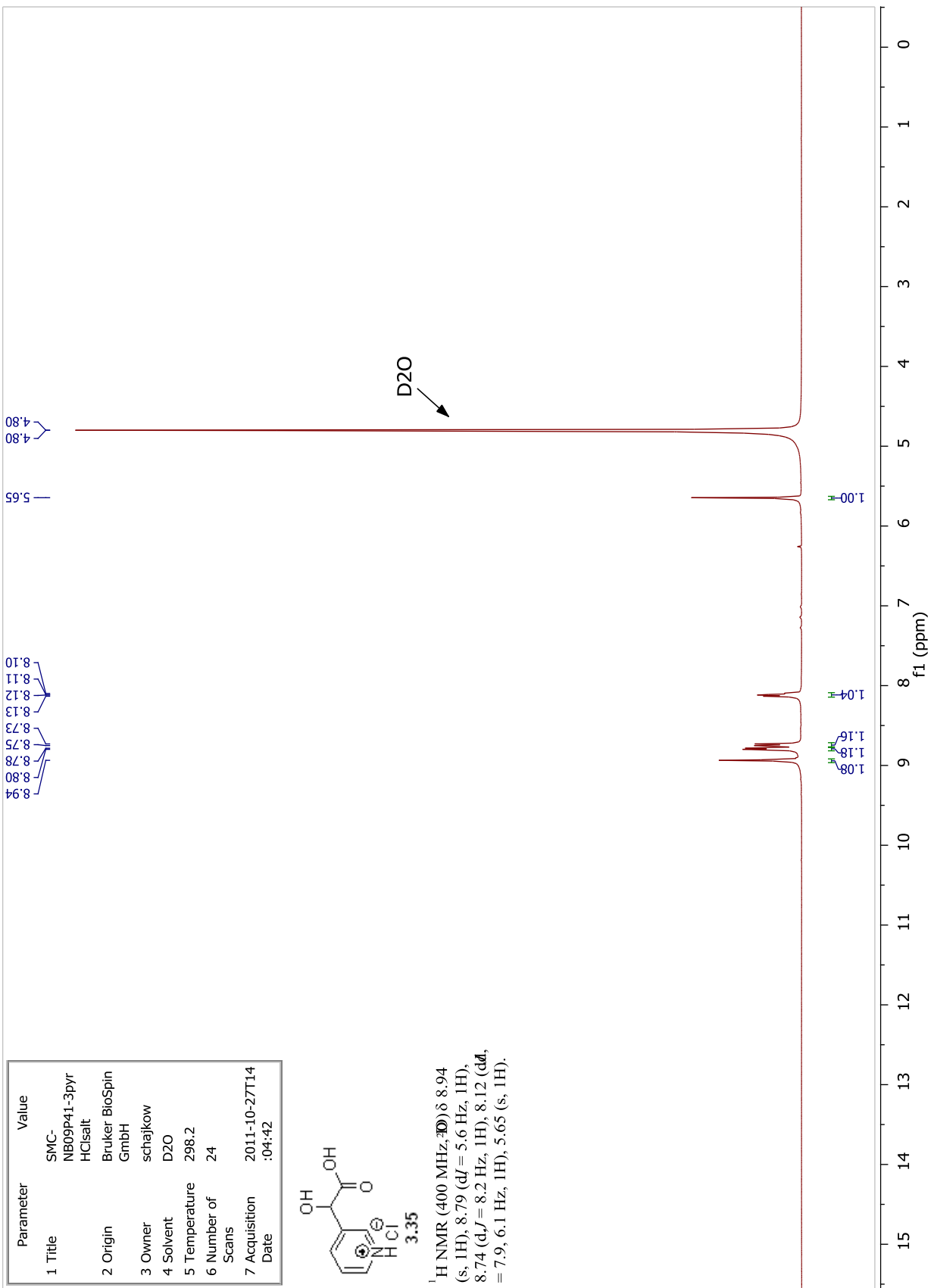
<sup>13</sup>C NMR (101 MHz,  
DMSO) δ 150.91, 150.60,  
150.03, 149.54, 149.18,  
149.01, 123.67, 123.24,  
123.17, 122.47, 121.76,  
121.71, 121.36, 76.66, 76.30.



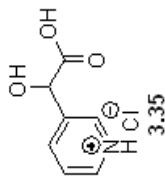
Parameter	Value
1 Title	SMC-NB09p411-3pyr
2 Origin	HCl salt Bruker BioSpin GmbH
3 Owner	schajkow
4 Solvent	D2O
5 Temperature	298.2
6 Number of Scans	24
7 Acquisition Date	2011-10-27T14:04:42



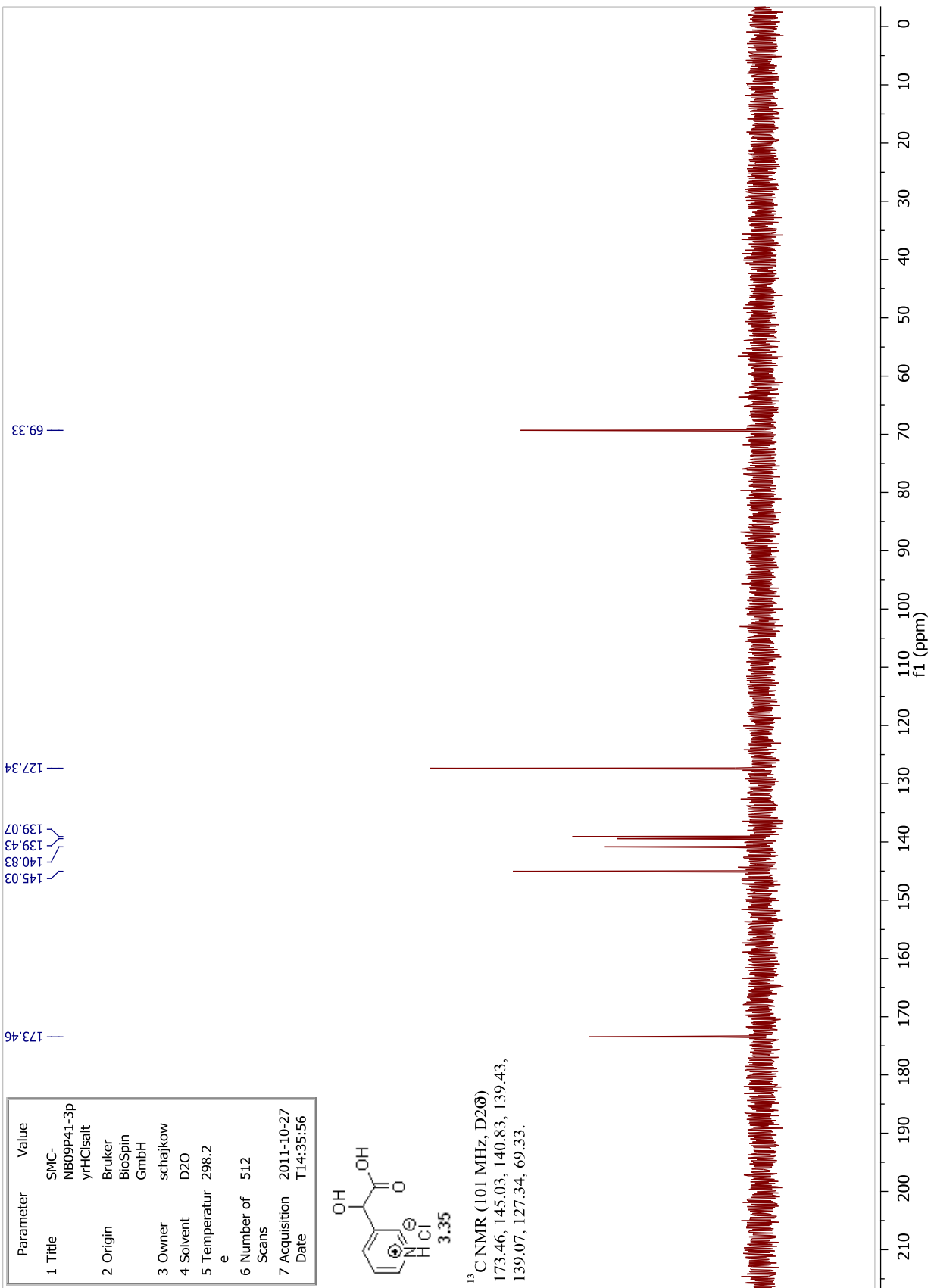
<sup>1</sup>H NMR (400 MHz, D<sub>2</sub>O) δ 8.94 (s, 1H), 8.79 (dJ = 5.6 Hz, 1H), 8.74 (dJ = 8.2 Hz, 1H), 8.12 (dd, = 7.9, 6.1 Hz, 1H), 5.65 (s, 1H).



Parameter	Value
1 Title	SMC-NB09P41-3p yHClSalt
2 Origin	Bruker BioSpin GmbH
3 Owner	schajkow
4 Solvent	D2O
5 Temperatur	298.2 e
6 Number of Scans	512
7 Acquisition Date	2011-10-27 T14:35:56

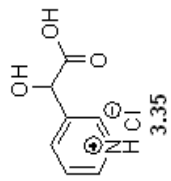


<sup>13</sup>C NMR (101 MHz, D2O)  
173.46, 145.03, 140.83, 139.43,  
139.07, 127.34, 69.33.

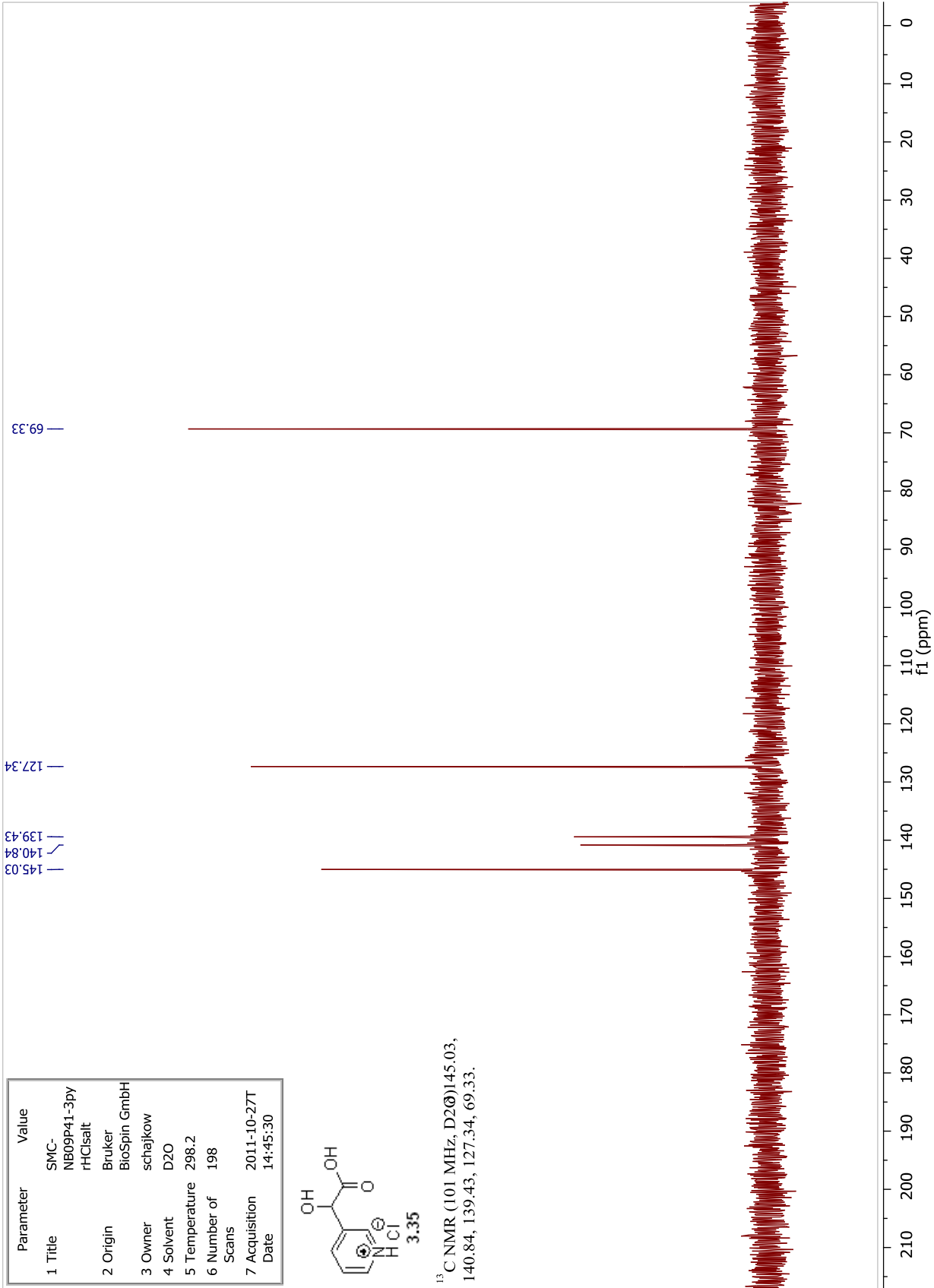




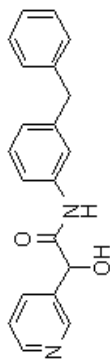
Parameter	Value
1 Title	SMC-NB09P41-3py rHCl salt
2 Origin	Bruker BioSpin GmbH
3 Owner	schajkow
4 Solvent	D2O
5 Temperature	298.2
6 Number of Scans	198
7 Acquisition Date	2011-10-27T14:45:30



<sup>13</sup>C NMR (101 MHz, D2O) 145.03, 140.84, 139.43, 127.34, 69.33.

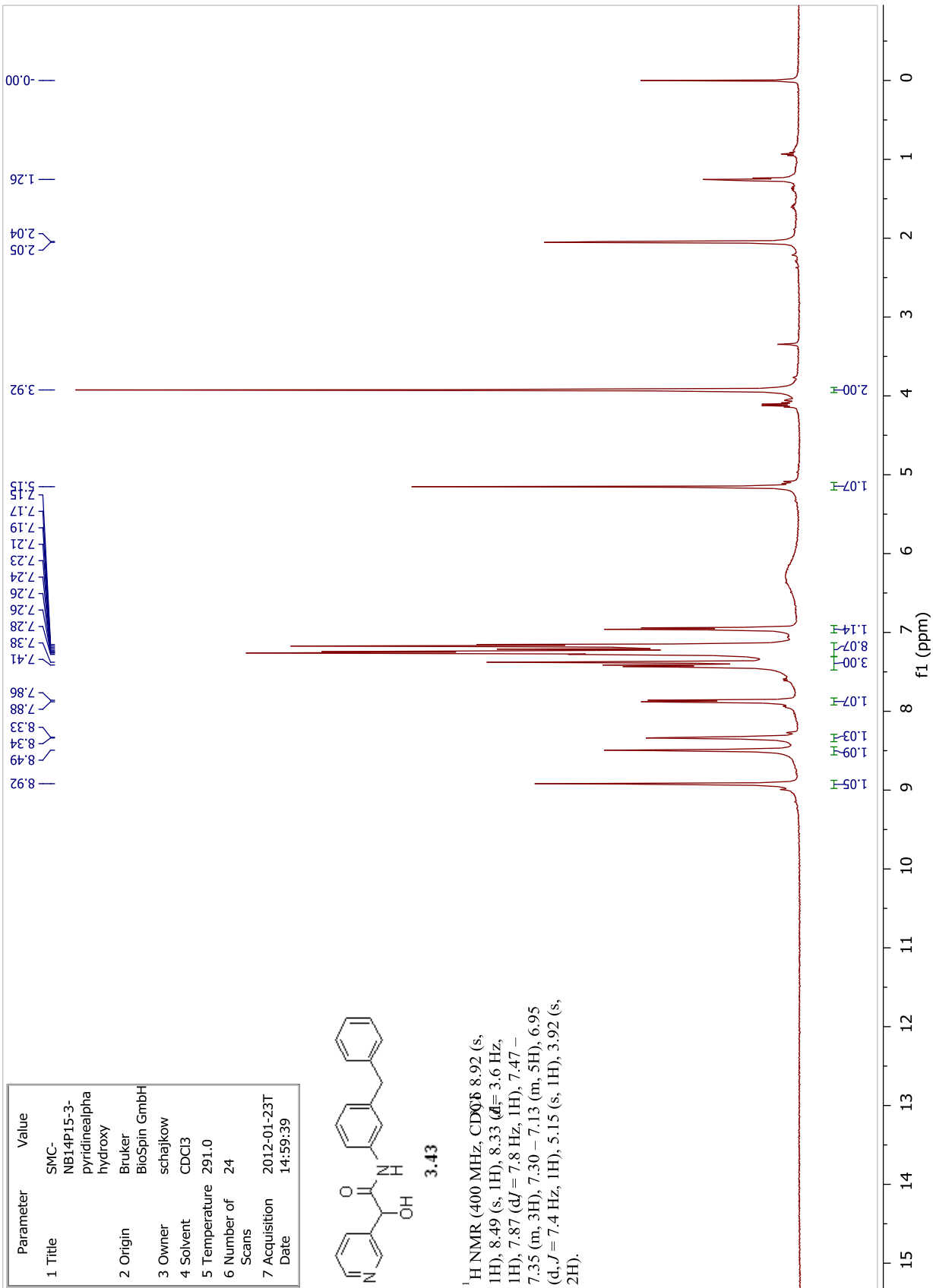


Parameter	Value
1 Title	SMC-NB14P15-3-pyridinealpha hydroxy
2 Origin	Bruker BioSpin GmbH
3 Owner	schajkow
4 Solvent	CDCl3
5 Temperature	291.0
6 Number of Scans	24
7 Acquisition Date	2012-01-23T14:59:39

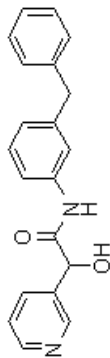


3.43

<sup>1</sup>H NMR (400 MHz, CDCl<sub>3</sub>) δ 8.92 (s, 1H), 8.49 (s, 1H), 8.33 (d, *d*= 3.6 Hz, 1H), 7.87 (d, *d* = 7.8 Hz, 1H), 7.47 – 7.35 (m, 3H), 7.30 – 7.13 (m, 5H), 6.95 (d, *J* = 7.4 Hz, 1H), 5.15 (s, 1H), 3.92 (s, 2H).

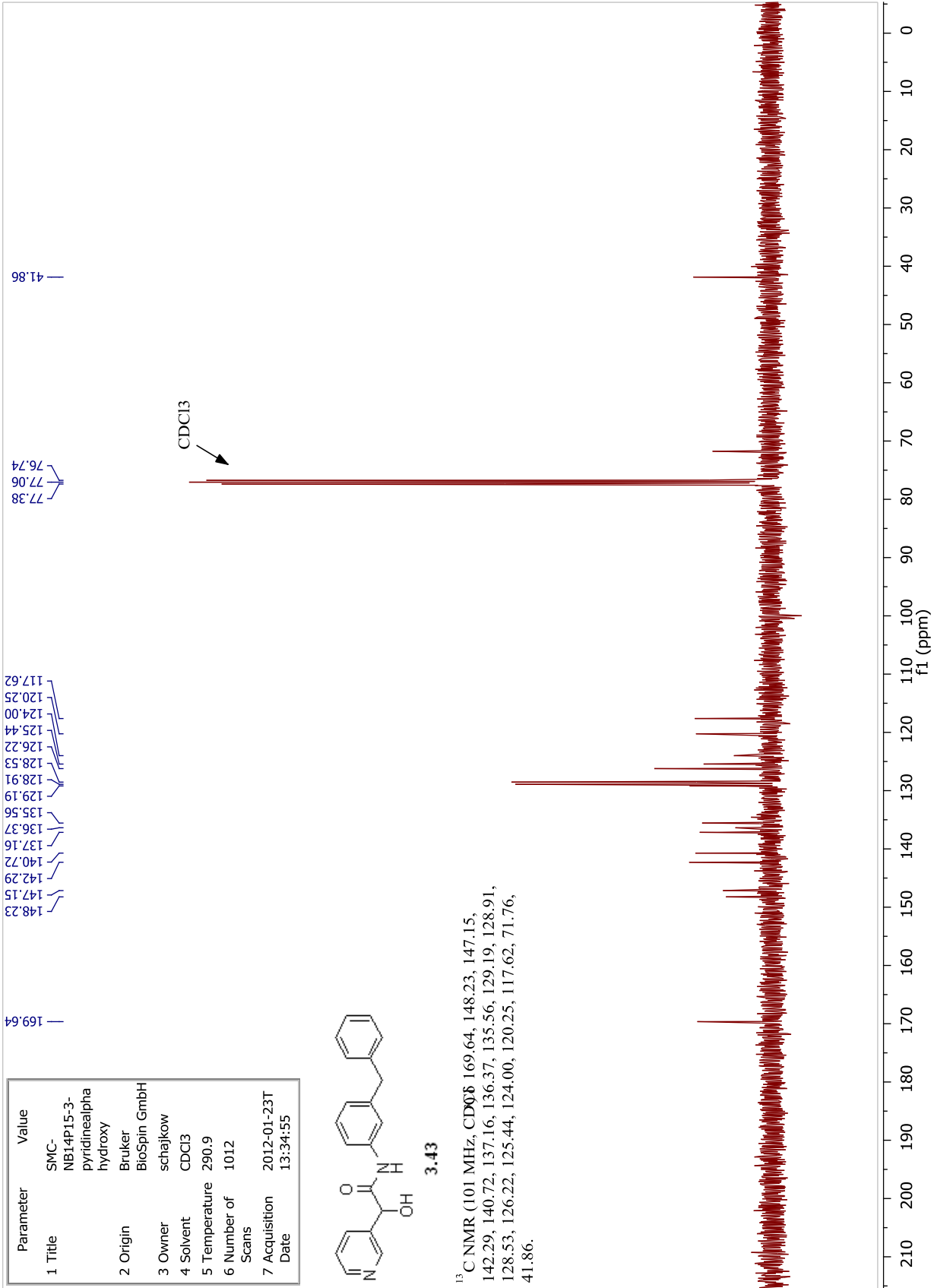


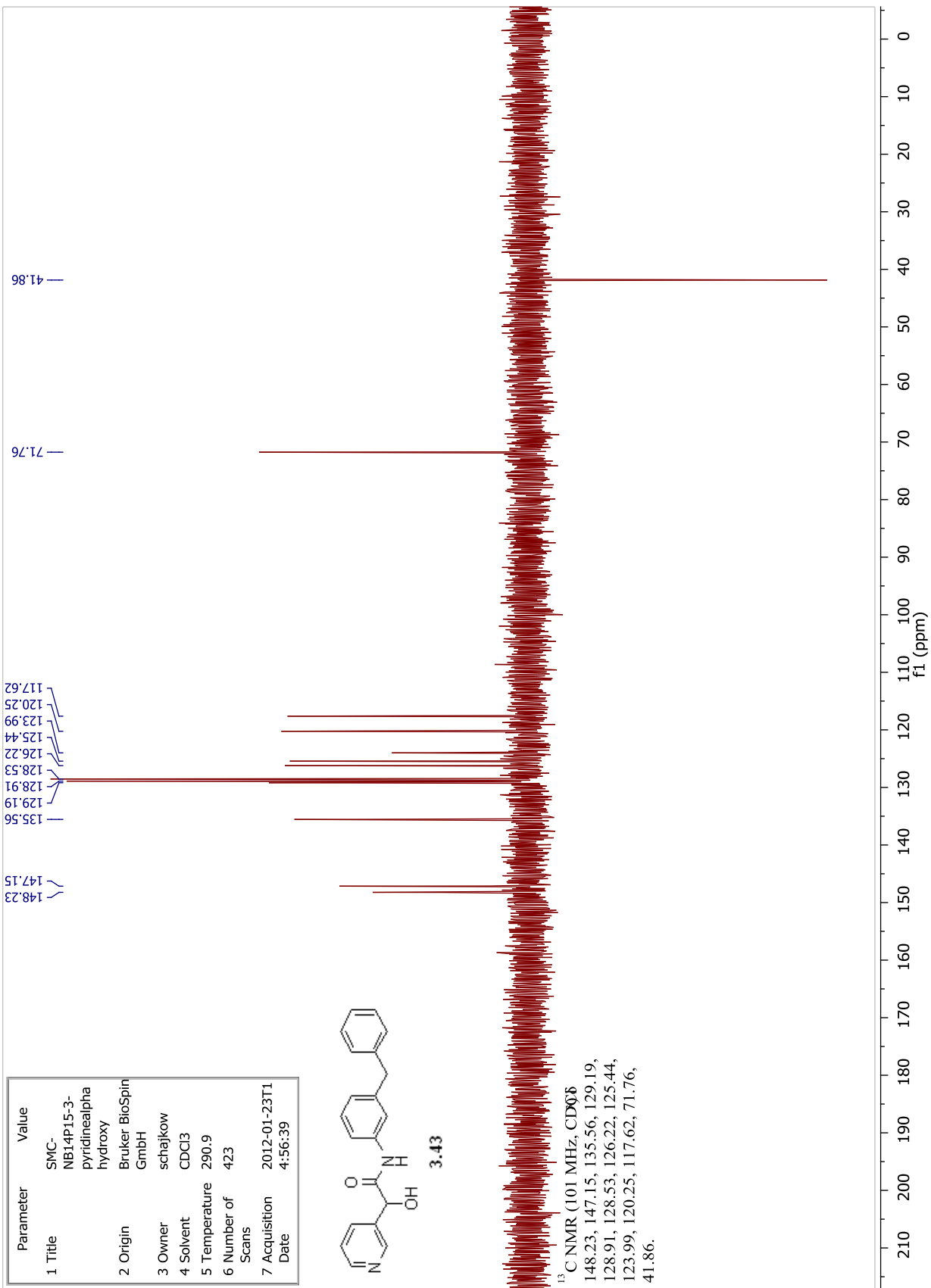
Parameter	Value
1 Title	SMC-NB14P15-3-pyridinealpha hydroxy
2 Origin	Bruker BioSpin GmbH
3 Owner	schajkow
4 Solvent	CDCl3
5 Temperature	290.9
6 Number of Scans	1012
7 Acquisition Date	2012-01-23T13:34:55



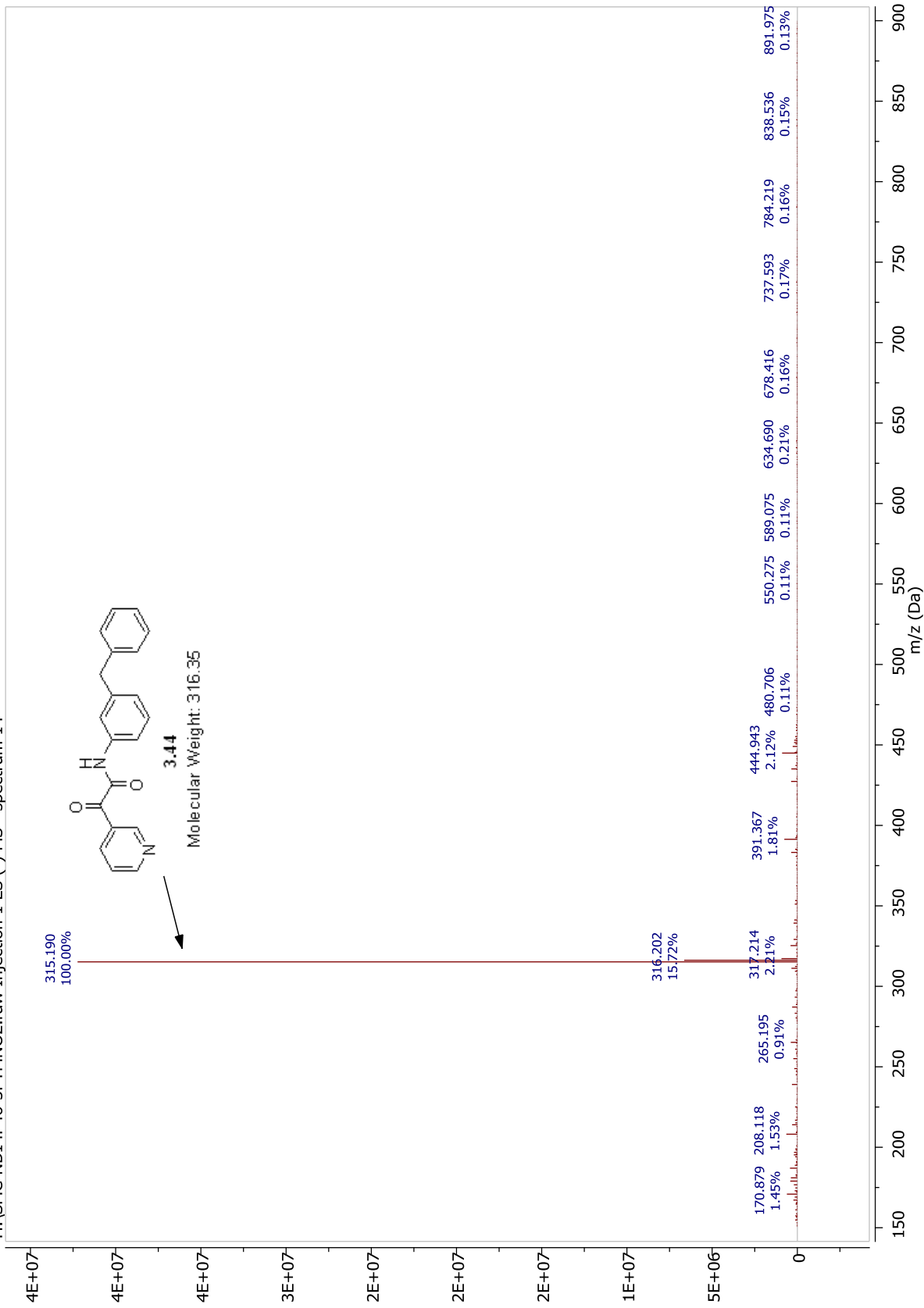
3.43

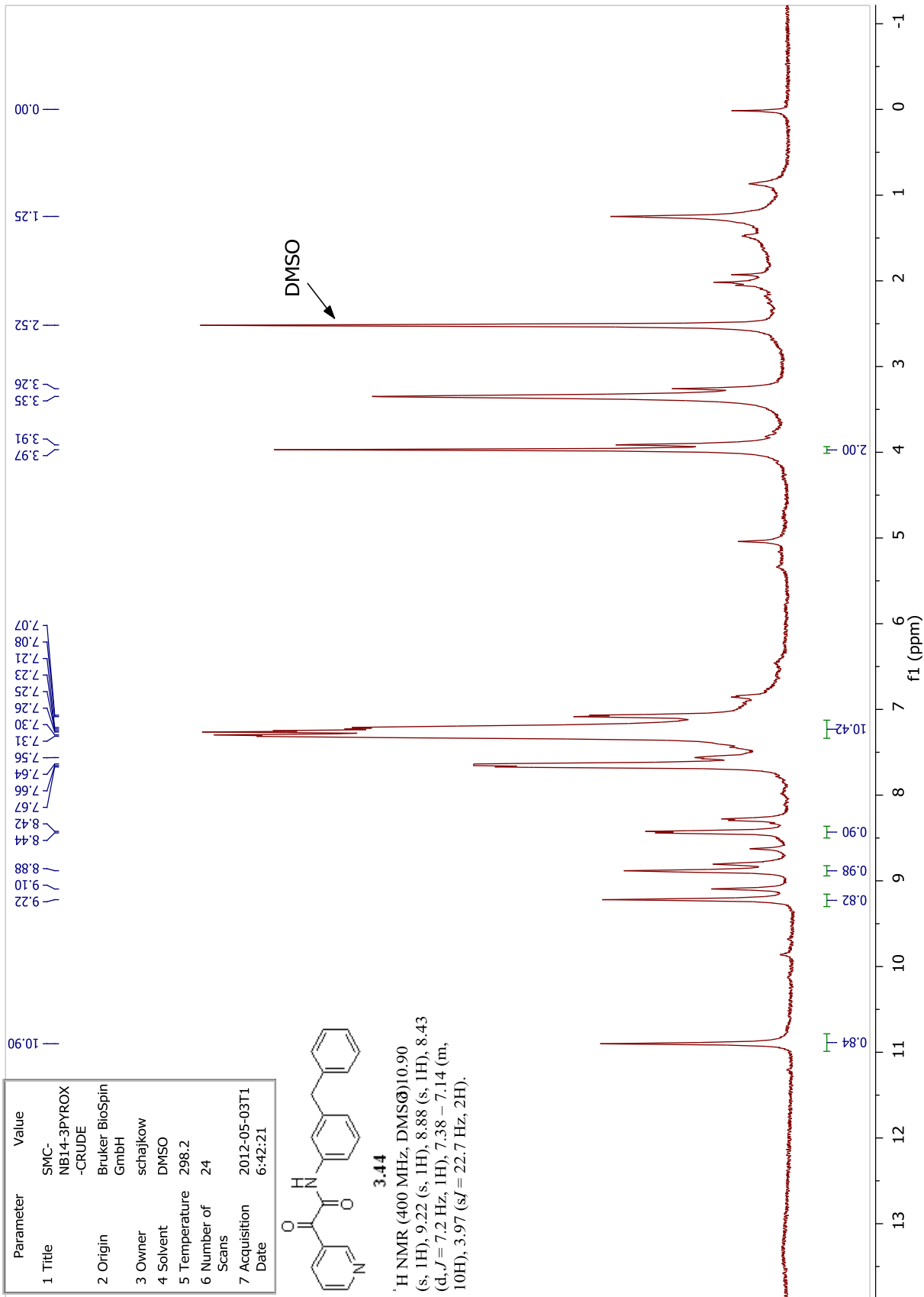
<sup>13</sup>C NMR (101 MHz, CDCl<sub>3</sub>) 169.64, 148.23, 147.15, 142.29, 140.72, 137.16, 136.37, 135.56, 129.19, 128.91, 128.53, 126.22, 125.44, 124.00, 120.25, 117.62, 71.76, 41.86.



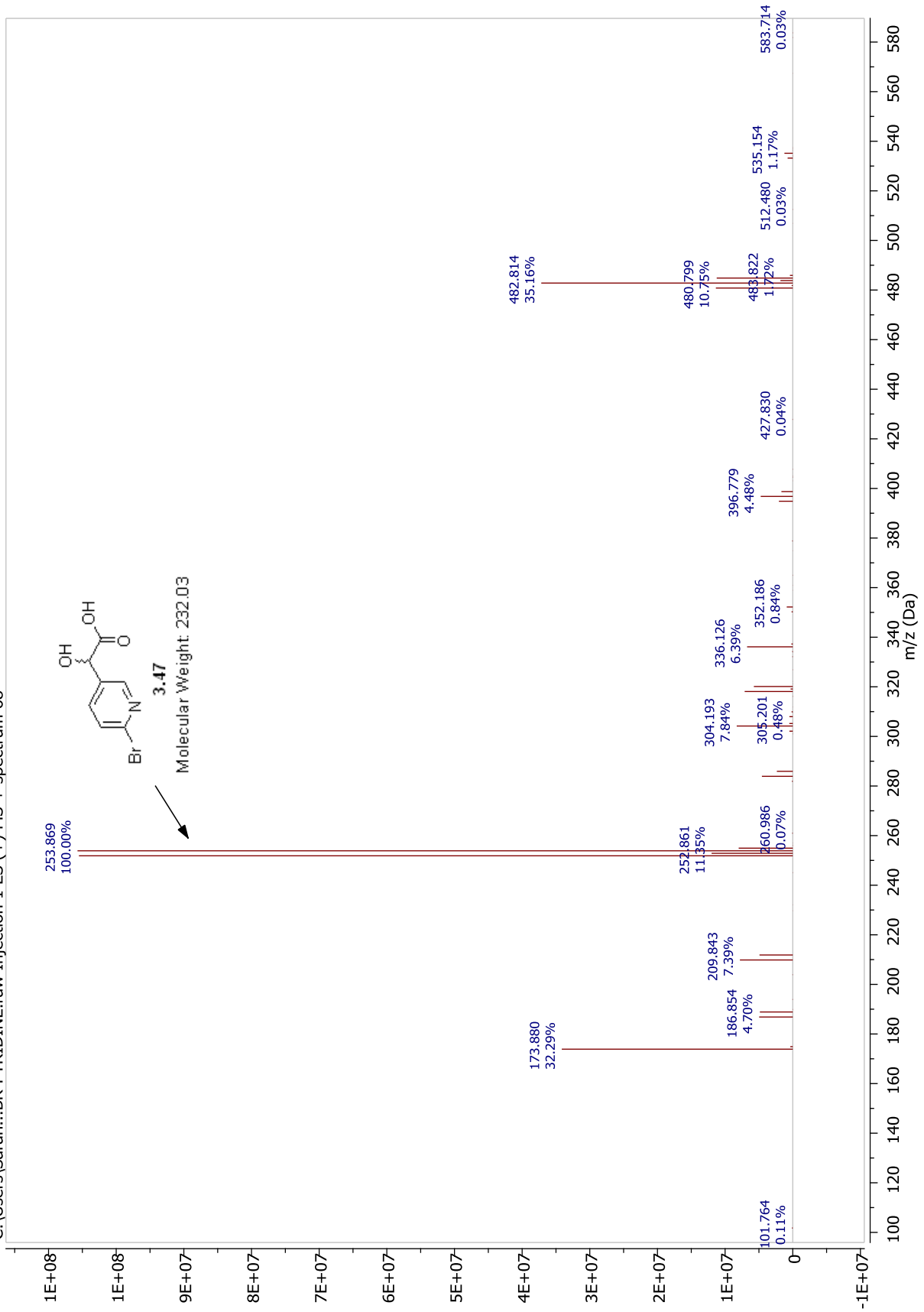


H:\SMC-NB14P46-3PYMNO2.raw Injection 1 ES (-) MS - spectrum 14

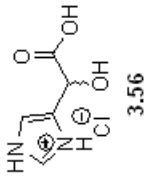




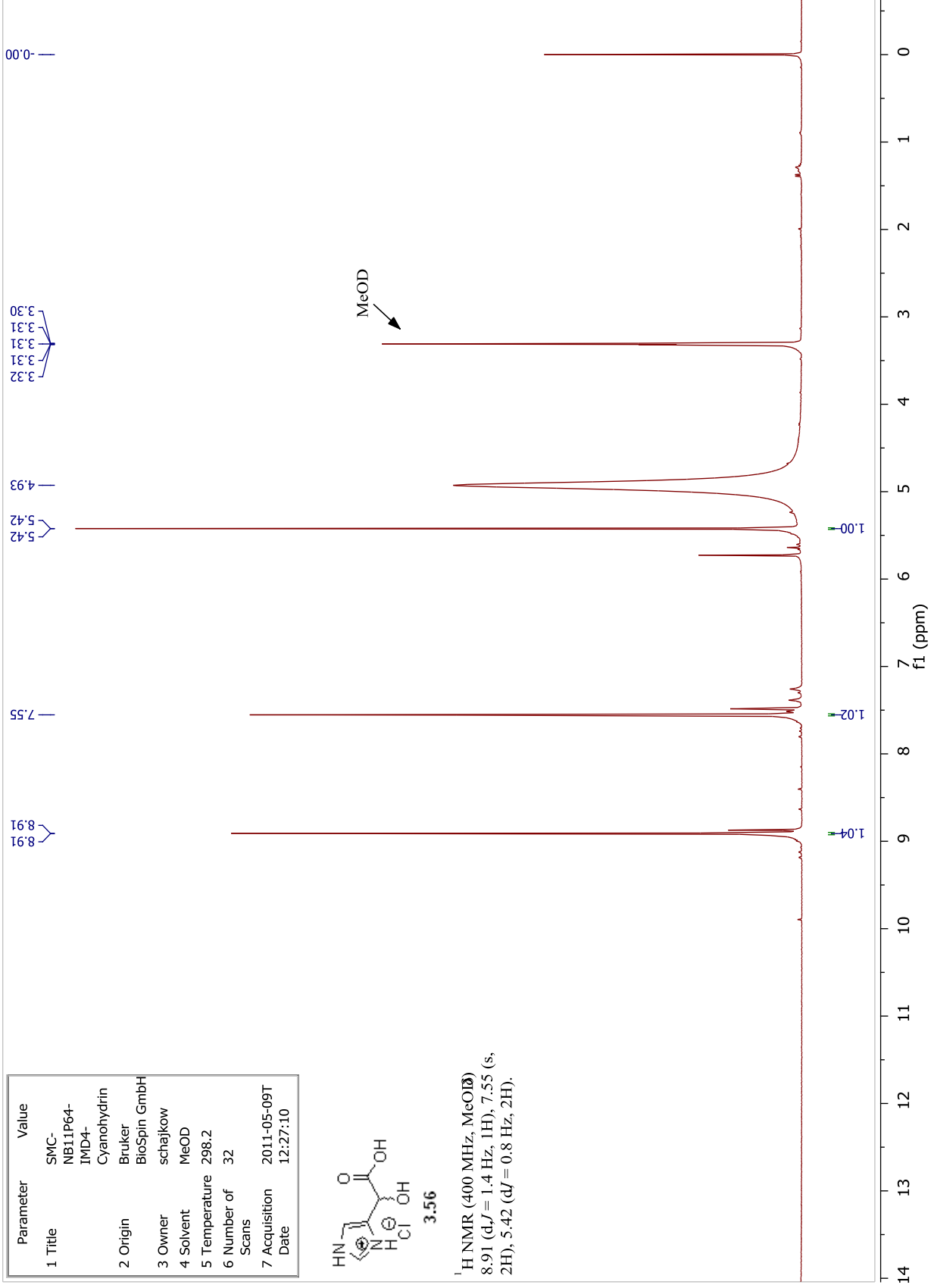
C:\Users\Sarah...\BR-PYRIDINE.raw Injection 1 ES (+) MS + spectrum 68



Parameter	Value
1 Title	SMC-NB11P64-IMD4-Cyanohydrin
2 Origin	Bruker BioSpin GmbH
3 Owner	schajkow
4 Solvent	MeOD
5 Temperature	298.2
6 Number of Scans	32
7 Acquisition Date	2011-05-09T12:27:10

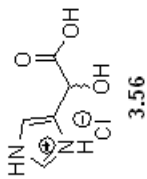


<sup>1</sup>H NMR (400 MHz, MeOD) 8.91 (d, *J* = 1.4 Hz, 1H), 7.55 (s, 2H), 5.42 (d, *J* = 0.8 Hz, 2H).

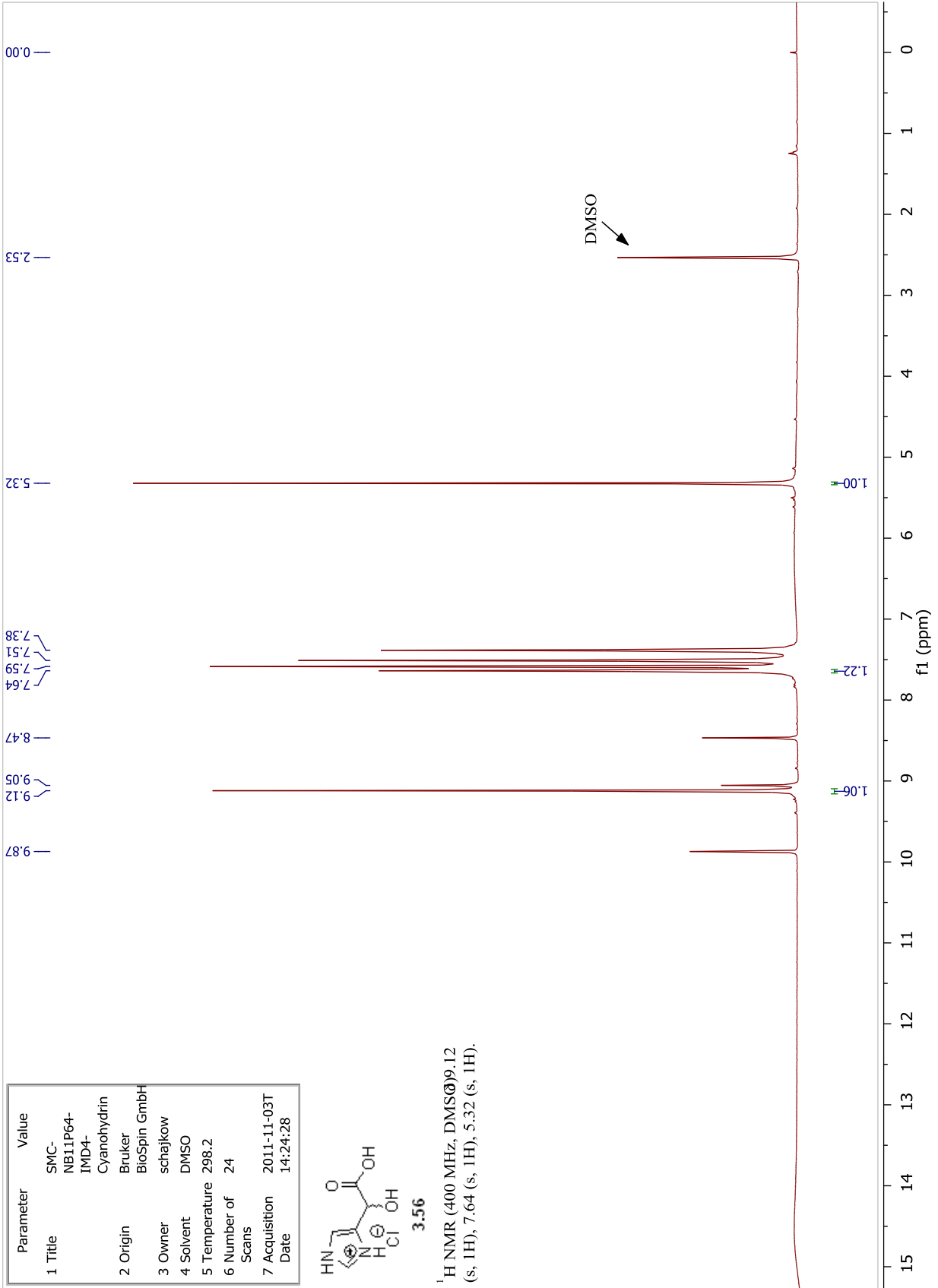




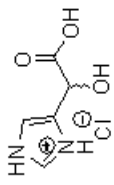
Parameter	Value
1 Title	SMC-NB11P64-IMD4-Cyanohydrin
2 Origin	Bruker BioSpin GmbH
3 Owner	schajkow
4 Solvent	DMSO
5 Temperature	298.2
6 Number of Scans	24
7 Acquisition Date	2011-11-03T14:24:28



<sup>1</sup>H NMR (400 MHz, DMSO-d<sub>6</sub>) 9.12 (s, 1H), 7.64 (s, 1H), 5.32 (s, 1H).

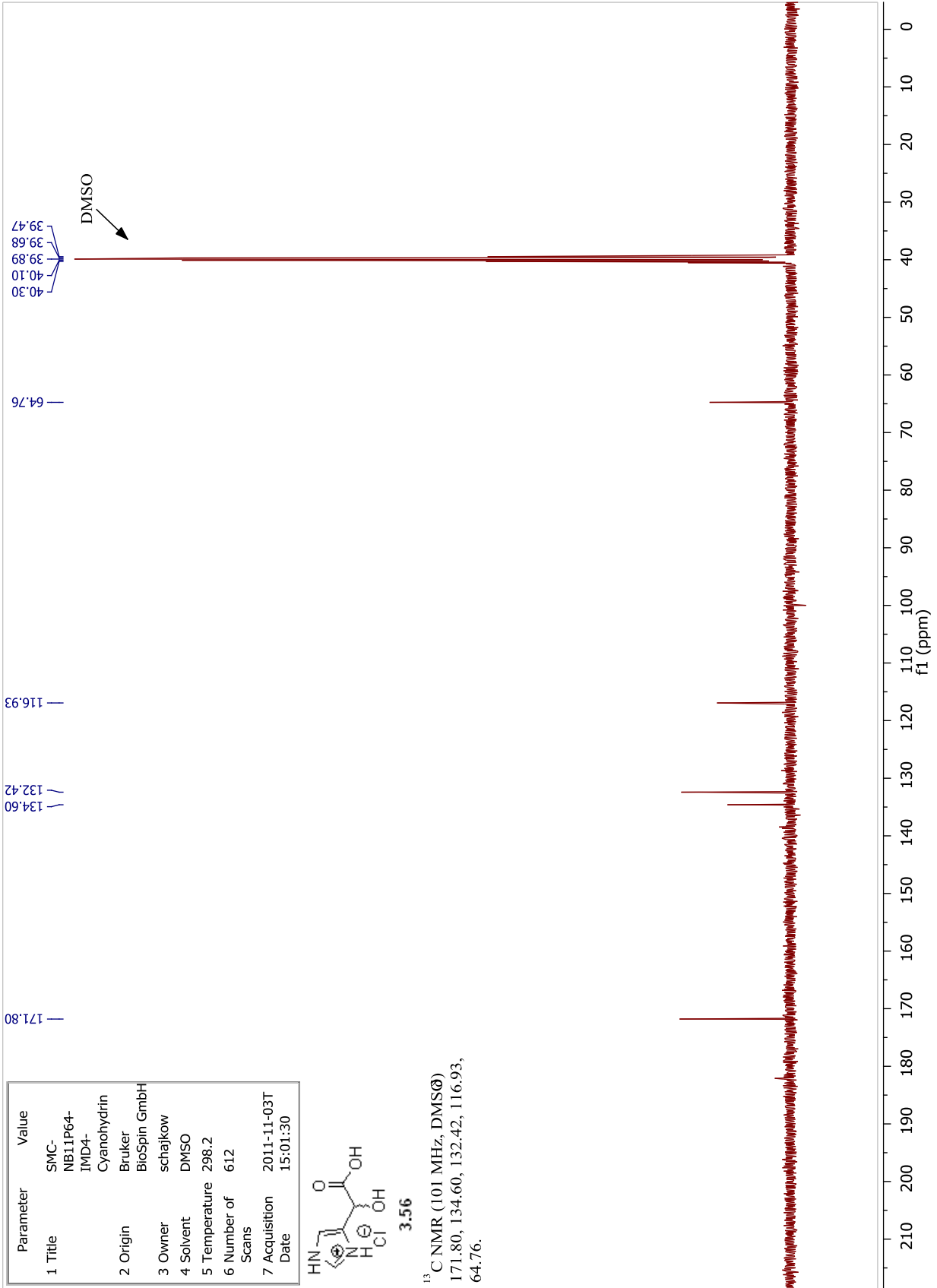


Parameter	Value
1 Title	SMC-NB11P64-IMD4-Cyanohydrin
2 Origin	Bruker BioSpin GmbH
3 Owner	schajkow
4 Solvent	DMSO
5 Temperature	298.2
6 Number of Scans	612
7 Acquisition Date	2011-11-03T15:01:30

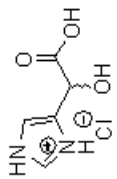


3.56

<sup>13</sup>C NMR (101 MHz, DMSO-d<sub>6</sub>)  
 171.80, 134.60, 132.42, 116.93,  
 64.76.

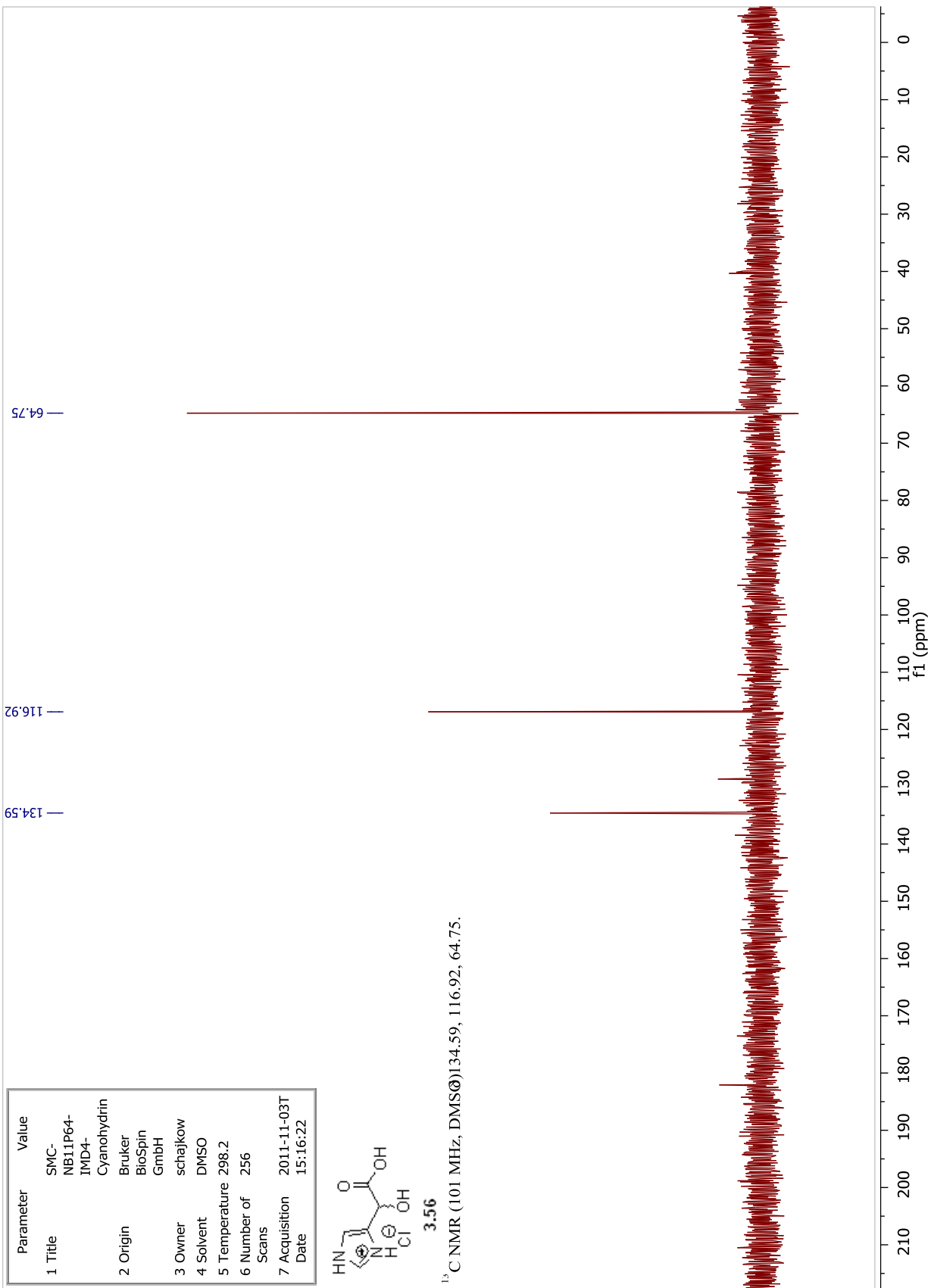


Parameter	Value
1 Title	SMC-NB11P64-IMD4-Cyanohydrin
2 Origin	Bruker BioSpin GmbH
3 Owner	schajkow
4 Solvent	DMSO
5 Temperature	298.2
6 Number of Scans	256
7 Acquisition Date	2011-11-03T15:16:22

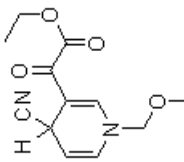


3.56

<sup>13</sup>C NMR (101 MHz, DMSO) 134.59, 116.92, 64.75.

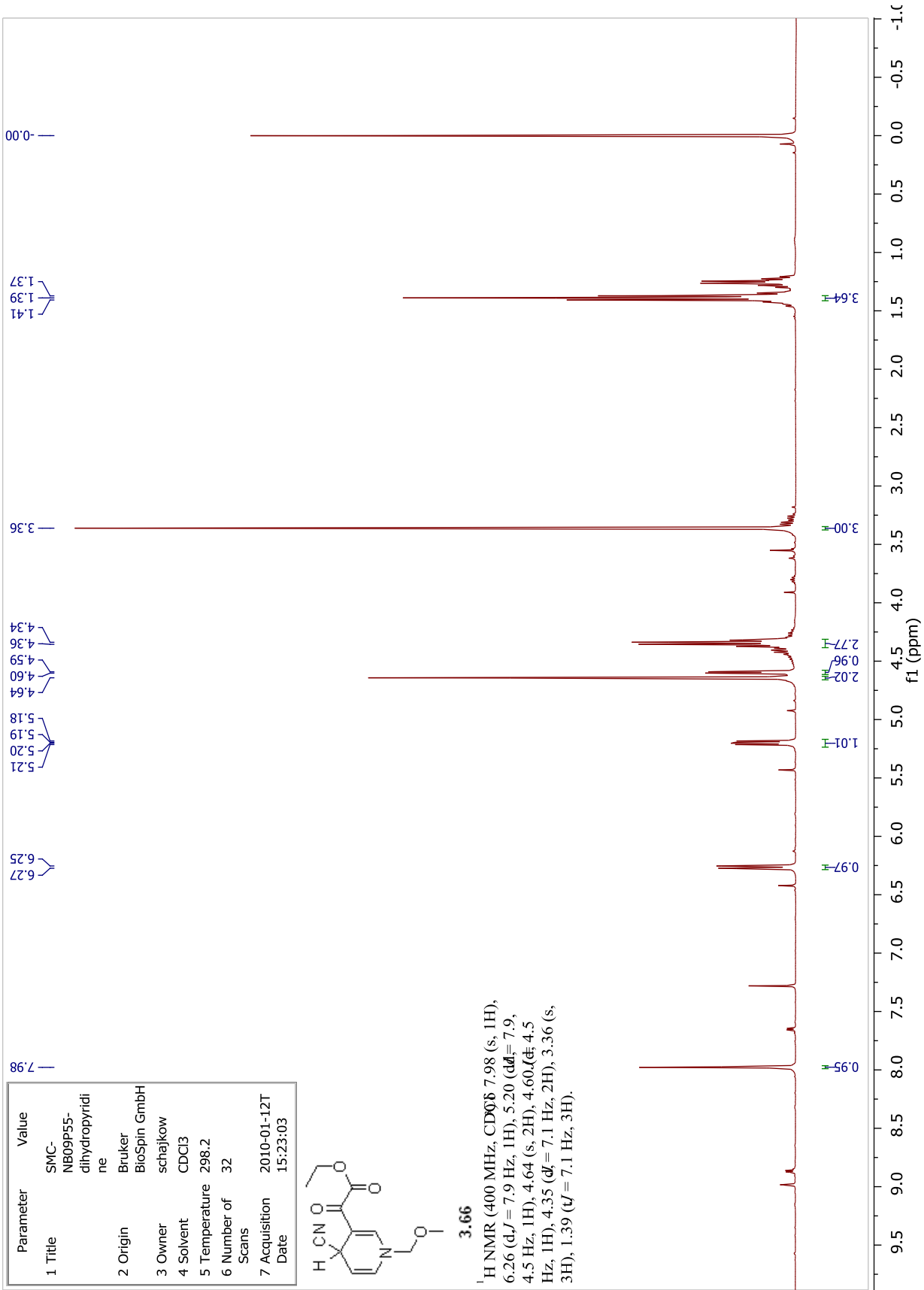


Parameter	Value
1 Title	SMC-NB09P55-dihydropyridine
2 Origin	Bruker Biospin GmbH
3 Owner	schajkow
4 Solvent	CDCl3
5 Temperature	298.2
6 Number of Scans	32
7 Acquisition Date	2010-01-12T15:23:03

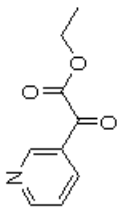


3.66

<sup>1</sup>H NMR (400 MHz, CDCl<sub>3</sub>) δ 7.98 (s, 1H), 6.26 (d, *J* = 7.9 Hz, 1H), 5.20 (dd, *J* = 7.9, 4.5 Hz, 1H), 4.64 (s, 2H), 4.60 (d, *J* = 4.5 Hz, 1H), 4.35 (d, *J* = 7.1 Hz, 2H), 3.36 (s, 3H), 1.39 (t, *J* = 7.1 Hz, 3H).

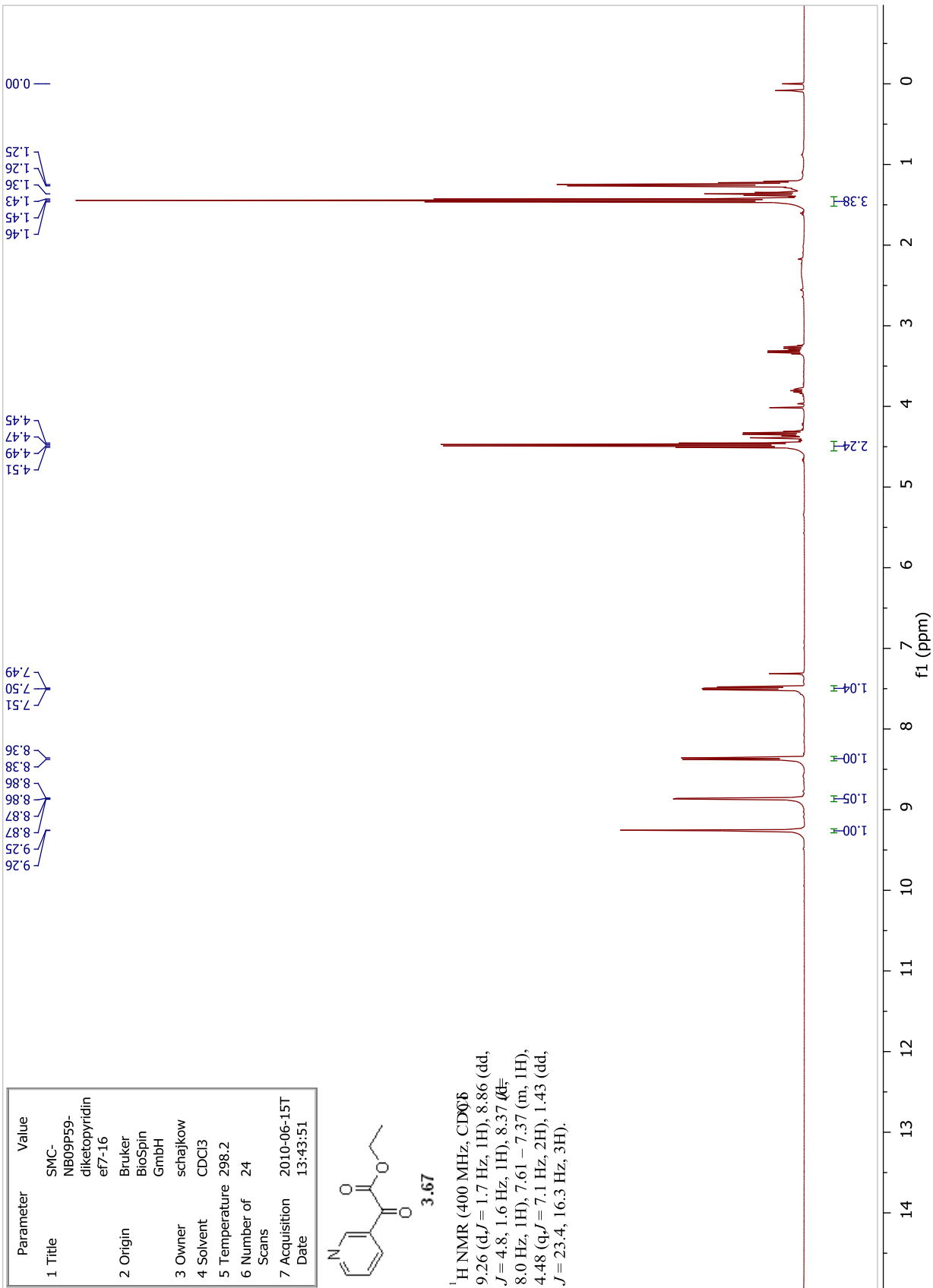


Parameter	Value
1 Title	SMC-NB09P59-diketopyridin eF7-16
2 Origin	Bruker BioSpin GmbH
3 Owner	schajkow
4 Solvent	CDCl3
5 Temperature	298.2
6 Number of Scans	24
7 Acquisition Date	2010-06-15T13:43:51

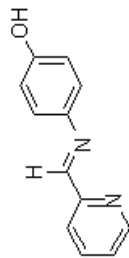


3.67

<sup>1</sup>H NMR (400 MHz, CDCl<sub>3</sub>)  
 9.26 (d, *J* = 1.7 Hz, 1H), 8.86 (dd, *J* = 4.8, 1.6 Hz, 1H), 8.37 (t, 8.0 Hz, 1H), 7.61 – 7.37 (m, 1H), 4.48 (q, *J* = 7.1 Hz, 2H), 1.43 (dd, *J* = 23.4, 16.3 Hz, 3H).

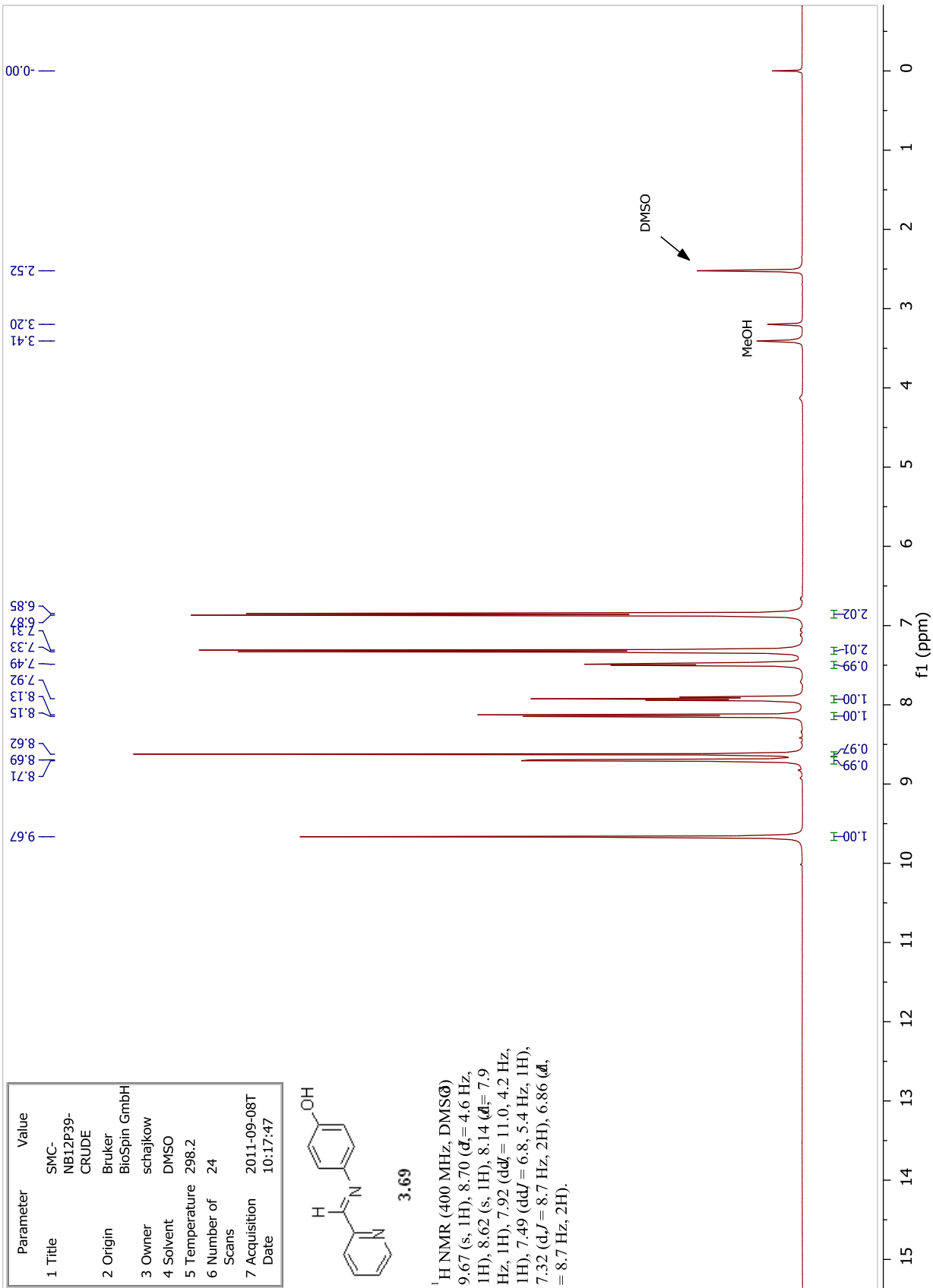


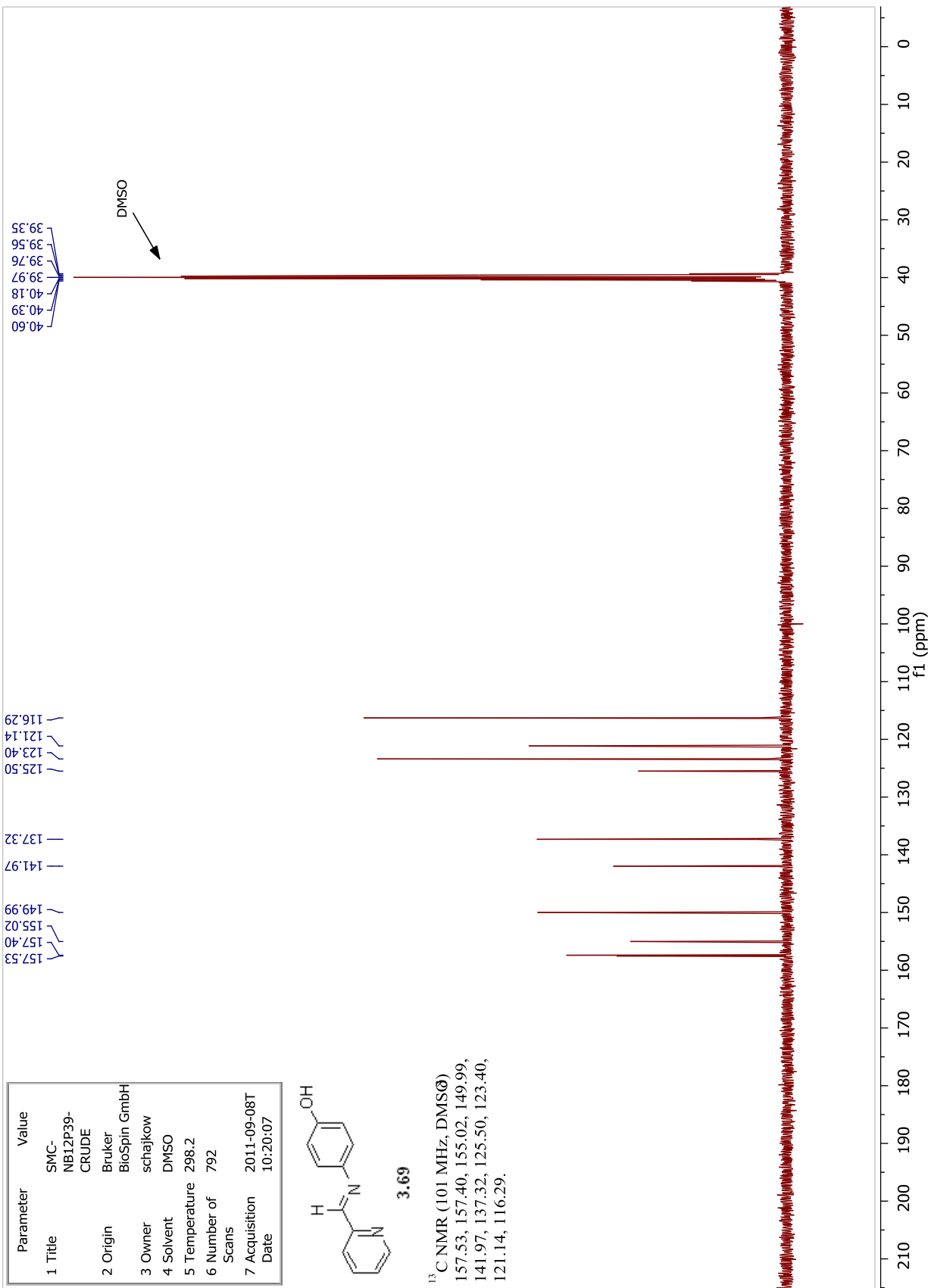
Parameter	Value
1 Title	SMC-NB12P39-CRUDE
2 Origin	Bruker BioSpin GmbH
3 Owner	schajkow
4 Solvent	DMSO
5 Temperature	298.2
6 Number of Scans	24
7 Acquisition Date	2011-09-08T10:17:47



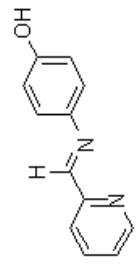
3.69

<sup>1</sup>H NMR (400 MHz, DMSO-d<sub>6</sub>)  
 9.67 (s, 1H), 8.70 (d, *d*<sub>H</sub> = 4.6 Hz, 1H), 8.62 (s, 1H), 8.14 (d, *d*<sub>H</sub> = 7.9 Hz, 1H), 7.92 (dd, *d*<sub>H</sub> = 11.0, 4.2 Hz, 1H), 7.49 (dd, *d*<sub>H</sub> = 6.8, 5.4 Hz, 1H), 7.32 (d, *d*<sub>H</sub> = 8.7 Hz, 2H), 6.86 (d, *d*<sub>H</sub> = 8.7 Hz, 2H).



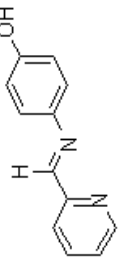


Parameter	Value
1 Title	SMC-NB12P39-CRUDE
2 Origin	Bruker BioSpin GmbH
3 Owner	schajkow
4 Solvent	DMSO
5 Temperature	298.2
6 Number of Scans	792
7 Acquisition Date	2011-09-08T10:20:07



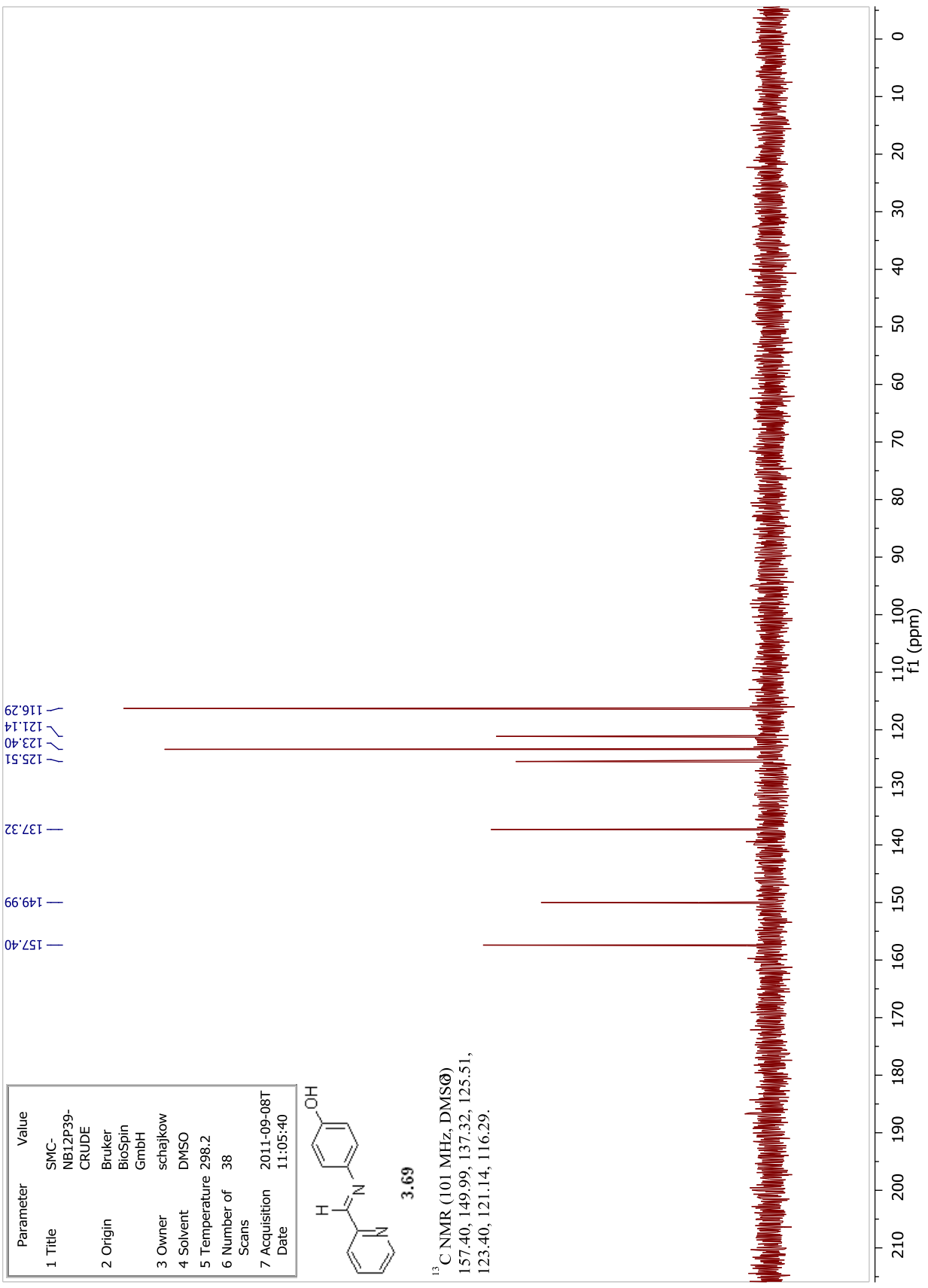
13C NMR (101 MHz, DMSO)  
 157.53, 157.40, 155.02, 149.99,  
 141.97, 137.32, 125.50, 123.40,  
 121.14, 116.29.

Parameter	Value
1 Title	SMC-NB12P39-CRUDE
2 Origin	Bruker BioSpin GmbH
3 Owner	schajkow
4 Solvent	DMSO
5 Temperature	298.2
6 Number of Scans	38
7 Acquisition Date	2011-09-08T11:05:40



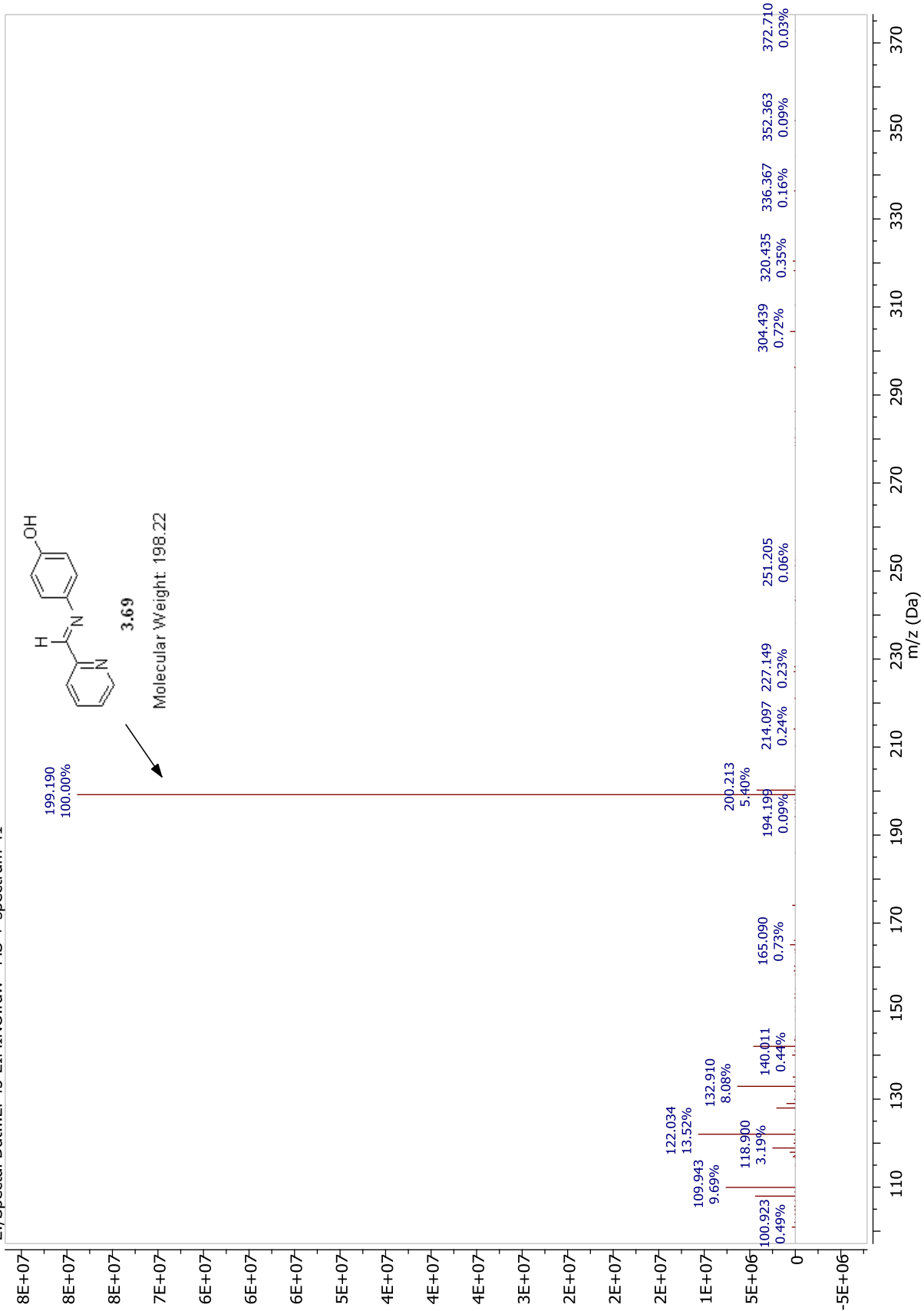
**3.69**

<sup>13</sup>C NMR (101 MHz, DMSO-*d*<sub>6</sub>)  
 157.40, 149.99, 137.32, 125.51,  
 123.40, 121.14, 116.29.

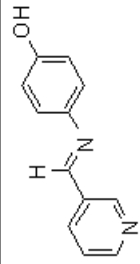




E:/Spectral Dat...2P45-2IMINO.raw MS + spectrum 41

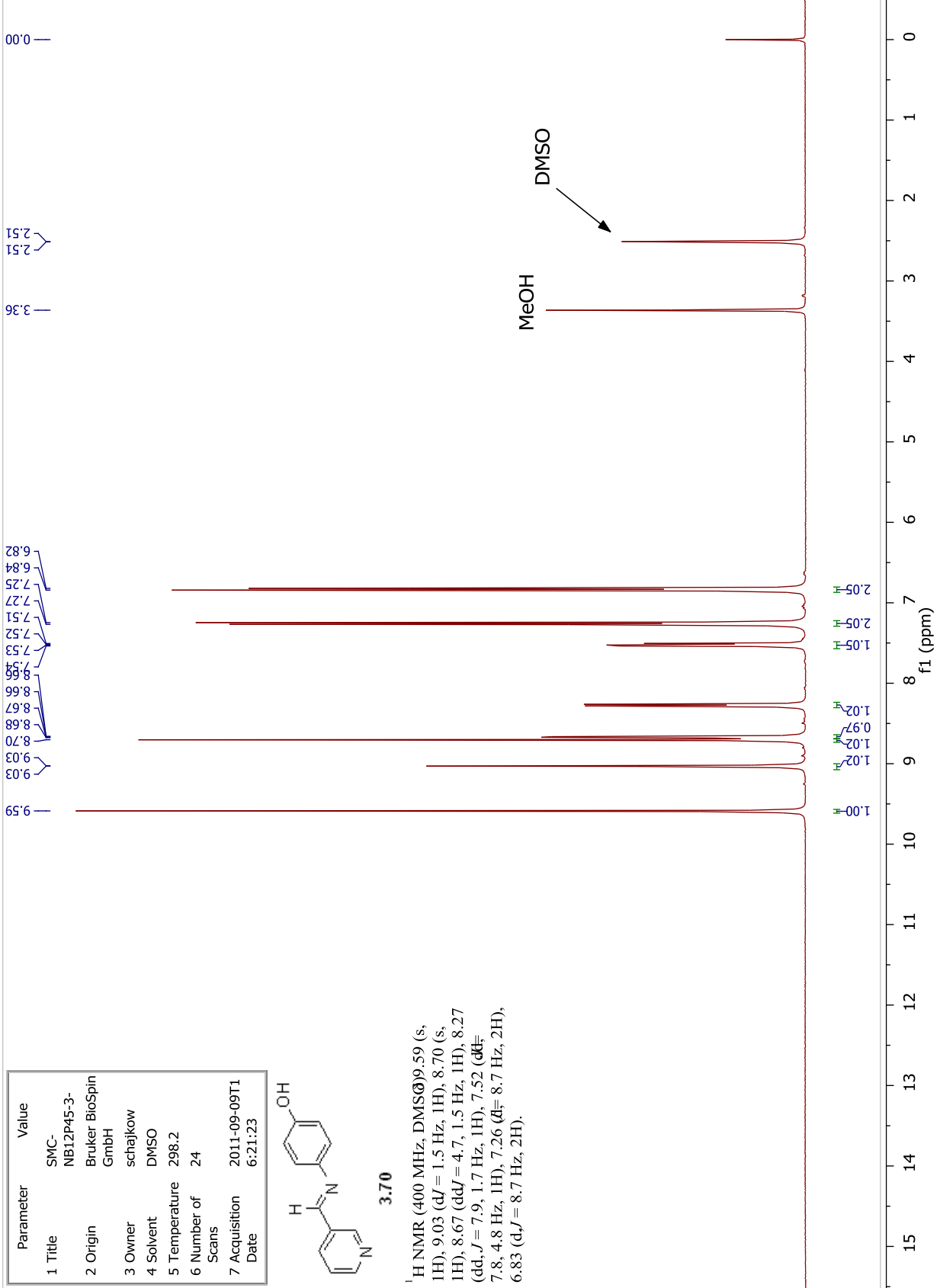


Parameter	Value
1 Title	SMC-NB12P45-3-
2 Origin	Bruker BioSpin GmbH
3 Owner	schajkowi
4 Solvent	DMSO
5 Temperature	298.2
6 Number of Scans	24
7 Acquisition Date	2011-09-09T16:21:23

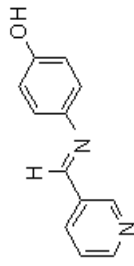


**3.70**

<sup>1</sup>H NMR (400 MHz, DMSO-d<sub>6</sub>) 9.59 (s, 1H), 9.03 (d, J = 1.5 Hz, 1H), 8.70 (s, 1H), 8.67 (dd, J = 4.7, 1.5 Hz, 1H), 8.27 (dd, J = 7.9, 1.7 Hz, 1H), 7.52 (dd, J = 7.8, 4.8 Hz, 1H), 7.26 (d, J = 8.7 Hz, 2H), 6.83 (d, J = 8.7 Hz, 2H).

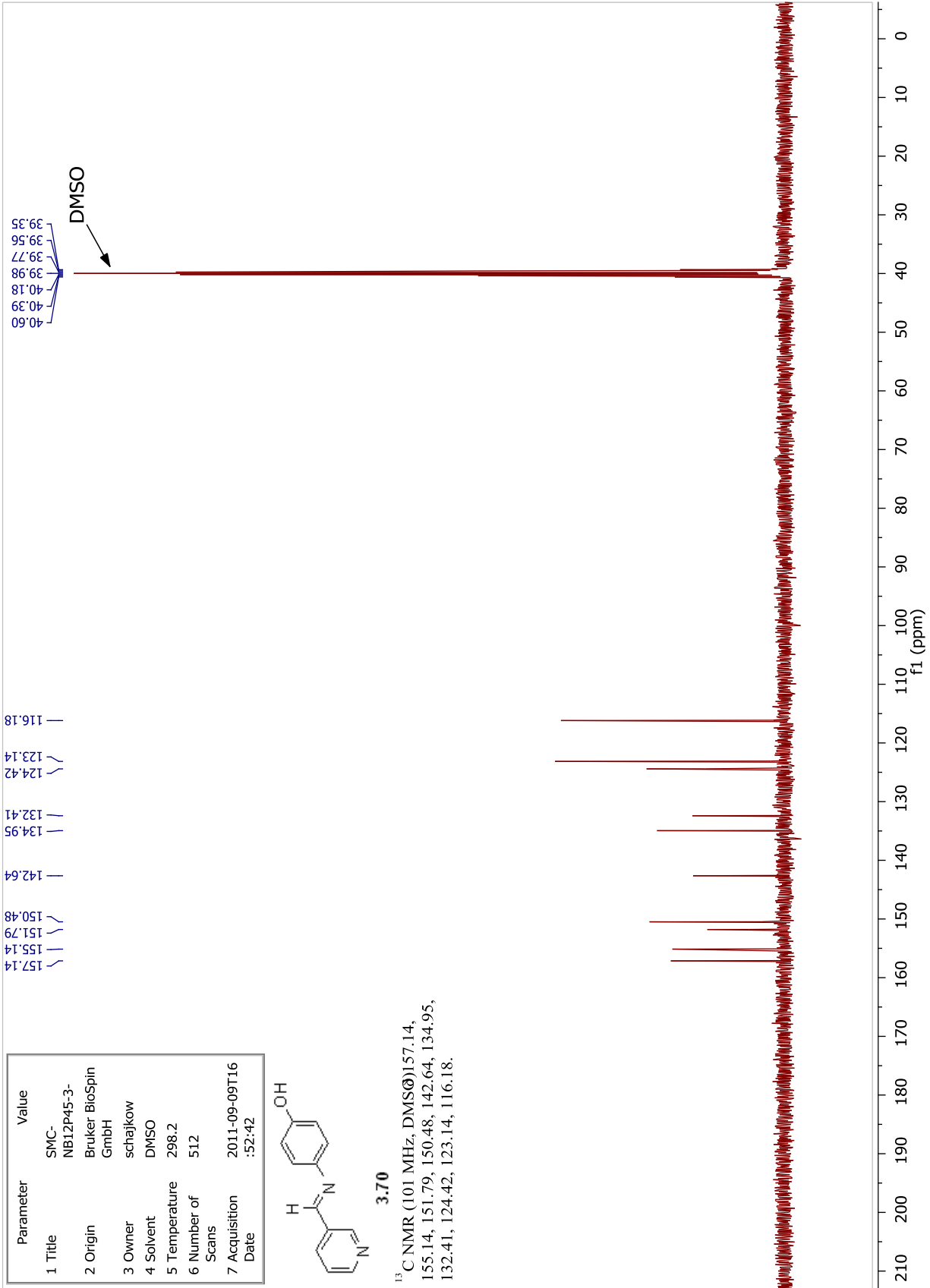


Parameter	Value
1 Title	SMC-NB12P45-3-
2 Origin	Bruker BioSpin GmbH
3 Owner	schajkow
4 Solvent	DMSO
5 Temperature	298.2
6 Number of Scans	512
7 Acquisition Date	2011-09-09T16:52:42

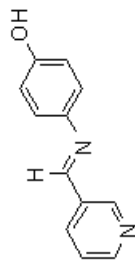


**3.70**

<sup>13</sup>C NMR (101 MHz, DMSO) 157.14, 155.14, 151.79, 150.48, 142.64, 134.95, 132.41, 124.42, 123.14, 116.18.

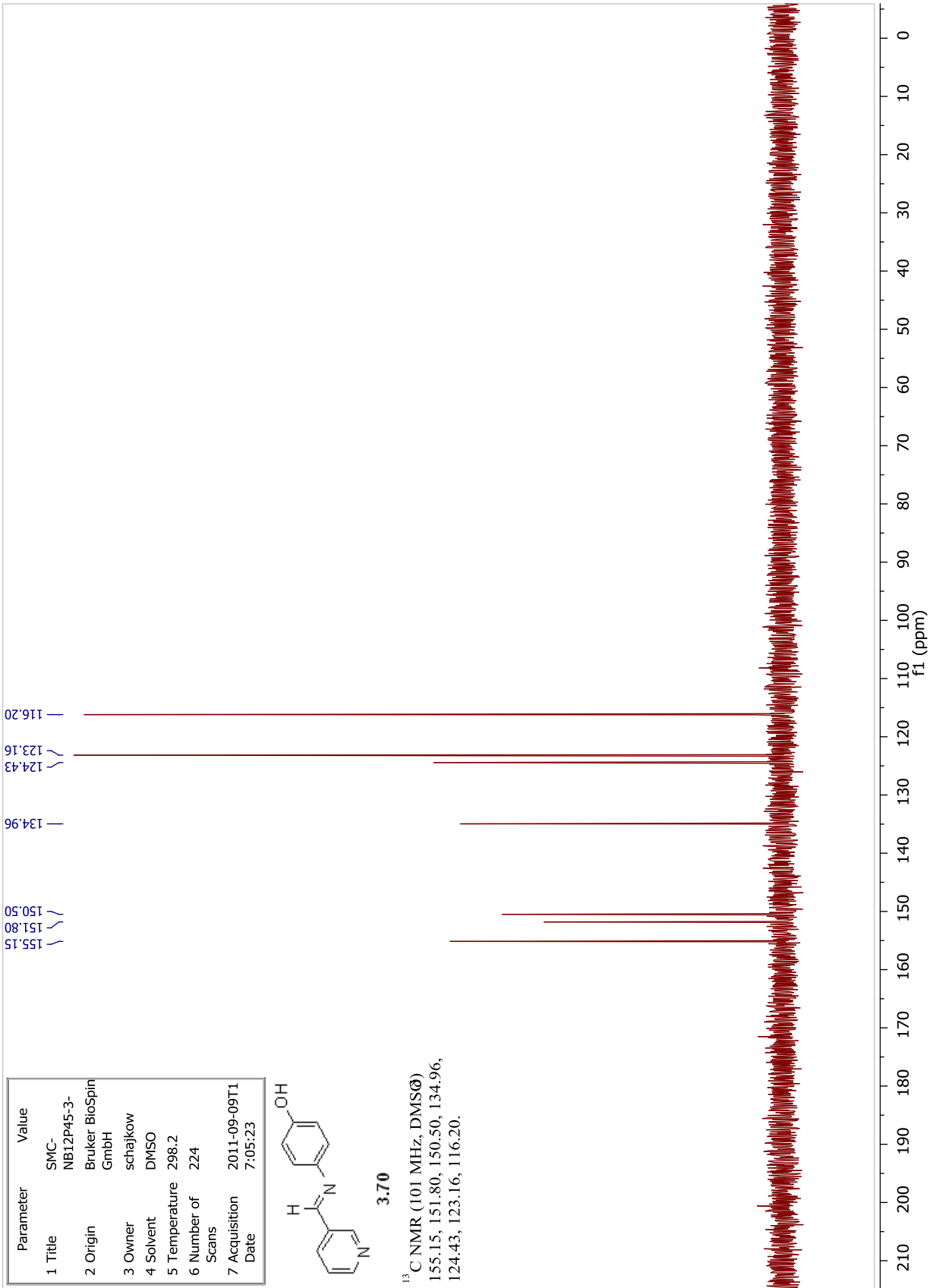


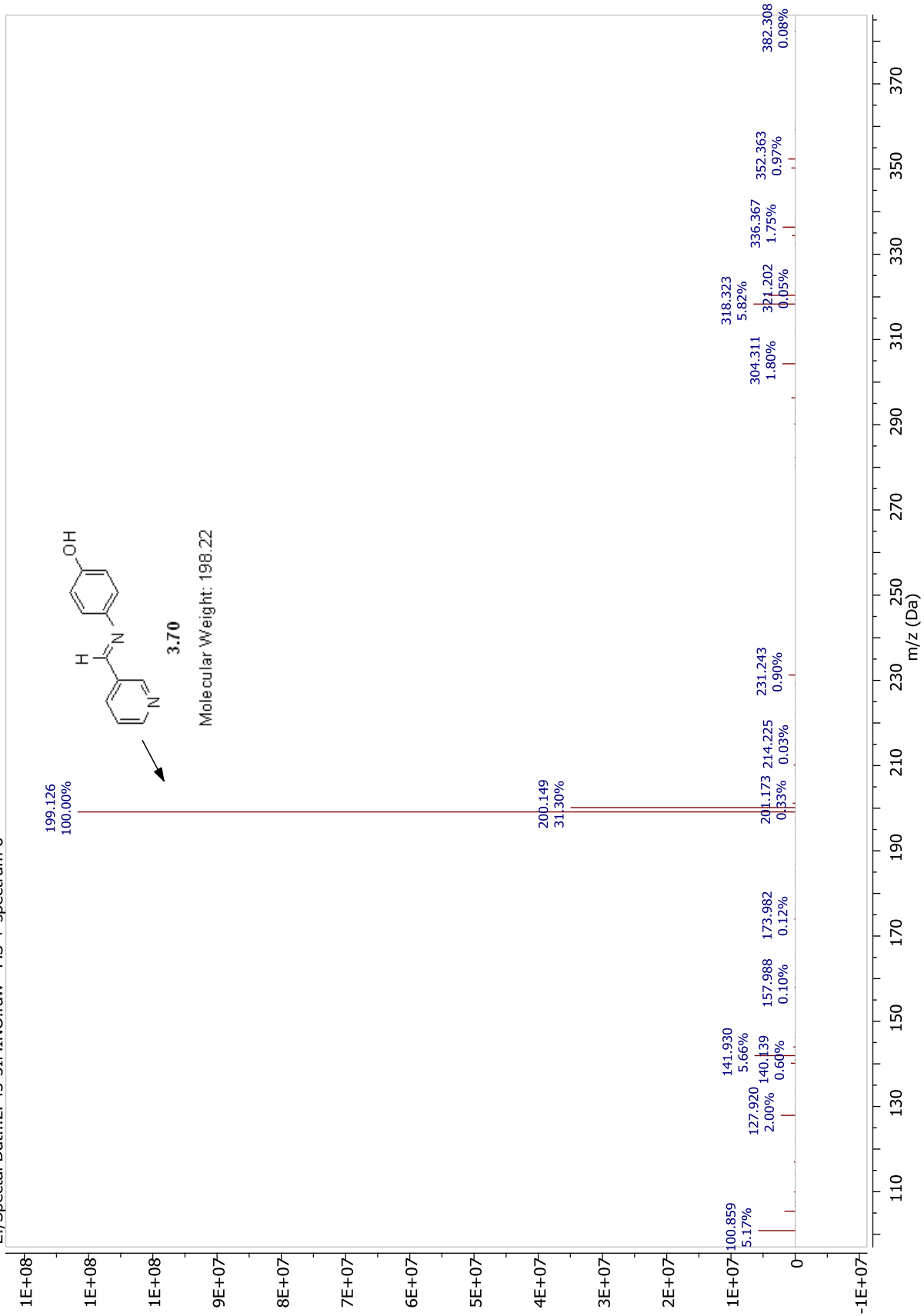
Parameter	Value
1 Title	SMC-NB12P45-3-
2 Origin	Bruker BioSpin GmbH
3 Owner	schajkow
4 Solvent	DMSO
5 Temperature	298.2
6 Number of Scans	224
7 Acquisition Date	2011-09-09T17:05:23



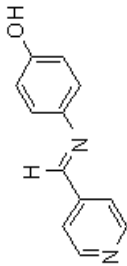
**3.70**

<sup>13</sup>C NMR (101 MHz, DMSO)  
 155.15, 151.80, 150.50, 134.96,  
 124.43, 123.16, 116.20.



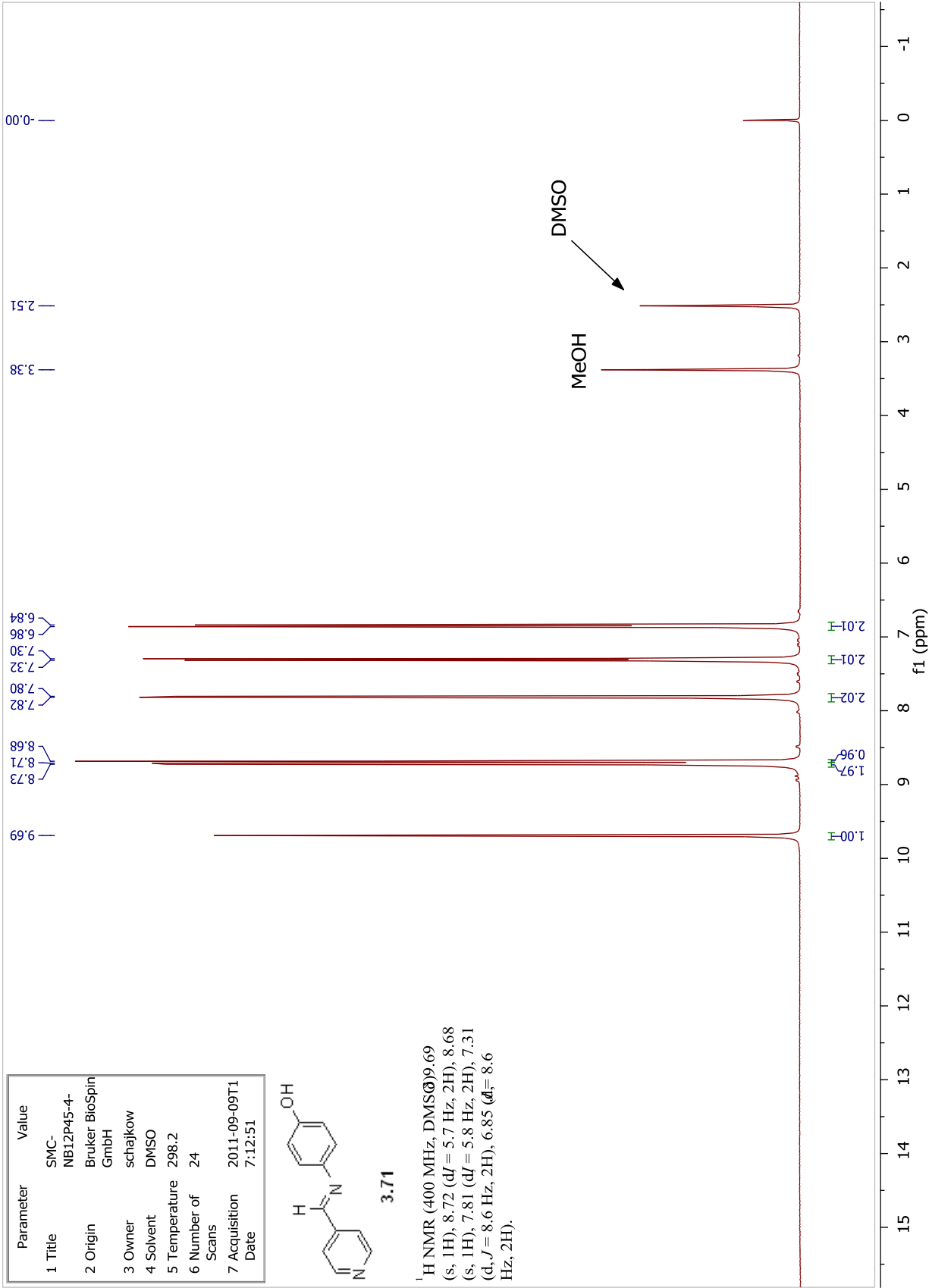


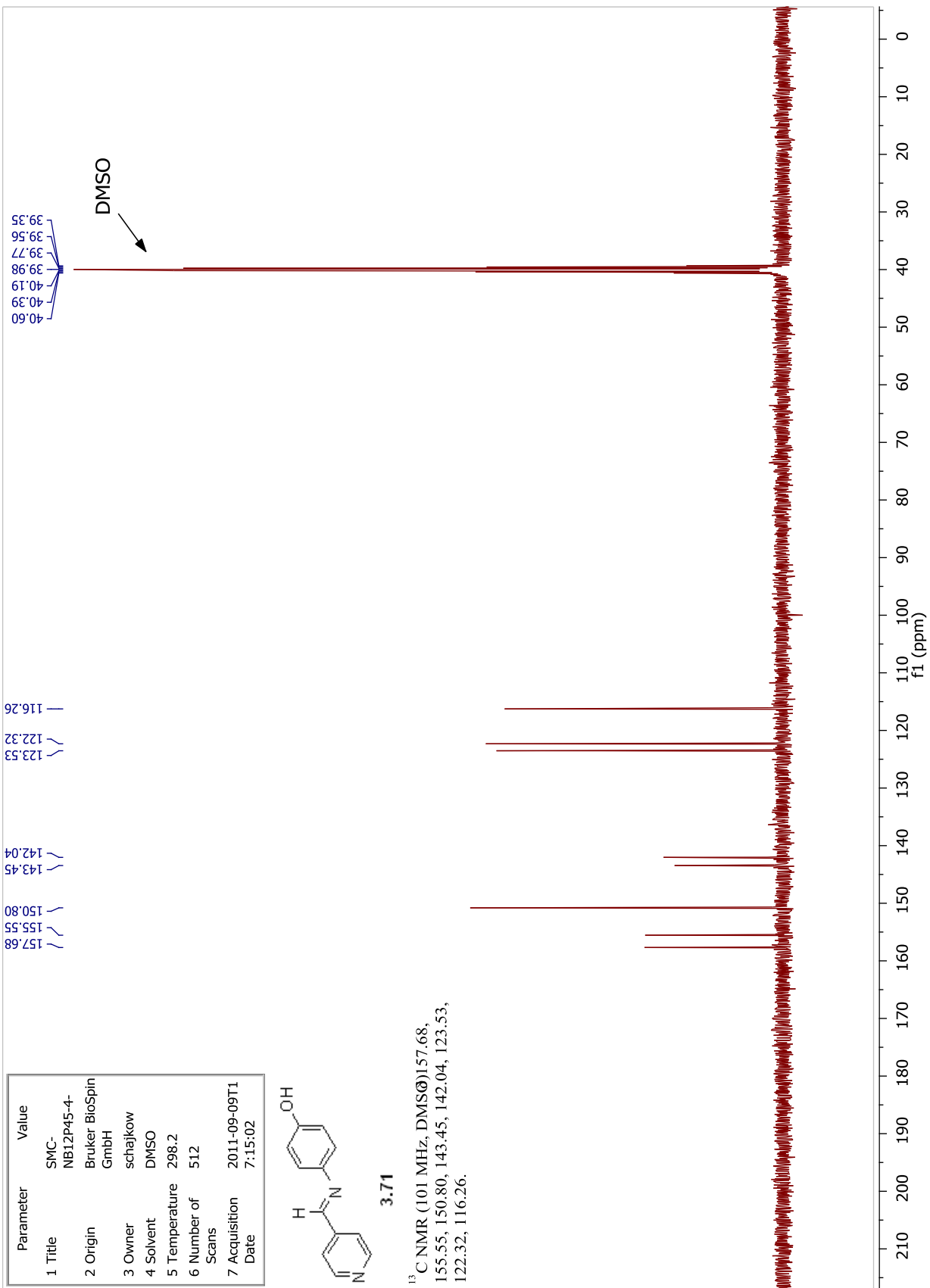
Parameter	Value
1 Title	SMC-NB12P45-4-
2 Origin	Bruker BioSpin GmbH
3 Owner	schajkow
4 Solvent	DMSO
5 Temperature	298.2
6 Number of Scans	24
7 Acquisition Date	2011-09-09T17:12:51



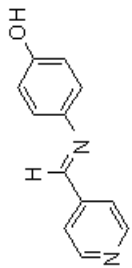
3.71

<sup>1</sup>H NMR (400 MHz, DMSO-d<sub>6</sub>) 9.69 (s, 1H), 8.72 (d, J = 5.7 Hz, 2H), 8.68 (s, 1H), 7.81 (d, J = 5.8 Hz, 2H), 7.31 (d, J = 8.6 Hz, 2H), 6.85 (d, J = 8.6 Hz, 2H).



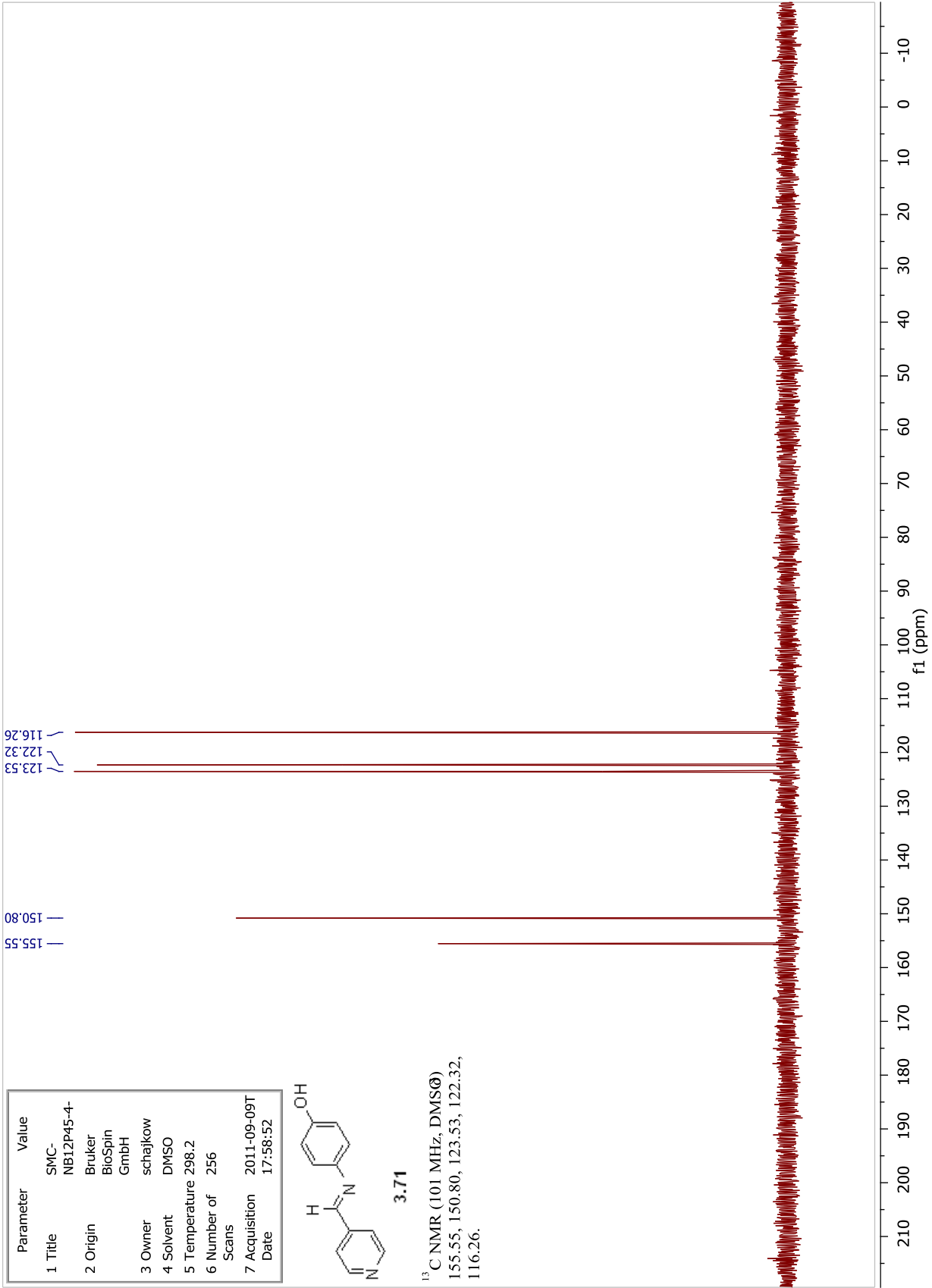


Parameter	Value
1 Title	SMC-NB12P45-4
2 Origin	Bruker BioSpin GmbH
3 Owner	schajkowi
4 Solvent	DMSO
5 Temperature	298.2
6 Number of Scans	256
7 Acquisition Date	2011-09-09T17:58:52

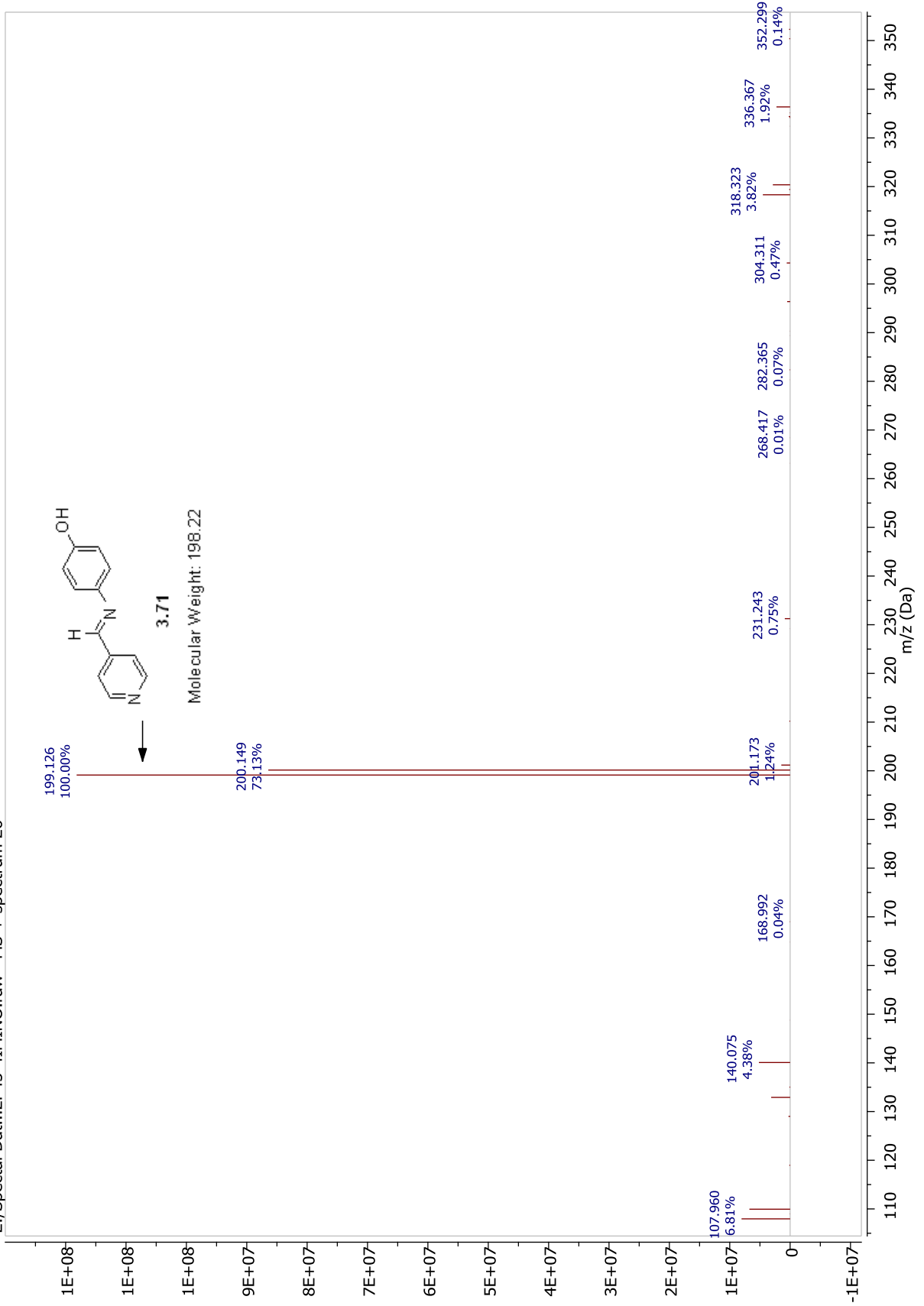


3.71

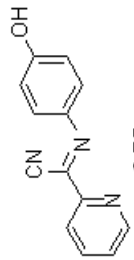
<sup>13</sup>C NMR (101 MHz, DMSO-d<sub>6</sub>)  
155.55, 150.80, 123.53, 122.32, 116.26.



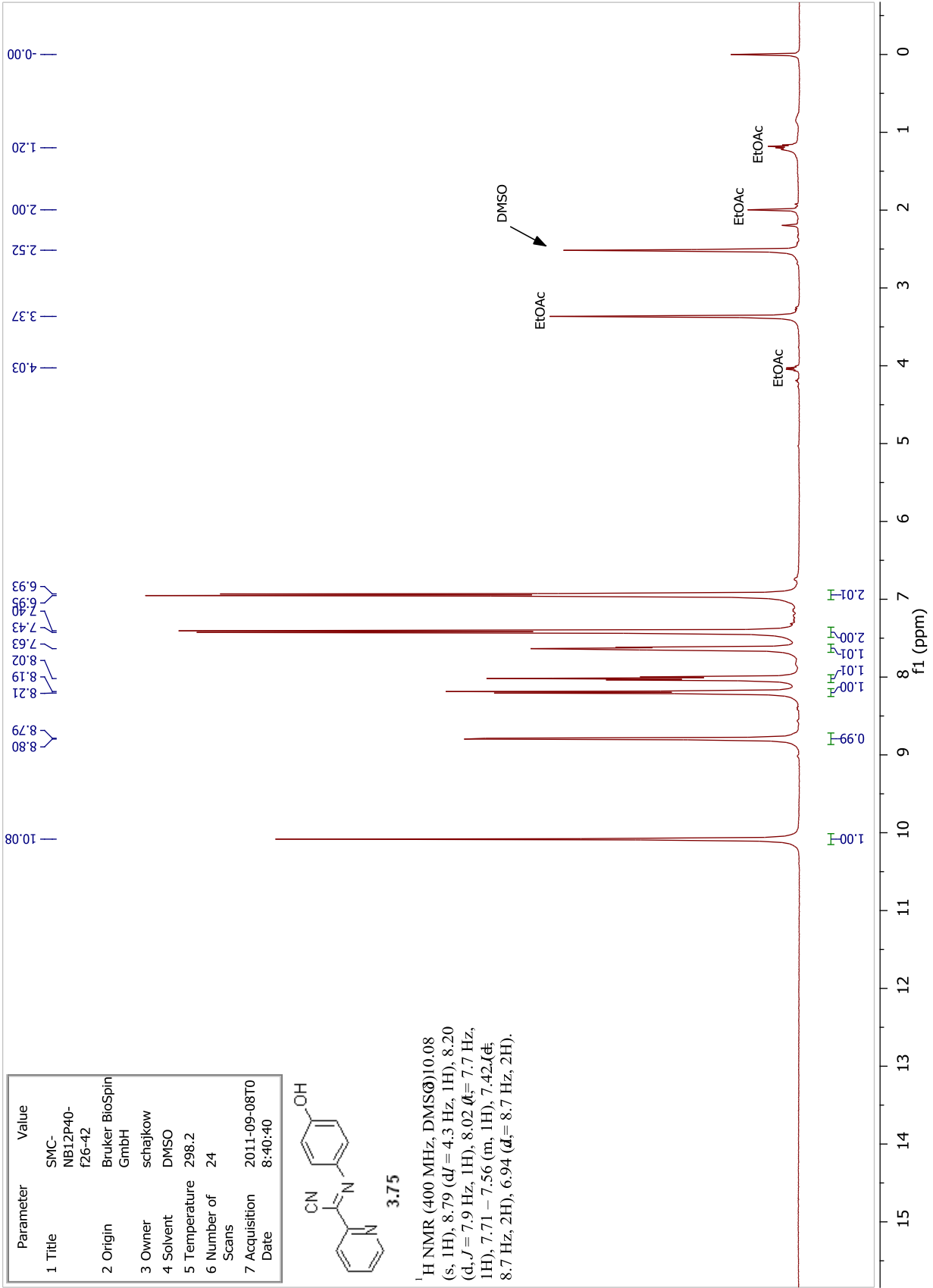


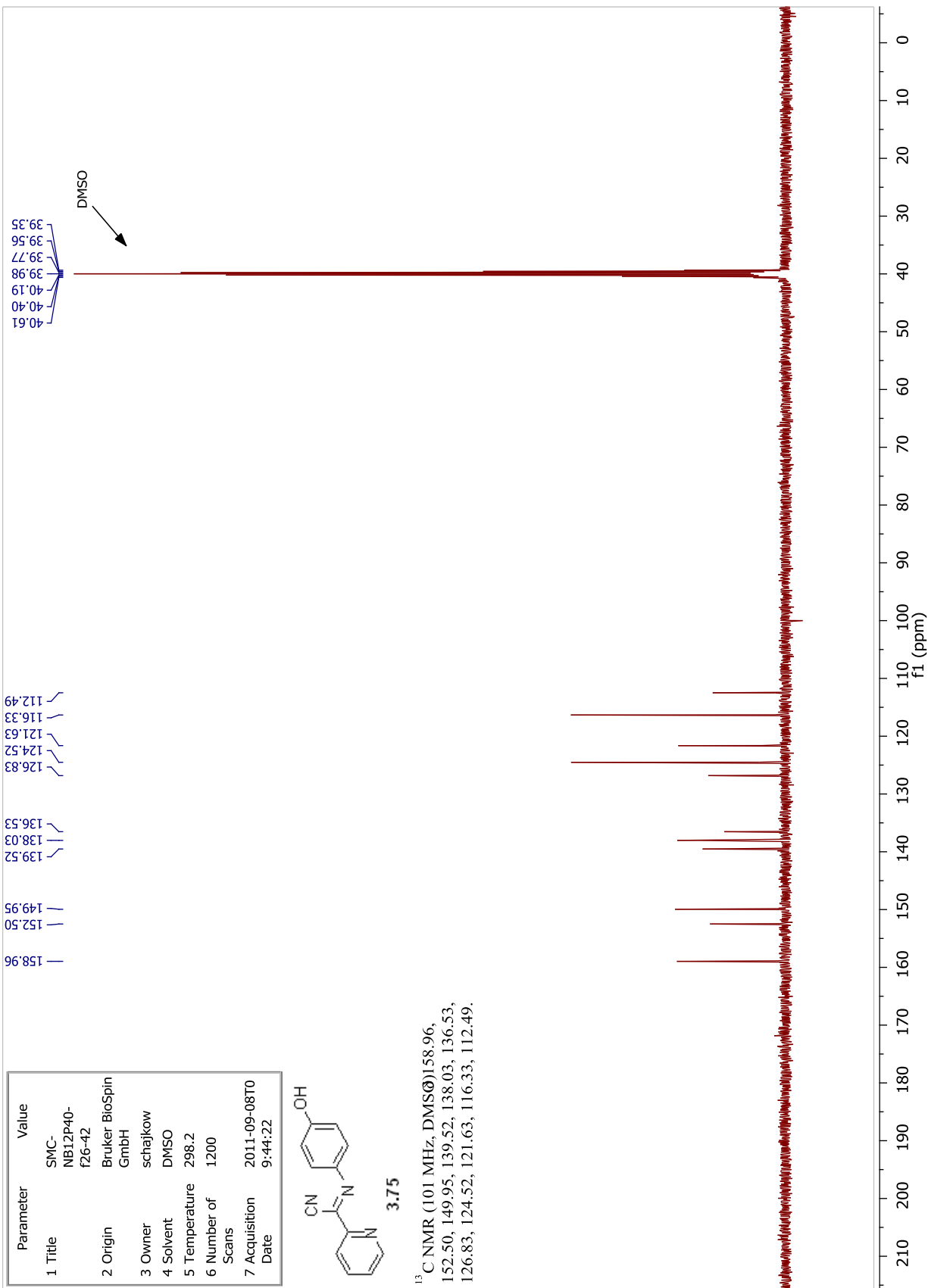


Parameter	Value
1 Title	SMC-NB12P40-f26-42
2 Origin	Bruker BioSpin GmbH
3 Owner	schajkow
4 Solvent	DMSO
5 Temperature	298.2
6 Number of Scans	24
7 Acquisition Date	2011-09-08T08:40:40

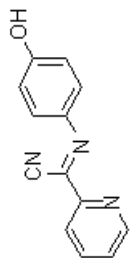


<sup>1</sup>H NMR (400 MHz, DMSO-d<sub>6</sub>) 10.08 (s, 1H), 8.79 (d, *d*<sub>J</sub> = 4.3 Hz, 1H), 8.20 (d, *J* = 7.9 Hz, 1H), 8.02 (t, *t*<sub>J</sub> = 7.7 Hz, 1H), 7.71 – 7.56 (m, 1H), 7.42 (d, 8.7 Hz, 2H), 6.94 (d, *d*<sub>J</sub> = 8.7 Hz, 2H).

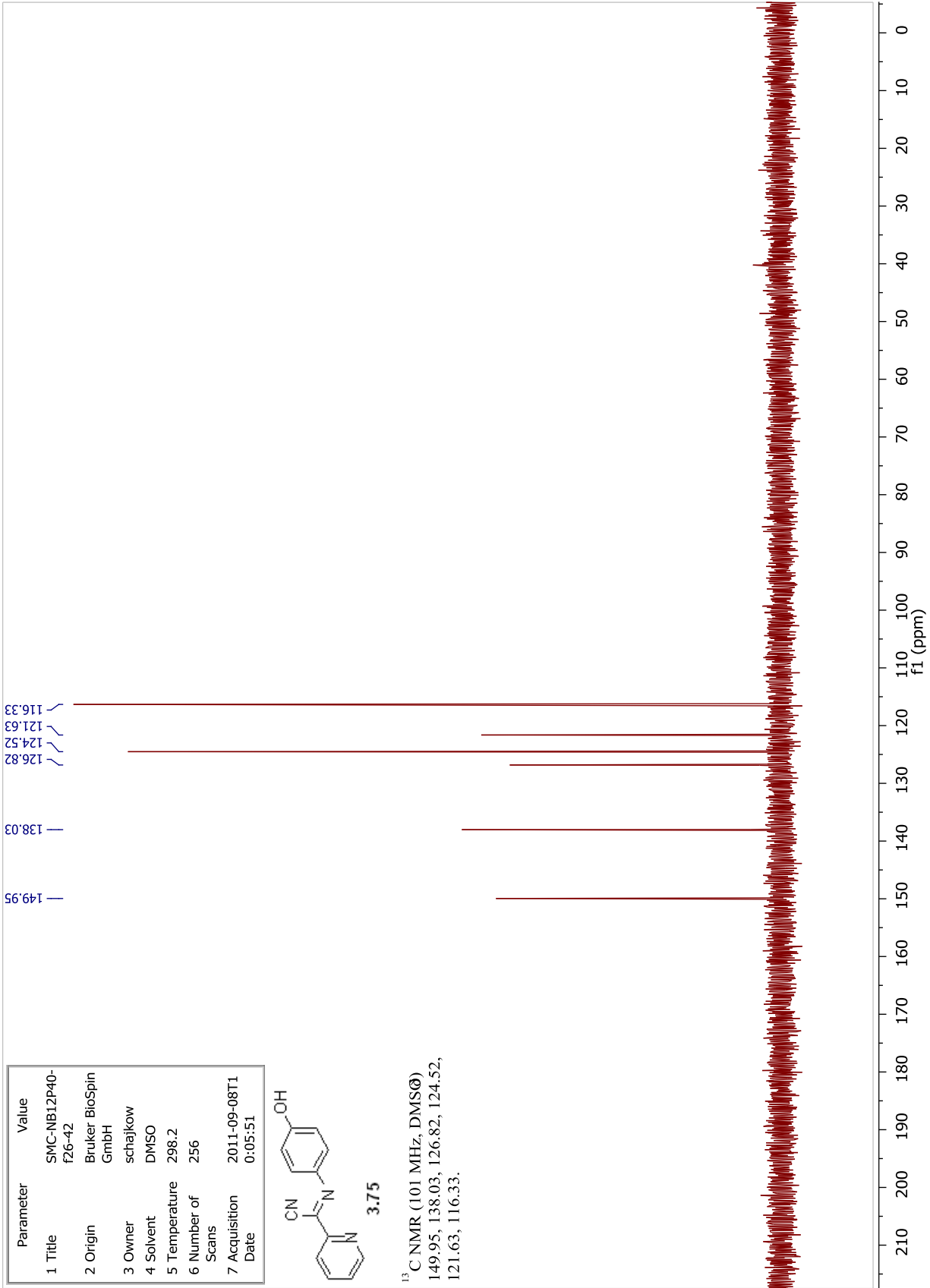


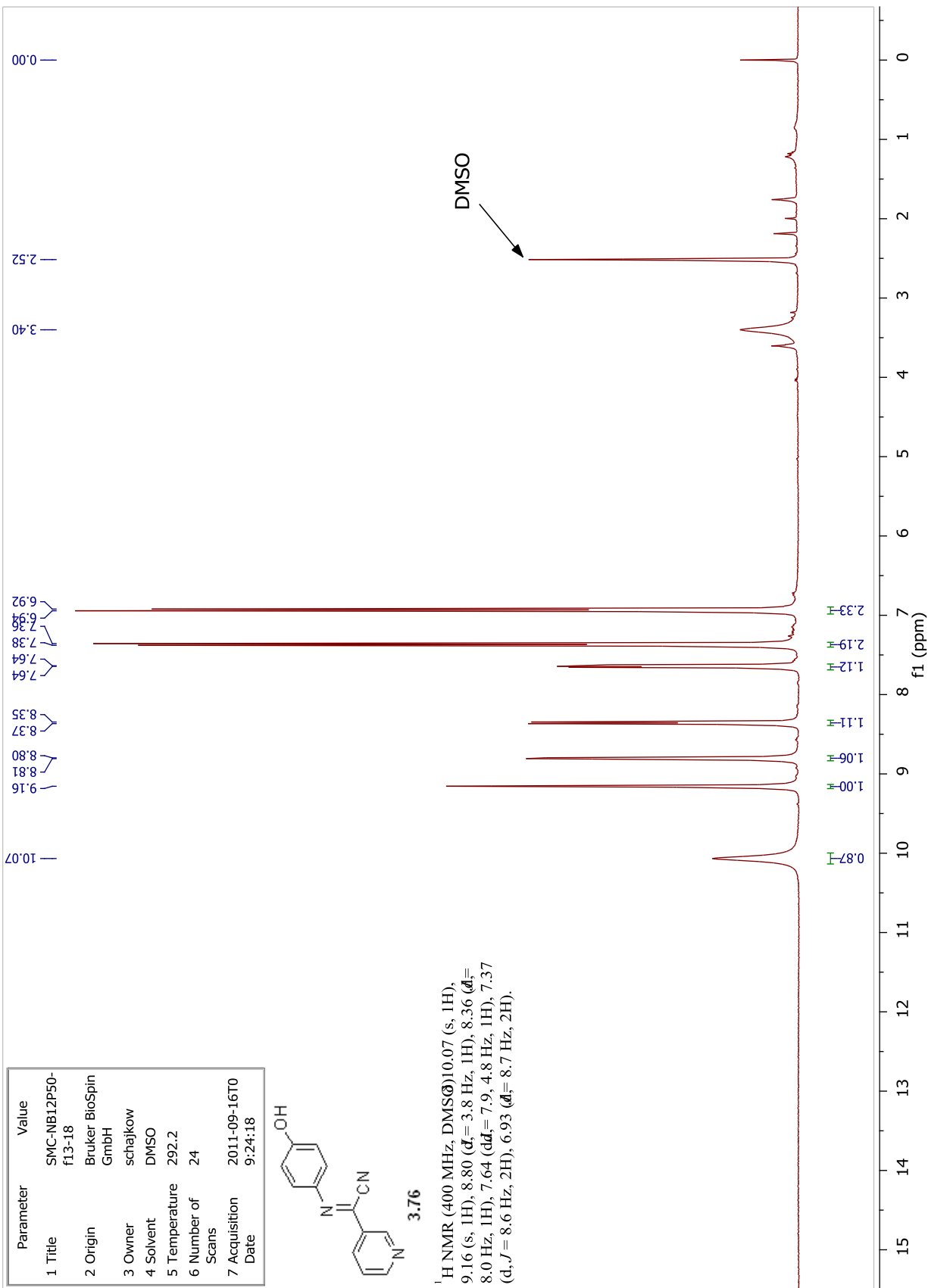


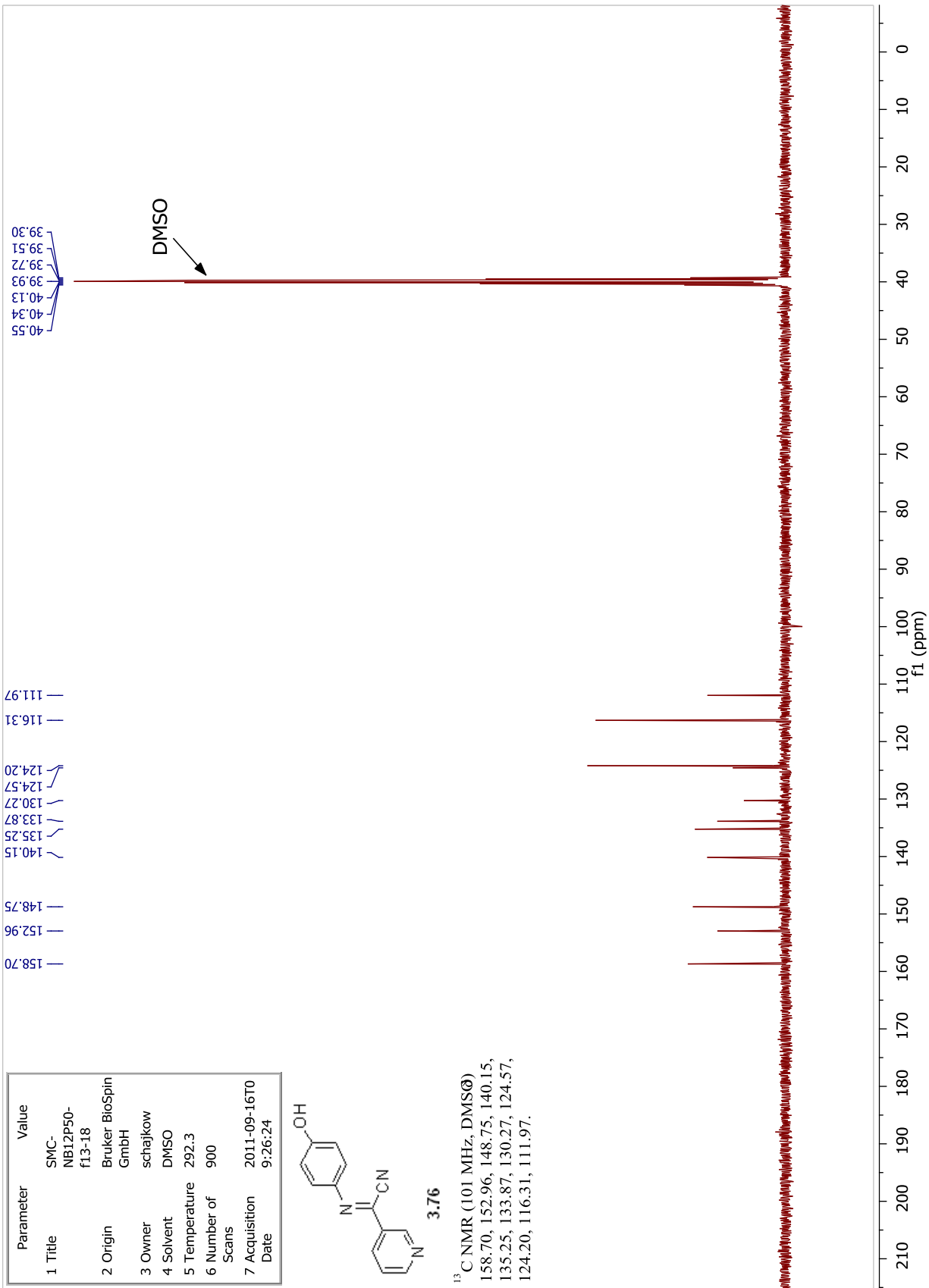
Parameter	Value
1 Title	SMC-NB12P40-f26-42
2 Origin	Bruker BioSpin GmbH
3 Owner	schajkow
4 Solvent	DMSO
5 Temperature	298.2
6 Number of Scans	256
7 Acquisition Date	2011-09-08T10:05:51



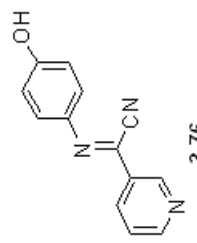
<sup>13</sup>C NMR (101 MHz, DMSO-*d*<sub>6</sub>)  
 149.95, 138.03, 126.82, 124.52,  
 121.63, 116.33.



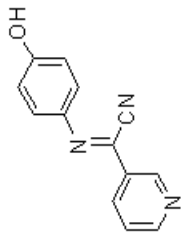




Parameter	Value
1 Title	SMC-NB12P50-f13-18
2 Origin	Bruker BioSpin GmbH
3 Owner	schajkow
4 Solvent	DMSO
5 Temperature	292.3
6 Number of Scans	900
7 Acquisition Date	2011-09-16T09:26:24

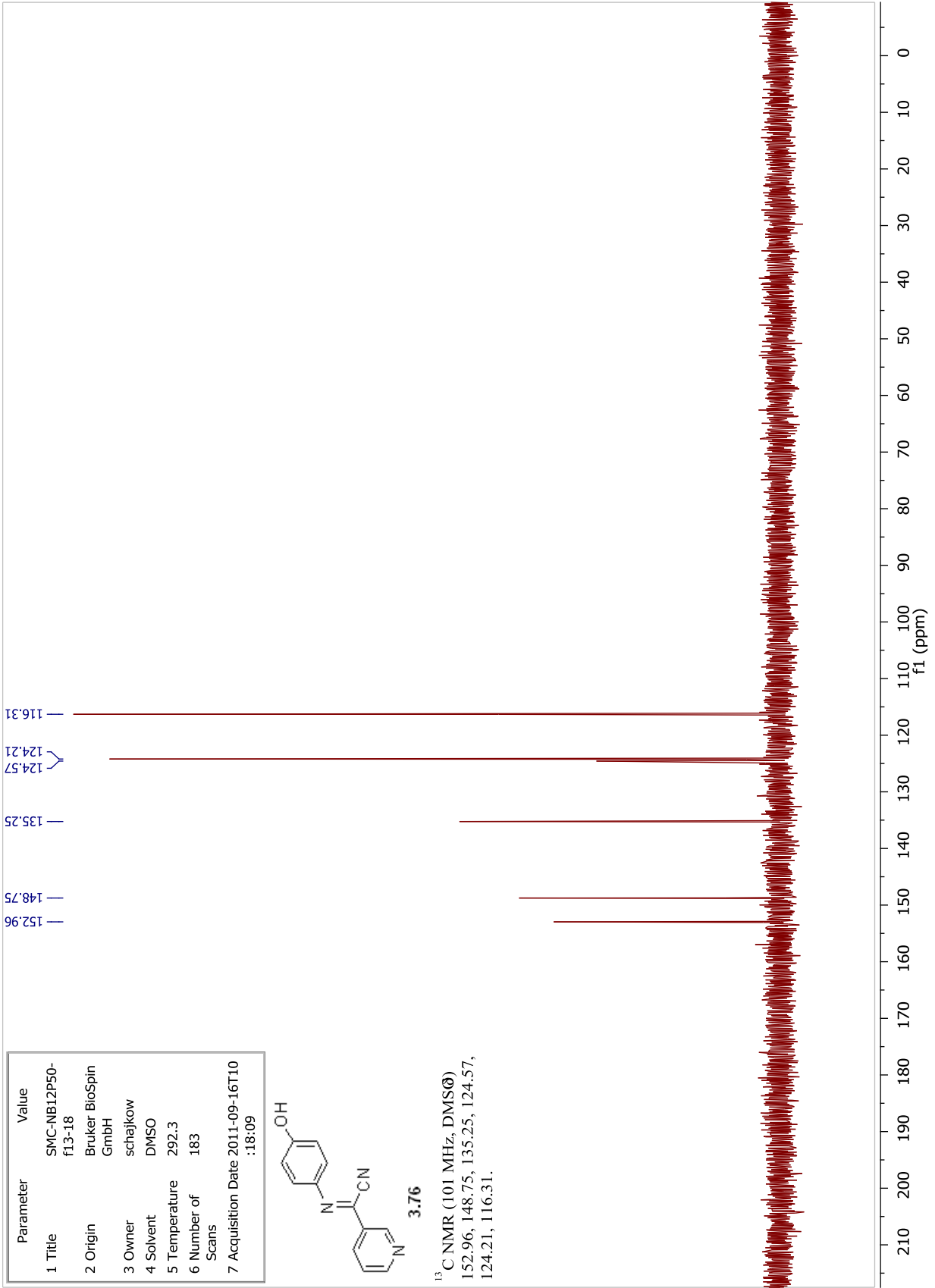


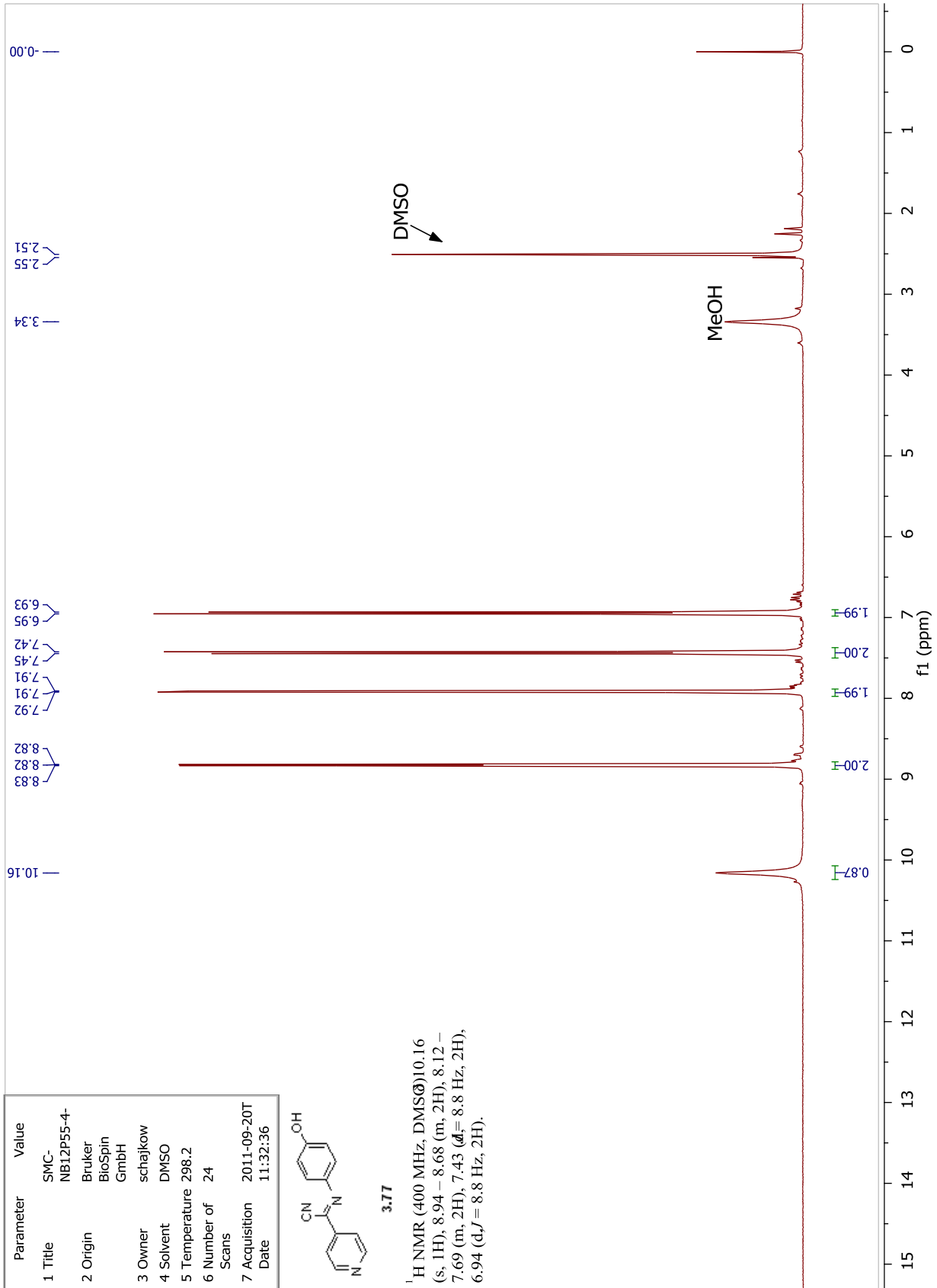
Parameter	Value
1 Title	SMC-NB12P50-f13-18
2 Origin	Bruker BioSpin GmbH
3 Owner	schajkow
4 Solvent	DMSO
5 Temperature	292.3
6 Number of Scans	183
7 Acquisition Date	2011-09-16T10:18:09



3.76

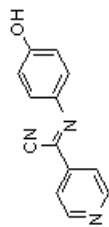
<sup>13</sup>C NMR (101 MHz, DMSO)  
 152.96, 148.75, 135.25, 124.57,  
 124.21, 116.31.





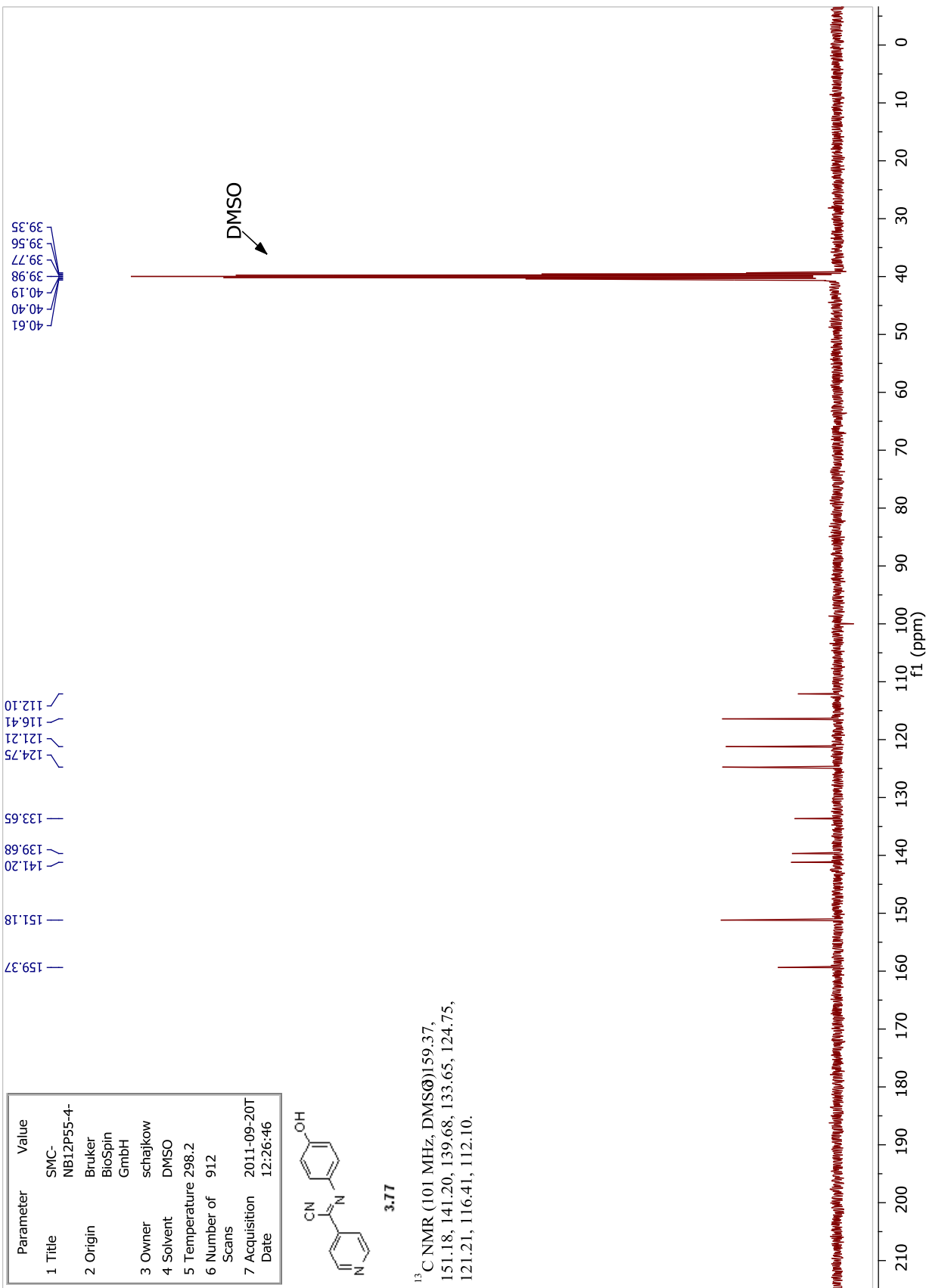


Parameter	Value
1 Title	SMC-NB12P55-4
2 Origin	Bruker BioSpin GmbH
3 Owner	schajkow
4 Solvent	DMSO
5 Temperature	298.2
6 Number of Scans	912
7 Acquisition Date	2011-09-20T12:26:46

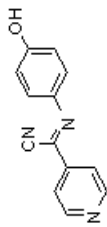


3.77

<sup>13</sup>C NMR (101 MHz, DMSO- $d_6$ ) 159.37, 151.18, 141.20, 139.68, 133.65, 124.75, 121.21, 116.41, 112.10.

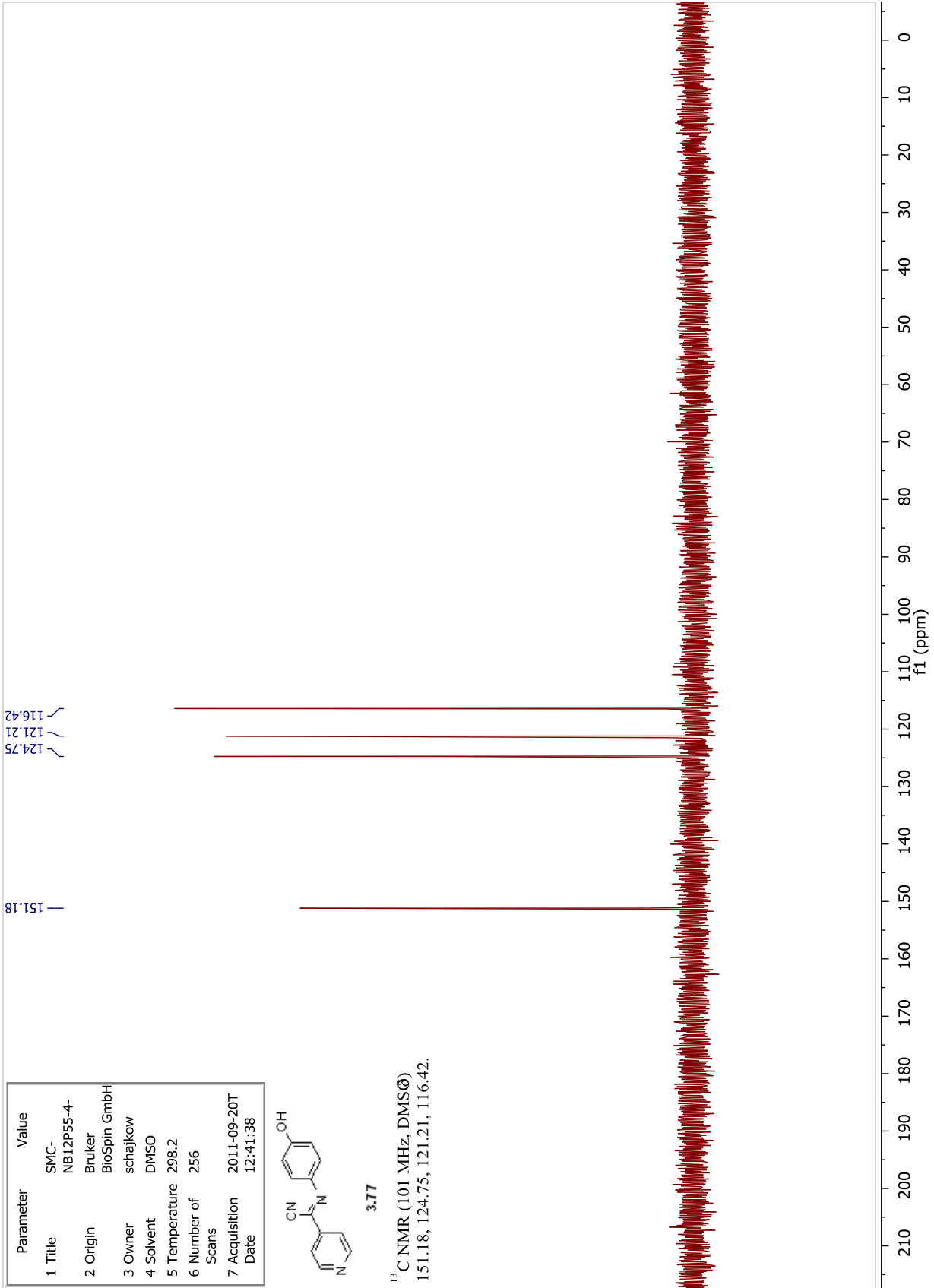


Parameter	Value
1 Title	SMC- NB12P55-4-
2 Origin	Bruker BioSpin GmbH
3 Owner	schajkow
4 Solvent	DMSO
5 Temperature	298.2
6 Number of Scans	256
7 Acquisition Date	2011-09-20T 12:41:38

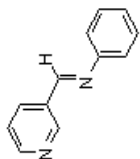


**3.77**

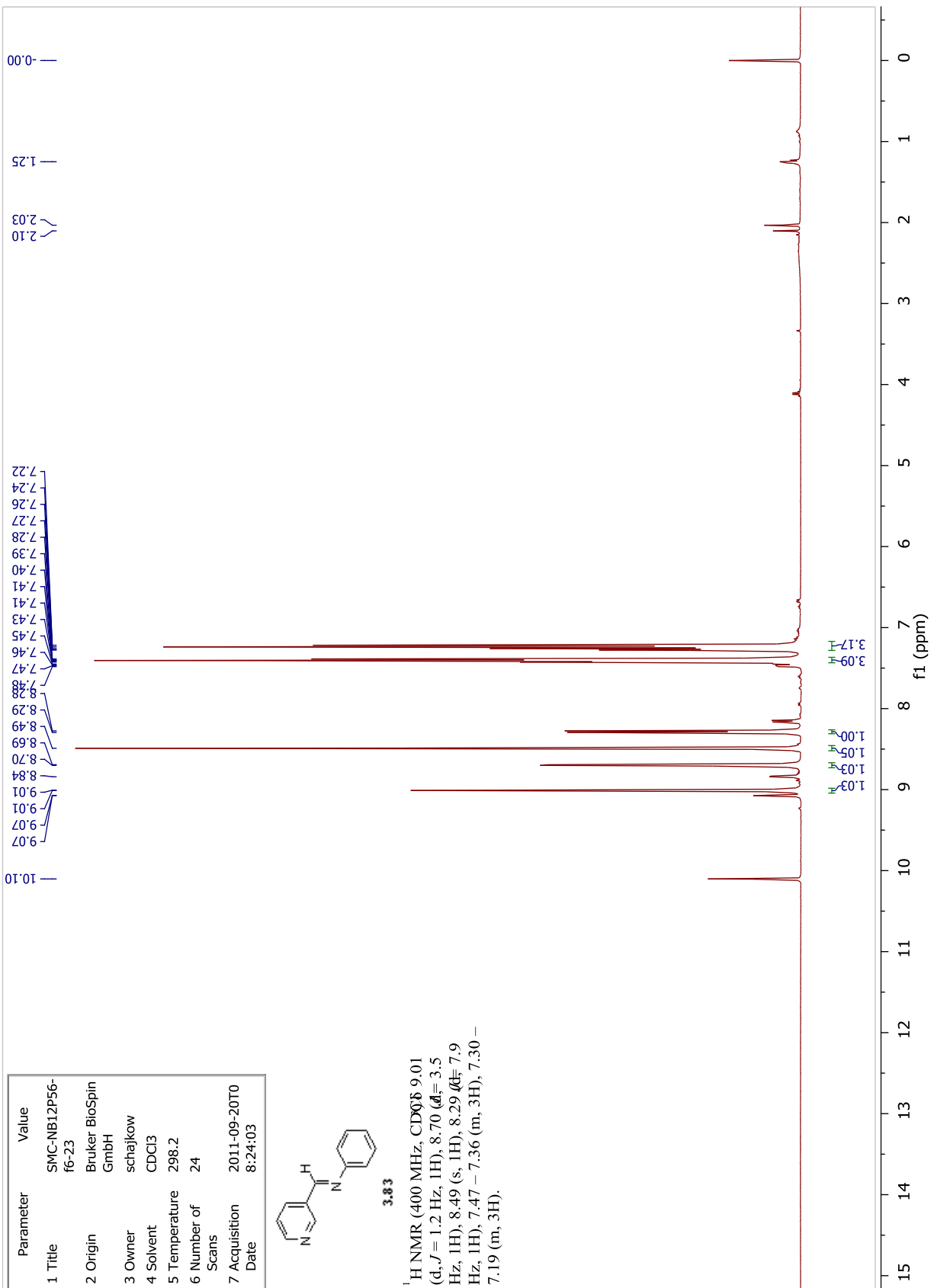
<sup>13</sup>C NMR (101 MHz, DMSO)  
151.18, 124.75, 121.21, 116.42.



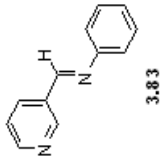
Parameter	Value
1 Title	SMC-NB12P56-f6-23
2 Origin	Bruker BioSpin GmbH
3 Owner	schajkowi
4 Solvent	CDCl <sub>3</sub>
5 Temperature	298.2
6 Number of Scans	24
7 Acquisition Date	2011-09-20T08:24:03



<sup>1</sup>H NMR (400 MHz, CDCl<sub>3</sub>) δ 9.01 (d, *J* = 1.2 Hz, 1H), 8.70 (d, *J* = 3.5 Hz, 1H), 8.49 (s, 1H), 8.29 (t, *J* = 7.9 Hz, 1H), 7.47 – 7.36 (m, 3H), 7.30 – 7.19 (m, 3H).



Parameter	Value
1 Title	SMC-NB12P56-f6-23
2 Origin	Bruker BioSpin GmbH
3 Owner	schajkow
4 Solvent	CDCl3
5 Temperature	298.2
6 Number of Scans	900
7 Acquisition Date	2011-09-20T08:26:23



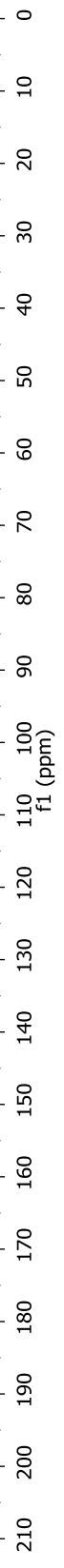
<sup>13</sup>C NMR (101 MHz, CDCl<sub>3</sub>)  
 157.18, 151.99, 151.43, 150.94,  
 134.89, 131.82, 129.25, 126.55,  
 123.80, 120.85.

77.40  
 77.09  
 76.77

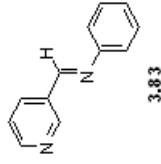
134.89  
 131.82  
 129.25  
 126.55  
 123.80  
 120.85

157.18  
 151.99  
 151.43  
 150.94

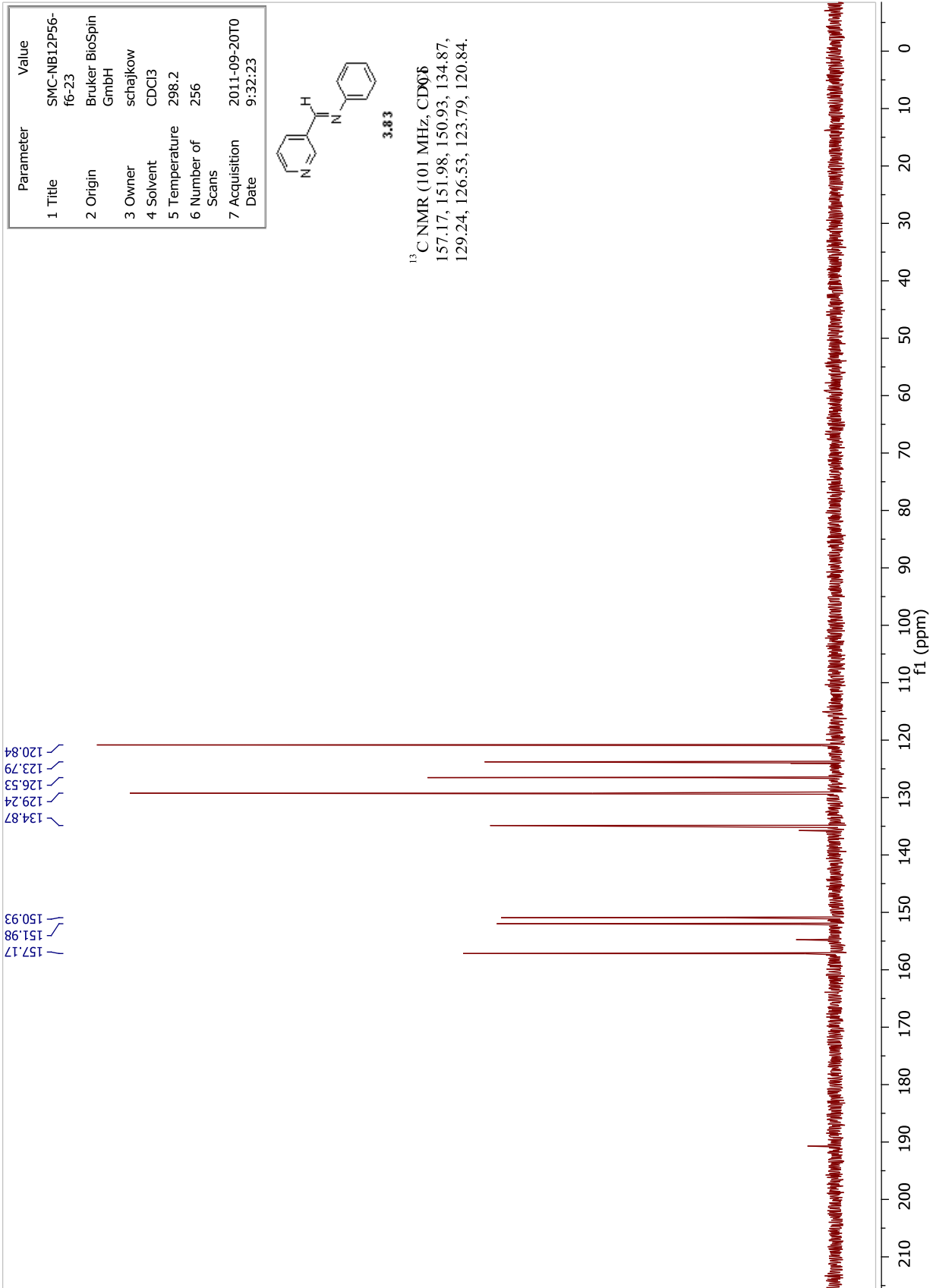
CDCl<sub>3</sub>

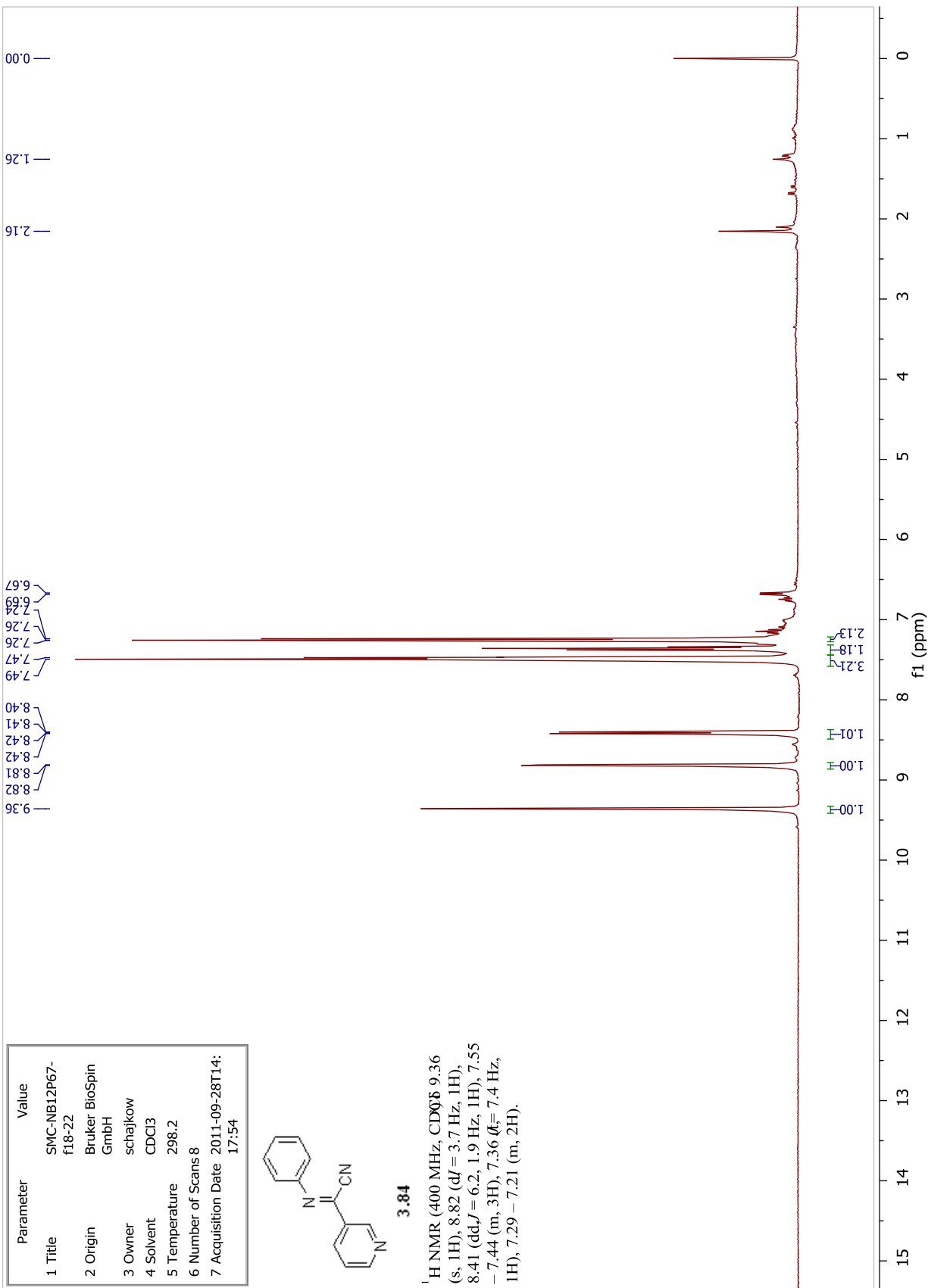


Parameter	Value
1 Title	SMC-NB12P56-f6-23
2 Origin	Bruker BioSpin GmbH
3 Owner	schajkow
4 Solvent	CDCl3
5 Temperature	298.2
6 Number of Scans	256
7 Acquisition Date	2011-09-20T09:32:23

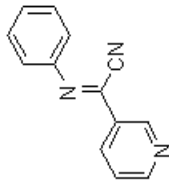


<sup>13</sup>C NMR (101 MHz, CDCl<sub>3</sub>)  
 157.17, 151.98, 150.93, 134.87,  
 129.24, 126.53, 123.79, 120.84.



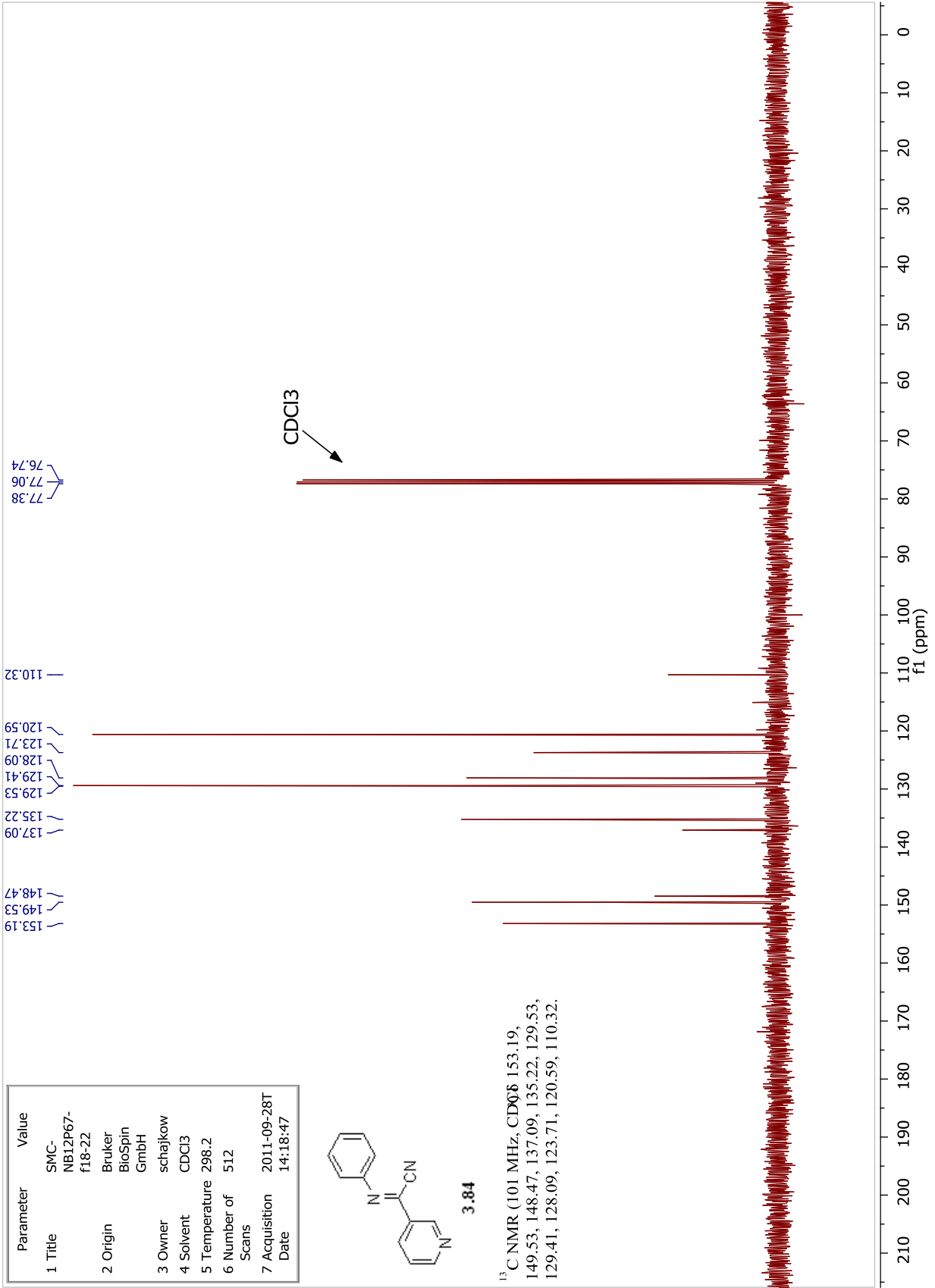


Parameter	Value
1 Title	SMC-NB12P67-f18-22
2 Origin	Bruker BioSpin GmbH
3 Owner	schajkow
4 Solvent	CDCl3
5 Temperature	298.2
6 Number of Scans	512
7 Acquisition Date	2011-09-28T14:18:47

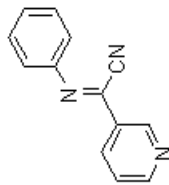


3.84

<sup>13</sup>C NMR (101 MHz, CDCl<sub>3</sub>) 153.19, 149.53, 148.47, 137.09, 135.22, 129.53, 129.41, 128.09, 123.71, 120.59, 110.32.

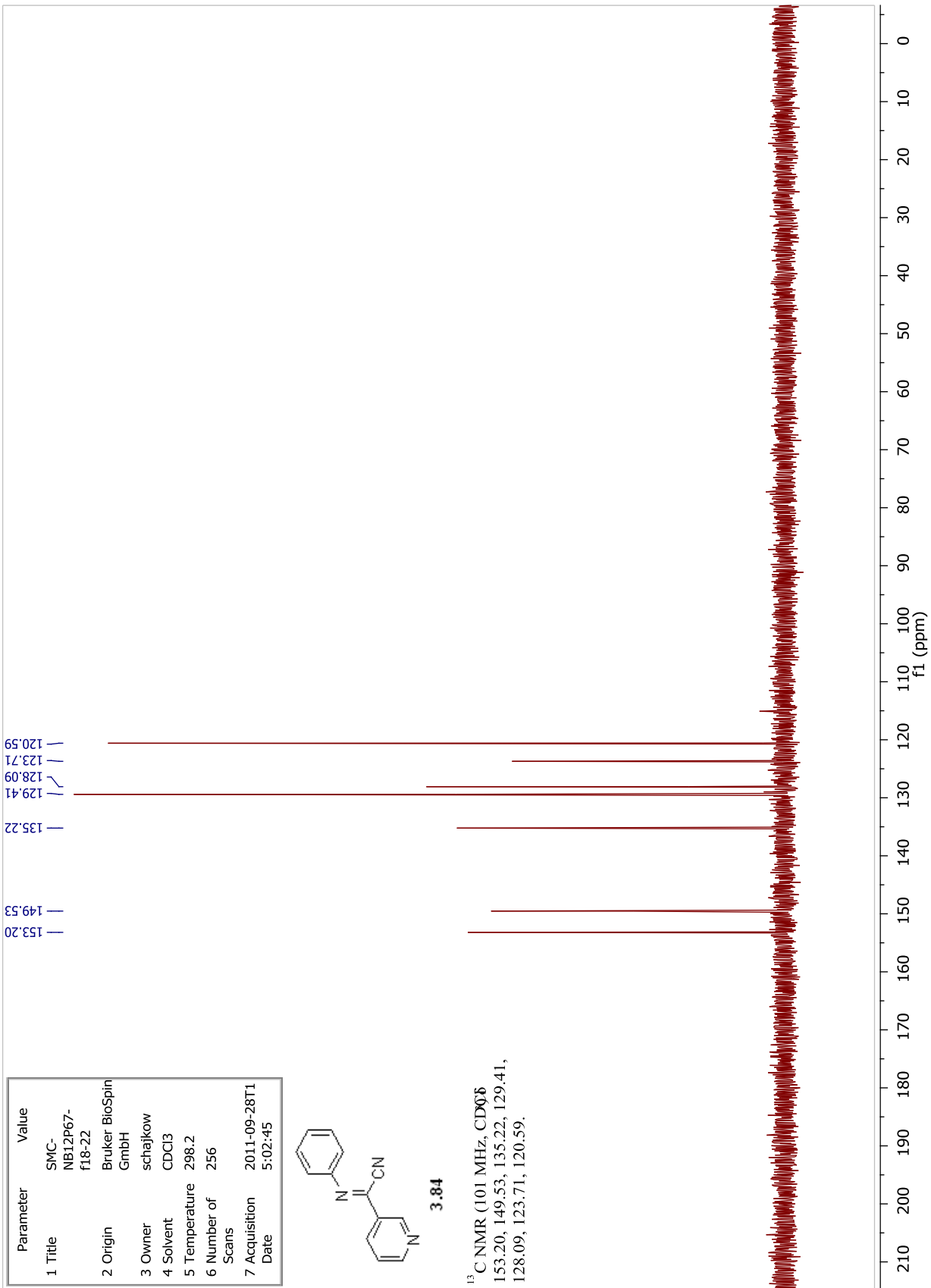


Parameter	Value
1 Title	SMC- NB12P67- f18-22
2 Origin	Bruker BioSpin GmbH
3 Owner	schajkow
4 Solvent	CDCl3
5 Temperature	298.2
6 Number of Scans	256
7 Acquisition Date	2011-09-28T1 5:02:45



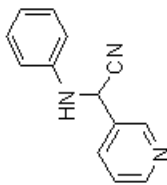
3.84

<sup>13</sup>C NMR (101 MHz, CDCl<sub>3</sub>)  
153.20, 149.53, 135.22, 129.41,  
128.09, 123.71, 120.59.



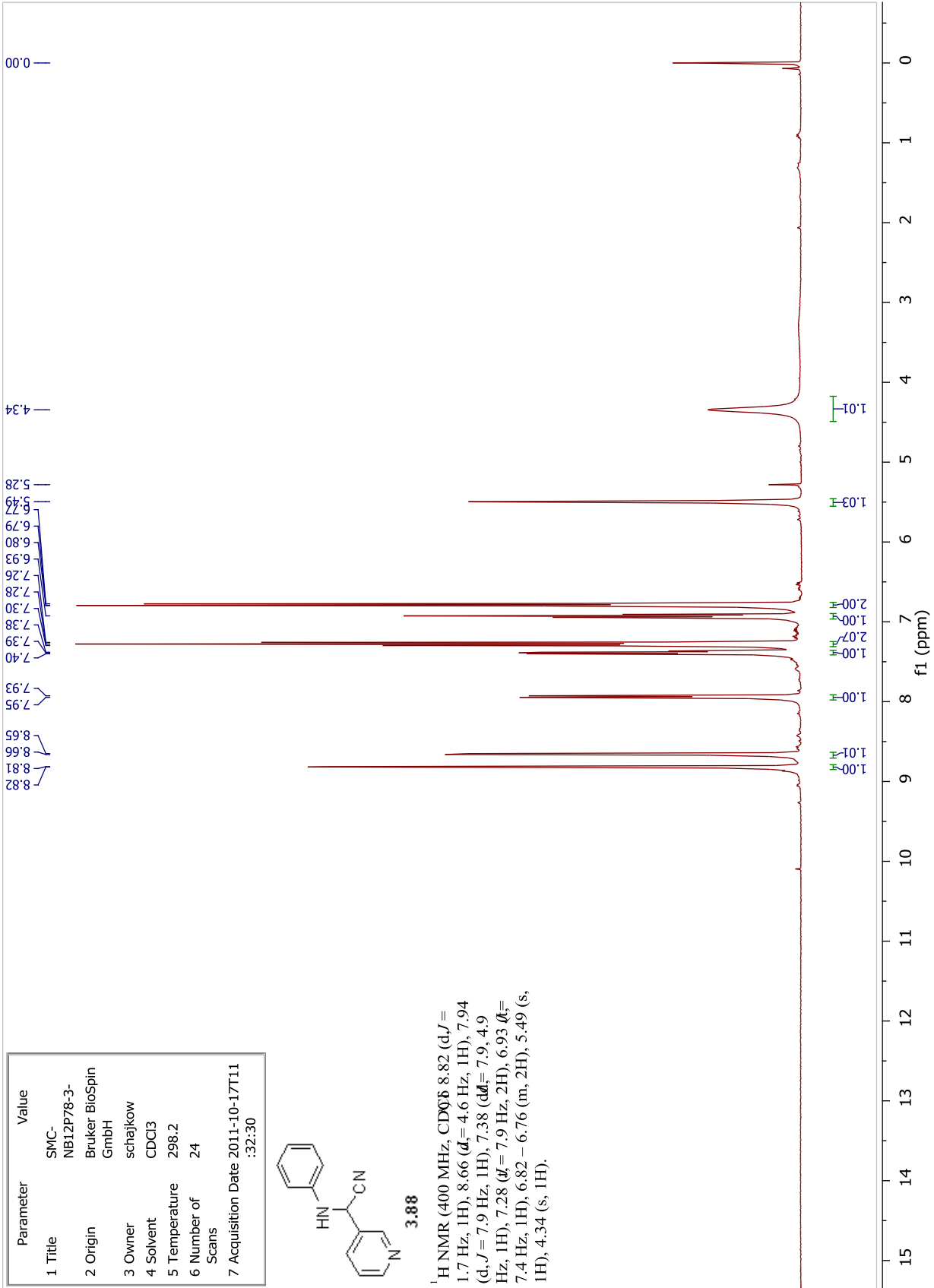


Parameter	Value
1 Title	SMC-NB12P78-3-
2 Origin	Bruker BioSpin GmbH
3 Owner	schajkow
4 Solvent	CDCl <sub>3</sub>
5 Temperature	298.2
6 Number of Scans	24
7 Acquisition Date	2011-10-17T11:32:30

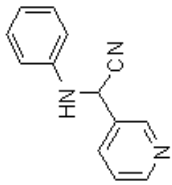


**3.88**

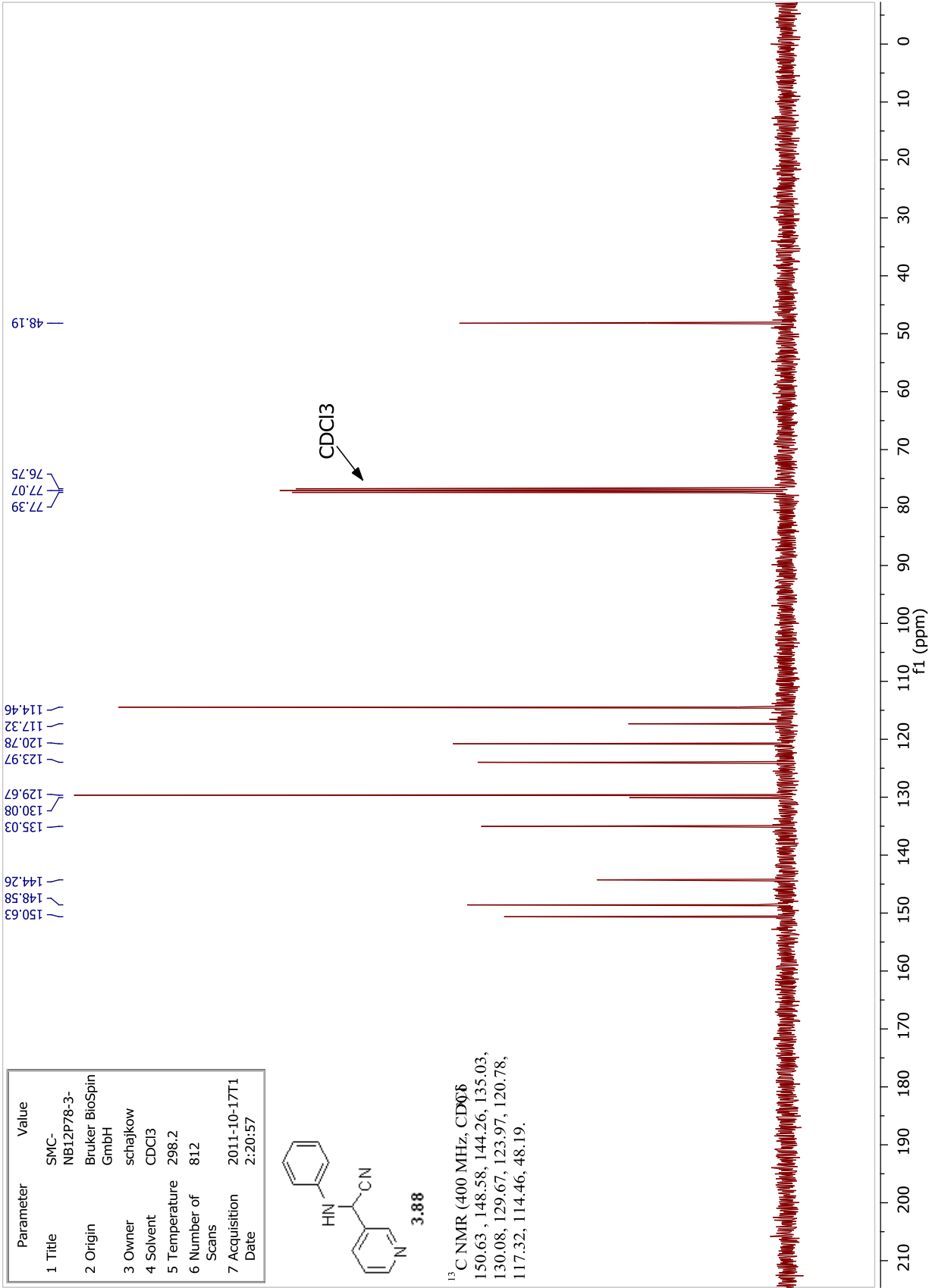
<sup>1</sup>H NMR (400 MHz, CDCl<sub>3</sub>) δ 8.82 (d, *J* = 1.7 Hz, 1H), 8.66 (d, *J* = 4.6 Hz, 1H), 7.94 (d, *J* = 7.9 Hz, 1H), 7.38 (dd, *J* = 7.9, 4.9 Hz, 1H), 7.28 (d, *J* = 7.9 Hz, 2H), 6.93 (t, *J* = 7.4 Hz, 1H), 6.82 – 6.76 (m, 2H), 5.49 (s, 1H), 4.34 (s, 1H).



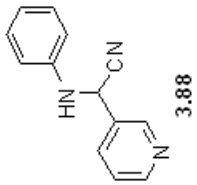
Parameter	Value
1 Title	SMC- NB12P78-3-
2 Origin	Bruker BioSpin GmbH
3 Owner	schajkowiak
4 Solvent	CDCl <sub>3</sub>
5 Temperature	298.2
6 Number of Scans	812
7 Acquisition Date	2011-10-17T1 2:20:57



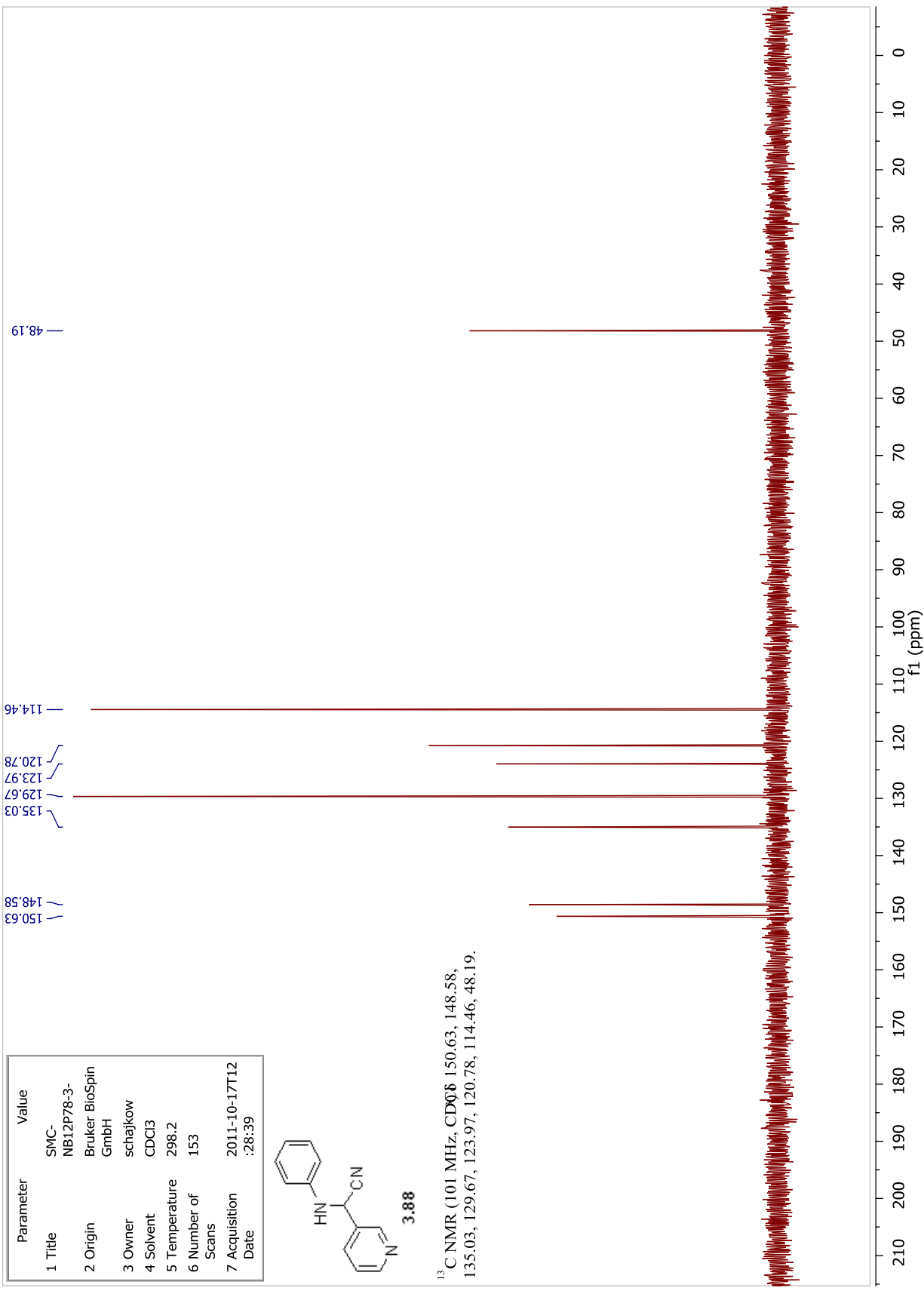
<sup>13</sup>C NMR (400 MHz, CDCl<sub>3</sub>)  
 150.63, 148.58, 144.26, 135.03,  
 130.08, 129.67, 123.97, 120.78,  
 117.32, 114.46, 48.19.



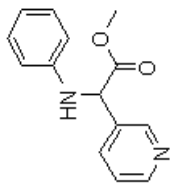
Parameter	Value
1 Title	SMC-NB12P78-3-
2 Origin	Bruker BioSpin GmbH
3 Owner	schajkow
4 Solvent	CDCl3
5 Temperature	298.2
6 Number of Scans	153
7 Acquisition Date	2011-10-17T12:28:39



<sup>13</sup>C NMR (101 MHz, CDCl<sub>3</sub>) 150.63, 148.58, 135.03, 129.67, 123.97, 120.78, 114.46, 48.19.

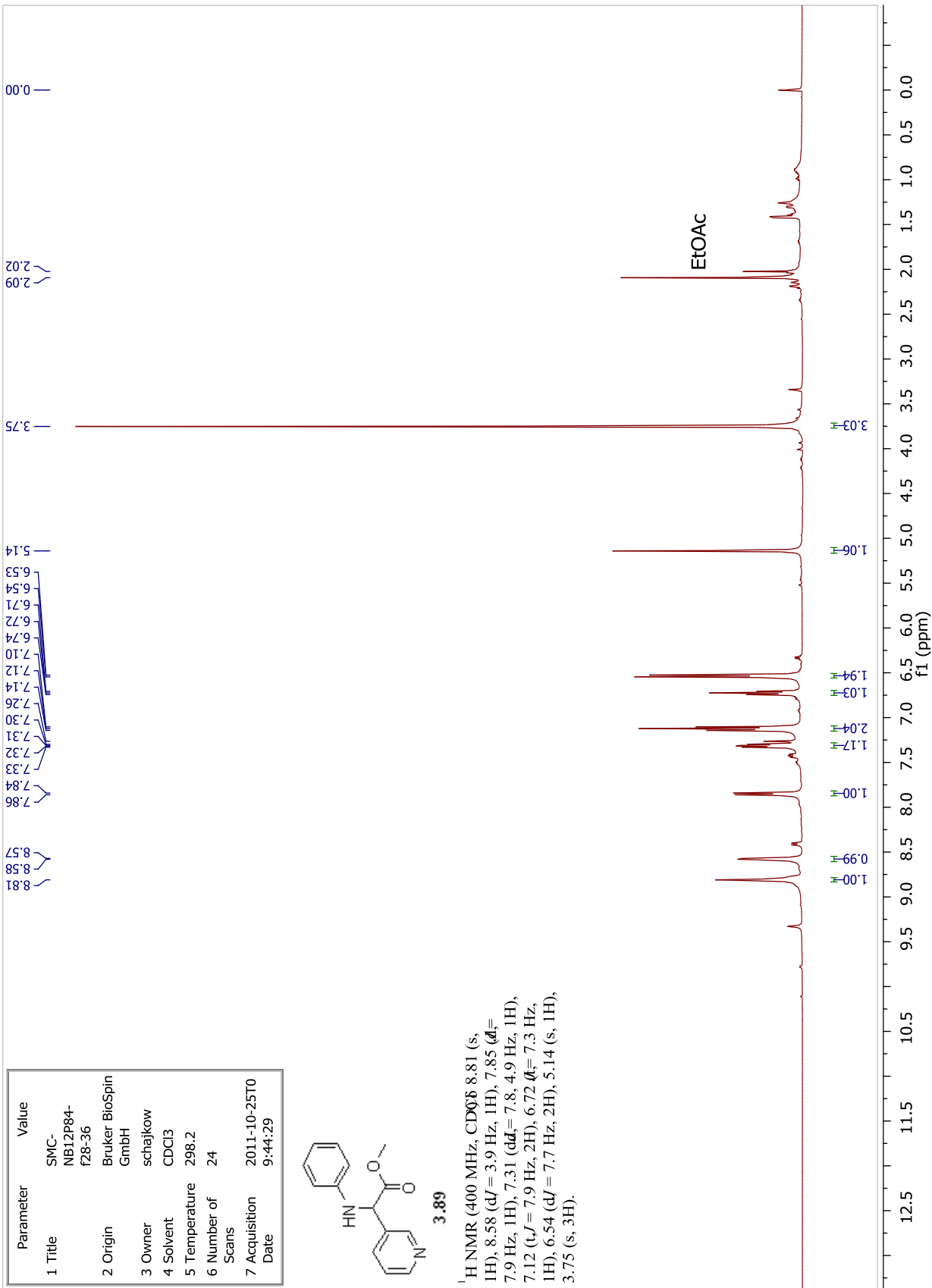


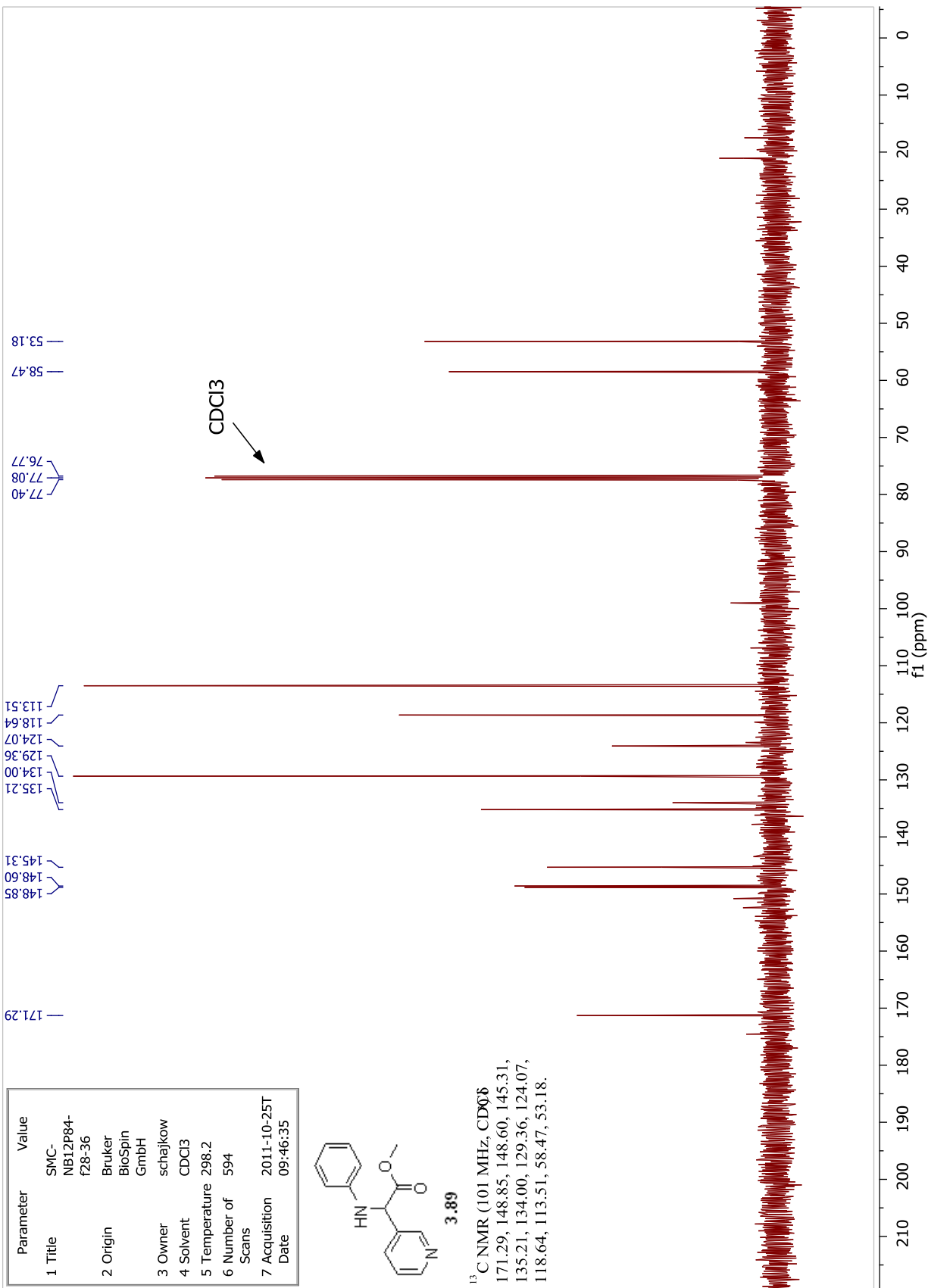
Parameter	Value
1 Title	SMC-NB12P84-f28-36
2 Origin	Bruker BioSpin GmbH
3 Owner	schajkow
4 Solvent	CDC13
5 Temperature	298.2
6 Number of Scans	24
7 Acquisition Date	2011-10-25T09:44:29



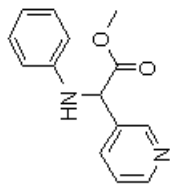
3.89

<sup>1</sup>H NMR (400 MHz, CDCl<sub>3</sub>) 8.81 (s, 1H), 8.58 (dJ = 3.9 Hz, 1H), 7.85 (dJ = 7.9 Hz, 1H), 7.31 (ddJ = 7.8, 4.9 Hz, 1H), 7.12 (tJ = 7.9 Hz, 2H), 6.72 (dJ = 7.3 Hz, 1H), 6.54 (dJ = 7.7 Hz, 2H), 5.14 (s, 1H), 3.75 (s, 3H).



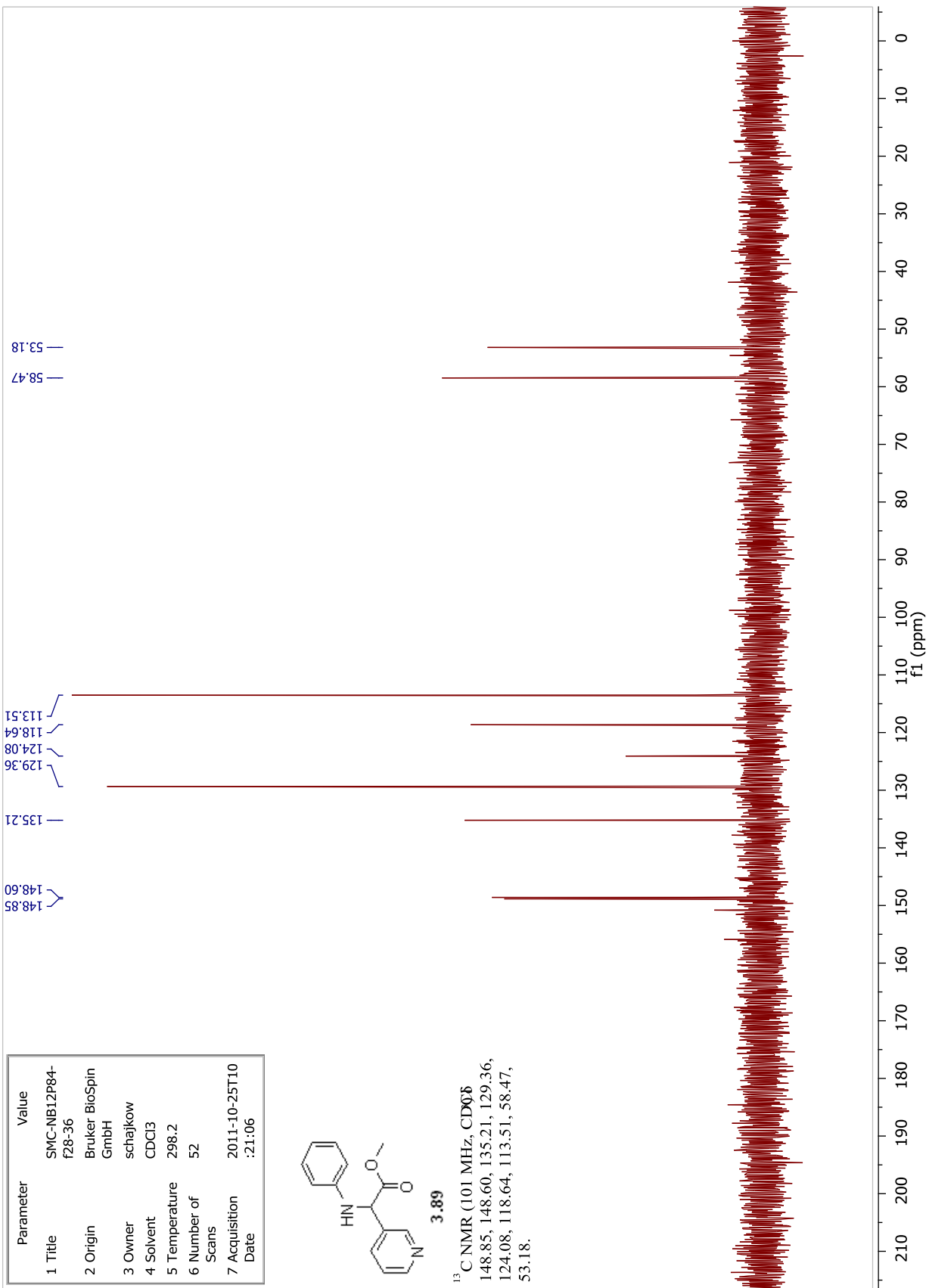


Parameter	Value
1 Title	SMC-NB12P84-f28-36
2 Origin	Bruker BioSpin GmbH
3 Owner	schajkow
4 Solvent	CDCl3
5 Temperature	298.2
6 Number of Scans	52
7 Acquisition Date	2011-10-25T10:21:06

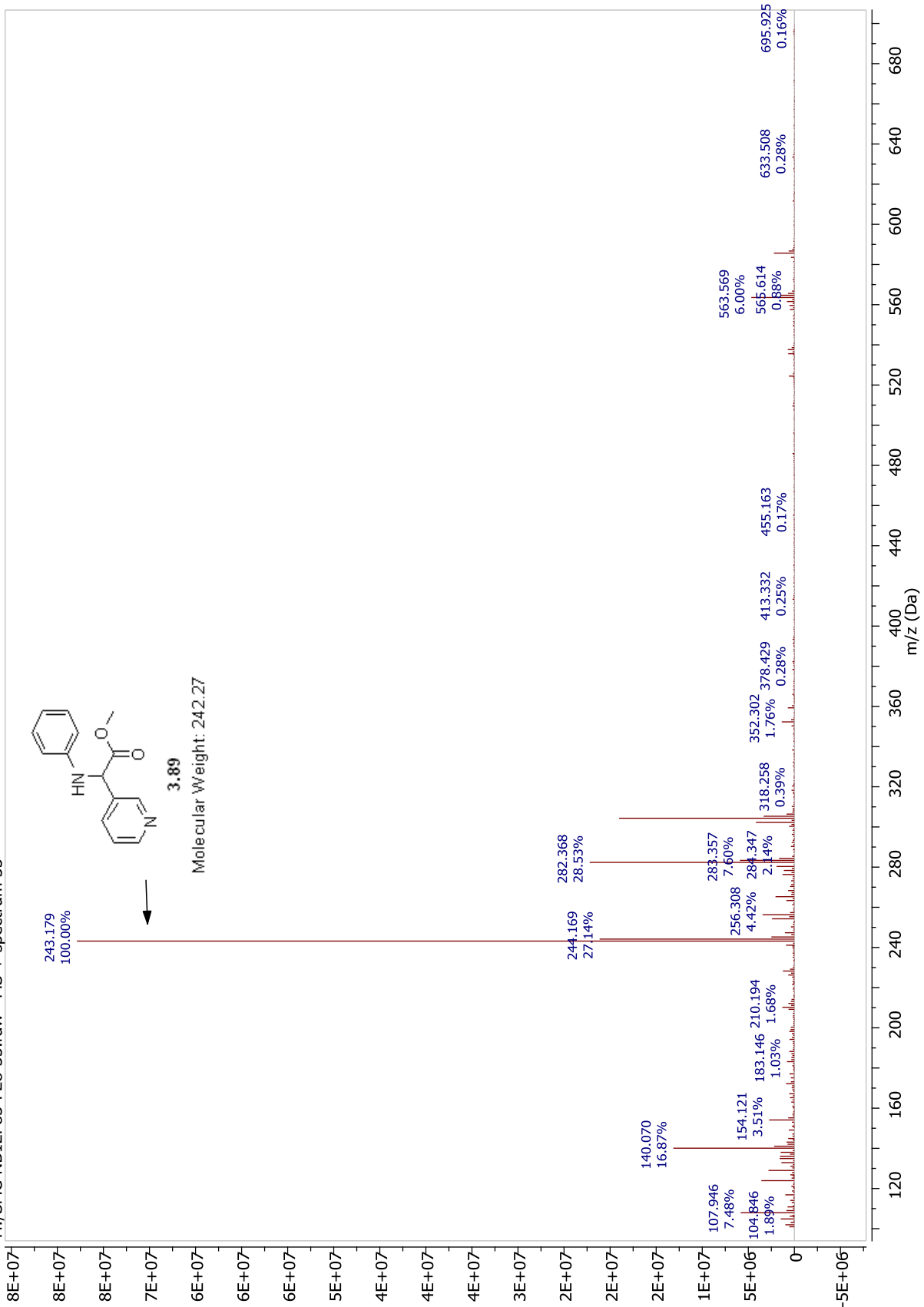


3.89

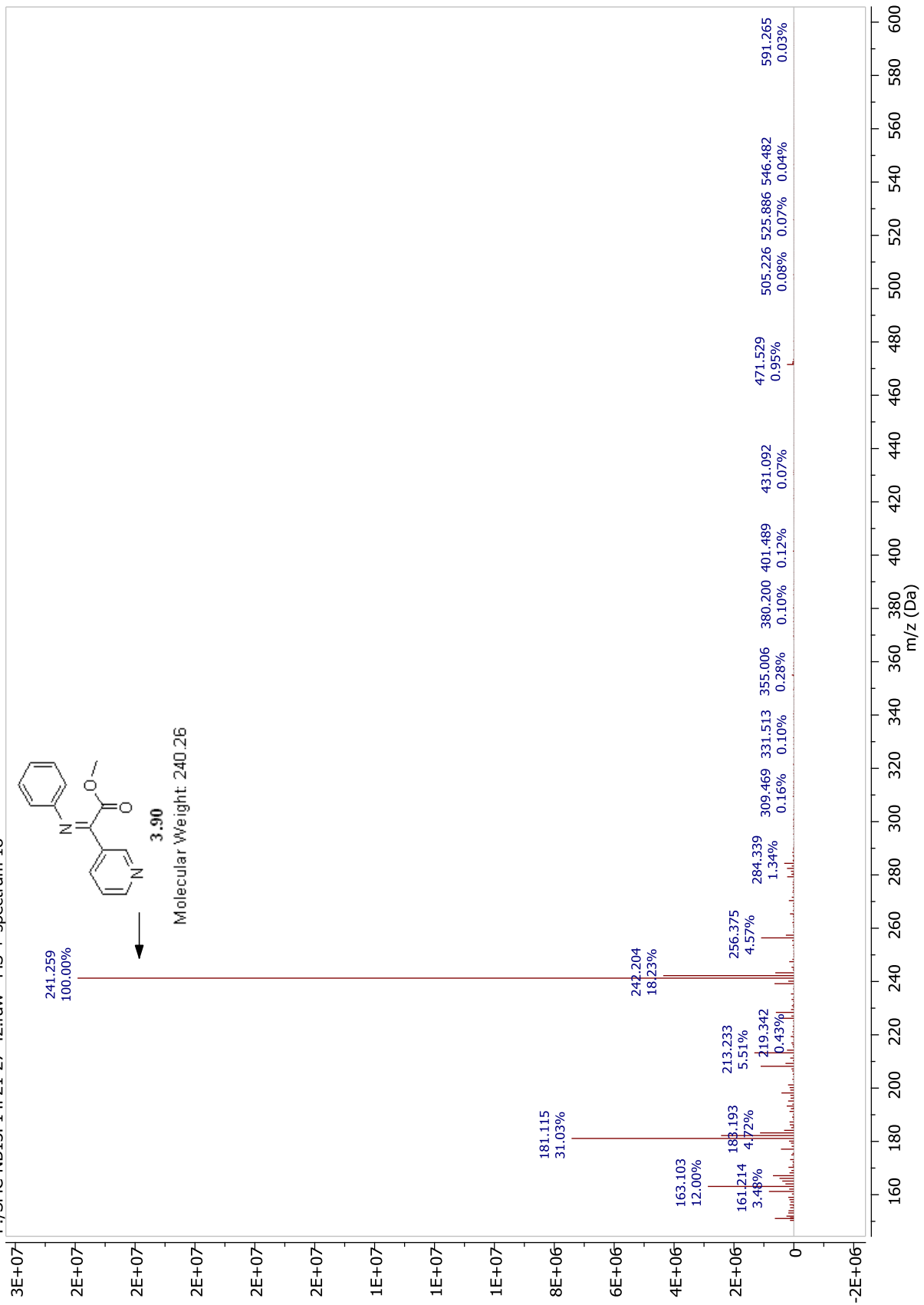
<sup>13</sup>C NMR (101 MHz, CDCl<sub>3</sub>)  
 148.85, 148.60, 135.21, 129.36,  
 124.08, 118.64, 113.51, 58.47,  
 53.18.



H:/SMC-NB12P83-F28-35.raw MS + spectrum 33

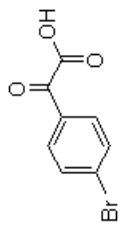


F:/SMC-NB13P14F21-27-42.raw MS + spectrum 18

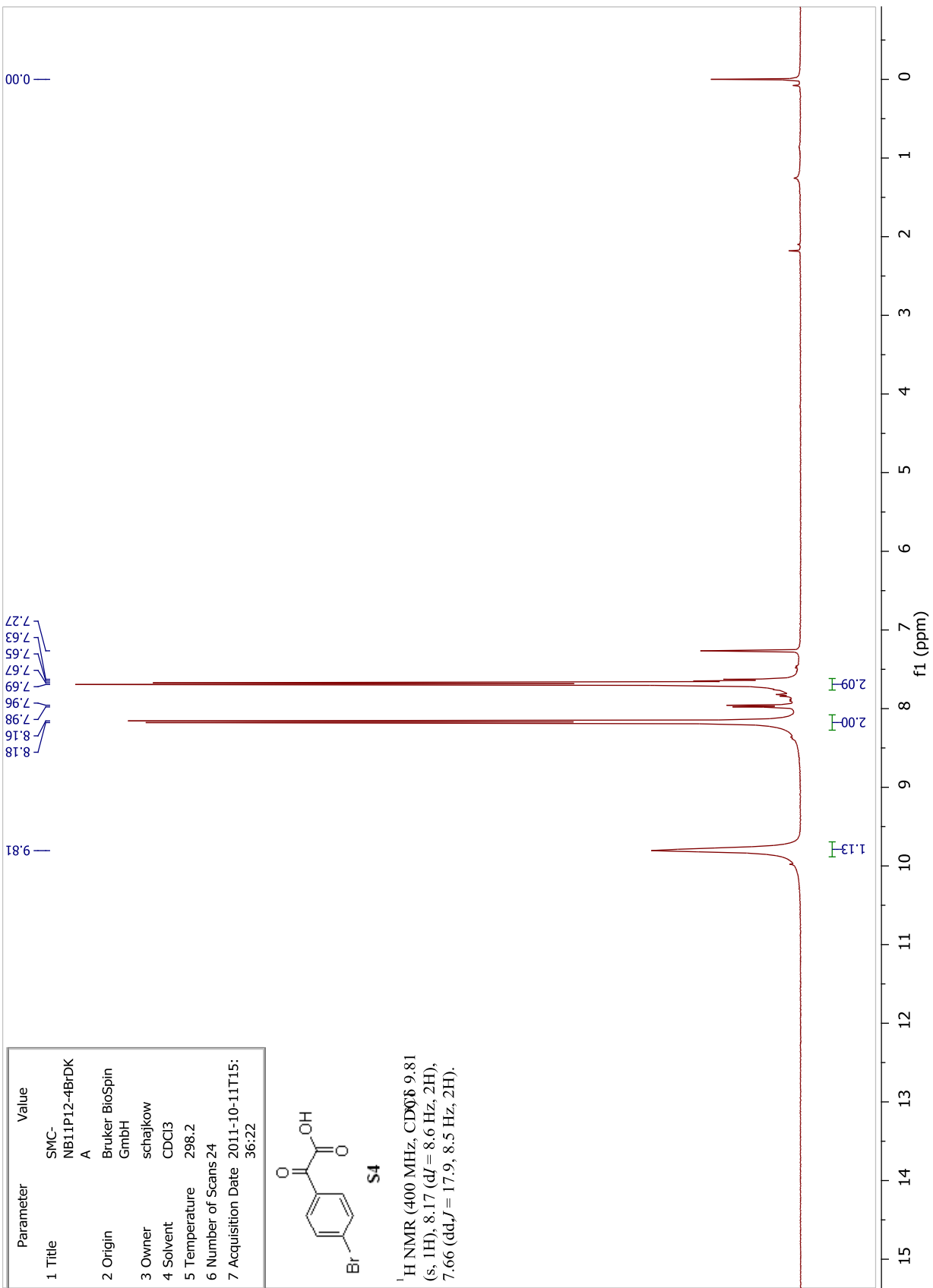




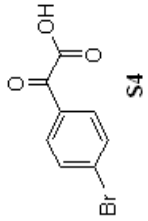
Parameter	Value
1 Title	SMC-NB11P12-4BRDK
2 Origin	A
3 Owner	Bruker BioSpin GmbH
4 Solvent	schajkow
5 Temperature	CDC13
6 Number of Scans	298.2
7 Acquisition Date	2011-10-11T15:36:22



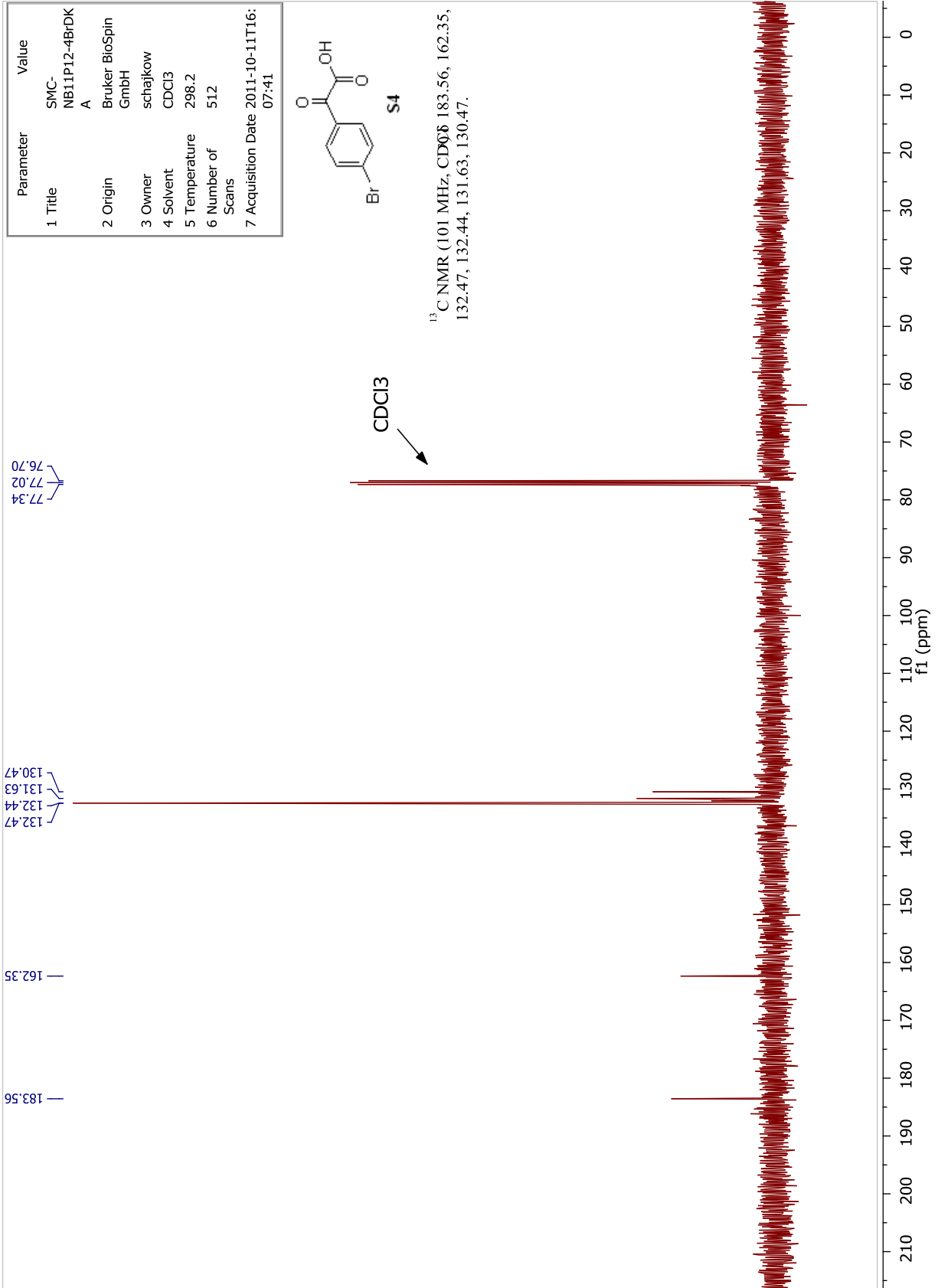
<sup>1</sup>H NMR (400 MHz, CDCl<sub>3</sub>) δ 9.81 (s, 1H), 8.17 (d, *J* = 8.6 Hz, 2H), 7.66 (dd, *J* = 17.9, 8.5 Hz, 2H).



Parameter	Value
1 Title	SMC-NB11P12-4BrDK
2 Origin	A
3 Owner	Bruker BioSpin GmbH
4 Solvent	schajkow CDCl3
5 Temperature	298.2
6 Number of Scans	512
7 Acquisition Date	2011-10-11T16:07:41



<sup>13</sup>C NMR (101 MHz, CDCl<sub>3</sub>) 183.56, 162.35, 132.47, 132.44, 131.63, 130.47.



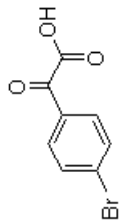
77.34  
77.02  
76.70

132.47  
132.44  
131.63  
130.47

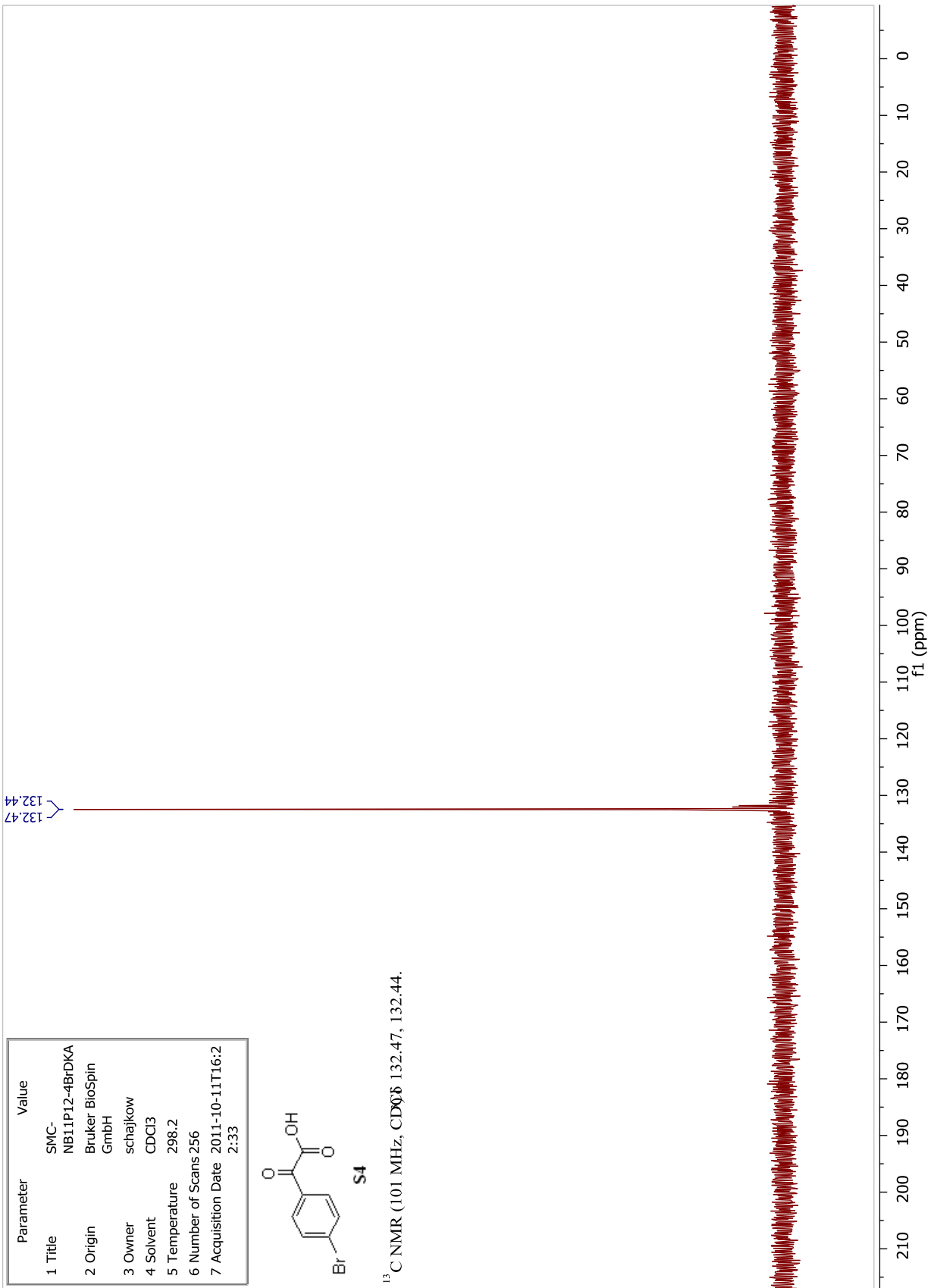
162.35

183.56

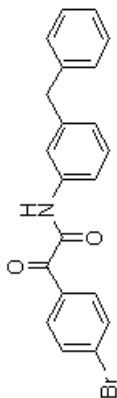
Parameter	Value
1 Title	SMC- NB11P12-4BrDKA
2 Origin	Bruker BioSpin GmbH
3 Owner	schajkow
4 Solvent	CDCI3
5 Temperature	298.2
6 Number of Scans	256
7 Acquisition Date	2011-10-11T16:2 2:33



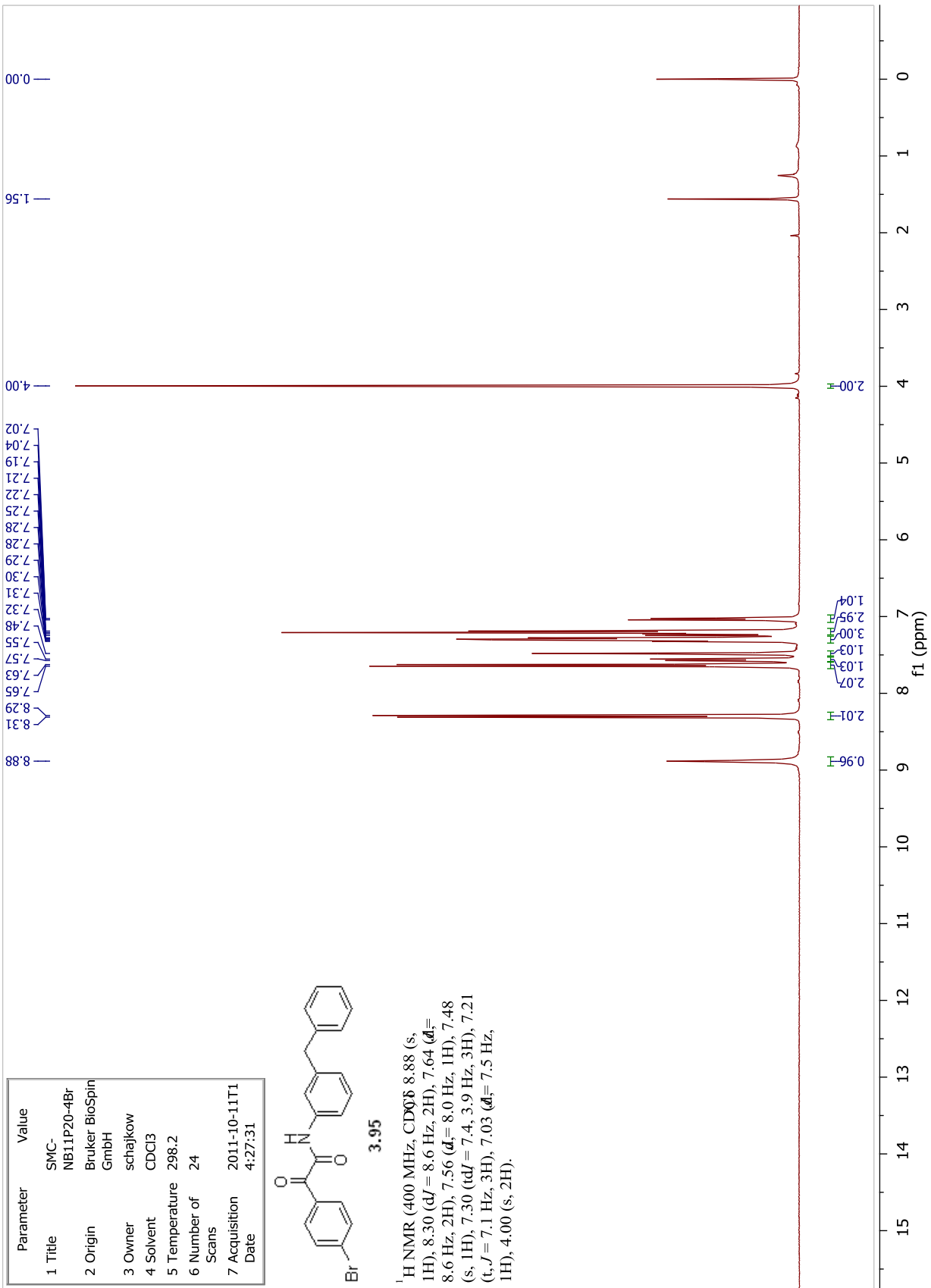
<sup>13</sup>C NMR (101 MHz, CDCl<sub>3</sub>) 132.47, 132.44.



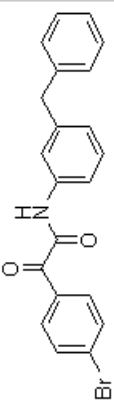
Parameter	Value
1 Title	SMC-NB11P20-4Br
2 Origin	Bruker BioSpin GmbH
3 Owner	schajkow
4 Solvent	CDCl3
5 Temperature	298.2
6 Number of Scans	24
7 Acquisition Date	2011-10-11T14:27:31



<sup>1</sup>H NMR (400 MHz, CDCl<sub>3</sub>) δ 8.88 (s, 1H), 8.30 (d, *d*<sub>H</sub> = 8.6 Hz, 2H), 7.64 (d, *d*<sub>H</sub> = 8.6 Hz, 2H), 7.56 (d, *d*<sub>H</sub> = 8.0 Hz, 1H), 7.48 (s, 1H), 7.30 (td, *t*<sub>H</sub> = 7.4, 3.9 Hz, 3H), 7.21 (t, *J* = 7.1 Hz, 3H), 7.03 (d, *d*<sub>H</sub> = 7.5 Hz, 1H), 4.00 (s, 2H).

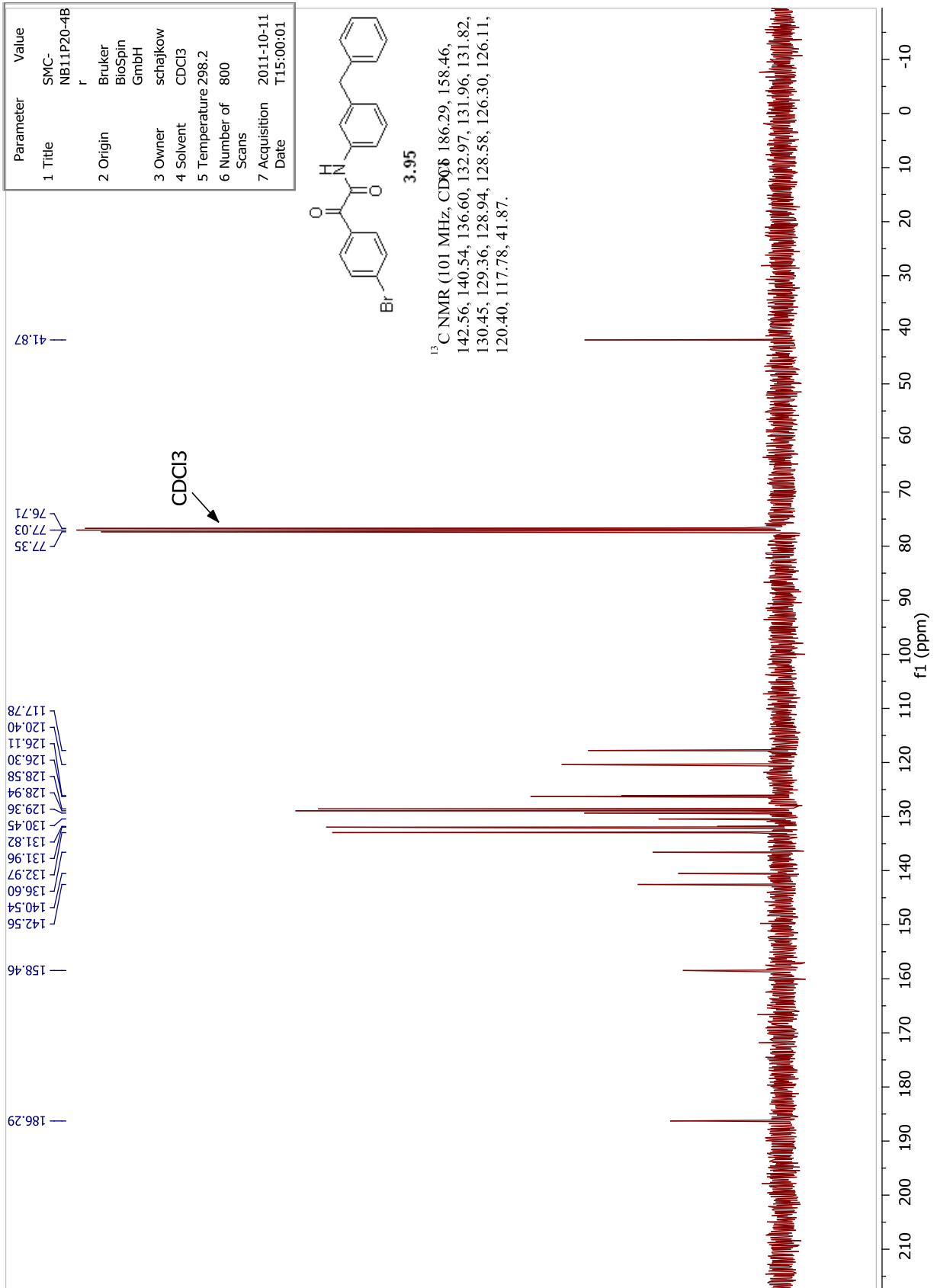


Parameter	Value
1 Title	SMC-NB11P20-4B
2 Origin	Bruker BioSpin GmbH
3 Owner	schajkow
4 Solvent	CDCl3
5 Temperature	298.2
6 Number of Scans	800
7 Acquisition Date	2011-10-11 15:00:01

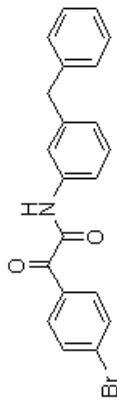


3.95

<sup>13</sup>C NMR (101 MHz, CDCl<sub>3</sub>) 186.29, 158.46, 142.56, 140.54, 136.60, 132.97, 131.96, 131.82, 130.45, 129.36, 128.94, 128.58, 126.30, 126.11, 120.40, 117.78, 41.87.

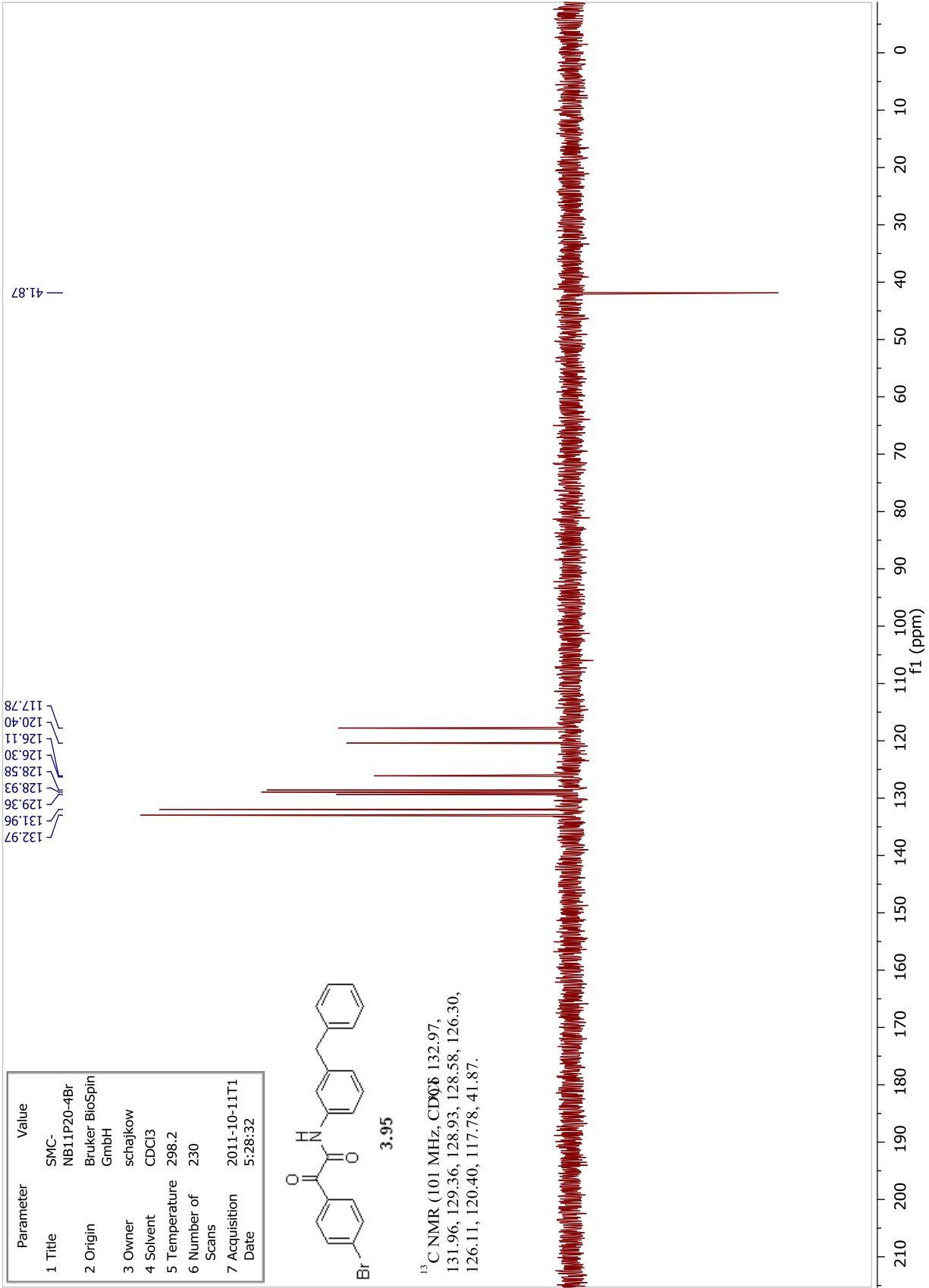


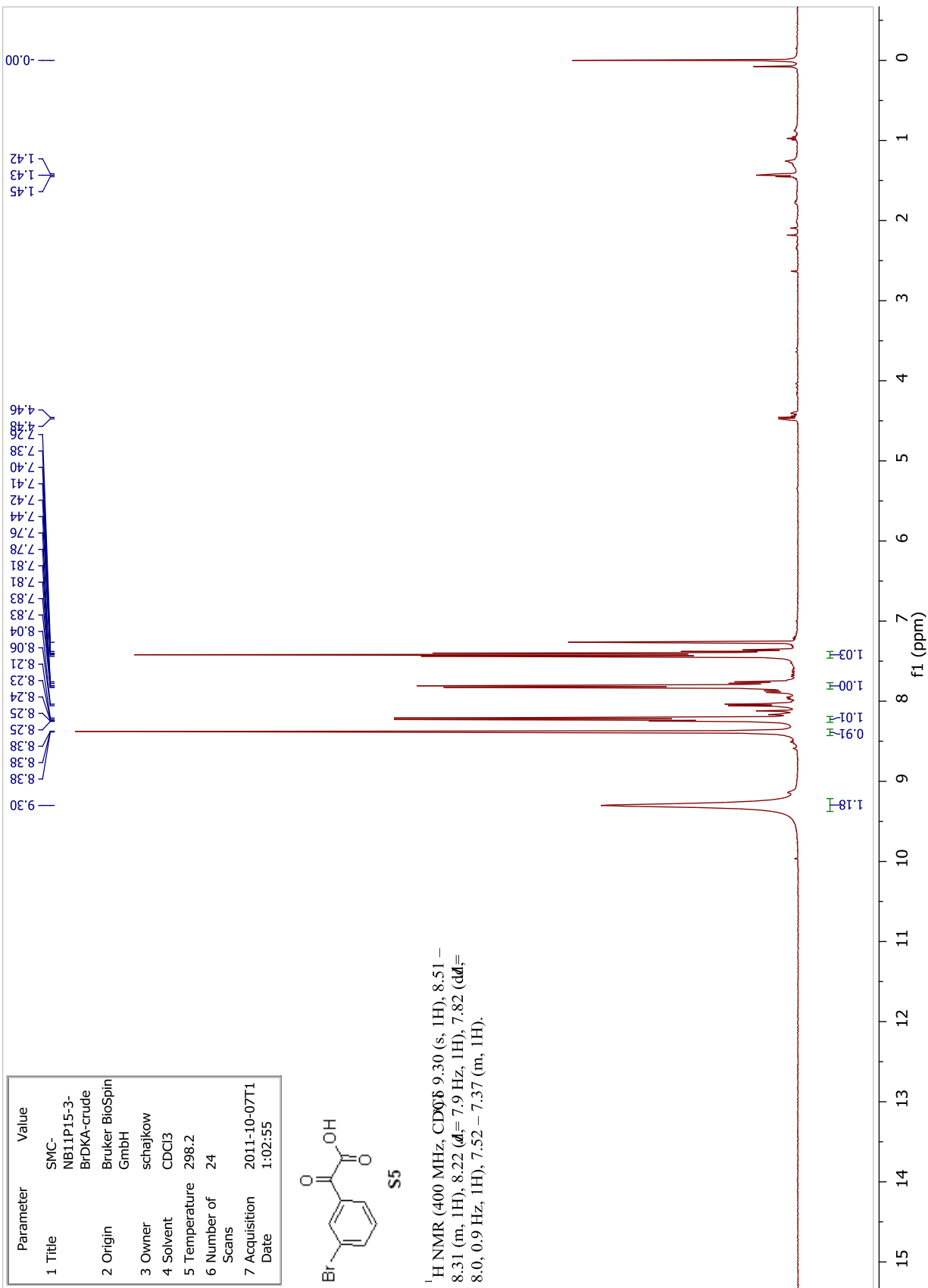
Parameter	Value
1 Title	SMC-NB11P20-4Br
2 Origin	Bruker BioSpin GmbH
3 Owner	schajkow
4 Solvent	CDCl3
5 Temperature	298.2
6 Number of Scans	230
7 Acquisition Date	2011-10-11T1 5:28:32

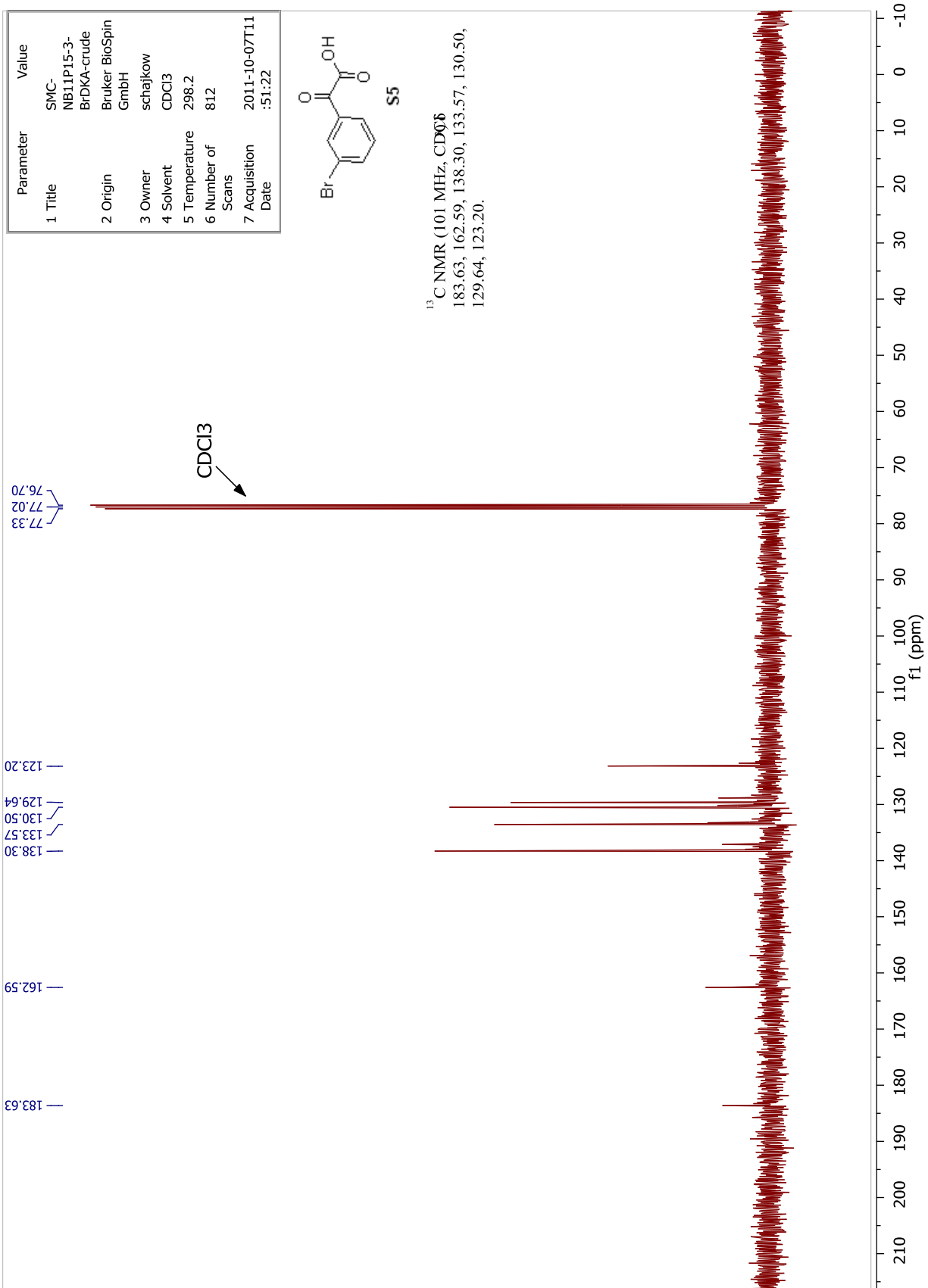


3.95

<sup>13</sup>C NMR (101 MHz, CDCl<sub>3</sub>) 132.97, 131.96, 129.36, 128.93, 128.58, 126.30, 126.11, 120.40, 117.78, 41.87.

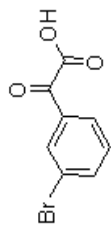






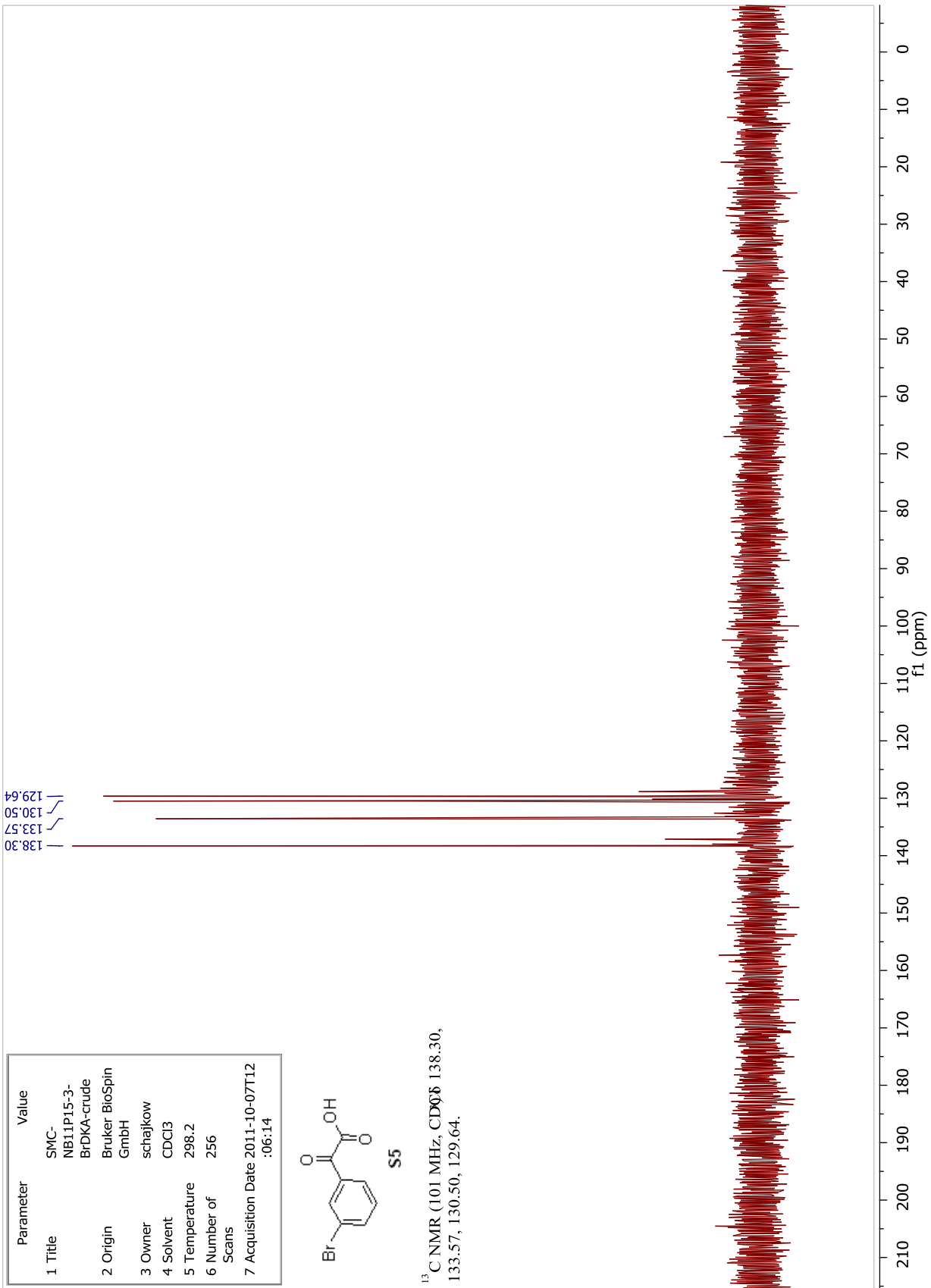


Parameter	Value
1 Title	SMC-NB11P15-3-BrDKA-crude
2 Origin	Bruker BioSpin GmbH
3 Owner	schajkow
4 Solvent	CDCl3
5 Temperature	298.2
6 Number of Scans	256
7 Acquisition Date	2011-10-07T12:06:14

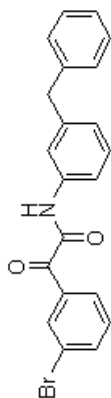


**S5**

<sup>13</sup>C NMR (101 MHz, CDCl<sub>3</sub>) 138.30, 133.57, 130.50, 129.64.

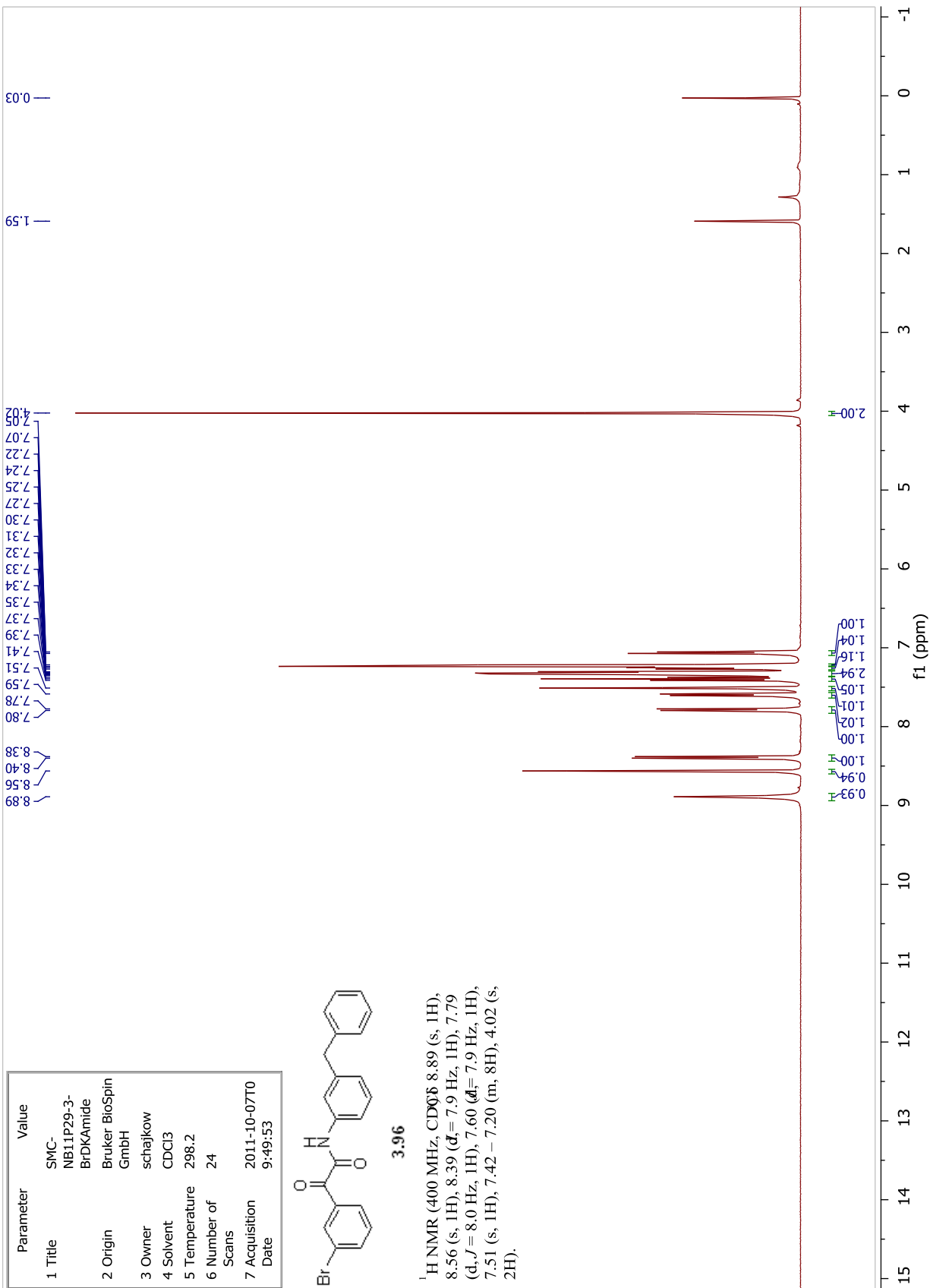


Parameter	Value
1 Title	SMC-NB11P29-3-BrDKAmide
2 Origin	Bruker BioSpin GmbH
3 Owner	schajkow
4 Solvent	CDCl3
5 Temperature	298.2
6 Number of Scans	24
7 Acquisition Date	2011-10-07T09:49:53

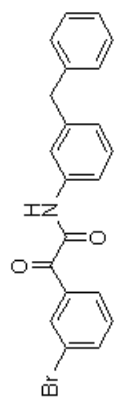


3.96

<sup>1</sup>H NMR (400 MHz, CDCl<sub>3</sub>) δ 8.89 (s, 1H), 8.56 (s, 1H), 8.39 (d, *d*<sub>1</sub> = 7.9 Hz, 1H), 7.79 (d, *J* = 8.0 Hz, 1H), 7.60 (d, *d*<sub>2</sub> = 7.9 Hz, 1H), 7.51 (s, 1H), 7.42 – 7.20 (m, 8H), 4.02 (s, 2H).

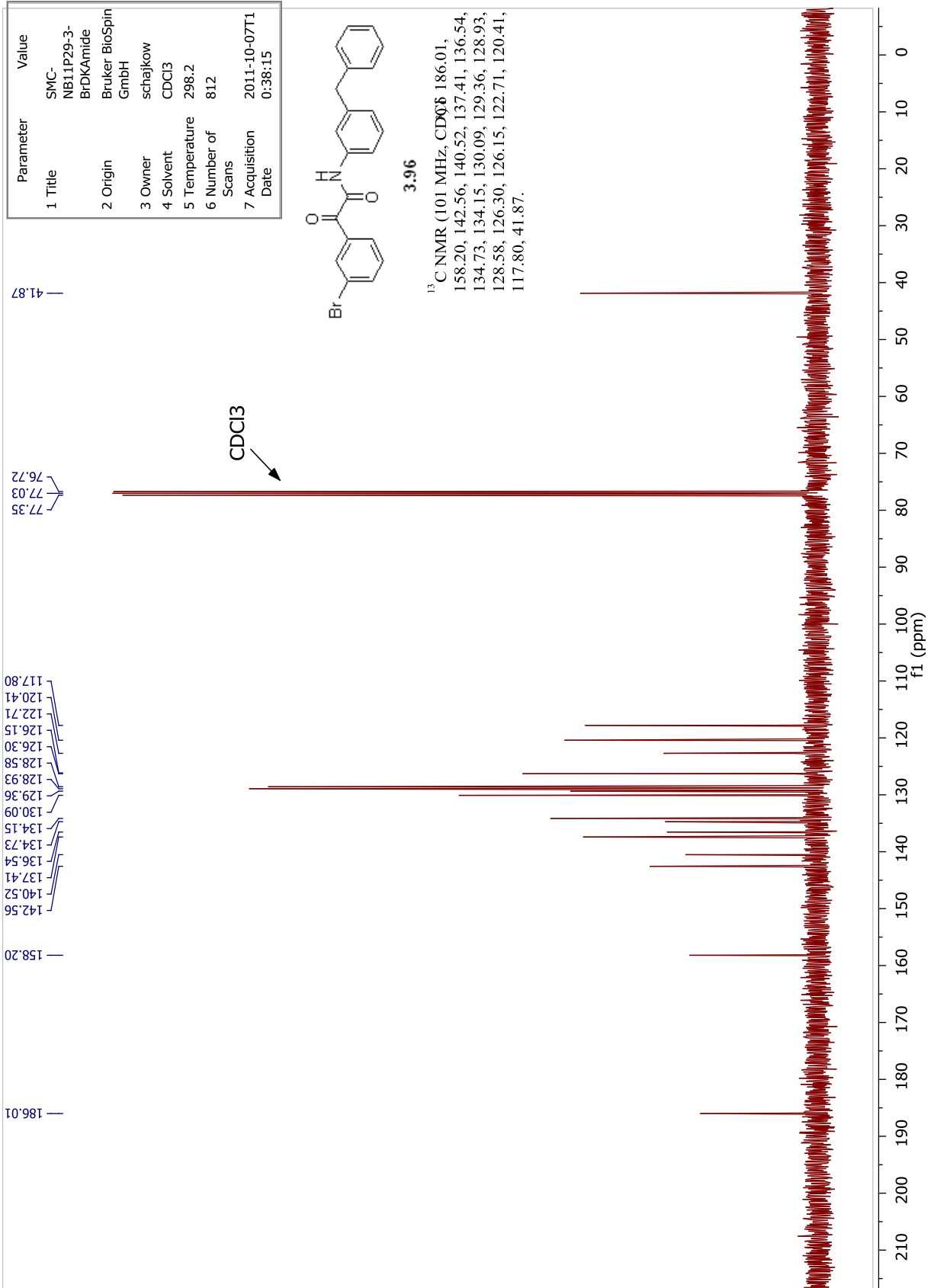


Parameter	Value
1 Title	SMC-NB11P29-3-BrDKAmide
2 Origin	Bruker BioSpin GmbH
3 Owner	schajkow
4 Solvent	CDCl3
5 Temperature	298.2
6 Number of Scans	812
7 Acquisition Date	2011-10-07T10:38:15

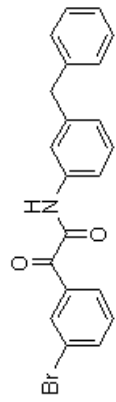


**3.96**

<sup>13</sup>C NMR (101 MHz, CDCl<sub>3</sub>) 186.01, 158.20, 142.56, 140.52, 137.41, 136.54, 134.73, 134.15, 130.09, 129.36, 128.93, 128.58, 126.30, 126.15, 122.71, 120.41, 117.80, 41.87.

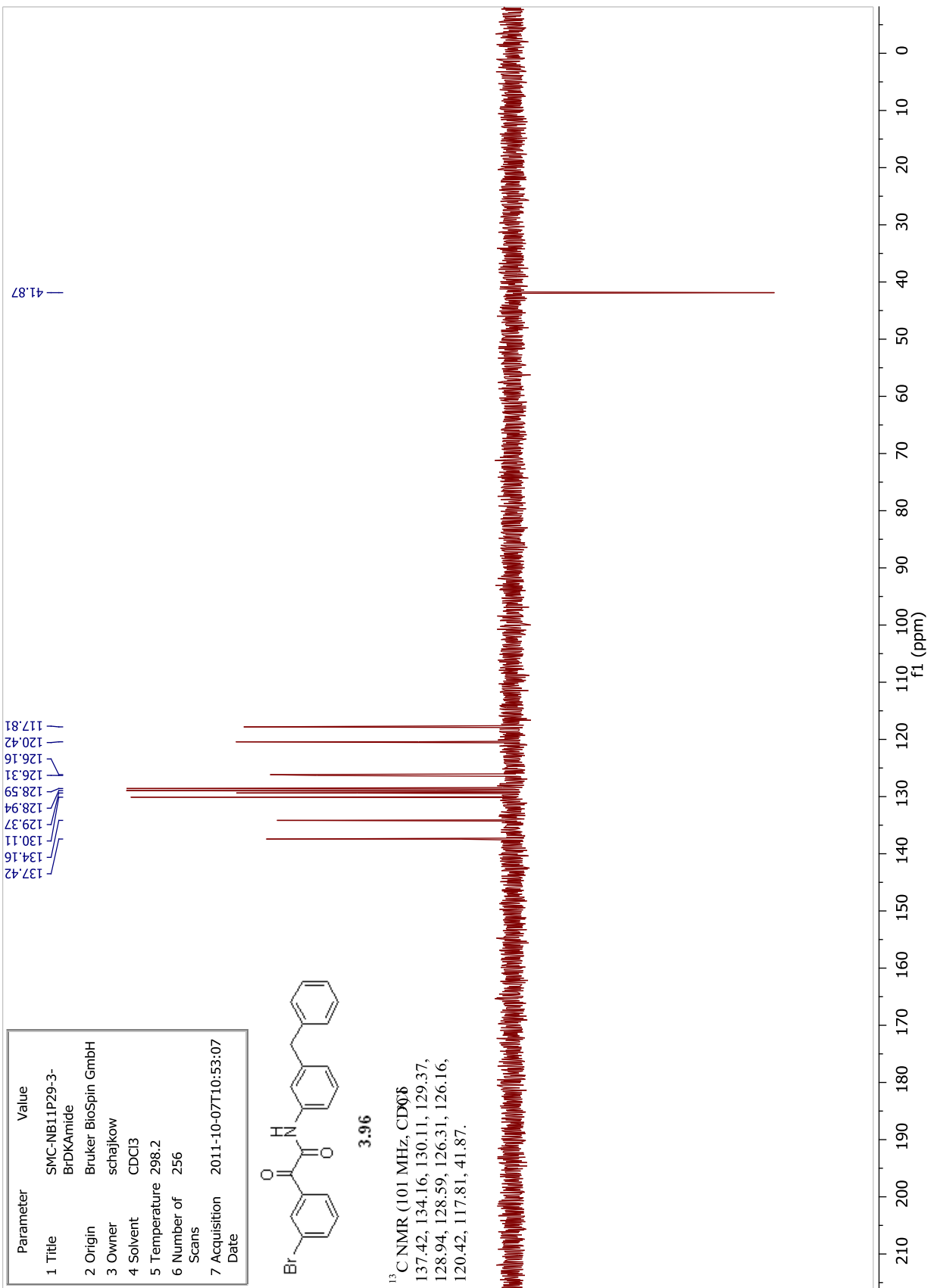


Parameter	Value
1 Title	SMC-NB11P29-3-BrDKAmide
2 Origin	Bruker BioSpin GmbH
3 Owner	schajkow
4 Solvent	CDCl3
5 Temperature	298.2
6 Number of Scans	256
7 Acquisition Date	2011-10-07T10:53:07

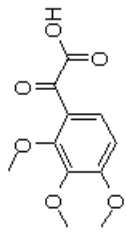


3.96

<sup>13</sup>C NMR (101 MHz, CDCl<sub>3</sub>)  
 137.42, 134.16, 130.11, 129.37,  
 128.94, 128.59, 126.31, 126.16,  
 120.42, 117.81, 41.87.

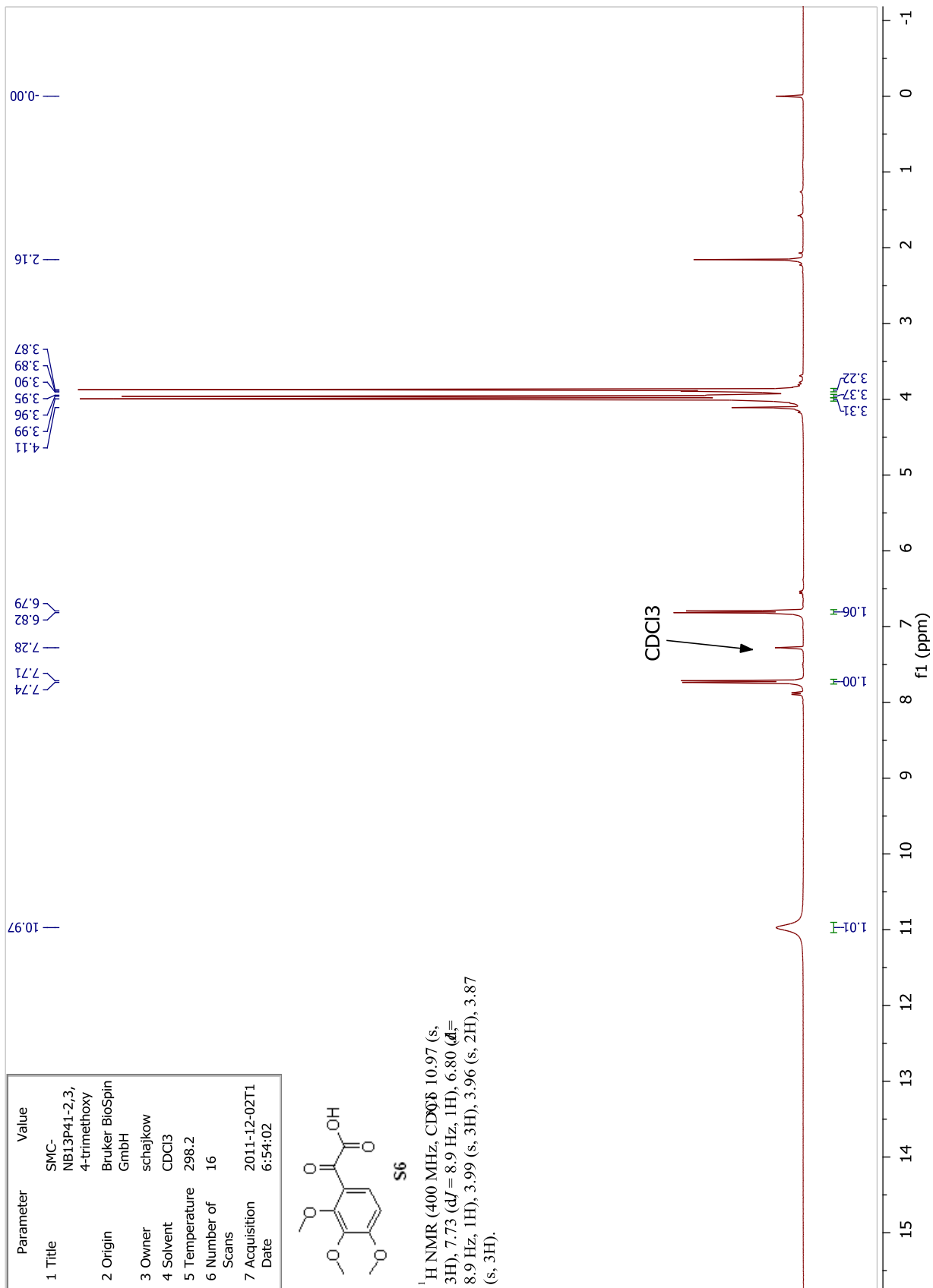


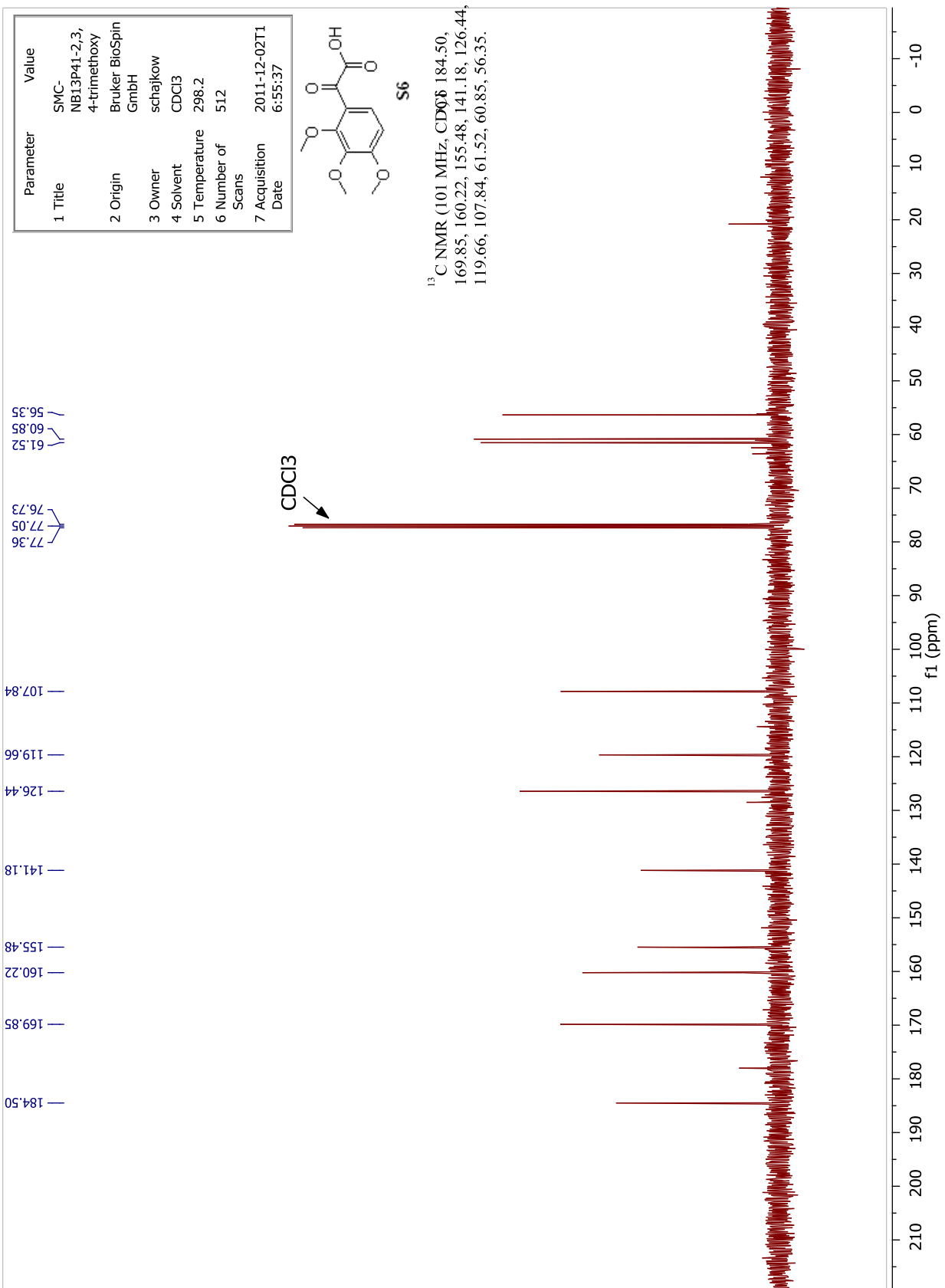
Parameter	Value
1 Title	SMC-NB13P41-2,3,4-trimethoxy
2 Origin	Bruker BioSpin GmbH
3 Owner	schajkowi
4 Solvent	CDCl <sub>3</sub>
5 Temperature	298.2
6 Number of Scans	16
7 Acquisition Date	2011-12-02T16:54:02



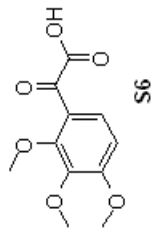
**S6**

<sup>1</sup>H NMR (400 MHz, CDCl<sub>3</sub>) 10.97 (s, 3H), 7.73 (dJ = 8.9 Hz, 1H), 6.80 (d, 8.9 Hz, 1H), 3.99 (s, 3H), 3.96 (s, 2H), 3.87 (s, 3H).



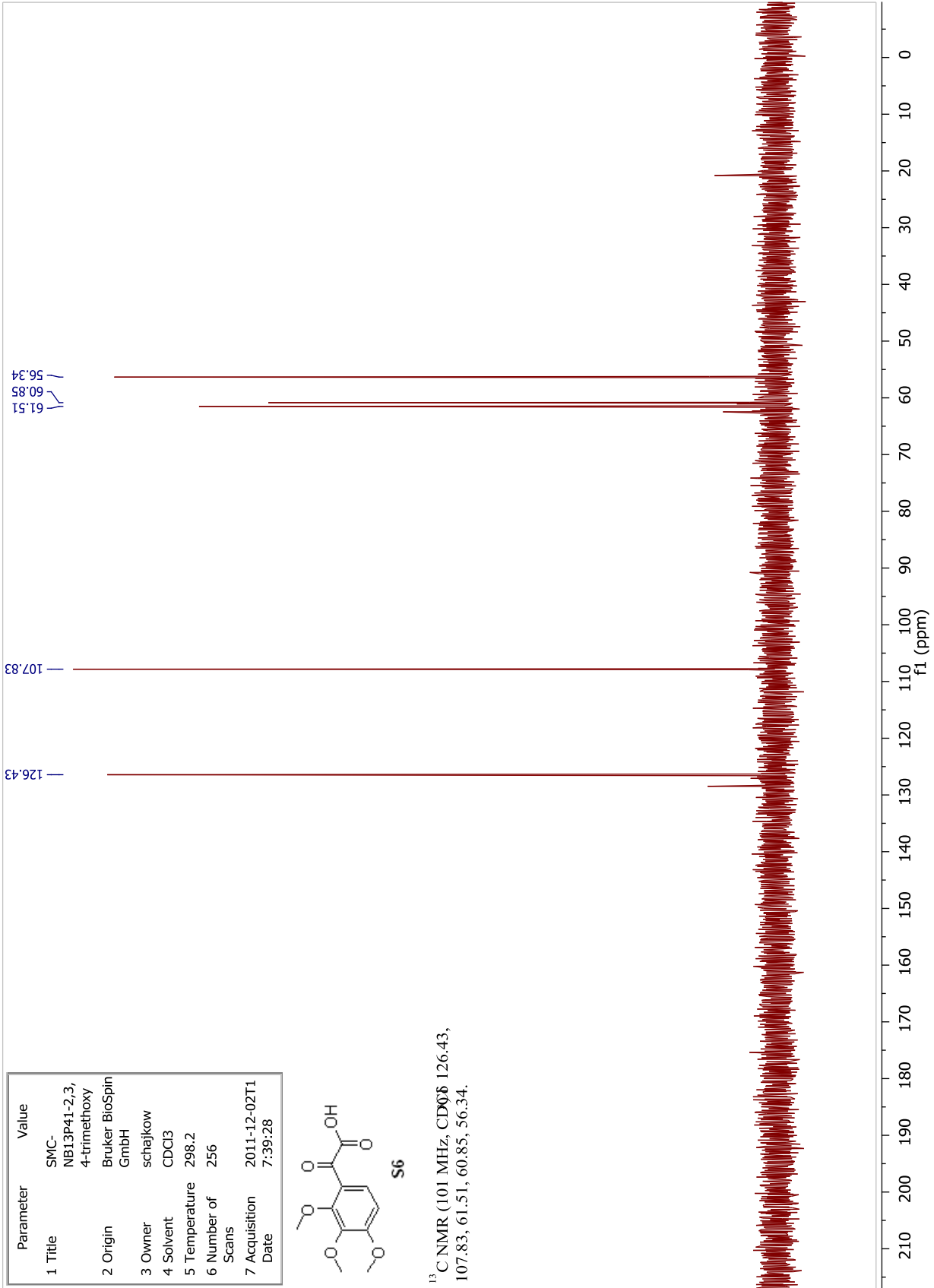


Parameter	Value
1 Title	SMC-NB13P41-2,3,4-trimethoxy
2 Origin	Bruker BioSpin GmbH
3 Owner	schajkowi
4 Solvent	CDCl <sub>3</sub>
5 Temperature	298.2
6 Number of Scans	256
7 Acquisition Date	2011-12-02T17:39:28

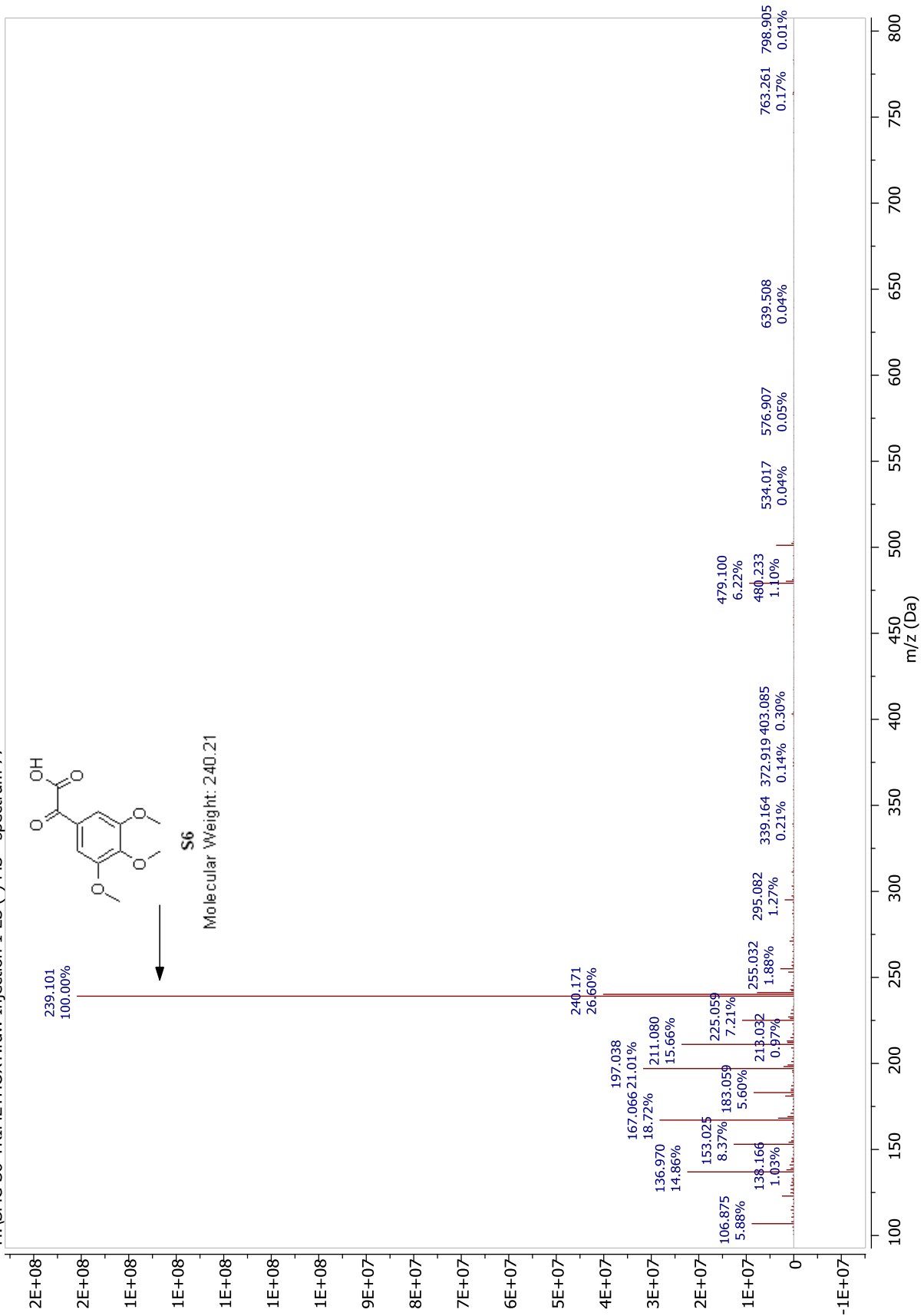


S6

<sup>13</sup>C NMR (101 MHz, CDCl<sub>3</sub>) 126.43, 107.83, 61.51, 60.85, 56.34.

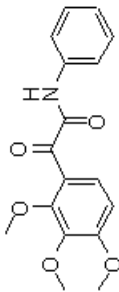


H:\SMC-S6-TRIMETHOXY.raw Injection 1 ES (-) MS - spectrum 77



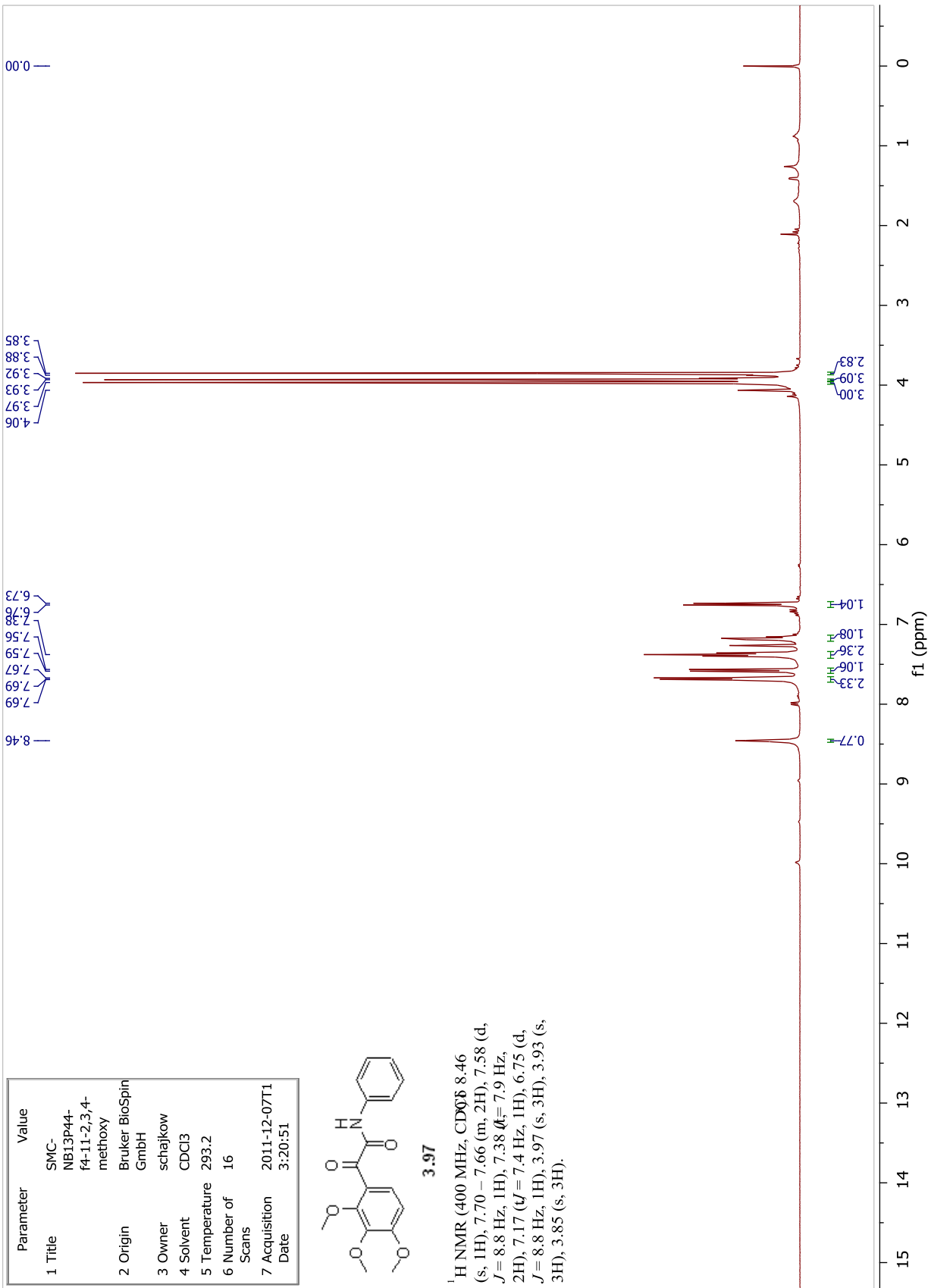


Parameter	Value
1 Title	SMC- NB13P44- f4-11-2,3,4- methoxy
2 Origin	Bruker BioSpin GmbH
3 Owner	schajkow
4 Solvent	CDCl <sub>3</sub>
5 Temperature	293.2
6 Number of Scans	16
7 Acquisition Date	2011-12-07T1 3:20:51

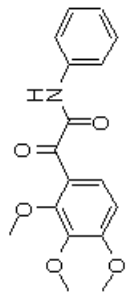


**3.97**

<sup>1</sup>H NMR (400 MHz, CDCl<sub>3</sub>) δ 8.46 (s, 1H), 7.70 – 7.66 (m, 2H), 7.58 (d, *J* = 8.8 Hz, 1H), 7.38 (t, *J* = 7.9 Hz, 2H), 7.17 (t, *J* = 7.4 Hz, 1H), 6.75 (d, *J* = 8.8 Hz, 1H), 3.97 (s, 3H), 3.93 (s, 3H), 3.85 (s, 3H).

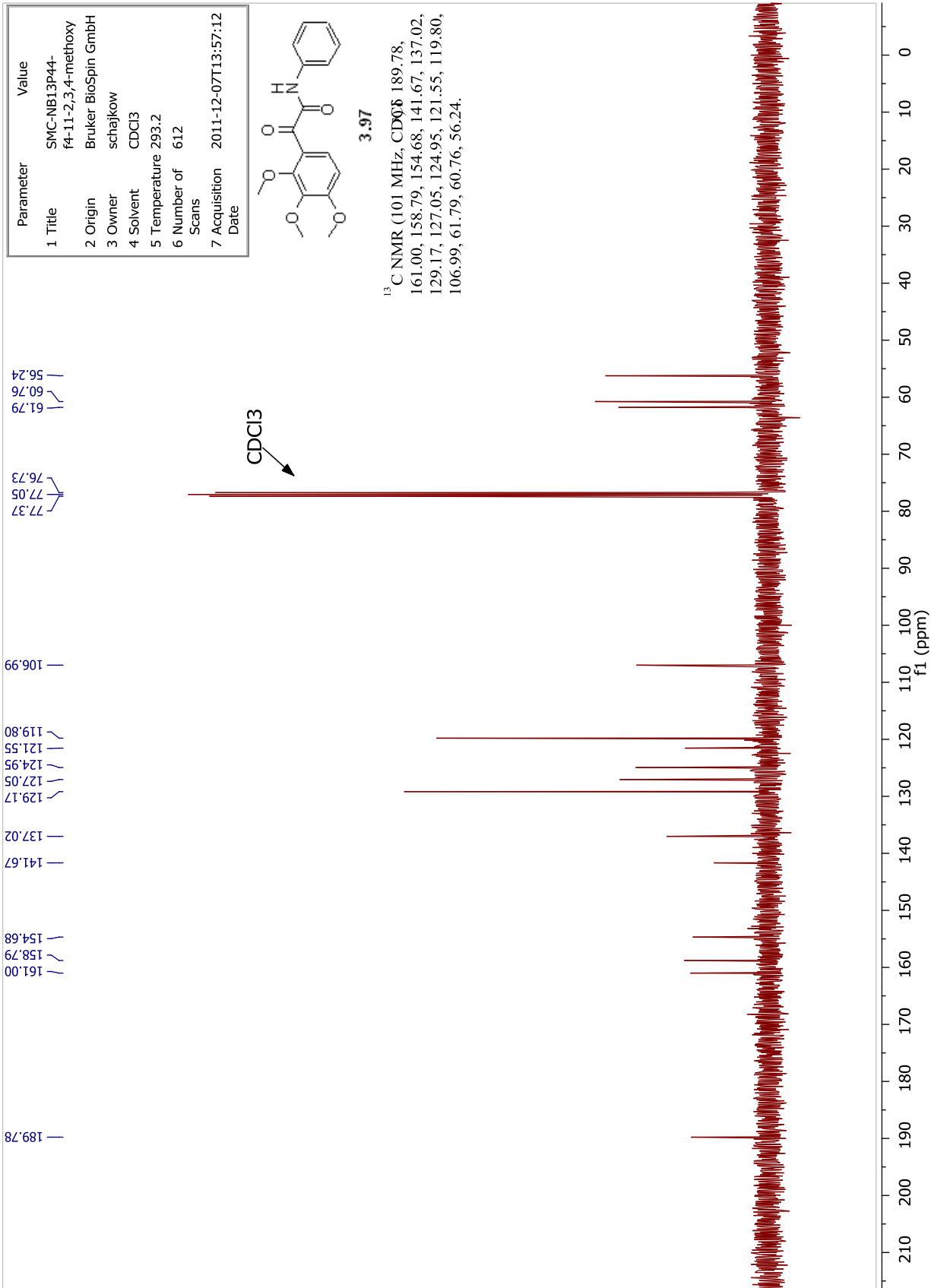


Parameter	Value
1 Title	SMC-NB13P44-f4-11-2,3,4-methoxy
2 Origin	Bruker BioSpin GmbH
3 Owner	schajkow
4 Solvent	CDCl3
5 Temperature	293.2
6 Number of Scans	612
7 Acquisition Date	2011-12-07T13:57:12

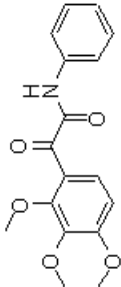


3.97

<sup>13</sup>C NMR (101 MHz, CDCl<sub>3</sub>) 189.78, 161.00, 158.79, 154.68, 141.67, 137.02, 129.17, 127.05, 124.95, 121.55, 119.80, 106.99, 61.79, 60.76, 56.24.

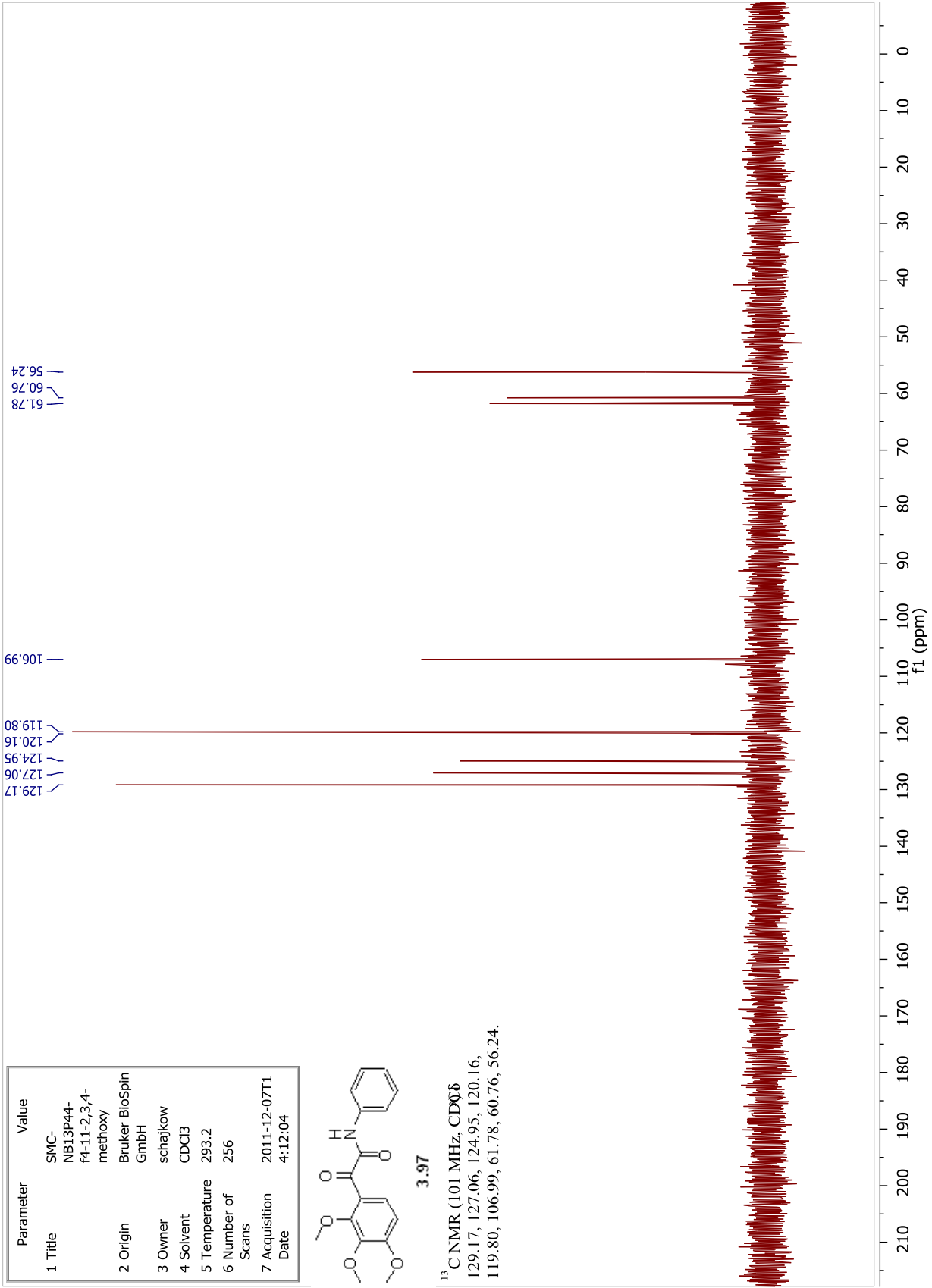


Parameter	Value
1 Title	SMC-NB13P44-f4-11-2,3,4-methoxy
2 Origin	Bruker BioSpin GmbH
3 Owner	schajkow
4 Solvent	CDCl <sub>3</sub>
5 Temperature	293.2
6 Number of Scans	256
7 Acquisition Date	2011-12-07T14:12:04

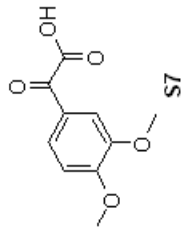


3.97

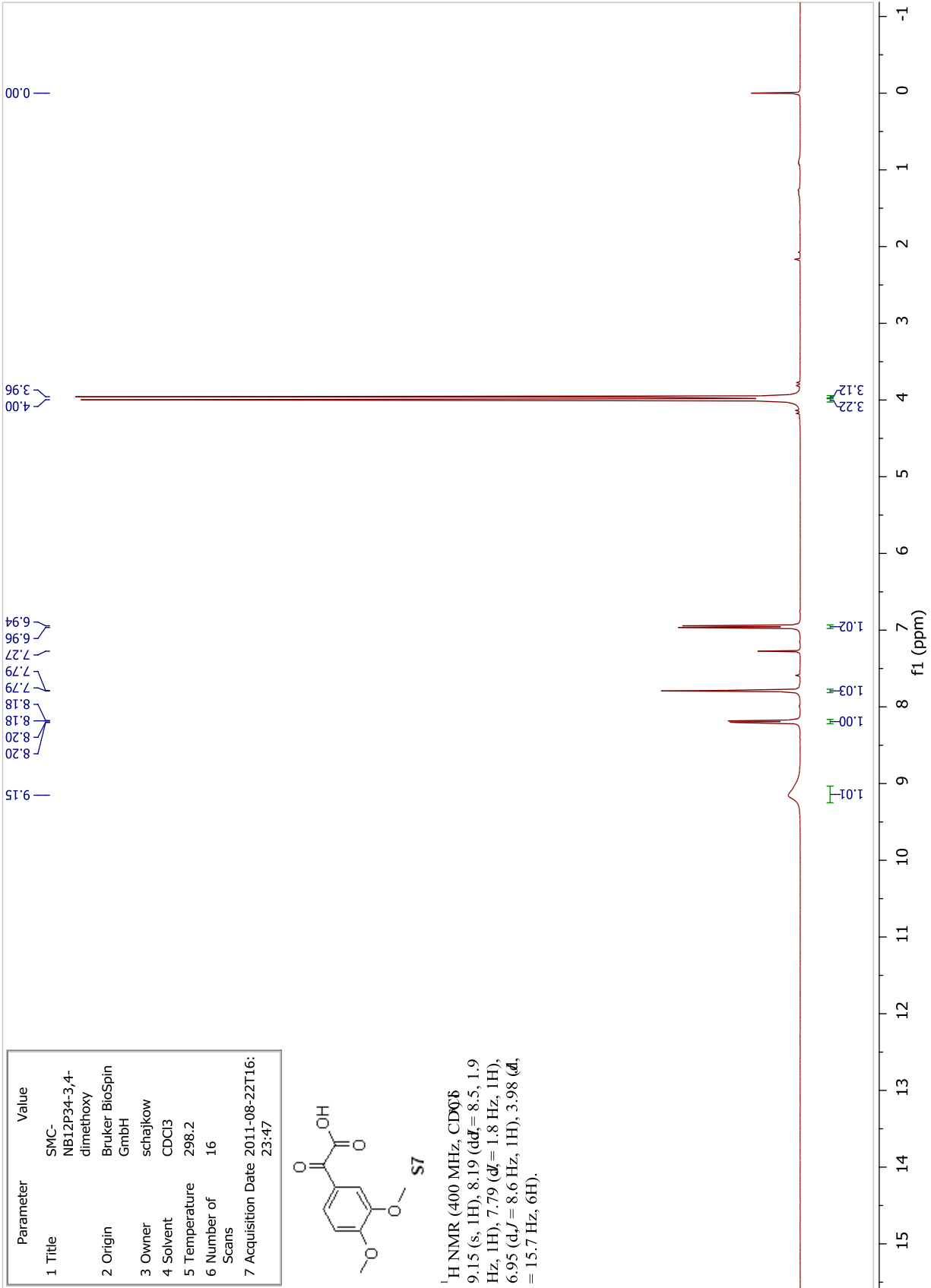
<sup>13</sup>C NMR (101 MHz, CDCl<sub>3</sub>)  
 129.17, 127.06, 124.95, 120.16,  
 119.80, 106.99, 61.78, 60.76, 56.24.



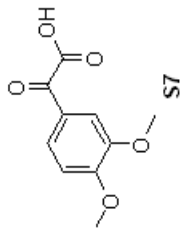
Parameter	Value
1 Title	SMC-NB12P34-3,4-dimethoxy
2 Origin	Bruker BioSpin GmbH
3 Owner	schajkowi
4 Solvent	CDCl <sub>3</sub>
5 Temperature	298.2
6 Number of Scans	16
7 Acquisition Date	2011-08-22T16:23:47



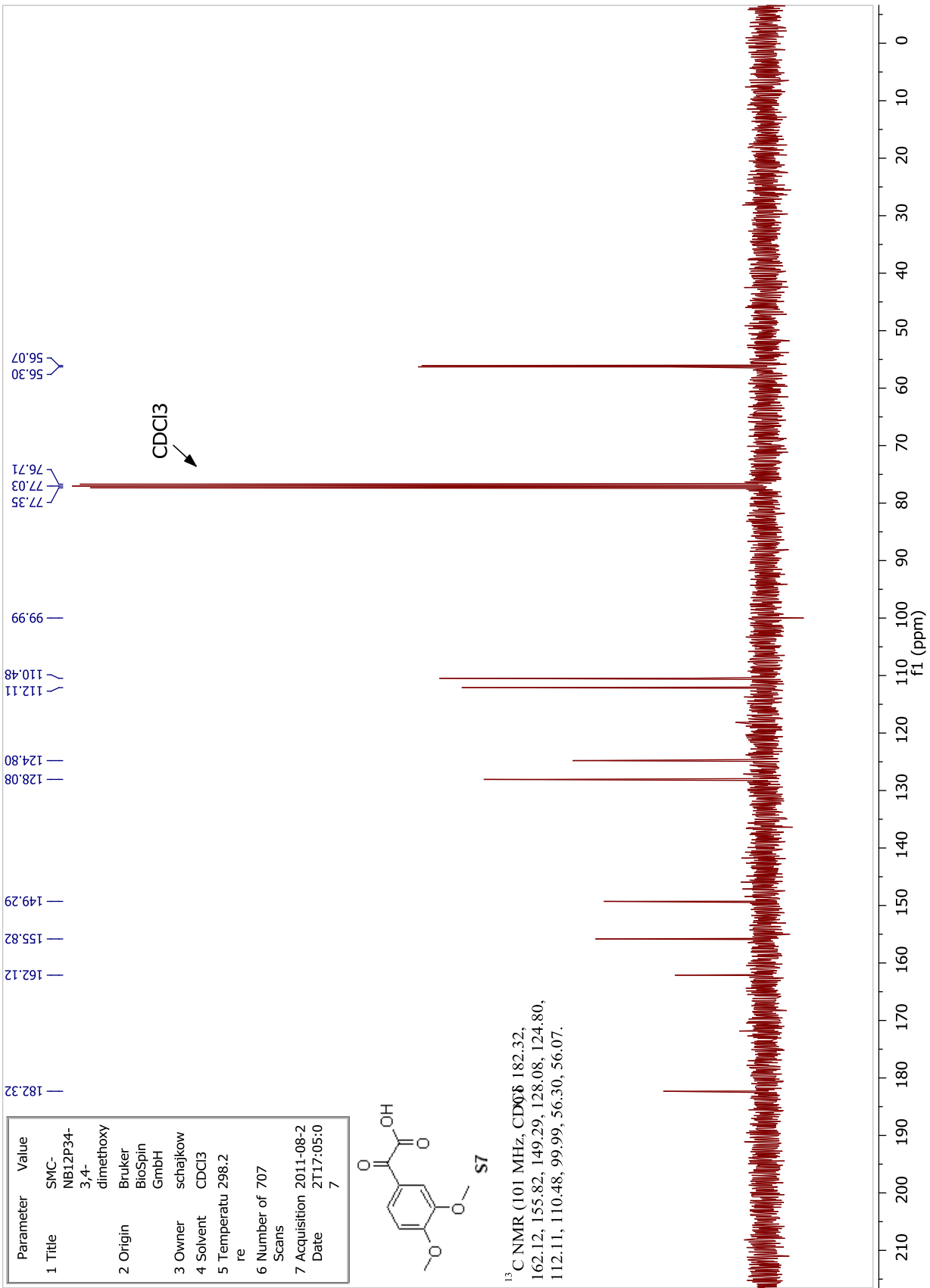
<sup>1</sup>H NMR (400 MHz, CDCl<sub>3</sub>)  
 9.15 (s, 1H), 8.19 (dd, *d*<sub>H</sub> = 8.5, 1.9 Hz, 1H), 7.79 (d, *d*<sub>H</sub> = 1.8 Hz, 1H), 6.95 (d, *J* = 8.6 Hz, 1H), 3.98 (d, *J* = 15.7 Hz, 6H).



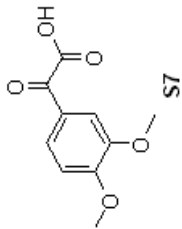
Parameter	Value
1 Title	SMC-NB12P34-3,4-dimethoxy
2 Origin	Bruker BioSpin GmbH
3 Owner	schajkowie
4 Solvent	CDCl <sub>3</sub>
5 Temperature	298.2
6 Number of Scans	707
7 Acquisition Date	2011-08-21 17:05:07



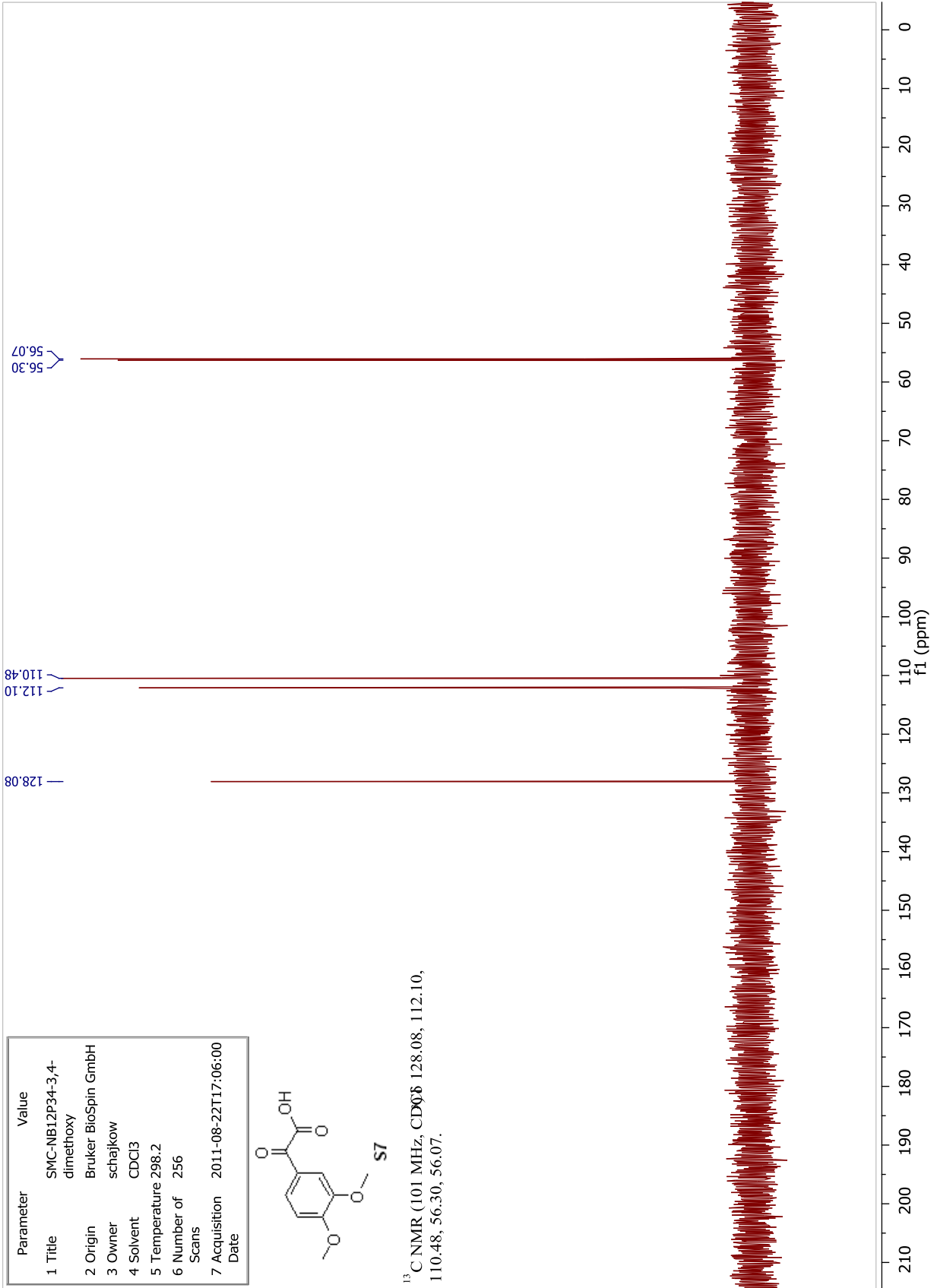
<sup>13</sup>C NMR (101 MHz, CDCl<sub>3</sub>) δ 182.32, 162.12, 155.82, 149.29, 128.08, 124.80, 112.11, 110.48, 99.99, 56.30, 56.07.



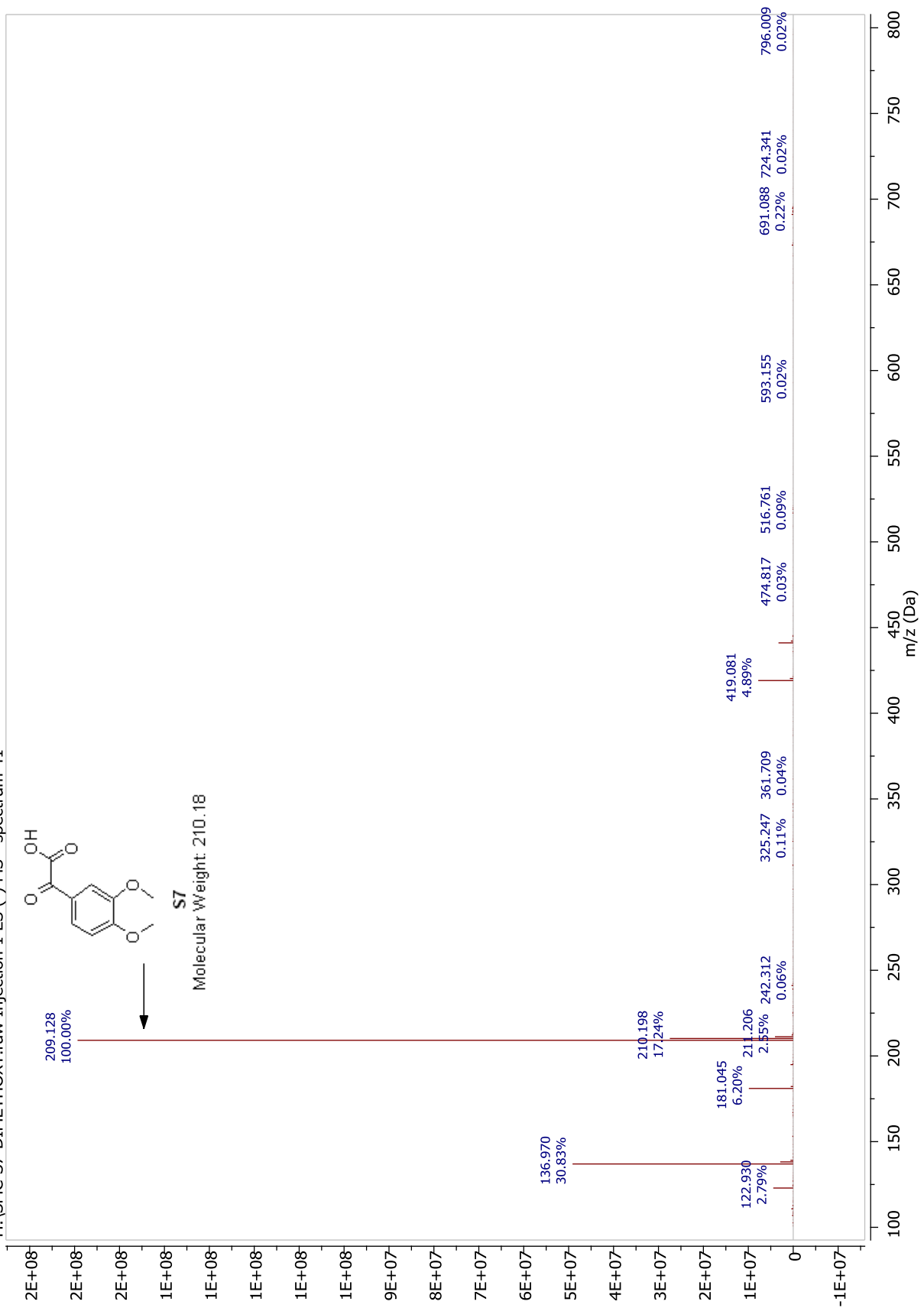
Parameter	Value
1 Title	SMC-NB12P34-3,4-dimethoxy
2 Origin	Bruker BioSpin GmbH
3 Owner	schajkow
4 Solvent	CDCl3
5 Temperature	298.2
6 Number of Scans	256
7 Acquisition Date	2011-08-22T17:06:00



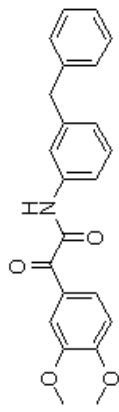
<sup>13</sup>C NMR (101 MHz, CDCl<sub>3</sub>) 128.08, 112.10, 110.48, 56.30, 56.07.



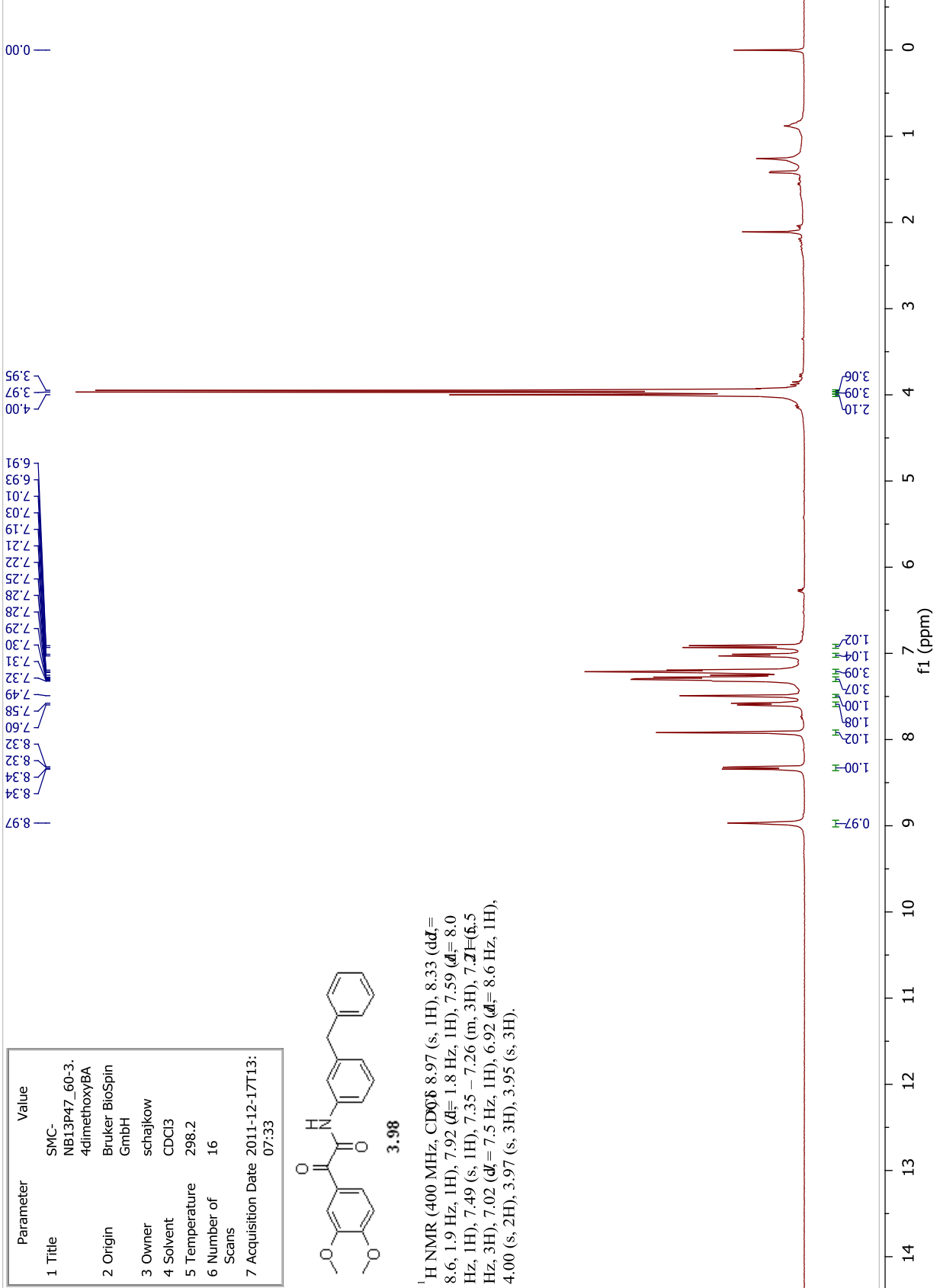
H:\SMC-S7-DIMETHOXY.raw Injection 1 ES (-) MS - spectrum 41



Parameter	Value
1 Title	SMC-NB13P47_60-3-4dimethoxyBA
2 Origin	Bruker BioSpin GmbH
3 Owner	schajkowi
4 Solvent	CDCl3
5 Temperature	298.2
6 Number of Scans	16
7 Acquisition Date	2011-12-17T13:07:33

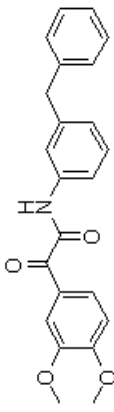


<sup>1</sup>H NMR (400 MHz, CDCl<sub>3</sub>) δ 8.97 (s, 1H), 8.33 (dd, = 8.6, 1.9 Hz, 1H), 7.92 (d, = 1.8 Hz, 1H), 7.59 (d, = 8.0 Hz, 1H), 7.49 (s, 1H), 7.35 – 7.26 (m, 3H), 7.21 (s, 3H), 7.02 (d, = 7.5 Hz, 1H), 6.92 (d, = 8.6 Hz, 1H), 4.00 (s, 2H), 3.97 (s, 3H), 3.95 (s, 3H).



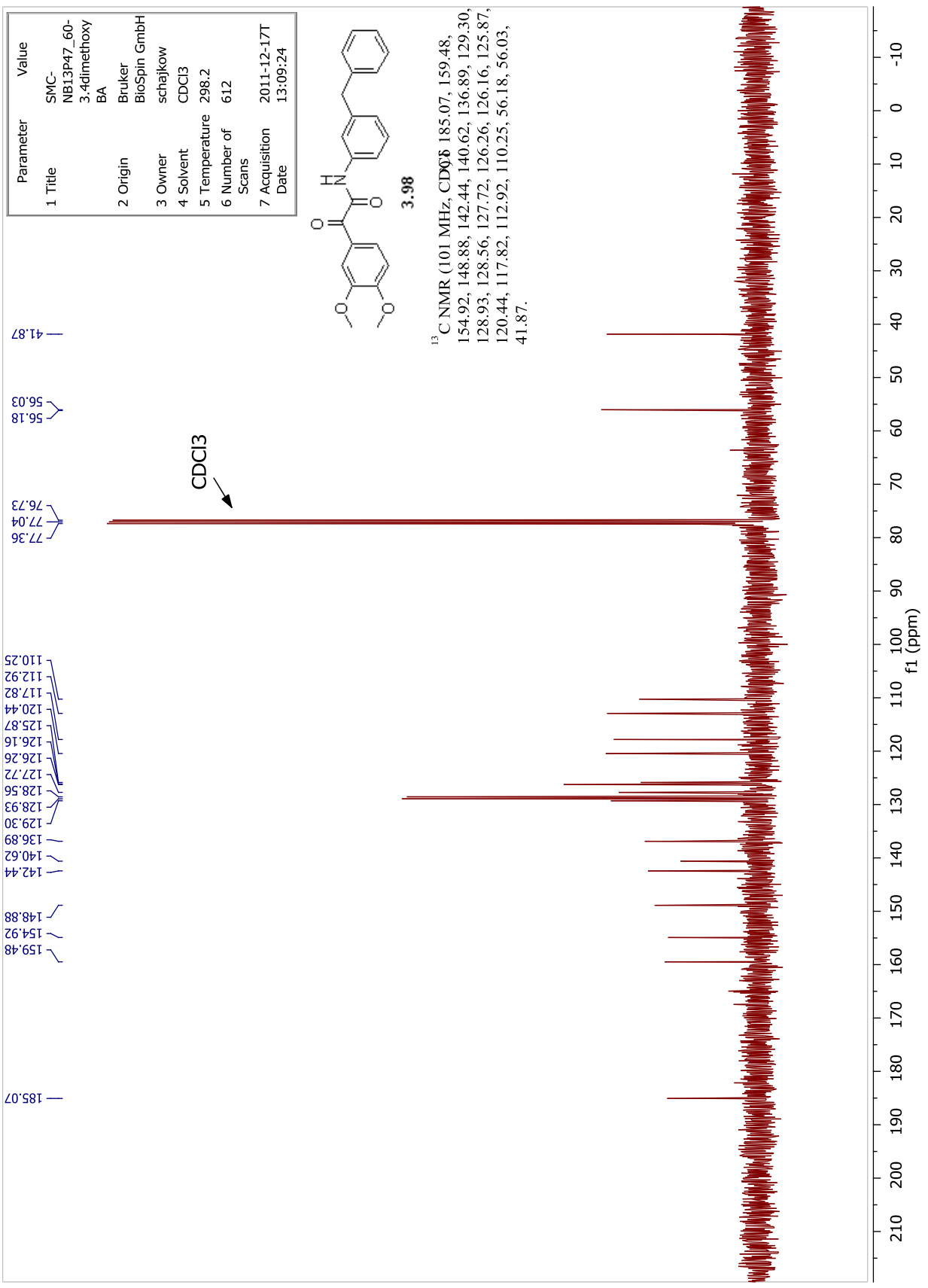


Parameter	Value
1 Title	SMC-NB13P47_60-3-4dimethoxy BA
2 Origin	Bruker BioSpin GmbH
3 Owner	schajkow
4 Solvent	CDCl3
5 Temperature	298.2
6 Number of Scans	612
7 Acquisition Date	2011-12-17T13:09:24

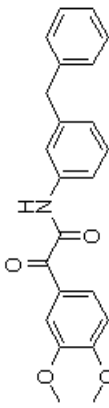


**3.98**

<sup>13</sup>C NMR (101 MHz, CDCl<sub>3</sub>) δ 185.07, 159.48, 154.92, 148.88, 142.44, 140.62, 136.89, 129.30, 128.93, 128.56, 127.72, 126.26, 126.16, 125.87, 120.44, 117.82, 112.92, 110.25, 56.18, 56.03, 41.87.

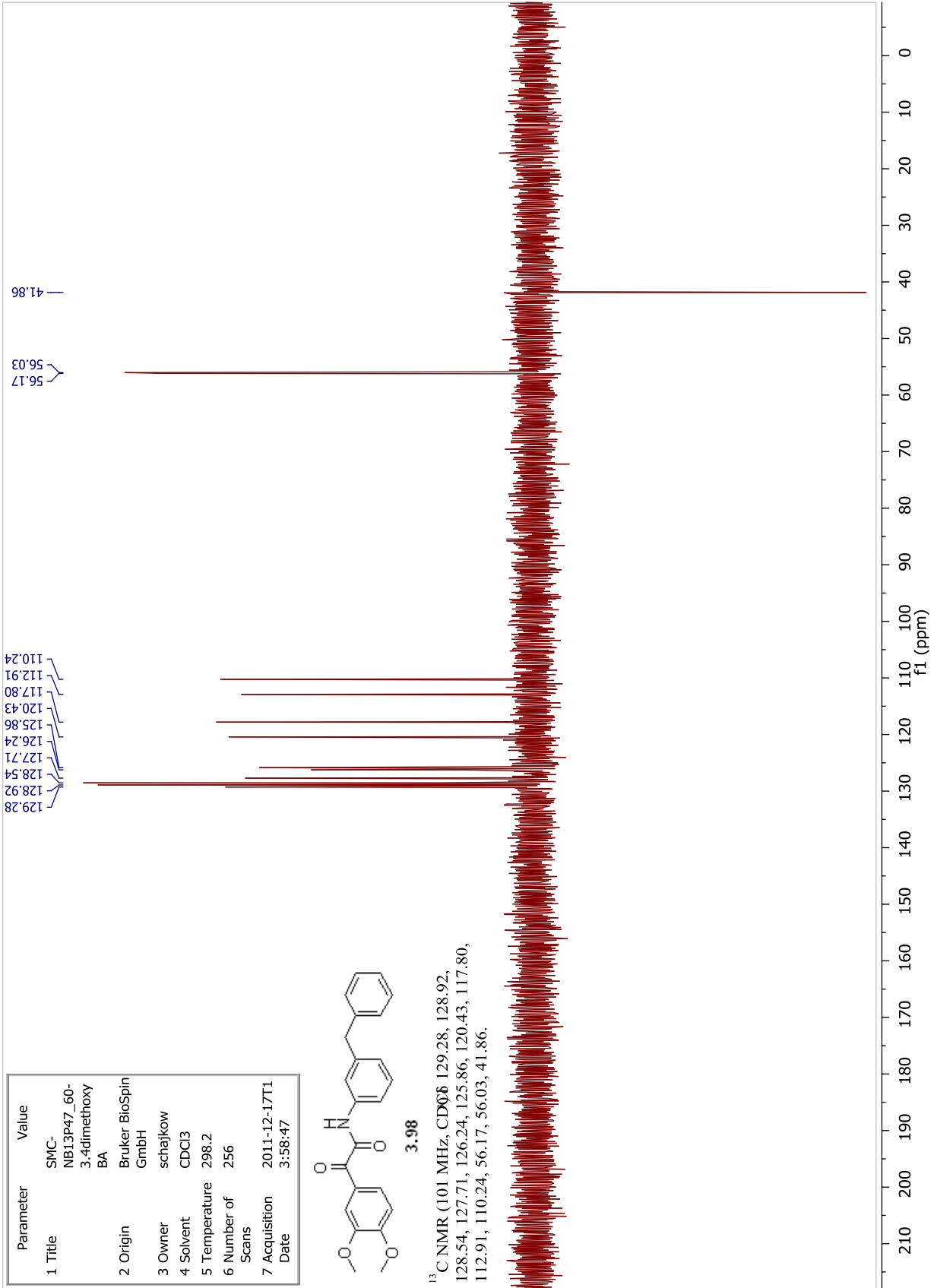


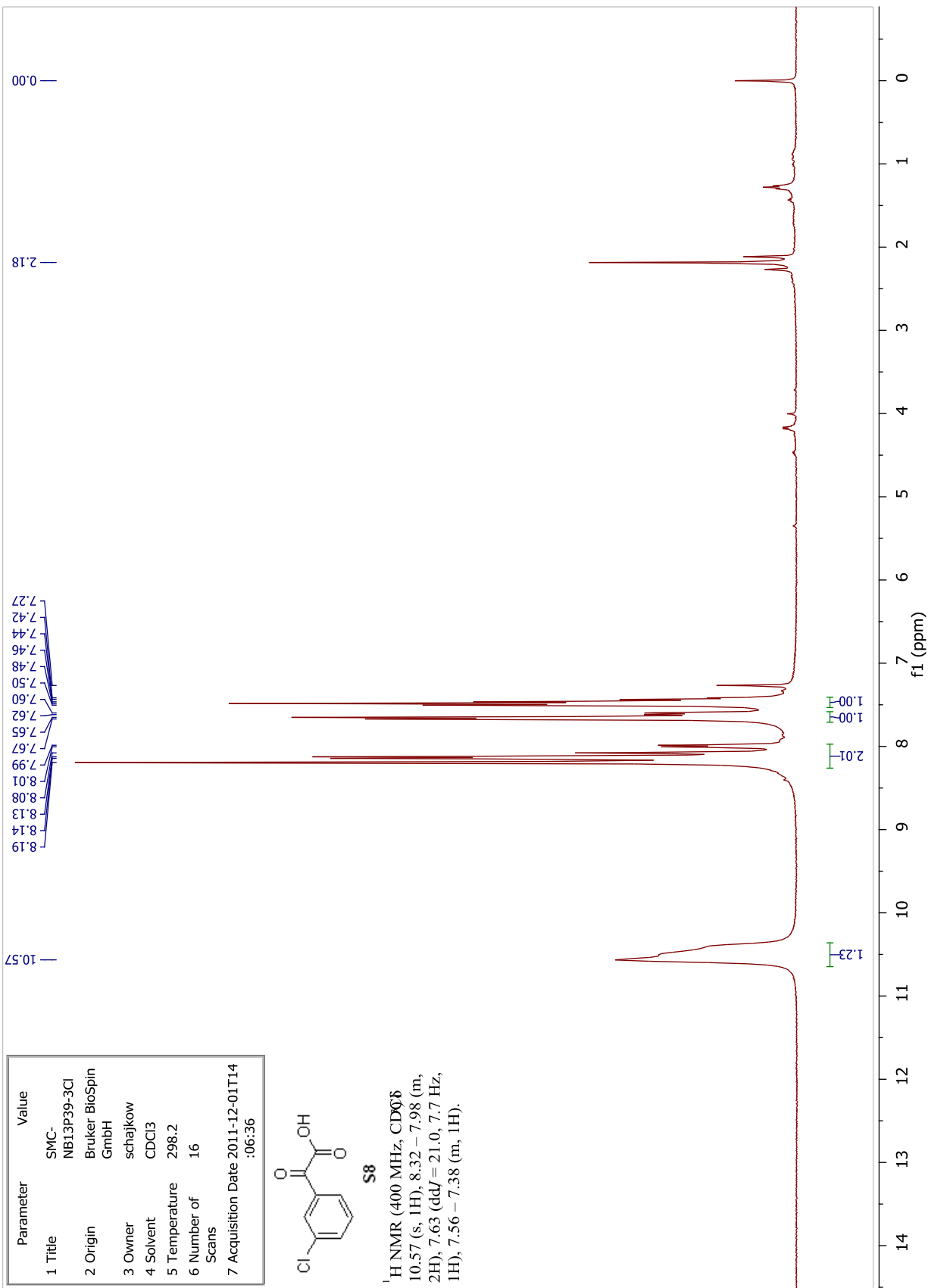
Parameter	Value
1 Title	SMC- NB13P47_60- 3,4-dimethoxy BA
2 Origin	Bruker BioSpin GmbH
3 Owner	schajkow
4 Solvent	CDCl3
5 Temperature	298.2
6 Number of Scans	256
7 Acquisition Date	2011-12-17T1 3:58:47



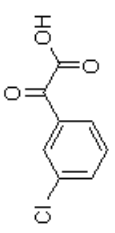
3.98

<sup>13</sup>C NMR (101 MHz, CDCl<sub>3</sub>) 129.28, 128.92, 128.54, 127.71, 126.24, 125.86, 120.43, 117.80, 112.91, 110.24, 56.17, 56.03, 41.86.





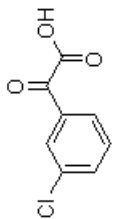
Parameter	Value
1 Title	SMC-NB13P39-3Cl
2 Origin	Bruker BioSpin GmbH
3 Owner	schajkow
4 Solvent	CDCl3
5 Temperature	298.2
6 Number of Scans	16
7 Acquisition Date	2011-12-01T14:06:36



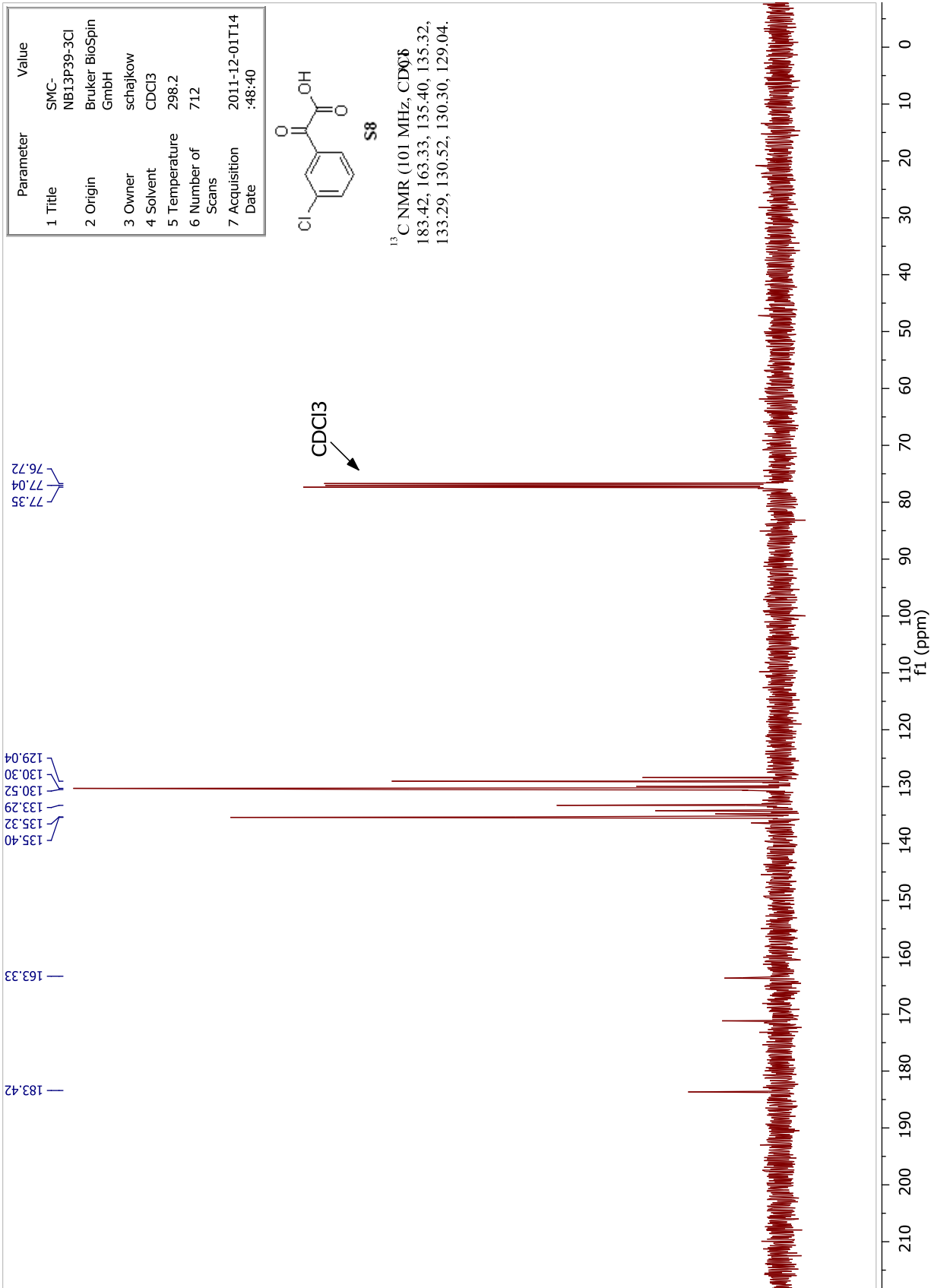
S8

<sup>1</sup>H NMR (400 MHz, CDCl<sub>3</sub>)  
 10.57 (s, 1H), 8.32 – 7.98 (m, 2H), 7.63 (dd, J = 21.0, 7.7 Hz, 1H), 7.56 – 7.38 (m, 1H).

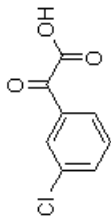
Parameter	Value
1 Title	SMC-NB13P39-3CI
2 Origin	Bruker BioSpin GmbH
3 Owner	schajkowi
4 Solvent	CDCl <sub>3</sub>
5 Temperature	298.2
6 Number of Scans	712
7 Acquisition Date	2011-12-01T14:48:40



<sup>13</sup>C NMR (101 MHz, CDCl<sub>3</sub>)  
 183.42, 163.33, 135.40, 135.32,  
 133.29, 130.52, 130.30, 129.04.

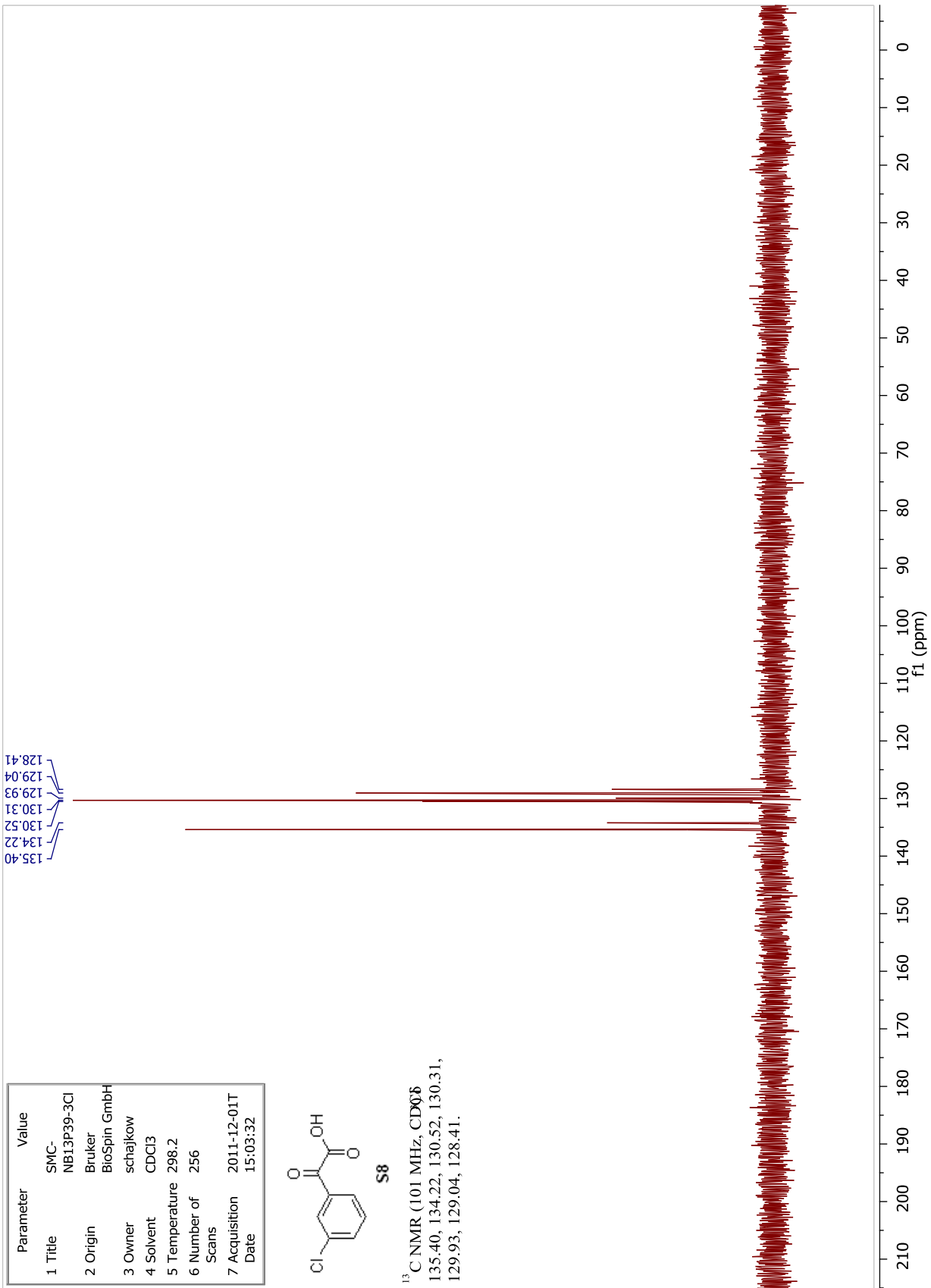


Parameter	Value
1 Title	SMC-NB13P39-3Cl
2 Origin	Bruker BioSpin GmbH
3 Owner	schajkow
4 Solvent	CDCl3
5 Temperature	298.2
6 Number of Scans	256
7 Acquisition Date	2011-12-01T15:03:32

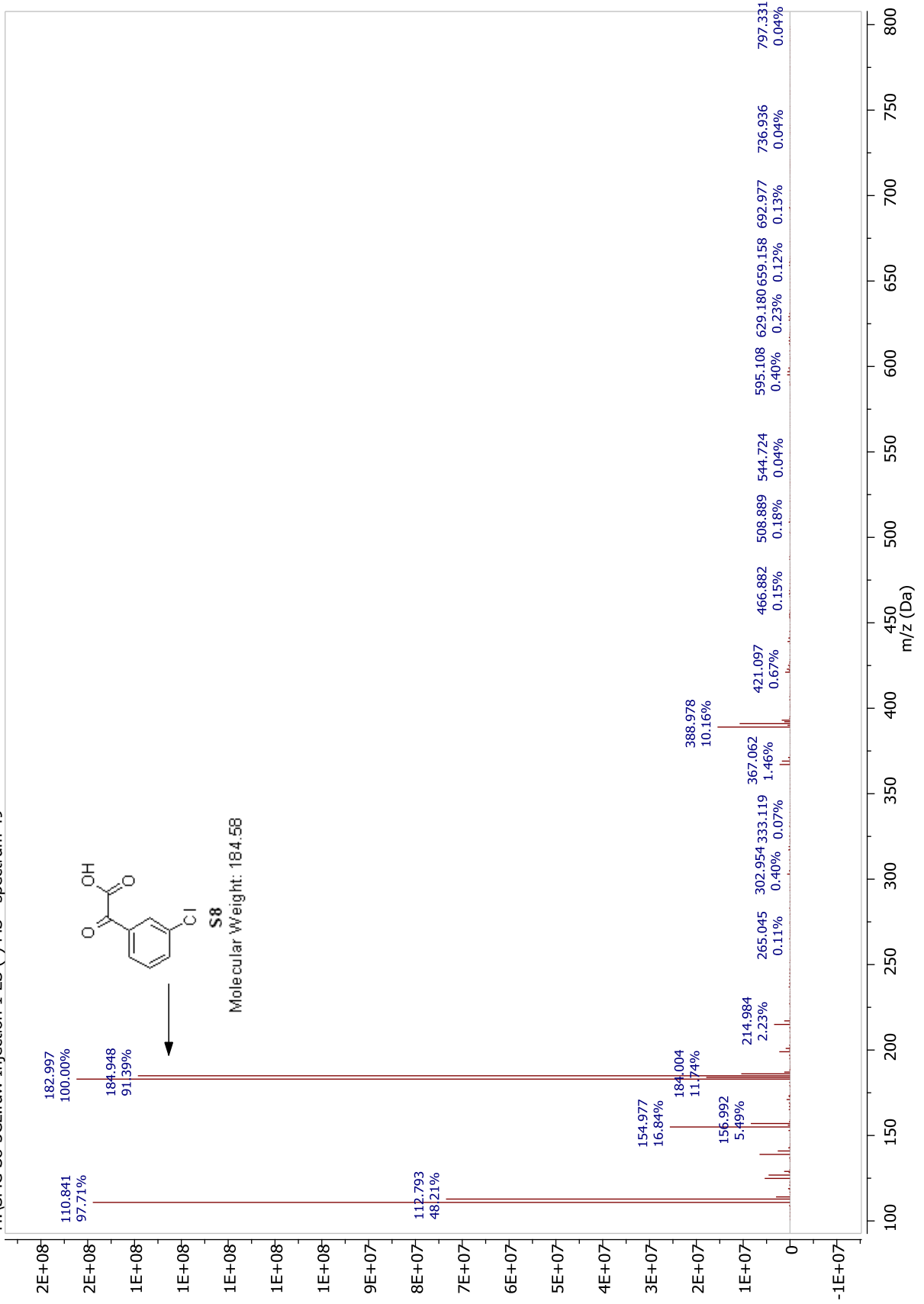


S8

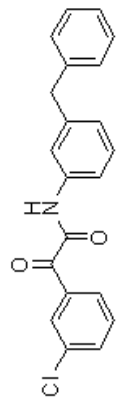
<sup>13</sup>C NMR (101 MHz, CDCl<sub>3</sub>)  
 135.40, 134.22, 130.52, 130.31,  
 129.93, 129.04, 128.41.



H:\SMC-S8-3CL.raw Injection 1 ES (-) MS - spectrum 49

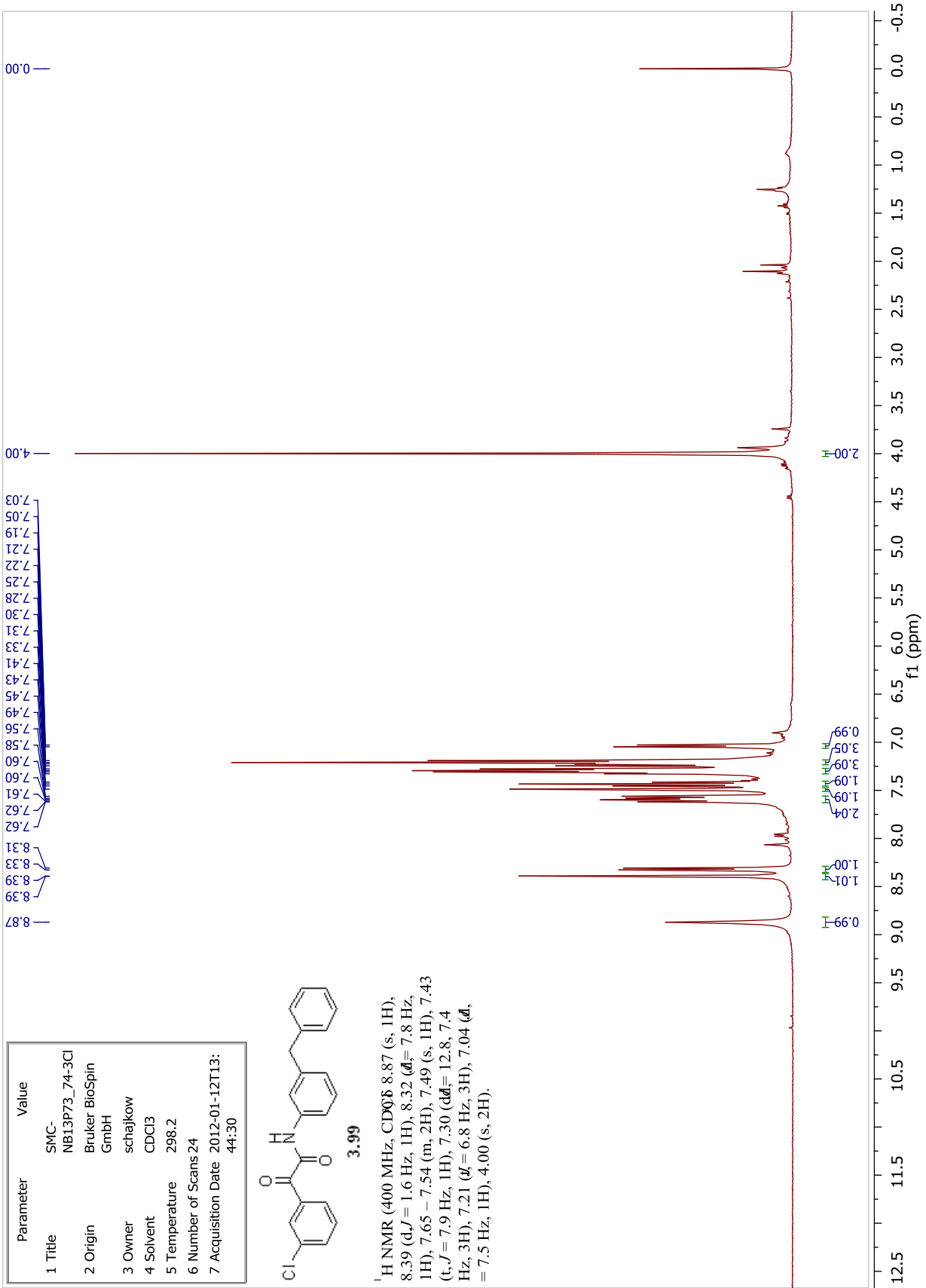


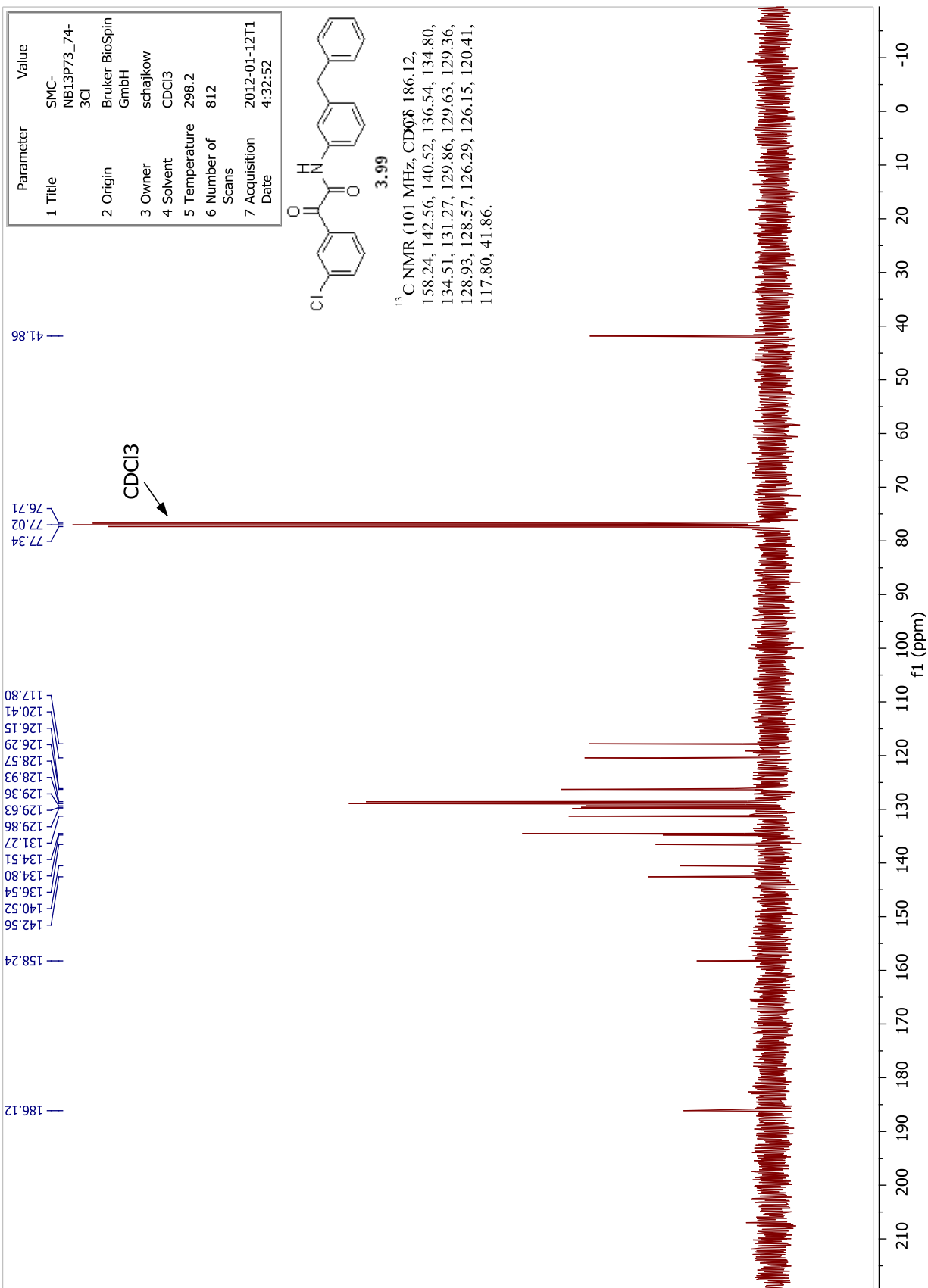
Parameter	Value
1 Title	SMC- NB13P73_74-3Cl
2 Origin	Bruker BioSpin GmbH
3 Owner	schajkow
4 Solvent	CDCl <sub>3</sub>
5 Temperature	298.2
6 Number of Scans	24
7 Acquisition Date	2012-01-12T13: 44:30



**3.99**

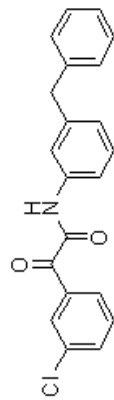
<sup>1</sup>H NMR (400 MHz, CDCl<sub>3</sub>) δ 8.87 (s, 1H), 8.39 (d, *J* = 1.6 Hz, 1H), 8.32 (d, *J* = 7.8 Hz, 1H), 7.65 – 7.54 (m, 2H), 7.49 (s, 1H), 7.43 (t, *J* = 7.9 Hz, 1H), 7.30 (dd, *J* = 12.8, 7.4 Hz, 3H), 7.21 (d, *J* = 6.8 Hz, 3H), 7.04 (d, *J* = 7.5 Hz, 1H), 4.00 (s, 2H).





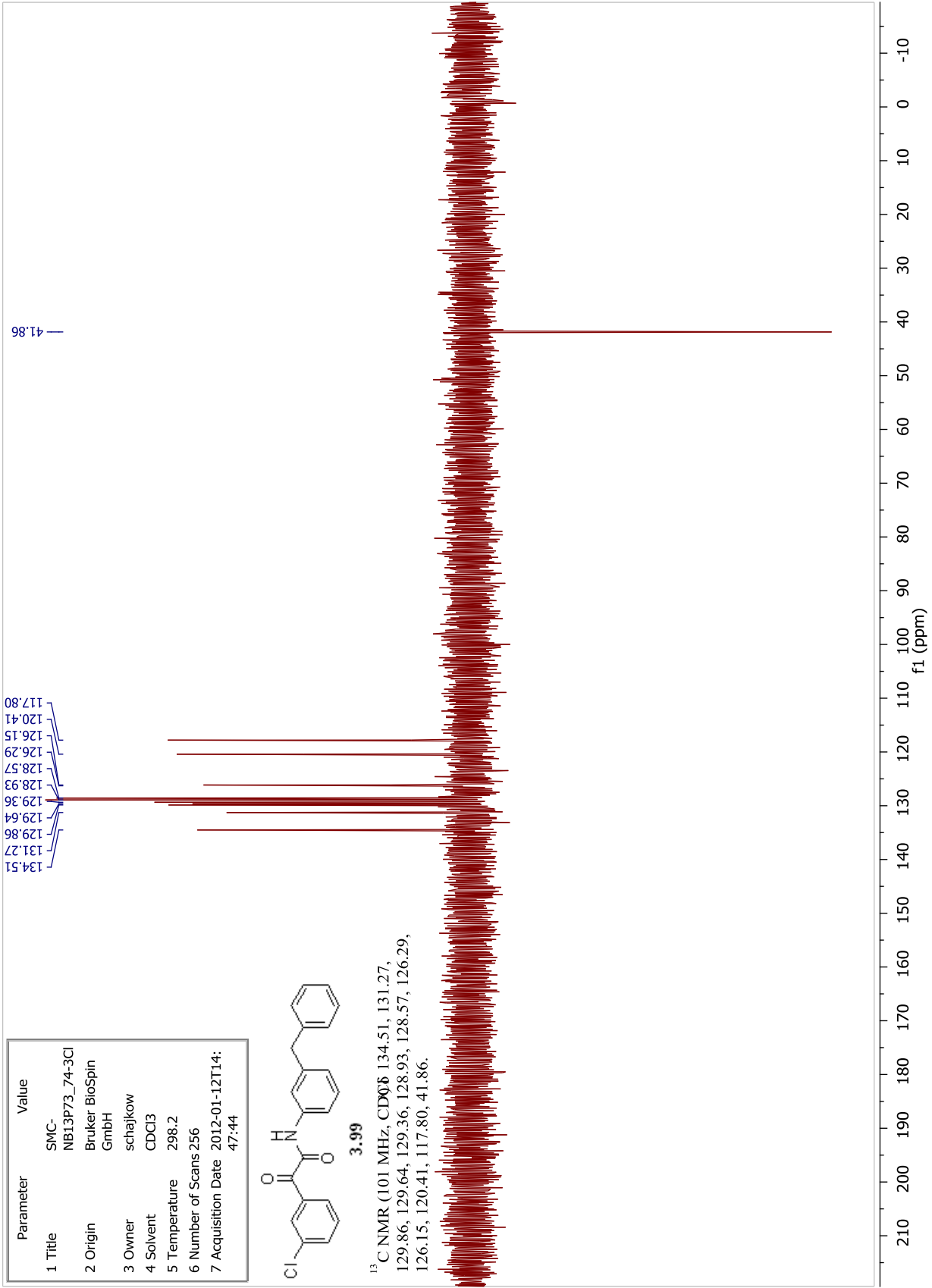


Parameter	Value
1 Title	SMC- NB13P73_74-3Cl
2 Origin	Bruker BioSpin GmbH
3 Owner	schajkow
4 Solvent	CDCI3
5 Temperature	298.2
6 Number of Scans	256
7 Acquisition Date	2012-01-12T14: 47:44

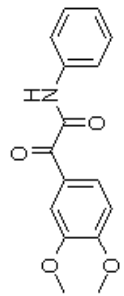


**3.99**

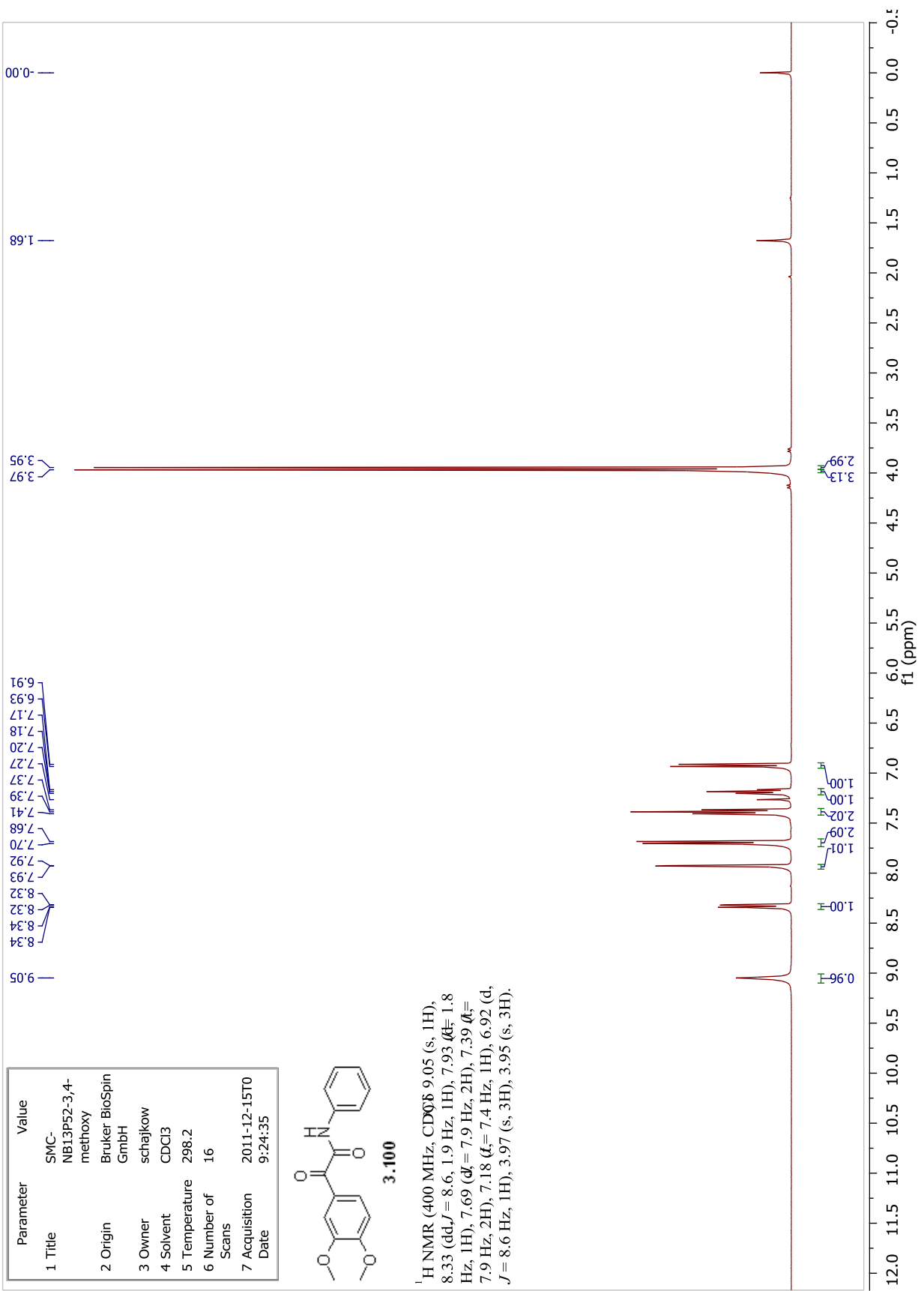
<sup>13</sup>C NMR (101 MHz, CDCl<sub>3</sub>) 134.51, 131.27, 129.86, 129.64, 129.36, 128.93, 128.57, 126.29, 126.15, 120.41, 117.80, 41.86.



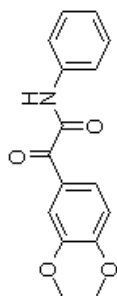
Parameter	Value
1 Title	SMC-NB13P52-3,4-methoxy
2 Origin	Bruker BioSpin GmbH
3 Owner	schajkow
4 Solvent	CDCl3
5 Temperature	298.2
6 Number of Scans	16
7 Acquisition Date	2011-12-15T09:24:35



<sup>1</sup>H NMR (400 MHz, CDCl<sub>3</sub>) 9.05 (s, 1H), 8.33 (dd, *J* = 8.6, 1.9 Hz, 1H), 7.93 (dt, 1.8 Hz, 1H), 7.69 (dt, 7.9 Hz, 2H), 7.39 (d, 7.9 Hz, 2H), 7.18 (t, 7.4 Hz, 1H), 6.92 (d, *J* = 8.6 Hz, 1H), 3.97 (s, 3H), 3.95 (s, 3H).

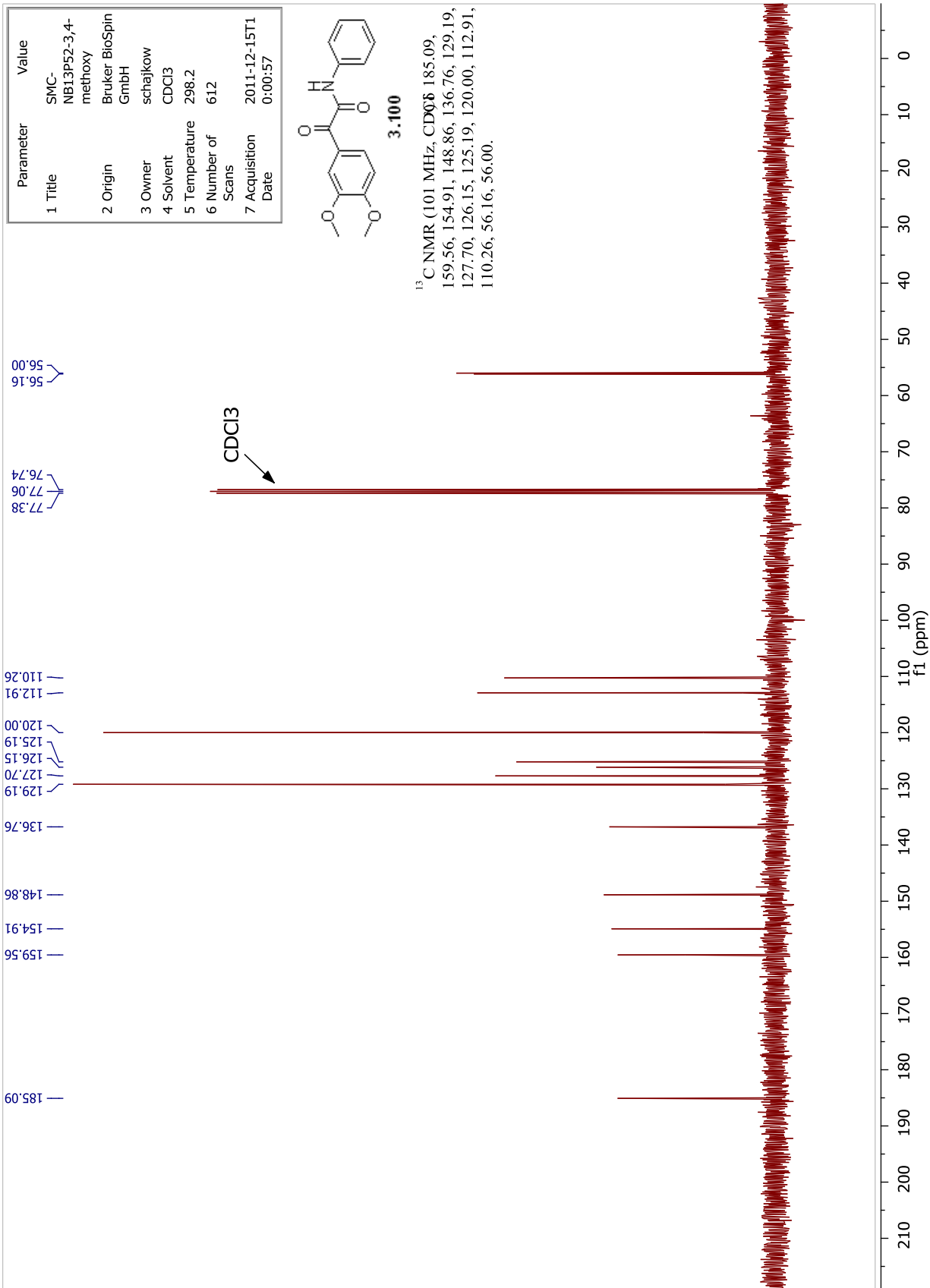


Parameter	Value
1 Title	SMC-NB13P52-3,4-methoxy
2 Origin	Bruker BioSpin GmbH
3 Owner	schajkow
4 Solvent	CDCl3
5 Temperature	298.2
6 Number of Scans	612
7 Acquisition Date	2011-12-15T10:00:57

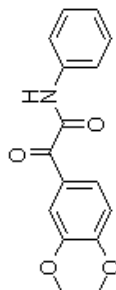


**3-100**

<sup>13</sup>C NMR (101 MHz, CDCl<sub>3</sub>) 185.09, 159.56, 154.91, 148.86, 136.76, 129.19, 127.70, 126.15, 125.19, 120.00, 112.91, 110.26, 56.16, 56.00.

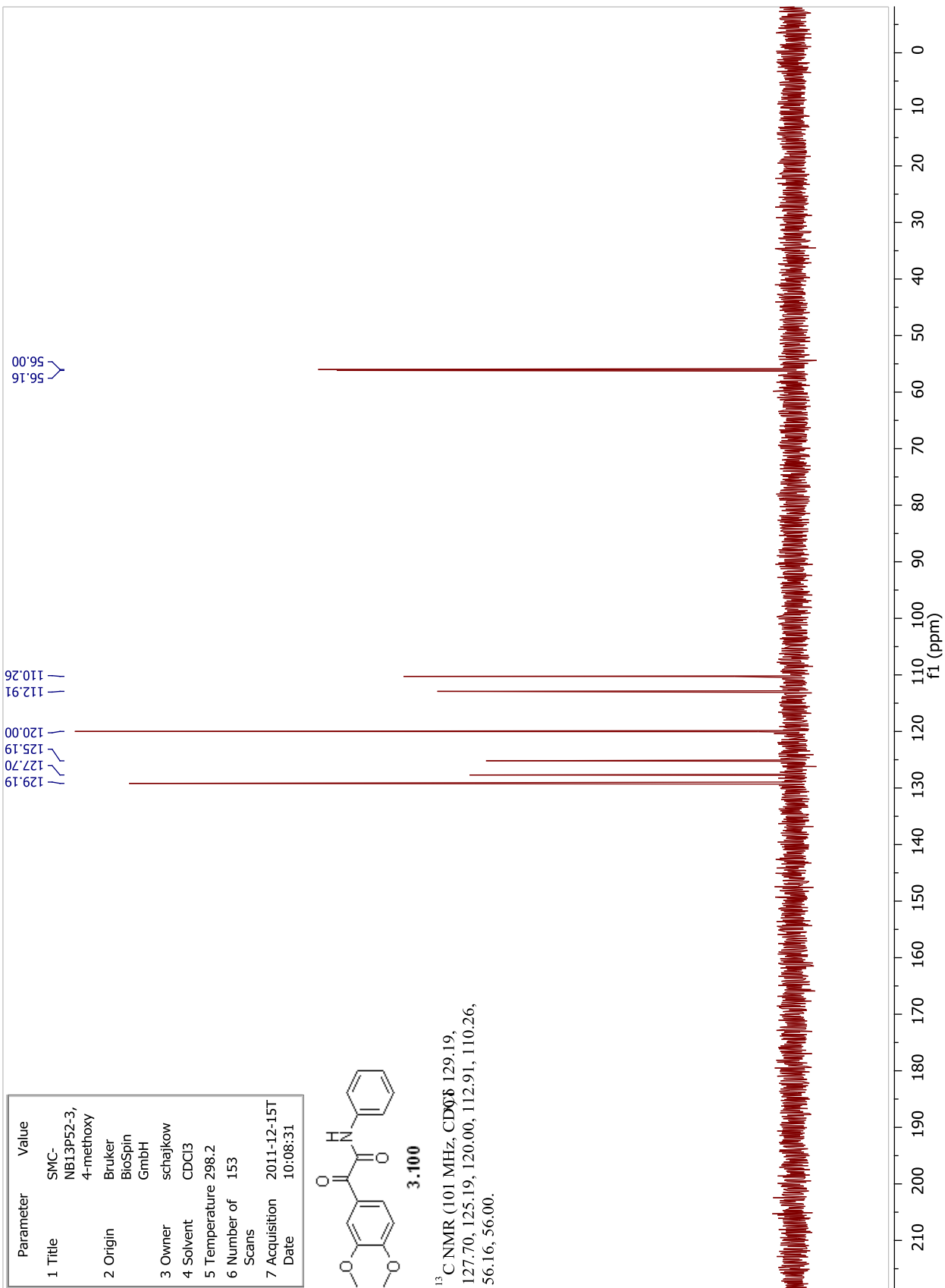


Parameter	Value
1 Title	SMC-NB13P52-3, 4-methoxy
2 Origin	Bruker BioSpin GmbH
3 Owner	schajkow
4 Solvent	CDCI3
5 Temperature	298.2
6 Number of Scans	153
7 Acquisition Date	2011-12-15T10:08:31

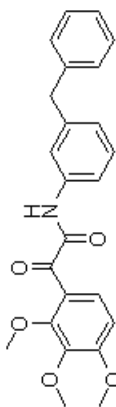


**3.100**

<sup>13</sup>C NMR (101 MHz, CDCl<sub>3</sub>) 129.19, 127.70, 125.19, 120.00, 112.91, 110.26, 56.16, 56.00.

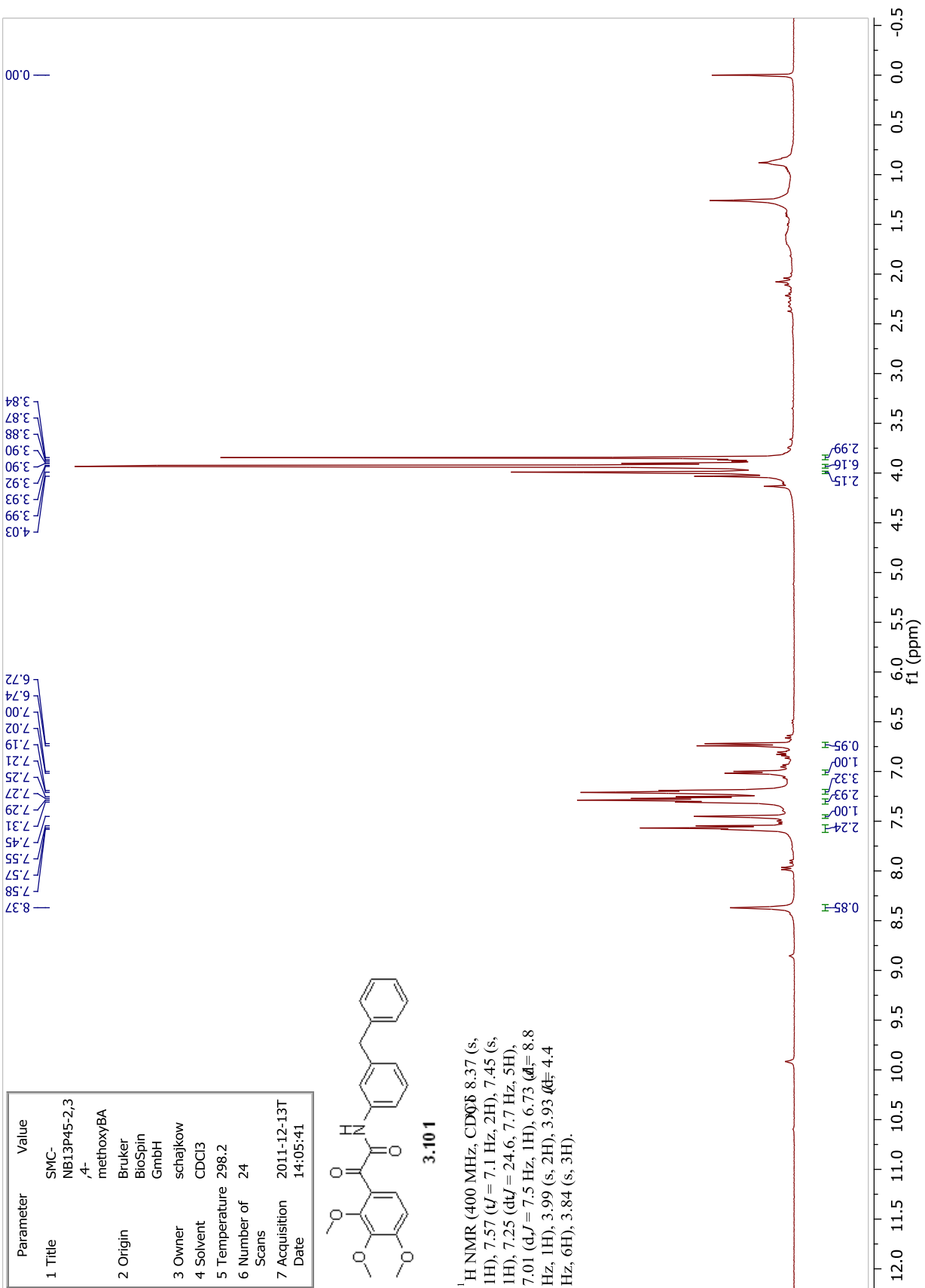


Parameter	Value
1 Title	SMC-NB13p45-2,3,4-methoxyBA
2 Origin	Bruker BioSpin GmbH
3 Owner	schajkow
4 Solvent	CDCl3
5 Temperature	298.2
6 Number of Scans	24
7 Acquisition Date	2011-12-13T14:05:41

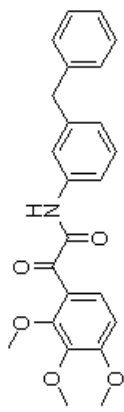


**3.101**

<sup>1</sup>H NMR (400 MHz, CDCl<sub>3</sub>) δ 8.37 (s, 1H), 7.57 (d, J = 7.1 Hz, 2H), 7.45 (s, 1H), 7.25 (dt, J = 24.6, 7.7 Hz, 5H), 7.01 (d, J = 7.5 Hz, 1H), 6.73 (d, J = 8.8 Hz, 1H), 3.99 (s, 2H), 3.93 (d, J = 4.4 Hz, 6H), 3.84 (s, 3H).

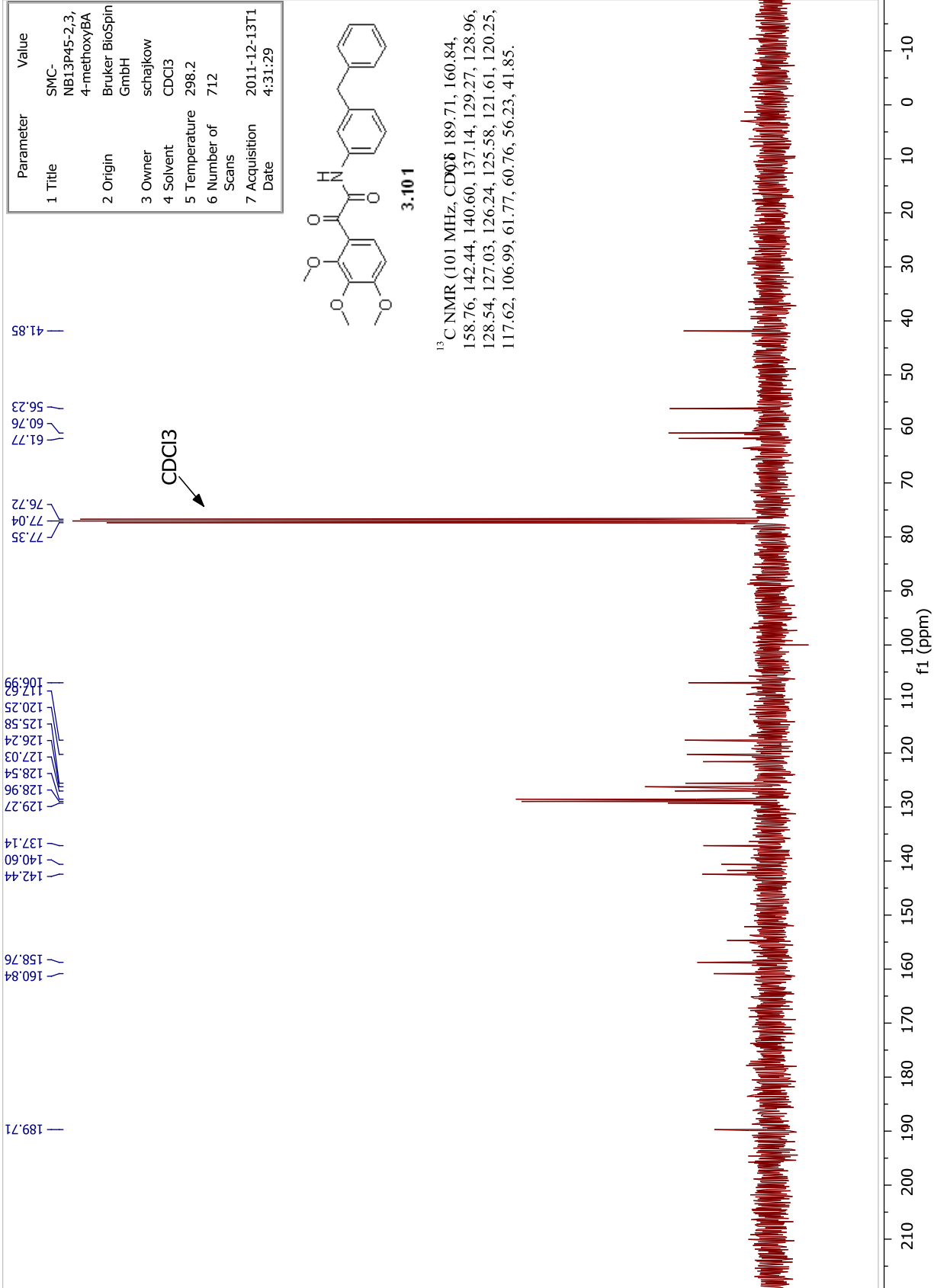


Parameter	Value
1 Title	SMC-NB13P45-2,3,4-methoxyBA
2 Origin	Bruker BioSpin GmbH
3 Owner	schajkow
4 Solvent	CDCl3
5 Temperature	298.2
6 Number of Scans	712
7 Acquisition Date	2011-12-13T14:31:29

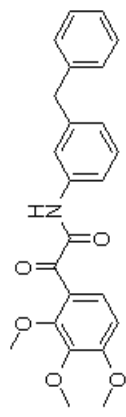


3.101

<sup>13</sup>C NMR (101 MHz, CDCl<sub>3</sub>) 189.71, 160.84, 158.76, 142.44, 140.60, 137.14, 129.27, 128.96, 128.54, 127.03, 126.24, 125.58, 121.61, 120.25, 117.62, 106.99, 61.77, 60.76, 56.23, 41.85.

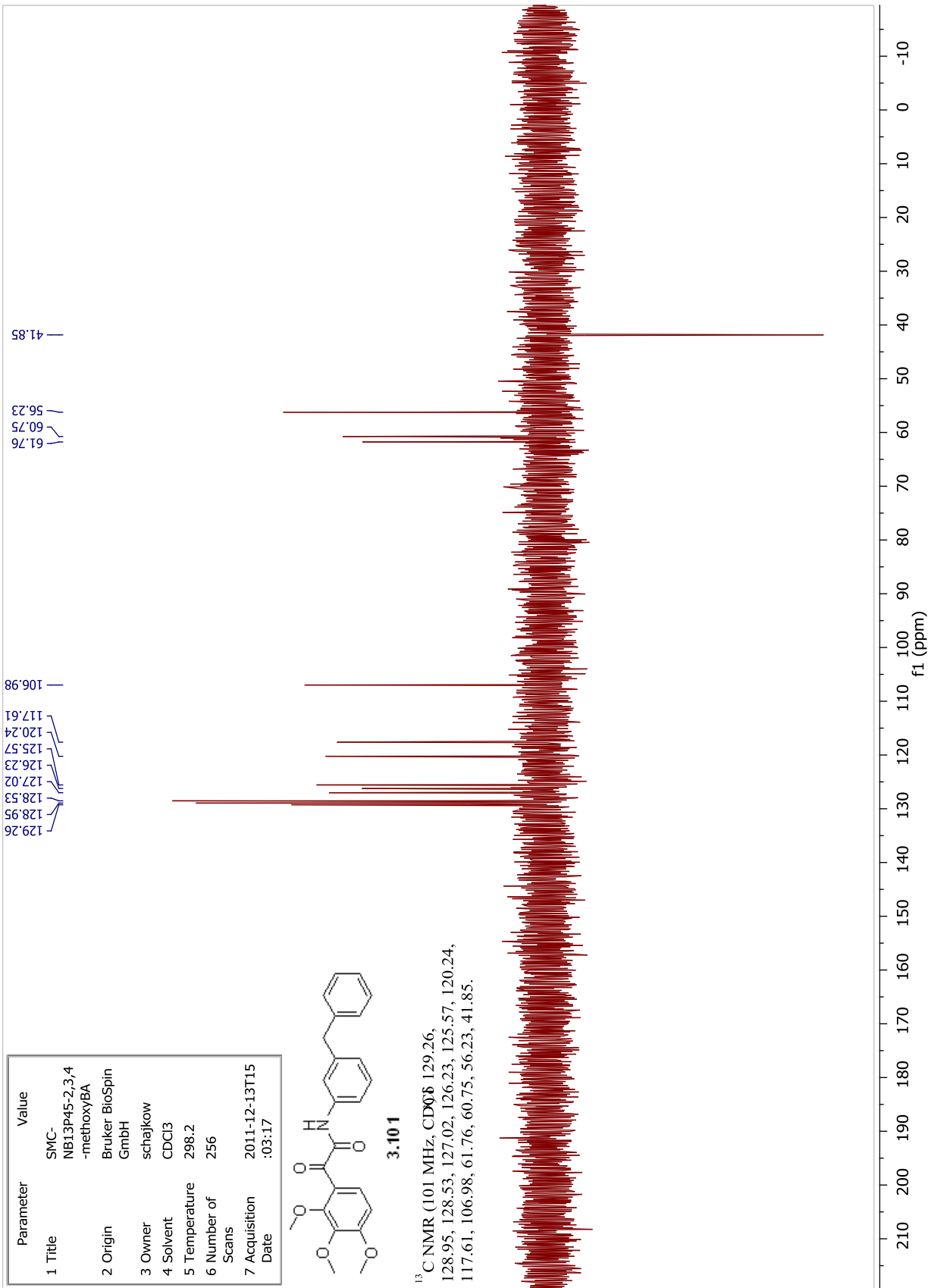


Parameter	Value
1 Title	SMC-NB13P45-2,3,4-methoxyBA
2 Origin	Bruker BioSpin GmbH
3 Owner	schajkow
4 Solvent	CDCl3
5 Temperature	298.2
6 Number of Scans	256
7 Acquisition Date	2011-12-13T15:03:17

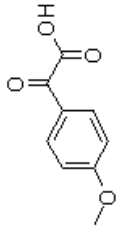


**3.101**

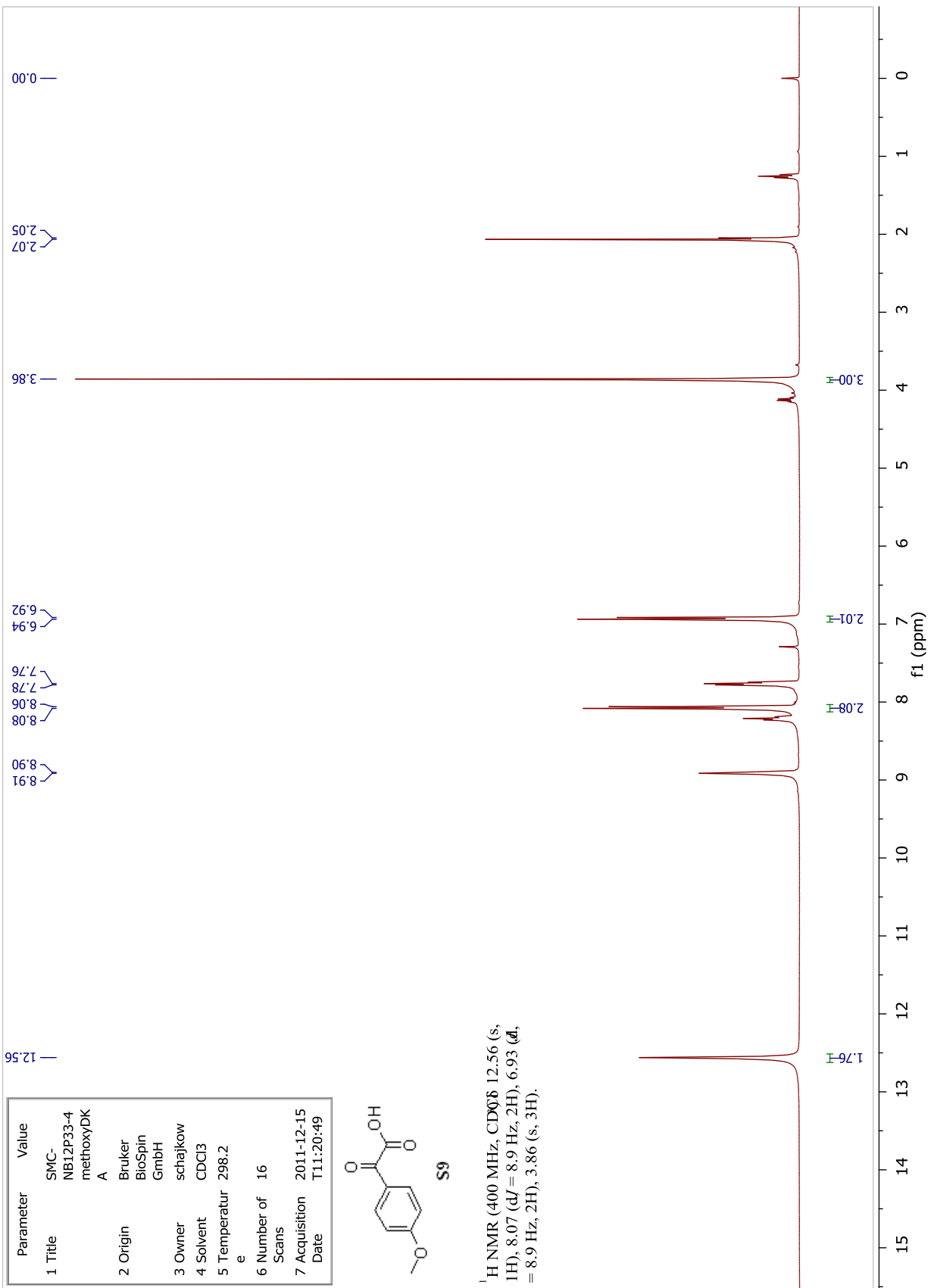
<sup>13</sup>C NMR (101 MHz, CDCl<sub>3</sub>) 129.26, 128.95, 128.53, 127.02, 126.23, 125.57, 120.24, 117.61, 106.98, 61.76, 60.75, 56.23, 41.85.



Parameter	Value
1 Title	SMC-NB12P33-4 methoxyDK A
2 Origin	Bruker BioSpin GmbH
3 Owner	schajkowi
4 Solvent	CDCl <sub>3</sub>
5 Temperatur	298.2 e
6 Number of Scans	16
7 Acquisition Date	2011-12-15 T11:20:49

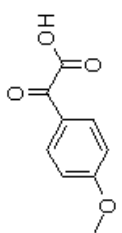


<sup>1</sup>H NMR (400 MHz, CDCl<sub>3</sub>) δ 12.56 (s, 1H), 8.07 (d, J = 8.9 Hz, 2H), 6.93 (d, J = 8.9 Hz, 2H), 3.86 (s, 3H).



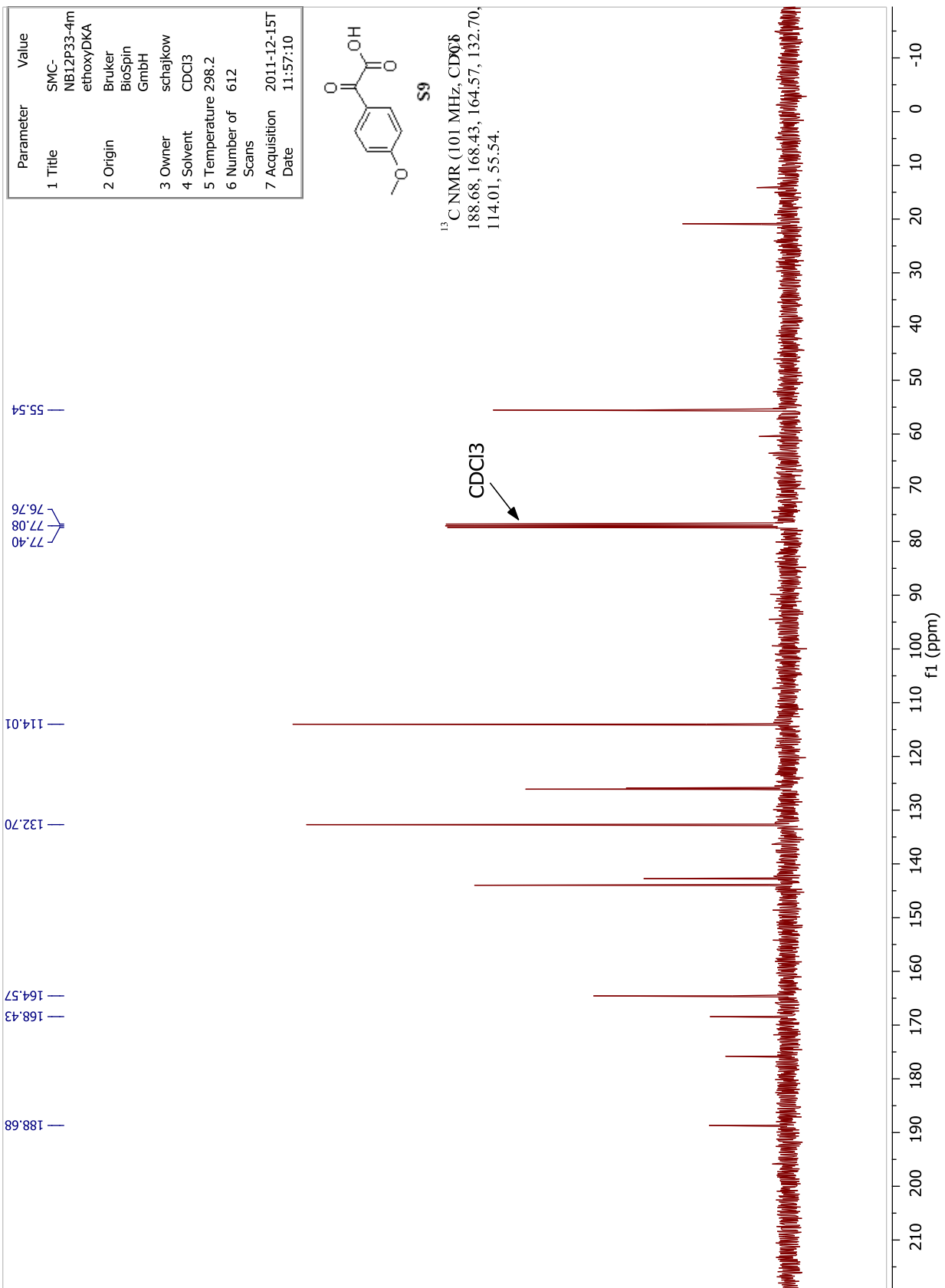


Parameter	Value
1 Title	SMC-NB12P33-4m ethoxyDKA
2 Origin	Bruker BioSpin GmbH
3 Owner	schajkow
4 Solvent	CDCl3
5 Temperature	298.2
6 Number of Scans	612
7 Acquisition Date	2011-12-15T 11:57:10

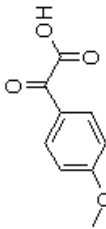


**S9**

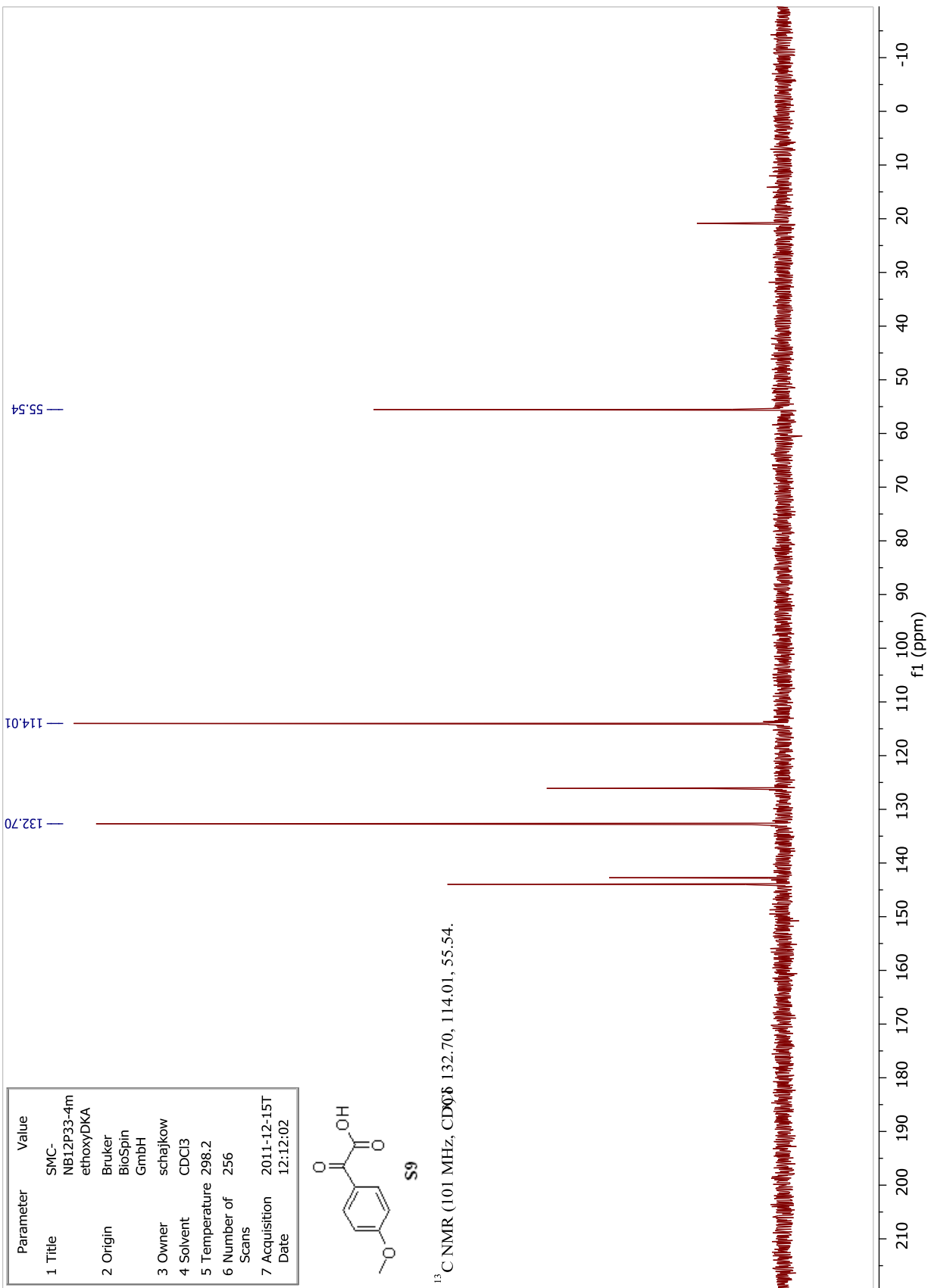
<sup>13</sup>C NMR (101 MHz, CDCl<sub>3</sub>)  
 188.68, 168.43, 164.57, 132.70,  
 114.01, 55.54.



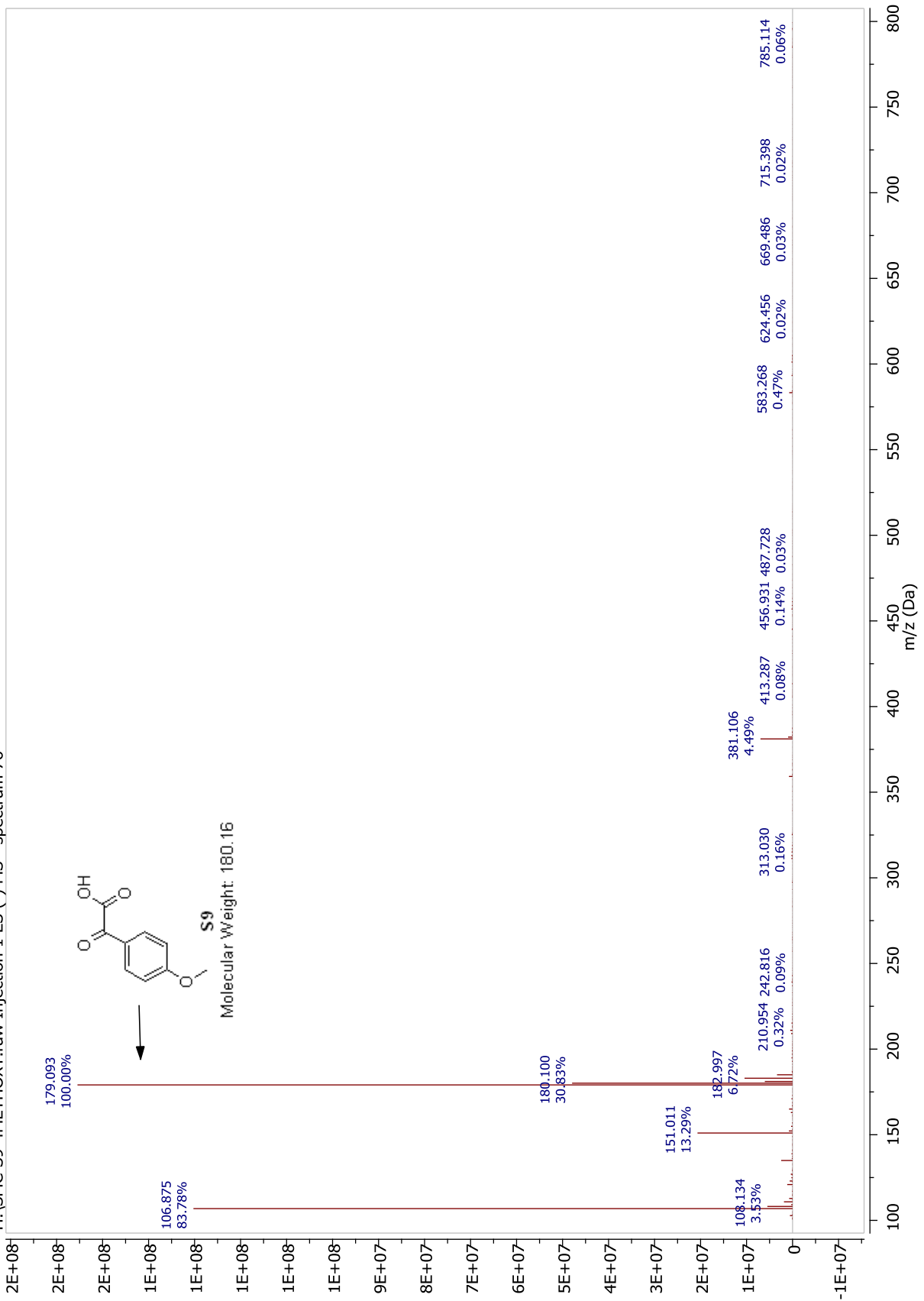
Parameter	Value
1 Title	SMC- NB12P33-4m ethoxyDKA
2 Origin	Bruker BioSpin GmbH
3 Owner	schajkow
4 Solvent	CDCl3
5 Temperature	298.2
6 Number of Scans	256
7 Acquisition Date	2011-12-15T 12:12:02



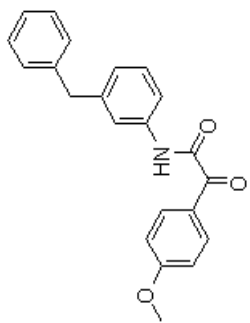
<sup>13</sup>C NMR (101 MHz, CDCl<sub>3</sub>) 132.70, 114.01, 55.54.



H:\SMC-S9-4METHOXY.raw Injection 1 ES (-) MS - spectrum 76

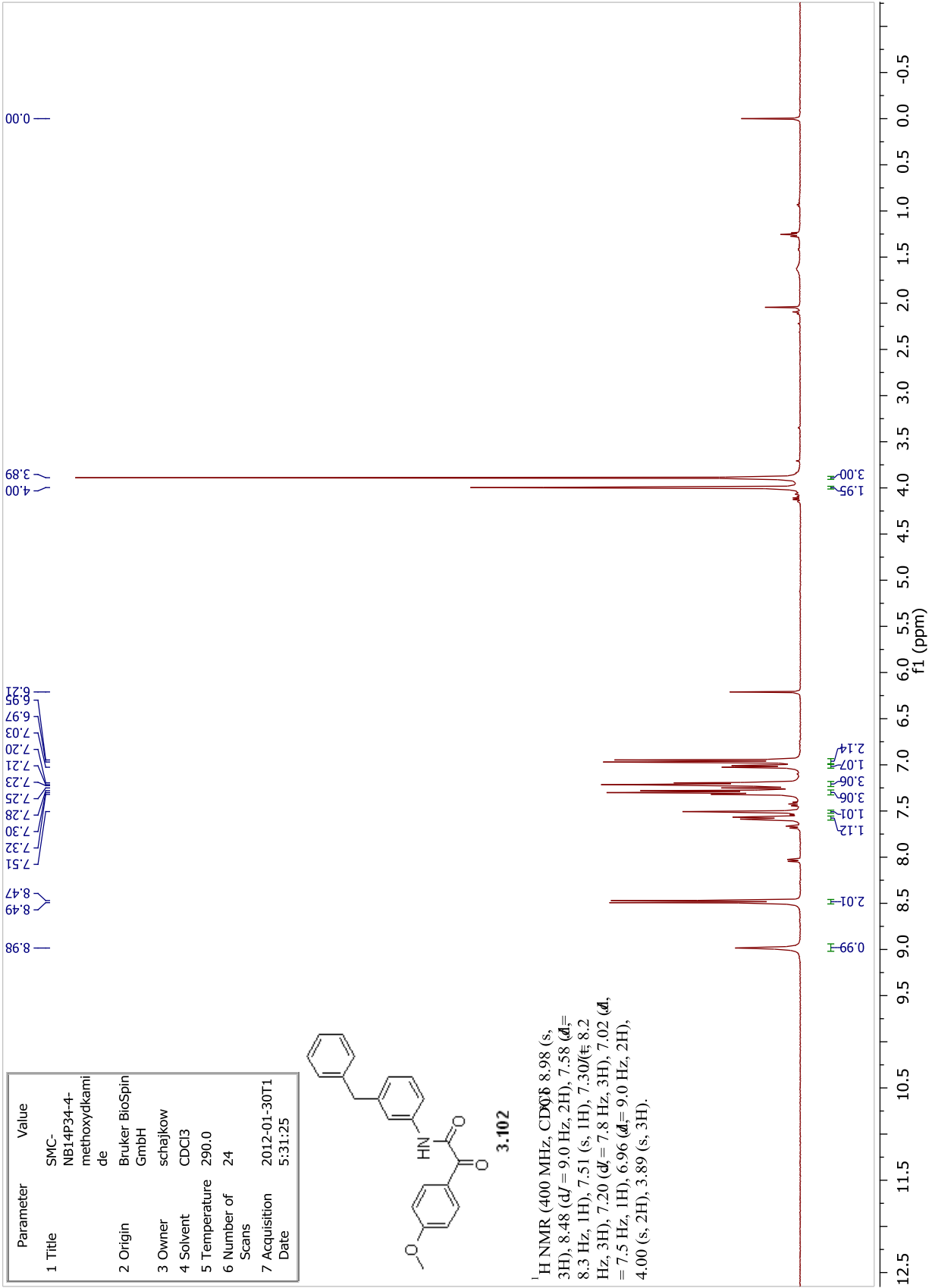


Parameter	Value
1 Title	SMC-NB14P34-4-methoxydkami de
2 Origin	Bruker BioSpin GmbH
3 Owner	schajkow
4 Solvent	CDCl3
5 Temperature	290.0
6 Number of Scans	24
7 Acquisition Date	2012-01-30T15:31:25

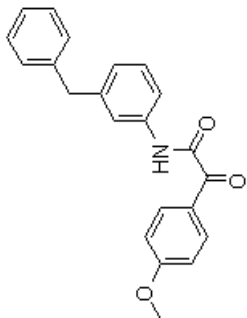


**3.102**

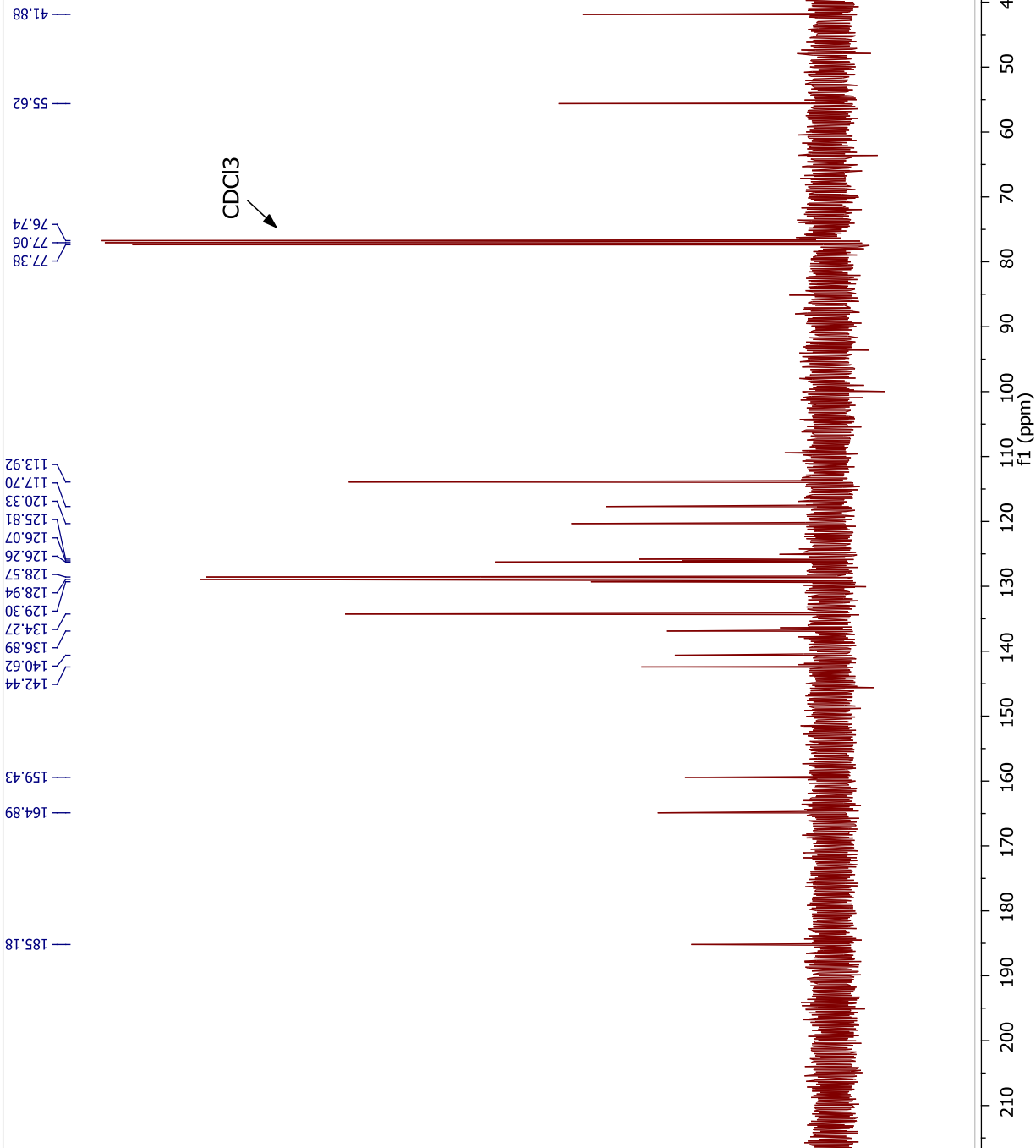
<sup>1</sup>H NMR (400 MHz, CDCl<sub>3</sub>) δ 8.98 (s, 3H), 8.48 (dJ = 9.0 Hz, 2H), 7.58 (dJ = 8.3 Hz, 1H), 7.51 (s, 1H), 7.30 (t, 8.2 Hz, 3H), 7.20 (dJ = 7.8 Hz, 3H), 7.02 (d, = 7.5 Hz, 1H), 6.96 (dJ = 9.0 Hz, 2H), 4.00 (s, 2H), 3.89 (s, 3H).



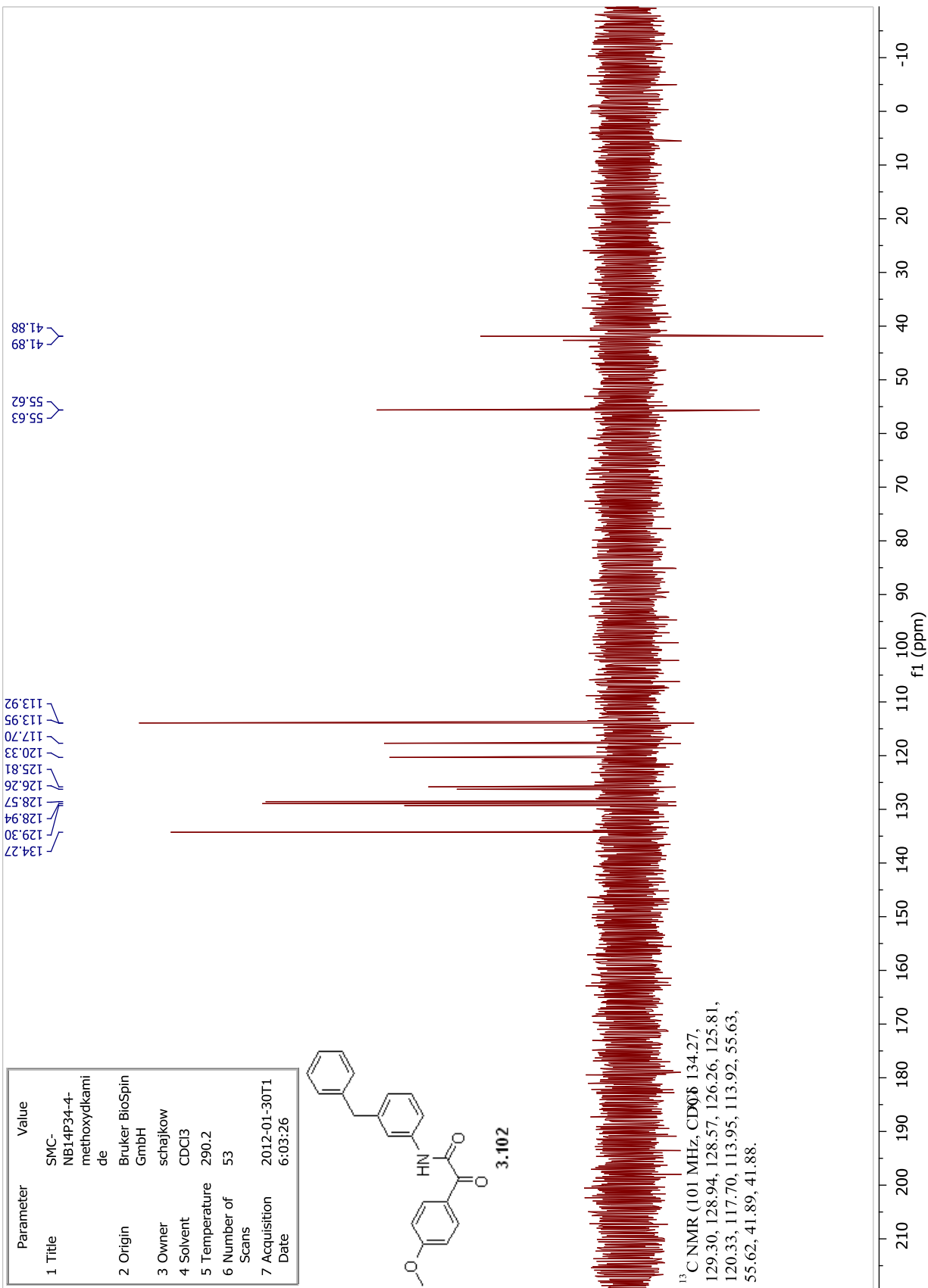
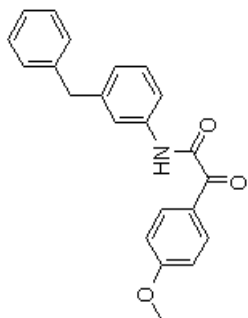
Parameter	Value
1 Title	SMC-NB14P34-4-methoxydkamid e
2 Origin	Bruker BioSpin GmbH
3 Owner	schajkow
4 Solvent	CDCl3
5 Temperature	290.1
6 Number of Scans	516
7 Acquisition Date	2012-01-30T15:57:52



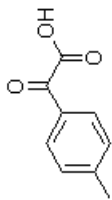
<sup>13</sup>C NMR (101 MHz, CDCl<sub>3</sub>)  
 185.18, 164.89, 159.43, 142.44,  
 140.62, 136.89, 134.27, 129.30,  
 128.94, 128.57, 126.26, 126.07,  
 125.81, 120.33, 117.70, 113.92,  
 55.62, 41.88.



Parameter	Value
1 Title	SMC- NB14P34-4- methoxydkami de
2 Origin	Bruker BioSpin GmbH
3 Owner	schajkow
4 Solvent	CDCl <sub>3</sub>
5 Temperature	290.2
6 Number of Scans	53
7 Acquisition Date	2012-01-30T1 6:03:26

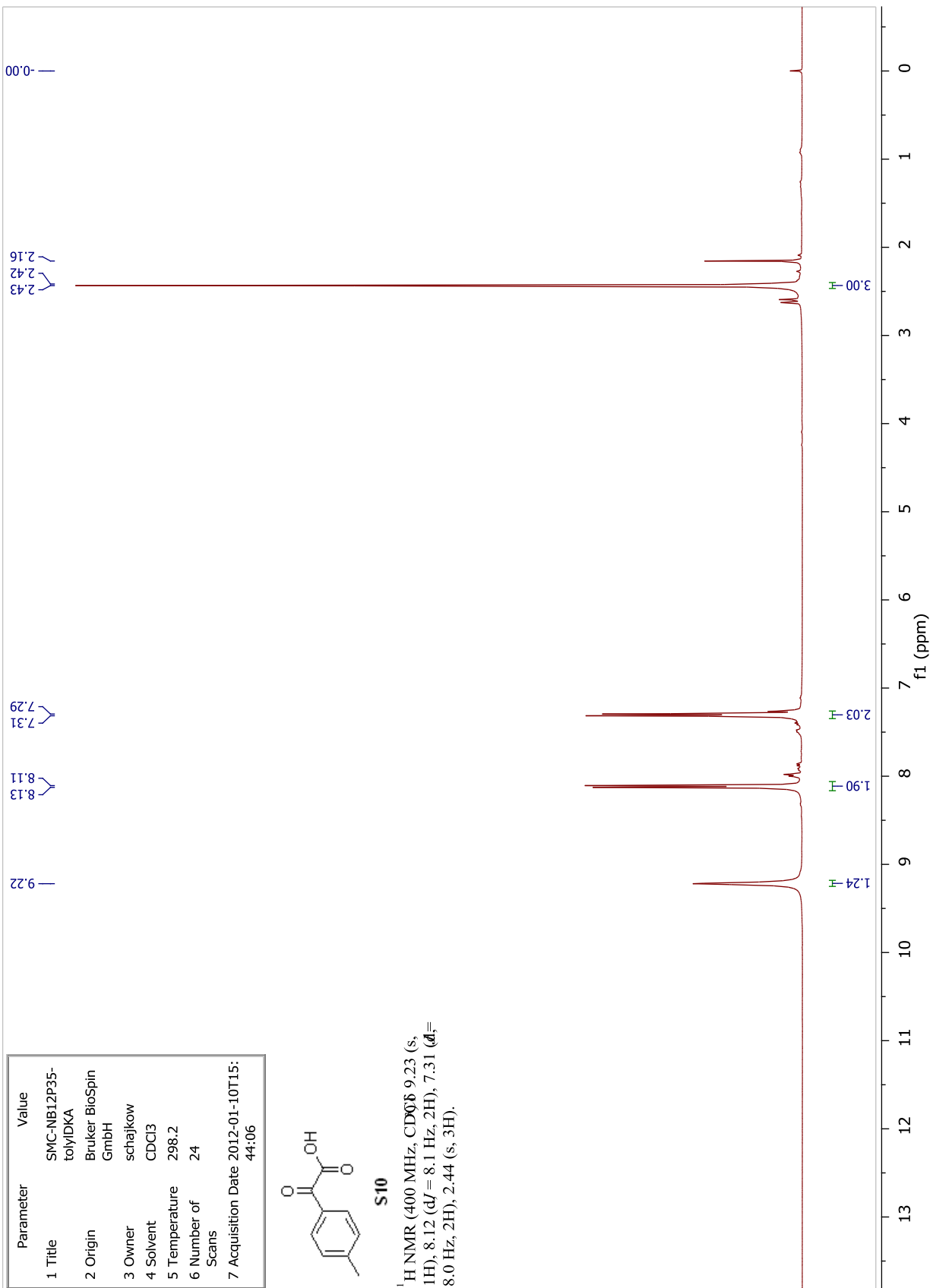


Parameter	Value
1 Title	SMC-NB12P35-tolyDKA
2 Origin	Bruker BioSpin GmbH
3 Owner	schajkow
4 Solvent	CDCl3
5 Temperature	298.2
6 Number of Scans	24
7 Acquisition Date	2012-01-10T11:44:06

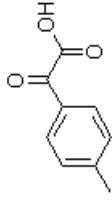


**S10**

<sup>1</sup>H NMR (400 MHz, CDCl<sub>3</sub>) δ 9.23 (s, 1H), 8.12 (d, *J* = 8.1 Hz, 2H), 7.31 (d, *J* = 8.0 Hz, 2H), 2.44 (s, 3H).

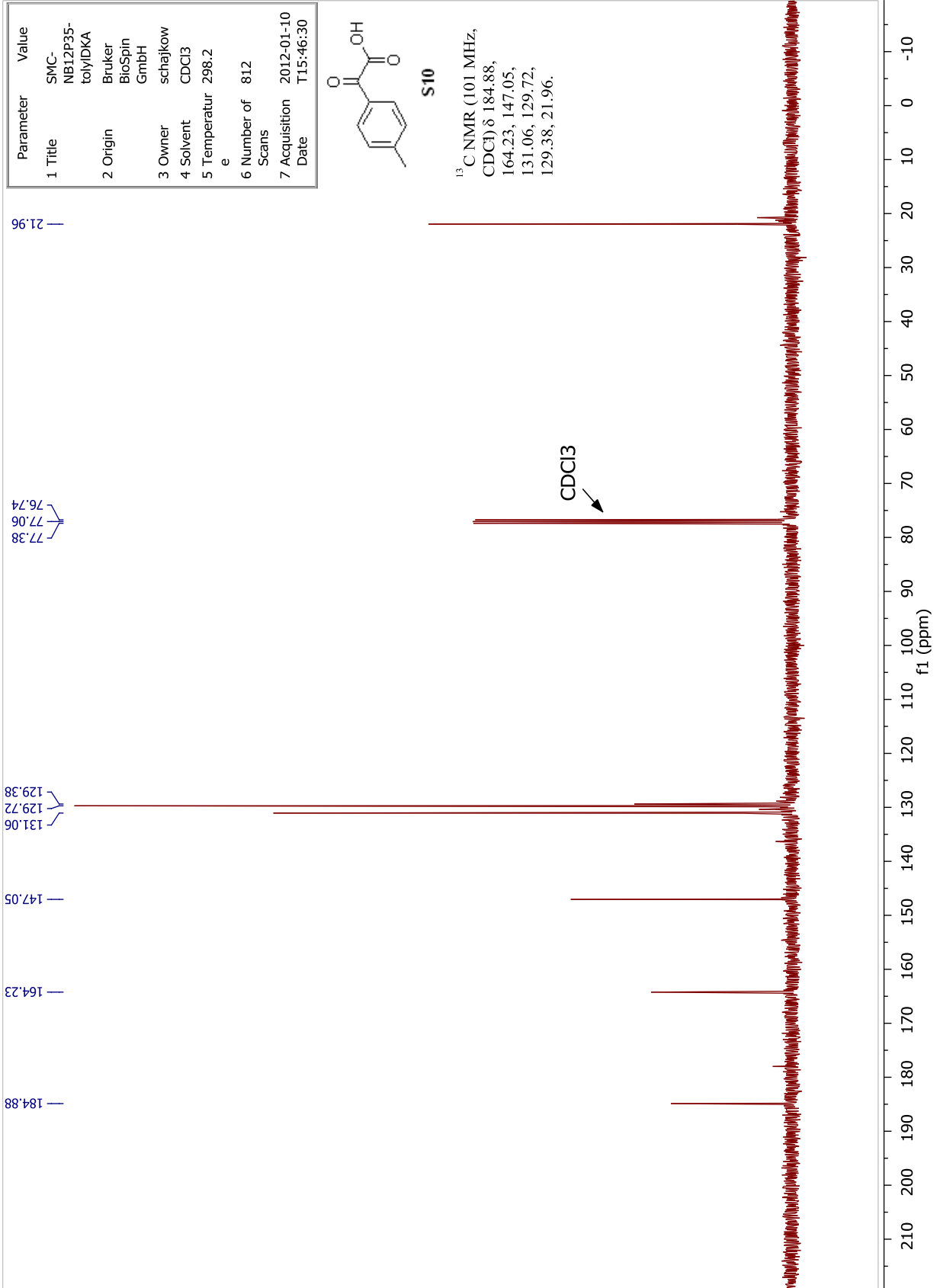


Parameter	Value
1 Title	SMC-NB12P35-toylidKA
2 Origin	Bruker BioSpin GmbH
3 Owner	schajkow
4 Solvent	CDCl3
5 Temperatur	298.2 e
6 Number of Scans	812
7 Acquisition Date	2012-01-10 T15:46:30



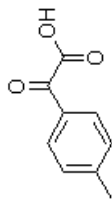
S10

<sup>13</sup>C NMR (101 MHz, CDCl<sub>3</sub>) δ 184.88, 164.23, 147.05, 131.06, 129.72, 129.38, 21.96.



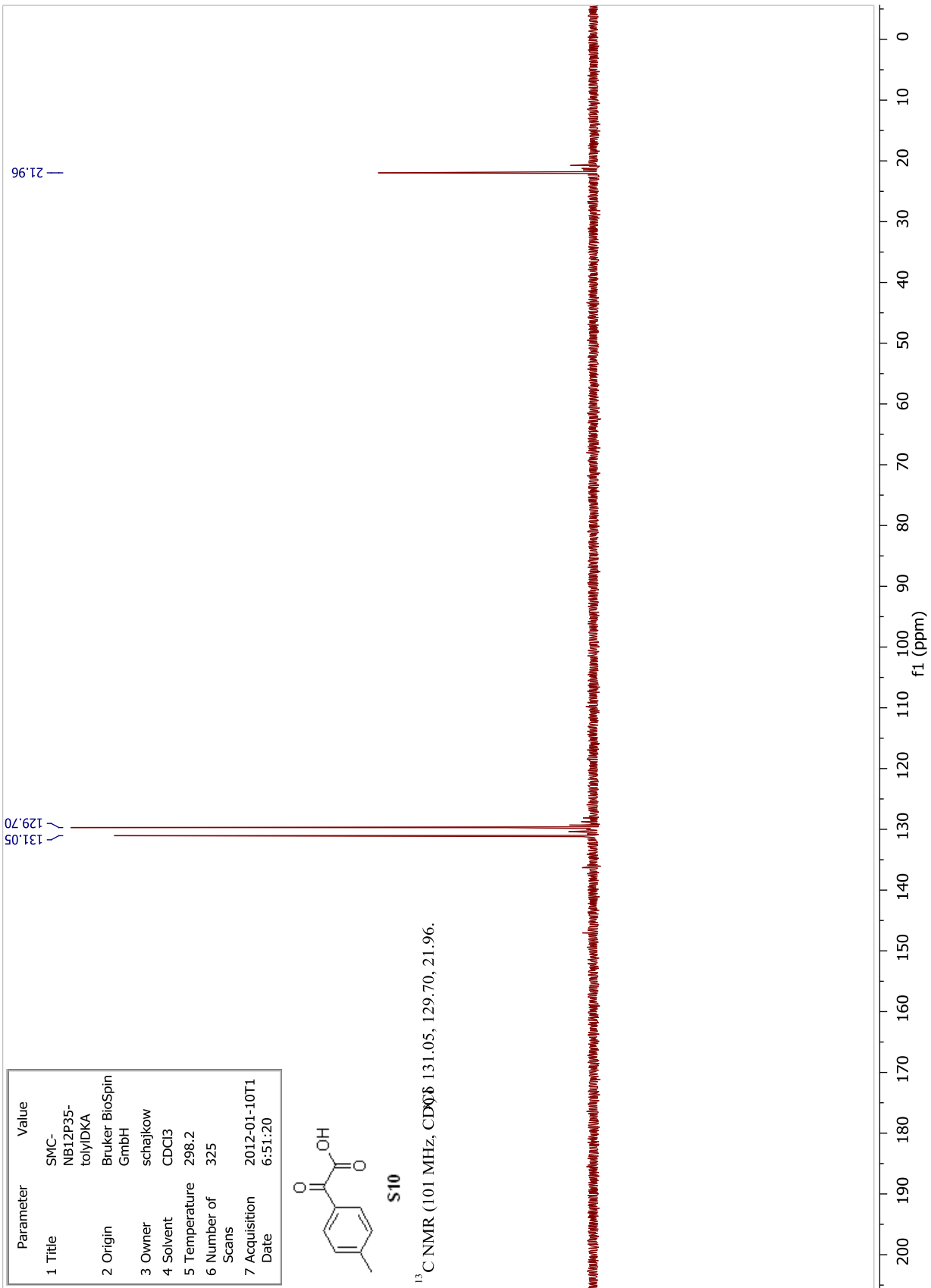


Parameter	Value
1 Title	SMC-NB12P35-tolyDKA
2 Origin	Bruker BioSpin GmbH
3 Owner	schajkowi
4 Solvent	CDCl3
5 Temperature	298.2
6 Number of Scans	325
7 Acquisition Date	2012-01-10T16:51:20

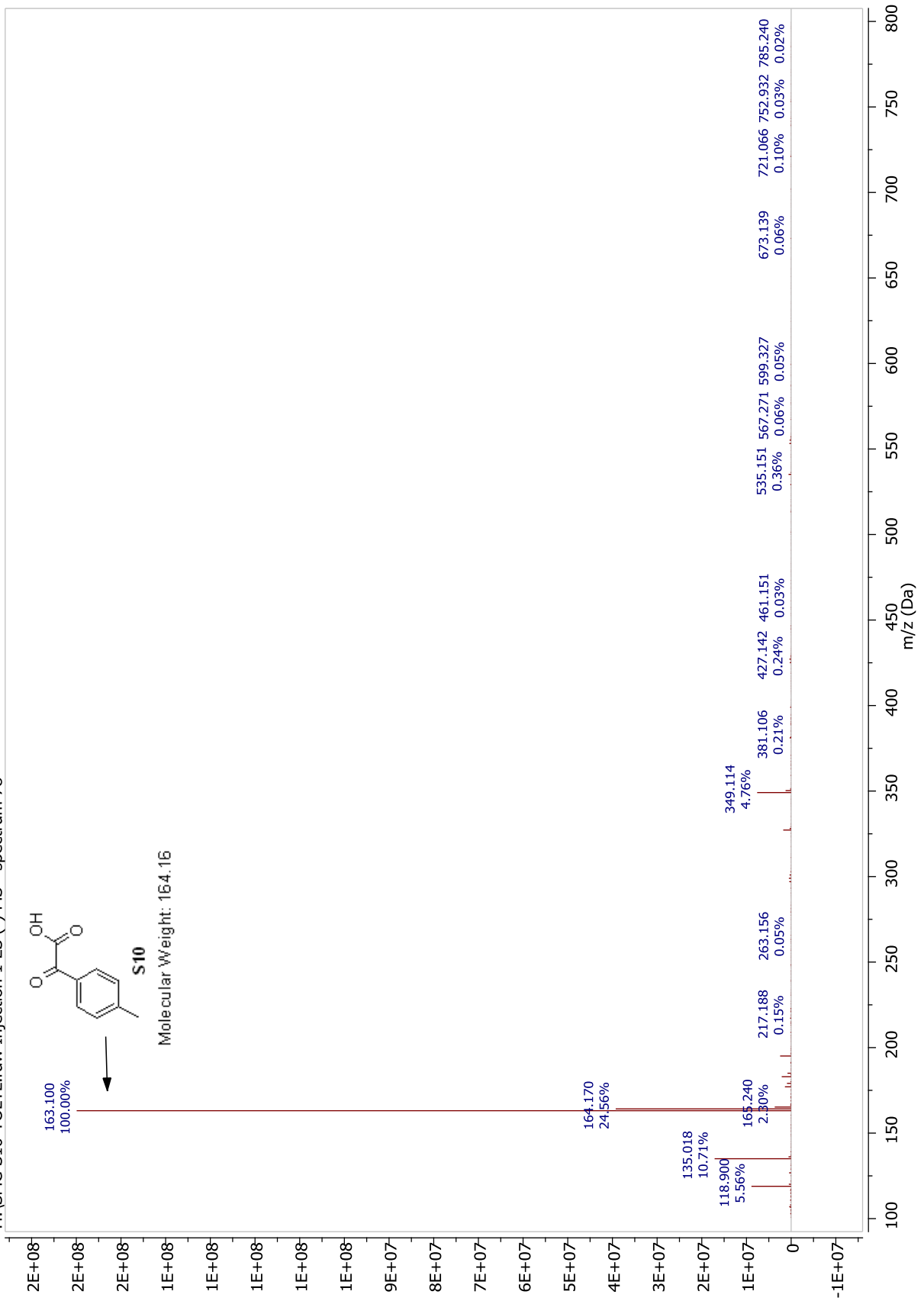


**S10**

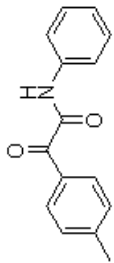
<sup>13</sup>C NMR (101 MHz, CDCl<sub>3</sub>) 131.05, 129.70, 21.96.



H:\SMC-S10-TOLYL.raw Injection 1 ES (-) MS - spectrum 78

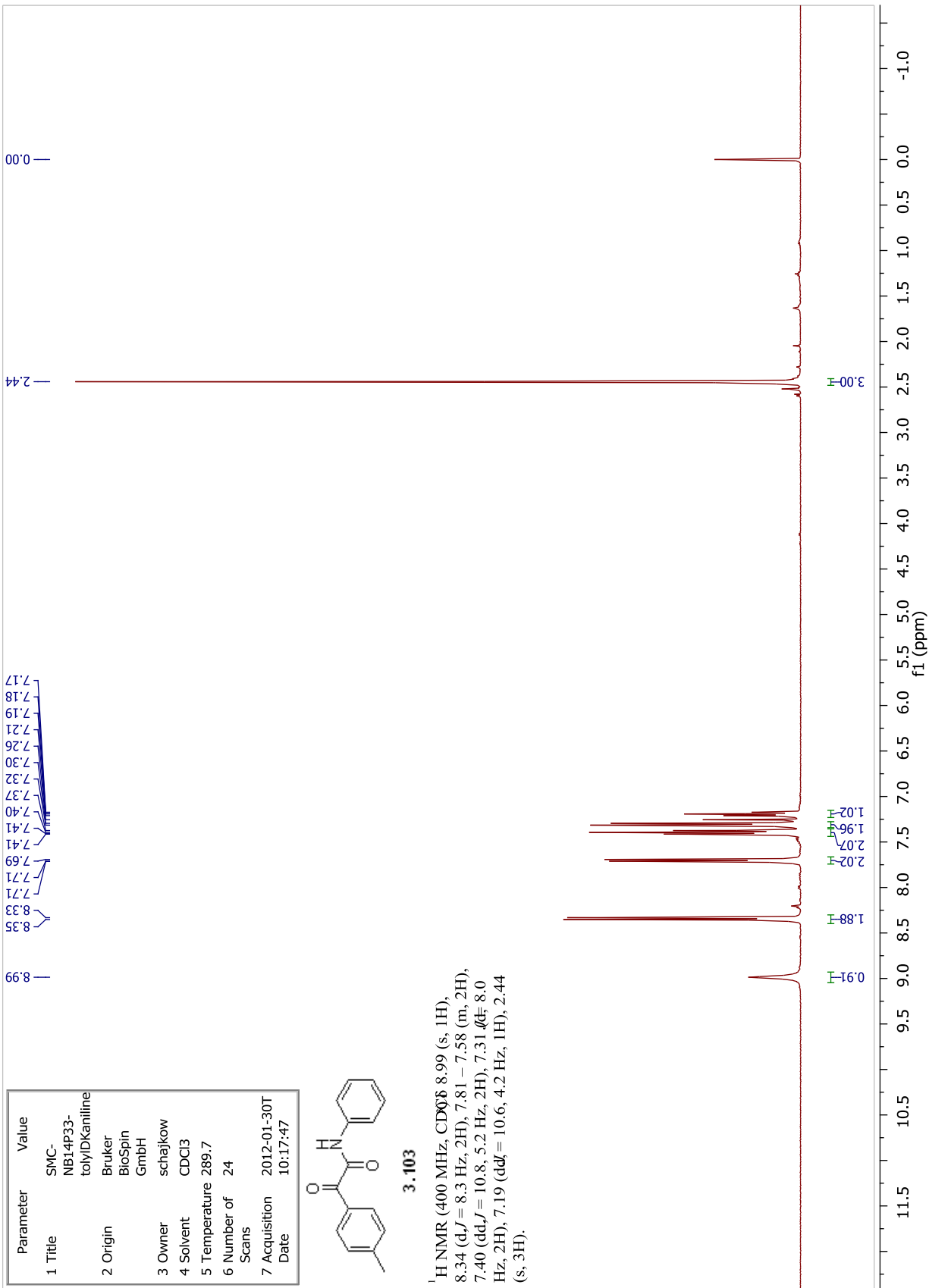


Parameter	Value
1 Title	SMC-NB14P33-tolylDKaniline
2 Origin	Bruker BioSpin GmbH
3 Owner	schajkow
4 Solvent	CDCl3
5 Temperature	289.7
6 Number of Scans	24
7 Acquisition Date	2012-01-30T 10:17:47

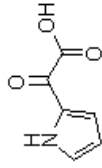


**3.103**

<sup>1</sup>H NMR (400 MHz, CDCl<sub>3</sub>) δ 8.99 (s, 1H), 8.34 (d, J = 8.3 Hz, 2H), 7.81 – 7.58 (m, 2H), 7.40 (dd, J = 10.8, 5.2 Hz, 2H), 7.31 (dd, J = 8.0 Hz, 2H), 7.19 (dd, J = 10.6, 4.2 Hz, 1H), 2.44 (s, 3H).

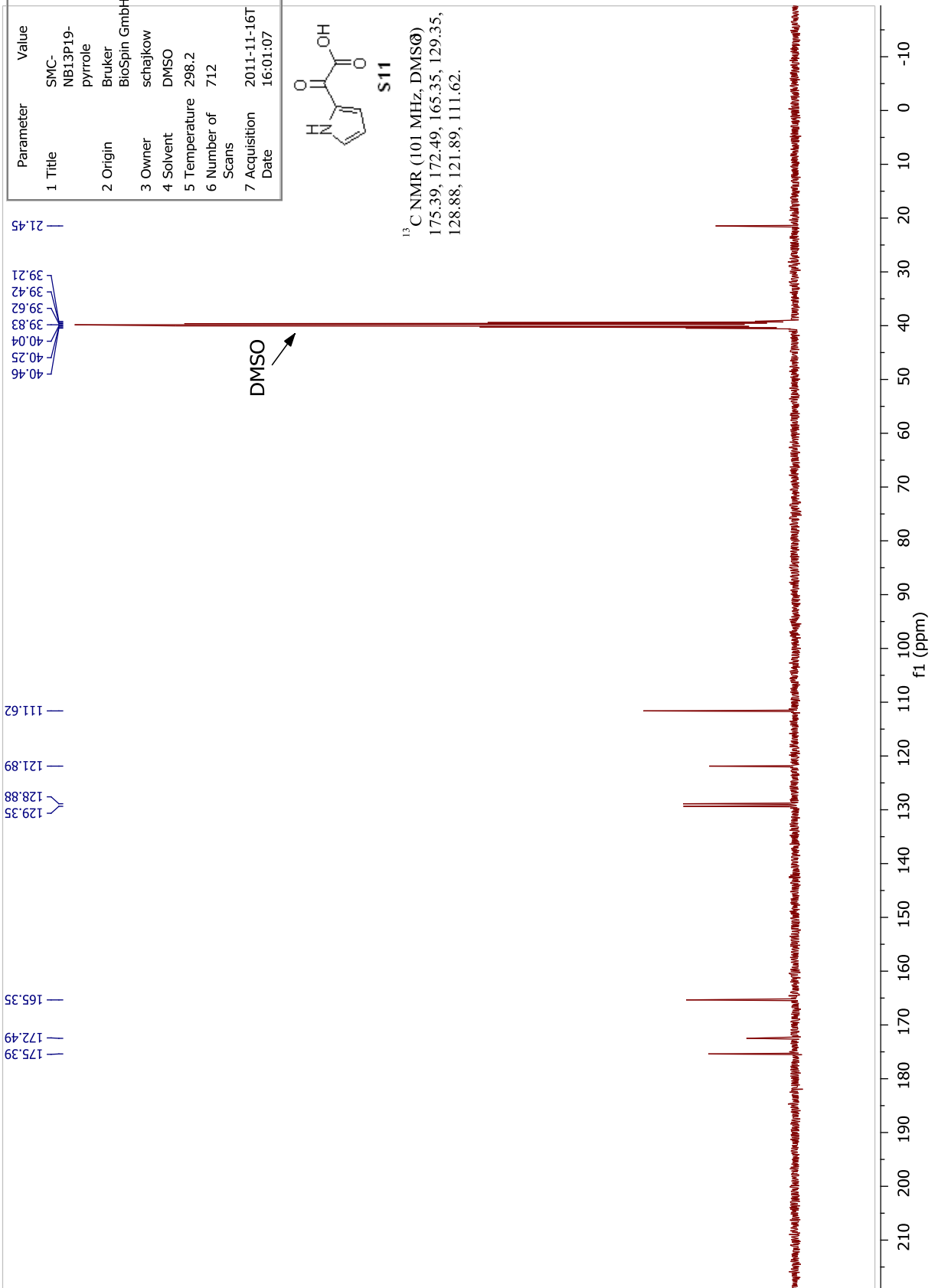


Parameter	Value
1 Title	SMC-NB13P19-pyrrole
2 Origin	Bruker BioSpin GmbH
3 Owner	schajkow
4 Solvent	DMSO
5 Temperature	298.2
6 Number of Scans	712
7 Acquisition Date	2011-11-16T16:01:07

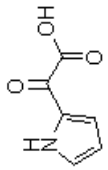


**S11**

<sup>13</sup>C NMR (101 MHz, DMSO)  
 175.39, 172.49, 165.35, 129.35,  
 128.88, 121.89, 111.62.

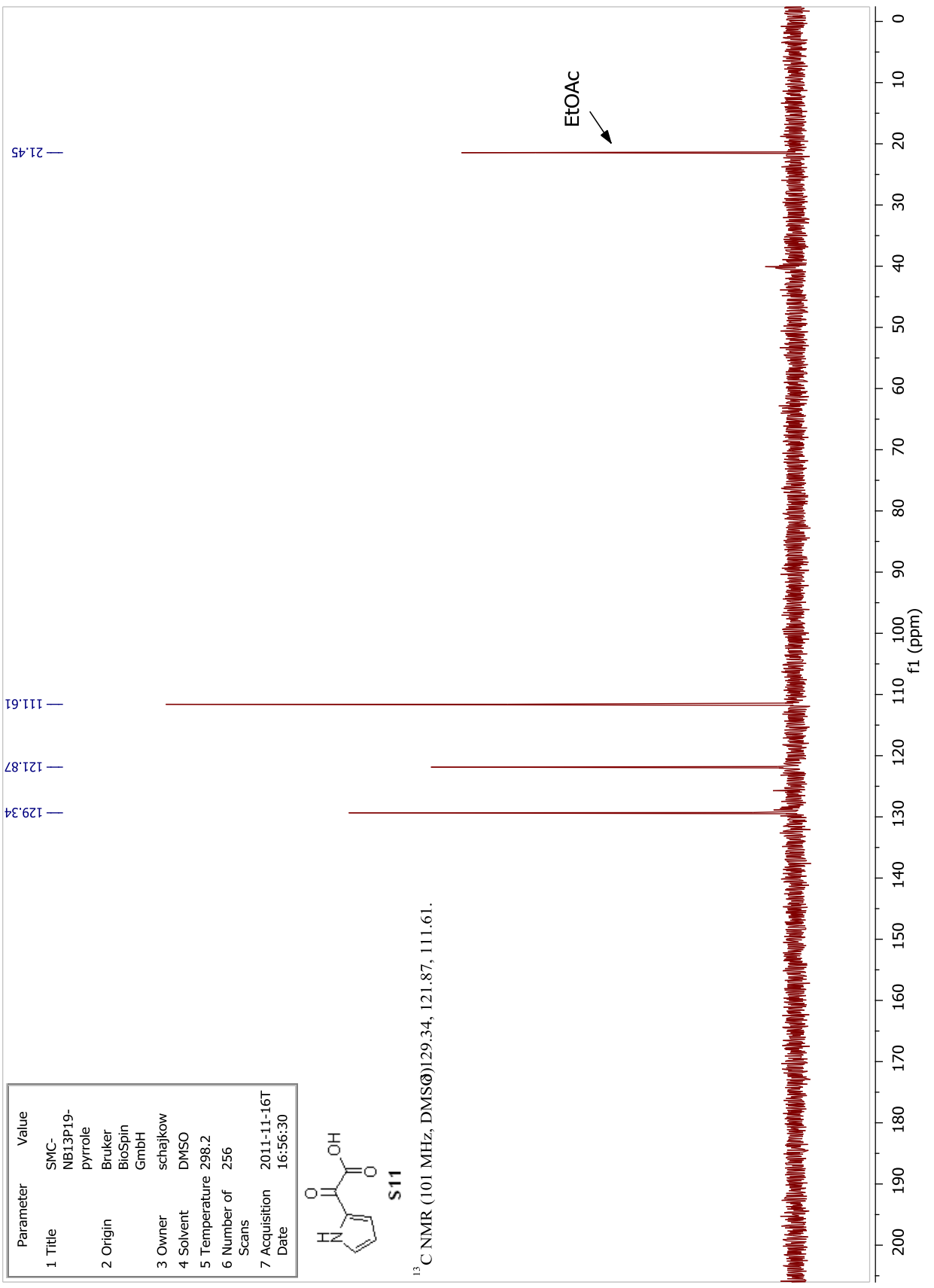


Parameter	Value
1 Title	SMC-NB13P19-pyrrole
2 Origin	Bruker BioSpin GmbH
3 Owner	schajkow
4 Solvent	DMSO
5 Temperature	298.2
6 Number of Scans	256
7 Acquisition Date	2011-11-16T16:56:30

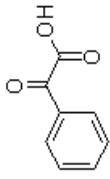


**S11**

<sup>13</sup>C NMR (101 MHz, DMSO) 129.34, 121.87, 111.61.

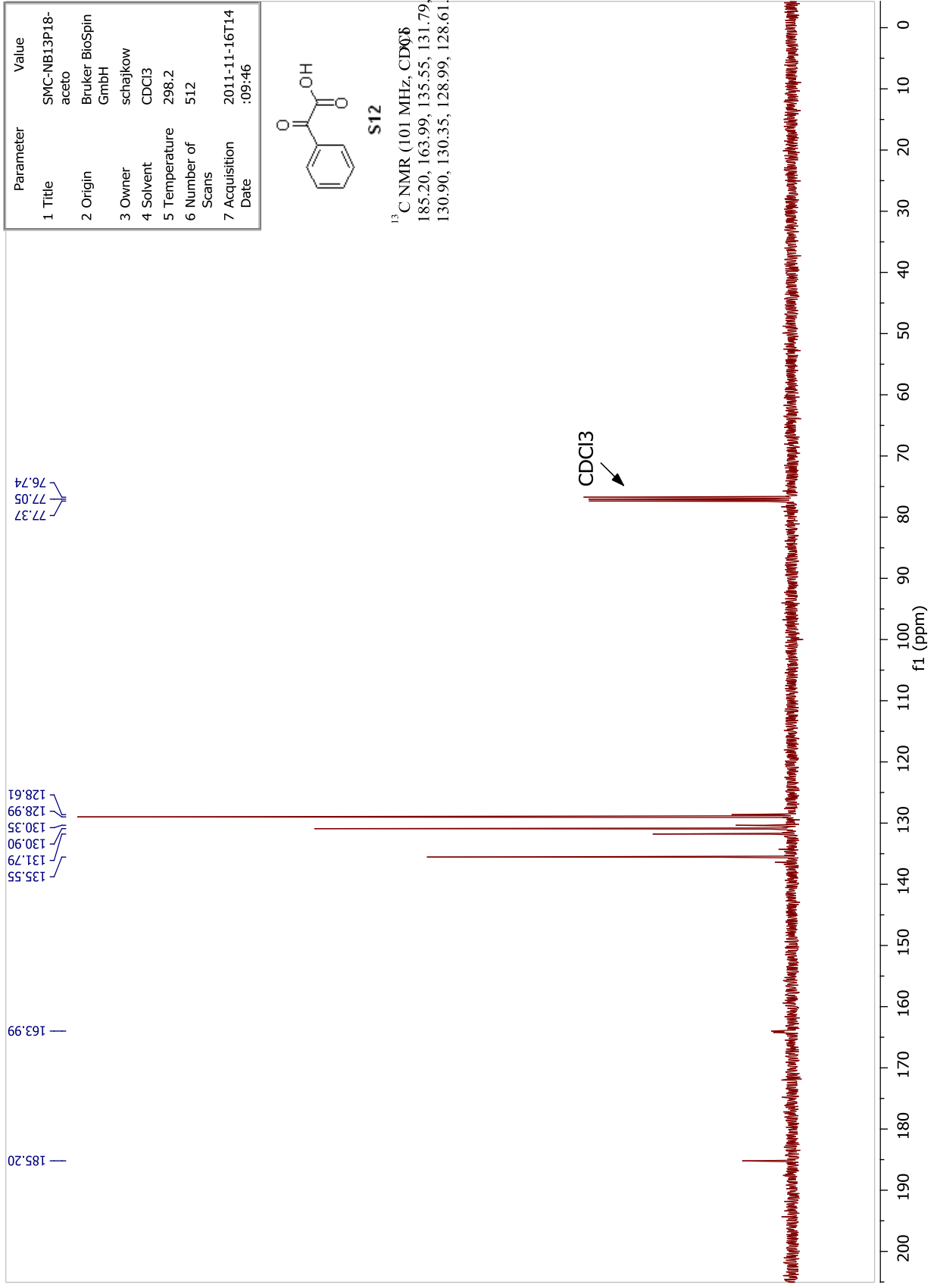


Parameter	Value
1 Title	SMC-NB13P18-aceto
2 Origin	Bruker BioSpin GmbH
3 Owner	schajjkow
4 Solvent	CDCl3
5 Temperature	298.2
6 Number of Scans	512
7 Acquisition Date	2011-11-16T14:09:46

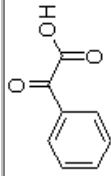


S12

<sup>13</sup>C NMR (101 MHz, CDCl<sub>3</sub>)  
 185.20, 163.99, 135.55, 131.79,  
 130.90, 130.35, 128.99, 128.61.

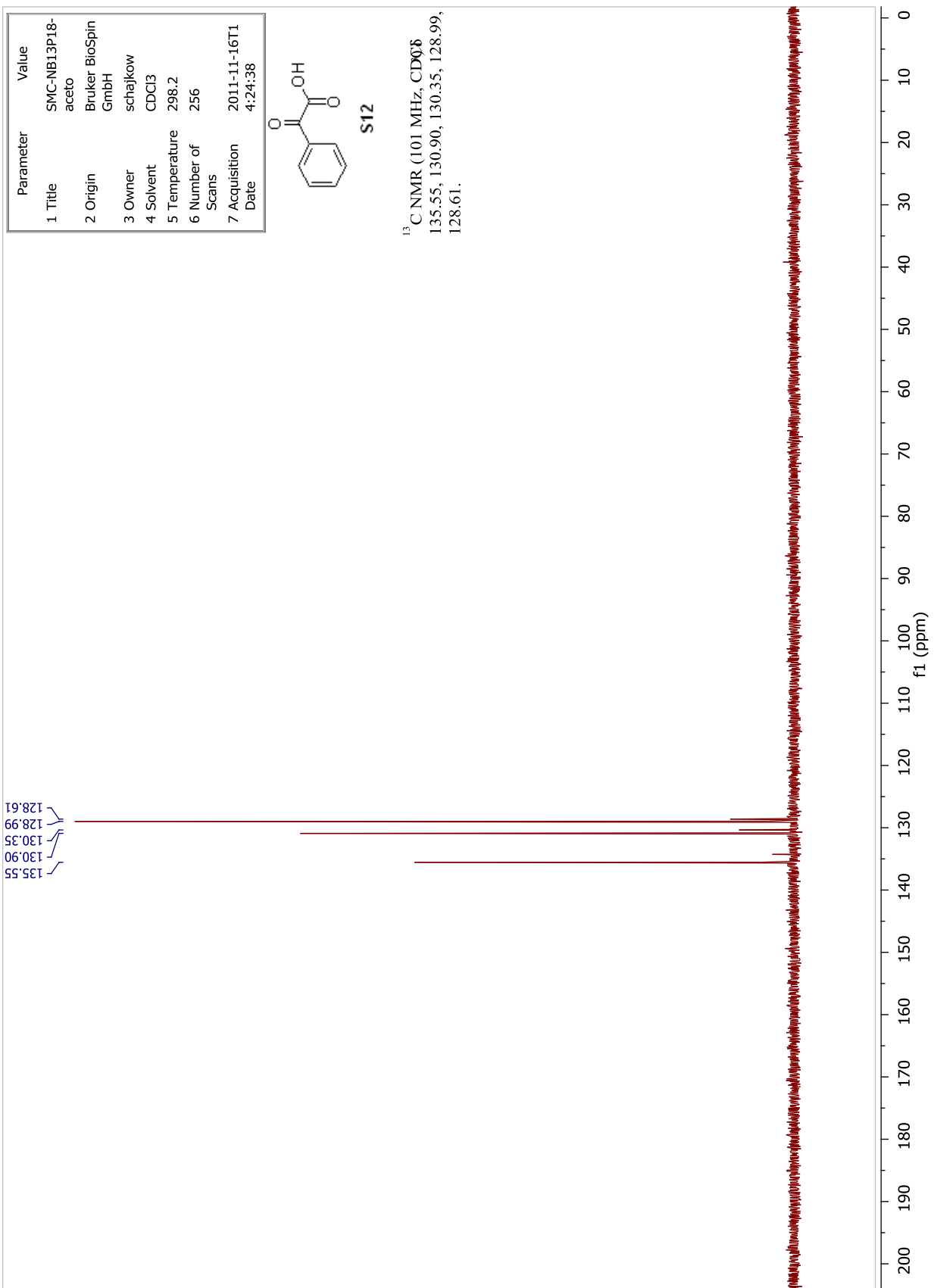


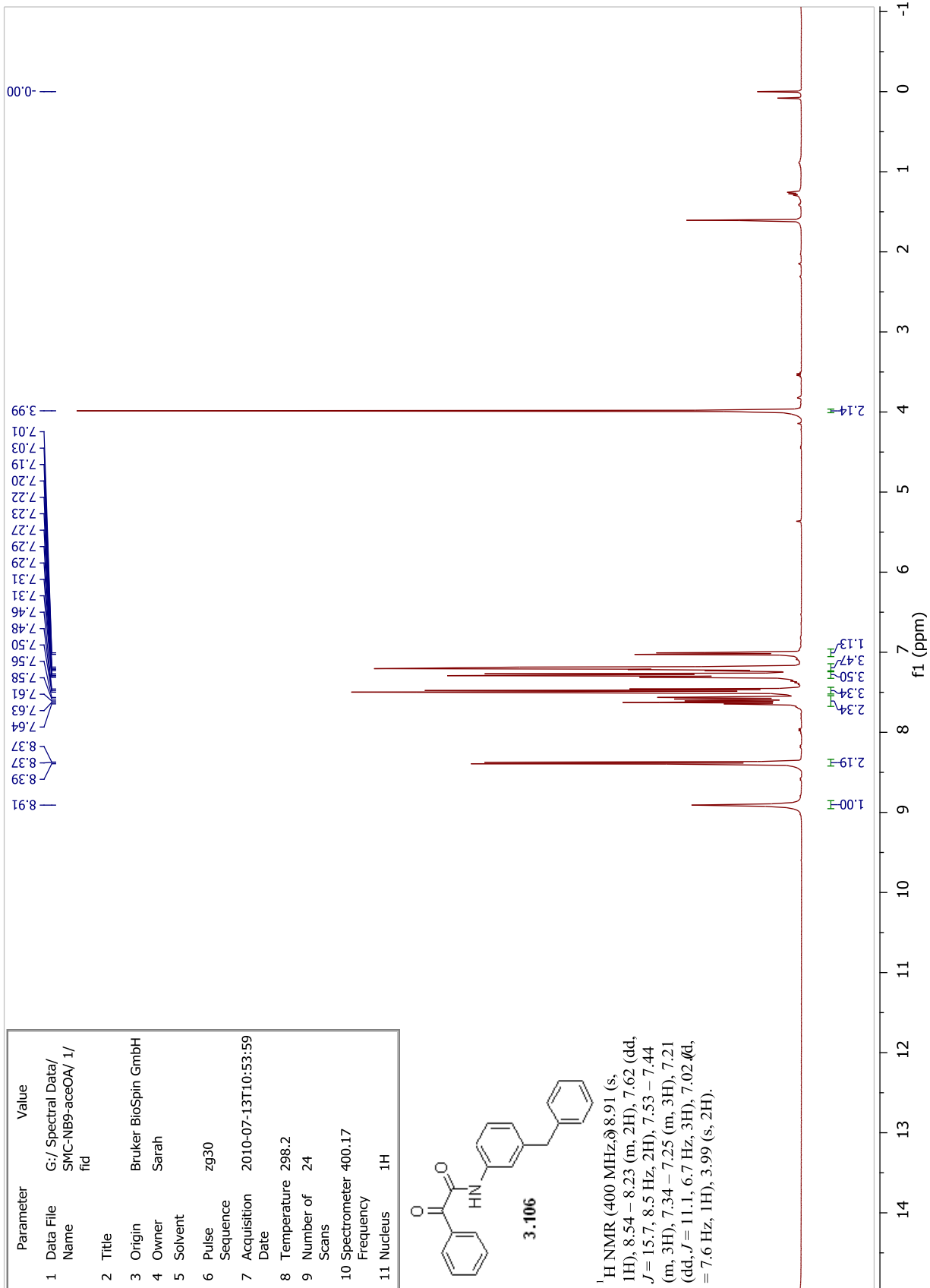
Parameter	Value
1 Title	SMC-NB13P18-aceto
2 Origin	Bruker BioSpin GmbH
3 Owner	schajkow
4 Solvent	CDCl3
5 Temperature	298.2
6 Number of Scans	256
7 Acquisition Date	2011-11-16T14:24:38



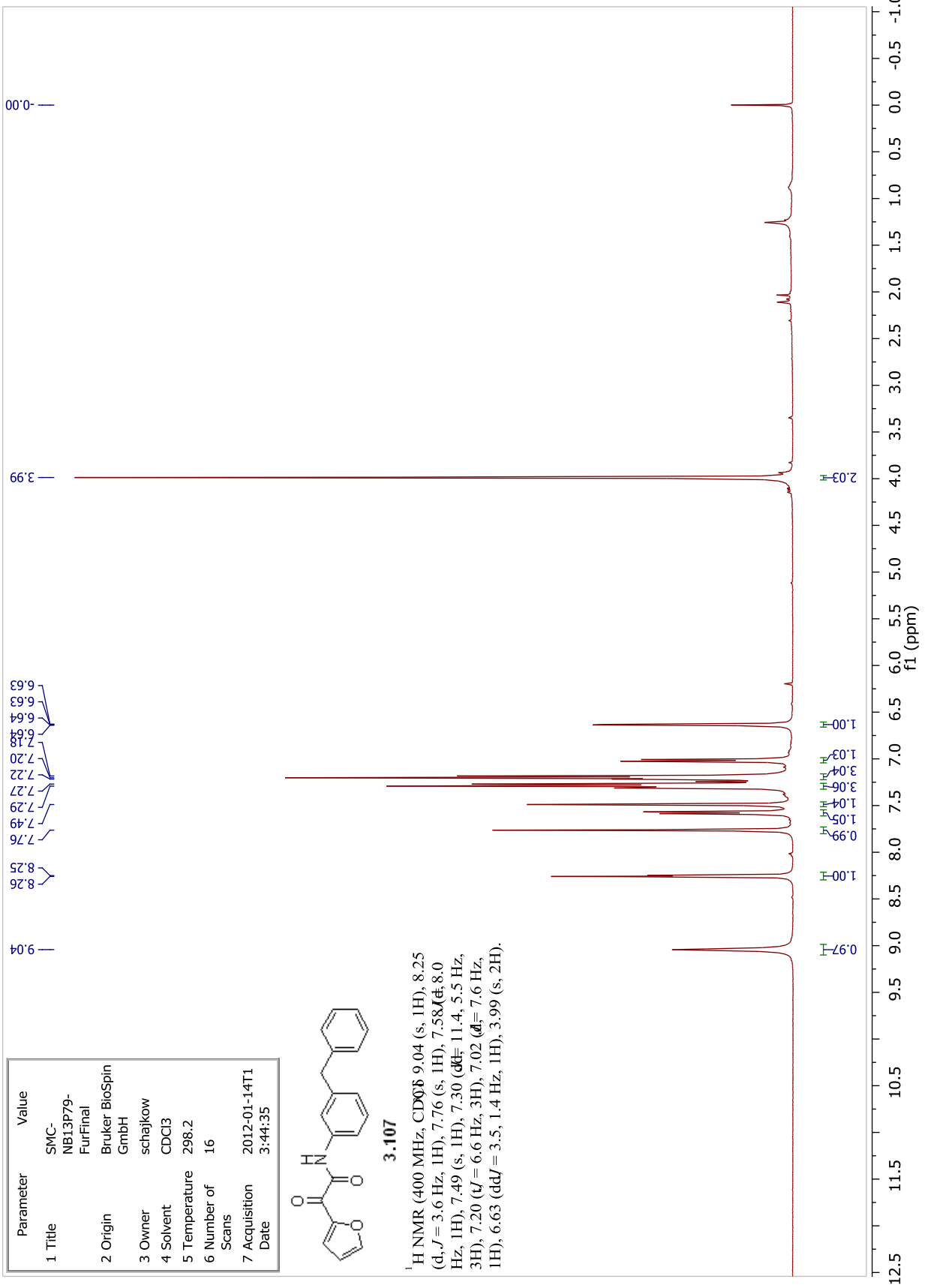
**S12**

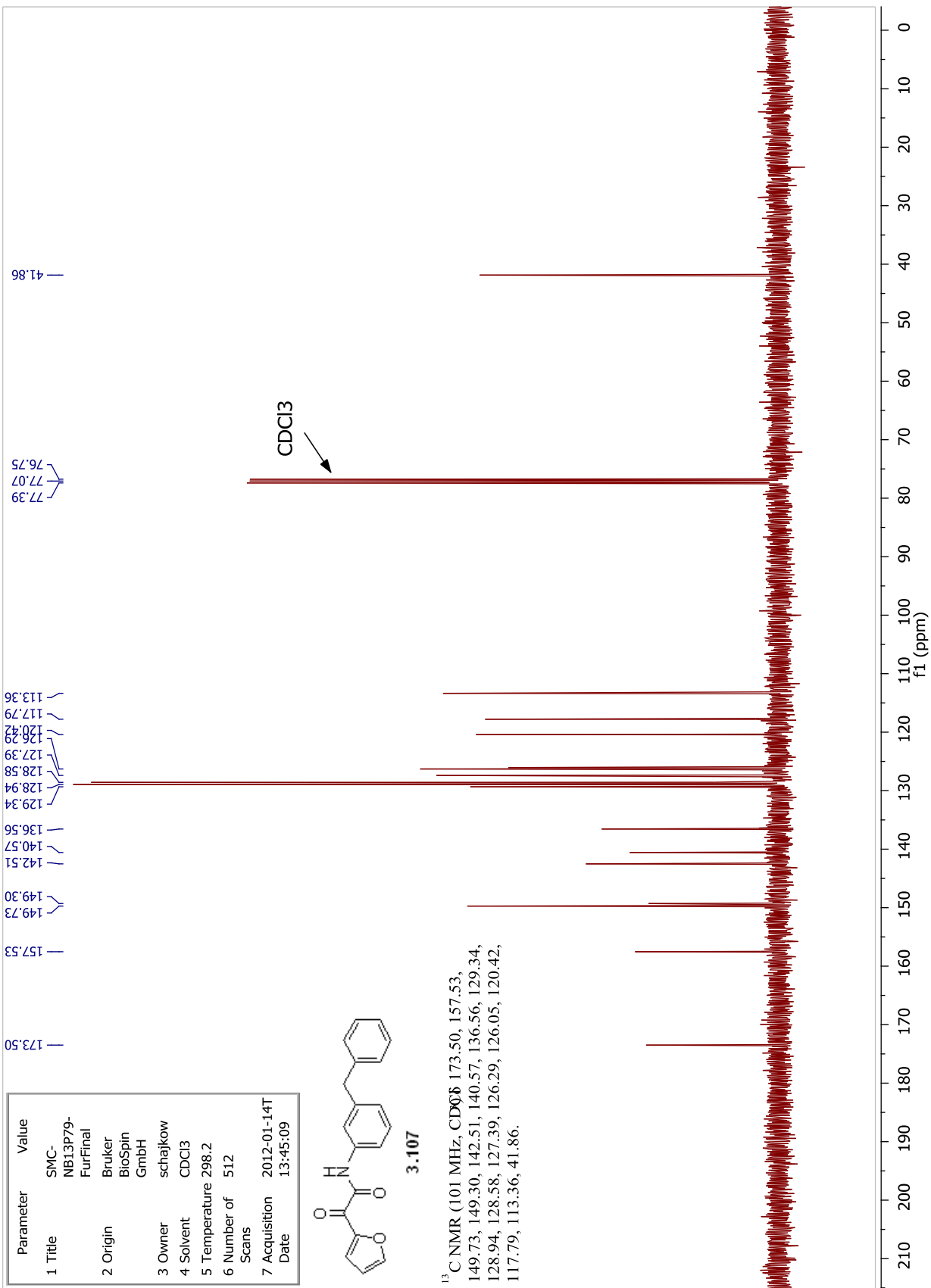
<sup>13</sup>C NMR (101 MHz, CDCl<sub>3</sub>)  
135.55, 130.90, 130.35, 128.99,  
128.61.

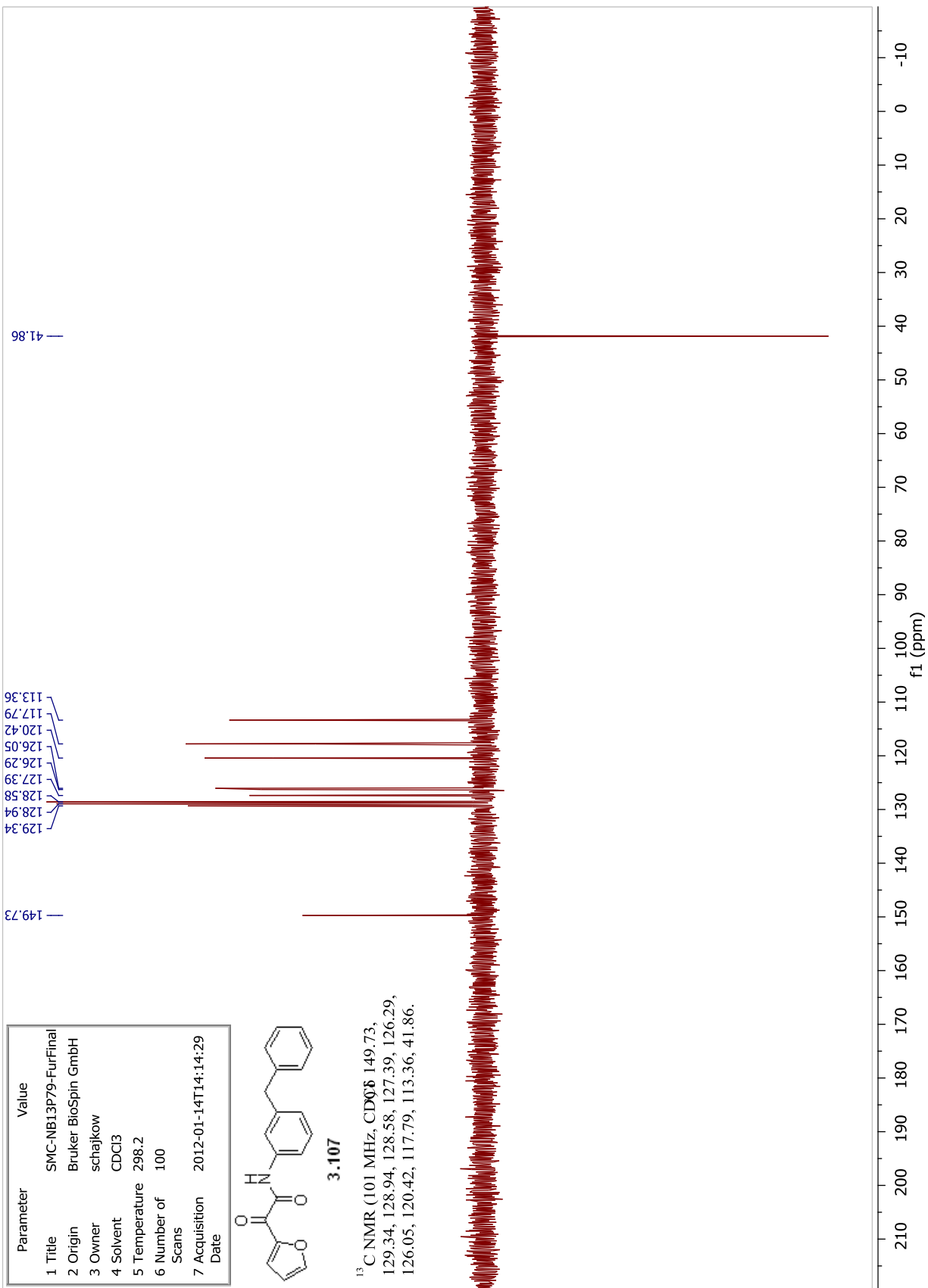




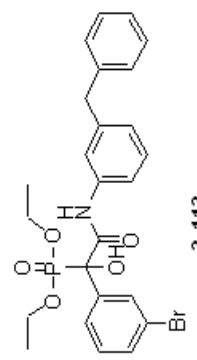




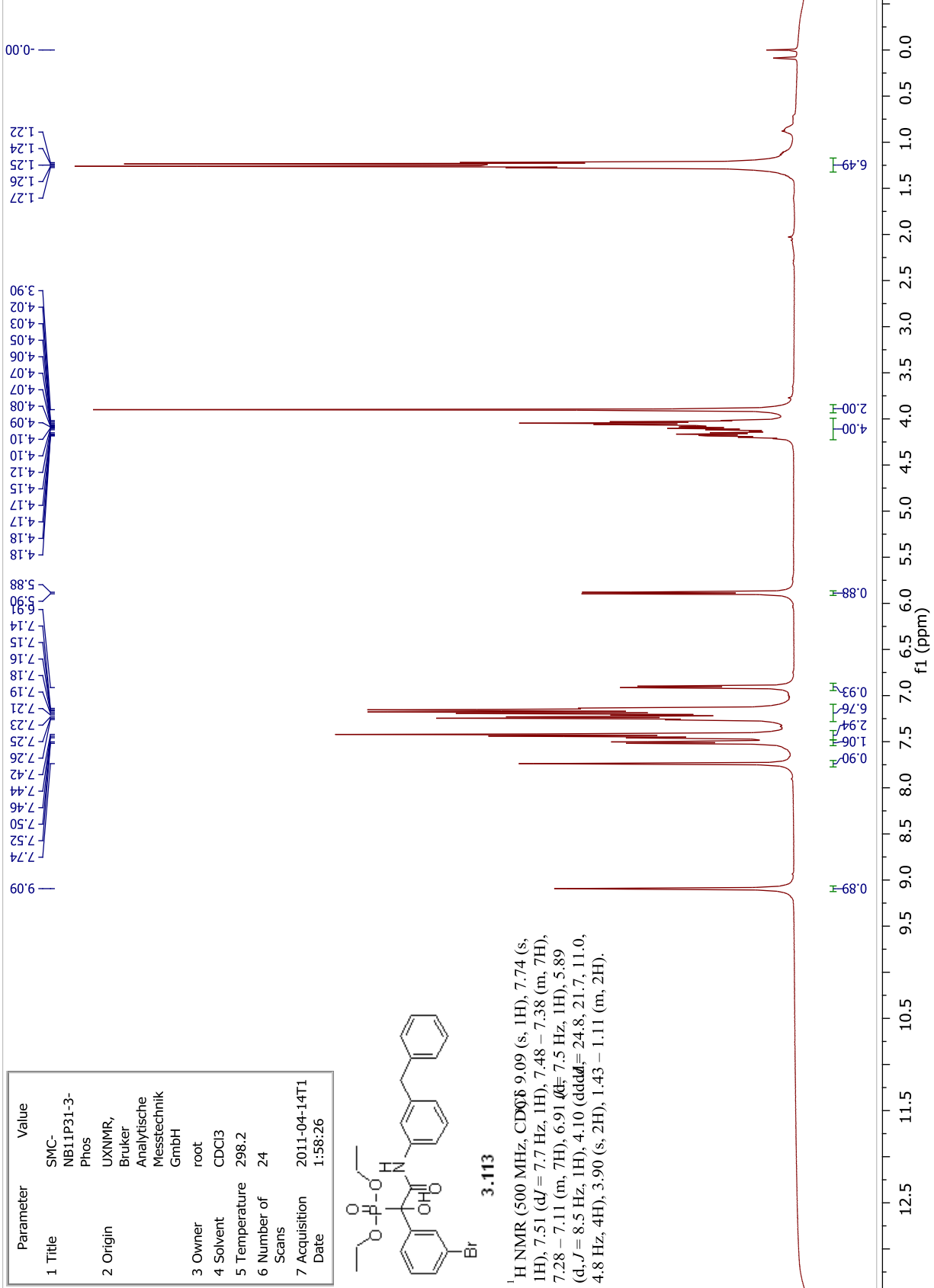




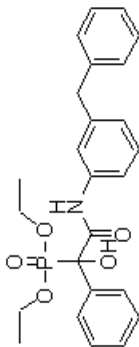
Parameter	Value
1 Title	SMC-NB11P31-3-Phos
2 Origin	UXNMR, Bruker Analytische Messtechnik GmbH
3 Owner	root
4 Solvent	CDCl3
5 Temperature	298.2
6 Number of Scans	24
7 Acquisition Date	2011-04-14T11:58:26



<sup>1</sup>H NMR (500 MHz, CDCl<sub>3</sub>) δ 9.09 (s, 1H), 7.74 (s, 1H), 7.51 (d, J = 7.7 Hz, 1H), 7.48 – 7.38 (m, 7H), 7.28 – 7.11 (m, 7H), 6.91 (d, J = 7.5 Hz, 1H), 5.89 (d, J = 8.5 Hz, 1H), 4.10 (dddd, J = 24.8, 21.7, 11.0, 4.8 Hz, 4H), 3.90 (s, 2H), 1.43 – 1.11 (m, 2H).

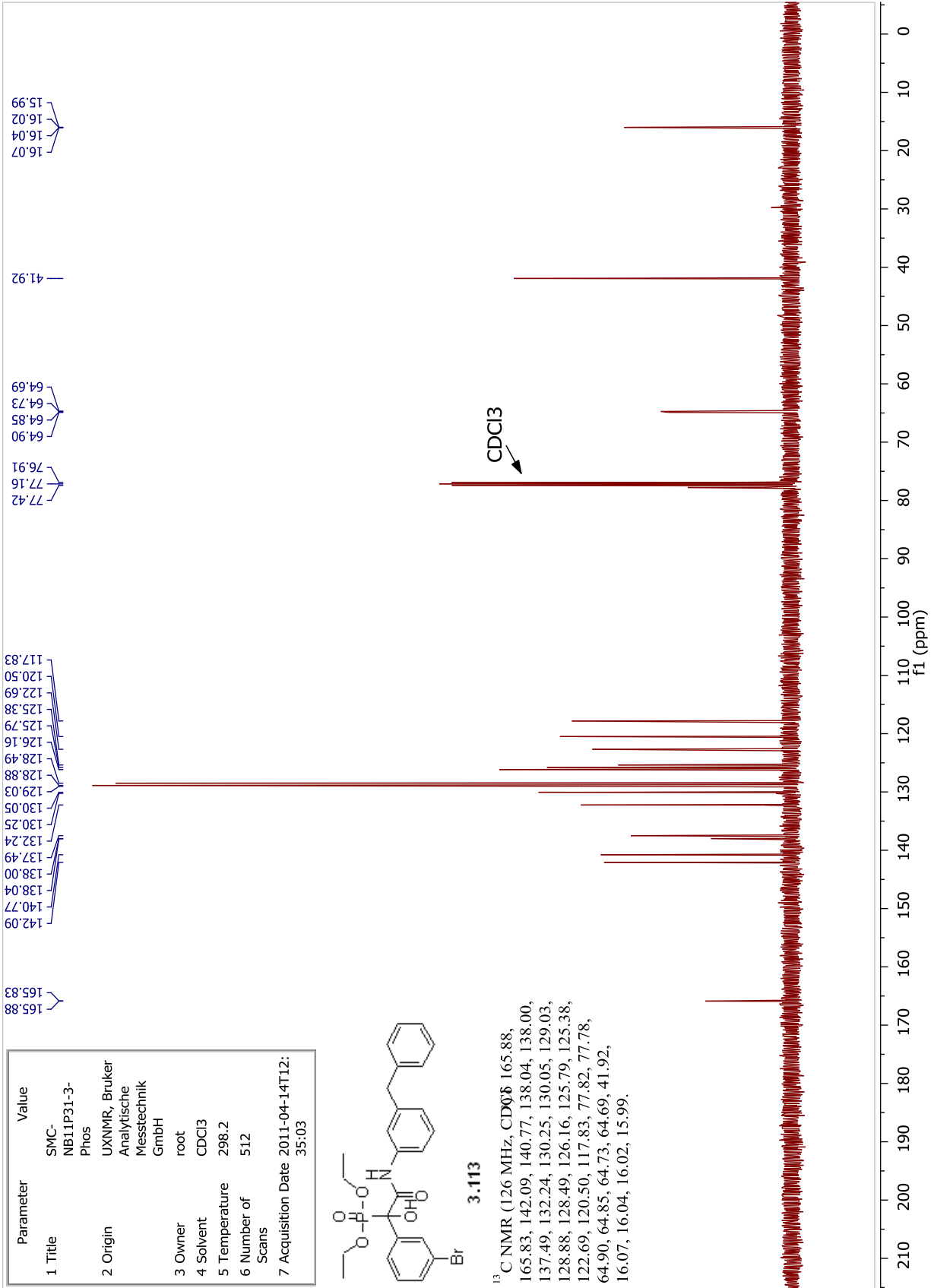


Parameter	Value
1 Title	SMC-NB11P31-3-Phos
2 Origin	UXNMR, Bruker Analytische Messtechnik GmbH
3 Owner	root
4 Solvent	CDCl3
5 Temperature	298.2
6 Number of Scans	512
7 Acquisition Date	2011-04-14T12:35:03

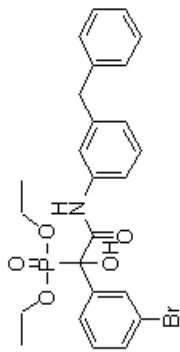


3.113

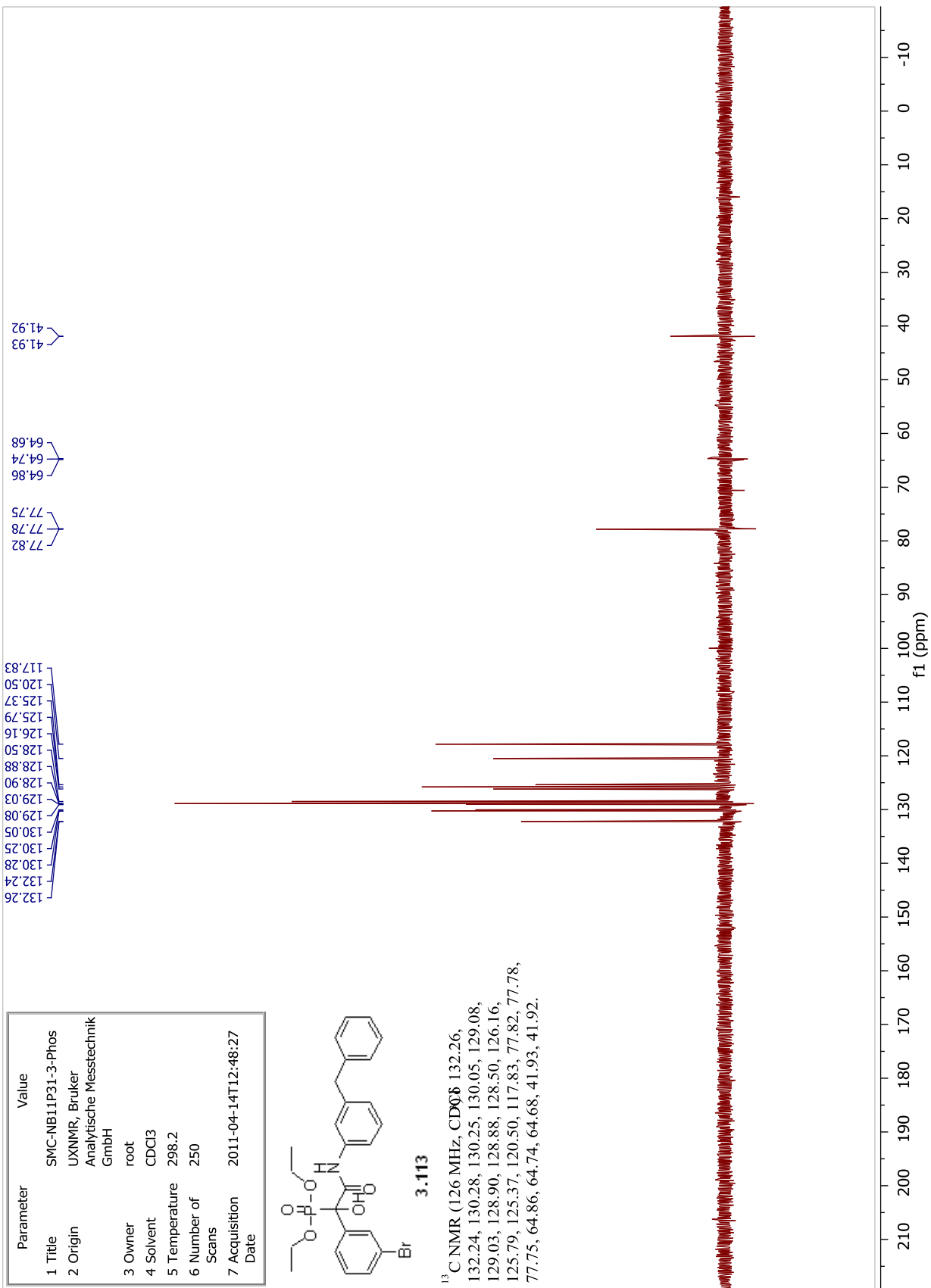
<sup>13</sup>C NMR (126 MHz, CDCl<sub>3</sub>) 165.88, 165.83, 142.09, 140.77, 138.04, 138.00, 137.49, 132.24, 130.25, 130.05, 129.03, 128.88, 128.49, 126.16, 125.79, 125.38, 122.69, 120.50, 117.83, 77.82, 77.78, 64.90, 64.85, 64.73, 64.69, 41.92, 16.07, 16.04, 16.02, 15.99.



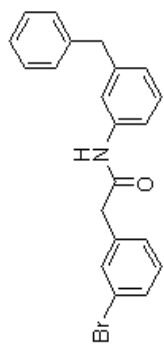
Parameter	Value
1 Title	SMC-NB11P31-3-Phos
2 Origin	UXNMR, Bruker Analytische Messtechnik GmbH
3 Owner	root
4 Solvent	CDCl3
5 Temperature	298.2
6 Number of Scans	250
7 Acquisition Date	2011-04-14T12:48:27



<sup>13</sup>C NMR (126 MHz, CDCl<sub>3</sub>) 132.26, 132.24, 130.28, 130.25, 130.05, 129.08, 129.03, 128.90, 128.88, 128.50, 126.16, 125.79, 125.37, 120.50, 117.83, 77.82, 77.78, 77.75, 64.86, 64.74, 64.68, 41.93, 41.92.

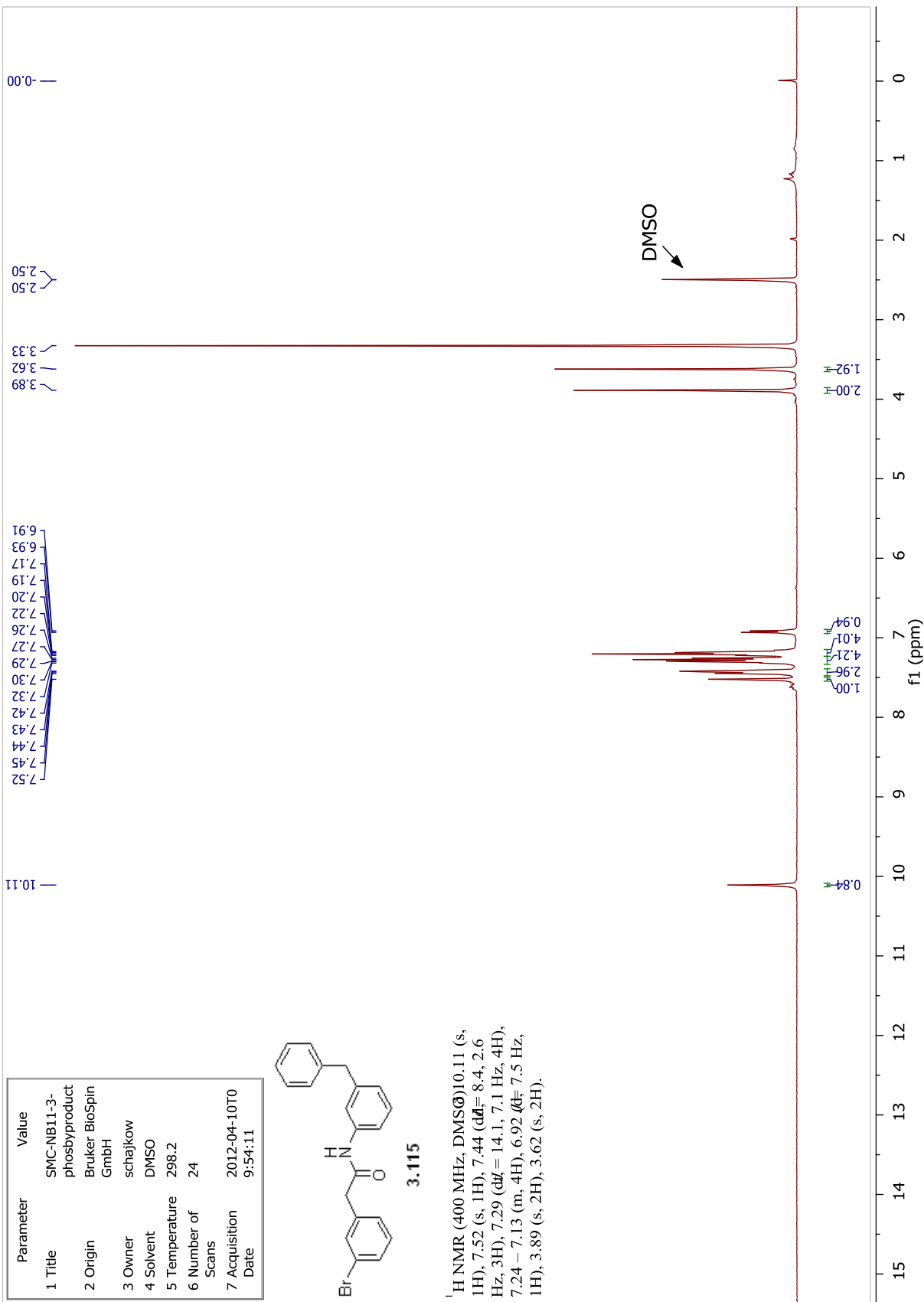


Parameter	Value
1 Title	SMC-NB11-3-phosbyproduct
2 Origin	Bruker BioSpin GmbH
3 Owner	schajkow
4 Solvent	DMSO
5 Temperature	298.2
6 Number of Scans	24
7 Acquisition Date	2012-04-10T09:54:11

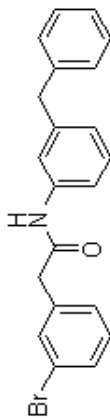


**3.115**

<sup>1</sup>H NMR (400 MHz, DMSO-d<sub>6</sub>) 10.11 (s, 1H), 7.52 (s, 1H), 7.44 (dd, *J* = 8.4, 2.6 Hz, 3H), 7.29 (dd, *J* = 14.1, 7.1 Hz, 4H), 7.24–7.13 (m, 4H), 6.92 (t, *J* = 7.5 Hz, 1H), 3.89 (s, 2H), 3.62 (s, 2H).

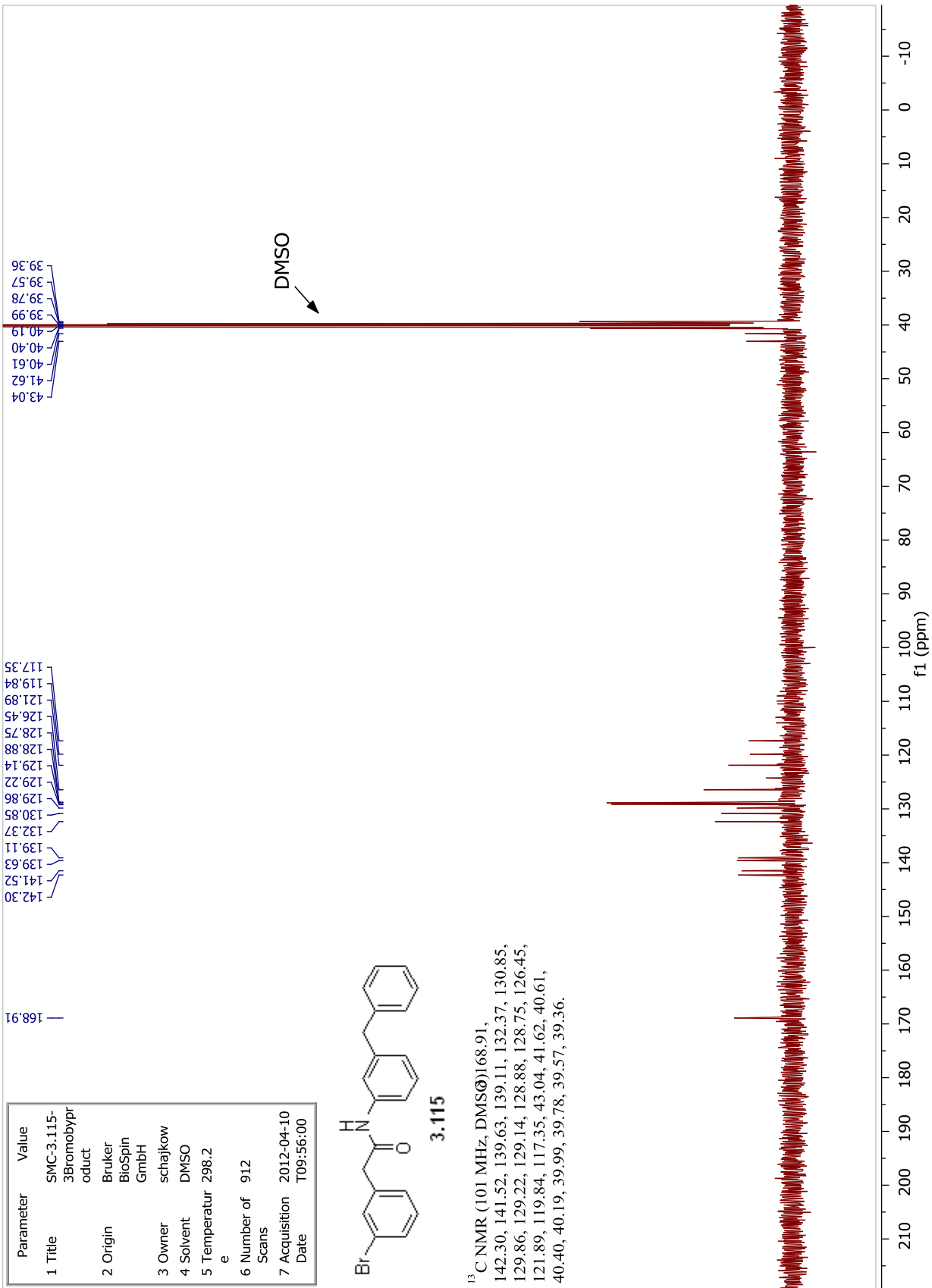


Parameter	Value
1 Title	SMC-3.115-3Bromobyprioduct
2 Origin	Bruker BioSpin GmbH
3 Owner	schajkow
4 Solvent	DMSO
5 Temperatur	298.2 e
6 Number of Scans	912
7 Acquisition Date	2012-04-10 T09:56:00



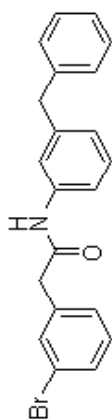
**3.115**

<sup>13</sup>C NMR (101 MHz, DMSO) 168.91, 142.30, 141.52, 139.63, 139.11, 132.37, 130.85, 129.86, 129.22, 129.14, 128.88, 128.75, 126.45, 121.89, 119.84, 117.35, 43.04, 41.62, 40.61, 40.40, 40.19, 39.99, 39.78, 39.57, 39.36.



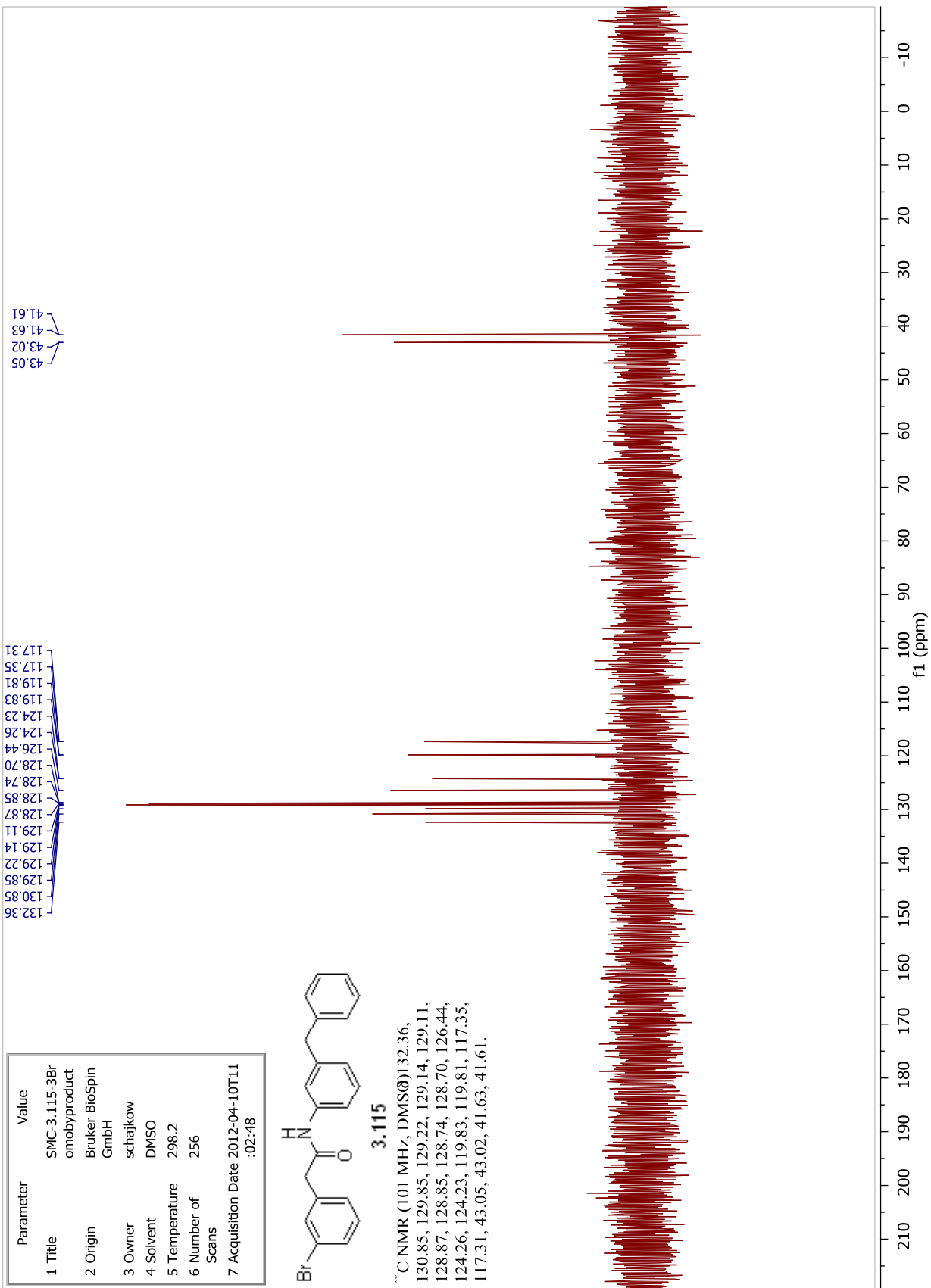


Parameter	Value
1 Title	SMC-3.115-3Br omobyproduct
2 Origin	Braker BioSpin GmbH
3 Owner	schajkow
4 Solvent	DMSO
5 Temperature	298.2
6 Number of Scans	256
7 Acquisition Date	2012-04-10T11 :02:48

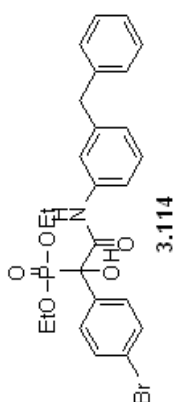


### 3.115

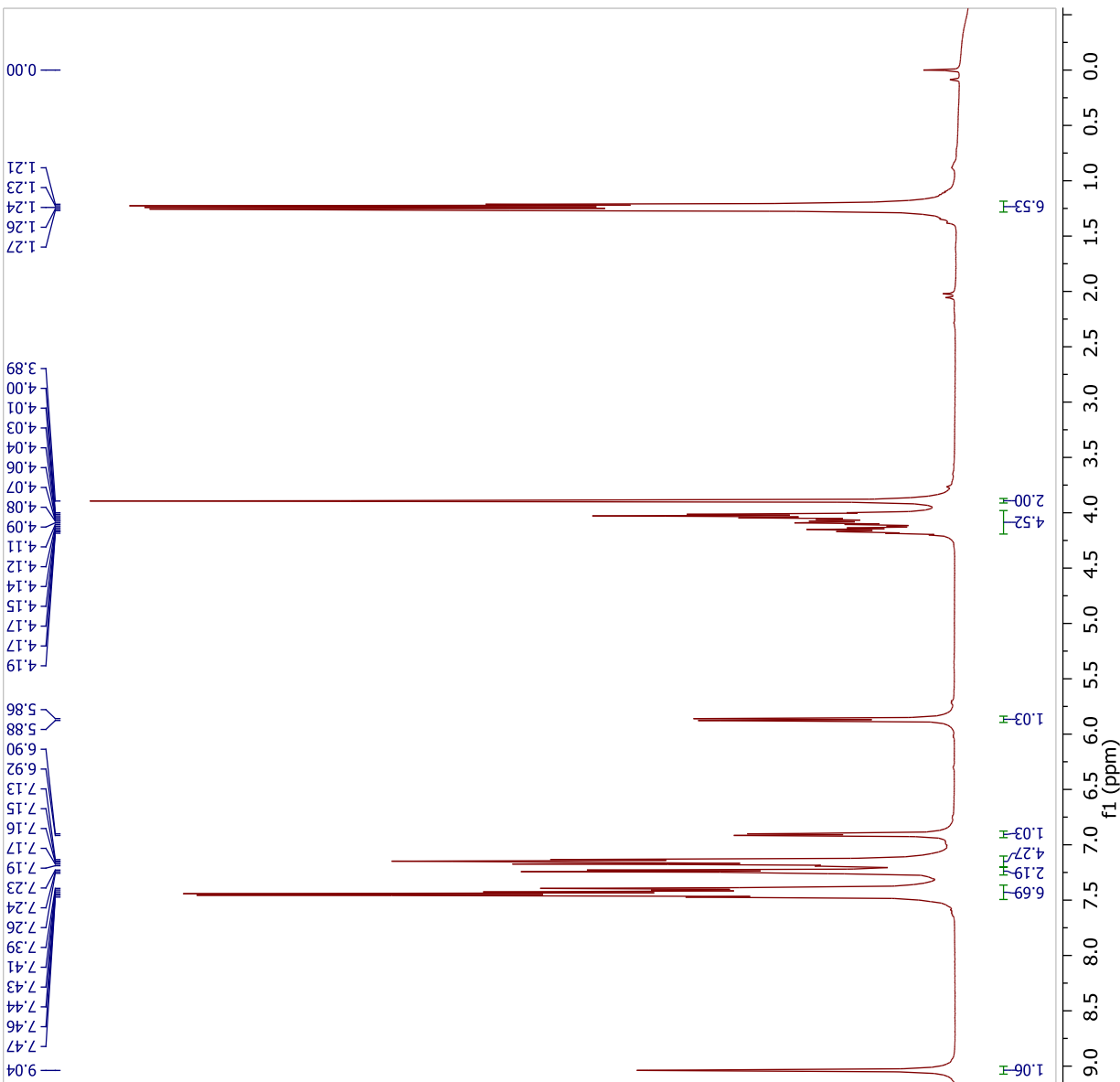
<sup>13</sup>C NMR (101 MHz, DMSO-d<sub>6</sub>) 132.36, 130.85, 129.85, 129.22, 129.14, 129.11, 128.87, 128.85, 128.74, 128.70, 126.44, 124.26, 124.23, 119.83, 119.81, 117.35, 117.31, 43.05, 41.63, 41.61.

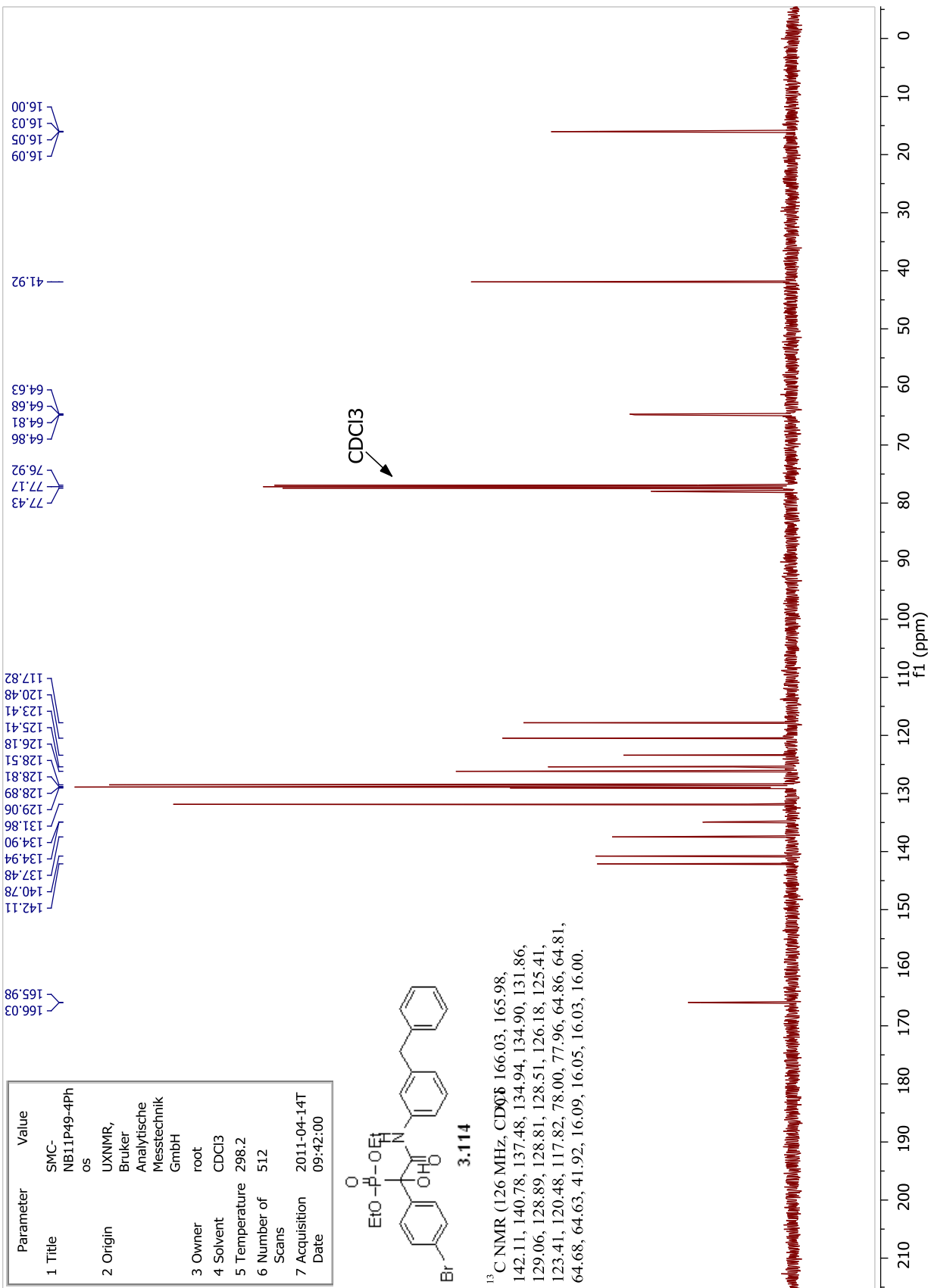


Parameter	Value
1 Title	SMC-NB11P49-4P
2 Origin	hos UXNMR, Bruker Analytische Messtechnik GmbH
3 Owner	root
4 Solvent	CDCl3
5 Temperature	298.2
6 Number of Scans	24
7 Acquisition Date	2011-04-14 T09:22:00



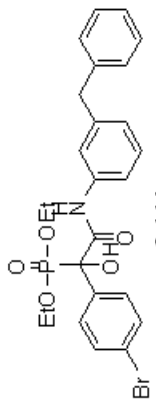
<sup>1</sup>H NMR (500 MHz, CDCl<sub>3</sub>) 9.04 (s, 1H), 7.43 (dt, *J* = 24.3, 7.9 Hz, 6H), 7.24 (t, *J* = 7.4 Hz, 2H), 7.21 – 7.10 (m, 4H), 6.91 (d, *J* = 7.4 Hz, 1H), 5.87 (dd, *J* = 8.5 Hz, 1H), 4.22 – 3.97 (m, 4H), 3.89 (s, 2H), 1.24 (dt, *J* = 14.4, 7.0 Hz, 6H).



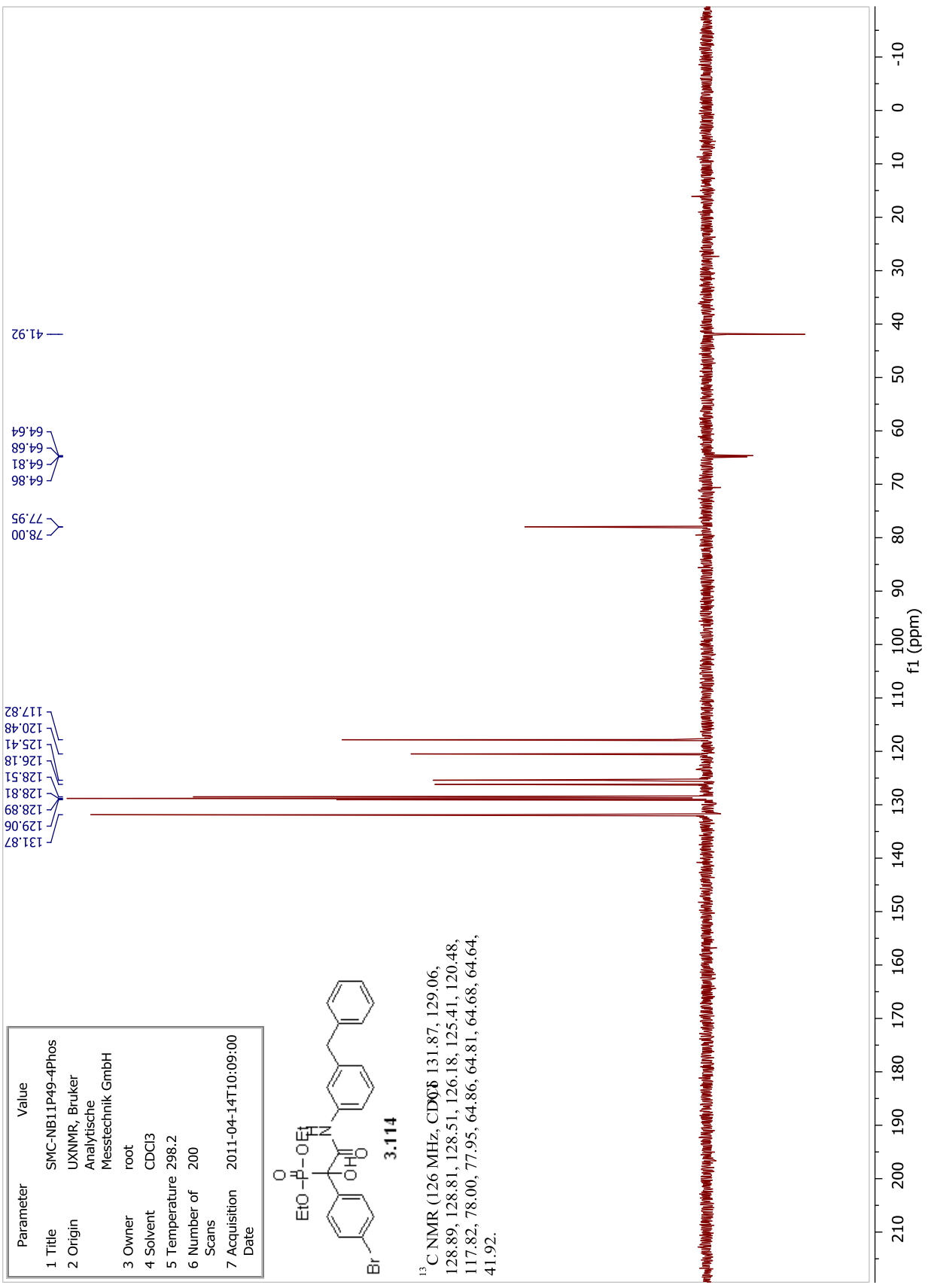


Parameter	Value
1 Title	SMC-NB11P49-4ph os
2 Origin	UXNMR, Bruker Analytische Messtechnik GmbH
3 Owner	root
4 Solvent	CDCl <sub>3</sub>
5 Temperature	298.2
6 Number of Scans	512
7 Acquisition Date	2011-04-14T 09:42:00

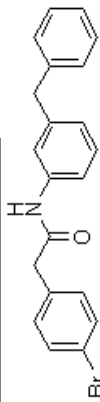
Parameter	Value
1 Title	SMC-NB11P49-4Phos
2 Origin	UXNMR, Bruker Analytische Messtechnik GmbH
3 Owner	root
4 Solvent	CDCl3
5 Temperature	298.2
6 Number of Scans	200
7 Acquisition Date	2011-04-14T10:09:00



<sup>13</sup>C NMR (126 MHz, CDCl<sub>3</sub>) 131.87, 129.06, 128.89, 128.81, 126.18, 125.41, 120.48, 117.82, 78.00, 77.95, 64.86, 64.81, 64.68, 64.64, 41.92.

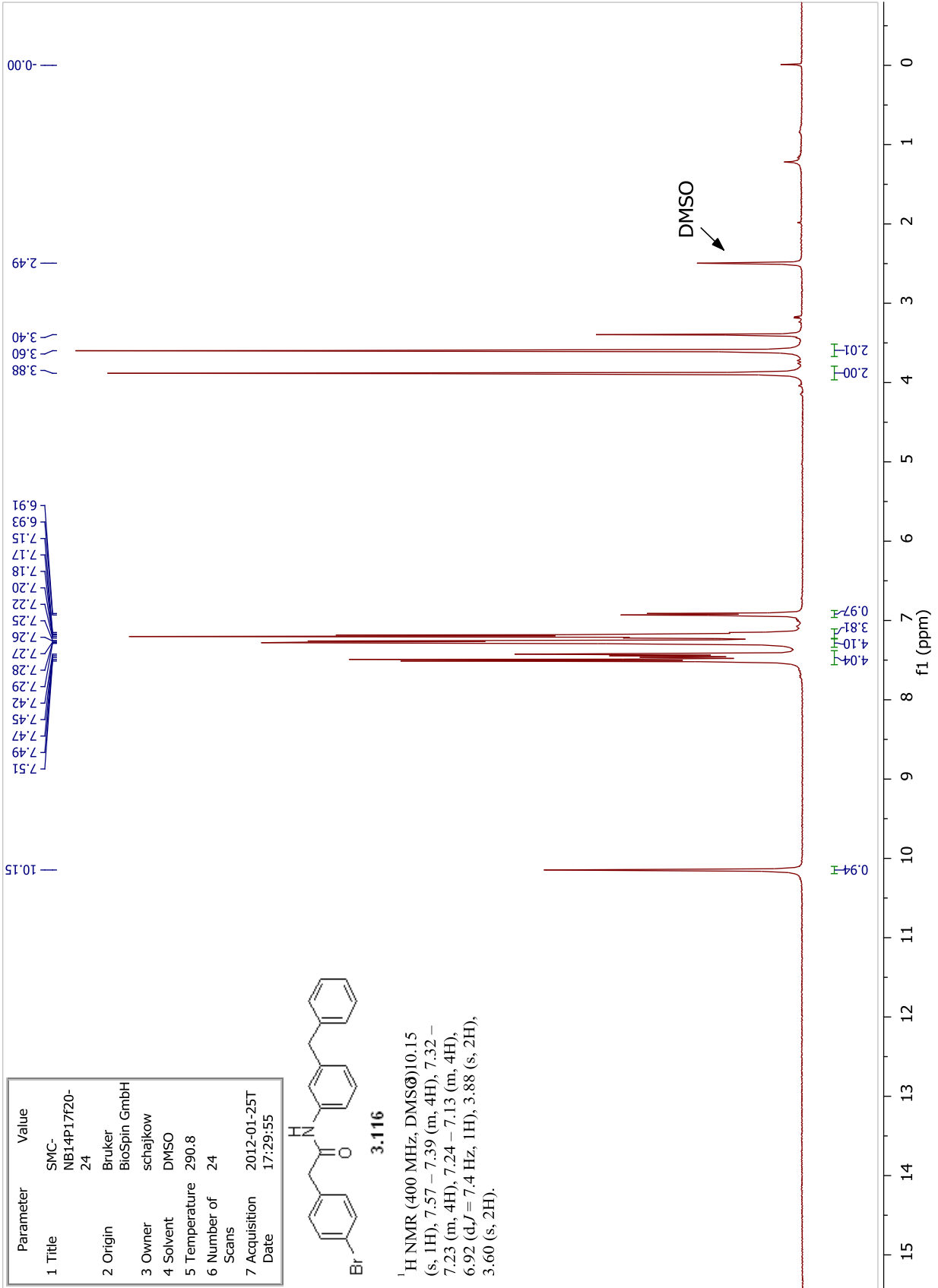


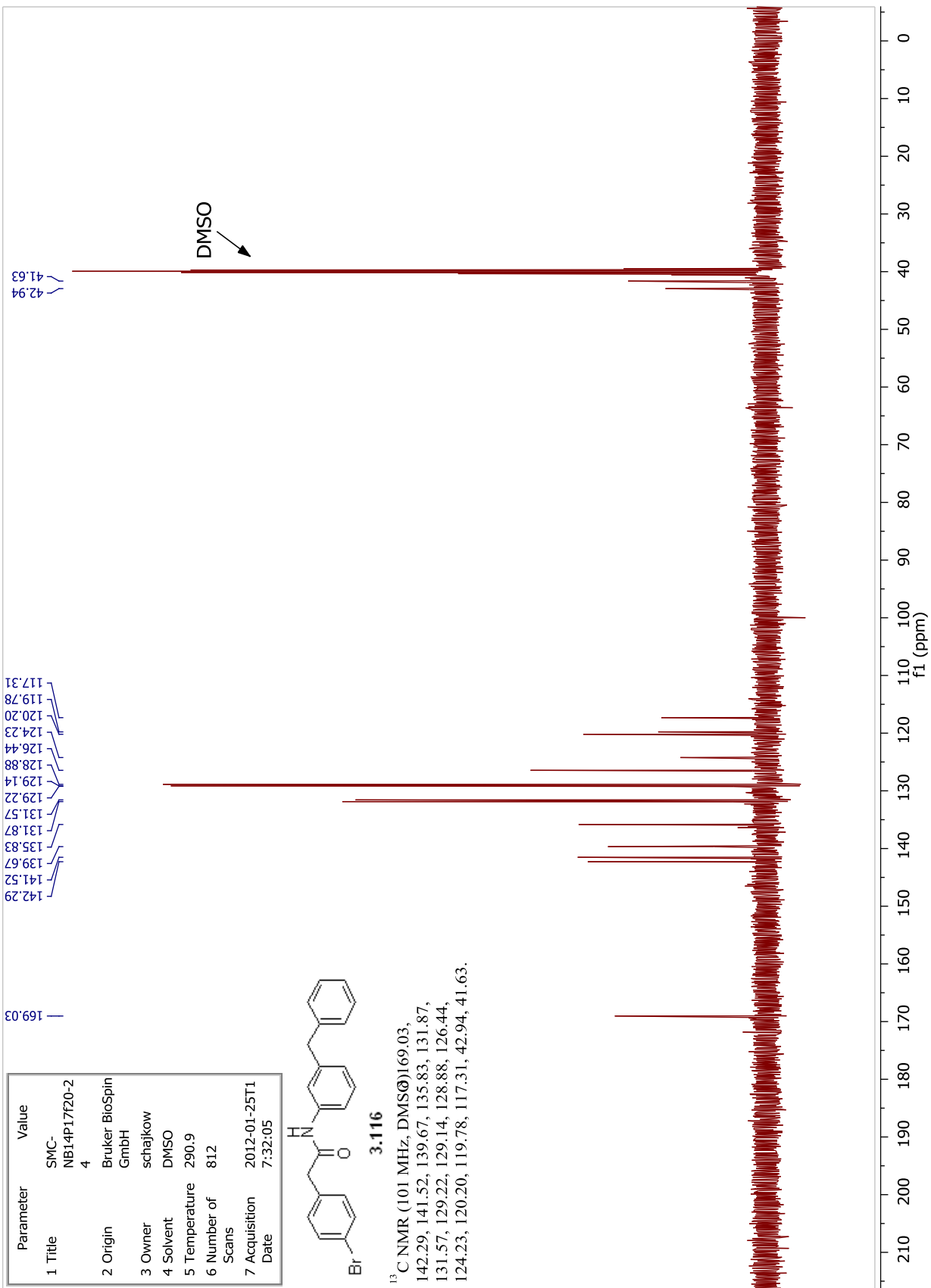
Parameter	Value
1 Title	SMC-NB14P1720-24
2 Origin	Bruker BioSpin GmbH
3 Owner	schajkow
4 Solvent	DMSO
5 Temperature	290.8
6 Number of Scans	24
7 Acquisition Date	2012-01-25T17:29:55



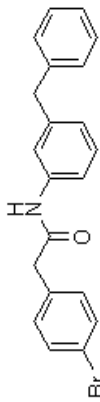
**3.116**

<sup>1</sup>H NMR (400 MHz, DMSO-d<sub>6</sub>) 10.15 (s, 1H), 7.57 – 7.39 (m, 4H), 7.32 – 7.23 (m, 4H), 7.24 – 7.13 (m, 4H), 6.92 (d, J = 7.4 Hz, 1H), 3.88 (s, 2H), 3.60 (s, 2H).



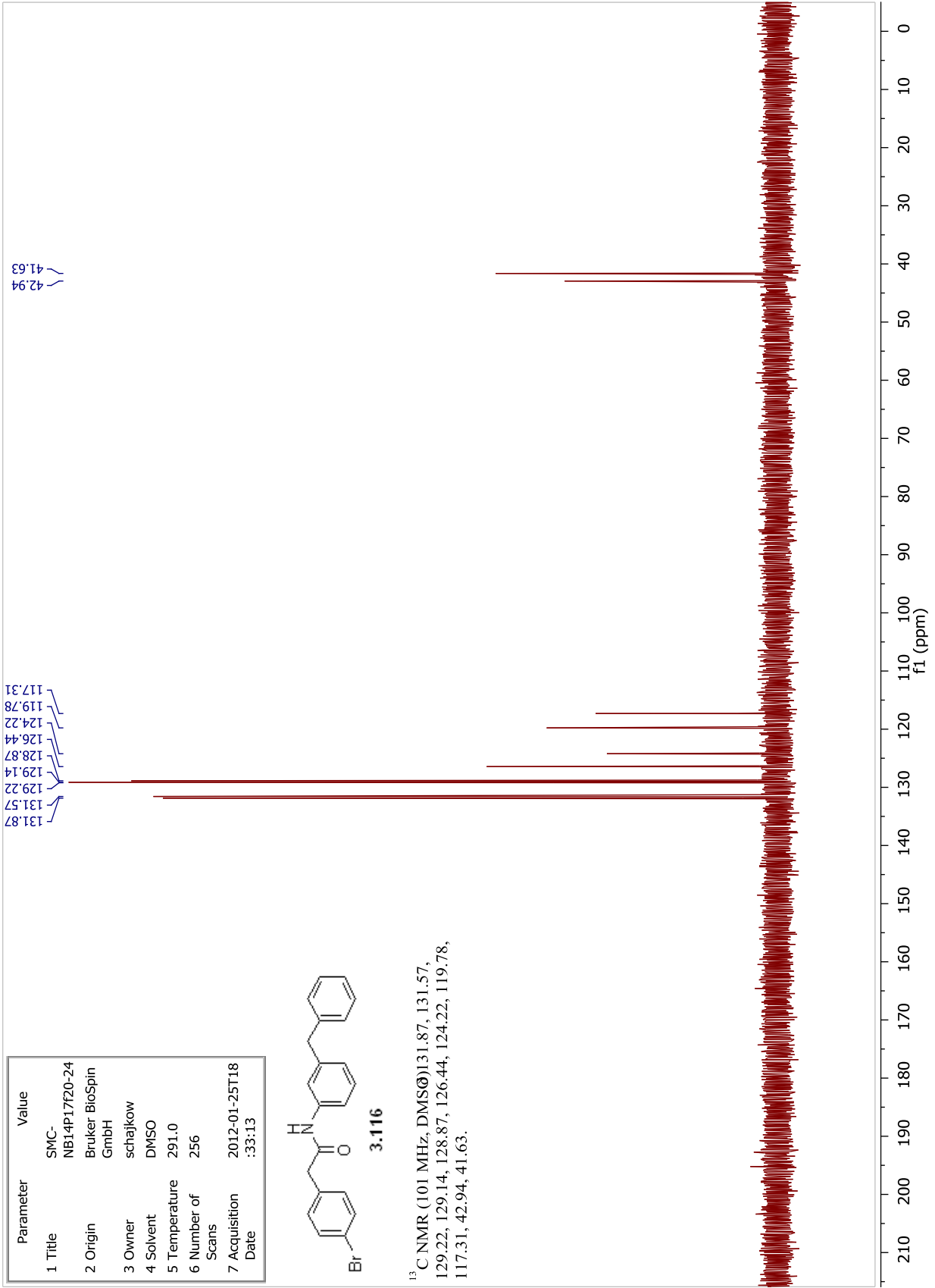


Parameter	Value
1 Title	SMC-NB14P17F20-24
2 Origin	Bruker BioSpin GmbH
3 Owner	schajkow
4 Solvent	DMSO
5 Temperature	291.0
6 Number of Scans	256
7 Acquisition Date	2012-01-25T18:33:13

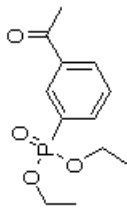


3.116

<sup>13</sup>C NMR (101 MHz, DMSO-d<sub>6</sub>) 131.87, 131.57, 129.22, 129.14, 128.87, 126.44, 124.22, 119.78, 117.31, 42.94, 41.63.

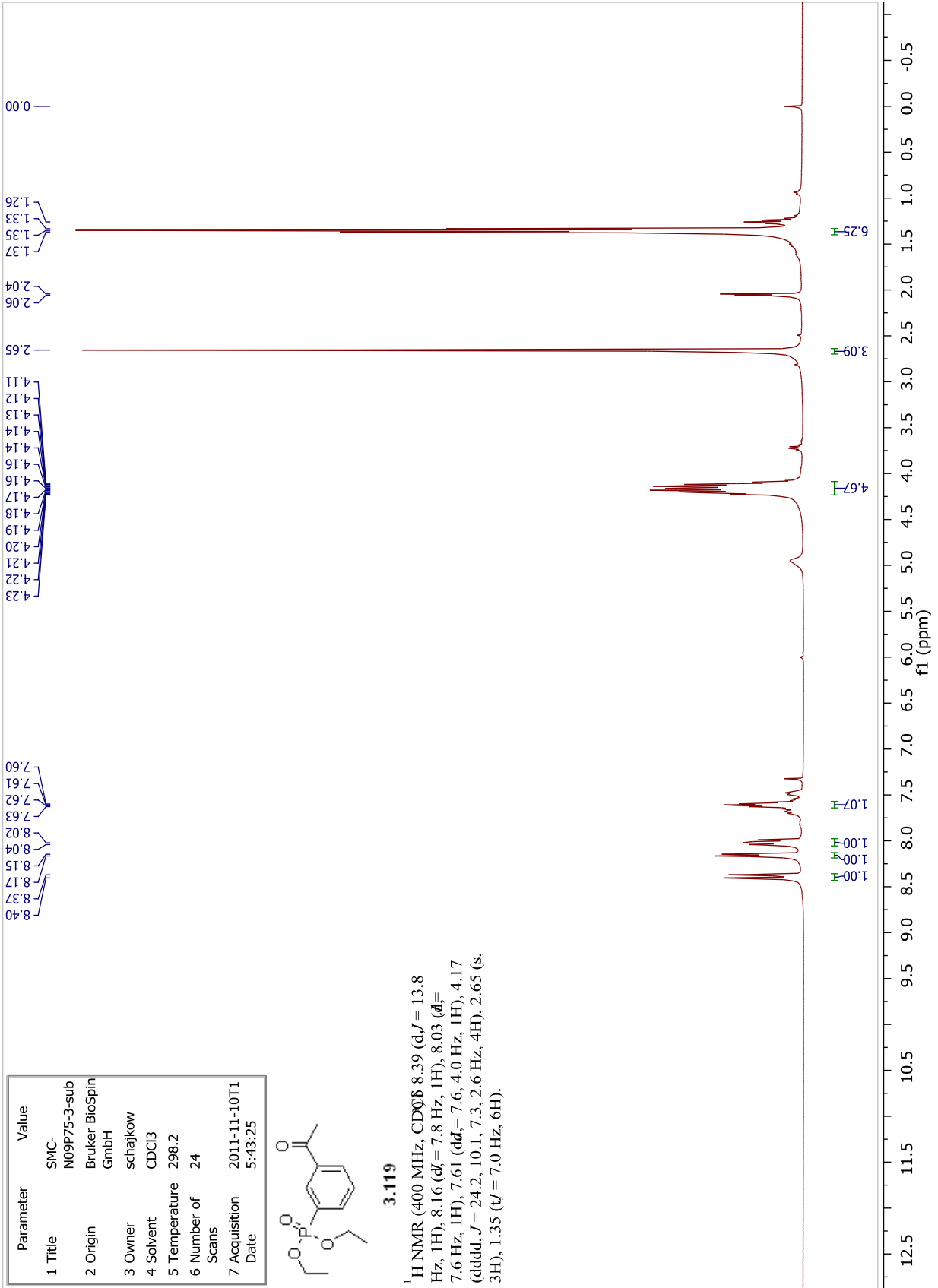


Parameter	Value
1 Title	SMC-N09P75-3-sub
2 Origin	Bruker BioSpin GmbH
3 Owner	schajkow
4 Solvent	CDCl3
5 Temperature	298.2
6 Number of Scans	24
7 Acquisition Date	2011-11-10T15:43:25

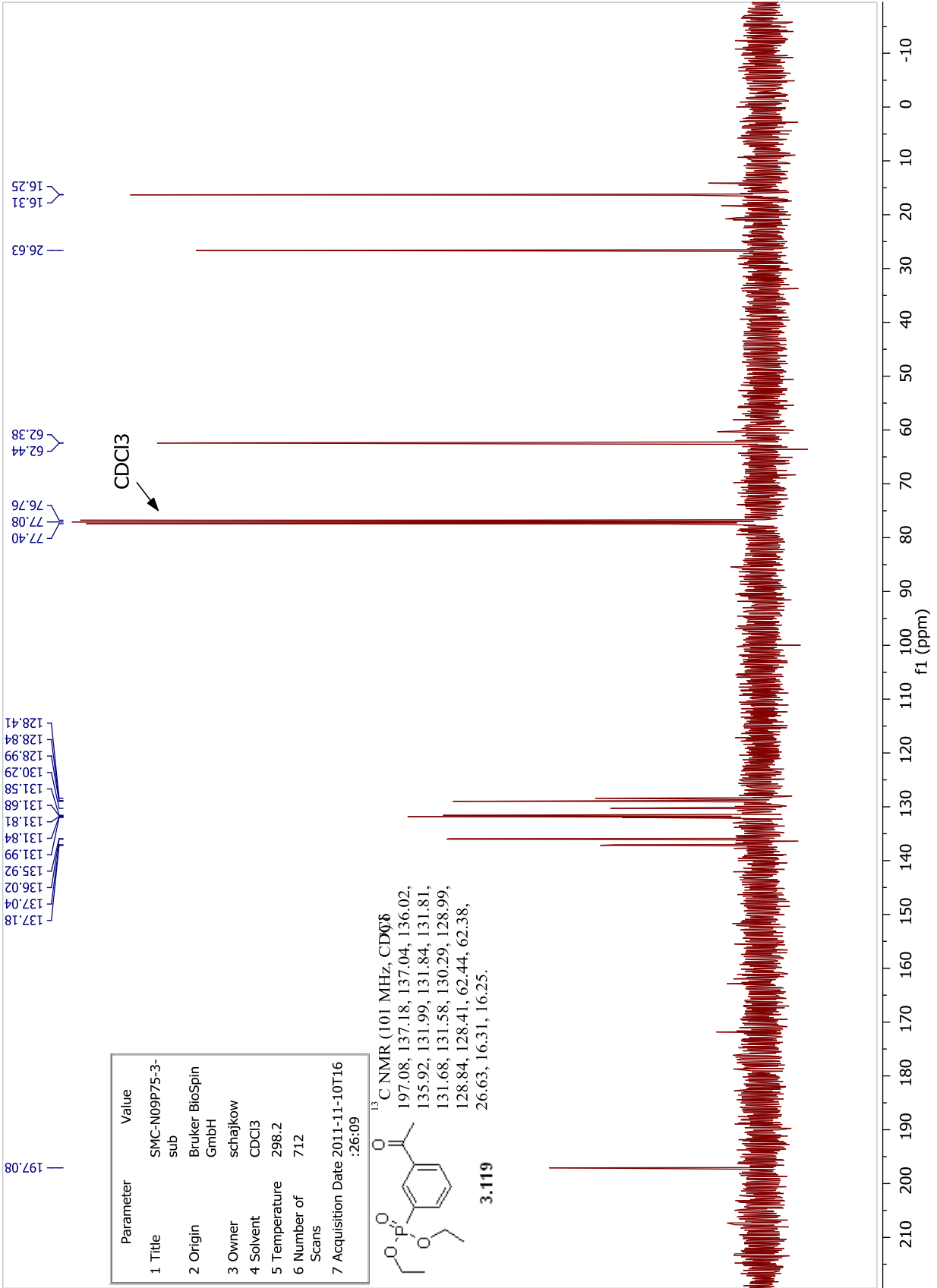


**3.119**

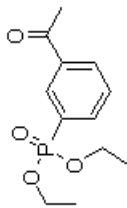
<sup>1</sup>H NMR (400 MHz, CDCl<sub>3</sub>) δ 8.39 (d, *J* = 13.8 Hz, 1H), 8.16 (d, *dJ* = 7.8 Hz, 1H), 8.03 (d, *dJ* = 7.6 Hz, 1H), 7.61 (dd, *dJ* = 7.6, 4.0 Hz, 1H), 4.17 (dddd, *J* = 24.2, 10.1, 7.3, 2.6 Hz, 4H), 2.65 (s, 3H), 1.35 (*tJ* = 7.0 Hz, 6H).



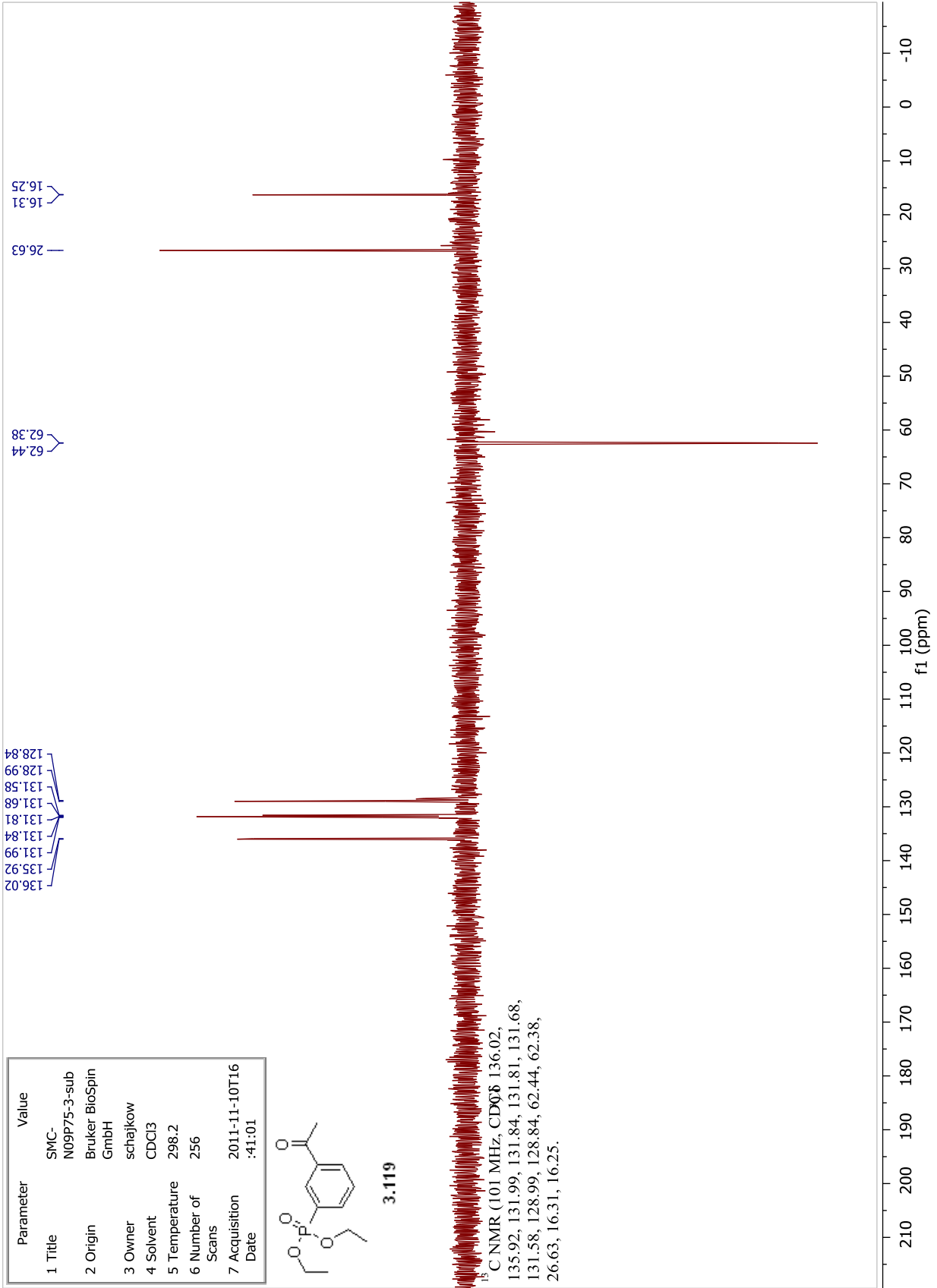


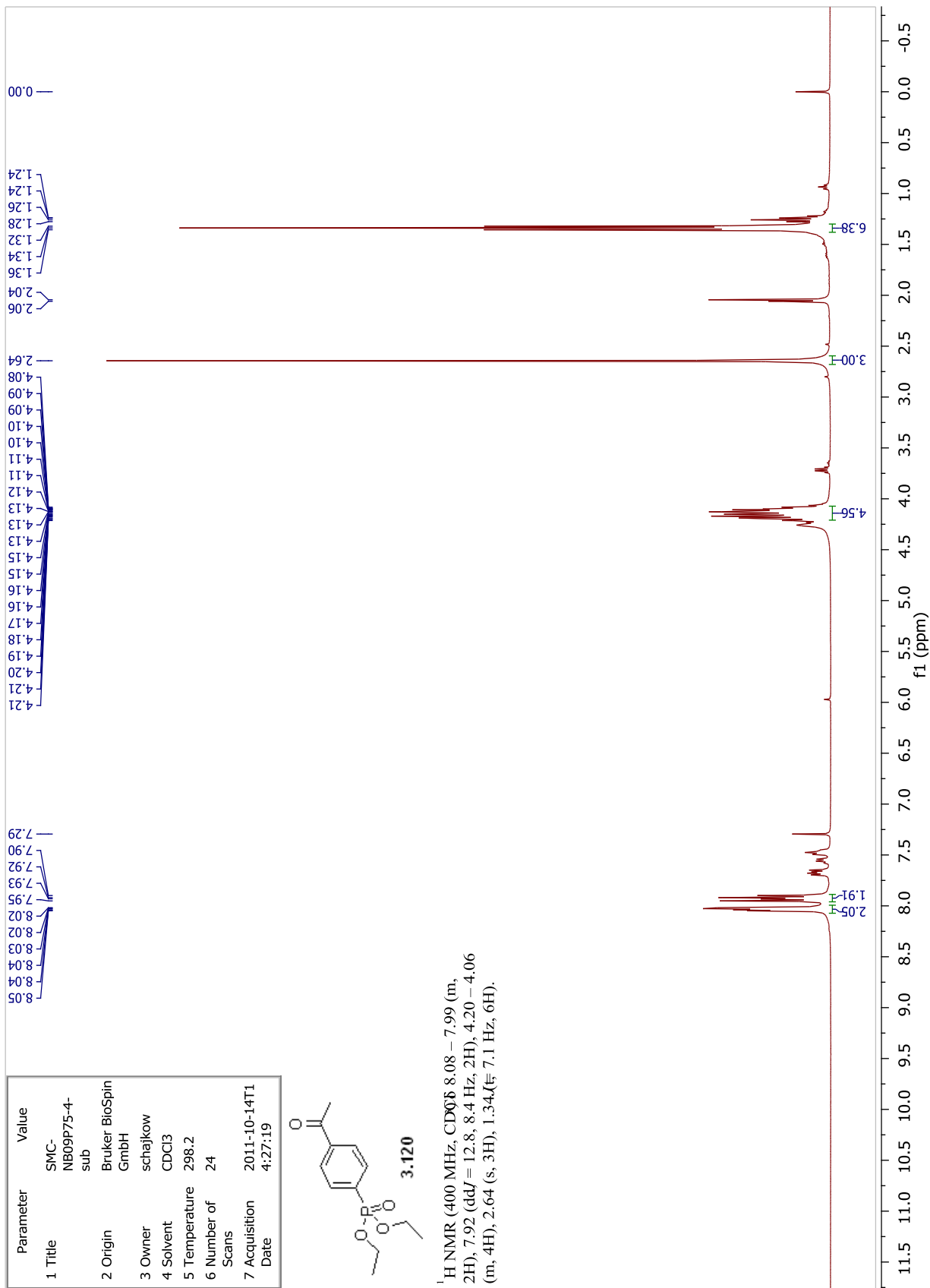


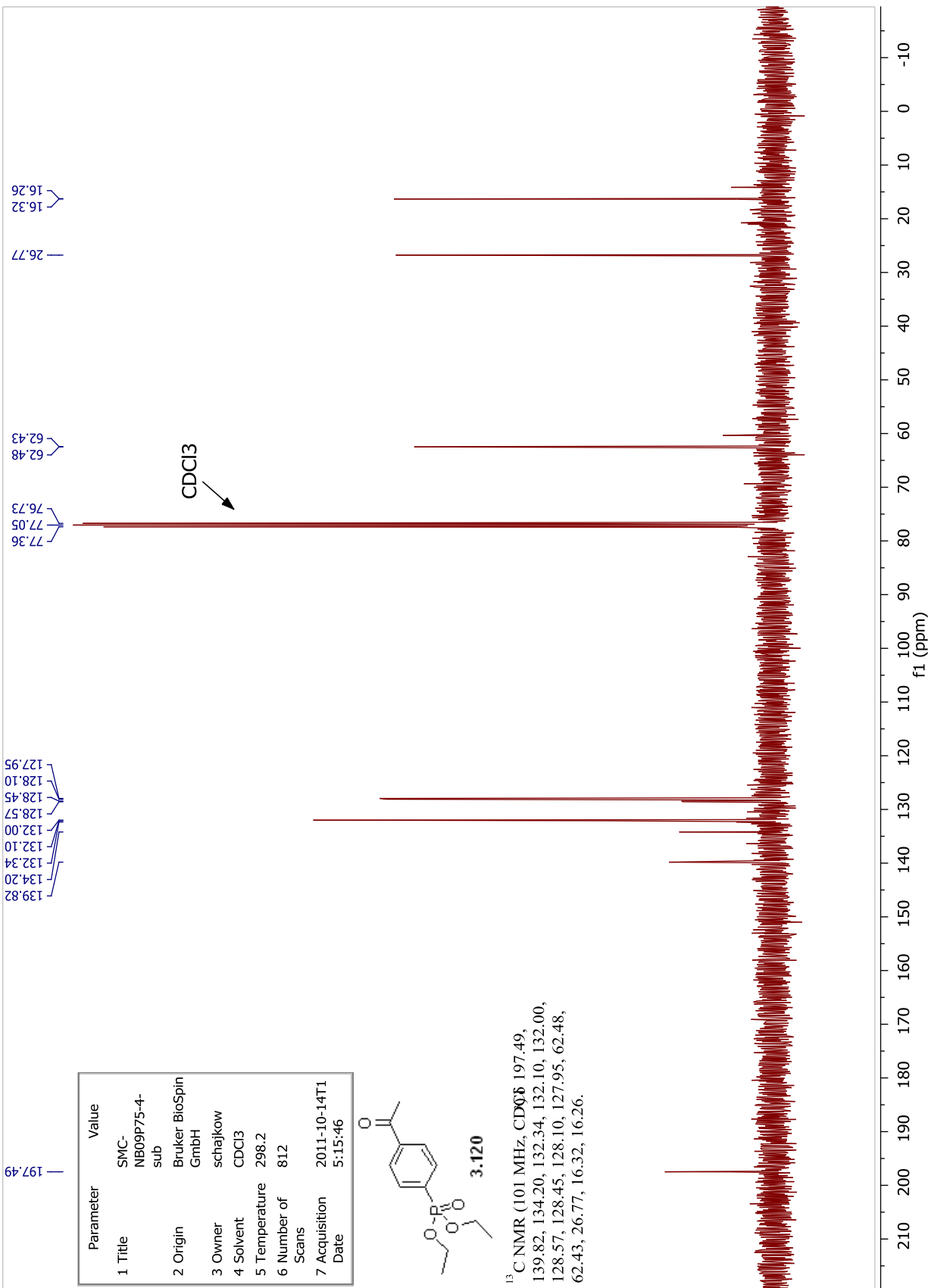
Parameter	Value
1 Title	SMC-N09P75-3-sub
2 Origin	Bruker BioSpin GmbH
3 Owner	schajkow
4 Solvent	CDCl3
5 Temperature	298.2
6 Number of Scans	256
7 Acquisition Date	2011-11-10T16:41:01



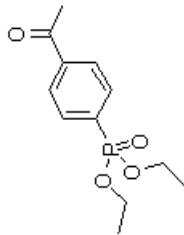
3.119



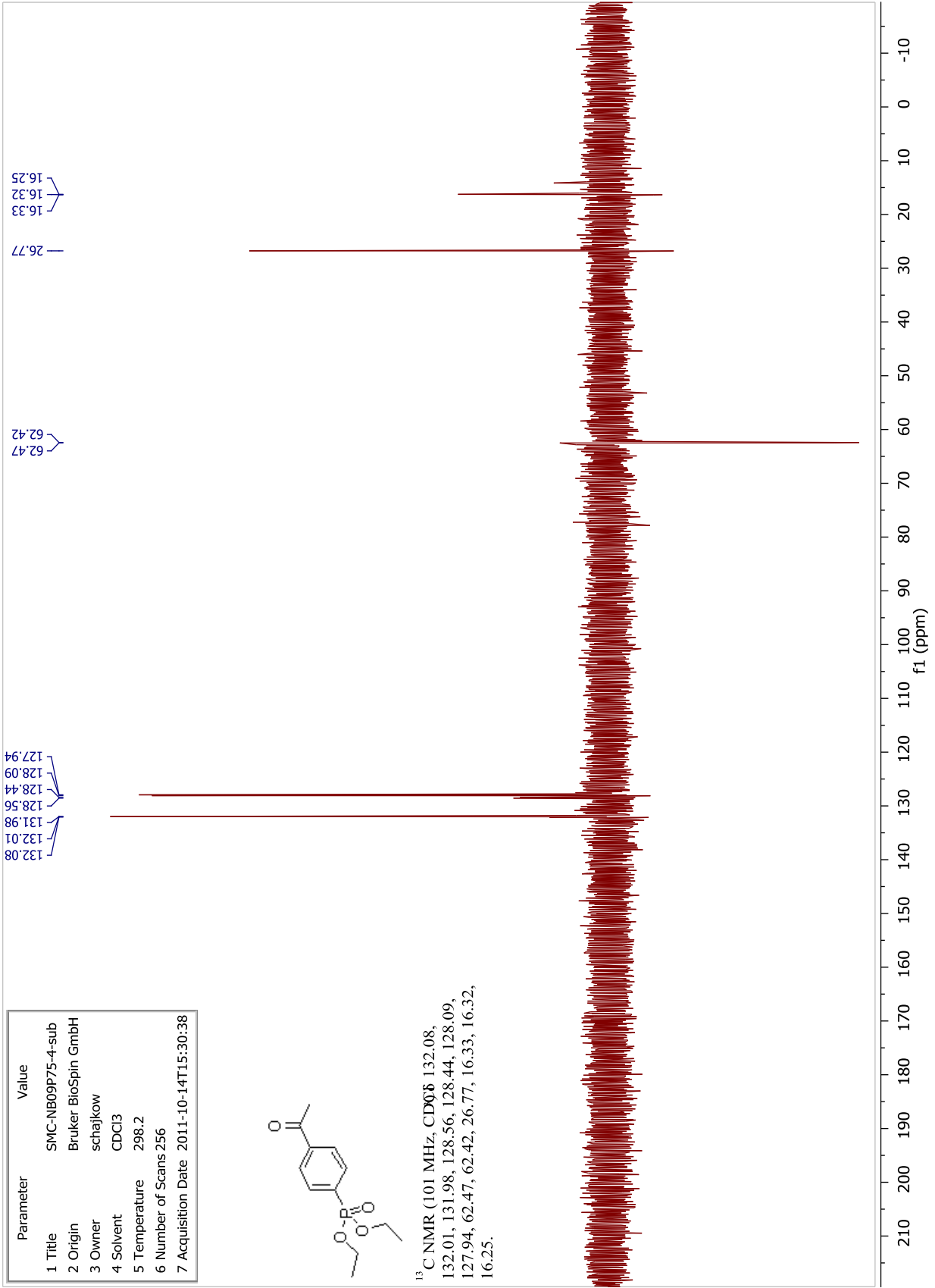




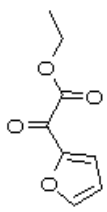
Parameter	Value
1 Title	SMC-NB09P75-4-sub
2 Origin	Bruker BioSpin GmbH
3 Owner	schajkowi
4 Solvent	CDCl3
5 Temperature	298.2
6 Number of Scans	256
7 Acquisition Date	2011-10-14T15:30:38



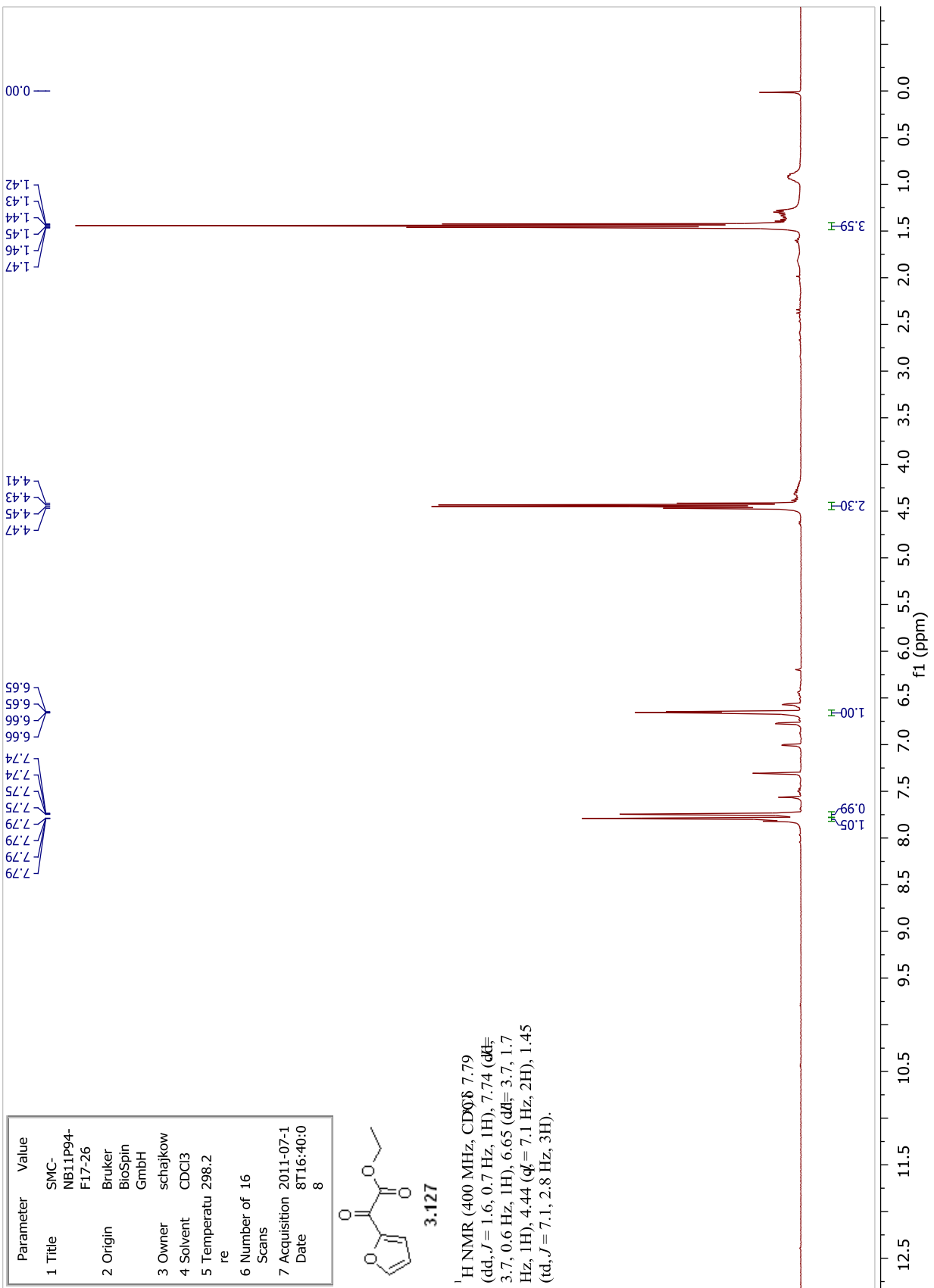
<sup>13</sup>C NMR (101 MHz, CDCl<sub>3</sub>) 132.08, 132.01, 131.98, 128.56, 128.44, 128.09, 127.94, 62.47, 62.42, 26.77, 16.33, 16.32, 16.25.



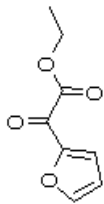
Parameter	Value
1 Title	SMC-NB11P94-F17-26
2 Origin	Bruker BioSpin GmbH
3 Owner	schajkowi
4 Solvent	CDCl <sub>3</sub>
5 Temperature	298.2
6 Number of Scans	16
7 Acquisition Date	2011-07-18 16:40:08



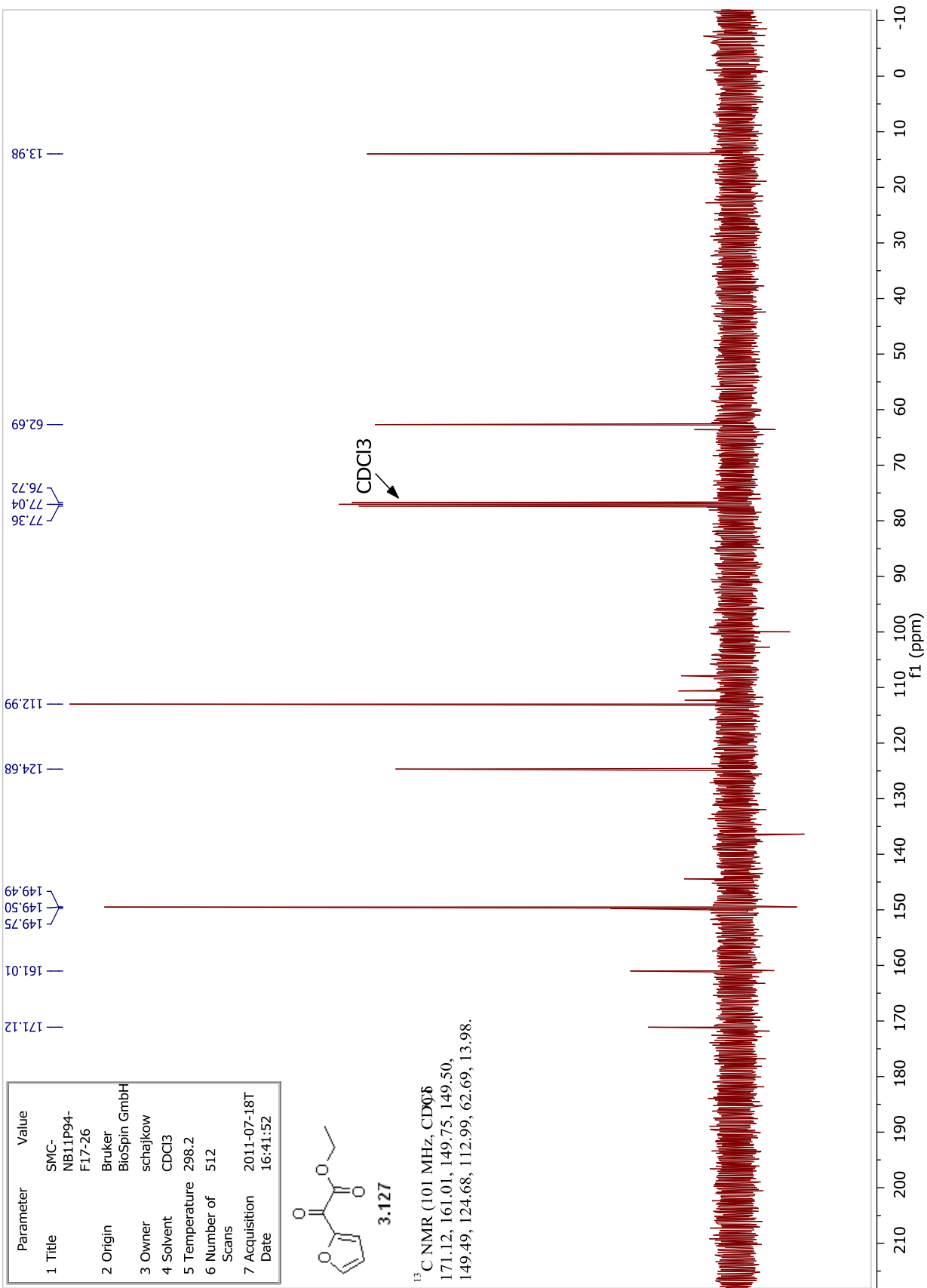
<sup>1</sup>H NMR (400 MHz, CDCl<sub>3</sub>) δ 7.79 (dd, *J* = 1.6, 0.7 Hz, 1H), 7.74 (dd, *J* = 3.7, 0.6 Hz, 1H), 6.65 (dd, *J* = 3.7, 1.7 Hz, 1H), 4.44 (q, *J* = 7.1 Hz, 2H), 1.45 (td, *J* = 7.1, 2.8 Hz, 3H).

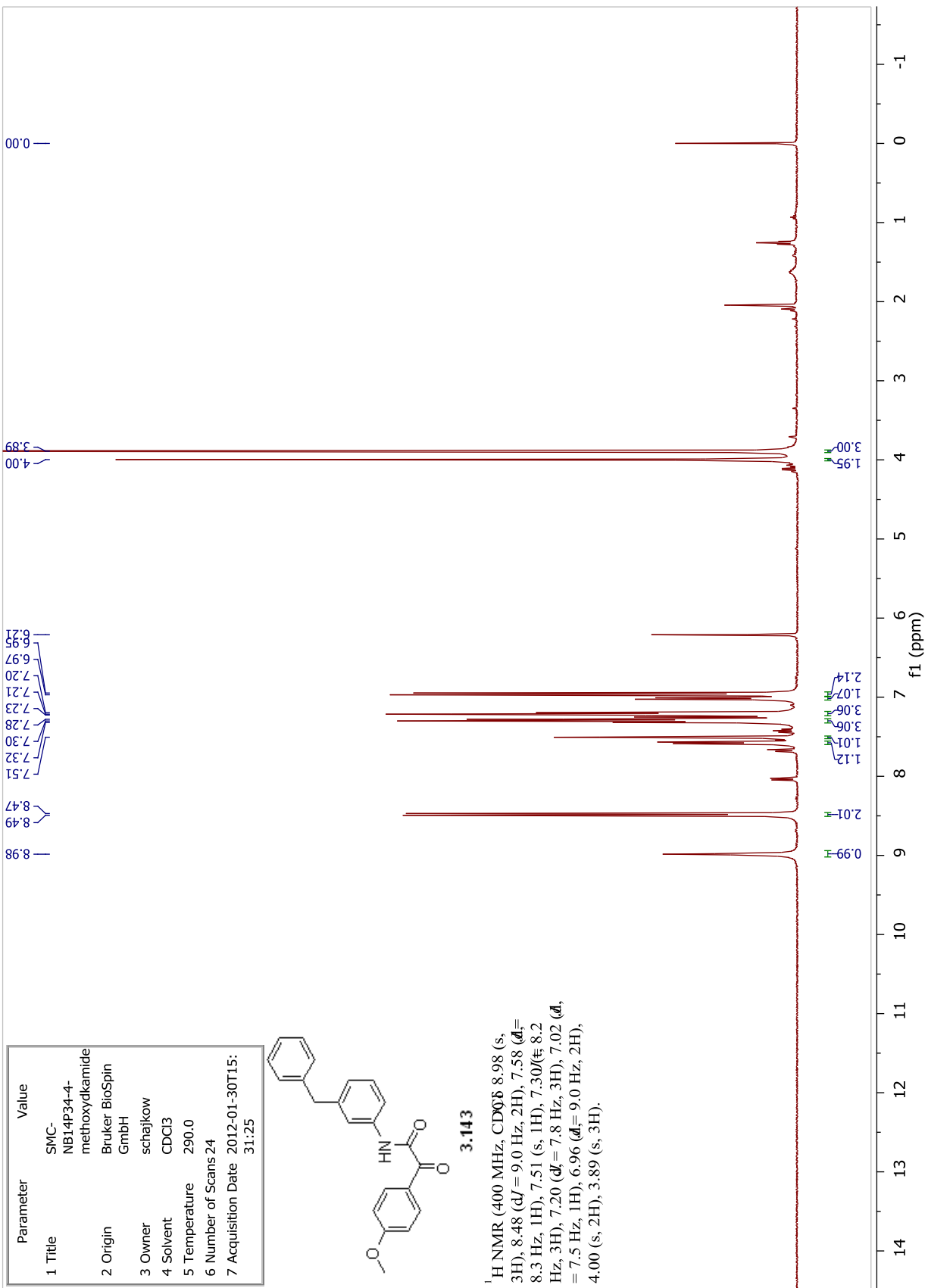


Parameter	Value
1 Title	SMC-NB11P94-F17-26
2 Origin	Bruker BioSpin GmbH
3 Owner	schajkow
4 Solvent	CDCl3
5 Temperature	298.2
6 Number of Scans	512
7 Acquisition Date	2011-07-18T16:41:52



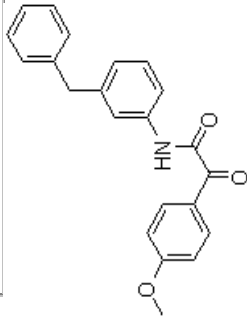
<sup>13</sup>C NMR (101 MHz, CDCl<sub>3</sub>)  
 171.12, 161.01, 149.75, 149.50,  
 149.49, 124.68, 112.99, 62.69, 13.98.





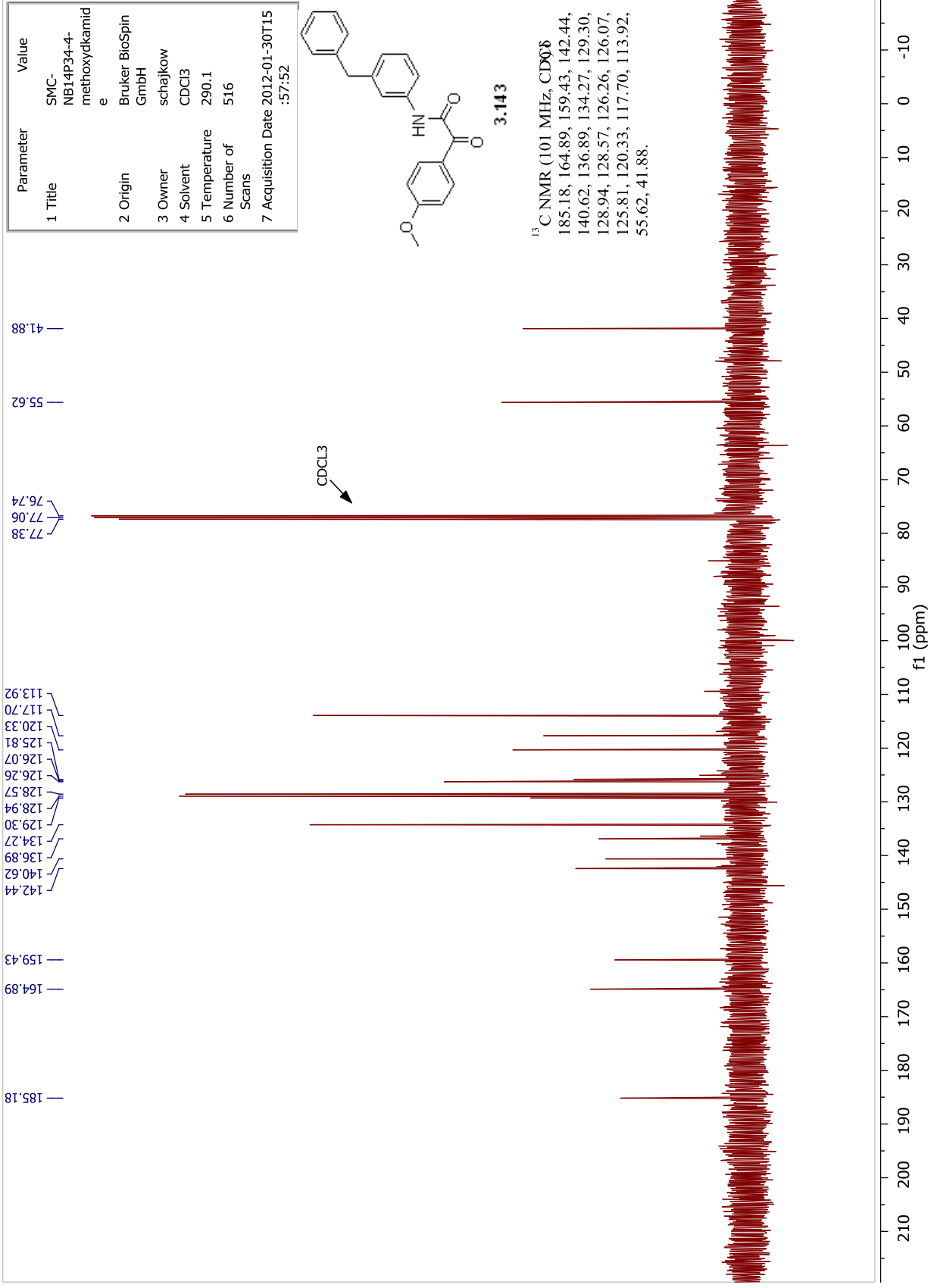


Parameter	Value
1 Title	SMC-NB14P34-4-methoxydkamid e
2 Origin	Bruker BioSpin GmbH
3 Owner	schajkow
4 Solvent	CDCl3
5 Temperature	290.1
6 Number of Scans	516
7 Acquisition Date	2012-01-30T15:57:52

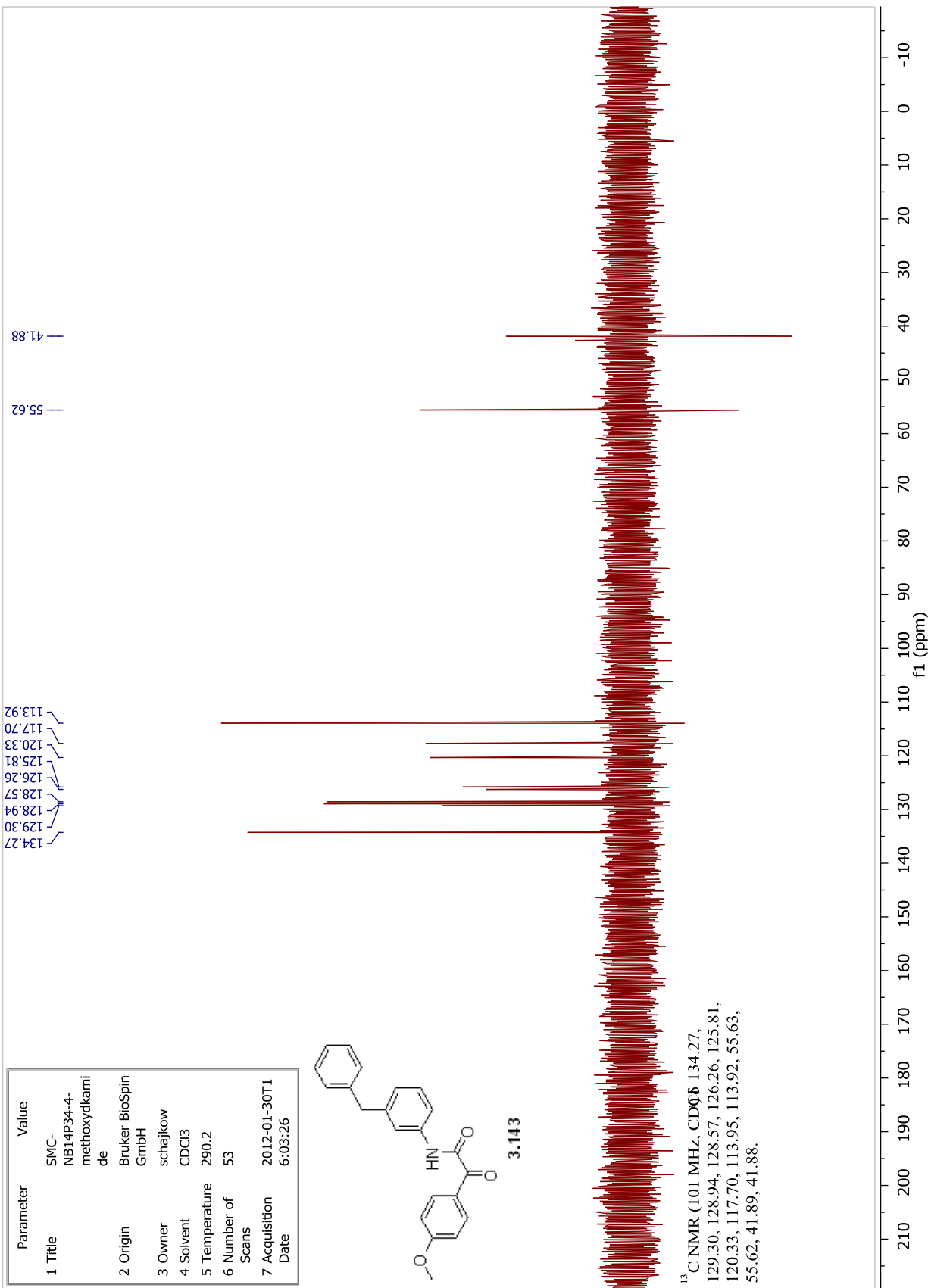
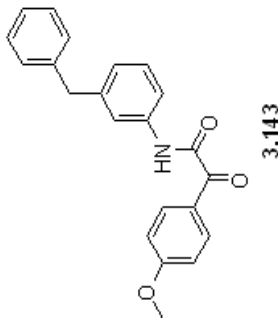


3.143

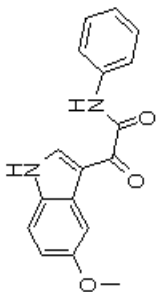
<sup>13</sup>C NMR (101 MHz, CDCl<sub>3</sub>)  
 185.18, 164.89, 159.43, 142.44,  
 140.62, 136.89, 134.27, 129.30,  
 128.94, 128.57, 126.26, 126.07,  
 125.81, 120.33, 117.70, 113.92,  
 55.62, 41.88.



Parameter	Value
1 Title	SMC-NB14P34-4-methoxydkami de
2 Origin	Bruker BioSpin GmbH
3 Owner	schajkow
4 Solvent	CDCl3
5 Temperature	290.2
6 Number of Scans	53
7 Acquisition Date	2012-01-30T16:03:26

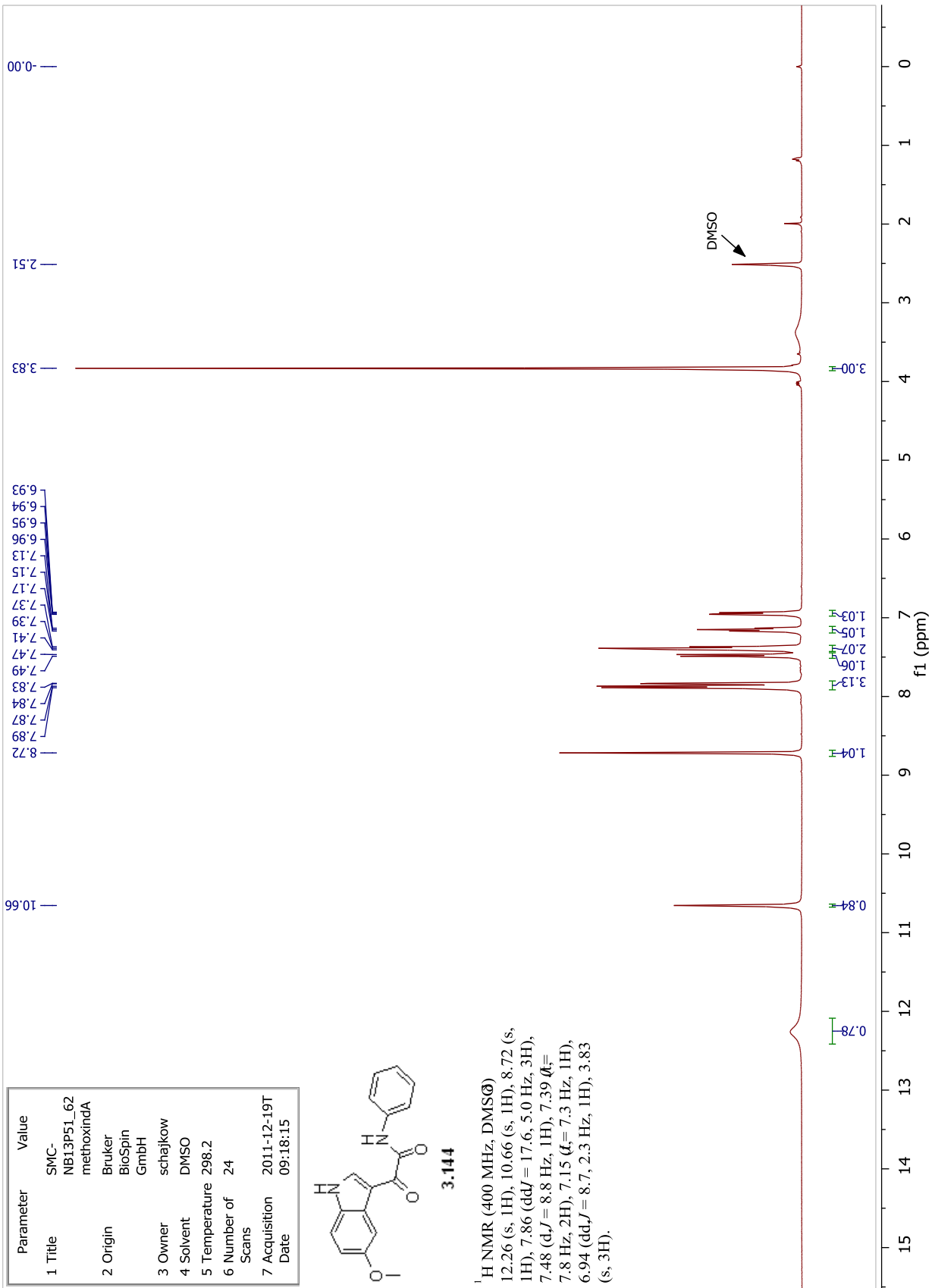


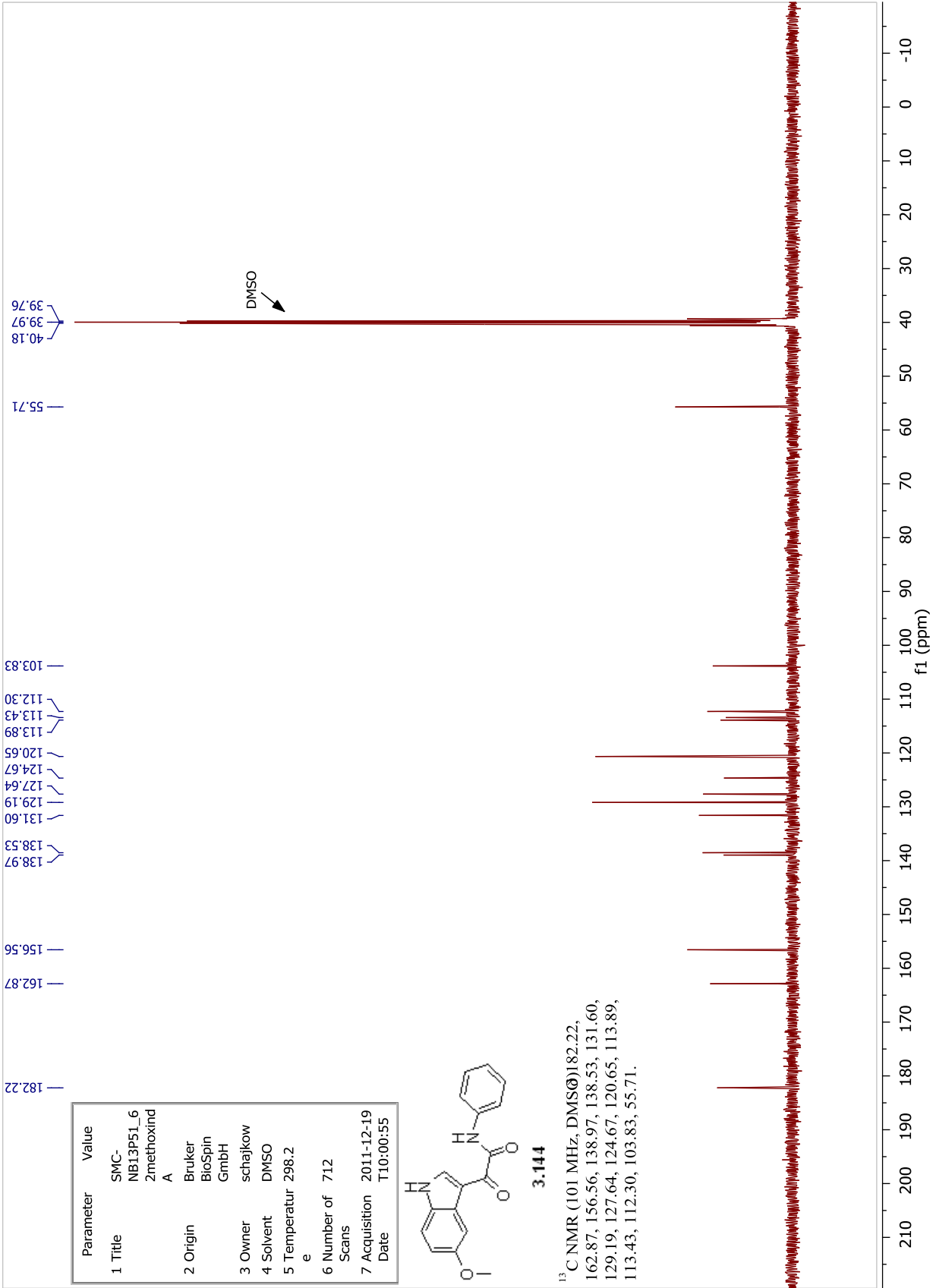
Parameter	Value
1 Title	SMC- NB13P51_62 methoxinda
2 Origin	Bruker BioSpin GmbH
3 Owner	schajkow
4 Solvent	DMSO
5 Temperature	298.2
6 Number of Scans	24
7 Acquisition Date	2011-12-19T 09:18:15



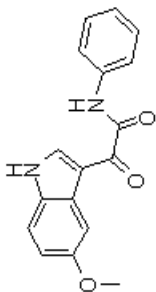
**3.144**

<sup>1</sup>H NMR (400 MHz, DMSO-d<sub>6</sub>)  
 12.26 (s, 1H), 10.66 (s, 1H), 8.72 (s, 1H), 7.86 (dd, *J* = 17.6, 5.0 Hz, 3H), 7.48 (d, *J* = 8.8 Hz, 1H), 7.39 (t, *J* = 7.8 Hz, 2H), 7.15 (t, *J* = 7.3 Hz, 1H), 6.94 (dd, *J* = 8.7, 2.3 Hz, 1H), 3.83 (s, 3H).



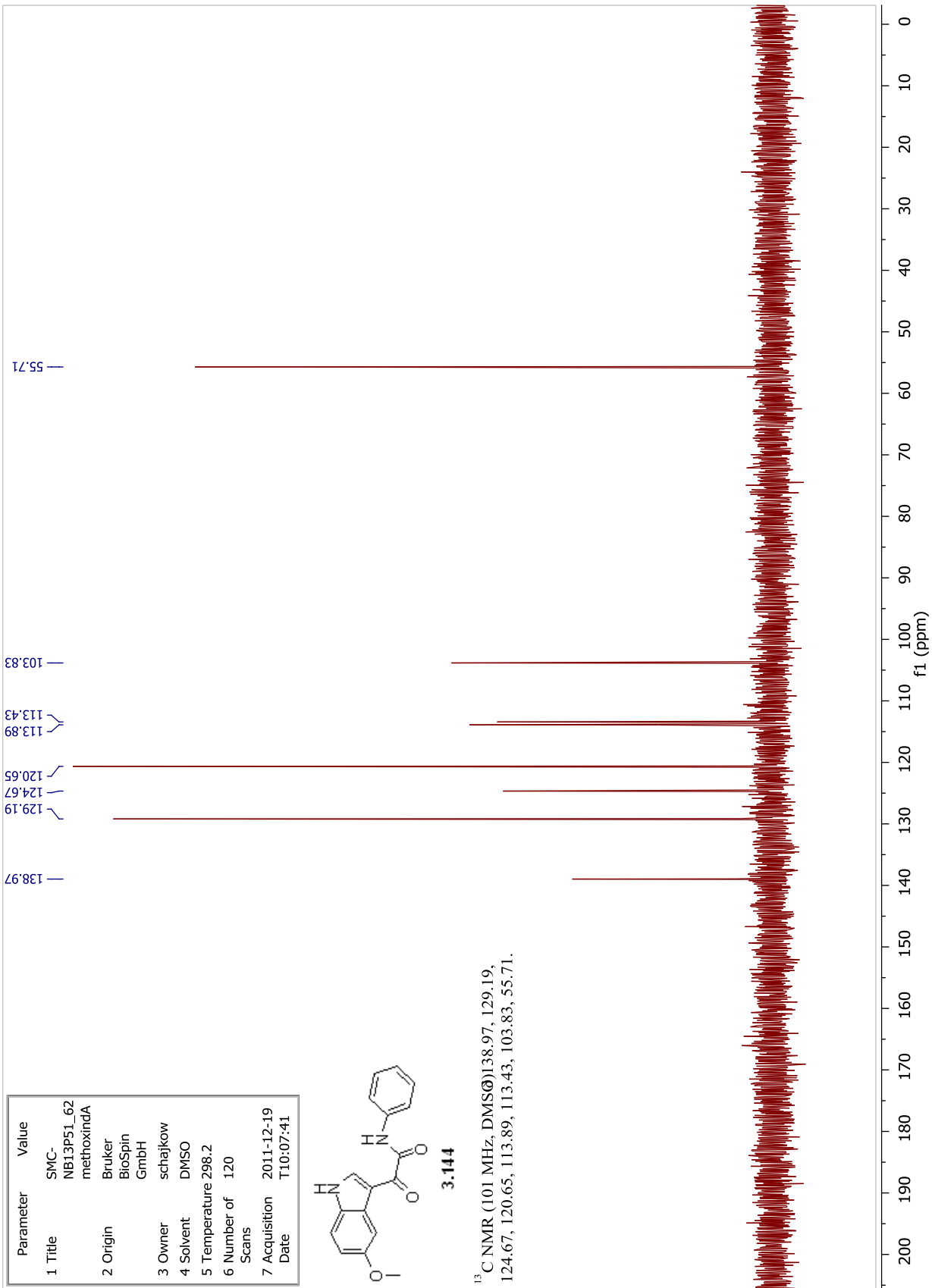


Parameter	Value
1 Title	SMC-NB13P51_62 methoxinda
2 Origin	Bruker BioSpin GmbH
3 Owner	schajkow
4 Solvent	DMSO
5 Temperature	298.2
6 Number of Scans	120
7 Acquisition Date	2011-12-19 T10:07:41

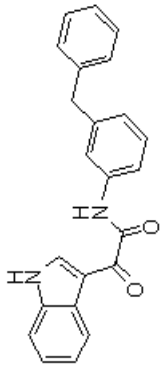


**3.144**

<sup>13</sup>C NMR (101 MHz, DMSO-d<sub>6</sub>) 138.97, 129.19, 124.67, 120.65, 113.89, 113.43, 103.83, 55.71.

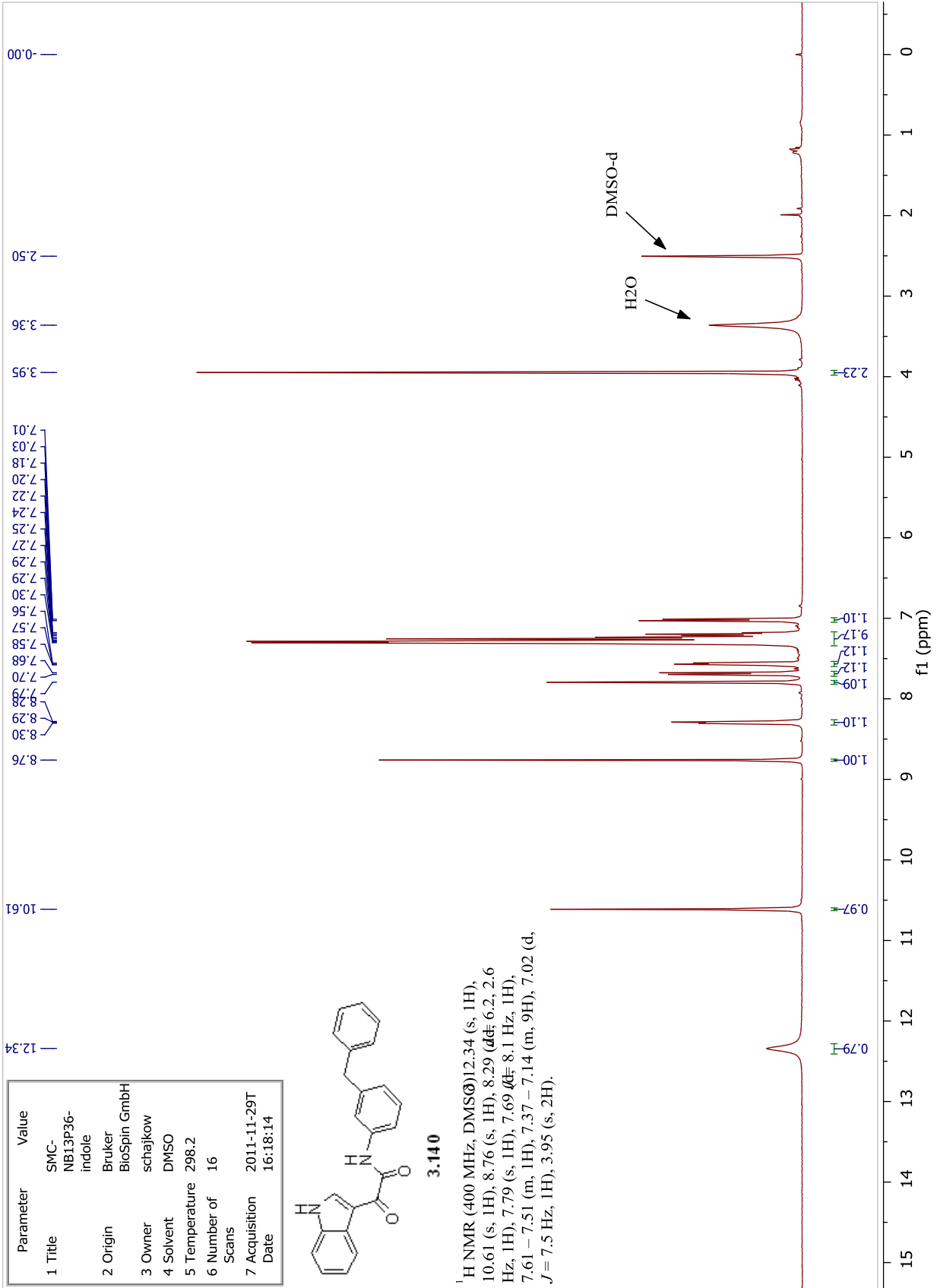


Parameter	Value
1 Title	SMC-NB13P36-indole
2 Origin	Bruker BioSpin GmbH
3 Owner	schajkow
4 Solvent	DMSO
5 Temperature	298.2
6 Number of Scans	16
7 Acquisition Date	2011-11-29T16:18:14

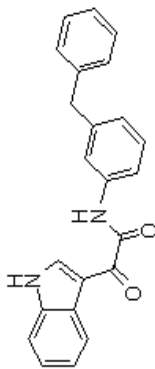


**3.140**

<sup>1</sup>H NMR (400 MHz, DMSO-d<sub>6</sub>) 12.34 (s, 1H), 10.61 (s, 1H), 8.76 (s, 1H), 8.29 (dd, 6.2, 2.6 Hz, 1H), 7.79 (s, 1H), 7.69 (dd, 8.1 Hz, 1H), 7.61 – 7.51 (m, 1H), 7.37 – 7.14 (m, 9H), 7.02 (d, J = 7.5 Hz, 1H), 3.95 (s, 2H).

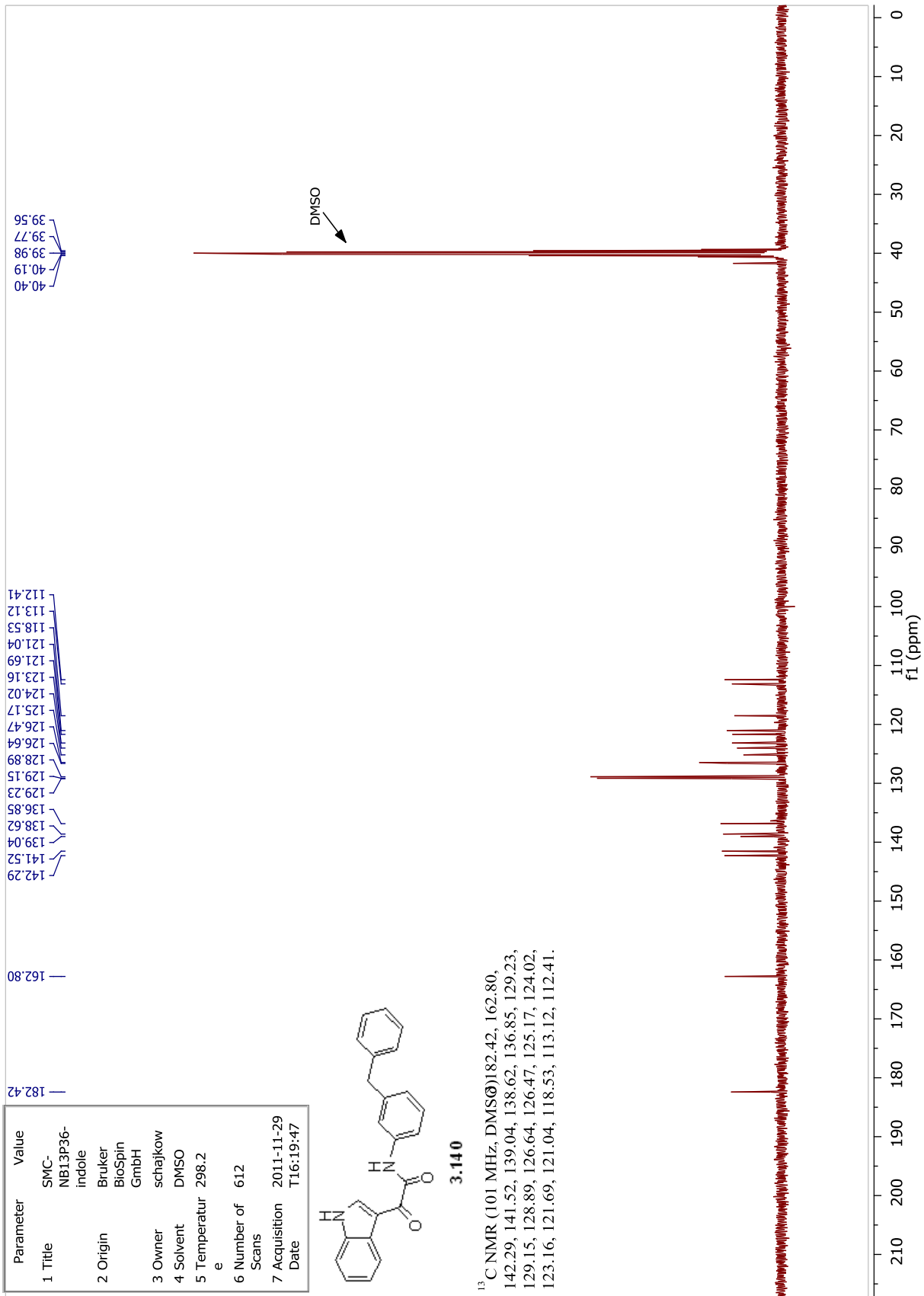


Parameter	Value
1 Title	SMC- NB13P36- indole
2 Origin	Bruker BioSpin GmbH
3 Owner	schajkow
4 Solvent	DMSO
5 Temperatur	298.2 e
6 Number of Scans	612
7 Acquisition Date	2011-11-29 T16:19:47

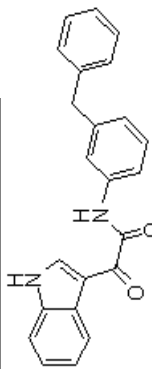


**3.140**

<sup>13</sup>C NMR (101 MHz, DMSO-d<sub>6</sub>) 182.42, 162.80, 142.29, 141.52, 139.04, 138.62, 136.85, 129.23, 129.15, 128.89, 126.64, 126.47, 125.17, 124.02, 123.16, 121.69, 121.04, 118.53, 113.12, 112.41.

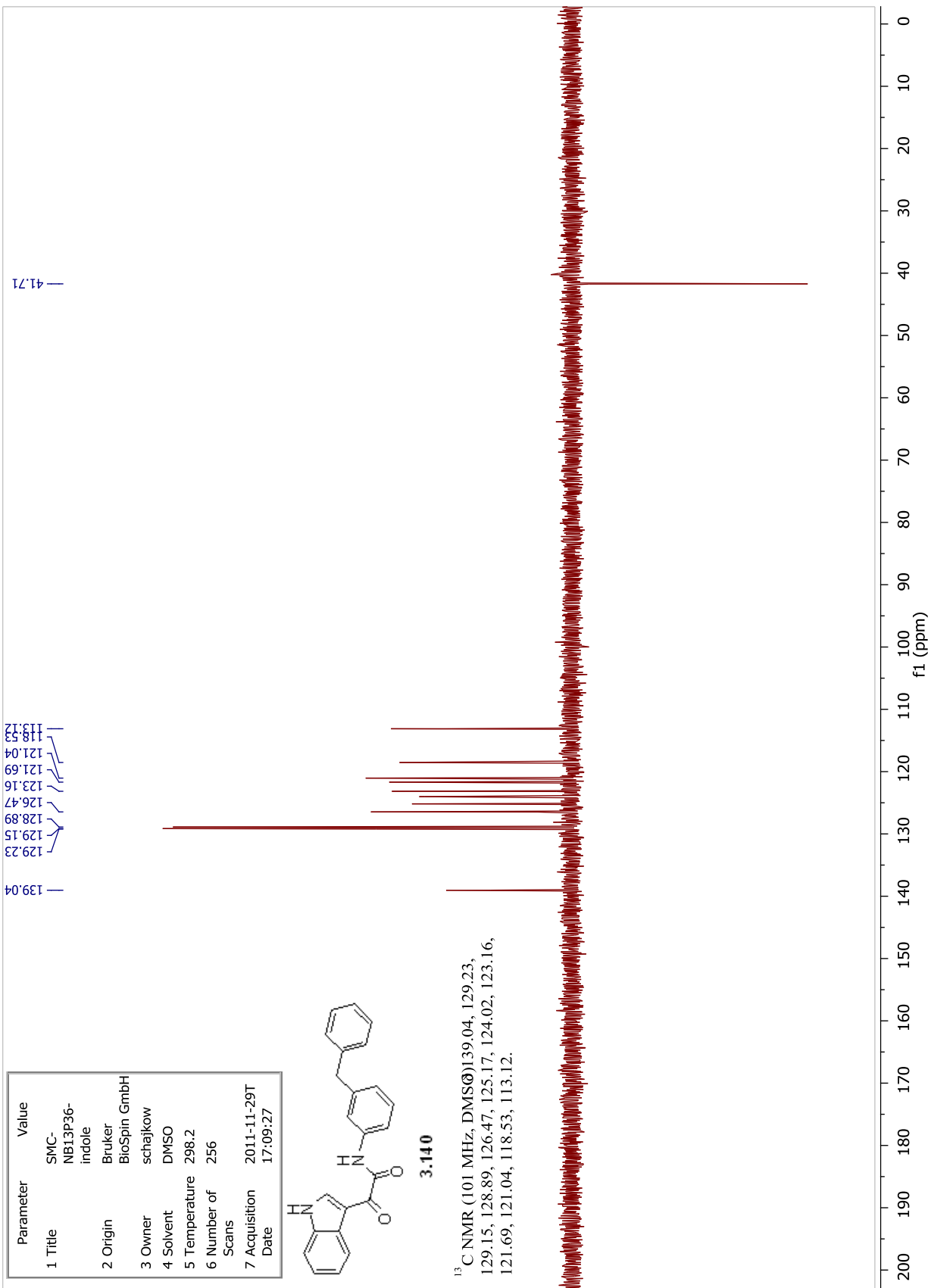


Parameter	Value
1 Title	SMC- NB13P36- indole
2 Origin	Bruker BioSpin GmbH
3 Owner	schajkow
4 Solvent	DMSO
5 Temperature	298.2
6 Number of Scans	256
7 Acquisition Date	2011-11-29T 17:09:27



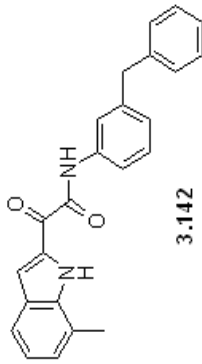
3.140

<sup>13</sup>C NMR (101 MHz, DMSO) 139.04, 129.23, 129.15, 128.89, 126.47, 125.17, 124.02, 123.16, 121.69, 121.04, 118.53, 113.12.

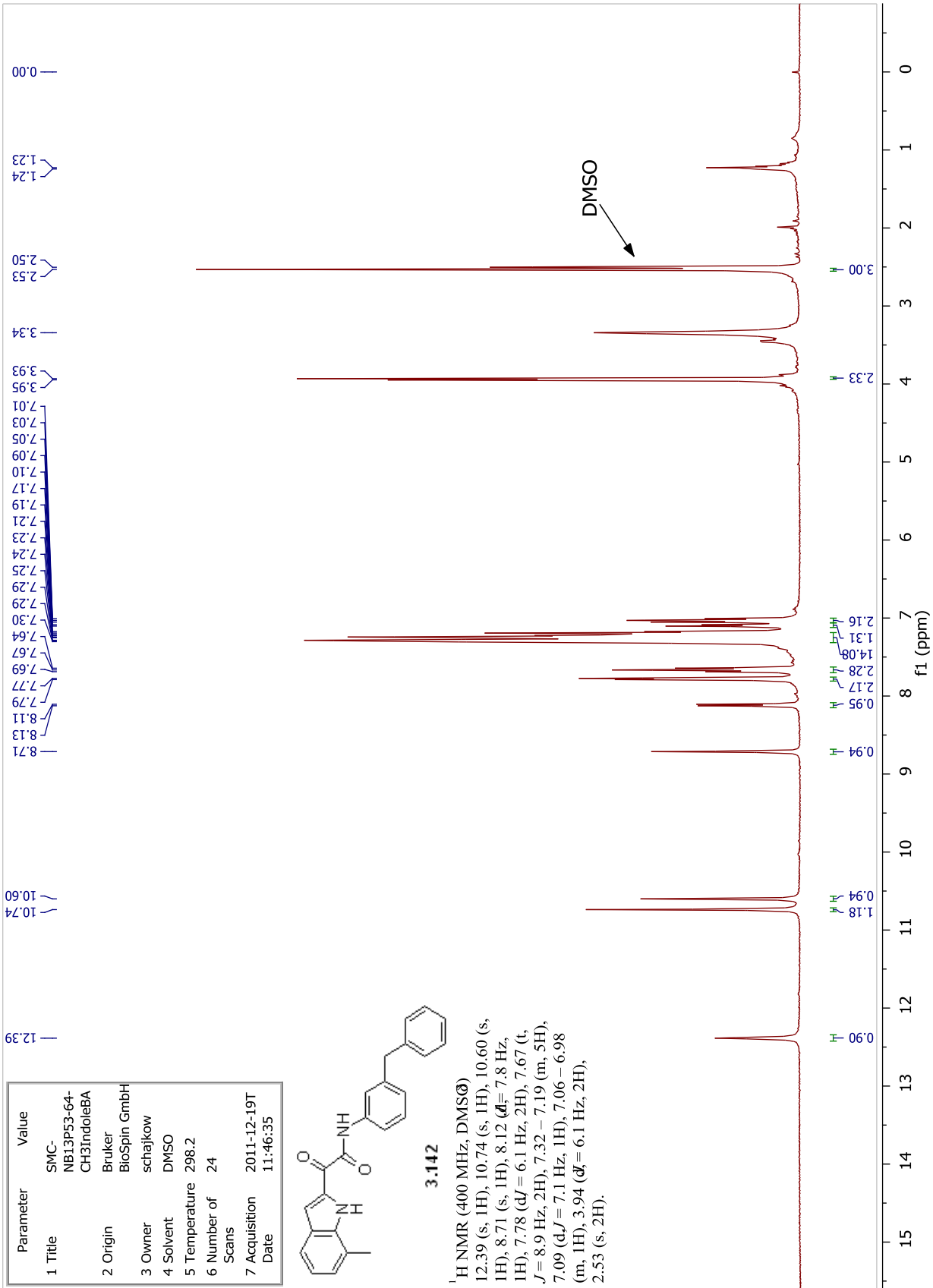


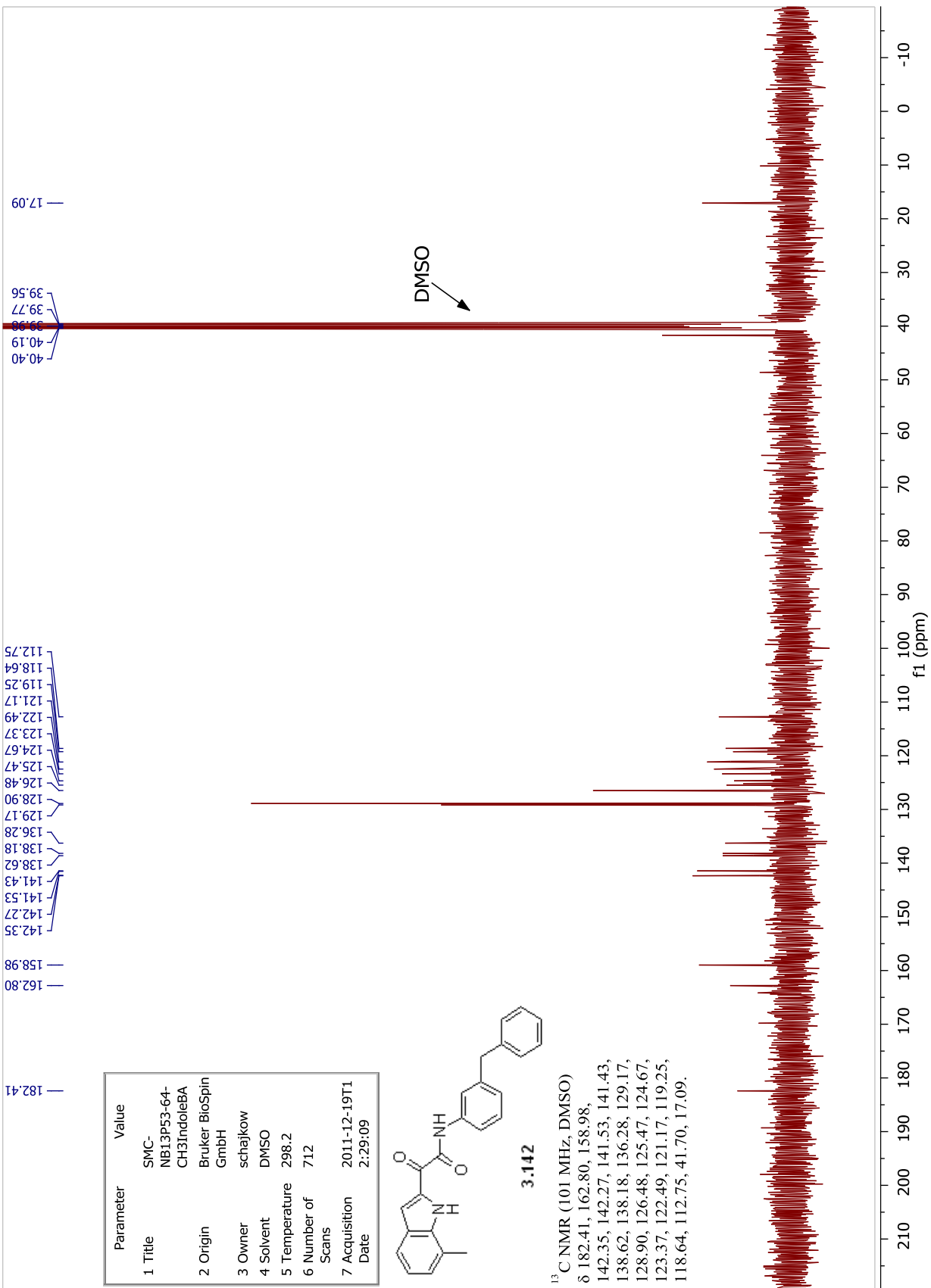


Parameter	Value
1 Title	SMC- NB13P53-64- CH3IndoleBA
2 Origin	Bruker BioSpin GmbH
3 Owner	schajkow
4 Solvent	DMSO
5 Temperature	298.2
6 Number of Scans	24
7 Acquisition Date	2011-12-19T 11:46:35

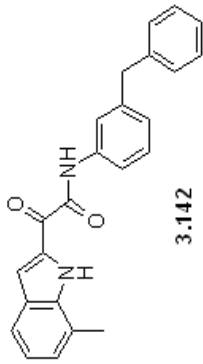


<sup>1</sup>H NMR (400 MHz, DMSO-*d*<sub>6</sub>)  
 12.39 (s, 1H), 10.74 (s, 1H), 10.60 (s, 1H), 8.71 (s, 1H), 8.12 (d, *d*<sub>H</sub> = 7.8 Hz, 1H), 7.78 (d, *d*<sub>H</sub> = 6.1 Hz, 2H), 7.67 (t, *J* = 8.9 Hz, 2H), 7.32 – 7.19 (m, 5H), 7.09 (d, *J* = 7.1 Hz, 1H), 7.06 – 6.98 (m, 1H), 3.94 (d, *d*<sub>H</sub> = 6.1 Hz, 2H), 2.53 (s, 2H).

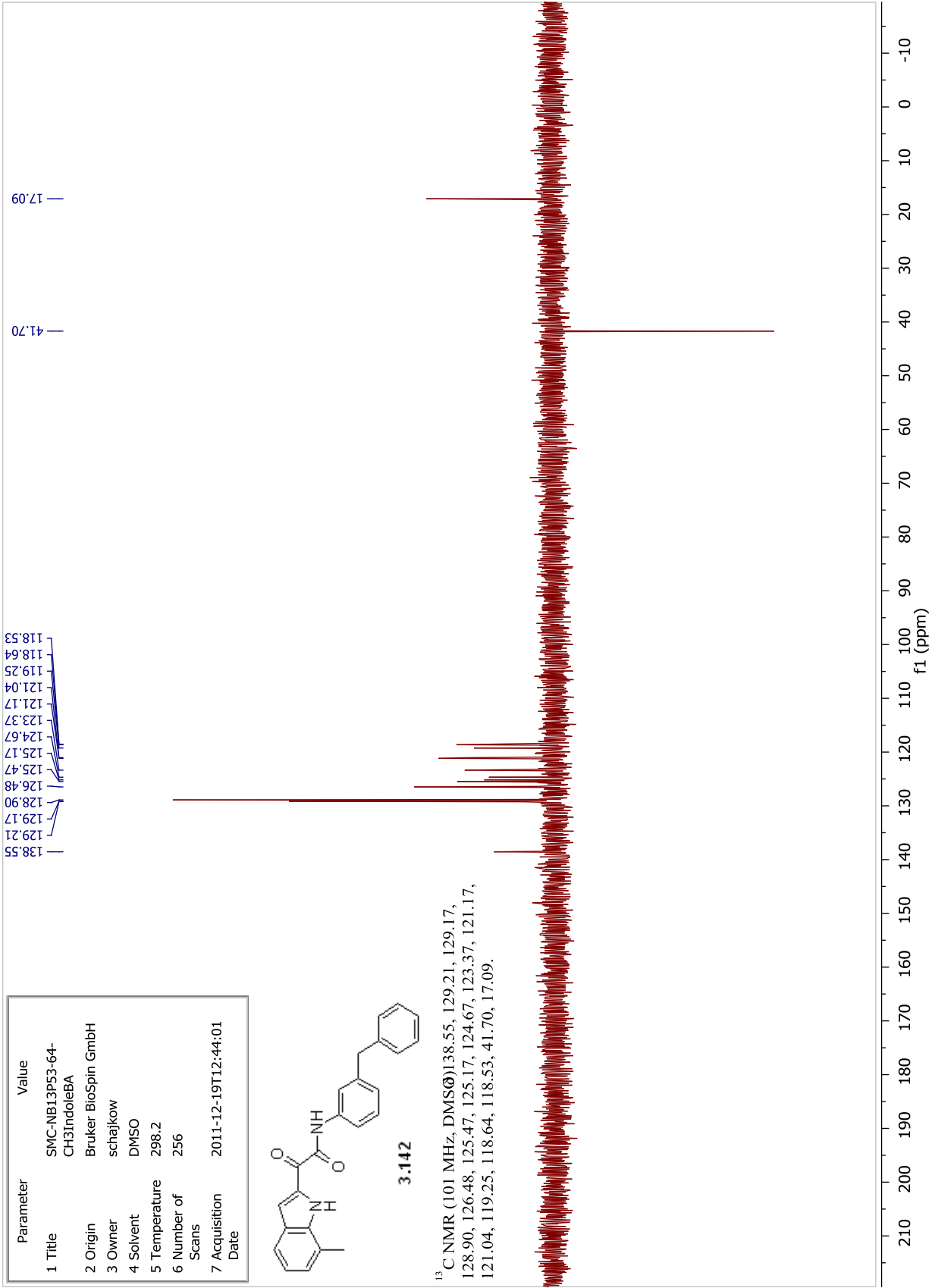


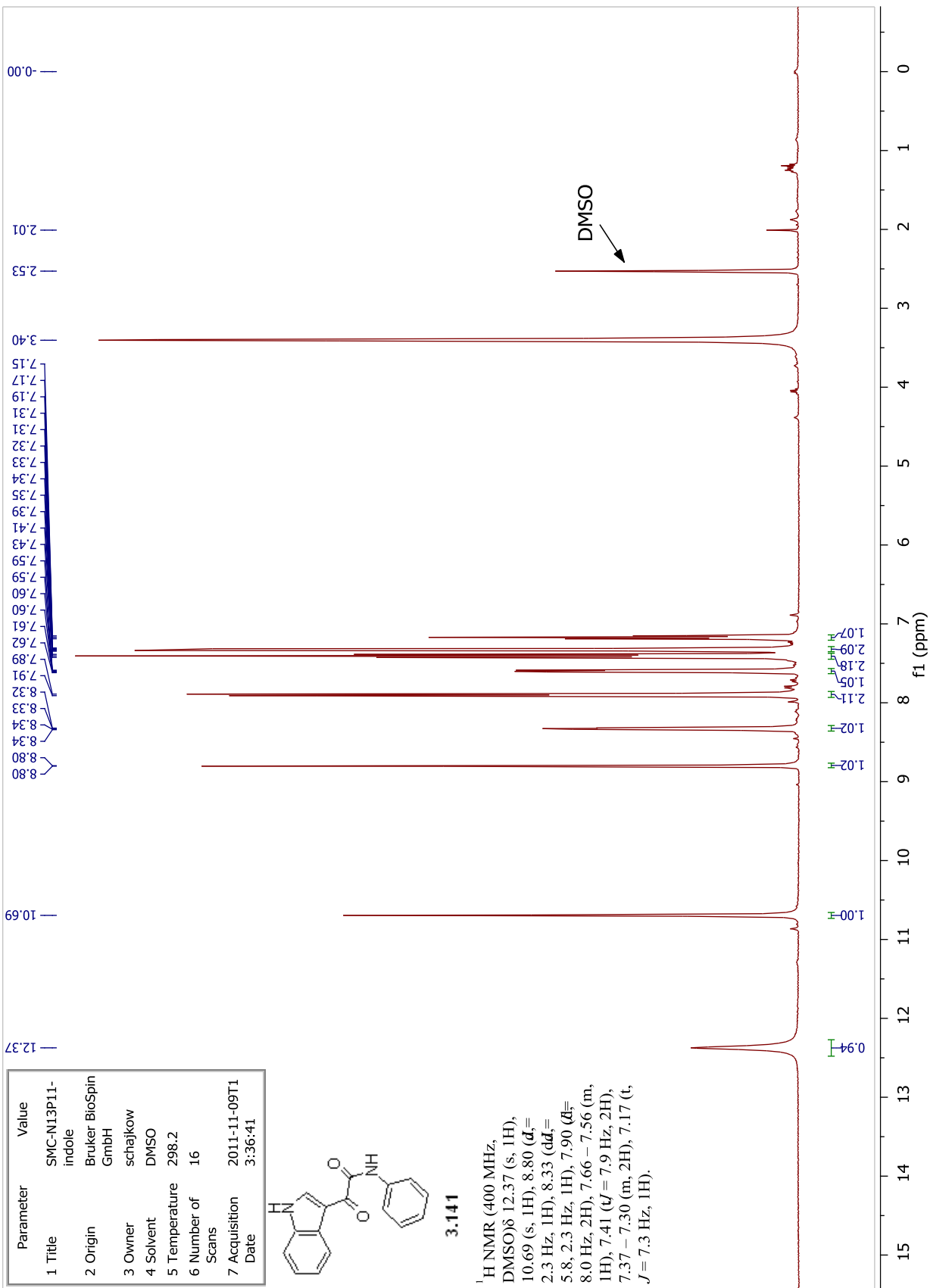


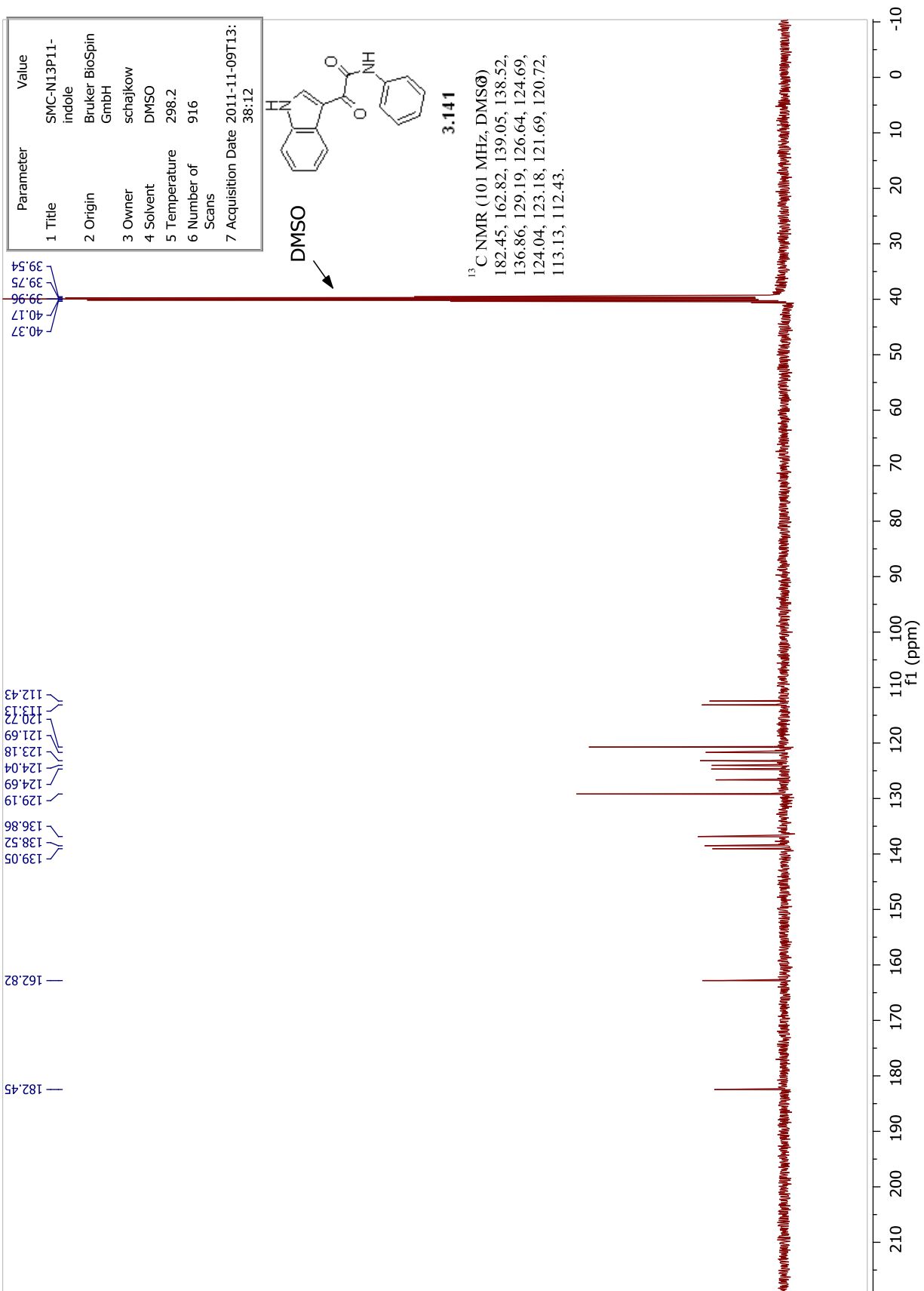
Parameter	Value
1 Title	SMC-NB13P53-64-CH3IndoleBA
2 Origin	Bruker BioSpin GmbH
3 Owner	schajkow
4 Solvent	DMSO
5 Temperature	298.2
6 Number of Scans	256
7 Acquisition Date	2011-12-19T12:44:01



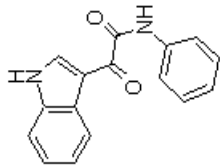
<sup>13</sup>C NMR (101 MHz, DMSO) 138.55, 129.21, 129.17, 128.90, 126.48, 125.47, 125.17, 124.67, 123.37, 121.17, 121.04, 119.25, 118.64, 118.53, 41.70, 17.09.





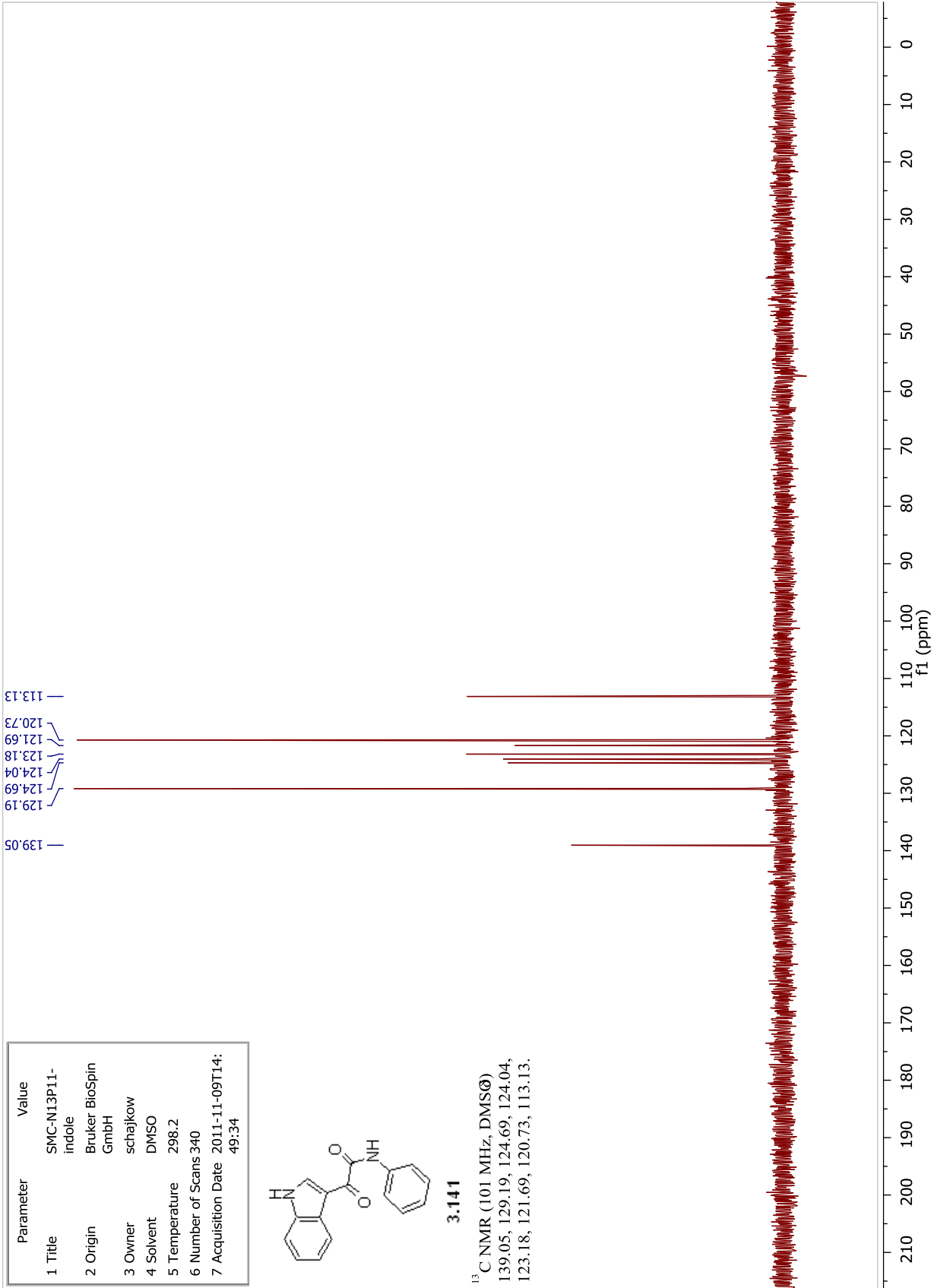


Parameter	Value
1 Title	SMC-N13P11-indole
2 Origin	Bruker BioSpin GmbH
3 Owner	schajkow
4 Solvent	DMSO
5 Temperature	298.2
6 Number of Scans	340
7 Acquisition Date	2011-11-09T14:49:34

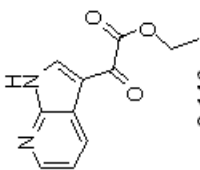


**3.141**

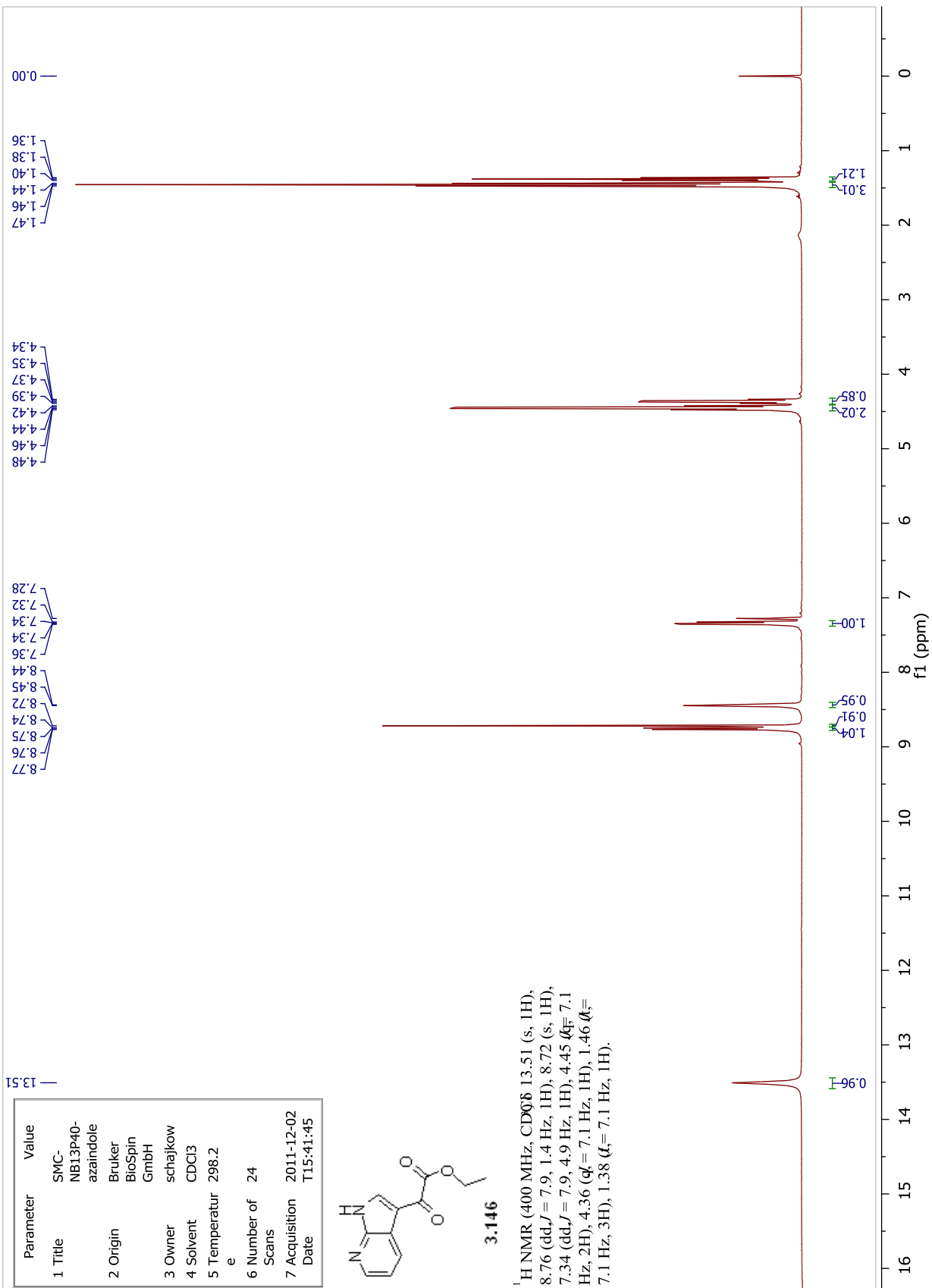
<sup>13</sup>C NMR (101 MHz, DMSO)  
 139.05, 129.19, 124.69, 124.04,  
 123.18, 121.69, 120.73, 113.13.

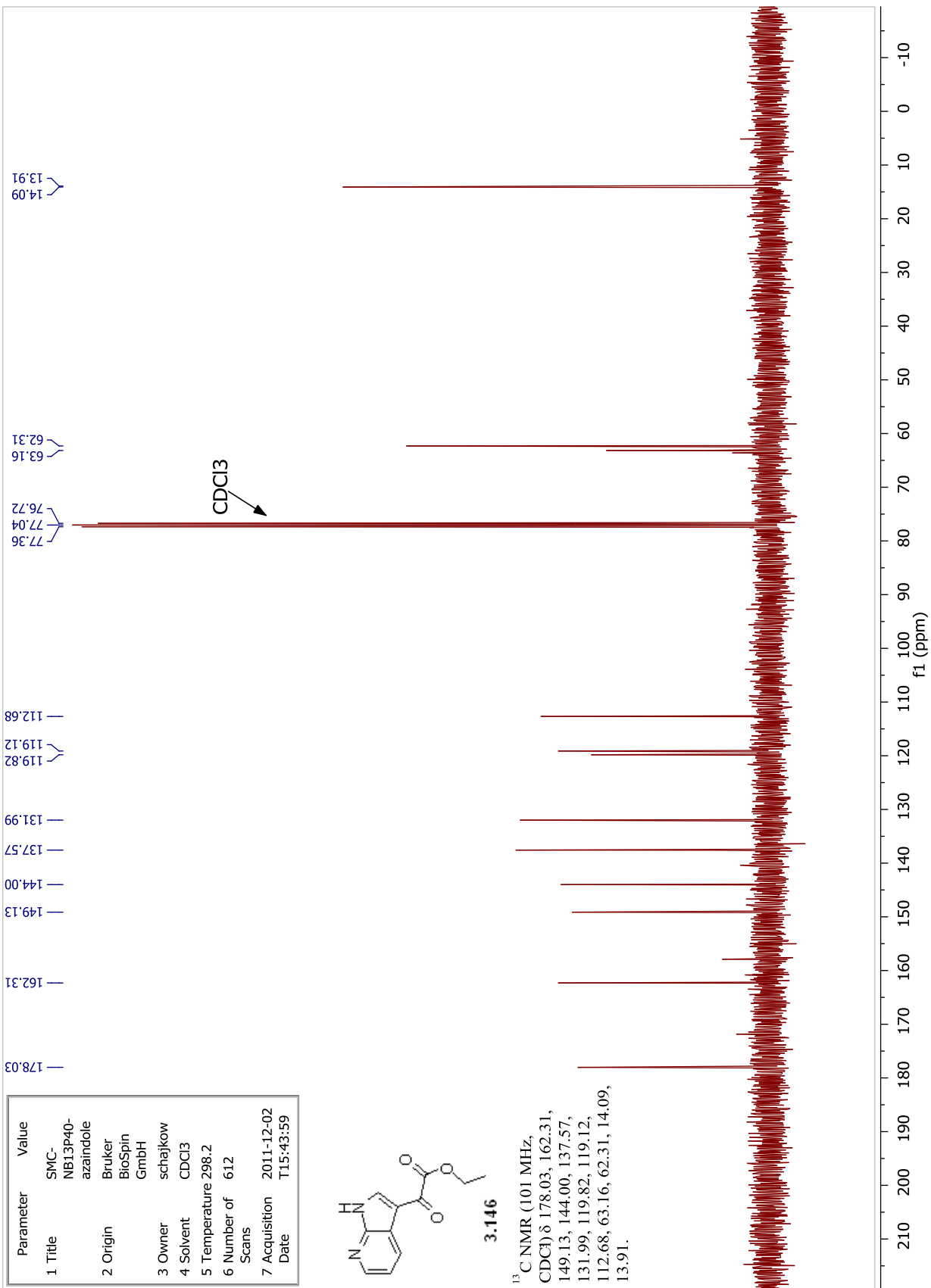


Parameter	Value
1 Title	SMC-NB13P40-azaindole
2 Origin	Bruker BioSpin GmbH
3 Owner	schajkowi
4 Solvent	CDCl <sub>3</sub>
5 Temperatur	298.2
6 Number of Scans	24
7 Acquisition Date	2011-12-02 T15:41:45

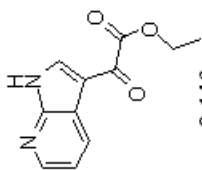


<sup>1</sup>H NMR (400 MHz, CDCl<sub>3</sub>) δ 13.51 (s, 1H), 8.76 (dd, *J* = 7.9, 1.4 Hz, 1H), 8.72 (s, 1H), 7.34 (dd, *J* = 7.9, 4.9 Hz, 1H), 4.45 (q, *J* = 7.1 Hz, 2H), 4.36 (q, *J* = 7.1 Hz, 1H), 1.46 (t, *J* = 7.1 Hz, 3H), 1.38 (t, *J* = 7.1 Hz, 1H).



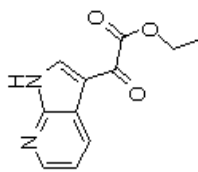


Parameter	Value
1 Title	SMC-NB13P40-azaindole
2 Origin	Bruker BioSpin GmbH
3 Owner	schajkow
4 Solvent	CDCl <sub>3</sub>
5 Temperature	298.2
6 Number of Scans	612
7 Acquisition Date	2011-12-02 T15:43:59



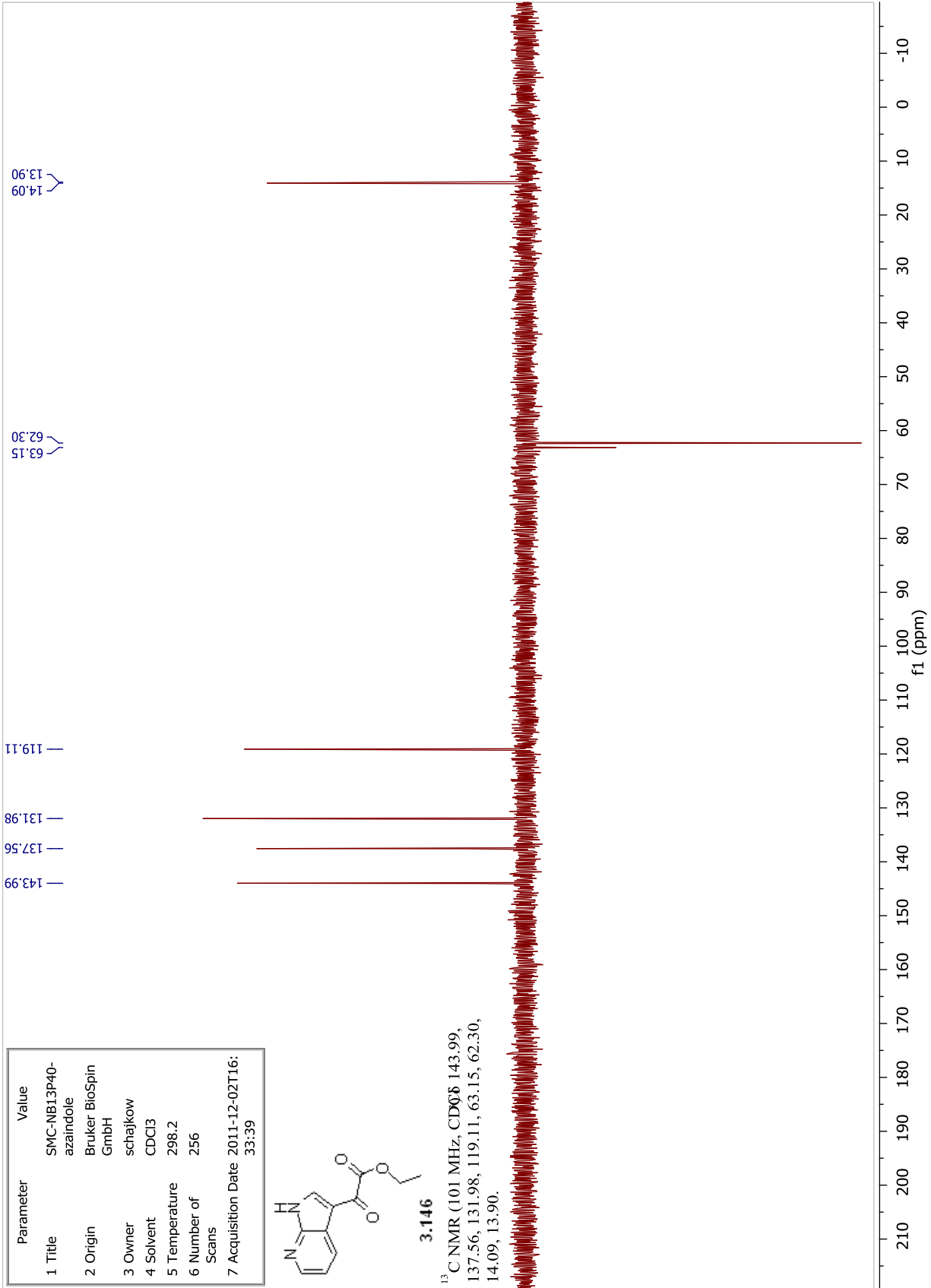


Parameter	Value
1 Title	SMC-NB13P40-azaindole
2 Origin	Bruker BioSpin GmbH
3 Owner	schajkow
4 Solvent	CDCl3
5 Temperature	298.2
6 Number of Scans	256
7 Acquisition Date	2011-12-02T16:33:39

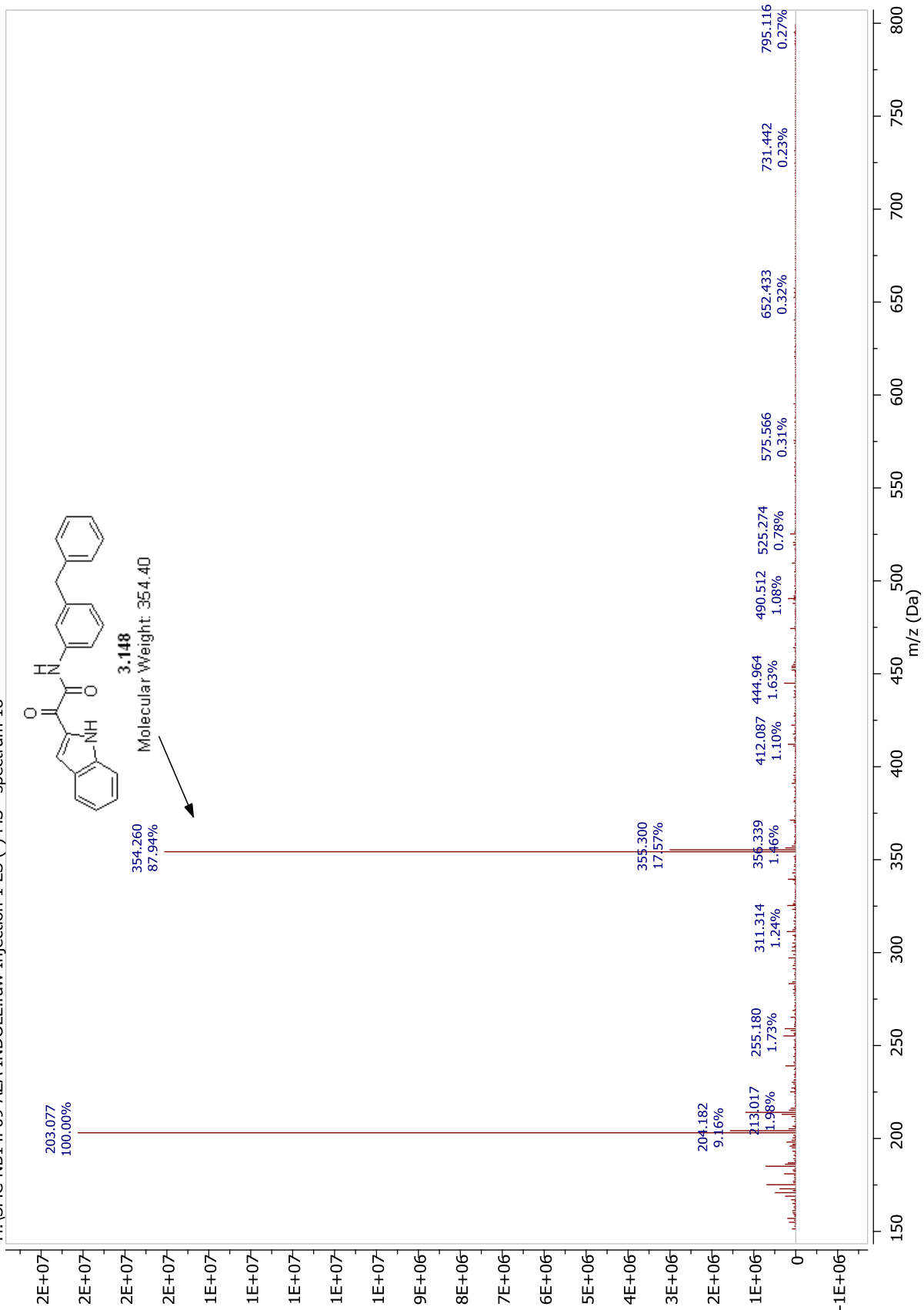


3.146

<sup>13</sup>C NMR (101 MHz, CDCl<sub>3</sub>) 143.99, 137.56, 131.98, 119.11, 63.15, 62.30, 14.09, 13.90.



H:\SMC-NB14P09-AZA INDOLE.raw Injection 1 ES (-) MS - spectrum 18



**Appendix: B**  
**Copyright Permissions**

Rightslink Printable License

[https://s100.copyright.com/CustomerAdmin/PLF.jsp?IID=2012021\\_1329760716388](https://s100.copyright.com/CustomerAdmin/PLF.jsp?IID=2012021_1329760716388)[5/3/2012 4:53:05 PM]

## **NATURE PUBLISHING GROUP LICENSE TERMS AND CONDITIONS**

May 03, 2012

This is a License Agreement between Sarah C. Scarry ("You") and Nature Publishing Group ("Nature Publishing Group") provided by Copyright Clearance Center ("CCC"). The license consists of your order details, the terms and conditions provided by Nature Publishing Group, and the payment terms and conditions.

**All payments must be made in full to CCC. For payment instructions, please see information listed at the bottom of this form.**

License Number 2853160924388

License date Feb 20, 2012

Licensed content publisher Nature Publishing Group

Licensed content publication Nature Biotechnology

Licensed content title Structure-based maximal affinity model predicts small-molecule druggability

Licensed content author Alan C Cheng, Ryan G Coleman, Kathleen T Smyth, Qing Cao, Patricia Soulard

Licensed content date Jan 1, 2007

Volume number 25

Issue number 1

Type of Use reuse in a thesis/dissertation

Requestor type academic/educational

Format print and electronic

Portion figures/tables/illustrations

Number of  
figures/tables/illustrations

1

High-res required no

Figures The figure that I am requesting to use is (Figure 2. Calculated druggability for a set of 27 target binding sites, Page 72 of the publication).

Author of this NPG article no

Your reference number

Title of your thesis /  
dissertation

The Synthesis of HIV-1 IN Inhibitors

Expected completion date May 2012

Estimated size (number of  
pages)

350

Total 0.00 USD

[Terms and Conditions](#)

### Terms and Conditions for Permissions

Nature Publishing Group hereby grants you a non-exclusive license to reproduce this material for this purpose, and for no other use, subject to the conditions

Rightslink Printable License

[https://s100.copyright.com/CustomerAdmin/PLF.jsp?IID=2012021\\_1329760716388](https://s100.copyright.com/CustomerAdmin/PLF.jsp?IID=2012021_1329760716388)[5/3/2012 4:57:09 PM]

## **NATURE PUBLISHING GROUP LICENSE TERMS AND CONDITIONS**

May 03, 2012

This is a License Agreement between Sarah C. Scarry ("You") and Nature Publishing Group ("Nature Publishing Group") provided by Copyright Clearance Center ("CCC"). The license consists of your order details, the terms and conditions provided by Nature Publishing Group, and the payment terms and conditions.

**All payments must be made in full to CCC. For payment instructions, please see information listed at the bottom of this form.**

License Number 2853160924388

License date Feb 20, 2012

Licensed content publisher Nature Publishing Group

Licensed content publication Nature Biotechnology

Licensed content title Structure-based maximal affinity model predicts small-molecule druggability

Licensed content author Alan C Cheng, Ryan G Coleman, Kathleen T Smyth, Qing Cao, Patricia Soulard

Licensed content date Jan 1, 2007

Volume number 25

Issue number 1

Type of Use reuse in a thesis/dissertation

Requestor type academic/educational

Format print and electronic

Portion figures/tables/illustrations

Number of  
figures/tables/illustrations

1

High-res required no

Figures The figure that I am requesting to use is (Figure 2. Calculated druggability for a set of 27 target binding sites, Page 72 of the publication).

Author of this NPG article no

Your reference number

Title of your thesis /  
dissertation

The Synthesis of HIV-1 IN Inhibitors

Expected completion date May 2012

Estimated size (number of  
pages)

350

Total 0.00 USD

[Terms and Conditions](#)

**Terms and Conditions for Permissions**

Nature Publishing Group hereby grants you a non-exclusive license to reproduce this material for this purpose, and for no other use, subject to the conditions

**From:** Sarah Marie Scarry

**To:** JOHN M RIMOLDI

**Subject:** FW: 87551 Form to request permission to reproduce or reprint WHO copyrighted material

**Date:** Thursday, May 03, 2012 4:55:51 PM

**From:** CAMPANARIO, Dolores [mailto:campanariod@who.int]

**Sent:** Monday, February 27, 2012 5:51 AM

**To:** schajkow@olemiss.edu

**Subject:** ID: 87551 Form to request permission to reproduce or reprint WHO copyrighted material

Dear MS Scarry,

Thank you for your enquiry. On behalf of the World Health Organization, we are pleased to grant you permission to reproduce the following WHO item/s, as indicated in your message below:

The Global Summary of the AIDS epidemic, 2009.

([http://www.searo.who.int/linkfiles/facts\\_and\\_figures\\_hiv\\_globalsituationpdf](http://www.searo.who.int/linkfiles/facts_and_figures_hiv_globalsituationpdf) (page 5: Adults and Children estimated to be living with HIV, 2009))

Please note that this permission is granted under the following terms:

- This is a non-exclusive permission to reproduce the material detailed below.
- WHO material should not be reproduced for use in association with commercial nor promotional activities
- There should be no suggestion that WHO endorses any specific company nor products in the (article, book etc.) nor in the manner of distribution of the article, book etc.).
- The material will be reproduced as it was published by WHO and no changes should be made to the content or meaning. Publishers may reformat the material in the style of the publication.
- The WHO Logo/Emblem should not be reproduced, unless it appears on an original WHO publication or unless a specific permission is given by WHO for its use.
- Please ensure that the original WHO source is appropriately acknowledged with either (i) the appropriate bibliographical reference (including publication title, author, publisher, volume/edition number, page numbers, copyright notice year) or (ii) in the case of materials published on the WHO web site, the URL reference and the date accessed.
- WHO will not charge any fee for the above permission, however we would like you to please provide me with 1 original hard copy or 2 of your final publication for our records, specifically showing where/how WHO material appears and how it is referenced on your product . Also indicate the attached Permission ID....

Number and please send directly to this address:

Ms Dolores Campanario

World Health Organization Press

WHP (Permissions Management and Reprint Rights)

20 Avenue Appia, Office 4152

CH-1211 Genève 27, Switzerland

Please also send as well a copy by e-mail to: [permissions@who.int](mailto:permissions@who.int) If available on CD/DVD please send me copies or if web page (send the direct link to where WHO is indicated on your site as well).

We thank you for your interest in WHO Information products. We wish you all the best with your project.

With kind regards.

Ms Dolores Campanario

WHO Press - (Permissions Management, Licensing and Reprint Rights)

Department of Knowledge Management and Sharing

Innovation, Information, Evidence and Research Cluster

World Health Organization Press

20 Avenue Appia, CH-1211 Genève 27, Switzerland

Tel: +41 22 791 24 83 - Fax: +41 22 791 4857 - Office: 4152 - E-mail: [campanariod@who.int](mailto:campanariod@who.int)

Direct Links:

To request for permission to reproduce parts or complete reprints of WHO copyrighted materials, complete this form - [http://www.who.int/about/licensing/copyright\\_form/en/index.html](http://www.who.int/about/licensing/copyright_form/en/index.html)

Information on Permissions and Licensing - <http://www.who.int/about/licensing/en/>

To order WHO publications on sale - <http://apps.who.int/bookorders/>

"Please note that if the requested item was jointly produced with other organization/s outside WHO or if not originally produced by WHO source, then please, also make every effort to obtain permissions from the appropriate external sources as mentioned on the original product details."

-----Original Message-----

From: [internet@who.int](mailto:internet@who.int) [<mailto:internet@who.int>]

Sent: lundi 20 février 2012 19:49

To: permissions; [schajkow@olemiss.edu](mailto:schajkow@olemiss.edu)

Subject: [DataCol Web] Form to request permission to reproduce or reprint WHO copyrighted material  
DataCol Web: Form to request permission to reproduce or reprint WHO copyrighted material

=====

ID: 87551

Section: Contact details

-----  
\* Title

\* Ms

-----  
\* First name

\* Sarah

-----  
\* Family name

\* Scarry

-----  
\* Organization/affiliation

\* The University of Mississippi

-----  
\* Web site address

\* [www.olemiss.edu](http://www.olemiss.edu)

-----  
\* Type of organization/affiliation

\* Academic

**From:** Sarah Marie Scarry  
**To:** JOHN M RIMOLDI  
**Subject:** FW: C-Query: Permission Requests  
**Date:** Thursday, May 03, 2012 4:55:31 PM  
**From:** AMBREEN IRSHAD - BSP [mailto:ambreenirshad@benthamscience.org]  
**Sent:** Tuesday, February 21, 2012 4:28 AM  
**To:** schajkow@olemiss.edu  
**Cc:** m.ahmed@benthamscience.org  
**Subject:** RE: C-Query: Permission Requests

## Grant of Permission

Dear Dr. Scarry:

Thank you for your interest in our copyrighted material, and for requesting permission for its use.

Permission is granted for the following subject to the conditions outlined below:

Figure 2 : Marchand, C.; Maddali, K.; Métifiot, M.; Pommier, Y., HIV-1 IN Inhibitors: 2010 Update and Perspectives. Current Topics in Medicinal Chemistry 2009, 9, (11), 1016-1037

To be used in the following manner:

1. Bentham Science Publishers grants you the right to reproduce the material indicated above on a one-time, non-exclusive basis, solely for the purpose described. Permission must be requested separately for any future or additional use.
2. For an article, the copyright notice must be printed on the first page of article or book chapter. For figures, photographs, covers, or tables, the notice may appear with the material, in a footnote, or in the reference list.

Thank you for your patience while your request was being processed. If you wish to contact us further, please use the address below.

Sincerely,

**AMBREEN IRSHAD**

**Permissions & Rights Manager**

Bentham Science Publishers Ltd

Email: [permission@benthamscience.org](mailto:permission@benthamscience.org)

URL: [www.benthamscience.com](http://www.benthamscience.com)



-----Original Message-----

From: [schajkow@olemiss.edu](mailto:schajkow@olemiss.edu) [mailto:[schajkow@olemiss.edu](mailto:schajkow@olemiss.edu)]

Sent: Monday, February 20, 2012 10:51 PM

To: [permission@benthamscience.org](mailto:permission@benthamscience.org)

Subject: C-Query: Permission Requests

Rightslink Printable License

[https://s100.copyright.com/CustomerAdmin/PLF.jsp?IID=2012021\\_1330398492210](https://s100.copyright.com/CustomerAdmin/PLF.jsp?IID=2012021_1330398492210)[5/3/2012 5:03:54 PM]

## ELSEVIER LICENSE

### TERMS AND CONDITIONS

May 03, 2012

This is a License Agreement between Sarah C. Scarry ("You") and Elsevier ("Elsevier") provided by Copyright Clearance Center ("CCC"). The license consists of your order details, the terms and conditions provided by Elsevier, and the payment terms and conditions.

**All payments must be made in full to CCC. For payment instructions, please see information listed at the bottom of this form.**

Supplier Elsevier Limited

The Boulevard, Langford Lane

Kidlington, Oxford, OX5 1GB, UK

Registered Company Number 1982084

Customer name Sarah C. Scarry

Customer address 4749 Sardis Lake Drive

Batesville, MS 38606

License number 2857380636210

License date Feb 27, 2012

Licensed content publisher Elsevier

Licensed content publication Trends in Microbiology

Licensed content title HIV-1 and the host cell: an intimate association

Licensed content author Eric O Freed

Licensed content date April 2004

Licensed content volume

number

12

Licensed content issue

number

4

Number of pages 8

Start Page 170

End Page 177

Type of Use reuse in a thesis/dissertation

Intended publisher of new

work

other

Portion figures/tables/illustrations

Number of

figures/tables/illustrations

1

Format both print and electronic

Are you the author of this

Elsevier article?

No

Will you be translating? No

Order reference number

Title of your

thesis/dissertation

The Synthesis of HIV-1 IN Inhibitors

Rightslink Printable License

[https://s100.copyright.com/CustomerAdmin/PLF.jsp?IID=2012021\\_1330398492210](https://s100.copyright.com/CustomerAdmin/PLF.jsp?IID=2012021_1330398492210)[5/3/2012 5:03:54 PM]

[Expected completion date](#) May 2012

[Estimated size \(number of pages\)](#)

350

[Elsevier VAT number](#) GB 494 6272 12

[Permissions price](#) 0.00 USD

[VAT/Local Sales Tax](#) 0.0 USD / 0.0 GBP

[Total](#) 0.00 USD

[Terms and Conditions](#)

## **INTRODUCTION**

1. The publisher for this copyrighted material is Elsevier. By clicking "accept" in connection with completing this licensing transaction, you agree that the following terms and conditions apply to this transaction (along with the Billing and Payment terms and conditions established by Copyright Clearance Center, Inc. ("CCC"), at the time that you opened your Rightslink account and that are available at any time at <http://myaccount.copyright.com>).

## **GENERAL TERMS**

2. Elsevier hereby grants you permission to reproduce the aforementioned material subject to the terms and conditions indicated.

3. Acknowledgement: If any part of the material to be used (for example, figures) has appeared in our publication with credit or acknowledgement to another source, permission must also be sought from that source. If such permission is not obtained then that material may not be included in your publication/copies. Suitable acknowledgement to the source must be made, either as a footnote or in a reference list at the end of your publication, as follows:

"Reprinted from Publication title, Vol /edition number, Author(s), Title of article / title of chapter, Pages No., Copyright (Year), with permission from Elsevier [OR APPLICABLE SOCIETY COPYRIGHT OWNER]." Also Lancet special credit -

"Reprinted from The Lancet, Vol. number, Author(s), Title of article, Pages No., Copyright (Year), with permission from Elsevier."

4. Reproduction of this material is confined to the purpose and/or media for which permission is hereby given.

5. Altering/Modifying Material: Not Permitted. However figures and illustrations may be altered/adapted minimally to serve your work. Any other abbreviations, additions, deletions and/or any other alterations shall be made only with prior written authorization of Elsevier Ltd. (Please contact Elsevier at [permissions@elsevier.com](mailto:permissions@elsevier.com))

6. If the permission fee for the requested use of our material is waived in this instance, please be advised that your future requests for Elsevier materials may attract a fee.

7. Reservation of Rights: Publisher reserves all rights not specifically granted in the combination of (i) the license details provided by you and accepted in the course of this licensing transaction, (ii) these terms and conditions and (iii) CCC's Billing and Payment terms and conditions.

8. License Contingent Upon Payment: While you may exercise the rights licensed immediately upon issuance of the license at the end of the licensing process for the

Rightslink Printable License

[https://s100.copyright.com/CustomerAdmin/PLF.jsp?IID=2012021\\_1330398492210](https://s100.copyright.com/CustomerAdmin/PLF.jsp?IID=2012021_1330398492210)[5/3/2012 5:10:05 PM]

## **ELSEVIER LICENSE TERMS AND CONDITIONS**

May 03, 2012

This is a License Agreement between Sarah C. Scarry ("You") and Elsevier ("Elsevier") provided by Copyright Clearance Center ("CCC"). The license consists of your order details, the terms and conditions provided by Elsevier, and the payment terms and conditions.

**All payments must be made in full to CCC. For payment instructions, please see information listed at the bottom of this form.**

Supplier Elsevier Limited

The Boulevard, Langford Lane

Kidlington, Oxford, OX5 1GB, UK

Registered Company Number 1982084

Customer name Sarah C. Scarry

Customer address 4749 Sardis Lake Drive

Batesville, MS 38606

License number 2857380636210

License date Feb 27, 2012

Licensed content publisher Elsevier

Licensed content publication Trends in Microbiology

Licensed content title HIV-1 and the host cell: an intimate association

Licensed content author Eric O Freed

Licensed content date April 2004

Licensed content volume

number

12

Licensed content issue

number

4

Number of pages 8

Start Page 170

End Page 177

Type of Use reuse in a thesis/dissertation

Intended publisher of new

work

other

Portion figures/tables/illustrations

Number of

figures/tables/illustrations

1

Format both print and electronic

Are you the author of this

Elsevier article?

No

Will you be translating? No

Order reference number

Title of your

thesis/dissertation

The Synthesis of HIV-1 IN Inhibitors

Rightslink Printable License

[https://s100.copyright.com/CustomerAdmin/PLF.jsp?IID=2012021\\_1330398492210](https://s100.copyright.com/CustomerAdmin/PLF.jsp?IID=2012021_1330398492210)[5/3/2012 5:10:05 PM]

Expected completion date May 2012

Estimated size (number of

pages)

350

Elsevier VAT number GB 494 6272 12  
Permissions price 0.00 USD  
VAT/Local Sales Tax 0.0 USD / 0.0 GBP  
Total 0.00 USD  
[Terms and Conditions](#)

## **INTRODUCTION**

1. The publisher for this copyrighted material is Elsevier. By clicking "accept" in connection with completing this licensing transaction, you agree that the following terms and conditions apply to this transaction (along with the Billing and Payment terms and conditions established by Copyright Clearance Center, Inc. ("CCC"), at the time that you opened your Rightslink account and that are available at any time at <http://myaccount.copyright.com>).

## **GENERAL TERMS**

2. Elsevier hereby grants you permission to reproduce the aforementioned material subject to the terms and conditions indicated.

3. Acknowledgement: If any part of the material to be used (for example, figures) has appeared in our publication with credit or acknowledgement to another source, permission must also be sought from that source. If such permission is not obtained then that material may not be included in your publication/copies. Suitable acknowledgement to the source must be made, either as a footnote or in a reference list at the end of your publication, as follows:

"Reprinted from Publication title, Vol /edition number, Author(s), Title of article / title of chapter, Pages No., Copyright (Year), with permission from Elsevier [OR APPLICABLE SOCIETY COPYRIGHT OWNER]." Also Lancet special credit -

"Reprinted from The Lancet, Vol. number, Author(s), Title of article, Pages No., Copyright (Year), with permission from Elsevier."

4. Reproduction of this material is confined to the purpose and/or media for which permission is hereby given.

5. Altering/Modifying Material: Not Permitted. However figures and illustrations may be altered/adapted minimally to serve your work. Any other abbreviations, additions, deletions and/or any other alterations shall be made only with prior written authorization of Elsevier Ltd. (Please contact Elsevier at [permissions@elsevier.com](mailto:permissions@elsevier.com))

6. If the permission fee for the requested use of our material is waived in this instance, please be advised that your future requests for Elsevier materials may attract a fee.

7. Reservation of Rights: Publisher reserves all rights not specifically granted in the combination of (i) the license details provided by you and accepted in the course of this licensing transaction, (ii) these terms and conditions and (iii) CCC's Billing and Payment terms and conditions.

8. License Contingent Upon Payment: While you may exercise the rights licensed immediately upon issuance of the license at the end of the licensing process for the

**NATURE PUBLISHING GROUP LICENSE  
TERMS AND CONDITIONS**

May 03, 2012

This is a License Agreement between Sarah C. Scarry ("You") and Nature Publishing Group ("Nature Publishing Group") provided by Copyright Clearance Center ("CCC"). The license consists of your order details, the terms and conditions provided by Nature Publishing Group, and the payment terms and conditions.

**All payments must be made in full to CCC. For payment instructions, please see information listed at the bottom of this form.**

License Number 2861640773877

License date Mar 03, 2012

Licensed content publisher Nature Publishing Group

Licensed content publication Nature Reviews Drug Discovery

Licensed content title The design of drugs for HIV and HCV

Licensed content author Erik De Clercq

Licensed content date Dec 1, 2007

Type of Use reuse in a thesis/dissertation

Requestor type academic/educational

Format print and electronic

Portion figures/tables/illustrations

Number of

figures/tables/illustrations

1

High-res required no

Figures Figure 1(a). Simplified flow charts of the life cycle of human immunodeficiency virus (HIV)

Author of this NPG article no

Your reference number

Title of your thesis /  
dissertation

The Synthesis of HIV-1 IN Inhibitors

Expected completion date May 2012

Estimated size (number of  
pages)

350

Total 0.00 USD

[Terms and Conditions](#)

**Terms and Conditions for Permissions**

Nature Publishing Group hereby grants you a non-exclusive license to reproduce this material for this purpose, and for no other use, subject to the conditions below:

1. NPG warrants that it has, to the best of its knowledge, the rights to license reuse of this material. However, you should ensure that the material you are requesting is original to Nature Publishing Group and does not carry the

Rightslink Printable License

[https://s100.copyright.com/CustomerAdmin/PLF.jsp?IID=2012030\\_1330826741877](https://s100.copyright.com/CustomerAdmin/PLF.jsp?IID=2012030_1330826741877)[5/3/2012 5:11:37 PM]

copyright of another entity (as credited in the published version). If the credit line on any part of the material you have requested indicates that it was reprinted or adapted by NPG with permission from another source, then you should also seek permission from that source to reuse the material.

2. Permission granted free of charge for material in print is also usually granted

for any electronic version of that work, provided that the material is incidental to the work as a whole and that the electronic version is essentially equivalent to, or substitutes for, the print version. Where print permission has been granted for a fee, separate permission must be obtained for any additional, electronic re-use (unless, as in the case of a full paper, this has already been accounted for during your initial request in the calculation of a print run). NB: In all cases, web-based use of full-text articles must be authorized separately through the 'Use on a Web Site' option when requesting permission.

3. Permission granted for a first edition does not apply to second and subsequent editions and for editions in other languages (except for signatories to the STM Permissions Guidelines, or where the first edition permission was granted for free).

4. Nature Publishing Group's permission must be acknowledged next to the figure, table or abstract in print. In electronic form, this acknowledgement must be visible at the same time as the figure/table/abstract, and must be hyperlinked to the journal's homepage.

5. The credit line should read:

Reprinted by permission from Macmillan Publishers Ltd: [JOURNAL NAME] (reference citation), copyright (year of publication)

For AOP papers, the credit line should read:

Reprinted by permission from Macmillan Publishers Ltd: [JOURNAL NAME], advance online publication, day month year (doi: 10.1038/sj.[JOURNAL ACRONYM].XXXXX)

**Note: For republication from the British Journal of Cancer, the following credit lines apply.**

Reprinted by permission from Macmillan Publishers Ltd on behalf of Cancer Research UK: [JOURNAL NAME] (reference citation), copyright (year of publication) For AOP papers, the credit line should read:

Reprinted by permission from Macmillan Publishers Ltd on behalf of Cancer Research UK: [JOURNAL NAME], advance online publication, day month year (doi: 10.1038/sj.[JOURNAL ACRONYM].XXXXX)

6. Adaptations of single figures do not require NPG approval. However, the adaptation should be credited as follows:

Adapted by permission from Macmillan Publishers Ltd: [JOURNAL NAME] (reference citation), copyright (year of publication)

**Note: For adaptation from the British Journal of Cancer, the following credit line applies.**

Adapted by permission from Macmillan Publishers Ltd on behalf of Cancer Research UK: [JOURNAL NAME] (reference citation), copyright (year of publication)

7. Translations of 401 words up to a whole article require NPG approval. Please

Rightslink Printable License

[https://s100.copyright.com/CustomerAdmin/PLF.jsp?IID=2012030\\_1330826902330](https://s100.copyright.com/CustomerAdmin/PLF.jsp?IID=2012030_1330826902330)[5/3/2012 5:17:21 PM]

## **NATURE PUBLISHING GROUP LICENSE**

### **TERMS AND CONDITIONS**

May 03, 2012

This is a License Agreement between Sarah C. Scarry ("You") and Nature Publishing Group ("Nature Publishing Group") provided by Copyright Clearance Center ("CCC"). The license consists of your order details, the terms and conditions provided by Nature Publishing Group, and the payment terms and conditions.

**All payments must be made in full to CCC. For payment instructions, please see information listed at the bottom of this form.**

License Number 2861640934330

License date Mar 03, 2012

Licensed content publisher Nature Publishing Group

Licensed content publication Nature Reviews Drug Discovery

Licensed content title The design of drugs for HIV and HCV

Licensed content author Erik De Clercq

Licensed content date Dec 1, 2007

Type of Use reuse in a thesis/dissertation

Requestor type academic/educational

Format print and electronic

Portion figures/tables/illustrations

Number of

figures/tables/illustrations

1

High-res required no

Figures Figure 3 (a). Nucleoside and non-nucleoside reverse transcriptase inhibitors/Mechanism of action of NRTIs

Author of this NPG article no

Your reference number

Title of your thesis /  
dissertation

The Synthesis of HIV-1 IN Inhibitors

Expected completion date May 2012

Estimated size (number of  
pages)

350

Total 0.00 USD

[Terms and Conditions](#)

### Terms and Conditions for Permissions

Nature Publishing Group hereby grants you a non-exclusive license to reproduce this material for this purpose, and for no other use, subject to the conditions below:

1. NPG warrants that it has, to the best of its knowledge, the rights to license reuse of this material. However, you should ensure that the material you are requesting is original to Nature Publishing Group and does not carry the

Rightslink Printable License

[https://s100.copyright.com/CustomerAdmin/PLF.jsp?IID=2012030\\_1330826902330](https://s100.copyright.com/CustomerAdmin/PLF.jsp?IID=2012030_1330826902330)[5/3/2012 5:17:21 PM]

copyright of another entity (as credited in the published version). If the credit line on any part of the material you have requested indicates that it was reprinted or adapted by NPG with permission from another source, then you should also seek permission from that source to reuse the material.

2. Permission granted free of charge for material in print is also usually granted

for any electronic version of that work, provided that the material is incidental to the work as a whole and that the electronic version is essentially equivalent to, or substitutes for, the print version. Where print permission has been granted for a fee, separate permission must be obtained for any additional, electronic re-use (unless, as in the case of a full paper, this has already been accounted for during your initial request in the calculation of a print run). NB: In all cases, web-based use of full-text articles must be authorized separately through the 'Use on a Web Site' option when requesting permission.

3. Permission granted for a first edition does not apply to second and subsequent editions and for editions in other languages (except for signatories to the STM Permissions Guidelines, or where the first edition permission was granted for free).

4. Nature Publishing Group's permission must be acknowledged next to the figure, table or abstract in print. In electronic form, this acknowledgement must be visible at the same time as the figure/table/abstract, and must be hyperlinked to the journal's homepage.

5. The credit line should read:

Reprinted by permission from Macmillan Publishers Ltd: [JOURNAL NAME] (reference citation), copyright (year of publication)

For AOP papers, the credit line should read:

Reprinted by permission from Macmillan Publishers Ltd: [JOURNAL NAME], advance online publication, day month year (doi: 10.1038/sj.[JOURNAL ACRONYM].XXXXX)

**Note: For republication from the British Journal of Cancer, the following credit lines apply.**

Reprinted by permission from Macmillan Publishers Ltd on behalf of Cancer Research UK: [JOURNAL NAME] (reference citation), copyright (year of publication) For AOP papers, the credit line should read:

Reprinted by permission from Macmillan Publishers Ltd on behalf of Cancer Research UK: [JOURNAL NAME], advance online publication, day month year (doi: 10.1038/sj.[JOURNAL ACRONYM].XXXXX)

6. Adaptations of single figures do not require NPG approval. However, the adaptation should be credited as follows:

Adapted by permission from Macmillan Publishers Ltd: [JOURNAL NAME] (reference citation), copyright (year of publication)

**Note: For adaptation from the British Journal of Cancer, the following credit line applies.**

Adapted by permission from Macmillan Publishers Ltd on behalf of Cancer Research UK: [JOURNAL NAME] (reference citation), copyright (year of publication)

7. Translations of 401 words up to a whole article require NPG approval. Please



Rightslink Printable License

[https://s100.copyright.com/CustomerAdmin/PLF.jsp?IID=2012030\\_1330826902330](https://s100.copyright.com/CustomerAdmin/PLF.jsp?IID=2012030_1330826902330)[5/3/2012 5:30:41 PM]

## **NATURE PUBLISHING GROUP LICENSE TERMS AND CONDITIONS**

May 03, 2012

This is a License Agreement between Sarah C. Scarry ("You") and Nature Publishing Group ("Nature Publishing Group") provided by Copyright Clearance Center ("CCC"). The license consists of your order details, the terms and conditions provided by Nature Publishing Group, and the payment terms and conditions.

**All payments must be made in full to CCC. For payment instructions, please see information listed at the bottom of this form.**

License Number 2861640934330

License date Mar 03, 2012

Licensed content publisher Nature Publishing Group

Licensed content publication Nature Reviews Drug Discovery

Licensed content title The design of drugs for HIV and HCV

Licensed content author Erik De Clercq

Licensed content date Dec 1, 2007

Type of Use reuse in a thesis/dissertation

Requestor type academic/educational

Format print and electronic

Portion figures/tables/illustrations

Number of

figures/tables/illustrations

1

High-res required no

Figures Figure 3 (a). Nucleoside and non-nucleoside reverse transcriptase inhibitors/Mechanism of action of NRTIs

Author of this NPG article no

Your reference number

Title of your thesis /  
dissertation

The Synthesis of HIV-1 IN Inhibitors

Expected completion date May 2012

Estimated size (number of  
pages)

350

Total 0.00 USD

[Terms and Conditions](#)

### Terms and Conditions for Permissions

Nature Publishing Group hereby grants you a non-exclusive license to reproduce this material for this purpose, and for no other use, subject to the conditions below:

1. NPG warrants that it has, to the best of its knowledge, the rights to license reuse of this material. However, you should ensure that the material you are requesting is original to Nature Publishing Group and does not carry the

Rightslink Printable License

[https://s100.copyright.com/CustomerAdmin/PLF.jsp?IID=2012030\\_1330826902330](https://s100.copyright.com/CustomerAdmin/PLF.jsp?IID=2012030_1330826902330)[5/3/2012 5:30:41 PM]

copyright of another entity (as credited in the published version). If the credit line on any part of the material you have requested indicates that it was reprinted or adapted by NPG with permission from another source, then you should also seek permission from that source to reuse the material.

2. Permission granted free of charge for material in print is also usually granted

for any electronic version of that work, provided that the material is incidental to the work as a whole and that the electronic version is essentially equivalent to, or substitutes for, the print version. Where print permission has been granted for a fee, separate permission must be obtained for any additional, electronic re-use (unless, as in the case of a full paper, this has already been accounted for during your initial request in the calculation of a print run). NB: In all cases, web-based use of full-text articles must be authorized separately through the 'Use on a Web Site' option when requesting permission.

3. Permission granted for a first edition does not apply to second and subsequent editions and for editions in other languages (except for signatories to the STM Permissions Guidelines, or where the first edition permission was granted for free).

4. Nature Publishing Group's permission must be acknowledged next to the figure, table or abstract in print. In electronic form, this acknowledgement must be visible at the same time as the figure/table/abstract, and must be hyperlinked to the journal's homepage.

5. The credit line should read:

Reprinted by permission from Macmillan Publishers Ltd: [JOURNAL NAME] (reference citation), copyright (year of publication)

For AOP papers, the credit line should read:

Reprinted by permission from Macmillan Publishers Ltd: [JOURNAL NAME], advance online publication, day month year (doi: 10.1038/sj.[JOURNAL ACRONYM].XXXXX)

**Note: For republication from the British Journal of Cancer, the following credit lines apply.**

Reprinted by permission from Macmillan Publishers Ltd on behalf of Cancer Research UK: [JOURNAL NAME] (reference citation), copyright (year of publication) For AOP papers, the credit line should read:

Reprinted by permission from Macmillan Publishers Ltd on behalf of Cancer Research UK: [JOURNAL NAME], advance online publication, day month year (doi: 10.1038/sj.[JOURNAL ACRONYM].XXXXX)

6. Adaptations of single figures do not require NPG approval. However, the adaptation should be credited as follows:

Adapted by permission from Macmillan Publishers Ltd: [JOURNAL NAME] (reference citation), copyright (year of publication)

**Note: For adaptation from the British Journal of Cancer, the following credit line applies.**

Adapted by permission from Macmillan Publishers Ltd on behalf of Cancer Research UK: [JOURNAL NAME] (reference citation), copyright (year of publication)

7. Translations of 401 words up to a whole article require NPG approval. Please

Rightslink Printable License

[https://s100.copyright.com/CustomerAdmin/PLF.jsp?IID=2012030\\_1330826741877](https://s100.copyright.com/CustomerAdmin/PLF.jsp?IID=2012030_1330826741877)[5/3/2012 5:32:14 PM]

## **NATURE PUBLISHING GROUP LICENSE**

### **TERMS AND CONDITIONS**

May 03, 2012

This is a License Agreement between Sarah C. Scarry ("You") and Nature Publishing Group ("Nature Publishing Group") provided by Copyright Clearance Center ("CCC"). The license consists of your order details, the terms and conditions provided by Nature Publishing Group, and the payment terms and conditions.

**All payments must be made in full to CCC. For payment instructions, please see information listed at the bottom of this form.**

License Number 2861640773877

License date Mar 03, 2012

Licensed content publisher Nature Publishing Group

Licensed content publication Nature Reviews Drug Discovery

Licensed content title The design of drugs for HIV and HCV

Licensed content author Erik De Clercq

Licensed content date Dec 1, 2007

Type of Use reuse in a thesis/dissertation

Requestor type academic/educational

Format print and electronic

Portion figures/tables/illustrations

Number of

figures/tables/illustrations

1

High-res required no

Figures Figure 1(a). Simplified flow charts of the life cycle of human immunodeficiency virus (HIV)

Author of this NPG article no

Your reference number

Title of your thesis /  
dissertation

The Synthesis of HIV-1 IN Inhibitors

Expected completion date May 2012

Estimated size (number of  
pages)

350

Total 0.00 USD

[Terms and Conditions](#)

### Terms and Conditions for Permissions

Nature Publishing Group hereby grants you a non-exclusive license to reproduce this material for this purpose, and for no other use, subject to the conditions below:

1. NPG warrants that it has, to the best of its knowledge, the rights to license reuse of this material. However, you should ensure that the material you are requesting is original to Nature Publishing Group and does not carry the

Rightslink Printable License

[https://s100.copyright.com/CustomerAdmin/PLF.jsp?IID=2012030\\_1330826741877](https://s100.copyright.com/CustomerAdmin/PLF.jsp?IID=2012030_1330826741877)[5/3/2012 5:32:14 PM]

copyright of another entity (as credited in the published version). If the credit line on any part of the material you have requested indicates that it was reprinted or adapted by NPG with permission from another source, then you should also seek permission from that source to reuse the material.

2. Permission granted free of charge for material in print is also usually granted

for any electronic version of that work, provided that the material is incidental to the work as a whole and that the electronic version is essentially equivalent to, or substitutes for, the print version. Where print permission has been granted for a fee, separate permission must be obtained for any additional, electronic re-use (unless, as in the case of a full paper, this has already been accounted for during your initial request in the calculation of a print run). NB: In all cases, web-based use of full-text articles must be authorized separately through the 'Use on a Web Site' option when requesting permission.

3. Permission granted for a first edition does not apply to second and subsequent editions and for editions in other languages (except for signatories to the STM Permissions Guidelines, or where the first edition permission was granted for free).

4. Nature Publishing Group's permission must be acknowledged next to the figure, table or abstract in print. In electronic form, this acknowledgement must be visible at the same time as the figure/table/abstract, and must be hyperlinked to the journal's homepage.

5. The credit line should read:

Reprinted by permission from Macmillan Publishers Ltd: [JOURNAL NAME] (reference citation), copyright (year of publication)

For AOP papers, the credit line should read:

Reprinted by permission from Macmillan Publishers Ltd: [JOURNAL NAME], advance online publication, day month year (doi: 10.1038/sj.[JOURNAL ACRONYM].XXXXX)

**Note: For republication from the British Journal of Cancer, the following credit lines apply.**

Reprinted by permission from Macmillan Publishers Ltd on behalf of Cancer Research UK: [JOURNAL NAME] (reference citation), copyright (year of publication) For AOP papers, the credit line should read:

Reprinted by permission from Macmillan Publishers Ltd on behalf of Cancer Research UK: [JOURNAL NAME], advance online publication, day month year (doi: 10.1038/sj.[JOURNAL ACRONYM].XXXXX)

6. Adaptations of single figures do not require NPG approval. However, the adaptation should be credited as follows:

Adapted by permission from Macmillan Publishers Ltd: [JOURNAL NAME] (reference citation), copyright (year of publication)

**Note: For adaptation from the British Journal of Cancer, the following credit line applies.**

Adapted by permission from Macmillan Publishers Ltd on behalf of Cancer Research UK: [JOURNAL NAME] (reference citation), copyright (year of publication)

7. Translations of 401 words up to a whole article require NPG approval. Please

## **NATURE PUBLISHING GROUP LICENSE TERMS AND CONDITIONS**

May 03, 2012

This is a License Agreement between Sarah C. Scarry ("You") and Nature Publishing Group ("Nature Publishing Group") provided by Copyright Clearance Center ("CCC"). The license consists of your order details, the terms and conditions provided by Nature Publishing Group, and the payment terms and conditions.

**All payments must be made in full to CCC. For payment instructions, please see information listed at the bottom of this form.**

License Number 2861640934330

License date Mar 03, 2012

Licensed content publisher Nature Publishing Group

Licensed content publication Nature Reviews Drug Discovery

Licensed content title The design of drugs for HIV and HCV

Licensed content author Erik De Clercq

Licensed content date Dec 1, 2007

Type of Use reuse in a thesis/dissertation

Requestor type academic/educational

Format print and electronic

Portion figures/tables/illustrations

Number of

figures/tables/illustrations

1

High-res required no

Figures Figure 3 (a). Nucleoside and non-nucleoside reverse transcriptase inhibitors/Mechanism of action of NRTIs

Author of this NPG article no

Your reference number

Title of your thesis /  
dissertation

The Synthesis of HIV-1 IN Inhibitors

Expected completion date May 2012

Estimated size (number of  
pages)

350

Total 0.00 USD

[Terms and Conditions](#)

### Terms and Conditions for Permissions

Nature Publishing Group hereby grants you a non-exclusive license to reproduce this material for this purpose, and for no other use, subject to the conditions below:

1. NPG warrants that it has, to the best of its knowledge, the rights to license reuse of this material. However, you should ensure that the material you are requesting is original to Nature Publishing Group and does not carry the

Rightslink Printable License

[https://s100.copyright.com/CustomerAdmin/PLF.jsp?IID=2012030\\_1330826902330](https://s100.copyright.com/CustomerAdmin/PLF.jsp?IID=2012030_1330826902330)[5/3/2012 5:39:27 PM]

copyright of another entity (as credited in the published version). If the credit line on any part of the material you have requested indicates that it was reprinted or adapted by NPG with permission from another source, then you should also seek permission from that source to reuse the material.

2. Permission granted free of charge for material in print is also usually granted

for any electronic version of that work, provided that the material is incidental to the work as a whole and that the electronic version is essentially equivalent to, or substitutes for, the print version. Where print permission has been granted for a fee, separate permission must be obtained for any additional, electronic re-use (unless, as in the case of a full paper, this has already been accounted for during your initial request in the calculation of a print run). NB: In all cases, web-based use of full-text articles must be authorized separately through the 'Use on a Web Site' option when requesting permission.

3. Permission granted for a first edition does not apply to second and subsequent editions and for editions in other languages (except for signatories to the STM Permissions Guidelines, or where the first edition permission was granted for free).

4. Nature Publishing Group's permission must be acknowledged next to the figure, table or abstract in print. In electronic form, this acknowledgement must be visible at the same time as the figure/table/abstract, and must be hyperlinked to the journal's homepage.

5. The credit line should read:

Reprinted by permission from Macmillan Publishers Ltd: [JOURNAL NAME] (reference citation), copyright (year of publication)

For AOP papers, the credit line should read:

Reprinted by permission from Macmillan Publishers Ltd: [JOURNAL NAME], advance online publication, day month year (doi: 10.1038/sj.[JOURNAL ACRONYM].XXXXX)

**Note: For republication from the British Journal of Cancer, the following credit lines apply.**

Reprinted by permission from Macmillan Publishers Ltd on behalf of Cancer Research UK: [JOURNAL NAME] (reference citation), copyright (year of publication) For AOP papers, the credit line should read:

Reprinted by permission from Macmillan Publishers Ltd on behalf of Cancer Research UK: [JOURNAL NAME], advance online publication, day month year (doi: 10.1038/sj.[JOURNAL ACRONYM].XXXXX)

6. Adaptations of single figures do not require NPG approval. However, the adaptation should be credited as follows:

Adapted by permission from Macmillan Publishers Ltd: [JOURNAL NAME] (reference citation), copyright (year of publication)

**Note: For adaptation from the British Journal of Cancer, the following credit line applies.**

Adapted by permission from Macmillan Publishers Ltd on behalf of Cancer Research UK: [JOURNAL NAME] (reference citation), copyright (year of publication)

7. Translations of 401 words up to a whole article require NPG approval. Please

Rightslink Printable License

[https://s100.copyright.com/CustomerAdmin/PLF.jsp?IID=2012030\\_1330974521001](https://s100.copyright.com/CustomerAdmin/PLF.jsp?IID=2012030_1330974521001)[5/3/2012 5:48:11 PM]

## **NATURE PUBLISHING GROUP LICENSE TERMS AND CONDITIONS**

May 03, 2012

This is a License Agreement between Sarah C. Scarry ("You") and Nature Publishing Group ("Nature Publishing Group") provided by Copyright Clearance Center ("CCC"). The license consists of your order details, the terms and conditions provided by Nature Publishing Group, and the payment terms and conditions.

**All payments must be made in full to CCC. For payment instructions, please see information listed at the bottom of this form.**

License Number 2862620377001

License date Mar 05, 2012

Licensed content publisher Nature Publishing Group

Licensed content publication Nature Reviews Drug Discovery

Licensed content title Integrase inhibitors to treat HIV/Aids

Licensed content author Yves Pommier, Allison A. Johnson, Christophe Marchand

Licensed content date Feb 24, 2005

Type of Use reuse in a thesis/dissertation

Requestor type academic/educational

Format print and electronic

Portion figures/tables/illustrations

Number of

figures/tables/illustrations

1

High-res required no

Figures Figure 2. The two integrase catalytic reactions (3'-processing and strand transfer)

Author of this NPG article no

Your reference number

Title of your thesis /  
dissertation

The Synthesis of HIV-1 IN Inhibitors

Expected completion date May 2012

Estimated size (number of  
pages)

350

Total 0.00 USD

[Terms and Conditions](#)

### Terms and Conditions for Permissions

Nature Publishing Group hereby grants you a non-exclusive license to reproduce this material for this purpose, and for no other use, subject to the conditions below:

1. NPG warrants that it has, to the best of its knowledge, the rights to license reuse of this material. However, you should ensure that the material you are requesting is original to Nature Publishing Group and does not carry the

Rightslink Printable License

[https://s100.copyright.com/CustomerAdmin/PLF.jsp?IID=2012030\\_1330974521001](https://s100.copyright.com/CustomerAdmin/PLF.jsp?IID=2012030_1330974521001)[5/3/2012 5:48:11 PM]

copyright of another entity (as credited in the published version). If the credit line on any part of the material you have requested indicates that it was reprinted or adapted by NPG with permission from another source, then you should also seek permission from that source to reuse the material.

2. Permission granted free of charge for material in print is also usually granted

for any electronic version of that work, provided that the material is incidental to the work as a whole and that the electronic version is essentially equivalent to, or substitutes for, the print version. Where print permission has been granted for a fee, separate permission must be obtained for any additional, electronic re-use (unless, as in the case of a full paper, this has already been accounted for during your initial request in the calculation of a print run). NB: In all cases, web-based use of full-text articles must be authorized separately through the 'Use on a Web Site' option when requesting permission.

3. Permission granted for a first edition does not apply to second and subsequent editions and for editions in other languages (except for signatories to the STM Permissions Guidelines, or where the first edition permission was granted for free).

4. Nature Publishing Group's permission must be acknowledged next to the figure, table or abstract in print. In electronic form, this acknowledgement must be visible at the same time as the figure/table/abstract, and must be hyperlinked to the journal's homepage.

5. The credit line should read:

Reprinted by permission from Macmillan Publishers Ltd: [JOURNAL NAME] (reference citation), copyright (year of publication)

For AOP papers, the credit line should read:

Reprinted by permission from Macmillan Publishers Ltd: [JOURNAL NAME], advance online publication, day month year (doi: 10.1038/sj.[JOURNAL ACRONYM].XXXXX)

**Note: For republication from the British Journal of Cancer, the following credit lines apply.**

Reprinted by permission from Macmillan Publishers Ltd on behalf of Cancer Research UK: [JOURNAL NAME] (reference citation), copyright (year of publication) For AOP papers, the credit line should read:

Reprinted by permission from Macmillan Publishers Ltd on behalf of Cancer Research UK: [JOURNAL NAME], advance online publication, day month year (doi: 10.1038/sj.[JOURNAL ACRONYM].XXXXX)

6. Adaptations of single figures do not require NPG approval. However, the adaptation should be credited as follows:

Adapted by permission from Macmillan Publishers Ltd: [JOURNAL NAME] (reference citation), copyright (year of publication)

**Note: For adaptation from the British Journal of Cancer, the following credit line applies.**

Adapted by permission from Macmillan Publishers Ltd on behalf of Cancer Research UK: [JOURNAL NAME] (reference citation), copyright (year of publication)

7. Translations of 401 words up to a whole article require NPG approval. Please



Rightslink Printable License

[https://s100.copyright.com/CustomerAdmin/PLF.jsp?IID=2012030\\_1330974521001](https://s100.copyright.com/CustomerAdmin/PLF.jsp?IID=2012030_1330974521001)[5/3/2012 5:50:19 PM]

## **NATURE PUBLISHING GROUP LICENSE**

### **TERMS AND CONDITIONS**

May 03, 2012

This is a License Agreement between Sarah C. Scarry ("You") and Nature Publishing Group ("Nature Publishing Group") provided by Copyright Clearance Center ("CCC"). The license consists of your order details, the terms and conditions provided by Nature Publishing Group, and the payment terms and conditions.

**All payments must be made in full to CCC. For payment instructions, please see information listed at the bottom of this form.**

License Number 2862620377001

License date Mar 05, 2012

Licensed content publisher Nature Publishing Group

Licensed content publication Nature Reviews Drug Discovery

Licensed content title Integrase inhibitors to treat HIV/Aids

Licensed content author Yves Pommier, Allison A. Johnson, Christophe Marchand

Licensed content date Feb 24, 2005

Type of Use reuse in a thesis/dissertation

Requestor type academic/educational

Format print and electronic

Portion figures/tables/illustrations

Number of

figures/tables/illustrations

1

High-res required no

Figures Figure 2. The two integrase catalytic reactions (3'-processing and strand transfer)

Author of this NPG article no

Your reference number

Title of your thesis /  
dissertation

The Synthesis of HIV-1 IN Inhibitors

Expected completion date May 2012

Estimated size (number of  
pages)

350

Total 0.00 USD

[Terms and Conditions](#)

### Terms and Conditions for Permissions

Nature Publishing Group hereby grants you a non-exclusive license to reproduce this material for this purpose, and for no other use, subject to the conditions below:

1. NPG warrants that it has, to the best of its knowledge, the rights to license reuse of this material. However, you should ensure that the material you are requesting is original to Nature Publishing Group and does not carry the

Rightslink Printable License

[https://s100.copyright.com/CustomerAdmin/PLF.jsp?IID=2012030\\_1330974521001](https://s100.copyright.com/CustomerAdmin/PLF.jsp?IID=2012030_1330974521001)[5/3/2012 5:50:19 PM]

copyright of another entity (as credited in the published version). If the credit line on any part of the material you have requested indicates that it was reprinted or adapted by NPG with permission from another source, then you should also seek permission from that source to reuse the material.

2. Permission granted free of charge for material in print is also usually granted

for any electronic version of that work, provided that the material is incidental to the work as a whole and that the electronic version is essentially equivalent to, or substitutes for, the print version. Where print permission has been granted for a fee, separate permission must be obtained for any additional, electronic re-use (unless, as in the case of a full paper, this has already been accounted for during your initial request in the calculation of a print run). NB: In all cases, web-based use of full-text articles must be authorized separately through the 'Use on a Web Site' option when requesting permission.

3. Permission granted for a first edition does not apply to second and subsequent editions and for editions in other languages (except for signatories to the STM Permissions Guidelines, or where the first edition permission was granted for free).

4. Nature Publishing Group's permission must be acknowledged next to the figure, table or abstract in print. In electronic form, this acknowledgement must be visible at the same time as the figure/table/abstract, and must be hyperlinked to the journal's homepage.

5. The credit line should read:

Reprinted by permission from Macmillan Publishers Ltd: [JOURNAL NAME] (reference citation), copyright (year of publication)

For AOP papers, the credit line should read:

Reprinted by permission from Macmillan Publishers Ltd: [JOURNAL NAME], advance online publication, day month year (doi: 10.1038/sj.[JOURNAL ACRONYM].XXXXX)

**Note: For republication from the British Journal of Cancer, the following credit lines apply.**

Reprinted by permission from Macmillan Publishers Ltd on behalf of Cancer Research UK: [JOURNAL NAME] (reference citation), copyright (year of publication) For AOP papers, the credit line should read:

Reprinted by permission from Macmillan Publishers Ltd on behalf of Cancer Research UK: [JOURNAL NAME], advance online publication, day month year (doi: 10.1038/sj.[JOURNAL ACRONYM].XXXXX)

6. Adaptations of single figures do not require NPG approval. However, the adaptation should be credited as follows:

Adapted by permission from Macmillan Publishers Ltd: [JOURNAL NAME] (reference citation), copyright (year of publication)

**Note: For adaptation from the British Journal of Cancer, the following credit line applies.**

Adapted by permission from Macmillan Publishers Ltd on behalf of Cancer Research UK: [JOURNAL NAME] (reference citation), copyright (year of publication)

7. Translations of 401 words up to a whole article require NPG approval. Please

Rightslink Printable License

[https://s100.copyright.com/CustomerAdmin/PLF.jsp?IID=2012030\\_1331076497751](https://s100.copyright.com/CustomerAdmin/PLF.jsp?IID=2012030_1331076497751)[5/3/2012 5:51:11 PM]

## **OXFORD UNIVERSITY PRESS LICENSE TERMS AND CONDITIONS**

May 03, 2012

This is a License Agreement between Sarah C. Scarry ("You") and Oxford University Press ("Oxford University Press") provided by Copyright Clearance Center ("CCC"). The license consists of your order details, the terms and conditions provided by Oxford University Press, and the payment terms and conditions.

**All payments must be made in full to CCC. For payment instructions, please see information listed at the bottom of this form.**

License Number 2863291049751

License date Mar 06, 2012

Licensed content publisher Oxford University Press

Licensed content publication Journal of Antimicrobial Chemotherapy

Licensed content title Resistance to enfuvirtide, the first HIV fusion inhibitor:

Licensed content author Michael L. Greenberg, Nick Cammack

Licensed content date 08/01/2004

Type of Use Thesis/Dissertation

Institution name

Title of your work The Synthesis of HIV-1 IN Inhibitors

Publisher of your work n/a

Expected publication date May 2012

Permissions cost 0.00 USD

Value added tax 0.00 USD

Total 0.00 USD

Total 0.00 USD

[Terms and Conditions](#)

## **STANDARD TERMS AND CONDITIONS FOR REPRODUCTION OF MATERIAL FROM AN OXFORD UNIVERSITY PRESS JOURNAL**

1. Use of the material is restricted to the type of use specified in your order details.
2. This permission covers the use of the material in the English language in the following territory: world. If you have requested additional permission to translate this material, the terms and conditions of this reuse will be set out in clause 12.
3. This permission is limited to the particular use authorized in (1) above and does not allow you to sanction its use elsewhere in any other format other than specified above, nor does it apply to quotations, images, artistic works etc that have been reproduced from other sources which may be part of the material to be used.
4. No alteration, omission or addition is made to the material without our written consent. Permission must be re-cleared with Oxford University Press if/when you decide to reprint.
5. The following credit line appears wherever the material is used: author, title, journal, year, volume, issue number, pagination, by permission of Oxford University Press or the sponsoring society if the journal is a society journal. Where a journal is being published on behalf of a learned society, the details of that society must be included in the credit line.
6. For the reproduction of a full article from an Oxford University Press journal for

whatever purpose, the corresponding author of the material concerned should be informed of the proposed use. Contact details for the corresponding authors of all Oxford University Press journal contact can be found alongside either the abstract or full text of the article concerned, accessible from [www.oxfordjournals.org](http://www.oxfordjournals.org) Should there be a problem clearing these rights, please contact [journals.permissions@oxfordjournals.org](mailto:journals.permissions@oxfordjournals.org)

7. If the credit line or acknowledgement in our publication indicates that any of the figures, images or photos was reproduced, drawn or modified from an earlier source it will be necessary for you to clear this permission with the original publisher as well. If this permission has not been obtained, please note that this material cannot be included in your publication/photocopies.

8. While you may exercise the rights licensed immediately upon issuance of the license at the end of the licensing process for the transaction, provided that you have disclosed complete and accurate details of your proposed use, no license is finally effective unless and until full payment is received from you (either by Oxford University Press or by Copyright Clearance Center (CCC)) as provided in CCC's Billing and Payment terms and conditions. If full payment is not received on a timely basis, then any license preliminarily granted shall be deemed automatically revoked and shall be void as if never granted. Further, in the event that you breach any of these terms and conditions or any of CCC's Billing and Payment terms and conditions, the license is automatically revoked and shall be void as if never granted. Use of materials as described in a revoked license, as well as any use of the materials beyond the scope of an unrevoked license, may constitute copyright infringement and Oxford University Press reserves the right to take any and all action to protect its copyright in the materials.

9. This license is personal to you and may not be sublicensed, assigned or transferred by you to any other person without Oxford University Press's written permission.

10. Oxford University Press reserves all rights not specifically granted in the combination of (i) the license details provided by you and accepted in the course of this licensing transaction, (ii) these terms and conditions and (iii) CCC's Billing and Payment terms and conditions.

11. You hereby indemnify and agree to hold harmless Oxford University Press and CCC, and their respective officers, directors, employs and agents, from and against any and all claims arising out of your use of the licensed material other than as specifically authorized pursuant to this license.

12. Other Terms and Conditions:

v1.4

**If you would like to pay for this license now, please remit this license along with your payment made payable to "COPYRIGHT CLEARANCE CENTER" otherwise you will be invoiced within 48 hours of the license date. Payment should be in the form of a check**

Rightslink Printable License

[https://s100.copyright.com/CustomerAdmin/PLF.jsp?IID=2012030\\_1331138797497](https://s100.copyright.com/CustomerAdmin/PLF.jsp?IID=2012030_1331138797497)[5/3/2012 5:55:01 PM]

## **ELSEVIER LICENSE TERMS AND CONDITIONS**

May 03, 2012

This is a License Agreement between Sarah C. Scarry ("You") and Elsevier ("Elsevier") provided by Copyright Clearance Center ("CCC"). The license consists of your order details, the terms and conditions provided by Elsevier, and the payment terms and conditions.

**All payments must be made in full to CCC. For payment instructions, please see information listed at the bottom of this form.**

Supplier Elsevier Limited

The Boulevard, Langford Lane  
Kidlington, Oxford, OX5 1GB, UK

Registered Company

Number

1982084

Customer name Sarah C. Scarry

Customer address 4749 Sardis Lake Drive  
Batesville, MS 38606

License number 2863701357497

License date Mar 07, 2012

Licensed content publisher Elsevier

Licensed content publication Structure

Licensed content title HIV-1 Transcription: Activation Mediated by Acetylation of Tat

Licensed content author Yoshihiro Nakatani

Licensed content date April 2002

Licensed content volume

number

10

Licensed content issue

number

4

Number of pages 2

Start Page 443

End Page 444

Type of Use reuse in a thesis/dissertation

Intended publisher of new

work

other

Portion figures/tables/illustrations

Number of

figures/tables/illustrations

1

Format both print and electronic

Are you the author of this

Elsevier article?

No

Will you be translating? No

Order reference number

Title of your The Synthesis of HIV-1 IN Inhibitors

Rightslink Printable License

[https://s100.copyright.com/CustomerAdmin/PLF.jsp?IID=2012030\\_1331138797497](https://s100.copyright.com/CustomerAdmin/PLF.jsp?IID=2012030_1331138797497)[5/3/2012 5:55:01 PM]

thesis/dissertation

Expected completion date May 2012

Estimated size (number of

pages)

350

Elsevier VAT number GB 494 6272 12

Permissions price 0.00 USD

VAT/Local Sales Tax 0.0 USD / 0.0 GBP

Total 0.00 USD

[Terms and Conditions](#)

## **INTRODUCTION**

1. The publisher for this copyrighted material is Elsevier. By clicking "accept" in connection with completing this licensing transaction, you agree that the following terms and conditions apply to this transaction (along with the Billing and Payment terms and conditions established by Copyright Clearance Center, Inc. ("CCC"), at the time that you opened your Rightslink account and that are available at any time at <http://myaccount.copyright.com>).

## **GENERAL TERMS**

2. Elsevier hereby grants you permission to reproduce the aforementioned material subject to the terms and conditions indicated.

3. Acknowledgement: If any part of the material to be used (for example, figures) has appeared in our publication with credit or acknowledgement to another source, permission must also be sought from that source. If such permission is not obtained then that material may not be included in your publication/copies. Suitable acknowledgement to the source must be made, either as a footnote or in a reference list at the end of your publication, as follows:

"Reprinted from Publication title, Vol /edition number, Author(s), Title of article / title of chapter, Pages No., Copyright (Year), with permission from Elsevier [OR APPLICABLE SOCIETY COPYRIGHT OWNER]." Also Lancet special credit -

"Reprinted from The Lancet, Vol. number, Author(s), Title of article, Pages No., Copyright (Year), with permission from Elsevier."

4. Reproduction of this material is confined to the purpose and/or media for which permission is hereby given.

5. Altering/Modifying Material: Not Permitted. However figures and illustrations may be altered/adapted minimally to serve your work. Any other abbreviations, additions, deletions and/or any other alterations shall be made only with prior written authorization of Elsevier Ltd. (Please contact Elsevier at [permissions@elsevier.com](mailto:permissions@elsevier.com))

6. If the permission fee for the requested use of our material is waived in this instance, please be advised that your future requests for Elsevier materials may attract a fee.

7. Reservation of Rights: Publisher reserves all rights not specifically granted in the combination of (i) the license details provided by you and accepted in the course of this licensing transaction, (ii) these terms and conditions and (iii) CCC's Billing and Payment terms and conditions.

8. License Contingent Upon Payment: While you may exercise the rights licensed

Rightslink Printable License

[https://s100.copyright.com/CustomerAdmin/PLF.jsp?IID=2012030\\_1331138797497](https://s100.copyright.com/CustomerAdmin/PLF.jsp?IID=2012030_1331138797497)[5/3/2012 5:57:30 PM]

## **ELSEVIER LICENSE TERMS AND CONDITIONS**

May 03, 2012

This is a License Agreement between Sarah C. Scarry ("You") and Elsevier ("Elsevier") provided by Copyright Clearance Center ("CCC"). The license consists of your order details, the terms and conditions provided by Elsevier, and the payment terms and conditions.

**All payments must be made in full to CCC. For payment instructions, please see information listed at the bottom of this form.**

Supplier Elsevier Limited

The Boulevard, Langford Lane  
Kidlington, Oxford, OX5 1GB, UK

Registered Company

Number

1982084

Customer name Sarah C. Scarry

Customer address 4749 Sardis Lake Drive  
Batesville, MS 38606

License number 2863701357497

License date Mar 07, 2012

Licensed content publisher Elsevier

Licensed content publication Structure

Licensed content title HIV-1 Transcription: Activation Mediated by Acetylation of Tat

Licensed content author Yoshihiro Nakatani

Licensed content date April 2002

Licensed content volume

number

10

Licensed content issue

number

4

Number of pages 2

Start Page 443

End Page 444

Type of Use reuse in a thesis/dissertation

Intended publisher of new

work

other

Portion figures/tables/illustrations

Number of

figures/tables/illustrations

1

Format both print and electronic

Are you the author of this

Elsevier article?

No

Will you be translating? No

Order reference number

Title of your The Synthesis of HIV-1 IN Inhibitors

Rightslink Printable License

[https://s100.copyright.com/CustomerAdmin/PLF.jsp?IID=2012030\\_1331138797497](https://s100.copyright.com/CustomerAdmin/PLF.jsp?IID=2012030_1331138797497)[5/3/2012 5:57:30 PM]

thesis/dissertation

Expected completion date May 2012

Estimated size (number of

pages)

350

Elsevier VAT number GB 494 6272 12

Permissions price 0.00 USD

VAT/Local Sales Tax 0.0 USD / 0.0 GBP

Total 0.00 USD

[Terms and Conditions](#)

## **INTRODUCTION**

1. The publisher for this copyrighted material is Elsevier. By clicking "accept" in connection with completing this licensing transaction, you agree that the following terms and conditions apply to this transaction (along with the Billing and Payment terms and conditions established by Copyright Clearance Center, Inc. ("CCC"), at the time that you opened your Rightslink account and that are available at any time at <http://myaccount.copyright.com>).

## **GENERAL TERMS**

2. Elsevier hereby grants you permission to reproduce the aforementioned material subject to the terms and conditions indicated.

3. Acknowledgement: If any part of the material to be used (for example, figures) has appeared in our publication with credit or acknowledgement to another source, permission must also be sought from that source. If such permission is not obtained then that material may not be included in your publication/copies. Suitable acknowledgement to the source must be made, either as a footnote or in a reference list at the end of your publication, as follows:

"Reprinted from Publication title, Vol /edition number, Author(s), Title of article / title of chapter, Pages No., Copyright (Year), with permission from Elsevier [OR APPLICABLE SOCIETY COPYRIGHT OWNER]." Also Lancet special credit -

"Reprinted from The Lancet, Vol. number, Author(s), Title of article, Pages No., Copyright (Year), with permission from Elsevier."

4. Reproduction of this material is confined to the purpose and/or media for which permission is hereby given.

5. Altering/Modifying Material: Not Permitted. However figures and illustrations may be altered/adapted minimally to serve your work. Any other abbreviations, additions, deletions and/or any other alterations shall be made only with prior written authorization of Elsevier Ltd. (Please contact Elsevier at [permissions@elsevier.com](mailto:permissions@elsevier.com))

6. If the permission fee for the requested use of our material is waived in this instance, please be advised that your future requests for Elsevier materials may attract a fee.

7. Reservation of Rights: Publisher reserves all rights not specifically granted in the combination of (i) the license details provided by you and accepted in the course of this licensing transaction, (ii) these terms and conditions and (iii) CCC's Billing and Payment terms and conditions.

8. License Contingent Upon Payment: While you may exercise the rights licensed



## **NATURE PUBLISHING GROUP LICENSE**

### **TERMS AND CONDITIONS**

May 03, 2012

This is a License Agreement between Sarah C. Scarry ("You") and Nature Publishing Group ("Nature Publishing Group") provided by Copyright Clearance Center ("CCC"). The license consists of your order details, the terms and conditions provided by Nature Publishing Group, and the payment terms and conditions.

**All payments must be made in full to CCC. For payment instructions, please see information listed at the bottom of this form.**

License Number 2863790346117

License date Mar 07, 2012

Licensed content publisher Nature Publishing Group

Licensed content publication Nature Medicine

Licensed content title Charting HIV's remarkable voyage through the cell: Basic science as a passport to future therapy

Licensed content author Warner C. Greene, B. Matija Peterlin

Licensed content date Jul 1, 2002

Type of Use reuse in a thesis/dissertation

Requestor type academic/educational

Format print and electronic

Portion figures/tables/illustrations

Number of

figures/tables/illustrations

1

High-res required no

Figures Figure 2. Schematic of Early Events Occurring after HIV infection.

Author of this NPG article no

Your reference number

Title of your thesis /  
dissertation

The Synthesis of HIV-1 IN Inhibitors

Expected completion date May 2012

Estimated size (number of  
pages)

350

Total 0.00 USD

[Terms and Conditions](#)

### Terms and Conditions for Permissions

Nature Publishing Group hereby grants you a non-exclusive license to reproduce this material for this purpose, and for no other use, subject to the conditions below:

1. NPG warrants that it has, to the best of its knowledge, the rights to license reuse of this material. However, you should ensure that the material you are requesting is original to Nature Publishing Group and does not carry the

Rightslink Printable License

[https://s100.copyright.com/CustomerAdmin/PLF.jsp?IID=2012030\\_1331151394117](https://s100.copyright.com/CustomerAdmin/PLF.jsp?IID=2012030_1331151394117)[5/3/2012 6:02:08 PM]

copyright of another entity (as credited in the published version). If the credit line on any part of the material you have requested indicates that it was reprinted or adapted by NPG with permission from another source, then you should also seek permission from that source to reuse the material.

2. Permission granted free of charge for material in print is also usually granted

for any electronic version of that work, provided that the material is incidental to the work as a whole and that the electronic version is essentially equivalent to, or substitutes for, the print version. Where print permission has been granted for a fee, separate permission must be obtained for any additional, electronic re-use (unless, as in the case of a full paper, this has already been accounted for during your initial request in the calculation of a print run). NB: In all cases, web-based use of full-text articles must be authorized separately through the 'Use on a Web Site' option when requesting permission.

3. Permission granted for a first edition does not apply to second and subsequent editions and for editions in other languages (except for signatories to the STM Permissions Guidelines, or where the first edition permission was granted for free).

4. Nature Publishing Group's permission must be acknowledged next to the figure, table or abstract in print. In electronic form, this acknowledgement must be visible at the same time as the figure/table/abstract, and must be hyperlinked to the journal's homepage.

5. The credit line should read:

Reprinted by permission from Macmillan Publishers Ltd: [JOURNAL NAME] (reference citation), copyright (year of publication)

For AOP papers, the credit line should read:

Reprinted by permission from Macmillan Publishers Ltd: [JOURNAL NAME], advance online publication, day month year (doi: 10.1038/sj.[JOURNAL ACRONYM].XXXXX)

**Note: For republication from the British Journal of Cancer, the following credit lines apply.**

Reprinted by permission from Macmillan Publishers Ltd on behalf of Cancer Research UK: [JOURNAL NAME] (reference citation), copyright (year of publication) For AOP papers, the credit line should read:

Reprinted by permission from Macmillan Publishers Ltd on behalf of Cancer Research UK: [JOURNAL NAME], advance online publication, day month year (doi: 10.1038/sj.[JOURNAL ACRONYM].XXXXX)

6. Adaptations of single figures do not require NPG approval. However, the adaptation should be credited as follows:

Adapted by permission from Macmillan Publishers Ltd: [JOURNAL NAME] (reference citation), copyright (year of publication)

**Note: For adaptation from the British Journal of Cancer, the following credit line applies.**

Adapted by permission from Macmillan Publishers Ltd on behalf of Cancer Research UK: [JOURNAL NAME] (reference citation), copyright (year of publication)

7. Translations of 401 words up to a whole article require NPG approval. Please

## **NATURE PUBLISHING GROUP LICENSE**

### **TERMS AND CONDITIONS**

May 03, 2012

This is a License Agreement between Sarah C. Scarry ("You") and Nature Publishing Group ("Nature Publishing Group") provided by Copyright Clearance Center ("CCC"). The license consists of your order details, the terms and conditions provided by Nature Publishing Group, and the payment terms and conditions.

**All payments must be made in full to CCC. For payment instructions, please see information listed at the bottom of this form.**

License Number 2863790346117

License date Mar 07, 2012

Licensed content publisher Nature Publishing Group

Licensed content publication Nature Medicine

Licensed content title Charting HIV's remarkable voyage through the cell: Basic science as a passport to future therapy

Licensed content author Warner C. Greene, B. Matija Peterlin

Licensed content date Jul 1, 2002

Type of Use reuse in a thesis/dissertation

Requestor type academic/educational

Format print and electronic

Portion figures/tables/illustrations

Number of

figures/tables/illustrations

1

High-res required no

Figures Figure 2. Schematic of Early Events Occurring after HIV infection.

Author of this NPG article no

Your reference number

Title of your thesis /  
dissertation

The Synthesis of HIV-1 IN Inhibitors

Expected completion date May 2012

Estimated size (number of  
pages)

350

Total 0.00 USD

[Terms and Conditions](#)

### Terms and Conditions for Permissions

Nature Publishing Group hereby grants you a non-exclusive license to reproduce this material for this purpose, and for no other use, subject to the conditions below:

1. NPG warrants that it has, to the best of its knowledge, the rights to license reuse of this material. However, you should ensure that the material you are requesting is original to Nature Publishing Group and does not carry the

Rightslink Printable License

[https://s100.copyright.com/CustomerAdmin/PLF.jsp?IID=2012030\\_1331151394117](https://s100.copyright.com/CustomerAdmin/PLF.jsp?IID=2012030_1331151394117)[5/3/2012 6:03:48 PM]

copyright of another entity (as credited in the published version). If the credit line on any part of the material you have requested indicates that it was reprinted or adapted by NPG with permission from another source, then you should also seek permission from that source to reuse the material.

2. Permission granted free of charge for material in print is also usually granted

for any electronic version of that work, provided that the material is incidental to the work as a whole and that the electronic version is essentially equivalent to, or substitutes for, the print version. Where print permission has been granted for a fee, separate permission must be obtained for any additional, electronic re-use (unless, as in the case of a full paper, this has already been accounted for during your initial request in the calculation of a print run). NB: In all cases, web-based use of full-text articles must be authorized separately through the 'Use on a Web Site' option when requesting permission.

3. Permission granted for a first edition does not apply to second and subsequent editions and for editions in other languages (except for signatories to the STM Permissions Guidelines, or where the first edition permission was granted for free).

4. Nature Publishing Group's permission must be acknowledged next to the figure, table or abstract in print. In electronic form, this acknowledgement must be visible at the same time as the figure/table/abstract, and must be hyperlinked to the journal's homepage.

5. The credit line should read:

Reprinted by permission from Macmillan Publishers Ltd: [JOURNAL NAME] (reference citation), copyright (year of publication)

For AOP papers, the credit line should read:

Reprinted by permission from Macmillan Publishers Ltd: [JOURNAL NAME], advance online publication, day month year (doi: 10.1038/sj.[JOURNAL ACRONYM].XXXXX)

**Note: For republication from the British Journal of Cancer, the following credit lines apply.**

Reprinted by permission from Macmillan Publishers Ltd on behalf of Cancer Research UK: [JOURNAL NAME] (reference citation), copyright (year of publication) For AOP papers, the credit line should read:

Reprinted by permission from Macmillan Publishers Ltd on behalf of Cancer Research UK: [JOURNAL NAME], advance online publication, day month year (doi: 10.1038/sj.[JOURNAL ACRONYM].XXXXX)

6. Adaptations of single figures do not require NPG approval. However, the adaptation should be credited as follows:

Adapted by permission from Macmillan Publishers Ltd: [JOURNAL NAME] (reference citation), copyright (year of publication)

**Note: For adaptation from the British Journal of Cancer, the following credit line applies.**

Adapted by permission from Macmillan Publishers Ltd on behalf of Cancer Research UK: [JOURNAL NAME] (reference citation), copyright (year of publication)

7. Translations of 401 words up to a whole article require NPG approval. Please

## **NATURE PUBLISHING GROUP LICENSE TERMS AND CONDITIONS**

May 03, 2012

This is a License Agreement between Sarah C. Scarry ("You") and Nature Publishing Group ("Nature Publishing Group") provided by Copyright Clearance Center ("CCC"). The license consists of your order details, the terms and conditions provided by Nature Publishing Group, and the payment terms and conditions.

**All payments must be made in full to CCC. For payment instructions, please see information listed at the bottom of this form.**

License Number 2863790720427

License date Mar 07, 2012

Licensed content publisher Nature Publishing Group

Licensed content publication Nature Medicine

Licensed content title Charting HIV's remarkable voyage through the cell: Basic science as a passport to future therapy

Licensed content author Warner C. Greene, B. Matija Peterlin

Licensed content date Jul 1, 2002

Type of Use reuse in a thesis/dissertation

Requestor type academic/educational

Format print and electronic

Portion figures/tables/illustrations

Number of

figures/tables/illustrations

1

High-res required no

Figures An overview of the organization of the ~9-kilobase genome of the HIV provirus and summary of its nine genes encoding 15 proteins.

Author of this NPG article no

Your reference number

Title of your thesis /  
dissertation

The Synthesis of HIV-1 IN Inhibitors

Expected completion date May 2012

Estimated size (number of  
pages)

350

Total 0.00 USD

[Terms and Conditions](#)

### Terms and Conditions for Permissions

Nature Publishing Group hereby grants you a non-exclusive license to reproduce this material for this purpose, and for no other use, subject to the conditions below:

1. NPG warrants that it has, to the best of its knowledge, the rights to license reuse of this material. However, you should ensure that the material you are requesting is original to Nature Publishing Group and does not carry the

Rightslink Printable License

[https://s100.copyright.com/CustomerAdmin/PLF.jsp?IID=2012030\\_1331151768427](https://s100.copyright.com/CustomerAdmin/PLF.jsp?IID=2012030_1331151768427)[5/3/2012 6:09:30 PM]

copyright of another entity (as credited in the published version). If the credit line on any part of the material you have requested indicates that it was reprinted or adapted by NPG with permission from another source, then you should also seek permission from that source to reuse the material.

2. Permission granted free of charge for material in print is also usually granted

for any electronic version of that work, provided that the material is incidental to the work as a whole and that the electronic version is essentially equivalent to, or substitutes for, the print version. Where print permission has been granted for a fee, separate permission must be obtained for any additional, electronic re-use (unless, as in the case of a full paper, this has already been accounted for during your initial request in the calculation of a print run). NB: In all cases, web-based use of full-text articles must be authorized separately through the 'Use on a Web Site' option when requesting permission.

3. Permission granted for a first edition does not apply to second and subsequent editions and for editions in other languages (except for signatories to the STM Permissions Guidelines, or where the first edition permission was granted for free).

4. Nature Publishing Group's permission must be acknowledged next to the figure, table or abstract in print. In electronic form, this acknowledgement must be visible at the same time as the figure/table/abstract, and must be hyperlinked to the journal's homepage.

5. The credit line should read:

Reprinted by permission from Macmillan Publishers Ltd: [JOURNAL NAME] (reference citation), copyright (year of publication)

For AOP papers, the credit line should read:

Reprinted by permission from Macmillan Publishers Ltd: [JOURNAL NAME], advance online publication, day month year (doi: 10.1038/sj.[JOURNAL ACRONYM].XXXXX)

**Note: For republication from the British Journal of Cancer, the following credit lines apply.**

Reprinted by permission from Macmillan Publishers Ltd on behalf of Cancer Research UK: [JOURNAL NAME] (reference citation), copyright (year of publication) For AOP papers, the credit line should read:

Reprinted by permission from Macmillan Publishers Ltd on behalf of Cancer Research UK: [JOURNAL NAME], advance online publication, day month year (doi: 10.1038/sj.[JOURNAL ACRONYM].XXXXX)

6. Adaptations of single figures do not require NPG approval. However, the adaptation should be credited as follows:

Adapted by permission from Macmillan Publishers Ltd: [JOURNAL NAME] (reference citation), copyright (year of publication)

**Note: For adaptation from the British Journal of Cancer, the following credit line applies.**

Adapted by permission from Macmillan Publishers Ltd on behalf of Cancer Research UK: [JOURNAL NAME] (reference citation), copyright (year of publication)

7. Translations of 401 words up to a whole article require NPG approval. Please

Rightslink Printable License

[https://s100.copyright.com/CustomerAdmin/PLF.jsp?IID=2012030\\_1331151768427](https://s100.copyright.com/CustomerAdmin/PLF.jsp?IID=2012030_1331151768427)[5/3/2012 6:11:11 PM]

## **NATURE PUBLISHING GROUP LICENSE TERMS AND CONDITIONS**

May 03, 2012

This is a License Agreement between Sarah C. Scarry ("You") and Nature Publishing Group ("Nature Publishing Group") provided by Copyright Clearance Center ("CCC"). The license consists of your order details, the terms and conditions provided by Nature Publishing Group, and the payment terms and conditions.

**All payments must be made in full to CCC. For payment instructions, please see information listed at the bottom of this form.**

License Number 2863790720427

License date Mar 07, 2012

Licensed content publisher Nature Publishing Group

Licensed content publication Nature Medicine

Licensed content title Charting HIV's remarkable voyage through the cell: Basic science as a passport to future therapy

Licensed content author Warner C. Greene, B. Matija Peterlin

Licensed content date Jul 1, 2002

Type of Use reuse in a thesis/dissertation

Requestor type academic/educational

Format print and electronic

Portion figures/tables/illustrations

Number of

figures/tables/illustrations

1

High-res required no

Figures An overview of the organization of the ~9-kilobase genome of the HIV provirus and summary of its nine genes encoding 15 proteins.

Author of this NPG article no

Your reference number

Title of your thesis /  
dissertation

The Synthesis of HIV-1 IN Inhibitors

Expected completion date May 2012

Estimated size (number of  
pages)

350

Total 0.00 USD

[Terms and Conditions](#)

### Terms and Conditions for Permissions

Nature Publishing Group hereby grants you a non-exclusive license to reproduce this material for this purpose, and for no other use, subject to the conditions below:

1. NPG warrants that it has, to the best of its knowledge, the rights to license reuse of this material. However, you should ensure that the material you are requesting is original to Nature Publishing Group and does not carry the

Rightslink Printable License

[https://s100.copyright.com/CustomerAdmin/PLF.jsp?IID=2012030\\_1331151768427](https://s100.copyright.com/CustomerAdmin/PLF.jsp?IID=2012030_1331151768427)[5/3/2012 6:11:11 PM]

copyright of another entity (as credited in the published version). If the credit line on any part of the material you have requested indicates that it was reprinted or adapted by NPG with permission from another source, then you should also seek permission from that source to reuse the material.

2. Permission granted free of charge for material in print is also usually granted

for any electronic version of that work, provided that the material is incidental to the work as a whole and that the electronic version is essentially equivalent to, or substitutes for, the print version. Where print permission has been granted for a fee, separate permission must be obtained for any additional, electronic re-use (unless, as in the case of a full paper, this has already been accounted for during your initial request in the calculation of a print run). NB: In all cases, web-based use of full-text articles must be authorized separately through the 'Use on a Web Site' option when requesting permission.

3. Permission granted for a first edition does not apply to second and subsequent editions and for editions in other languages (except for signatories to the STM Permissions Guidelines, or where the first edition permission was granted for free).

4. Nature Publishing Group's permission must be acknowledged next to the figure, table or abstract in print. In electronic form, this acknowledgement must be visible at the same time as the figure/table/abstract, and must be hyperlinked to the journal's homepage.

5. The credit line should read:

Reprinted by permission from Macmillan Publishers Ltd: [JOURNAL NAME] (reference citation), copyright (year of publication)

For AOP papers, the credit line should read:

Reprinted by permission from Macmillan Publishers Ltd: [JOURNAL NAME], advance online publication, day month year (doi: 10.1038/sj.[JOURNAL ACRONYM].XXXXX)

**Note: For republication from the British Journal of Cancer, the following credit lines apply.**

Reprinted by permission from Macmillan Publishers Ltd on behalf of Cancer Research UK: [JOURNAL NAME] (reference citation), copyright (year of publication) For AOP papers, the credit line should read:

Reprinted by permission from Macmillan Publishers Ltd on behalf of Cancer Research UK: [JOURNAL NAME], advance online publication, day month year (doi: 10.1038/sj.[JOURNAL ACRONYM].XXXXX)

6. Adaptations of single figures do not require NPG approval. However, the adaptation should be credited as follows:

Adapted by permission from Macmillan Publishers Ltd: [JOURNAL NAME] (reference citation), copyright (year of publication)

**Note: For adaptation from the British Journal of Cancer, the following credit line applies.**

Adapted by permission from Macmillan Publishers Ltd on behalf of Cancer Research UK: [JOURNAL NAME] (reference citation), copyright (year of publication)

7. Translations of 401 words up to a whole article require NPG approval. Please



Rightslink Printable License

[https://s100.copyright.com/CustomerAdmin/PLF.jsp?IID=2012030\\_1331599255927](https://s100.copyright.com/CustomerAdmin/PLF.jsp?IID=2012030_1331599255927)[5/3/2012 6:13:04 PM]

**ELSEVIER LICENSE  
TERMS AND CONDITIONS**

May 03, 2012

This is a License Agreement between Sarah C. Scarry ("You") and Elsevier ("Elsevier") provided by Copyright Clearance Center ("CCC"). The license consists of your order details, the terms and conditions provided by Elsevier, and the payment terms and conditions.

**All payments must be made in full to CCC. For payment instructions, please see information listed at the bottom of this form.**

Supplier Elsevier Limited

The Boulevard, Langford Lane  
Kidlington, Oxford, OX5 1GB, UK

Registered Company

Number

1982084

Customer name Sarah C. Scarry

Customer address 4749 Sardis Lake Drive

Batesville, MS 38606

License number 2866750655927

License date Mar 12, 2012

Licensed content publisher Elsevier

Licensed content publication Antiviral Research

Licensed content title Strand transfer inhibitors of HIV-1 integrase: Bringing IN a new era of antiretroviral therapy

Licensed content author Damian J. McColl, Xiaowu Chen

Licensed content date January 2010

Licensed content volume

number

85

Licensed content issue

number

1

Number of pages 18

Start Page 101

End Page 118

Type of Use reuse in a thesis/dissertation

Intended publisher of new

work

other

Portion figures/tables/illustrations

Number of

figures/tables/illustrations

1

Format both print and electronic

Are you the author of this

Elsevier article?

No

Will you be translating? No

Order reference number

Rightslink Printable License

[https://s100.copyright.com/CustomerAdmin/PLF.jsp?IID=2012030\\_1331599255927](https://s100.copyright.com/CustomerAdmin/PLF.jsp?IID=2012030_1331599255927)[5/3/2012 6:13:04 PM]

Title of your

thesis/dissertation

The Synthesis of HIV-1 IN Inhibitors

Expected completion date May 2012

Estimated size (number of pages)

350

Elsevier VAT number GB 494 6272 12

Permissions price 0.00 USD

VAT/Local Sales Tax 0.0 USD / 0.0 GBP

Total 0.00 USD

[Terms and Conditions](#)

## **INTRODUCTION**

1. The publisher for this copyrighted material is Elsevier. By clicking "accept" in connection with completing this licensing transaction, you agree that the following terms and conditions apply to this transaction (along with the Billing and Payment terms and conditions established by Copyright Clearance Center, Inc. ("CCC"), at the time that you opened your Rightslink account and that are available at any time at <http://myaccount.copyright.com>).

## **GENERAL TERMS**

2. Elsevier hereby grants you permission to reproduce the aforementioned material subject to the terms and conditions indicated.

3. Acknowledgement: If any part of the material to be used (for example, figures) has appeared in our publication with credit or acknowledgement to another source, permission must also be sought from that source. If such permission is not obtained then that material may not be included in your publication/copies.

Suitable acknowledgement to the source must be made, either as a footnote or in a reference list at the end of your publication, as follows:

"Reprinted from Publication title, Vol /edition number, Author(s), Title of article / title of chapter, Pages No., Copyright (Year), with permission from Elsevier [OR APPLICABLE SOCIETY COPYRIGHT OWNER]." Also Lancet special credit -

"Reprinted from The Lancet, Vol. number, Author(s), Title of article, Pages No., Copyright (Year), with permission from Elsevier."

4. Reproduction of this material is confined to the purpose and/or media for which permission is hereby given.

5. Altering/Modifying Material: Not Permitted. However figures and illustrations may be altered/adapted minimally to serve your work. Any other abbreviations, additions, deletions and/or any other alterations shall be made only with prior written authorization of Elsevier Ltd. (Please contact Elsevier at [permissions@elsevier.com](mailto:permissions@elsevier.com))

6. If the permission fee for the requested use of our material is waived in this instance, please be advised that your future requests for Elsevier materials may attract a fee.

7. Reservation of Rights: Publisher reserves all rights not specifically granted in the combination of (i) the license details provided by you and accepted in the course of this licensing transaction, (ii) these terms and conditions and (iii) CCC's Billing and Payment terms and conditions.

Rightslink Printable License

[https://s100.copyright.com/CustomerAdmin/PLF.jsp?IID=2012030\\_1331599255927](https://s100.copyright.com/CustomerAdmin/PLF.jsp?IID=2012030_1331599255927)[5/3/2012 6:14:35 PM]

**ELSEVIER LICENSE  
TERMS AND CONDITIONS**

May 03, 2012

This is a License Agreement between Sarah C. Scarry ("You") and Elsevier ("Elsevier") provided by Copyright Clearance Center ("CCC"). The license consists of your order details, the terms and conditions provided by Elsevier, and the payment terms and conditions.

**All payments must be made in full to CCC. For payment instructions, please see information listed at the bottom of this form.**

Supplier Elsevier Limited

The Boulevard, Langford Lane  
Kidlington, Oxford, OX5 1GB, UK

Registered Company

Number

1982084

Customer name Sarah C. Scarry

Customer address 4749 Sardis Lake Drive  
Batesville, MS 38606

License number 2866750655927

License date Mar 12, 2012

Licensed content publisher Elsevier

Licensed content publication Antiviral Research

Licensed content title Strand transfer inhibitors of HIV-1 integrase: Bringing IN a new era of antiretroviral therapy

Licensed content author Damian J. McColl, Xiaowu Chen

Licensed content date January 2010

Licensed content volume  
number

85

Licensed content issue  
number

1

Number of pages 18

Start Page 101

End Page 118

Type of Use reuse in a thesis/dissertation

Intended publisher of new  
work

other

Portion figures/tables/illustrations

Number of  
figures/tables/illustrations

1

Format both print and electronic

Are you the author of this  
Elsevier article?

No

Will you be translating? No

Order reference number

Rightslink Printable License

[https://s100.copyright.com/CustomerAdmin/PLF.jsp?IID=2012030\\_1331599255927](https://s100.copyright.com/CustomerAdmin/PLF.jsp?IID=2012030_1331599255927)[5/3/2012 6:14:35 PM]

Title of your

thesis/dissertation

The Synthesis of HIV-1 IN Inhibitors

Expected completion date May 2012

Estimated size (number of pages)

350

Elsevier VAT number GB 494 6272 12

Permissions price 0.00 USD

VAT/Local Sales Tax 0.0 USD / 0.0 GBP

Total 0.00 USD

[Terms and Conditions](#)

## **INTRODUCTION**

1. The publisher for this copyrighted material is Elsevier. By clicking "accept" in connection with completing this licensing transaction, you agree that the following terms and conditions apply to this transaction (along with the Billing and Payment terms and conditions established by Copyright Clearance Center, Inc. ("CCC"), at the time that you opened your Rightslink account and that are available at any time at <http://myaccount.copyright.com>).

## **GENERAL TERMS**

2. Elsevier hereby grants you permission to reproduce the aforementioned material subject to the terms and conditions indicated.

3. Acknowledgement: If any part of the material to be used (for example, figures) has appeared in our publication with credit or acknowledgement to another source, permission must also be sought from that source. If such permission is not obtained then that material may not be included in your publication/copies.

Suitable acknowledgement to the source must be made, either as a footnote or in a reference list at the end of your publication, as follows:

"Reprinted from Publication title, Vol /edition number, Author(s), Title of article / title of chapter, Pages No., Copyright (Year), with permission from Elsevier [OR APPLICABLE SOCIETY COPYRIGHT OWNER]." Also Lancet special credit -

"Reprinted from The Lancet, Vol. number, Author(s), Title of article, Pages No., Copyright (Year), with permission from Elsevier."

4. Reproduction of this material is confined to the purpose and/or media for which permission is hereby given.

5. Altering/Modifying Material: Not Permitted. However figures and illustrations may be altered/adapted minimally to serve your work. Any other abbreviations, additions, deletions and/or any other alterations shall be made only with prior written authorization of Elsevier Ltd. (Please contact Elsevier at [permissions@elsevier.com](mailto:permissions@elsevier.com))

6. If the permission fee for the requested use of our material is waived in this instance, please be advised that your future requests for Elsevier materials may attract a fee.

7. Reservation of Rights: Publisher reserves all rights not specifically granted in the combination of (i) the license details provided by you and accepted in the course of this licensing transaction, (ii) these terms and conditions and (iii) CCC's Billing and Payment terms and conditions.

Rightslink Printable License  
[https://s100.copyright.com/CustomerAdmin/PLF.jsp?IID=2012030\\_1331599560382](https://s100.copyright.com/CustomerAdmin/PLF.jsp?IID=2012030_1331599560382)[5/3/2012 6:17:29 PM]

## **ELSEVIER LICENSE TERMS AND CONDITIONS**

May 03, 2012

This is a License Agreement between Sarah C. Scarry ("You") and Elsevier ("Elsevier") provided by Copyright Clearance Center ("CCC"). The license consists of your order details, the terms and conditions provided by Elsevier, and the payment terms and conditions.

**All payments must be made in full to CCC. For payment instructions, please see information listed at the bottom of this form.**

Supplier Elsevier Limited

The Boulevard, Langford Lane  
Kidlington, Oxford, OX5 1GB, UK

Registered Company

Number

1982084

Customer name Sarah C. Scarry

Customer address 4749 Sardis Lake Drive  
Batesville, MS 38606

License number 2866750960382

License date Mar 12, 2012

Licensed content publisher Elsevier

Licensed content publication Antiviral Research

Licensed content title Strand transfer inhibitors of HIV-1 integrase: Bringing IN a new era of antiretroviral therapy

Licensed content author Damian J. McColl, Xiaowu Chen

Licensed content date January 2010

Licensed content volume

number

85

Licensed content issue

number

1

Number of pages 18

Start Page 101

End Page 118

Type of Use reuse in a thesis/dissertation

Intended publisher of new

work

other

Portion figures/tables/illustrations

Number of

figures/tables/illustrations

1

Format both print and electronic

Are you the author of this

Elsevier article?

No

Will you be translating? No

Order reference number

Rightslink Printable License

[https://s100.copyright.com/CustomerAdmin/PLF.jsp?IID=2012030\\_1331599560382](https://s100.copyright.com/CustomerAdmin/PLF.jsp?IID=2012030_1331599560382)[5/3/2012 6:17:29 PM]

Title of your

thesis/dissertation

The Synthesis of HIV-1 IN Inhibitors

Expected completion date May 2012

Estimated size (number of pages)

350

Elsevier VAT number GB 494 6272 12

Permissions price 0.00 USD

VAT/Local Sales Tax 0.0 USD / 0.0 GBP

Total 0.00 USD

[Terms and Conditions](#)

## **INTRODUCTION**

1. The publisher for this copyrighted material is Elsevier. By clicking "accept" in connection with completing this licensing transaction, you agree that the following terms and conditions apply to this transaction (along with the Billing and Payment terms and conditions established by Copyright Clearance Center, Inc. ("CCC"), at the time that you opened your Rightslink account and that are available at any time at <http://myaccount.copyright.com>).

## **GENERAL TERMS**

2. Elsevier hereby grants you permission to reproduce the aforementioned material subject to the terms and conditions indicated.

3. Acknowledgement: If any part of the material to be used (for example, figures) has appeared in our publication with credit or acknowledgement to another source, permission must also be sought from that source. If such permission is not obtained then that material may not be included in your publication/copies.

Suitable acknowledgement to the source must be made, either as a footnote or in a reference list at the end of your publication, as follows:

"Reprinted from Publication title, Vol /edition number, Author(s), Title of article / title of chapter, Pages No., Copyright (Year), with permission from Elsevier [OR APPLICABLE SOCIETY COPYRIGHT OWNER]." Also Lancet special credit -

"Reprinted from The Lancet, Vol. number, Author(s), Title of article, Pages No., Copyright (Year), with permission from Elsevier."

4. Reproduction of this material is confined to the purpose and/or media for which permission is hereby given.

5. Altering/Modifying Material: Not Permitted. However figures and illustrations may be altered/adapted minimally to serve your work. Any other abbreviations, additions, deletions and/or any other alterations shall be made only with prior written authorization of Elsevier Ltd. (Please contact Elsevier at [permissions@elsevier.com](mailto:permissions@elsevier.com))

6. If the permission fee for the requested use of our material is waived in this instance, please be advised that your future requests for Elsevier materials may attract a fee.

7. Reservation of Rights: Publisher reserves all rights not specifically granted in the combination of (i) the license details provided by you and accepted in the course of this licensing transaction, (ii) these terms and conditions and (iii) CCC's Billing and Payment terms and conditions.

Rightslink Printable License  
[https://s100.copyright.com/CustomerAdmin/PLF.jsp?IID=2012030\\_1331599560382](https://s100.copyright.com/CustomerAdmin/PLF.jsp?IID=2012030_1331599560382)[5/3/2012 6:19:25 PM]

## **ELSEVIER LICENSE TERMS AND CONDITIONS**

May 03, 2012

This is a License Agreement between Sarah C. Scarry ("You") and Elsevier ("Elsevier") provided by Copyright Clearance Center ("CCC"). The license consists of your order details, the terms and conditions provided by Elsevier, and the payment terms and conditions.

**All payments must be made in full to CCC. For payment instructions, please see information listed at the bottom of this form.**

Supplier Elsevier Limited

The Boulevard, Langford Lane  
Kidlington, Oxford, OX5 1GB, UK

Registered Company

Number

1982084

Customer name Sarah C. Scarry

Customer address 4749 Sardis Lake Drive  
Batesville, MS 38606

License number 2866750960382

License date Mar 12, 2012

Licensed content publisher Elsevier

Licensed content publication Antiviral Research

Licensed content title Strand transfer inhibitors of HIV-1 integrase: Bringing IN a new era of antiretroviral therapy

Licensed content author Damian J. McColl, Xiaowu Chen

Licensed content date January 2010

Licensed content volume  
number

85

Licensed content issue  
number

1

Number of pages 18

Start Page 101

End Page 118

Type of Use reuse in a thesis/dissertation

Intended publisher of new  
work

other

Portion figures/tables/illustrations

Number of  
figures/tables/illustrations

1

Format both print and electronic

Are you the author of this  
Elsevier article?

No

Will you be translating? No

Order reference number

Rightslink Printable License

[https://s100.copyright.com/CustomerAdmin/PLF.jsp?IID=2012030\\_1331599560382](https://s100.copyright.com/CustomerAdmin/PLF.jsp?IID=2012030_1331599560382)[5/3/2012 6:19:25 PM]

Title of your

thesis/dissertation

The Synthesis of HIV-1 IN Inhibitors

Expected completion date May 2012

Estimated size (number of pages)

350

Elsevier VAT number GB 494 6272 12

Permissions price 0.00 USD

VAT/Local Sales Tax 0.0 USD / 0.0 GBP

Total 0.00 USD

[Terms and Conditions](#)

## **INTRODUCTION**

1. The publisher for this copyrighted material is Elsevier. By clicking "accept" in connection with completing this licensing transaction, you agree that the following terms and conditions apply to this transaction (along with the Billing and Payment terms and conditions established by Copyright Clearance Center, Inc. ("CCC"), at the time that you opened your Rightslink account and that are available at any time at <http://myaccount.copyright.com>).

## **GENERAL TERMS**

2. Elsevier hereby grants you permission to reproduce the aforementioned material subject to the terms and conditions indicated.

3. Acknowledgement: If any part of the material to be used (for example, figures) has appeared in our publication with credit or acknowledgement to another source, permission must also be sought from that source. If such permission is not obtained then that material may not be included in your publication/copies.

Suitable acknowledgement to the source must be made, either as a footnote or in a reference list at the end of your publication, as follows:

"Reprinted from Publication title, Vol /edition number, Author(s), Title of article / title of chapter, Pages No., Copyright (Year), with permission from Elsevier [OR APPLICABLE SOCIETY COPYRIGHT OWNER]." Also Lancet special credit -

"Reprinted from The Lancet, Vol. number, Author(s), Title of article, Pages No., Copyright (Year), with permission from Elsevier."

4. Reproduction of this material is confined to the purpose and/or media for which permission is hereby given.

5. Altering/Modifying Material: Not Permitted. However figures and illustrations may be altered/adapted minimally to serve your work. Any other abbreviations, additions, deletions and/or any other alterations shall be made only with prior written authorization of Elsevier Ltd. (Please contact Elsevier at [permissions@elsevier.com](mailto:permissions@elsevier.com))

6. If the permission fee for the requested use of our material is waived in this instance, please be advised that your future requests for Elsevier materials may attract a fee.

7. Reservation of Rights: Publisher reserves all rights not specifically granted in the combination of (i) the license details provided by you and accepted in the course of this licensing transaction, (ii) these terms and conditions and (iii) CCC's Billing and Payment terms and conditions.



**From:** Sarah Marie Scarry  
**To:** JOHN M RIMOLDI  
**Subject:** FW: Kaiser Family Foundation permissions  
**Date:** Thursday, May 03, 2012 5:11:30 PM  
**From:** Kanani Kauka [mailto:KananiK@kff.org]  
**Sent:** Tuesday, March 13, 2012 5:16 PM  
**To:** 'schajkow@olemiss.edu'  
**Subject:** Kaiser Family Foundation permissions

Thank you for your copyright permission request. This is to grant permission to you and your organization for one-time use of the material cited in your e-mail below. Permission is granted with the understanding that the material is not to be altered or presented out of context.

Please source the material as follows:

**"Fact Sheet: The HIV/AIDS Epidemic in the United States"**, (#3029-12), The Henry J. Kaiser Family Foundation, February 2012

Our permission statement is:

This information was reprinted with permission from the Henry J. Kaiser Family Foundation. The Kaiser Family Foundation, a leader in health policy analysis, health journalism and communication, is dedicated to filling the need for trusted, independent information on the major health issues facing our nation and its people. The Foundation is a non-profit private operating foundation, based in Menlo Park, California.

Please let me know if you have questions.

Thanks,  
Kanani

---

**Kanani Kauka**  
**production assistant**

Kaiser Family Foundation  
2400 Sand Hill Road | Menlo Park, CA 94025  
kkauka@kff.org | 650.854.9400  
www.kff.org | www.kaiserhealthnews.org | www.statehealthfacts.org | www.kaiserEDU.org  
**SIGN UP FOR E-MAIL ALERTS AT:** [www.kff.org/email](http://www.kff.org/email)

Requester's Name\*: Sarah Scarry

Name of Organization\*: The University of Mississippi

Email Address\*: [schajkow@olemiss.edu](mailto:schajkow@olemiss.edu)

Phone\*: 662-915-8865

Fax:

Organization Web site: [www.olemiss.edu](http://www.olemiss.edu)

Kaiser Publication Title\*: HIV/AIDS Policy Fact Sheet: The HIV/AIDS Epidemic in the United States

Kaiser Publication URL\*: <http://www.kff.org/hivaids/upload/3029-12.pdf>

Kaiser Publication Number: <http://www.kff.org/hivaids/upload/3029-12.pdf>

Intended Use\*: This figure (Top Ten States by Cumulative AIDS Diagnoses and by AIDS Diagnosis Rate Per 100,000) will be used in a dissertation.

Distribution\*: Electronic and print. May 2012

Intent to Sell\*: No. Not for profit.

Comments:

**From:** Sarah Marie Scarry  
**To:** JOHN M RIMOLDI  
**Subject:** FW: Kaiser Family Foundation permissions  
**Date:** Thursday, May 03, 2012 5:11:49 PM  
**From:** Kanani Kauka [mailto:KananiK@kff.org]  
**Sent:** Tuesday, March 13, 2012 5:19 PM  
**To:** 'schajkow@olemiss.edu'  
**Subject:** Kaiser Family Foundation permissions

Thank you for your copyright permission request. This is to grant permission to you and your organization for one-time use of the material cited in your e-mail below. Permission is granted with the

understanding that the material is not to be altered or presented out of context.

Please source the material as follows:

**"Estimated Numbers of AIDS Diagnoses, All Ages, 2009"**, statehealthfacts.org, The Henry J. Kaiser Family Foundation, February 2011

Our permission statement is:

This information was reprinted with permission from the Henry J. Kaiser Family Foundation. The Kaiser Family Foundation, a leader in health policy analysis, health journalism and communication, is dedicated to filling the need for trusted, independent information on the major health issues facing our nation and its people. The Foundation is a non-profit private operating foundation, based in Menlo Park, California.

Please let me know if you have questions.

Thanks,

Kanani

---

**Kanani Kauka**

**production assistant**

Kaiser Family Foundation

2400 Sand Hill Road | Menlo Park, CA 94025

[kkauka@kff.org](mailto:kkauka@kff.org) | 650.854.9400

[www.kff.org](http://www.kff.org) | [www.kaiserhealthnews.org](http://www.kaiserhealthnews.org) | [www.statehealthfacts.org](http://www.statehealthfacts.org) | [www.kaiserEDU.org](http://www.kaiserEDU.org)

**SIGN UP FOR E-MAIL ALERTS AT:** [www.kff.org/email](http://www.kff.org/email)

Requester's Name\*: Sarah Scarry

Name of Organization\*: The University of Mississippi

Email Address\*: [schajkow@olemiss.edu](mailto:schajkow@olemiss.edu)

Phone\*: 662-915-8865

Fax:

Organization Web site: [www.olemiss.edu](http://www.olemiss.edu)

Kaiser Publication Title\*: Statehealthfacts.org Estimated Numbers of AIDS Diagnoses, All Ages, 2009

Kaiser Publication URL\*: [http://www.statehealthfacts.org/savemap.jsp?](http://www.statehealthfacts.org/savemap.jsp?ind=508&cat=11&sub=119&yr=92&typ=1&sort=a)

[ind=508&cat=11&sub=119&yr=92&typ=1&sort=a](http://www.statehealthfacts.org/savemap.jsp?ind=508&cat=11&sub=119&yr=92&typ=1&sort=a)

Kaiser Publication Number: [http://www.statehealthfacts.org/comparemaptable.jsp?](http://www.statehealthfacts.org/comparemaptable.jsp?ind=508&cat=11&sub=119&yr=92&typ=1&sort=a)

[ind=508&cat=11&sub=119&yr=92&typ=1&sort=a](http://www.statehealthfacts.org/comparemaptable.jsp?ind=508&cat=11&sub=119&yr=92&typ=1&sort=a)

Intended Use\*: This figure will be used in a dissertation.

Distribution\*: Electronic and print.

Intent to Sell\*: No. Not for profit.

Comments:

## VITA

Sarah Chajkowski Scarry was born in Pittsburgh, Pennsylvania, USA on March 3<sup>rd</sup>, 1984. She received his Bachelor of Science degree in Chemistry from Waynesburg University in May 2006, with the distinction of *cum laude*. She joined the doctoral program in the Department of Medicinal Chemistry at the University of Mississippi in the fall of 2006 and successfully completed all the requirements for a doctoral degree in the spring of 2012.